THE ANALYSIS OF ENGINEERING STRUCTURES

THE ANALYSIS OF ENGINEERING STRUCTURES

BY

A. J. S. PIPPARD, M.B.E., D.Sc.

MEMBER OF THE INSTITUTION OF CIVIL ENGINEERS ; MEMBER OF THE AMERICAN SOCIETY OF CIVIL ENGINEERS ; FELLOW OF THE ROYAL AERONAUTICAL SOCIETY.
PROFESSOR OF CIVIL ENGINEERING IN THE UNIVERSITY OF LONDON AT IMPERIAL COLLEGE ;

and

J. F. BAKER,

O.B.E., M.A., Sc.D. (Cantab.), D.Sc. (Wales).

ASSOCIATE MEMBER OF THE INSTITUTION OF CIVIL ENGINEERS ;
ASSOCIATE MEMBER OF THE AMERICAN SOCIETY OF CIVIL ENGINEERS ;
MEMBER OF THE INSTITUTION OF STRUCTURAL ENGINEERS.
PROFESSOR OF MECHANICAL SCIENCES IN THE UNIVERSITY OF CAMBRIDGE.
FORMERLY TECHNICAL OFFICER TO THE STEEL STRUCTURES RESEARCH COMMITTEE.

LONDON
EDWARD ARNOLD & CO.

FIRST PUBLISHED 1936
SECOND EDITION 1943
REPRINTED 1944, 1945, 1948, 1950, 1953

REPRINTED BY LITHOGRAPHY IN GREAT BRITAIN
BY JARROLD AND SONS, LIMITED NORWICH

PREFACE TO THE SECOND EDITION

The preparation of a second edition of this book under present conditions was not easy in view of other demands on the authors' time. Many of the good intentions made in peace-time had to be abandoned, but it has been possible to carry out some improvements and it is hoped that the result will justify the labour of revision.

In addition to the inclusion of new material in various sections of the book, two completely new chapters have been added. One, dealing with the voussoir arch, is largely the result of an experimental study of this type of structure made by one of the authors and his associates during the years immediately preceding the war. The other, which deals with the elasto-plastic behaviour of structures, is based to a considerable extent on researches made by the other author for The Institute of Welding.

The treatment of the theory of reinforced concrete has been simplified by the omission of a number of formulas which, though useful in the preparation of design curves, tend to confuse, rather than help, the study of fundamental principles.

The authors thank those readers who have taken the trouble to point out errors. As a result, one or two serious mistakes and a number of minor ones have been corrected. It is too much to hope that all have now been eradicated and the continued help of readers will be welcomed.

A. J. SUTTON PIPPARD.
J. F. BAKER.

LONDON, 1943.

PREFACE TO FIRST EDITION

The primary object of this book is to present to the student of engineering a general outline of the theories upon which the design of structures is based. Problems of practical design have been excluded as we believe that this side of the engineer's work cannot be effectively taught by means of text-books and must be acquired by experience in the shops and drawing office.

This point of view explains the omission of certain sections commonly found in books dealing with the theory of structures, but we hope that such omissions will be compensated by the inclusion of methods of analysis which are not usually given and which in some cases appear for the first time.

It is assumed that the student is reasonably familiar with simple analytical and graphical statics since the study of these subjects forms a normal part of an intermediate course in engineering or applied mathematics. Descriptions of stress diagrams, vector diagrams etc., have therefore been reduced to the minimum consistent with a continuous treatment of the subject.

The work during the last six years of the Steel Structures Research Committee of the Department of Scientific and Industrial Research has completely modified the outlook on the design of steel building frames. Both authors were members of this Committee, one of them being its Technical Officer for the greater part of its existence, and the results achieved are dealt with in sufficient detail to enable the student to appreciate the modern aspects of this important branch of structural engineering.

The authors are deeply indebted to Messrs. Longmans Green & Company, Limited, for their very generous permission to reproduce certain portions of books published by them * especially in connection with portions of Chapters 7 and 8 and those sections dealing with strain energy analysis.

In the troublesome work of proof reading we have been helped by Miss L. Chitty, M.A.; in the working of examples by Mr. S. R. Sparkes, B.Sc., and in the preparation of drawings by Mr. T. Bryce, all of the Imperial College and to them we offer our grateful thanks.

A. J. SUTTON PIPPARD.
J. F. BAKER.

September, 1936.

* "Aeroplane Structures" (A. J. S. Pippard and J. L. Pritchard) and "Strain Energy Methods of Stress Analysis" (A. J. S. Pippard).

CONTENTS

CHAPTER 1

DEFINITIONS AND GENERAL PRINCIPLES

CHAPTER 2

PRIMARY STRESS ANALYSIS OF STATICALLY DETERMINATE FRAMES

CHAPTER 3

THE STRESSES IN STRAIGHT AND CURVED BEAMS

CHAPTER 4

THEOREMS RELATING TO ELASTIC BODIES

CHAPTER 5

DISPLACEMENTS OF ELASTIC BODIES

CHAPTER 6

STRESS ANALYSIS OF REDUNDANT FRAMES

CHAPTER 7

STRUTS AND LATERALLY LOADED COLUMNS AND TIES

CHAPTER 8

CONTINUOUS BEAMS AND COLUMNS

CHAPTER 9

FRAMES WITH STIFF JOINTS

CHAPTER 10

SECONDARY STRESSES IN FRAMED STRUCTURES

CHAPTER 11

THE BEHAVIOUR OF CONNECTIONS IN STEEL FRAMES

CHAPTER 12

ELASTIC ARCHES AND RINGS

CHAPTER 13

THEORY OF COMPOSITE STRUCTURES AND REINFORCED CONCRETE

CHAPTER 14

INFLUENCE LINES FOR STATICALLY DETERMINATE STRUCTURES

CHAPTER 15

INFLUENCE LINES FOR STATICALLY INDETERMINATE STRUCTURES

CHAPTER 16

THE SUSPENSION BRIDGE

CHAPTER 17

THE BEAM CURVED IN PLAN

CHAPTER 18

NOTES ON FLAT SLABS AND PLATES

CHAPTER 19

THE DESIGN OF STEEL FRAMED BUILDINGS

CHAPTER 20

THE THEORY OF GRAVITY DAMS

CHAPTER 21

PRESSURE OF EARTH AND RETAINING WALLS

CHAPTER 22

MECHANICAL METHODS OF STRESS ANALYSIS

CHAPTER 23

THE VOUSSOIR ARCH

CHAPTER 24

THE BEHAVIOUR OF STRUCTURES IN THE ELASTO-PLASTIC RANGE

APPENDIX

BERRY FUNCTIONS

FOLDING TABLES

THE ANALYSIS OF ENGINEERING STRUCTURES

CHAPTER 1

DEFINITIONS AND GENERAL PRINCIPLES

1.1. Introduction.—Any assemblage of materials whose function is that of supporting loads is a structure. The term may be applied equally correctly to a large bridge or an aeroplane wing rib; to a masonry dam or the steel frame of a building. The component parts of a loaded structure are in a state of stress and the laws which govern the distribution of these stresses must be studied with a view to their calculation so that the different parts of the structure may be proportioned to take them with safety.

In most cases there are several methods by which loads can be supported, and the first stage in the design of a structure is to decide the most appropriate way of solving the particular problem which is presented. For instance, in choosing a bridge to carry a railway across a river the safety of the structure is not the only criterion; cost and appearance must be considered so that the choice of the best type is a matter requiring judgment, experience and taste.

When the general lines of the scheme have been settled the loads which the structure has to carry must be estimated as accurately as possible. The loads usually arise from a variety of causes and in the case taken as an example will include the weight of trains, the dynamic effects of the locomotive driving wheels, the dead weight of the bridge itself and the pressure of wind on trains and structure. When these loads have been estimated the forces in the different parts of the structure must be calculated and the dimensions fixed so that the stresses will be everywhere within safe limits. This stage of the design, for which a knowledge of the theory of structures is required, will be dealt with in this book.

1.2. Classification of structures.—Structures are often classified into the two main groups of framed structures and mass structures. The former comprises arrangements of separate bars or plates pinned or rivetted together as in a lattice girder or roof truss and such structures depend on the geometrical properties of the arrangement to resist

external loads. The latter group relies upon the weight of material in the structure to provide this resistance as in the case of a masonry dam. This classification is not complete or very satisfactory, but is sometimes useful as a broad division.

1.3. Factor of safety and load factor.—It is impossible to determine exactly either the external loads or the internal forces to which a structure is subjected. Moreover, the materials available are subject to certain variations in quality, and workmanship at times will fall below the average. It is therefore necessary in order to guard against these contingencies to allow a margin of strength over and above that which calculation indicates as being just right. This allowance is made by the introduction either of a factor of safety or a load factor and the distinction between these methods is important.

If the maximum stress which the material in any component of a structure can withstand is denoted by f and that component is designed so that at full load the working stress reaches f/n, n is known as the factor of safety. The maximum stress is advisably taken as the yield stress of the material and n is usually then about 2.

Another method however is to multiply the external loads by a load factor N and to design the structure so that the stress under the action of this factored load system reaches the maximum value f.

In other words when a factor of safety is adopted we ensure that under full working loads the stress will nowhere exceed a safe working limit: when a load factor is used we design so that under a specified number of times the full load the structure will just reach the failing point.

In many cases these two methods yield identical results but in others there is a considerable difference.

It is impossible at the present stage to indicate how these differences arise but the question will be dealt with more fully later and illustrated with reference to particular problems.

1.4. Frameworks.—An arrangement of bars, connected by joints incapable of transmitting bending moments, which is able to resist geometrical distortion under the action of any system of applied loads is known as a framework, pin-jointed frame, skeleton frame or truss.

When such a frame is loaded at the joints the internal forces in the bars composing it are simple tensions or compressions: loads acting on any member between its terminal joints will induce bending moments and shearing forces in that member only. The effect of the axial forces in the bars will be to elongate or shorten these bars to the extent of their elastic strains but this elastic deformation, which is necessarily very small, is the only alteration in the configuration of the frame.

It must be emphasized that to comply with the definition, the arrangement of bars must be able to resist deformation under the action of *any* load system. An arrangement which will resist a particular load distribution but which will deform or collapse under another is not a braced frame.

A frame of which all the bars lie in one plane is known as a plane

frame and will resist distortion only under systems of loads in that plane. When the bars lie in more than one plane the frame is a space frame and will resist distortion under loads in any direction.

1.5. Criterion for frameworks.—The simplest plane frame consists of a triangle of pin-jointed bars. If extra points are to be braced to this elementary frame each one will necessitate the addition of two extra bars. Thus, the first 3 joints of any plane frame having j joints or nodes require 3 bars to connect them, while the remaining $j-3$ joints require $2j-6$ extra bars. If then n is the total number of bars required to brace j joints together,

$$n=2j-3 \quad . \quad . \quad . \quad . \quad . \quad . \quad . \quad . \quad . \quad . \quad (1)$$

The simplest space frame consists of 4 joints connected by 6 members

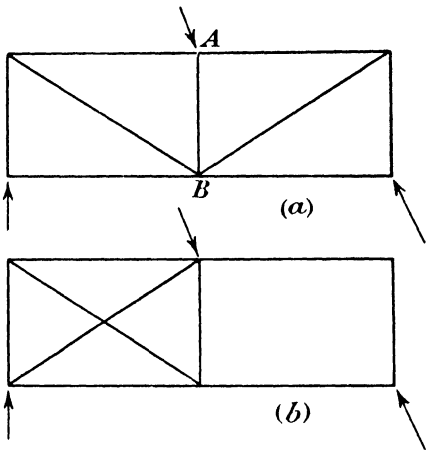

FIG. 1.1.

to form a skeleton tetrahedron. Additional nodes will each require 3 bars for connection to this tetrahedron, so that for this case,

$$n=3j-6 \quad . \quad . \quad . \quad . \quad . \quad . \quad . \quad . \quad . \quad . \quad (2)$$

These equations give the minimum number of bars necessary for the construction of frames with a specified number of joints and these are termed essential bars. An arrangement of bars containing less than the essential number cannot form a frame and will, except perhaps in special cases, collapse under load. If it contains more than the essential number the frame is said to be overbraced or redundant. If it contains the correct number of bars given by the appropriate criterion it is a simply stiff or just-stiff frame.

This statement is made with certain reservations : it is assumed that the disposition of the bars is satisfactory and that their character and strength are adequate for the loads which they may have to carry.

For example, in Fig. 1.1 there are 6 nodes to be connected by bars to form a plane frame. Equation (1) shows that 9 members are essential and if less than this number is provided it is impossible to brace these

points. The essential number of bars however can be disposed either as shown at (*a*) or at (*b*). In the first case the disposition is satisfactory but in the second, one panel is overbraced while the other is unbraced. Further, although (*a*) has a satisfactory disposition of bars it is necessary to ensure that these bars can fulfil the duties imposed upon them. Under the loading shown AB will be in compression ; under another system it may be in tension. All bars must therefore be capable of taking such tensile or compressive forces as may be imposed by any possible external load system.

In cases where a number of nodes have to be connected by bracing bars to certain fixed points it is clear that these fixed points are equivalent to an already existing frame, and the number of bars necessary to effect the bracing are $2n$ and $3n$ for plane and space frames respectively, where n is the number of free nodes.

1.6. Reactive forces.—The usual function of a frame, as already stated, is to transmit an external load system to a number of specified points, *e.g.* the load on a bridge has to be transmitted to the abutments. Since the external loading may vary, the supporting points must be capable of exerting reactive forces which will statically balance any such loading.

If a plane frame is supported at two points the reactive forces at these points together with the external loads form a system in static equilibrium and the necessary conditions which must be satisfied are three in number, as follows :—

1. The algebraic sum of the components of loads and reactions parallel to any axis in the plane must be zero.
2. The algebraic sum of the components of loads and reactions parallel to an axis perpendicular to the original axis and in the plane must be zero.
3. The algebraic sum of the moments about any point in the plane must be zero.

These conditions require three forces for their satisfaction and the nature of the supports must be such as to provide these forces. If one support is capable of exerting a force along one of the axes of resolution only while the other can exert forces along both axes of resolution, the necessary conditions are satisfied. Such supports may be provided by a frictionless roller and a pin joint respectively and these supply the statically essential reactive forces.

This arrangement is illustrated in Fig. 1.2 at (*a*) where the roof truss shown is supported at A on a pin joint which can exert a reaction in any direction and at B on a frictionless roller which can only exert a reaction normal to the bearing.

If both the supports are pin joints both the reactive forces are inclined and give components about the two chosen axes, thus introducing four forces. Since only three equations have to be satisfied the magnitude of these forces cannot be determined from purely statical considerations. This case is one in which a number of nodes are connected to two fixed points and the number of essential bars is

$2n$. In the example illustrated $n=4$ and 8 bars only are needed: a suitable frame is shown at (*b*).

In the case of a space frame the conditions of static equilibrium which have to be satisfied are six in number; the components of the external loads and of the reactive forces along three mutually perpendicular axes must be zero and the moments of the loads and forces about those axes must also be zero. The essential reactions for a space frame must therefore provide six component forces suitably disposed. If one support consists of a universal joint, this will account for three of the six components. Another support should then be such that movements of the supported point are restricted to a line; this introduces two restraints. The third support should be such that movements are restricted to a plane, which only requires one restraint. The

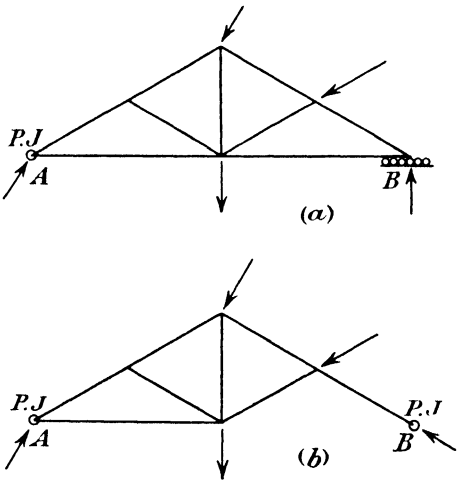

FIG. 1.2.

simplest illustration of the arrangement is that of the ball, groove and point used for mounting certain instruments. If more than the essential six reactive forces are provided the frame will be statically indeterminate unless the number of bars in it is correspondingly decreased.

1.7. Primary and secondary stresses.—The axial forces in the bars of a frame under loads applied to the nodes are known as the primary stresses. In actual structures the joints are seldom of the pinned type but are designed to transmit bending moments. The stresses in the bars are then no longer simple tensions and compressions but are complicated by the effects of bending. The extra stresses induced by the stiffness of the joints are known as secondary stresses; not because they are of secondary importance but because no estimate can be made of their magnitude until the primary stresses based on the assumption of pin joints have been calculated.

1.8. Self-straining.—If a just-stiff frame has one of its members removed the remaining bars form a mechanism. It is evident therefore

that the member which has been removed could within certain limits be replaced by another of a different length without causing any stresses in the remaining bars. The only effect would be an alteration in the configuration of the frame.

If, however, a redundant bar is to be inserted into a just-stiff frame without causing stresses in the existing bars it must be made of exactly the right length since the two joints to be connected are already fixed in position relative to each other. If by error or design the member is not of the exact length, force will have to be exerted to get it into position—the two points to be joined will have to be brought closer together or forced apart. This means that before any external load is applied to the frame its members are in a state of stress. This action is known as self-straining and any forces in the members due to initial stresses must be added to those caused by the action of the external load system in order to determine the total stress condition.

CHAPTER 2

PRIMARY STRESS ANALYSIS OF STATICALLY DETERMINATE FRAMES

2.1. The general problem.—The first step in the analysis of any braced structure is the determination of the stresses or forces in the bars of the frame on the assumptions that they are all pinned at the ends and that all loads are applied to the joints. Under these circumstances the internal forces are purely tensile or compressive, and although this ideal state of affairs does not completely represent the conditions in an actual structure the determination of these primary stresses is an essential preliminary to a more exact analysis. In the present chapter an account will therefore be given of the various methods in use for calculating such forces. Since certain of these are dealt with adequately in books on statics, which the student is presumed to have studied, it should not be necessary to elaborate them here : we shall be content to give examples which will serve as indications of the treatment.

A simply stiff framework, which will alone be considered in this chapter, can be completely analysed by the methods of statics since the number of unknowns is the same as the number of equations obtainable from the conditions of static equilibrium. The methods of stress analysis in use are therefore only variations of the application of the same fundamental principles.

2.2. The stress diagram.—One of the most generally useful methods is that of the stress diagram which is simply a continued application of the well-known polygon of forces. This theorem states that if any number of forces acting at a point are in equilibrium the vector diagram representing these forces in direction and magnitude consists of a closed polygon. In its simplest form when only three forces are acting the polygon becomes the triangle of forces.

In a braced frame every joint is in equilibrium under the action of the forces in the bars meeting at the joint and the external loads applied to the joint. Hence, a closed polygon can be drawn for every joint in the frame provided that not more than two unknown quantities appear at any joint. If the external loads are specified the unknowns may consist of the internal forces in two bars of the frame. For example, suppose Fig. 2.1 to represent a joint O in a frame carrying an external load W, and OA, OB and OC the bars connected to O. If the force in OA is known *e.g.* to be ·8W the forces in OB and OC can be determined. Using Bow's notation, *ab* is set out parallel to the line of action of W and equal to W to some selected scale. *bc* is then drawn parallel to OA and its length is made ·8W to the same scale. From *c*, *cd* is drawn

parallel to OB and from *a*, *ad* is drawn parallel to OC. These lines meet at *d*; *cd* and *ad* then represent to scale the magnitude of the forces in OB and OC respectively. The direction of arrows on the force polygon must be all in the same sense—in the present instance clockwise—and these arrows, transferred to the joint diagram give the direction of the force acting through the member on the joint.

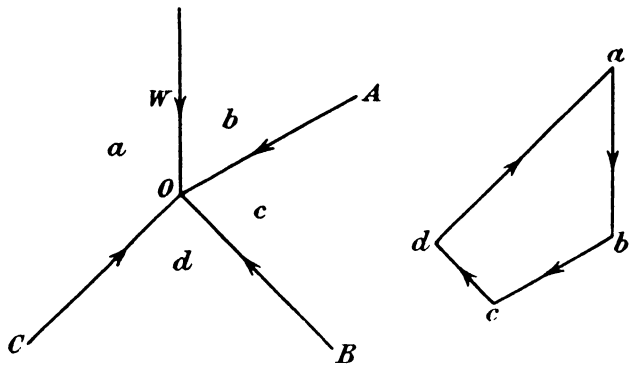

FIG. 2.1.

The two unknowns may however consist of a magnitude and a direction as in the case illustrated by Fig. 2.2, which represents the joint at the point where a truss is pinned to a support. The forces in OA, OB and OC are known and the reactive force has to be found both in magnitude and direction.

ab, *bc* and *cd* are drawn parallel to the lines of action of the three

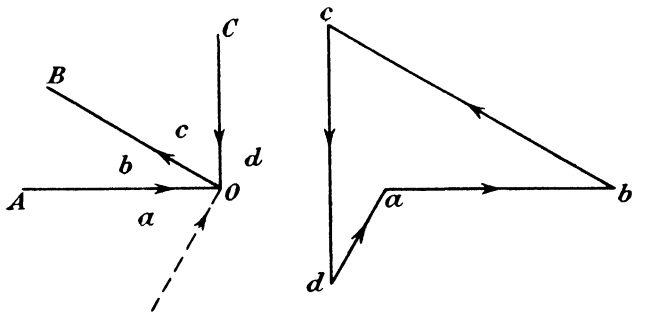

FIG. 2.2.

known forces and proportional to their magnitudes. The closing vector *da* then represents in magnitude and direction the reactive force at O.

This principle can be used to find graphically the reactions and primary stresses in any just-stiff braced framework, but instead of drawing separate polygons for each joint the work is simplified by combining them into one stress diagram.

As an illustration the quadrangular truss shown in Fig. 2.3 will be analysed. The truss is supported on rollers at the left-hand side, the

reaction there being consequently vertical, and by a pinned joint at the right-hand side where the reaction will be inclined.

The frame diagram is lettered in accordance with Bow's notation.

The first step is to determine the magnitude and line of action of the reactive forces and this may be done either by direct calculation from the static equations or graphically by the use of the funicular polygon. The process in the latter case is as follows. Set out the load line *abc* . . . . *k* to some convenient scale so that *ab* represents the force of 1 ton acting between A and B in magnitude and direction, *bc* the force between

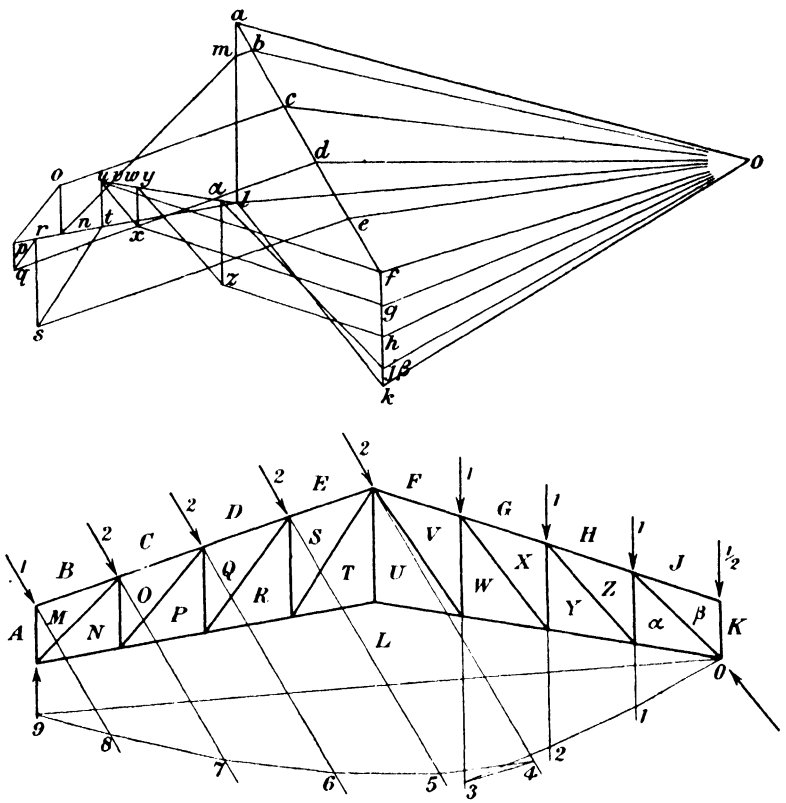

FIG. 2.3.

B and C and so on. Take any convenient pole O and join O*a*, O*b* . . . . O*k*, thus completing the vector diagram. Produce the lines of action of all the forces on the frame diagram as shown.

Starting at the pinned support draw the line 01 in the space J parallel to O*j*, cutting the line of action of HJ at 1. From 1 draw 12 in space H parallel to O*h* to cut the line of action of GH at 2. Similarly, 23, 34, 45, etc., are drawn in the spaces G, F, E, etc., parallel to O*g*, O*f*, O*e*, etc., until finally 89 in space A is parallel to O*a*. Complete the funicular polygon by joining 09.

From the pole O of the vector diagram draw O*l* parallel to 09 of the

funicular polygon to meet the vertical from *a* at *l*. *kl* is then the magnitude and direction of the reaction at the right-hand support.

To draw the stress diagram we start with joint ABM. *ab* has already been drawn to represent the external force in magnitude and direction, so from *a* and *b* we draw lines *am* and *bm* parallel to forces AM and BM. *abm* is then the triangle of forces for the joint considered and the lines *am* and *bm* give the magnitudes of the forces in the bars AM and BM and the direction in which these forces act on the joint. Thus *ab* is drawn in the direction of the external force and following round the triangle we see that *bm* acts towards the joint and BM is therefore in compression. Similarly *ma* acts towards the joint and MA is also in compression.

Proceeding now to joint AMNLA we find one external reaction and three internal forces acting. Of these *la* and *am* are known so that the polygon of forces could be drawn for this joint. *la* and *am* are, however, already drawn to scale so, if *mn* and *ln* are drawn parallel to MN and LN respectively the polygon is completed by these two additional lines. Following round the diagram in a clockwise direction to conform with the fact that *la* is an upward force we find *am* and *mn* act towards the joint, but that *nl* acts from the joint. Thus, NL is in tension. Joint BCONM and remaining joints are treated in the same way in succession until the whole stress diagram is completed. The test of accuracy is obtained when the line parallel to $\alpha\beta$ in the frame diagram drawn from α in the stress diagram gives β coinciding with *j*. This gives a zero force in $j\beta$ which is obviously correct from an examination of the conditions at joint KβJ.

2.3. Ritter's method of sections.—In many cases the method of sections can be used with advantage in stress analysis, especially when a knowledge of the forces in certain members only is required.

This method consists essentially of solving the equations of static equilibrium for a section of the framework and by judicious choice of such section the work is made very simple.

Fig. 2.4 shows a cantilever frame supported at A and D and carrying loads at E and B. The necessary dimensions are shown on the diagram.

The section of the frame GCBF is kept in equilibrium by the external load at B and the internal forces in GH, FH and FE which act on the joints G and F in the direction of the arrows at those joints. These four forces must therefore satisfy the conditions of static equilibrium and so the algebraic sum of their moments about any point must be zero. Now the lines of action of HG and FH meet at H and by taking moments about this point we eliminate the moments of these two forces and obtain

$$T_{EF} \times HE = 5EB$$

or

$$T_{EF} = \frac{5 \times 20}{10} = 10$$

where T_{EF} is the force in EF.

It is unnecessary to know the direction of T_{EF}. If it is assumed to be a tension and is actually a compression this will be indicated by a

negative value in the result. Again by taking moments about F the moments of the forces in EF and FH are eliminated and we obtain

$$T_{HG} \times Ff = 50$$

where Ff is the perpendicular from F on the line of action of HG.

Ff can often, as in the present case, be obtained geometrically, but if this is difficult it can be scaled from the frame diagram.

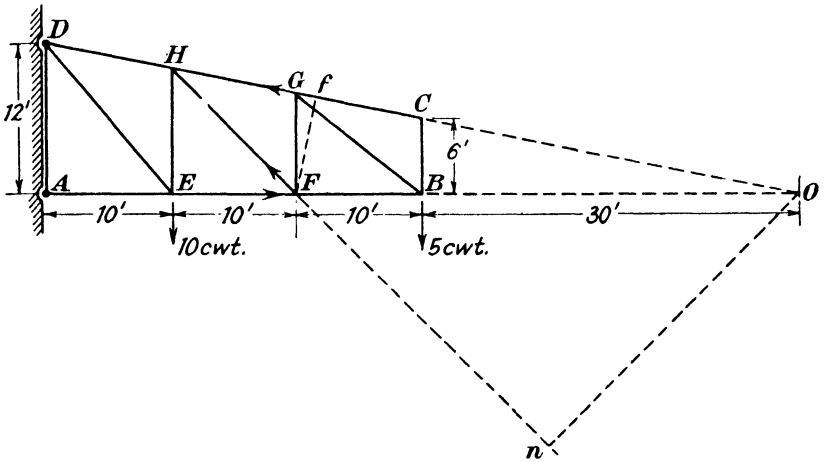

FIG. 2.4.

If DC and AB be produced to meet at O we have from the similar triangles FGf and ODA,

$$\frac{Ff}{GF} = \frac{OA}{OD}$$

or
$$Ff = \frac{8 \times 60}{\sqrt{60^2 + 12^2}} = 7{\cdot}84.$$

Hence
$$T_{HG} = \frac{50}{7{\cdot}84} = 6{\cdot}38.$$

Suppose now that the force in GF is to be calculated.

The section GCB of the frame is in equilibrium under the action of the external load at B and the internal forces GH, GF and BF.

The lines of action of GH and BF meet at O and so we take moments about this point and obtain

$$T_{GF} \times 40 = 30 \times 5$$

or
$$T_{GF} = 3{\cdot}75.$$

To calculate the force in FH we again consider the section GCBF and take moments about O where HG and EF meet.

Then
$$T_{HF} \times nO = 30 \times 5$$

It is best here to scale nO and so solve for T_{HF}.

For the members DH, DE and AE the procedure is the same as above, but both the loads at B and E now appear in the equations.

For example T_{AE} is found by taking moments about D, the equation being,

$$T_{AE} \times DA = (10 \times 10) + (30 \times 5)$$

or

$$T_{AE} = 20{\cdot}83.$$

2.4. Method of resolution at joints.—In certain simple forms of truss the forces in all the bars can be written down directly by considering the equilibrium of each joint in turn. This is a method which with a little practice is very quick and useful.

Suppose the forces in all the bars of the truss shown in Fig. 2.5 are required.

The reactions at A and B are first calculated. Consider first the equilibrium of joint A.

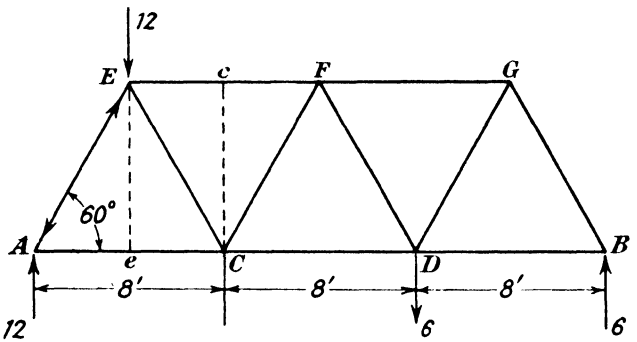

FIG. 2.5.

The vertical component of force in AE must balance the vertical reaction and so,

$$T_{AE} = 12 \text{ cosec } 60° = 13{\cdot}85.$$

The horizontal component of T_{AE} is balanced by the force in AC or

$$T_{AC} = T_{AE} \cos 60° = 6{\cdot}925.$$

The problem may also be treated by taking AE*e* as the triangle of forces for the joint A, where E*e* is perpendicular to AC.

Then,

$$\frac{T_{AE}}{12} = \frac{AE}{Ee}$$

or

$$T_{AE} = \frac{12 \times 8}{4\sqrt{3}} = 13{\cdot}85$$

and

$$\frac{T_{AC}}{T_{AE}} = \frac{Ae}{AE}$$

i.e.

$$T_{AC} = \tfrac{1}{2} T_{AE} = 6{\cdot}925.$$

Taking joint E next, the forces acting are 13·85 from AE and the vertical load at E.

These can be dealt with separately. A triangle of forces for AE, EC and EF is the equilateral triangle EFC and due to the force in AE, equal forces occur in EF and EC, EF being compressive and EC tensile.

For the vertical load at E we take ECc as the triangle of forces and obtain as the total forces in the bars,

$$T_{EC}=13{\cdot}85-12 \text{ cosec } 60^\circ=0$$
$$T_{EF}=-13{\cdot}85+\tfrac{1}{2}(13{\cdot}85)=-6{\cdot}925.$$

where the positive sign denotes tension and the negative sign compression.

Alternatively if a section be taken cutting EF, EC and CA the total shearing force across this section is zero, by summing forces to the left or right. Since EC is the only bar of the three which can have a vertical component of force, such component must be zero to balance the shearing force. Hence $T_{EC}=0$.

Similarly, $T_{CF}=T_{FD}=0$.

Therefore, by considering the equilibrium of joint F,

$$T_{EF}=T_{FG}=-6{\cdot}925.$$

Also from joint C, $T_{AC}=T_{CD}=6{\cdot}925$.

Treating joint B in the same way as A,

$$T_{BG}=-6{\cdot}925$$

and $$T_{BD}=\ 3{\cdot}462.$$

Also $$T_{GD}=\ 6{\cdot}925$$

and the forces are all determined.

2.5. Method of tension coefficients.—The methods described in the previous paragraphs are not easily applicable to space frames and although they may be adapted for such cases analysis by their means is laborious and liable to error. The most satisfactory treatment of space frames has been very fully described by Professor R. V. Southwell.* It is equally applicable to plane frames and is one of the simplest and most accurate methods of stress determination for such frames. The general case of the space frame will be considered first and its simplification when applied to a plane frame dealt with afterwards.

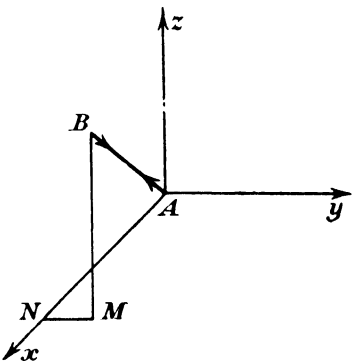

FIG. 2.6.

Let AB in Fig. 2.6 be any bar in a space frame,

T_{AB} the *tension* in this bar,

and L_{AB} the length of the bar.

* "Primary stress determination in space frames." R. V. Southwell, "Engineering," February 6th, 1920, p. 165.

This method is also used by Müller-Breslau in "Die Neueren Methoden der Festigkeitslehre" (Leipzig, 1924, and earlier editions).

The tension will be expressed in the form

$$T_{AB}=L_{AB}t_{AB}$$

where t_{AB} is known as a tension coefficient.

Through A take three mutually perpendicular axes, Ax, Ay, Az, and let the co-ordinates of A and B be (x_A, y_A, z_A) and (x_B, y_B, z_B).

Then, the component of T_{AB} acting at A in the direction Ax is

$$T_{AB}\cos BAx$$

or

$$T_{AB}\frac{x_B-x_A}{L_{AB}}$$

which from the expression for T_{AB} in terms of its tension coefficient can be written

$$t_{AB}(x_B-x_A).$$

Similarly, the components of T_{AB} along Ay and Az are $t_{AB}(y_B-y_A)$ and $t_{AB}(z_B-z_A)$ respectively.

At B, the other end of the bar, the components along the three axes will be

$$t_{AB}(x_A-x_B),\quad t_{AB}(y_A-y_B)\quad \text{and } t_{AB}(z_A-z_B).$$

Suppose now that at a joint A in a space frame there are connected any number of bars AB, AC . . . . AQ, and that the components of external load acting at this joint along the directions of the x, y and z axes are X_A, Y_A and Z_A respectively. The equilibrium of the joint requires that the components of all the forces along three mutually perpendicular axes shall be zero so that the conditions for equilibrium are

$$\left.\begin{aligned} t_{AB}(x_B-x_A)+t_{AC}(x_C-x_A)+\ \ldots\ +t_{AQ}(x_Q-x_A)+X_A&=0\\ t_{AB}(y_B-y_A)+t_{AC}(y_C-y_A)+\ \ldots\ +t_{AQ}(y_Q-y_A)+Y_A&=0\\ t_{AB}(z_B-z_A)+t_{AC}(z_C-z_A)+\ \ldots\ +t_{AQ}(z_Q-z_A)+Z_A&=0 \end{aligned}\right\} \quad (1)$$

Three equations such as these can be formed for each joint in the framework. They involve the quantities (x_B-x_A), (y_B-y_A), (z_B-z_A), etc., which are the projected lengths of the bars on the x, y and z axes respectively and therefore known from the drawings of the frame, and the unknown quantities t_{AB}, t_{AC}, etc., which are to be calculated.

For every term such as $t_{AB}(x_B-x_A)$ in one equation there will be a term $t_{AB}(x_A-x_B)$ in another equation, these being numerically equal but opposite in sign since $(x_B-x_A)=-(x_A-x_B)$. If, therefore, the x equations for all the joints are added we obtain

$$\left.\begin{aligned} X_A+X_B+\ \ldots\ &=0\\ \text{and similarly, by adding the } y \text{ and } z \text{ equations,}&\\ Y_A+Y_B+\ \ldots\ &=0,\\ \text{and}\qquad Z_A+Z_B+\ \ldots\ &=0. \end{aligned}\right\} \quad \ldots\ldots\ (2)$$

These equations express three of the essential conditions for the static equilibrium of the frame as a whole, viz., that the sum of the

components of the external forces along three perpendicular axes must be zero.

Again, if the first of the equations in (1) be multiplied by y_A and the second of these equations by $-x_A$ we obtain

$$t_{AB}(x_By_A-x_Ay_A)+t_{AC}(x_Cy_A-x_Ay_A)+ \ldots . t_{AQ}(x_Qy_A-x_Ay_A)+X_Ay_A=0$$
$$t_{AB}(-y_Bx_A+y_Ax_A)+t_{AC}(-y_Cx_A+y_Ax_A)+ \ldots . +t_{AQ}(-y_Qx_A+y_Ax_A) -Y_Ax_A=0,$$

and adding these we get

$$t_{AB}(x_By_A-x_Ay_B)+t_{AC}(x_Cy_A-x_Ay_C)+ \ldots . +t_{AQ}(x_Qy_A-x_Ay_Q)+X_Ay_A -Y_Ax_A=0 \quad . \quad . \quad (3)$$

If this is done for the corresponding equation for each joint we shall obtain similar results to (3), and for every term such as $t_{AB}(x_By_A-x_Ay_B)$ there will appear another, numerically equal but opposite in sign, $t_{AB}(x_Ay_B-x_By_A)$.

Hence, by adding all these equations we obtain

$$\left.\begin{aligned} &(y_AX_A-x_AY_A)+(y_BX_B-x_BY_B)+ \ldots =0 \\ &\text{and similarly from the other equations of (1)} \\ &(z_AY_A-y_AZ_A)+(z_BY_B-y_BZ_B)+ \ldots =0 \\ &\text{and} \quad (x_AZ_A-z_AX_A)+(x_BZ_B-z_BX_B)+ \ldots . =0 \end{aligned}\right\} \quad . \quad . \quad . \quad (4)$$

These equations express the remaining three essential conditions for the static equilibrium of the frame as a whole, viz., that the moments about three perpendicular axes shall be zero.

It has already been shown that the essential reactive forces for a space frame are six in number. If the frame is supported at A, B and C, for example, it is necessary for one point, say A, to be pinned, for another, B, to be restrained to move along a line in one plane, and for the third C, to be simply restrained in a plane. Thus, at A we shall have three reactive forces X_A, Y_A and Z_A, at B two reactive forces X_B, Z_B, and at C, one reactive force only, Z_C. The equations (2) and (4) enable these six unknown forces to be determined.

Having found the reactive forces the equations corresponding to (1) are used to find the values of the tension coefficients. It should be pointed out that these equations do not all have to be solved simultaneously and the work is neither difficult nor involved. Once the tension coefficients have been evaluated the loads in the members are found by multiplying the coefficients by the lengths of the appropriate members, *e.g.*,

$$T_{AB}=t_{AB}\sqrt{(x_B-x_A)^2+(y_B-y_A)^2+(z_B-z_A)^2}.$$

In forming the equations the load in a member is always assumed to be tensile and the terms in the equation are positive or negative as they tend to move the joint in the positive or negative direction of x, y or z. A negative result for the tension coefficient signifies that the force in that member is compressive.

As an example of this method the space frame shown in Fig. 2.7 will be analysed. It consists of a cantilever structure formed of three

longitudinal members ABC, GHJ and DEF braced together and arranged so that at any section they lie at the corners of an equilateral triangle.

As there are six points to be braced to the wall, eighteen members are necessary. These are provided by the six longitudinal members, six struts and six diagonal panel members.

The loading is as shown on the diagram.

Taking the co-ordinate axes positive in the directions indicated and starting with point F, the equations of equilibrium are formed as follows :—

The members meeting at this joint are FE, FC, FJ, FH, FB, and by

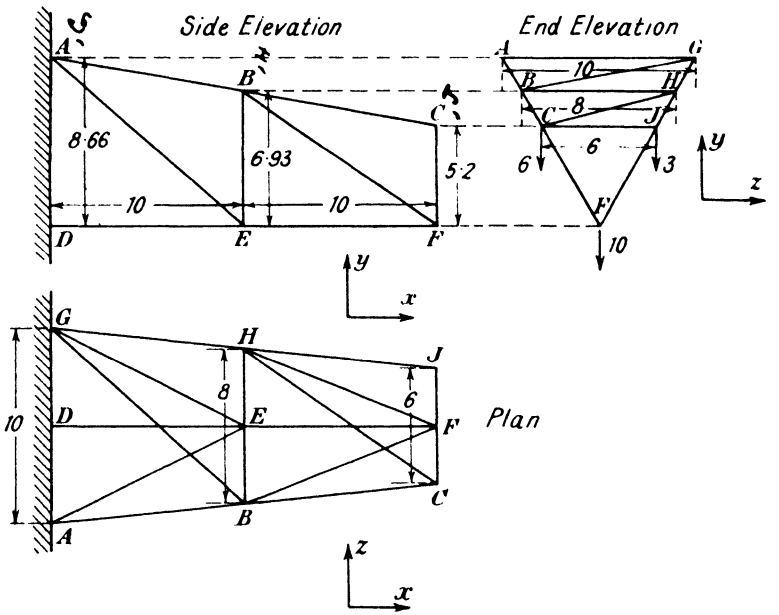

FIG. 2.7.

considering first the equation for the x axis, it is clear that FC and FJ have no components.

The projection of FE on this axis is -10, that of FB is -10, and that of FH is -10, so that the equation is

$$-10t_{FE}-10t_{FB}-10t_{FH}=0.$$

Considering now the y axis, the members concerned are FC, FJ, FB and FH. The projections on the y axis of FC and FJ are both 5·2, and of FB and FH are 6·93. The load is 10 acting in a negative direction so that the equation is

$$5{\cdot}2t_{FC}+5{\cdot}2t_{FJ}+6{\cdot}93t_{FB}+6{\cdot}93t_{FH}=10.$$

Similarly, for the z axis we get

$$3t_{FJ}-3t_{FC}+4t_{FH}-4t_{FB}=0.$$

Following the same procedure at every joint the necessary equations are formed and are best set out as shown in Table 2.1.

TABLE 2.1.

Joint		Equations
F	x	$-10t_{FE}-10t_{FB}-10t_{FH}=0.$
	y	$5{\cdot}2t_{FC}+5{\cdot}2t_{FJ}+6{\cdot}93t_{FB}+6{\cdot}93t_{FH}-10=0.$
	z	$3t_{FJ}-3t_{FC}+4t_{FH}-4t_{FB}=0.$
C	x	$-10t_{CB}-10t_{CH}=0.$
	y	$-5{\cdot}2t_{CF}+1{\cdot}73t_{CB}+1{\cdot}73t_{CH}-6=0.$
	z	$6t_{CJ}+7t_{CH}-t_{CB}+3t_{CF}=0.$
J	x	$-10t_{JH}=0.$
	y	$1{\cdot}73t_{JH}-5{\cdot}2t_{JF}-3=0.$
	z	$-6t_{JC}+t_{JH}-3t_{JF}=0.$
E	x	$10t_{EF}-10t_{ED}-10t_{EA}-10t_{EG}=0.$
	y	$6{\cdot}93t_{EB}+8{\cdot}66t_{EA}+6{\cdot}93t_{EH}+8{\cdot}66t_{EG}=0.$
	z	$4t_{EH}-4t_{EB}+5t_{EG}-5t_{EA}=0.$
B	x	$10t_{BC}-10t_{BA}-10t_{BG}+10t_{BF}=0.$
	y	$-6{\cdot}93t_{BE}+1{\cdot}73t_{BA}+1{\cdot}73t_{BG}-1{\cdot}73t_{BC}-6{\cdot}93t_{BF}=0.$
	z	$8t_{BH}+9t_{BG}+t_{BC}-t_{BA}+4t_{BE}+4t_{BF}=0.$
H	x	$10t_{HJ}-10t_{HG}+10t_{HC}+10t_{HF}=0.$
	y	$1{\cdot}73t_{HG}-1{\cdot}73t_{HJ}-1{\cdot}73t_{HC}-6{\cdot}93t_{HE}-6{\cdot}93t_{HF}=0.$
	z	$-8t_{HB}-7t_{HC}-t_{HJ}+t_{HG}-4t_{HF}-4t_{HE}=0.$

TABLE 2.2.

Member	Tension-coefficient t	Length L	Load Lt
FC	−1·15	6·0	− 6·9
FJ	−0·576	6·0	− 3·46
FB	1·59	12·8	20·3
FE	−2·75	10·0	−27·5
FH	1·16	12·8	14·85
CB	−0·215	10·2	− 2·19
CJ	0·288	6·0	1·73
CH	0·215	12·3	2·64
JH	0	10·2	0
EB	−1·194	8·0	− 9·55
ED	−4·4	10·0	−44·0
EA	0·961	14·14	13·60
EG	0·684	14·14	9·7
EH	−0·86	8·0	− 7·08
BA	1·28	10·2	13·06
BG	0·133	13·56	1·80
BH	−0·166	8·0	− 1·328
HG	1·375	10·2	14·02

These equations must now be solved. In the present instance joint J is taken first and the equation Jx for forces along the x axis gives $t_{JH}=0$. Substituting this value in Jy we find t_{JF} to be $-0{\cdot}576$ and $t_{JC}=0{\cdot}288$ follows at once from Jz.

If joint C be now considered it will be seen from Cx that $t_{CB}+t_{CH}=0$ which can be substituted in Cy to obtain $t_{CF}=-1{\cdot}15$. If we use this and the known value of t_{CJ} in Cz, an equation in t_{CH} and t_{CB} is obtained which with Cx enables these two coefficients to be evaluated.

This process is continued until all the coefficients have been determined and these, multiplied by the respective lengths of the members, give the loads in the members as set out in Table 2.2, p. 17.

When the method of tension coefficients is applied to the stress analysis of plane frames the work is considerably simplified since there are no components along the z axis, and all the data are contained in a single view of the framework.

As an illustration the roof truss shown in Fig. 2.8 will be analysed.

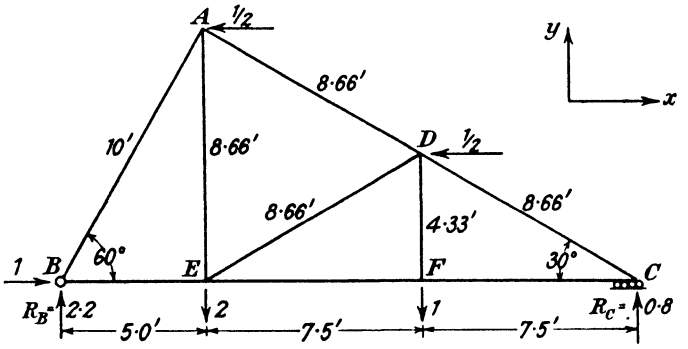

FIG. 2.8.

If R_B and R_C are the reactions at B and C respectively we obtain by taking moments about B

$$20R_C=10+12{\cdot}5-\frac{4{\cdot}33}{2}-4{\cdot}33$$

or

$$R_C=0{\cdot}8.$$

Therefore the vertical component of $R_B=2{\cdot}2$ and the horizontal component of $R_B=1{\cdot}0$.

The positive directions of x and y are indicated on the diagram and the equations for the various joints in terms of tension coefficients are given in Table 2.3, p. 19.

t_{CD} is obtained directly from equation Cy and is $-{\cdot}1846$ which is entered in the Table.

From Cx and Fx, $t_{CF}=-t_{CD}=t_{FE}$ and from Fy, $t_{FD}=$[illegible]1.

The values of t_{DC} and t_{DF} thus found are substituted in Dx and Dy leaving simultaneous equations in t_{DE} and t_{DA} which give on solution $t_{DE}=-{\cdot}1488$ and $t_{DA}=-{\cdot}1025$.

t_{AB} is found directly from By and substitution of its value in Bx gives t_{BE}.

TABLE 2.3.

Joint		Equation	Bar	t	L	T
C	x	$-7{\cdot}5t_{CF}-7{\cdot}5t_{CD}=0$	CD	$-{\cdot}1846$	8·66	$-1{\cdot}6^{e}$
	y	$4{\cdot}33t_{CD}+0{\cdot}8=0$	CF	$+{\cdot}1846$	7·5	$+1{\cdot}385$
F	x	$t_{FC}-t_{FE}=0$	FD	$+{\cdot}231$	4·33	$+1{\cdot}000$
	y	$4{\cdot}33t_{FD}-1=0$	FE	$+{\cdot}1846$	7·5	$+1{\cdot}385$
D	x	$7{\cdot}5t_{DC}-7{\cdot}5t_{DE}-7{\cdot}5t_{DA}-\frac{1}{2}=0$	BA	$-{\cdot}254$	10·0	$-2{\cdot}54$
	y	$-4{\cdot}33(t_{DF}+t_{DC}+t_{DE}-t_{DA})=0$	BE	$+{\cdot}054$	5·0	$+0{\cdot}27$
A	x	$7{\cdot}5t_{AD}-5t_{AB}-\frac{1}{2}=0$	DE	$-{\cdot}1488$	8·66	$-1{\cdot}29$
	y	$-8{\cdot}66t_{AE}-4{\cdot}33t_{AD}-8{\cdot}66t_{AB}=0$	DA	$-{\cdot}1025$	8·66	$-{\cdot}888$
B	x	$5t_{BE}+5t_{BA}+1=0$	AE	$+{\cdot}305$	8·66	$+2{\cdot}64$
	y	$8{\cdot}66t_{BA}+2{\cdot}2=0$				
E	x	$7{\cdot}5t_{EF}+7{\cdot}5t_{ED}-5t_{EB}=0$				
	y	$8{\cdot}66t_{EA}+4{\cdot}33t_{ED}-2=0$				

Ay then gives t_{AE}.

The remaining three equations Ax, Ex and Ey afford a check upon the accuracy of the work, since they are satisfied when the values of the tension coefficients already found are substituted in them. Instead of calculating the reactions directly they could have been dealt with as unknown forces, V_C, V_B and H_B.

The equations for B and C would then have been :—

Joint		Equations
B	x	$5t_{BE}+5t_{BA}+H_B=0$
	y	$8{\cdot}66t_{BA}+V_B=0$
C	x	$-7{\cdot}5t_{CF}-7{\cdot}5t_{CD}=0$
	y	$4{\cdot}33t_{CD}+V_C=0$

and there would be twelve equations to solve for the nine bar forces and the three reactive forces, H_B, V_B and V_C.

EXERCISES

(1) Determine by inspection the forces in the truss shown in diagram 2*a*.

(*FG*$=-3$; *GH*$=$*HJ*$=-6$; *JK*$=-4{\cdot}5$;
AC$=0$; *CD*$=3$; *DE*$=4{\cdot}5$; *EB*$=0$;
FC$=$*GD*$=5$; *DJ*$=2{\cdot}5$; *EK*$=7{\cdot}5$;
AF$=$*CG*$=-4$; *HD*$=0$; *JE*$=$*KB*$=-6$.)

(2) The frame shown at 2*b* is pinned at A, B and C to a rigid support. Comment on the adequacy or otherwise of the bracing and if necessary modify it.

Make a neat sketch of the frame and mark on it the internal stresses in all members.

($AD=DG=CF=GH=-W$;
$EH=EF=W$; $BE=DE=0$;
$FH=-W\sqrt{2}$; $AE=W\sqrt{2}$.)

(3) The pin-jointed frame shown at 2*c* is supported at A and D. The sides AB, BC and CD are equal in length. Using the method of tension coefficients, find the forces in all members of the frame.

($AB=-5{\cdot}78$; $CD=-4{\cdot}04$; $AD=2{\cdot}02$;
$AC=1{\cdot}00$; $BC=-2{\cdot}89$.)

(4) Determine by calculation the forces in all members of the pin-jointed frame shown in diagram 2*d*.

($AB=-5{\cdot}0$; $CD=-7{\cdot}96$; $BC=7{\cdot}10$; $DE=11{\cdot}07$;
$AC=0$; $CE=5{\cdot}99$; $BD=-15{\cdot}95$; $DF=-24{\cdot}20$.)

(5) Using the method of tension coefficients, obtain the forces in all bars of the frame shown in diagram 2*e*.

($AB=18{\cdot}25$; $AC=-17{\cdot}51$; $BC=-14{\cdot}58$;
$BD=18{\cdot}00$; $CD=3{\cdot}33$; $CE=-26{\cdot}98$.)

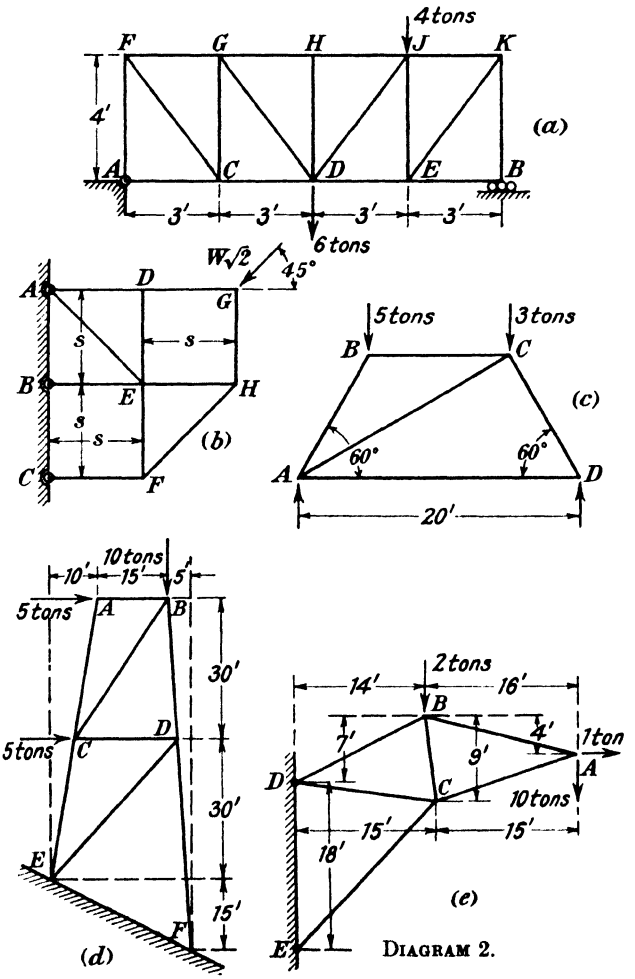

DIAGRAM 2.

CHAPTER 3

THE STRESSES IN STRAIGHT AND CURVED BEAMS

3.1. Shearing force and bending moment.—The theory of flexure is fully dealt with in standard text-books on Strength of Materials. Only those portions of the subject, therefore, which are referred to in later chapters will be outlined here.

For our present purpose a beam can be defined as a member supporting transverse loads or subjected to other bending actions.

The *shearing force* or *shear* at any section of a beam is the algebraic sum of all the external forces, including the reactions, acting on either side of the section, resolved normal to the axis of the beam.

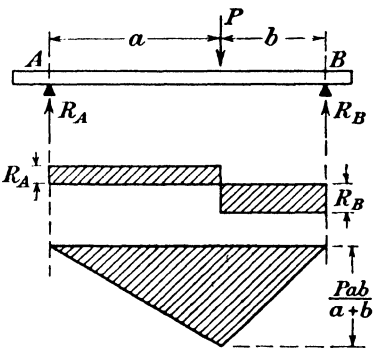

FIG. 3.1.

The *bending moment* at any section of a beam is the algebraic sum of the moments of all the applied forces, including the reactions, on either side of the section.

Shearing force and bending moment diagrams for a freely supported beam of length $a+b$ carrying a concentrated load P at a distance a from the left-hand support are shown in Fig. 3.1.

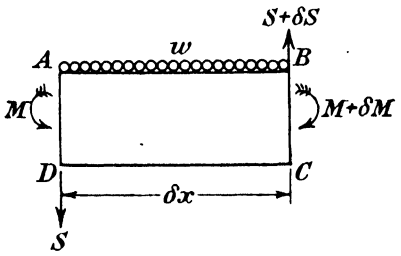

FIG. 3.2.

3.2. Relationship between loading, shearing force and bending moment.—In Fig. 3.2, DA and CB represent two sections of a beam under load separated by a small distance δx.

The bending moment at AD is M, and at BC is M+δM. The shearing force at AD is S, and at BC is S+δS.

The intensity of loading over the small length δx is w. Considering the equilibrium of the length of the beam shown we have by equating vertical forces

$$S+w\delta x=S+\delta S,$$

whence, on making δx and δS infinitely small,

$$\frac{dS}{dx}=w,$$

and by taking moments about D

$$M+\delta M+\frac{w(\delta x)^2}{2}-(S+\delta S)\delta x-M=0$$

i.e.

$$\frac{dM}{dx}=S.$$

Putting these relationships into integral form we have

$$\int w dx=\int dS=S$$

and

$$\int S dx=\int dM=M,$$

i.e. the integral of the load diagram between any limits gives the change of shearing force between those limits and the integral of the shearing force diagram similarly gives the change of bending moment.

3.3. Theory of simple bending.—The relation must now be found between the external forces acting on the beam and the internal stresses which keep it in equilibrium.

The assumptions made in the theory of simple bending and throughout this chapter are, except when otherwise stated,

(1) The beam is not stressed beyond the proportional limit of the material.
(2) Young's modulus is the same for tension and compression.
(3) A plane cross-section at right angles to the plane of bending before strain remains plane after strain.
(4) There is no resultant axial force on the beam.
(5) The cross-section of the beam is symmetrical about an axis through its centroid parallel to the plane of bending.

In Fig. 3.3, let ED, BC be two adjacent cross-sections of the beam, and after bending by pure couples applied to the ends of the beam let them be as shown at E′D′, B′C′. They will clearly not be parallel since, due to bending, the fibres parallel and close to CD will have stretched, while those parallel and close to EB will have shortened. It is also clear that there is some plane between CD and EB where the material is neither stretched nor compressed. This plane is called the neutral plane or surface, and its line of intersection with the cross-section of the beam is called the neutral axis of the section.

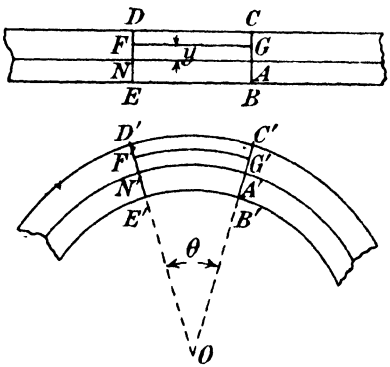

FIG. 3.3.

Let the sections E′D′, B′C′, inclined after bending at a small angle θ to one another, meet in a line perpendicular to the plane of the paper. Let this line intersect the plane of the paper in O. Let NA be the line in which the neutral surface cuts the plane of the paper before bending, and N′A′ be that

line after bending. Let y be the distance from the neutral surface of any layer of the material FG parallel to that surface.

Then if R is the radius of curvature we have

$$\frac{F'G'}{N'A'}=\frac{(R+y)\theta}{R\theta}=\frac{R+y}{R}.$$

The strain at the layer F'G' is

$$e=\frac{F'G'-FG}{FG}=\frac{F'G'-N'A'}{N'A'}=\frac{(R+y)\theta-R\theta}{R\theta}=\frac{y}{R}.$$

The longitudinal tensile stress intensity is

$$Ee=E\frac{y}{R}=p, \text{ say.}$$

This is equal to the compressive stress at the same distance below the neutral surface, *i.e.* the intensity of the direct longitudinal stress at any point in the cross-section is proportional to the distance of that point from the neutral axis, reaching a maximum at the boundary farthest from the neutral surface.

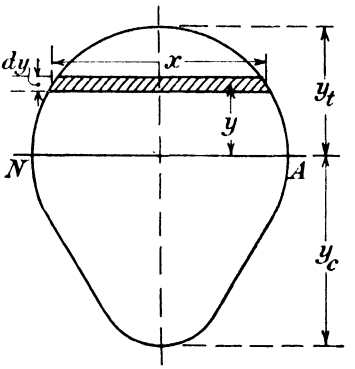

FIG. 3.4.

3.4. Moment of resistance.—The longitudinal internal forces, which are tensile on one side of the neutral surface and compressive on the other, clearly form a couple which must at any section, since the beam is in equilibrium, be equal and opposite to the bending moment at that section. This couple is called the moment of resistance.

In Fig. 3.4, let the shaded area be an elementary strip at a distance y from the neutral axis. The total force on the elementary area is $pxdy$ and the moment of this force is $pxydy$.

The total moment across the section is

$$M=\int pxydy=\int\frac{Ey}{R}xydy$$
$$=\frac{E}{R}\int xy^2dy$$
$$=\frac{EI}{R},$$

where I is the second moment of area or the moment of inertia of the section about the neutral axis;

therefore
$$\frac{M}{I}=\frac{E}{R}=\frac{p}{y}.$$

The maximum intensities of stress occur at the outer boundaries of the surface and if these are f_t and f_c respectively,

$$f_t=\frac{My_t}{I} \quad \text{and} \quad f_c=\frac{My_c}{I},$$

where y_t, y_c are the distances of the most distant tensile and compressive fibres from the neutral axis.

The quantity I/y, where y is the distance of the neutral axis from the most highly stressed fibre, is called the modulus of the section and is usually denoted by Z, so that we have the relation $f=M/Z$. There are two moduli for every section which is not symmetrical about the neutral axis.

Since there is no axial load on the beam the sum of the forces on the elementary areas must be zero, *i.e.*

$$\int px dy=0,$$

or

$$\frac{E}{R}\int xy dy=0.$$

The term covered by the integral sign is the first moment of area about the neutral axis and since this is zero the neutral axis must pass through the centroid of the section.

3.5. Stresses when loads are not normal to the beam.—When a beam is subjected to an oblique load the longitudinal stress at any point in the cross-section is made up of two parts, one due to bending action and the other to the effect of the component of the oblique load along the axis of the beam. Thus in the cantilever shown in Fig. 3.5 subjected to a load P, the line of action of which makes an angle θ with the axis of the beam, the stress at a section which is x from the point of application of the load will be due to a bending moment $Px \sin \theta$ and to a thrust $P \cos \theta$. The maximum compressive and tensile stresses due to bending will be $\frac{(Px \sin \theta)y_c}{I}$ and $\frac{(Px \sin \theta)y_t}{I}$ respectively, while, if A is the cross-sectional area of the beam, the stress due to the thrust will be $\frac{P}{A} \cos \theta$ uniformly distributed over the cross-section.

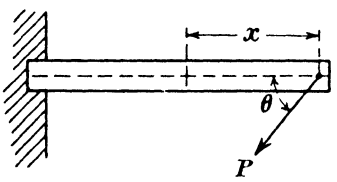

FIG. 3.5.

Therefore the total maximum compressive stress will be

$$\frac{(Px \sin \theta)y_c}{I}+\frac{P}{A} \cos \theta,$$

and the total maximum tensile stress will be

$$\frac{(Px \sin \theta)y_t}{I}-\frac{P}{A} \cos \theta.$$

This result assumes that the flexibility of the beam is not so great as to cause secondary effects. The general problem, when this condition is not fulfilled, will be dealt with in Chapter 7.

3.6. Unsymmetrical bending.—It was assumed in the derivation of the expression for the bending stress at any point in a beam given in paragraph 3.3 that the cross-section of the beam was symmetrical about an axis through its centroid parallel to the plane of bending. Such an axis of symmetry must be a principal axis of inertia of the cross-section and the assumption (5) of paragraph 3.3 could, in fact, have been expressed more generally as follows :

"The axis through the centroid of the cross-section of the beam parallel to the plane of bending must be a principal axis of inertia of the cross-section."

If the plane containing the applied bending moment is not parallel to a principal axis of inertia of the beam section the bending stresses cannot be found by the direct application of the formula of paragraph 3.3.

Fig. 3.6 shows the cross-section of a beam in the shape of an unequal angle, carrying vertical loads. The angle is supported with its short leg horizontal so that the plane of the applied bending moment is parallel to the vertical axis vv. The principal axes of inertia, about which the second moments of area of the section are a maximum and a minimum, are xx and yy respectively. Before the formula of paragraph 3.3 can be used to determine the bending stress at any point the applied bending moment must be resolved into its components about the principal axes. If, at the section under consideration, the applied bending moment acting parallel to the vertical plane vv is M, then its components in the planes parallel to xx and yy will be M sin α and M cos α respectively.

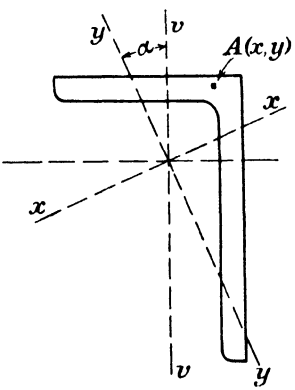

FIG. 3.6.

At a point A (x, y) in the cross-section the bending stress due to the first of these moments will be

$$\frac{x\mathrm{M}\sin\alpha}{\mathrm{I}_y}$$

and due to the second,

$$\frac{y\mathrm{M}\cos\alpha}{\mathrm{I}_x},$$

where I_x and I_y are the second moments of area of the section about the axes xx and yy respectively.

The total bending stress at the point A due to the applied moment M is therefore

$$p=\frac{\mathrm{M}x\sin\alpha}{\mathrm{I}_y}+\frac{\mathrm{M}y\cos\alpha}{\mathrm{I}_x}.$$

Since the bending stress at the neutral axis is zero, the equation to the neutral axis is

$$\frac{x \sin \alpha}{I_y} + \frac{y \cos \alpha}{I_x} = 0.$$

In many cases of unsymmetrical bending there is a tendency for the beam to twist. This is not, in general, a serious matter in practice as a beam is usually constrained, for example, by the floor slab in the case of a floor beam and by the roof covering in the case of a purlin and the resulting torsional stresses are small. Where a beam is not so constrained particular care must be taken in its design, as even in a symmetrical section such as a solid steel I, subjected to what appears to be symmetrical bending, large torsional distortions may occur due to a small unintentional eccentricity of loading.

3.7. Distribution of shear stress.—The distribution and value of the shear stress at any section of a beam may be found as follows :—

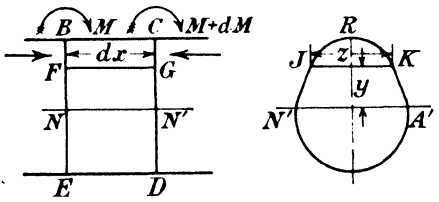

FIG. 3.7.

In Fig. 3.7, let BE, CD be two cross-sections of the beam at a small distance dx from one another, and let the bending moments at these sections be M and M+dM respectively. Let the breadth of the section at any height y be z=JK.

Then the longitudinal stress intensity at height y above the neutral axis N'A' is, as already shown,

$$p = \frac{My}{I},$$

where I is the second moment of area of the section about N'A'.

The longitudinal thrust on any element of cross-section at BF is $pzdy$, where zdy is the area of this element, *i.e.*

$$\frac{My}{I} zdy$$

and the thrust at CG on an element at the same height is

$$\frac{(M+dM)y}{I} zdy.$$

Therefore the excess of thrust on the element of area at CG over that at BF is the difference of the above quantities,

i.e.

$$\frac{dMy}{I} zdy$$

and the total difference of thrusts on the areas CG, BF is

$$\int_y^{y_0} \frac{dMy}{I} zdy,$$

where y_0=BN.

But since BFGC is in equilibrium, the excess of thrust must be balanced by the longitudinal shearing force across the surface FG. Let q be the intensity of the shear stress across FG.

The shearing force across FG is

$$qzdx=\int_y^{y_0}\frac{dMy}{I}zdy$$

$$=\frac{dM}{I}\int_y^{y_0}yzdy,$$

therefore

$$q=\frac{dM}{dx}\frac{1}{Iz}\int_y^{y_0}yzdy=\frac{S}{Iz}\int_y^{y_0}yzdy$$

where S is the total shearing force on the cross-section of the beam.

Now

$$\int_y^{y_0}yzdy$$

is the moment of the area JRK about N'A' and is equal to $A\bar{y}$, where A is the area of JRK and $\bar{y}$ the distance of its centroid from the neutral axis.

The shearing stress at the neutral axis is equal to $\frac{S}{Ib}A\bar{y}$ where b is the breadth of the section at the neutral axis and $A\bar{y}$ is the moment of the area of the section above the neutral axis.

The distribution of shearing stress is given for the two sections most commonly met with, *i.e.* rectangular and I section.

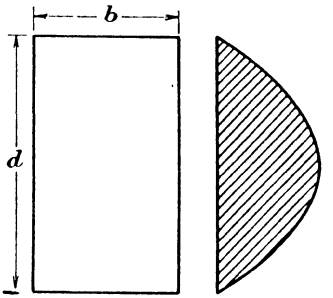

FIG. 3.8.

Rectangular Section.—

$$q=\frac{S}{I}\int_y^{\frac{d}{2}}ydy$$

since $z=b=$constant

$$=\frac{S}{2I}\left(\frac{d^2}{4}-y^2\right),$$

$$=\frac{6S}{bd^3}\left(\frac{d^2}{4}-y^2\right),$$

since

$$I=\frac{bd^3}{12}.$$

This is a parabola the maximum shear stress being $\frac{3S}{2bd}$ at the neutral axis (Fig. 3.8).

I *Section.*—Let dimensions be as in Fig. 3.9. Then the shear stress intensity at any height y above the neutral axis is

$$\frac{S}{Ib}\times\text{moment of area above height } y \text{ about the neutral axis.}$$

The shear stress diagram is shown in Fig. 3.9.

On the inner edge of the flange

$$q=\frac{S}{8I}(D^2-d^2)$$

and just inside the web

$$q=\frac{S}{8I}(D^2-d^2)\frac{B}{b}.$$

At the neutral axis the maximum shear stress is

$$\frac{S}{I}\left(\frac{D^2-d^2}{8}\cdot\frac{B}{b}+\frac{d^2}{8}\right).$$

3.8. Deflection of beams.—For a straight beam of uniform section we have the relation

$$\frac{1}{R}=\frac{M}{EI}.$$

In Fig. 3.10 let PQ be a small length of such a beam when deflected

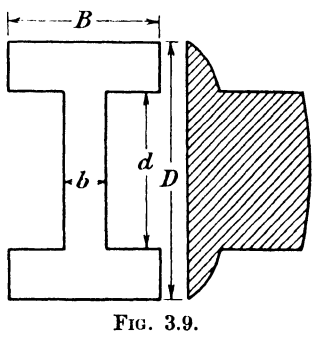

FIG. 3.9.

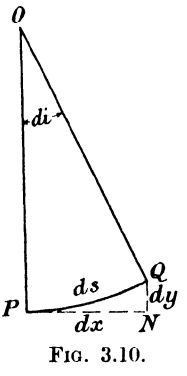

FIG. 3.10.

under load The co-ordinates of P and Q referred to rectangular axes are (x, y), $(x+\delta x)(y+\delta y)$, and the angles which the tangents at P and Q make with the axis of x are i and $i+\delta i$.

The deflection δy is so small that δx and δs may be taken to be equal.

Then
$$\frac{1}{R}=\frac{\delta i}{\delta s}=\frac{\delta i}{\delta x},$$

but
$$i=\tan i=\frac{dy}{dx},$$

hence in the limit when δx and δy become infinitely small

$$\frac{1}{R}=\frac{d^2y}{dx^2},$$

therefore
$$\frac{dy}{dx}=\text{slope of beam}=\int\frac{1}{R}dx=\int\frac{M}{EI}dx$$

between suitable limits ;

and $$y=\text{deflection}=\int\int\frac{M}{EI}dxdx$$

between suitable limits.

From this and the results of paragraph 3.2 the following relations are obtained :—

$$w=\frac{dS}{dx}=\frac{d^2M}{dx^2}=EI\frac{d^4y}{dx^4}, \quad \ldots\ldots\ldots \quad (1)$$

$$S=\frac{dM}{dx}=EI\frac{d^3y}{dx^3}, \quad \ldots\ldots\ldots \quad (2)$$

$$M=EI\frac{d^2y}{dx^2}, \quad \ldots\ldots\ldots \quad (3)$$

$$\text{slope}=i=\int\frac{Mdx}{EI}, \quad \ldots\ldots\ldots \quad (4)$$

$$\text{deflection}=y=\int\int\frac{Mdxdx}{EI}. \quad \ldots\ldots\ldots \quad (5)$$

These five relations are important. From them, for example, if the loading on a beam is known, the shearing force, bending moment, slope and deflection can be obtained by successive integration, the proper constant of integration being added at each step. Alternatively, if the bending moment is given for every point along the beam, the loading, shear, deflection and slope may be deduced.

It should be noted that $\frac{d^2y}{dx^2}$, *i.e.* $\frac{d}{dx}\left(\frac{dy}{dx}\right)$ is the rate of change of slope and is positive or negative in any particular case according to the positive direction chosen for the measurement of y. Bending moments which produce a positive change of slope must therefore be taken as positive and vice versa in forming the equation (3). For example in Fig. 3.11, y is measured positive downwards from the unstrained axis of the beam and the slope, which is everywhere negative, increases with x until it reaches its maximum value of zero at the fixed end. Hence, positive bending moments are those which tend to produce concavity downwards.

The deflection of beams loaded in different ways will now be considered in some detail.

3.9. Uniformly loaded cantilever.—Fig. 3.11 shows in its unstrained position, a cantilever of uniform cross-section and length l. If the x

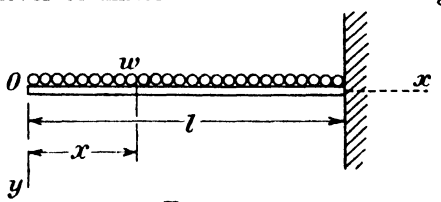

FIG. 3.11.

axis is taken along the unstrained axis of the beam, which is assumed horizontal, and y is measured downwards, we shall have, when M is a "hogging" bending moment, *i.e.* one which causes the beam to become concave downwards,

$$EI\frac{d^2y}{dx^2}=M \quad . \quad . \quad . \quad . \quad . \quad . \quad . \quad . \quad . \quad (1)$$

Under the action of a uniformly distributed load of intensity w per unit length the bending moment at a distance x from the free end is

$$M=\frac{wx^2}{2}=EI\frac{d^2y}{dx^2}$$

therefore

$$\frac{dy}{dx}=\frac{wx^3}{6EI}+A \quad . \quad . \quad . \quad . \quad . \quad . \quad . \quad . \quad . \quad . \quad (2)$$

and

$$y=\frac{wx^4}{24EI}+Ax+B. \quad . \quad . \quad . \quad . \quad . \quad . \quad . \quad . \quad . \quad (3)$$

where A and B are constants of integration, the values of which must be found from a consideration of the end conditions of the beam.

Since the beam is a cantilever it will suffer no change of slope at the fixed end, that is to say when $x=l$, $\frac{dy}{dx}=0$ and so from equation (2),

$$A=-\frac{wl^3}{6EI}$$

and

$$\frac{dy}{dx}=\frac{wx^3}{6EI}-\frac{wl^3}{6EI}.$$

There is, further, no deflection at the fixed end, *i.e.* $y=0$ when $x=l$ and equation (3) then gives

$$B=\frac{wl^4}{8EI}$$

and

$$y=\frac{wx^4}{24EI}-\frac{wl^3x}{6EI}+\frac{wl^4}{8EI}$$

which is the equation of the deflected form of the cantilever.

3.10. Simply supported beam carrying a concentrated load.—Fig. 3.12 shows a beam of uniform cross-section and length l resting on simple supports which offer no resistance to bending. A concentrated load W is applied at a distance a from the left-hand support which is taken as the origin of co-ordinates. The supports apply to the beam vertical reactions R_A and R_B of magnitudes $\frac{W(l-a)}{l}$ and $\frac{Wa}{l}$ respectively.

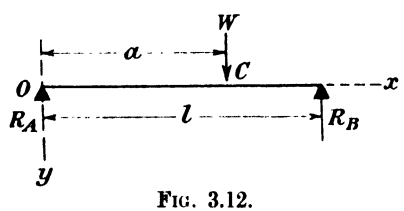

FIG. 3.12.

It is convenient in the first place to form separate expressions for the bending moments at sections to the left and right of the concentrated load respectively, thus :

when $x<a$	when $x>a$
$M=-R_A x$	$M=-R_A x+W[x-a]$
therefore $EI\frac{d^2y}{dx^2}=-R_A x$	$EI\frac{d^2y}{dx^2}=-R_A x+W[x-a]$
and $EI\frac{dy}{dx}=-R_A\frac{x^2}{2}+A$	$EI\frac{dy}{dx}=-R_A\frac{x^2}{2}+\frac{W[x-a]^2}{2}+A'$

where A and A′ are constants of integration.

The left-hand expression holds for all sections of the beam between the left-hand support and the point of application of the load, C. The right-hand expression holds for all sections between C and the right-hand support. They will both, therefore, give the slope of the beam under the load at C, that is when $x=a$ and we have

$$EI\left(\frac{dy}{dx}\right)_c=-R_A\frac{a^2}{2}+A \qquad EI\left(\frac{dy}{dx}\right)_c=-R_A\frac{a^2}{2}+A'$$

it follows that $A=A'$.

Using the same argument, on integrating once more it will be found that

$$EIy=-R_A\frac{x^3}{6}+Ax+B \qquad EIy=-R_A\frac{x^3}{6}+W\frac{[x-a]^3}{6}+Ax+B.$$

If it is stipulated that the terms inside the square brackets are omitted when $x<a$, the right-hand expressions are capable of expressing the bending moment, slope and deflection at any section of the beam thus :

$$EI\frac{d^2y}{dx^2}=-R_A x+W[x-a] \quad \ldots\ldots\ldots \quad (1)$$

$$EI\frac{dy}{dx}=-R_A\frac{x^2}{2}+\frac{W[x-a]^2}{2}+A \quad \ldots\ldots\ldots \quad (2)$$

and

$$EIy=-R_A\frac{x^3}{6}+\frac{W[x-a]^3}{6}+Ax+B \quad \ldots\ldots \quad (3)$$

The constants A and B are evaluated from a consideration of the end conditions. If there is no sinking of the supports under load we have $y=0$ when $x=0$ and from (3), the term in the bracket being omitted since $x<a$, we obtain $B=0$.

When $x=l$, $y=0$ so that

$$A=R_A\frac{l^2}{6}-\frac{W[l-a]^3}{6l}=\frac{Wa(l-a)(2l-a)}{6l}.$$

The deflection under the load is

$$y_c=\frac{1}{EI}\left[-R_A\frac{a^3}{6}+Aa\right]=\frac{Wa^2(l-a)^2}{3EIl}.$$

The maximum deflection will occur at the point where $\frac{dy}{dx}=0$ which, if $a>\frac{l}{2}$, will be found in the length of beam between the left-hand support and C.

In this length

$$\frac{dy}{dx}=\frac{1}{EI}\left[-R_A\frac{x^2}{2}+A\right]$$

and equating this to zero it follows that the maximum deflection occurs at

$$x=\sqrt{\frac{a(2l-a)}{3}}.$$

Substituting this value of x in equation (3) we have

$$y_{max}=\frac{W(l-a)(2al-a^2)^{3/2}}{9\sqrt{3}EIl}.$$

The method outlined above, due to W. H. Macaulay,* can be applied to a beam carrying any number of concentrated loads W_1, W_2, W_3, etc., at distances a, b, c, etc., from the left-hand support. The expression for the bending moment at any point in the beam, from which those giving the slopes and deflections are derived, is best found by writing down the bending moment at the section just to the left of the right-hand support, taking moments to the left of the section, thus

$$EI\frac{d^2y}{dx^2}=-R_Ax+W_1[x-a]+W_2[x-b]+W_3[x-c]+\text{ etc.}$$

Care must be taken when integrating to retain intact the expressions in the square brackets and to omit those which do not apply when considering a particular section. Errors can be avoided if it is remembered that the term inside a bracket must be omitted when, on substituting for x, it has a negative value.

3.11. Simply supported beam carrying a distributed load.—Macaulay's method will now be used to determine the deflections of a beam carrying a load of intensity w which extends from a point at a distance a from the left-hand support to the right-hand support (Fig. 3.13).

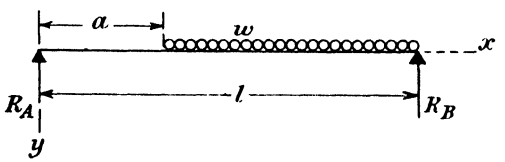

FIG. 3.13.

* "Note on the Deflection of Beams." Messenger of Mathematics, Vol. 48 (1919), p. 129.

With the stipulation set out in the last paragraph the equation which holds over the whole length of the beam is

$$EI\frac{d^2y}{dx^2}=-R_Ax+\frac{w}{2}[x-a]^2 \quad . \quad . \quad . \quad . \quad . \quad . \quad . \quad . \quad (1)$$

Upon integrating this twice we have

$$EI\frac{dy}{dx}=-R_A\frac{x^2}{2}+\frac{w}{6}[x-a]^3+A \quad . \quad . \quad . \quad . \quad . \quad . \quad (2)$$

and

$$EIy=-R_A\frac{x^3}{6}+\frac{w}{24}[x-a]^4+Ax+B \quad . \quad . \quad . \quad . \quad . \quad (3)$$

When $x=0$, $y=0$ and so $B=0$.
When $x=l$, $y=0$

$$\therefore \qquad 0=-\frac{w(l-a)^2}{2l}\cdot\frac{l^3}{6}+\frac{w(l-a)^4}{24}+Al$$

and

$$A=\frac{w(l-a)^2(l^2+2al-a^2)}{24l}.$$

The final equation for the deflection at any point in the beam is then

$$y=\frac{1}{EI}\left[-\frac{w(l-a)^2x^3}{12l}+\frac{w[x-a]^4}{24}+\frac{w(l-a)^2(l^2+2al-a^2)x}{24l}\right] \quad (4)$$

It will be realised that the method set out above can only be used when the distributed load stretches to the right-hand support. The

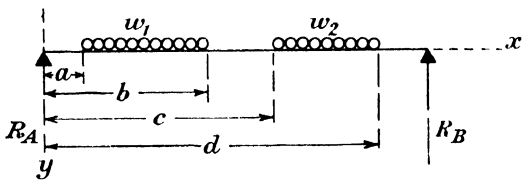

FIG. 3.14.

general case of a beam carrying a load distributed over a short length only of the span can however be covered by the use of a simple artifice.

If the beam AB carries a load of intensity w per unit length extending between points C and D which are a and b respectively from the left-hand support the behaviour of the beam is the same as if it were loaded uniformly to an intensity w over the length CB and to an intensity $-w$ over the length DB. By this arrangement the loads are made continuous to the right-hand support.

Macaulay's method can be applied and the deflection derived as before from the equation

$$EI\frac{d^2y}{dx^2}=-R_Ax+\frac{w[x-a]^2}{2}-\frac{w[x-b]^2}{2} \quad . \quad . \quad . \quad . \quad (5)$$

When loads of different intensities are distributed over two portions of the beam as shown in Fig. 3.14 the equation will be

$$EI\frac{d^2y}{dx^2}=-R_Ax+\frac{w_1[x-a]^2}{2}-\frac{w_1[x-b]^2}{2}+\frac{w_2[x-c]^2}{2}-\frac{w_2[x-d]^2}{2}. \quad (6)$$

3.12. Simply supported beam subjected to a couple applied at a point.—The slopes and deflections of a beam of uniform cross-section subjected to a couple M applied to a point C at a distance a from the left-hand support (Fig. 3.15) can be found without difficulty. The reactions, R, supplied by the supports act as shown in the figure and are of magnitude $\frac{M}{l}$. If the couple is replaced by an upward vertical force $W=\frac{M}{b}$ acting through C and an equal and opposite force acting through a point at a distance b to the right of C the equations can be formed in the usual way. If, in the limit, b is made to approach zero while keeping $M=Wb$, the required solution is obtained.

A more elegant method is obtained, however, by extending Macaulay's

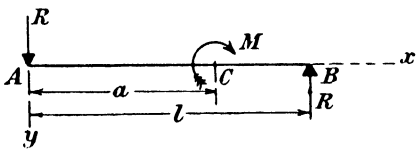

FIG. 3.15.

notation. The equation which holds over the whole length of the beam can be written

$$EI\frac{d^2y}{dx^2}=Rx-[M] \quad . \quad . \quad . \quad . \quad . \quad . \quad . \quad . \quad (1)$$

the significance of the square bracket being, as before, that the term inside it shall be neglected when $x<a$.

Integrating equation (1) we can write

$$EI\frac{dy}{dx}=\frac{Rx^2}{2}-[M(x-a)]+A \quad . \quad . \quad . \quad . \quad . \quad . \quad . \quad (2)$$

and

$$EIy=\frac{Rx^3}{6}-\left[\frac{M(x-a)^2}{2}\right]+Ax+B \quad . \quad . \quad . \quad . \quad . \quad (3)$$

Since $y=0$ when $x=0$ and when $x=l$ we have

$$B=0$$

and

$$A=\frac{M}{6l}(2l^2-6al+3a^2).$$

The equation for the deflection at any point is then

$$y=\frac{1}{EI}\left\{\frac{Mx^3}{6l}-\tfrac{1}{2}[M(x-a)^2]+\frac{M}{6l}(2l^2-6al+3a^2)x\right\} \quad . \quad . \quad . \quad (4)$$

3.13. Simply supported beam subjected to transverse loads and end couples.—General expressions for the slopes at the ends of a beam of uniform cross-section subjected to any system of transverse loads and to couples at its ends will be needed later and will be derived at this stage.

Fig. 3.16 shows a beam subjected to any distribution of transverse loads and to couples M_A and M_B at its ends A and B respectively.

If the hogging bending moment at a section x from the left-hand support due to the transverse loads alone is M'_x then the total bending moment at that point is

$$M'_x+M_A\frac{(l-x)}{l}+\frac{x}{l}M_B.$$

We may, therefore, write

$$EI\frac{d^2y}{dx^2}=M'_x+M_A\frac{(l-x)}{l}+\frac{x}{l}M_B \quad . \quad . \quad . \quad . \quad . \quad . \quad (1)$$

Multiplying equation (1) by x and integrating between the limits $x=0$ and $x=l$, we obtain

$$EI\left[x\frac{dy}{dx}-y\right]_0^l=\int_0^l M'_x x\,dx+\left[\frac{M_A}{l}\left(\frac{lx^2}{2}-\frac{x^3}{3}\right)+\frac{x^3}{3l}M_B\right]_0^l \quad . \quad . \quad (2)$$

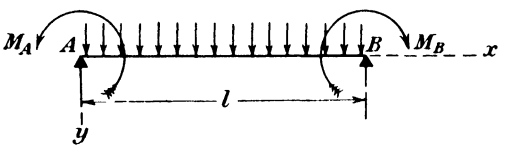

FIG. 3.16.

If it is assumed that there is no sinking of the supports, that is to say $y=0$ when $x=0$ and when $x=l$, equation (2) may be written

$$\theta_{BA}=\frac{1}{EIl}\int_0^l M'_x x\,dx+\frac{l}{6EI}(M_A+2M_B) \quad . \quad . \quad . \quad . \quad . \quad (3)$$

where θ_{BA} is the slope of the beam at the end B where $x=l$.

Integrating (1) between the limits $x=0$ and $x=l$ we have

$$EI\left[\frac{dy}{dx}\right]_0^l=\int_0^l M'_x dx+\left[\frac{M_A}{l}\left(lx-\frac{x^2}{2}\right)+\frac{x^2}{2l}M_B\right]_0^l$$

or

$$\theta_{BA}-\theta_{AB}=\frac{1}{EI}\int_0^l M'_x dx+\frac{l}{2EI}(M_A+M_B) \quad . \quad . \quad . \quad . \quad . \quad (4)$$

where θ_{AB} is the slope of the beam at the end A where $x=0$.

Substituting in this equation the value of θ_{BA} given by equation (3) it will be found that

$$\theta_{AB}=-\frac{1}{EI}\int_0^l M'_x dx+\frac{1}{EIl}\int_0^l M'_x x\,dx-\frac{l}{6EI}(2M_A+M_B) \quad . \quad . \quad (5)$$

Now $\int_0^l M'_x dx$ is the total area of the bending moment diagram due to the transverse loads alone and will be denoted by A.

$\int_0^l M'_x x dx$ is the moment of this area about the left-hand end of the beam where $x=0$, and will be denoted by $A\bar{x}$, $\bar{x}$ being the distance of the centroid of the area from the end where $x=0$.

Then

$$l\int_0^l M'_x dx - \int_0^l M'_x x dx = l\int_0^l M'_x dx - \bar{x}\int_0^l M'_x dx = (l-\bar{x})\int_0^l M'_x dx$$

which is the moment of the area of the bending moment diagram about the right-hand end of the beam, where $x=l$ and will be denoted by $A\bar{x}'$, $\bar{x}'$ being the distance of the centroid of the area from the end where $x=l$.

Equations (3) and (5) may then be written

$$\theta_{BA} = \frac{l}{6EI}\left(M_A + 2M_B + \frac{6A\bar{x}}{l^2}\right) \quad . \quad . \quad . \quad . \quad . \quad . \quad (6)$$

and

$$\theta_{AB} = -\frac{l}{6EI}\left(2M_A + M_B + \frac{6A\bar{x}'}{l^2}\right) \quad . \quad . \quad . \quad . \quad . \quad (7)$$

If the supports sink when the load is applied to the beam so that the end B has a deflection δ relative to A, then the slope everywhere on the beam will be increased by an amount $\frac{\delta}{l}$ and the slopes at the ends will be

$$\theta_{BA} = \frac{l}{6EI}\left(M_A + 2M_B + \frac{6A\bar{x}}{l^2}\right) + \frac{\delta}{l} \quad . \quad . \quad . \quad . \quad . \quad (8)$$

$$\theta_{AB} = -\frac{l}{6EI}\left(2M_A + M_B + \frac{6A\bar{x}'}{l^2}\right) + \frac{\delta}{l} \quad . \quad . \quad . \quad . \quad (9)$$

3.14. Encastré beams.—An encastré beam is one in which the ends are built into the supports or otherwise fixed so that the slope of the beam at those points cannot change. When load is applied the supports exert restraining moments on the ends of the beams. The magnitudes of these moments can be found directly from the expressions for the slopes at the ends of a beam derived in the preceding paragraph and the deflection at any point can then be determined by the method set out in paragraphs 3.10–3.12.

An encastré beam is so constrained that no change of slope occurs at the ends hence, if the axis of the beam was originally horizontal and the end B deflects under load a distance δ relative to A, we may write from equations (8) and (9) of paragraph 3.13

$$\frac{l}{6EI}\left(M_A + 2M_B + \frac{6A\bar{x}}{l^2}\right) + \frac{\delta}{l} = 0$$

and

$$-\frac{l}{6EI}\left(2M_A + M_B + \frac{6A\bar{x}'}{l^2}\right) + \frac{\delta}{l} = 0.$$

Solving these equations we obtain

$$M_A=\frac{2A\bar{x}}{l^2}-\frac{4A\bar{x}'}{l^2}+\frac{6EI\delta}{l^2} \quad \ldots\ldots\ldots \quad (1)$$

and

$$M_B=-\frac{4A\bar{x}}{l^2}+\frac{2A\bar{x}'}{l^2}-\frac{6EI\delta}{l^2} \quad \ldots\ldots\ldots \quad (2)$$

In the case of a beam carrying a uniformly distributed load of intensity w over the whole span

$$\bar{x}=\bar{x}'=\frac{l}{2}, \quad A=\frac{2}{3}\times l\times\frac{wl^2}{8}=\frac{wl^3}{12}$$

and the end fixing moments are

$$M_A=\frac{wl^2}{12}+\frac{6EI\delta}{l^2} \quad \ldots\ldots\ldots \quad (3)$$

and

$$M_B=\frac{wl^2}{12}-\frac{6EI\delta}{l^2} \quad \ldots\ldots\ldots \quad (4)$$

The effect of the downward deflection of the end B relative to the end A is to increase the moment M_A. The importance of this increase is most easily appreciated from a consideration of a special case.

Suppose a total load of 12 tons uniformly distributed is to be carried over a span of 20 feet by means of a steel beam having a relevant second moment of area $I=220$ (ins.)^4 and a depth of 12 inches.

If the beam were simply supported at its ends the maximum bending moment, occurring at the centre of the span, would be $M_{max}=\frac{wl^2}{8}$ $=360$ tons-ins. and the maximum longitudinal flexural stress would be $p_{max}=\frac{360\times 6}{220}=9{\cdot}8$ tons/sq. in.

If the ends of the beam were encastré and it were assumed that no relative deflection of the ends occurred the restraining moments exerted on the beam at the supports would be :—

$$M_A=M_B=\frac{wl^2}{12}=240 \text{ tons-ins.}$$

This is the greatest bending moment occurring in the beam as will be seen if the bending moment diagram for the encastré beam is drawn, and the resulting maximum longitudinal stress is 6·55 tons per square inch.

It is interesting to determine what relative sinking of the supports could occur before the maximum stress reached the permissible limit.

A stress of 8 tons per square inch would be produced by a bending moment of $\frac{8\times 220}{6}$ tons-inches so that, from equation (3), the limiting deflection is given by

$$\frac{8\times 220}{6}=240+\frac{6\times 13{,}000\times 220}{240\times 240}\delta \qquad \text{or} \qquad \delta=0{\cdot}18 \text{ inch.}$$

This comparatively small deflection would produce in this particular beam, with ends encastré, an increase in the maximum stress of more than 20 per cent. No such increase in the maximum stress would have been produced by the deflection had the ends of the beam been simply supported.

3.15. Beams of varying section subjected to any load system.—The formulas derived in paragraphs 3.2 to 3.8 have been applied so far to beams of uniform cross-section throughout their length. They are applicable, however, for all practical purposes, to beams in which the cross-section is not uniform.

From equation (3), paragraph 3.8

$$\frac{d^2y}{dx^2}=\frac{M}{EI}.$$

Integrating this $$\frac{dy}{dx}=\frac{1}{E}\int\frac{M}{I}dx+A$$

and $$y=\frac{1}{E}\int\int\frac{M}{I}dxdx+Ax+B.$$

Where $\frac{M}{I}$ is not an easily integrable function of x, recourse must be had to graphical methods for the determination of

$$\int\frac{M}{I}dx \quad \text{and} \quad \int\int\frac{M}{I}dxdx.$$

When these integrals have been evaluated the constants of integration A and B can be found and the equations for the slopes and deflections follow as in paragraphs 3.9–3.13.

As an example we shall consider the case of a cantilever of length L and constant depth d, which tapers linearly in plan view from a breadth b at the fixed end to nothing at the free end and carries a concentrated load W at the free end.

The relevant second moment of area at a section distance x from the free end is $\frac{1}{12}\frac{bd^3x}{L}$ and the bending moment there is Wx so that

$$\frac{d^2y}{dx^2}=\frac{M}{EI}=\frac{12WL}{bd^3E}$$

Hence $$\frac{dy}{dx}=\frac{12WLx}{bd^3E}+A$$

and $$y=\frac{6WLx^2}{bd^3E}+Ax+B$$

when $x=L$, $\frac{dy}{dx}=0$ $\quad\therefore A=-\frac{12WL^2}{bd^3E}$

when $x=L$, $y=0$ $\quad\therefore B=\frac{12WL^3}{bd^3E}-\frac{6WL^3}{bd^3E}=\frac{6WL^3}{bd^3E}.$

At the free end where the load is applied, $x=0$ and the deflection is

$$\frac{6WL^3}{bd^3E}.$$

A beam which is designed to be economical as far as weight of material is concerned must vary in cross-section from point to point in a manner dependent upon the variation of the bending moment to which it is subjected.

The design of a member of this type, particularly when it forms part of a continuous structure such as one built of reinforced concrete, presents no fundamental difficulty but is laborious. A general method has been published in the Proceedings of the American Society of Civil Engineers.*

3.16. Moment area and shear area methods.—There is a considerable literature dealing with more specialised methods of determining the slopes and deflections of beams.

The best known of these is the moment area method. If a beam of uniform cross-section, initially straight, is subjected to any load system so that M_x is the bending moment at any section at a distance x from the origin, which we have in earlier paragraphs taken as the left-hand end of the beam, then $\Delta\theta$, the change in angle between the tangents at two points C and D on the beam, is given by

$$\Delta\theta=\frac{1}{EI}\int_C^D M_x dx.$$

$\int_C^D M_x dx$, sometimes called the moment area, is the area of the bending moment diagram between C and D and we have the theorem: *If C and D are any two points on a beam the change in angle between the tangent at C and the tangent at D is equal to the area of the bending moment diagram between these points divided by EI, the constant flexural rigidity of the beam.*

If C is taken as the origin of co-ordinates so that x is measured from C it will be seen from equation (2) of paragraph 3.13 that we may write

$$x_D\theta_D-y_D+y_C=\frac{1}{EI}\int_C^D M_x x dx.$$

The left-hand side of this equation is an expression for the deflection of C relative to the tangent at D, while the right-hand side is equivalent to the area of the bending moment diagram between C and D multiplied by the distance of the centroid of this area from C. We thus have the further theorem:—

The displacement of C relative to the tangent at D is equal to the moment of the area of the bending moment diagram between C and D about the ordinate through C divided by the flexural rigidity of the beam.

To find by this method the deflection at the centre of a beam of span l which carries a uniformly distributed load of intensity w it must

* "Tapered Structural Members: An Analytical Treatment." Weiskopf and Pickworth, Proc. Am. Soc. C.E., October, 1935.

be remembered that the tangent at the centre of the length is horizontal so that the deflection there will be equal in magnitude to the displacement of one end of the beam relative to the tangent at the centre of length.

The area of half the parabolic segment forming the bending moment diagram of the beam is $\frac{2}{3} \cdot \frac{l}{2} \cdot \frac{wl^2}{8} = \frac{wl^3}{24}$ and the distance of the centroid of this area from the end of the beam is $\frac{5l}{16}$ so that the required displacement is

$$\frac{wl^3}{24} \times \frac{5l}{16} \times \frac{1}{EI} = \frac{5wl^4}{384EI}.$$

It will be seen that in applying this method to beams with uniformly distributed loads a knowledge of the areas and the positions of the centroids of parabolic segments is required. This has led to the development of an analogous method * in which use is made of the area of the shearing force diagram, which is usually a simpler figure than the bending moment diagram.

While it is well for the student to be aware of the existence of these methods, he will not usually find them of any great benefit in practice. The straightforward method of determining slopes and deflections set out in paragraphs 3.9–3.15 will in all cases give results with little, if any, more labour and with much less liability to error.

Another special method is the Column Analogy, due to Professor Hardy Cross.† It provides a simple means of determining the carry-over and distribution factors, used in the moment distribution method (paragraph 8.4), for members of varying cross-section. It is also applicable to the stress analysis of arches and rings.

3.17. Bending stresses in curved beams.—The equations for bending stress obtained in paragraph 3.3 are only valid if the beam is initially

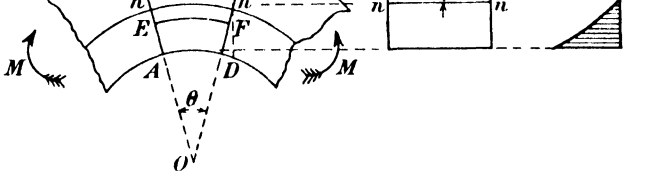

FIG. 3.17.

straight. If it has an appreciable curvature the application of these

* "The Shear Area Method." Compton and Dohrenwend, Proc. Am. Soc. C.E., May, 1935.

† "The Column Analogy." Hardy Cross, Bulletin No. 215. University of Illinois Engineering Experiment Station. A simple account will also be found in "Structural Theory," by Sutherland and Bowman. 3rd ed. Wiley, New York, 1942.

formulas may result in serious error and a more exact treatment, which is due to Winkler, is necessary.

Fig. 3.17 shows a beam, initially curved, subjected to a bending moment M tending to straighten it. BA and CD are two adjacent cross-sections initially separated by a small angle θ. The radius of curvature of the neutral surface *nn* over the small length of the beam between these sections is assumed to be constant and equal to r.

The same assumptions will be made as for the case of straight beams.

Under the action of M the section CD will rotate through a small angle $\delta\theta$ relative to AB.

Let EF be any surface at a distance y from *nn*, y being assumed to be positive when measured towards O, the centre of curvature of the short length of beam under consideration. The strain of a fibre in the surface EF is

$$e=\frac{y\delta\theta}{(r-y)\theta} \quad . \quad . \quad . \quad . \quad . \quad . \quad . \quad . \quad . \quad (1)$$

and, if lateral pressure between the fibres is neglected, the stress at EF is

$$f=\mathrm{E}e=\frac{\mathrm{E}y\delta\theta}{(r-y)\theta} \quad . \quad . \quad . \quad . \quad . \quad . \quad . \quad . \quad . \quad (2)$$

This is a hyperbolic curve of stress distribution as shown in Fig. 3.17 instead of the linear distribution obtained in the case of an initially straight beam.

Since there is no axial force acting on the beam the sum of the compressive forces in the fibres of the beam above the neutral axis must be equal to the sum of the tensile forces in the fibres below the neutral axis. If the beam is of constant width as shown in the diagram this entails that the area of the stress diagram above the neutral axis must be equal to the area of the diagram below it and so the neutral axis does not, as in the case of the straight beam, pass through the centroid of the section but is displaced towards the centre of curvature.

For equilibrium of the cross-section we have to satisfy two conditions :

(1) That already stated above, viz. that the total force on the cross-section is zero.

(2) The sum of the moments of forces on the cross-section about *nn* must be equal to the applied moment M.

If $d\mathrm{A}$ is an element of area of the cross-section at EF these conditions may be expressed as

$$\int f d\mathrm{A}=0$$
$$\int fy d\mathrm{A}=\mathrm{M}$$

and on substituting the value of f from (2) we obtain

$$\frac{\mathrm{E}\delta\theta}{\theta}\int\frac{y d\mathrm{A}}{r-y}=0 \quad . \quad . \quad . \quad . \quad . \quad . \quad . \quad . \quad (3)$$

and

$$\frac{\mathrm{E}\delta\theta}{\theta}\int\frac{y^2 d\mathrm{A}}{r-y}=\mathrm{M}. \quad . \quad . \quad . \quad . \quad . \quad . \quad . \quad (4)$$

The second of these equations may be rewritten in the form

$$\frac{E\delta\theta}{\theta}\left\{-\int y dA+\int\frac{ry dA}{r-y}\right\}=M.$$

The second integral is zero from equation (3) and the first represents the moment of area of the cross-section about *nn*, *i.e.* $-Ah$ where A is the total area of the cross-section and $-h$ is the distance of the neutral axis from the centroid.

So,
$$\frac{E\delta\theta}{\theta}Ah=M$$

or
$$\frac{E\delta\theta}{\theta}=\frac{M}{Ah} \quad . \quad . \quad . \quad . \quad . \quad . \quad . \quad . \quad . \quad . \quad (5)$$

Substituting this value of $\frac{E\delta\theta}{\theta}$ in (2) we have

$$f=\frac{My}{Ah(r-y)} \quad . \quad . \quad . \quad . \quad . \quad . \quad . \quad . \quad . \quad . \quad (6)$$

The maximum value of f occurs in the fibre AD and the minimum value in the fibre BC, so that if the distances of these fibres from the neutral axis are y_1 and $-y_2$ respectively, we have

$$\left.\begin{aligned} f_{max}&=\frac{My_1}{Ah(r-y_1)}\\ \text{and}\quad f_{min}&=-\frac{My_2}{Ah(r+y_2)}\end{aligned}\right\} \quad . \quad . \quad . \quad . \quad . \quad . \quad . \quad (7)$$

These equations cannot be used unless h and r are known.

Let y' be the distance of any element of cross-section from the axis through the centroid parallel to *nn* so that $y'=y+h$.

Substituting for y in equation (3) we have

$$\int\left(\frac{y'-h}{R-y'}\right)dA=0$$

where R is the radius measured to the axis through the centroid, *cc*.

Hence
$$\int\left(\frac{y'}{R-y'}\right)dA-\int\left(\frac{h}{R-y'}\right)dA=0. \quad . \quad . \quad . \quad . \quad . \quad (8)$$

The first integral in this equation represents a modified area and will be denoted by mA,

i.e.
$$\int\left(\frac{y'}{R-y'}\right)dA=mA \quad . \quad . \quad . \quad . \quad . \quad . \quad . \quad (9)$$

where m is a coefficient which must be calculated. The second integral in (8) can be written in the form

$$\int\left(\frac{h}{R-y'}\right)dA=\frac{h}{R}\int\left(1+\frac{y'}{R-y'}\right)dA=\frac{hA}{R}(1+m). \quad . \quad . \quad (10)$$

Substituting (9) and (10) in (8) we have

$$mA-\frac{hA}{R}(1+m)=0$$

or
$$h=R\frac{m}{1+m} \quad \ldots\ldots\ldots\ldots \quad (11)$$

The value of m may be found in some cases by direct integration, in others a graphical construction is preferable.

Suppose the section of the beam consists of a rectangle of width B and depth H.

Then
$$m=\frac{1}{A}\int_{-H/2}^{H/2}\left(\frac{y'}{R-y'}\right)dA$$

where
$$dA=Bdy' \text{ and } A=BH.$$

So,
$$m=\frac{1}{H}\int_{-H/2}^{H/2}\left(\frac{R}{R-y'}-1\right)dy'$$

or
$$m=\frac{R}{H}\log_e\frac{2R+H}{2R-H}-1. \quad \ldots\ldots\ldots \quad (12)$$

In the case of a circular section the integration is rather lengthy but gives the result

$$m=2\left(\frac{R^2}{a^2}-\frac{1}{2}\right)-\frac{2R}{a^2}\sqrt{R^2-a^2}$$

where a is the radius of the circle.

The value of m may also be found by taking a sufficient number of terms in the expansion of the expression $\frac{1}{R-y'}$, thus

$$m=\frac{1}{A}\int\frac{y'dA}{R-y'}$$
$$=\frac{1}{AR}\int y'\left(1+\frac{y'}{R}+\frac{y'^2}{R^2}+\frac{y'^3}{R^3}+\ldots\right)dA.$$

If dA can be expressed as a function of y' this series can readily be integrated. For a rectangle, for example, $dA=Bdy'$ and

$$m=\frac{B}{AR}\int_{-H/2}^{H/2}\left(y'+\frac{y'^2}{R}+\frac{y'^3}{R^2}+\frac{y'^4}{R^3}+\ldots\right)dy'$$
$$=\frac{B}{AR}\left[\frac{y'^2}{2}+\frac{y'^3}{3R}+\frac{y'^4}{4R^2}+\ldots\right]_{-H/2}^{H/2}$$

The even powers of y' vanish and we obtain

$$m=\frac{1}{HR}\left[\frac{H^3}{12R}+\frac{H^5}{80R^3}+\ldots\right]$$

or
$$m=\frac{1}{3}\left(\frac{H}{2R}\right)^2+\frac{1}{5}\left(\frac{H}{2R}\right)^4+\frac{1}{7}\left(\frac{H}{2R}\right)^6+\ldots, \quad \text{etc.}$$

In the same way the value for a circle of diameter D is found to be

$$m=\frac{1}{4}\left(\frac{D}{2R}\right)^2+\frac{1}{8}\left(\frac{D}{2R}\right)^4+\frac{5}{64}\left(\frac{D}{2R}\right)^6+\ldots \quad \text{etc.}$$

If the integral cannot be evaluated readily a graphical construction may be used as follows (Fig. 3.18):

AGBG′ is the cross-section, which is shown symmetrical about the axis AB. This is not necessary, but is the usual condition. The centre of curvature is O and G′G is the axis through the centroid. The length CD of any line parallel to G′G is proportional to an element of area dA at that level. Also FE$=y'$ and EO$=$R$-y'$. Join OD and produce this line to cut G′G at J. From J draw JH perpendicular to EH. Then the triangles JHD, OED are similar and

$$\text{DH} : \text{ED} :: \text{JH} : \text{EO},$$

i.e.
$$\text{DH}=\frac{\text{JH}}{\text{EO}}\text{ED}=\frac{y'}{\text{R}-y'}\,.\,\text{ED}$$

so DH is proportional to $\dfrac{y'}{\text{R}-y'}dA$ at this section.

Now consider another section KL which is above the axis G′G. As before join OL and from N the point where this line intersects G′G draw NM perpendicular to KL.

Then
$$\text{ML}=\frac{\text{MN}}{\text{OP}}\text{PL}=\frac{y'}{\text{R}-y'}dA.$$

It will be noticed that when the value of y' is negative, *i.e.* when the section considered lies above the axis through the centroid, the point on the derived figure lies inside the original diagram instead of outside it as for sections below the axis. This corresponds with the sign of the integral, which is positive when y' is positive and negative when y' is negative.

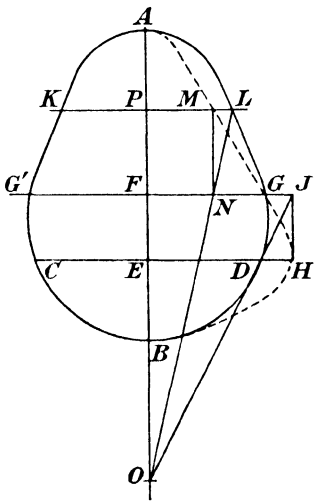

FIG. 3.18.

If a number of points are obtained in this way the derived figure is easily drawn and is indicated by dotted lines in Fig. 3.18.

The area included between this dotted line and the boundary of the original contour is a measure of $\frac{1}{2}\int\frac{y'}{\text{R}-y'}dA$ since one-half only of the symmetrical section shown has been treated.

If the section is not symmetrical about the line AO the diagram would of course be completed by a similar process on the other side.

Once the value of m has been found, h is calculated from equation (11), *i.e.* $h=\text{R}\left(\dfrac{m}{1+m}\right)$ and $r=\text{R}-h$. The stresses can then be found directly from equations (6) and (7).

As an example suppose a steel bar 2 inches square in cross-section

to be curved in a circular arc having a mean radius of 8 inches and to be loaded by end couples of 10 inch-tons. It is required to calculate the maximum and minimum stresses.

In the first place we will calculate m from the formula derived by direct integration

$$m=\frac{R}{H}\log_e\frac{2R+H}{2R-H}-1$$
$$=(4\times\cdot2513145)-1=\cdot005258.$$

As a check we may use the expansion

$$m=\tfrac{1}{3}(\tfrac{1}{8})^2+\tfrac{1}{5}(\tfrac{1}{8})^4+\tfrac{1}{7}(\tfrac{1}{8})^6+\ \ldots$$
$$=\cdot005208+\cdot000048$$
$$=\cdot005256.$$

Using the exact value we have

$$h=R\left(\frac{m}{1+m}\right)$$
$$=\frac{8\times\cdot005258}{1\cdot005258}=\cdot04184 \text{ inch.}$$

Then $r=8-\cdot04184=7\cdot95816$ inches

and $$f_{max}=\frac{My_1}{Ah(r-y_1)}$$

where $y_1=1-\cdot04184=\cdot95816$

$$\therefore\quad f_{max}=\frac{10\times\cdot95816}{4\times\cdot04184\times7}=8\cdot18 \text{ tons per square inch.}$$

Also $$f_{min}=\frac{-My_2}{Ah(r+y_2)}$$

where $-y_2=-(1+\cdot04184)=-1\cdot04184.$

$$\therefore\quad f_{min}=\frac{-10\times1\cdot04184}{4\times\cdot04184\times9}=-6\cdot92 \text{ tons per square inch.}$$

If the stresses are calculated by the formulas derived for initially straight beams we obtain

$$f=\frac{10\times3}{4}=7\cdot5 \text{ tons per square inch.}$$

The error is rather over 8 per cent. on the low side, and this error increases rapidly as the curvature is increased.

EXERCISES

(1) A wooden cantilever 12 feet long is 10 inches deep throughout but is tapered in plan in such a way that when a load is hung on the free end the maximum fibre stress is the same at all sections.

If this fibre stress is 1,200 lb. per square inch, calculate the deflection under the load.

$$E = 1{\cdot}5 \times 10^6 \text{ lb. per square inch.}$$

(1·66 inches)

(2) A cantilever of length L is propped at a distance L/4 from the free end to the level of the fixed end. It carries a load W at the free end. Determine the ratio of deflections at the free end for the prop in position and the prop removed.

(0·048)

(3) A cantilever of uniform cross-section and length L carries a load W at the free end and a distributed load varying linearly from w at the free end to $3w$ at the fixed end.

Calculate the deflection at the free end.

$$\frac{L^3}{3EI}\left(W + \frac{23wL}{40}\right)$$

(4) A vertical wooden mast 50 feet high tapers linearly from 9 inches diameter at the base to 4 inches diameter at the top. At what point will the mast break under a horizontal load applied at the top ?

If the ultimate strength of the wood is 5,000 lb. per square inch, calculate the magnitude of the load which will cause failure.

(20 feet from top : 442 lb.)

(5) A cantilever of length L has a constant breadth B and a varying depth given by $K\sqrt{x}$, where K is a constant and x is the distance from the free end. The cantilever carries a load W at the free end which causes a maximum fibre stress f in the material of the beam. Find the deflection at the free end if D is the depth of the beam at the root.

$$\left(\frac{8WL^3}{EBD^3}\right)$$

(6) A beam in cross-section is an equilateral triangle of 8-inch side, the line of the loading being perpendicular to one side.

If the total shearing force at a section is 5 tons, plot the distribution of shear stress across this section.

(Parabola with maximum value of ·27 tons per square inch at half depth)

(7) A beam freely supported over a span of 20 feet carries a load which varies uniformly from an intensity of 1 ton per foot at one end to 3 tons per foot at the other end. If the moment of inertia of the beam is 300 inch units and E is 30×10^6 lb. per square inch, calculate the deflection at the centre of the span.

(1·79 inches)

(8) A R.S.J. of $12'' \times 6'' \times \frac{1}{2}$ inch section is 12 feet long. It is fixed at one end and pinned at the other. A moment is applied to the pinned end tending to bend the beam in its strongest direction. If the maximum stress is 5 tons per square inch calculate the magnitude of the moment and the angle of slope at the pinned end of the beam.

(211·5 in.-tons ; 0·132 degrees)

(9) A beam AB of length L is freely supported at A and at a point C which is kL from the end B. If the load on AC is a uniformly distributed one of intensity w, find the value of k which will cause the upward deflection of B to equal the downward deflection midway between A and C.

(0·238)

(10) An encastré beam 20 feet span has a couple of 80 foot-tons applied at a point 5 feet from one support. Draw the bending moment diagram.

(11) A straight horizontal beam rests on supports 20 feet apart and overhangs each of these supports by 4 feet.

It carries loads of 10 and 8 tons at 5 and 14 feet respectively from the left-hand support.

Calculate what concentrated loads applied to the extreme ends of the beam will make it remain horizontal over both supports.

(9·55 tons at L.H. end
8·22 tons at R.H. end)

(12) The ends of a beam which carries a concentrated load at one-third of the span are so constrained that they assume slopes one-half of those which would occur if the beam were simply supported.

Sketch the bending moment and shearing force diagrams.

$$\begin{matrix} (\textit{End B.Ms.} = \frac{2}{27}WL \textit{ and } \frac{1}{27}WL \\ \textit{End S.Fs.} \quad = -\frac{10}{27}W \textit{ and } \frac{8}{27}W) \end{matrix}$$

(13) An encastré beam of span L has a moment of inertia varying uniformly from I_0 at the centre to $\frac{1}{2}I_0$ at each end. It carries a load uniformly varying from an intensity w at each end to $2w$ at the centre. Calculate the bending moments at the centre and ends and the central deflection.

$$\left(\begin{matrix} \textit{BM at centre} & -\dfrac{wL^2}{12} \\ \text{,,} \quad \text{,,} \textit{ ends} & +\dfrac{wL^2}{12} \\ \textit{Deflection} & = \dfrac{wL^4}{192I_0E} \end{matrix} \right)$$

(14) A circular link is made of square section steel bar of 1 inch side the junction being left unwelded.

The internal diameter is 3 inches. If the maximum stress in the steel is not to exceed 8 tons per square inch, calculate what diametrical pull the link can carry.

(·52 tons)

CHAPTER 4

THEOREMS RELATING TO ELASTIC BODIES

4.1. Elastic behaviour.—When loads are applied to a body—whether it be solid or a framework—the shape of that body is slightly changed. If, on the removal of the loads the body completely regains its original shape it is said to behave elastically. The curve obtained by plotting the displacements of any point against the loads causing these displacements is in most cases a straight line, but for certain types of bodies and for certain forms of loading the load-displacement curve is not linear although the behaviour is perfectly elastic.

Since many of the theorems relating to the behaviour of bodies under stress are only applicable if the displacements are proportional to the loads producing them, it is important to recognise the distinction between the two cases.

A thin rod of elastic material used as a tie rod, *i.e.* subjected to an axial tensile stress, will have a linear relationship between load and displacement, but if the same rod is subjected to a compressive load applied eccentrically the displacement of any point will increase at a greater rate than the load although such displacement will be elastic, *i.e.* it will disappear on the removal of the load.

4.2. Principle of superposition.—*If the displacements of all points in a body are proportional to the loads causing them the effect produced upon such body by a number of forces is the sum of the effects produced by the several forces when applied separately.*

This is a most important consequence of a linear load-displacement curve and renders possible the solution of many problems which would otherwise be intractable.

Its truth is readily seen by considering the case of a rod subjected to an axial tensile load of P+Q.

The extension of the rod under the load, if the material obeys Hooke's law, *i.e.* if it has a linear stress strain curve, is $\frac{(P+Q)L}{AE}$ where L is the length of the rod, A its cross-sectional area and E is Young's modulus for the material.

But this extension is $\frac{PL}{AE}+\frac{QL}{AE}$ which is the sum of the extensions of the rod under the two separate forces P and Q.

Fig. 4.1 (*a*) illustrates the point with reference to the actual load-extension diagram for the rod. Under tensions P and Q the extensions are represented by OA and OB respectively. If P+Q be applied to the rod the extension is represented by OC.

Since the triangles OBE and FGH are identical we can write,

$$OC=OA+FG=OA+OB$$

or extension due to P+Q=extension due to P+extension due to Q.

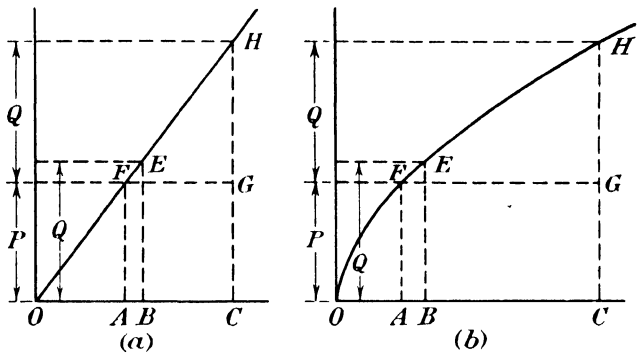

FIG. 4.1.

Next consider the case of a material which does not obey Hooke's law : the load extension curve for such a material is shown in Fig. 4.1 (*b*). As before, the extensions for loads P and Q are represented by OA and OB respectively. Under the action of P+Q the extension will be represented by OC and it is clear from the diagram that this is not equal to OA+OB. We are therefore unable to determine the extension of the rod under P+Q by adding those due to P and Q when applied separately.

To illustrate the principle, let Fig. 4.2 represent any body which obeys Hooke's law, carrying loads W_1 and W_2 as shown and supported at the points A and B.

The load system is the sum of the two systems shown in (*b*) and (*c*), and the stress at any point, such as D, which is produced by the load system (*a*) is the algebraic sum of the stresses produced by the load systems (*b*) and (*c*), whilst the displacement at any point due to (*a*) is the algebraic sum of the displacements due to (*b*) and (*c*). For the sake of brevity this statement will be expressed in the form

$$(a)=(b)+(c).$$

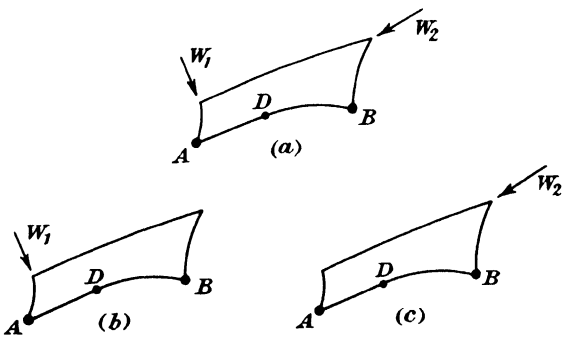

FIG. 4.2.

It is important to realise that the structures of (*a*), (*b*) and (*c*) are identical; no modification must be made. This warning is necessary since a so-called method of superposition is sometimes used in which a redundant structure is divided into two simply-stiff frames and the loading is applied half to one and half to the other. A solution obtained in this way is only approximate; it may in some cases be a good approximation but it cannot, in general, be exact. This method must not be confused with that now described, which furnishes exact solutions.

Suppose, for example, that the encastré beam shown in Fig. 4.3 carries a uniform load of intensity $2w$ over one-half of the span, and that it is required to determine the values of the end fixing moments M_A and M_B. The usual method necessitates either the use of a planimeter or the mathematical integration of the free bending moment diagram, and is unnecessarily lengthy. The load system (*a*) can, however, be replaced by the two systems shown in (*b*) and (*c*) respectively in Fig. 4.3; (*b*) consists of a uniform load of intensity w acting on the whole span, while (*c*) consists of a downward load of intensity w over one-half of the span and an upward load of intensity w over the other half.

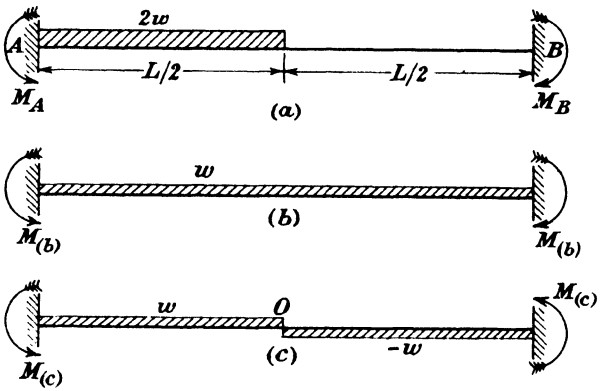

FIG. 4.3.

Then $$(a)=(b)+(c).$$

Now, the end fixing moment for (*b*) is

$$M_{(b)}=\frac{wL^2}{12}.$$

It is clear from the skew-symmetry of the arrangement that in (*c*) there is neither bending moment nor deflection at O, the centre of

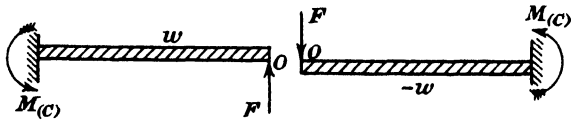

FIG. 4.4.

the beam. There is, however, a shearing force F, and the two halves of the beam are in equilibrium under the actions shown in Fig. 4.4.

Considering the left-hand half, the upward deflection of O due to F equals the downward deflection of O due to w.

That is, $$\frac{FL^3}{24EI}=\frac{wL^4}{128EI};$$

whence $$F=\frac{3}{16}wL,$$

and $$M_{(c)}=\frac{wL^2}{8}-\frac{3wL^2}{32}=\frac{wL^2}{32}.$$

Hence $$M_A=M_{(b)}+M_{(c)}=\frac{wL^2}{12}+\frac{wL^2}{32}=\frac{11wL^2}{96},$$

and $$M_B=M_{(b)}-M_{(c)}=\frac{wL^2}{12}-\frac{wL^2}{32}=\frac{5wL^2}{96}.$$

4.3. Strain energy.—When loads are applied to a body their points of application are displaced and the energy due to their movements is imparted to the body. If the strains are perfectly elastic this energy is stored in the body and is recoverable—when the loads are removed it is used in restoring the body to its original shape. If the strains are greater than those within which the body behaves elastically, part of the energy is used in permanently deforming the body and this portion is not recoverable. In general we are only concerned with strains of an elastic type and the energy stored under these conditions is known as strain energy. We shall also confine our attention to the case in which the load-displacement curve is linear.

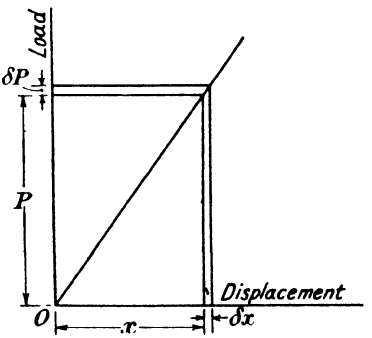

FIG. 4.5.

Fig. 4.5 represents the load displacement curve for a bar of material which obeys Hooke's law when subjected to a direct tensile or compressive force. The ordinates represent the loads applied to the bar and the abscissæ the displacements. These loads are applied in such a way that no kinetic energy is created, *i.e.* the bar does not vibrate longitudinally. The work done by the load is then all stored as strain energy in the bar.

Under a load P the displacement is x and under a load P+δP the displacement is $x+\delta x$.

The work done by the load during the increment of strain is its average value multiplied by the distance through which it moves, *i.e.* $\left(P+\frac{\delta P}{2}\right)\delta x$.

Since no kinetic energy is created this energy is stored in the bar and the increment of strain energy is therefore

$$\delta u = P\delta x$$

the second order term being neglected.

Since the load-displacement curve is linear

$$\delta x = \frac{L\delta P}{AE}$$

where L is the length of the bar, A is the cross-sectional area and E is Young's modulus.

Then $$\delta u = \frac{PL}{AE}\delta P.$$

Hence, the total strain energy of the bar as the load is increased from zero to P_0 is

$$u = \frac{L}{AE}\int_0^{P_0} P dP$$

or $$u = \frac{P_0^2 L}{2AE} \quad \ldots\ldots\ldots\ldots (1)$$

If the load is applied in such a way that kinetic energy is created the extra energy will cause the bar to vibrate. When these vibrations have ceased, however, the energy of the bar will be the same as found above. The strain energy does not depend upon the manner in which the load is applied but only upon the final value of the load. It is assumed that the strains during vibration are not such as to cause permanent deformation, *i.e.* the maximum stress at no time exceeds the limit of proportionality.

4.4. Force in a bar in terms of end displacements.—It is often convenient to express the force in a bar of a framework in terms of the displacements of its ends. Suppose P and Q are two nodes of a frame connected by the bar PQ.

Let the co-ordinates of P measured from any origin be (x_P, y_P, z_P) and the co-ordinates of Q be (x_Q, y_Q, z_Q).

When loads are applied to the frame P and Q will be displaced and the new co-ordinates will be

$(x_P+\alpha_P, y_P+\beta_P, z_P+\gamma_P)$ and $(x_Q+\alpha_Q, y_Q+\beta_Q, z_Q+\gamma_Q)$ respectively.

The initial length of the bar PQ is L, where

$$L^2=(x_Q-x_P)^2+(y_Q-y_P)^2+(z_Q-z_P)^2$$

and the final length is L+δL, where

$$\begin{aligned}(L+\delta L)^2&=(x_Q+\alpha_Q-x_P-\alpha_P)^2+(y_Q+\beta_Q-y_P-\beta_P)^2+(z_Q+\gamma_Q-z_P-\gamma_P)^2\\&=(x_Q-x_P)^2+(\alpha_Q-\alpha_P)^2+2(x_Q-x_P)(\alpha_Q-\alpha_P)\\&\quad+(y_Q-y_P)^2+(\beta_Q-\beta_P)^2+2(y_Q-y_P)(\beta_Q-\beta_P)\\&\quad+(z_Q-z_P)^2+(\gamma_Q-\gamma_P)^2+2(z_Q-z_P)(\gamma_Q-\gamma_P).\end{aligned}$$

Substituting for the appropriate terms from the equation for L^2 and neglecting the second order terms $(\alpha_Q-\alpha_P)^2$, $(\beta_Q-\beta_P)^2$ and $(\gamma_Q-\gamma_P)^2$

this becomes,

$$(L+\delta L)^2=L^2+2\{(x_Q-x_P)(\alpha_Q-\alpha_P)+(y_Q-y_P)(\beta_Q-\beta_P)+(z_Q-z_P)(\gamma_Q-\gamma_P)\}.$$

Neglecting the second order term $(\delta L)^2$ this can be written in the form,

$$e=\frac{\delta L}{L}=\frac{(x_Q-x_P)(\alpha_Q-\alpha_P)+(y_Q-y_P)(\beta_Q-\beta_P)+(z_Q-z_P)(\gamma_Q-\gamma_P)}{L^2}$$

where e is the strain in the bar.

The stress is then Ee, and the force in the bar is AEe where A is the area and E is Young's modulus.

4.5. Strain energy as a function of external loads.—If PQ is any bar in a plane frame and T_{PQ} is the force in it we can write from the result of the previous paragraph

$$\frac{T_{PQ}L}{AE}=\frac{(x_Q-x_P)(\alpha_Q-\alpha_P)+(y_Q-y_P)(\beta_Q-\beta_P)}{L}$$

and multiplying both sides of this equation by $\frac{1}{2}T_{PQ}$ we obtain

$$\frac{T^2_{PQ}L}{2AE}=\tfrac{1}{2}t_{PQ}[(x_Q-x_P)(\alpha_Q-\alpha_P)+(y_Q-y_P)(\beta_Q-\beta_P)]$$

where t_{PQ} is the tension coefficient for PQ.

This can be rewritten :

$$\frac{T^2_{PQ}L}{2AE}=\frac{\alpha_Q t_{PQ}}{2}(x_Q-x_P)+\frac{\beta_Q t_{PQ}}{2}(y_Q-y_P)+\frac{\alpha_P t_{PQ}}{2}(x_P-x_Q)+\frac{\beta_P t_{PQ}}{2}(y_P-y_Q).$$

Similar expressions can be written for every bar of the frame : α_Q and β_Q will be common factors for all the bars connected to the joint Q so that if all the expressions are added we shall obtain

$$\Sigma\frac{T^2L}{2AE}=\frac{\alpha_Q}{2}\{t_{QA}(x_Q-x_A)+t_{QB}(x_Q-x_B)+\ \ldots\ +t_{QP}(x_Q-x_P)\}$$
$$+\frac{\beta_Q}{2}\{t_{QA}(y_Q-y_A)+t_{QB}(y_Q-y_B)+\ \ldots\ +t_{QP}(y_Q-y_P)\}$$

+similar expressions for every other joint of the frame. If X_Q and Y_Q are the components of external force along the x and y axes at joint Q the equations of equilibrium for this joint are, from equation (1) of paragraph 2.5,

$$t_{QA}(x_A-x_Q)+t_{QB}(x_B-x_Q)+\ \ldots\ +t_{QP}(x_P-x_Q)+X_Q=0$$

and $$t_{QA}(y_A-y_Q)+t_{QB}(y_B-y_Q)+\ \ldots\ +t_{QP}(y_P-y_Q)+Y_Q=0.$$

Substituting the values of X_Q and Y_Q from these equations in the above we obtain,

$$\Sigma\frac{T^2L}{2AE}=\Sigma\left(\frac{\alpha_Q}{2}X_Q+\frac{\beta_Q}{2}Y_Q\right)$$

the summation of the left-hand side including all the bars of the frame and that of the right-hand side all the joints.

The left-hand expression is the internal work or strain energy of the frame produced *by the action of the external loads*, so that

$$U=\tfrac{1}{2}\Sigma(\alpha_Q X_Q+\beta_Q Y_Q). \quad . \quad . \quad . \quad . \quad . \quad . \quad . \quad . \quad (1)$$

If W_Q is the resultant force at Q of which X_Q and Y_Q are the components, and if Δ_Q is the displacement of Q in the line of action of W_Q, we have,

$$X_Q\alpha_Q+Y_Q\beta_Q=W_Q\Delta_Q$$

and (1) can be written,

$$U=\tfrac{1}{2}\Sigma W\Delta \quad . \quad . \quad . \quad . \quad . \quad . \quad . \quad . \quad (2)$$

i.e. the internal work of a frame which has a linear load-displacement relationship is half the sum of the products of the external forces and their respective displacements in their own lines of action.

This result depends only on the final values of the external loads and not upon the way in which they have been applied.

In the case of a space frame the same result is obtained in an exactly similar manner by introducing displacements and loads along the *z* axis of reference.

4.6. Strain energy due to bending.—Hitherto we have assumed that the bars with which we were dealing were subjected to pure tension or compression only, but as any action which stresses a body produces strain energy we shall now obtain expressions for that due to other actions.

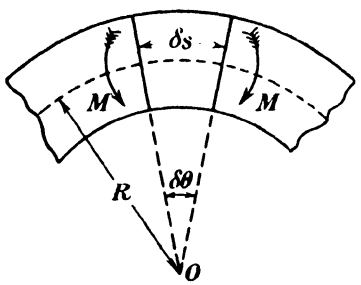

FIG. 4.6.

Suppose an initially straight beam to be subjected to a uniform bending moment M.

Under the action of this moment let two adjacent normal sections separated by a distance δs be inclined to each other so that δs subtends an angle $\delta\theta$ at the centre of curvature as in Fig. 4.6.

Since M could be replaced by equal and opposite forces acting at the outermost tensile and compressive fibres of the beam respectively and the external work could be expressed in terms of these equivalent forces it is clear that the result obtained in the previous paragraph holds true and we can write

$$\delta U_B=\tfrac{1}{2}M\delta\theta$$

where δU_B is the strain energy of the element due to bending.

If R is the radius of curvature of the element due to the action of M,

$$R\delta\theta=\delta s$$

and

$$\delta U_B=\frac{M\delta s}{2R}.$$

But from the ordinary theory of bending,

$$\frac{1}{R}=\frac{M}{EI} \qquad \therefore \qquad \delta U_B=\frac{M^2\delta s}{2EI}$$

and in the limit when δs is indefinitely decreased we can write

$$U_B = \int \frac{M^2 ds}{2EI}$$

which is the expression for the strain energy due to bending.

4.7. Strain energy due to shearing force.—Let AC and BD in Fig. 4.7 be two adjacent sections of a beam, separated by a distance δs, subjected to a shearing force F which will be supposed to be uniformly distributed over the cross-section of the beam.

Due to F let the shear strain be ϕ so that B and D move through a distance $\phi\delta s$ to B′ and D′ respectively.

Then $$\delta U_F = \tfrac{1}{2} F \phi \delta s,$$

where δU_F is the strain energy of the element due to shear.

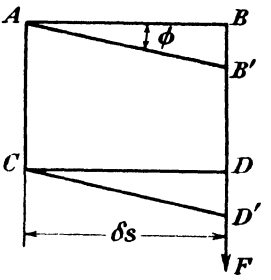

FIG. 4.7.

But $$\phi = \frac{\text{shear stress}}{N} = \frac{F}{AN}$$

where N is the modulus of rigidity of the material and A is the cross-sectional area of the beam.

$$\therefore \qquad \delta U_F = \tfrac{1}{2} \frac{F^2 \delta s}{AN}$$

and if δs is indefinitely reduced we have

$$U_F = \int \frac{F^2 ds}{2AN} \qquad \ldots\ldots\ldots \quad (1)$$

The shear stress is not in fact uniformly distributed over the cross-section: in a rectangular beam, for example, the distribution is parabolic and so the correct form of the above equation is,

$$U_F = k \int \frac{F^2 ds}{2AN} \qquad \ldots\ldots\ldots \quad (2)$$

where k is a coefficient which depends upon the shape of the section and the form of the loading.

4.8. Strain energy due to torsion.—Suppose that under the action of a torque T, two adjacent sections of a circular shaft δs apart are

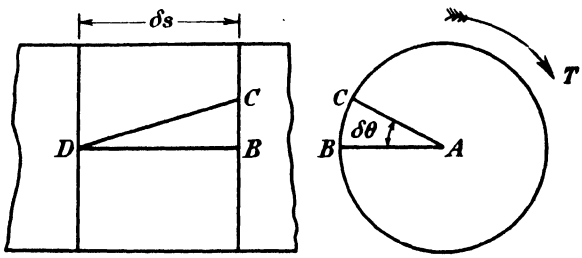

FIG. 4.8.

twisted through an angle $\delta\theta$ relative to each other as shown in Fig. 4.8. If the outer radius of the shaft is R the shear strain ϕ is

$$\phi=\frac{BC}{BD}=\frac{R\delta\theta}{\delta s}.$$

Also,
$$\phi=q/N=\frac{TR}{NJ}$$

where q is the shear stress at the radius R, N is the modulus of rigidity of the material and J is the polar second moment of area of the shaft.

Hence
$$\frac{R\delta\theta}{\delta s}=\frac{TR}{NJ}$$

or
$$\delta\theta=\frac{T\delta s}{NJ}.$$

The internal work of the element of the shaft is $\frac{1}{2}T\delta\theta$

$\therefore$
$$\delta u=\frac{T^2\delta s}{2NJ}$$

or
$$U_T=\int\frac{T^2ds}{2NJ}.$$

If the shaft is not circular in section, J is not the polar moment, but has a modified value which can be calculated * although in some cases an experimental determination may be the simpler procedure. For a general discussion of this problem reference may be made to text books on "Strength of Materials." †

4.9. The strain energy of curved beams.—When a beam has a large initial curvature the expression for the strain energy previously obtained for straight beams is not applicable.

Suppose ABCD in Fig. 4.9 is an element of a curved bar acted upon by a bending moment M, a shearing force F and an axial tension T.

From paragraph 3.17 we have,

$$\frac{E\delta\theta}{\theta}=\frac{M}{Ah}$$

so that
$$\delta\theta=\frac{M\theta}{AEh}=\frac{M\delta s}{RAEh}$$

which is the decrease of angle between AB and CD due to M.

Hence, if δU_B is the strain energy of the element due to bending,

$$\delta U_B=\frac{M^2\delta s}{2RAEh}. \quad . \quad . \quad . \quad . \quad . \quad . \quad . \quad . \quad . \quad (1)$$

Due to T the element elongates by an amount $\frac{T\delta s}{AE}$ and this *increases*

* See for example, "The determination of the stresses in a shaft of any cross section." Bairstow and Pippard. Proc. Inst. C.E., Vol. CCXIV, 1921–22.

† *E.g.* "Strength of Materials." J. Case. Arnold. Chapter XXX.

the angle θ by $\frac{T\delta s}{RAE}$ so that the work done by T if it acted alone would be $\frac{T\delta s}{RAE}\times\frac{TR}{2}=\frac{T^2\delta s}{2AE}$.

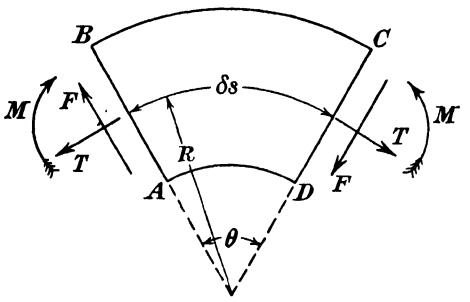

FIG. 4.9.

Part of this work, however, is done against the couple M and relieves the strain energy already stored by M. The amount used in this way is $\frac{MT\delta s}{RAE}$ and the net amount stored as strain energy in the element is therefore

$$\delta U_T=\frac{T^2\delta s}{2AE}-\frac{MT\delta s}{RAE}$$
$$=\frac{T\delta s}{AE}\left(\frac{T}{2}-\frac{M}{R}\right) \quad . \quad . \quad . \quad . \quad . \quad . \quad . \quad . \quad (2)$$

The shearing force F will cause sliding of one section relative to the other of an amount $\frac{kF\delta s}{AN}$ where k is a numerical factor depending on the shape of the cross-section.

So the strain energy of the element due to shearing force is

$$\delta U_F=\frac{kF^2\delta s}{2AN} \quad . \quad . \quad . \quad . \quad . \quad . \quad . \quad . \quad (3)$$

and the total strain energy of the element is

$$\delta U=\delta U_B+\delta U_T+\delta U_F$$
$$=\frac{M^2\delta s}{2RAEh}+\frac{T\delta s}{AE}\left(\frac{T}{2}-\frac{M}{R}\right)+\frac{kF^2\delta s}{2AN}$$

or,
$$U=\int\left\{\frac{M^2}{2RAEh}+\frac{T}{AE}\left(\frac{T}{2}-\frac{M}{R}\right)+\frac{kF^2}{2AN}\right\}ds \quad . \quad . \quad . \quad . \quad (4)$$

In many cases the effects of T and F are negligible compared with that of M and we have with sufficient accuracy

$$U=\int\frac{M^2ds}{2RAEh} \quad . \quad . \quad . \quad . \quad . \quad . \quad . \quad . \quad (5)$$

4.10. Clerk Maxwell's reciprocal theorem.—Suppose any elastic body,

either solid or a framework, is supported in such a way that the reactive forces do no work when loads are applied to the body. This result may be obtained by fixing the points of supports in space or by allowing them to rest on frictionless bearings. In the first case there is no movement of the supporting points and in the second, any movement is at right angles to the reactive force brought into action. The conditions for the sufficiency of the reactive forces as described in Chapter 1 must of course be observed. The body has a linear load-deflection relation such that when loads W_1 and W_2 are applied separately in specified directions to any two points A and B in the body,

Under the action of W_1 *alone :—*
A will move $W_1\Delta_1$ in the direction of W_1.
B will move $W_1\Delta'_2$ in the direction of W_2.

Under the action of W_2 *alone :—*
A will move $W_2\Delta'_1$ in the direction of W_1.
B will move $W_2\Delta_2$ in the direction of W_2.

If these two loads are applied simultaneously at such a rate that no kinetic energy is set up W_1 grows to its maximum value while A moves through the distance $W_1\Delta_1+W_2\Delta'_1$ and W_2 grows to its maximum while B moves through $W_2\Delta_2+W_1\Delta'_2$.

Hence the total strain energy of the body is

$$U=\tfrac{1}{2}W_1(W_1\Delta_1+W_2\Delta'_1)+\tfrac{1}{2}W_2(W_2\Delta_2+W_1\Delta'_2).$$

When W_1 alone acts on the body the strain energy is $\frac{1}{2}W_1^2\Delta_1$. If W_2 is then applied to point B it will move through a distance $W_2\Delta_2$ and the strain energy due to this will be $\frac{1}{2}W_2^2\Delta_2$. At the same time it will cause the load W_1 to move through a further distance $W_2\Delta'_1$ and since the value of W_1 is constant during this movement the work done on it is $W_1W_2\Delta'_1$.

Hence the total strain energy is

$$U=\tfrac{1}{2}W_1^2\Delta_1+\tfrac{1}{2}W_2^2\Delta_2+W_1W_2\Delta'_1.$$

It has been seen, however, that the manner in which the external loads reach their final values does not affect the value of the strain energy and the two expressions are therefore equal, *i.e.*

$$\tfrac{1}{2}W_1(W_1\Delta_1+W_2\Delta'_1)+\tfrac{1}{2}W_2(W_2\Delta_2+W_1\Delta'_2)$$
$$=\tfrac{1}{2}W_1^2\Delta_1+\tfrac{1}{2}W_2^2\Delta_2+W_1W_2\Delta'_1$$

Whence $\tfrac{1}{2}W_1W_2\Delta'_2=\tfrac{1}{2}W_1W_2\Delta'_1$

or $\Delta'_2=\Delta'_1$,

i.e. the deflection of B in the direction of W_2 when a unit load acts at A in the direction of W_1 is the same as the deflection of A in the direction of W_1 when a unit load acts at B in the direction of W_2.

This is the simplest form of Clerk Maxwell's reciprocal theorem. In its general form it may be stated as follows.*

Suppose that a number of forces P_1, P_2 . . . P_n, act simultaneously

* See "An introduction to the Theory of Elasticity." R. V. Southwell. Clarendon Press. pp. 11–12.

upon a body which obeys Hooke's Law and that the displacements in the lines of action of these forces are respectively Δ_1, Δ_2 . . . Δ_n. If these forces are replaced by a second system P'_1, P'_2 . . . P'_n acting at the same points and in the same directions as those of the first system, the corresponding displacements being Δ'_1, Δ'_2 . . . Δ'_n, then

$$P_1\Delta'_1+P_2\Delta'_2+ \ldots +P_n\Delta'_n=P'_1\Delta_1+P'_2\Delta_2+ \ldots +P'_n\Delta_n.$$

4.11. The first theorem of Castigliano.—Let any frame having a linear relationship between load and deflection be supported in such a way that the reactive forces do no work when loads are applied to the frame. If a number of loads, W_1, W_2 . . . . W_N, are applied to points 1, 2, ... N of the frame let the movement of point q in the direction of W_Q due to W_P be $W_P({}_p\delta_q)$ where q and p are any loaded points.

Thus the movement of point 3 in the direction of W_3 due to the load W_1 is $W_1({}_1\delta_3)$, etc.

The total movement of W_1 in its own line of action is then

$$\Delta_1=W_1({}_1\delta_1)+W_2({}_2\delta_1)+W_3({}_3\delta_1)+ \ldots . +W_N({}_N\delta_1),$$

and the movement of W_2 in its own line of action is

$$\Delta_2=W_1({}_1\delta_2)+W_2({}_2\delta_2)+W_3({}_3\delta_2)+ \ldots . +W_N({}_N\delta_2).$$

Using the result of equation (2) in paragraph 4.5 we can write

$$\tfrac{1}{2}W_1\Delta_1+\tfrac{1}{2}W_2\Delta_2+ \ldots . +\tfrac{1}{2}W_N\Delta_N=\sum\frac{(\alpha W_1+\beta W_2+ \ldots . +\nu W_N)^2L}{2AE}$$

where $\alpha W_1+\beta W_2+ \ldots . +\nu W_N$ is the load in any member due to the external load system.

If W_1 is removed the deflections of points 1, 2, . . ., etc., are

$$\begin{aligned}&\Delta_1-W_1({}_1\delta_1)\\&\Delta_2-W_1({}_1\delta_2)\\&\ldots\ldots\ldots\\&\Delta_N-W_1({}_1\delta_N).\end{aligned}$$

and as before,

$$\tfrac{1}{2}W_2\{\Delta_2-W_1({}_1\delta_2)\}+\tfrac{1}{2}W_3\{\Delta_3-W_1({}_1\delta_3)\}+ \ldots . +\tfrac{1}{2}W_N\{\Delta_N-W_1({}_1\delta_N)\}=\sum\frac{(\beta W_2+ \ldots +\nu W_N)^2L}{2AE}.$$

Subtracting this from the previous result we obtain

$$\tfrac{1}{2}W_1\Delta_1+\tfrac{1}{2}W_2W_1({}_1\delta_2)+\tfrac{1}{2}W_3W_1({}_1\delta_3)+ \ldots . +\tfrac{1}{2}W_NW_1({}_1\delta_N)=\sum\frac{\alpha W_1(\alpha W_1+2\beta W_2+ \ldots . +2\nu W_N)L}{2AE}.$$

By Clerk Maxwell's theorem we can put ${}_1\delta_2={}_2\delta_1$, ${}_1\delta_3={}_3\delta_1$, etc., and on substituting for Δ_1 the expression becomes

$$W_1[\tfrac{1}{2}W_1({}_1\delta_1)+W_2({}_2\delta_1)+W_3({}_3\delta_1)+ \ldots . +W_N({}_N\delta_1)]=\tfrac{1}{2}\sum\frac{\alpha W_1L}{AE}(\alpha W_1+2\beta W_2+ \ldots . +2\nu W_N).$$

If W_1 acts alone on the frame,

$$\tfrac{1}{2}W_1^2({}_1\delta_1)=\tfrac{1}{2}\sum\frac{\alpha^2W_1^2L}{AE}.$$

Adding this to the last result we obtain

$$W_1\Delta_1=W_1\sum\frac{\alpha L}{AE}(\alpha W_1+\beta W_2+\ \ldots\ .\ +\nu W_N)$$

or,
$$\Delta_1=\sum\frac{\partial u}{\partial W_1}$$

where u is the strain energy of a bar of the frame

Hence
$$\Delta_1=\frac{\partial U}{\partial W_1}$$

where U is the total strain energy of the frame or, extending the result to a solid body, the total strain energy of the body.

This is the first theorem of Castigliano,* and states that *if the total strain energy expressed in terms of the external loads be partially differentiated with respect to any one of the external loads, the result gives the displacement of that load in its own line of action.*

The applications of this theorem will be dealt with in the next Chapter.

4.12. The second theorem of Castigliano.—Suppose an elastic framework to be supported in such a way that no work is done by the reactive forces, and further let this frame be subjected to a system of external loads and to self-straining forces due to the presence of imperfectly fitting redundant members.

Let A and B in Fig. 4.10 be two adjacent nodes of the frame, the original distance between them before the application of either external or self-straining forces being L.

Suppose forces P and Q to act on the joints A and B along the line joining them as shown in the figure and let P and Q be functions of some variable R. Then if U′ is the strain energy of the frame due to the external loads and the self-straining forces we can write by the first theorem of Castigliano :—

The movement of A in the direction of $AB=\frac{\partial U'}{\partial P}$ and the movement of B in the direction of $BA=\frac{\partial U'}{\partial Q}$.

Also,
$$\frac{\partial U'}{\partial R}=\frac{\partial U'}{\partial P}\frac{dP}{dR}+\frac{\partial U'}{\partial Q}\frac{dQ}{dR}$$

If we put P=Q=R this becomes $\frac{\partial U'}{\partial R}=\frac{\partial U'}{\partial P}+\frac{\partial U'}{\partial Q}$=total shortening

* This theorem and the next were enunciated and fully discussed by Castigliano in his book "Théorème de l'équilibre des systèmes élastiques et ses applications" (Paris, 1879). An English translation by E. S. Andrews entitled "Elastic Stresses in Structures" (Scott Greenwood) is now available.

of AB.

Suppose now that A and B are connected by a redundant bar of the

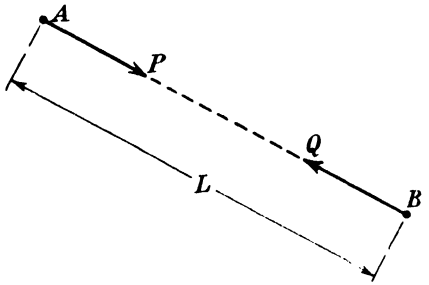

FIG. 4.10.

frame so that R is the load in this member. Also let the original length of this bar be $L-\lambda$ where λ is small compared with L.

The final length of the bar is $(L-\lambda)\left(1+\frac{R}{AE}\right)$, R being a tensile force.

But since the initial distance between A and B was L these points have approached each other by an amount

$$L-(L-\lambda)\left(1+\frac{R}{AE}\right)=\lambda-\frac{RL}{AE},$$

the second order term $\frac{\lambda R}{AE}$ being neglected.

Hence $$\lambda-\frac{RL}{AE}=\frac{\partial U'}{\partial R}.$$

Now $$\frac{RL}{AE}=\frac{\partial}{\partial R}\left(\frac{R^2L}{2AE}\right)=\frac{\partial u}{\partial R}$$

where u is the strain energy of the bar AB.

Hence $$\frac{\partial U'}{\partial R}+\frac{\partial u}{\partial R}=\lambda.$$

But $$\frac{\partial U'}{\partial R}+\frac{\partial u}{\partial R}=\frac{\partial U}{\partial R}$$

where U is the total strain energy of the frame including the bar AB.

$\therefore$ $$\frac{\partial U}{\partial R}=\lambda$$

or the partial differential coefficient of the total strain energy of a frame with respect to the load in a redundant member is equal to the initial lack of fit of that member.

Attention must be paid to the signs in using this result. In order to keep them correct the load in the member should always be made consistent with the initial lack of fit: if the member is initially too short the force R should be assumed to be tensile and if initially too long it should be assumed to be compressive. If this rule is observed the theorem will hold in all cases.

This is the second theorem of Castigliano in its general form. If the member AB were originally of just the correct length we put $\lambda=0$ and the result is

$$\frac{\partial U}{\partial R}=0.$$

This gives the value of R which will make the strain energy of the frame a minimum and in consequence this form of the theorem is often called the principle of least work. It is, however, only a special case of the more general result.

4.13. Differential coefficients of strain energy with respect to a moment.—In the previous paragraphs the differentiation of the expression for the strain energy of an elastic body has been done with respect to an axial force. It will now be shown that the theorems of Castigliano can be extended to include the case when the action considered is a moment.

Suppose two external loads, P_1 and P_2, to act at any section of an elastic body.

Then the displacement of P_1 in its line of action $=\delta_1=\frac{\partial U}{\partial P_1}$ and the displacement of P_2 in its line of action $=\delta_2=\frac{\partial U}{\partial P_2}$.

If these loads are functions of P,

$$\frac{\partial U}{\partial P}=\frac{\partial U}{\partial P_1}\cdot\frac{dP_1}{dP}+\frac{\partial U}{\partial P_2}\cdot\frac{dP_2}{dP}$$

and if $P_1=P_2=P$ we have

$$\frac{\partial U}{\partial P}=\frac{\partial U}{\partial P_1}+\frac{\partial U}{\partial P_2}=\delta_1+\delta_2.$$

If P_1 and P_2 are equal and opposite forces separated by a distance a they apply a couple $Pa=M$ to the body

and
$$\frac{1}{a}\frac{\partial U}{\partial P}=\frac{1}{a}(\delta_1+\delta_2).$$

But
$$\frac{1}{a}\frac{\partial U}{\partial P}=\frac{\partial U}{\partial Pa}=\frac{\partial U}{\partial M}.$$

Also $\frac{\delta_1+\delta_2}{a}=\theta$ is the angular rotation of the line joining the points of application of P_1 and P_2.

Hence
$$\frac{\partial U}{\partial M}=\theta$$

Or the differential coefficient of the strain energy with respect to an external moment is the rotation of that moment in radians. This is the first theorem of Castigliano when the applied external action is a moment.

If P_1 and P_2 are internal redundant actions

$$\frac{\partial U}{\partial P_1}=\frac{\partial U}{\partial P_2}=0$$

and then $$\frac{\partial U}{\partial M}=0$$

which is the second theorem of Castigliano when the redundant action is a moment.

4.14. Principle of Saint Venant.—This principle, known as the " elastic equivalence of statically equipollent systems of load," states that the strains which are produced in a body by the application to a small part of its surface of a system of forces statically equivalent to zero force and zero couple are of negligible magnitude at distances which are large compared with the linear dimensions of the part.

Suppose such a system of forces is divided into two parts which we will call A and B, these two parts being such that they produce equal and opposite resultant actions on the small part considered.

By Saint Venant's Principle the strain at any point some distance from the part upon which A+B acts is very nearly zero. When A acts alone let the strain at this point be e. Then clearly the effect of B alone must be to cause a strain approximating to $-e$ since by the principle of superposition the effect of A+B must be the same as the sum of the separate effects. Thus the system of forces B whose resultant actions are equal in magnitude but opposite in sign to those of A produces nearly equal and opposite strains to those produced by A.

The principle of Saint Venant can therefore be restated and we may say that *forces applied at one part of an elastic structure will induce stresses which except in a region close to that part, will depend almost entirely upon their resultant action, and very little upon their distribution.*

The principle was originally stated without proof but having restated it in the form just quoted Professor R. V. Southwell, from consideration of strain energy,* gave a proof which is reproduced here in its original form.

" Let us consider the case of a long girder, or braced framework, which is loaded at its two ends by forces applied in any given way; and let us employ the symbol A to denote those regions which immediately adjoin the parts at which the forces are applied, and the symbol B for the remainder. The conditions of equilibrium require merely that the resultant action transmitted by B shall have a definite value; but the conditions of continuity (or of compatibility of strains) will not be satisfied unless the total increase of the strain energy stored in A and B has its minimum value. Evidently, then, the equilibrium configuration may be regarded as in the nature of a compromise between the requirements of A and B. To reduce to a minimum the strain energy stored in A, the reactions between A and B would require to distribute themselves in a manner which will depend upon the distribution of the forces applied to A; the requirements of B, on the other hand, will not vary, since there must be some definite distribution of stresses, in an otherwise unloaded body, which will entail the minimum storage of strain energy in transmitting a given resultant action.

* " Castigliano's Theorem of Least Work and the Principle of Saint Venant." R. V. Southwell. Phil. Mag., Vol. XLV, January, 1923, p. 193.

Thus, in the process of adjustment which results in the actual distribution corresponding to equilibrium, we may picture a contest between the unloaded portions,* which strive always after 'standardisation,' and the loaded portions, which demand a particular solution for every specified distribution of the forces acting on them. As we pass from the regions of application of load through successive sections of the unloaded portion B, there will be a steady tendency for the claims of standardisation to prevail. The theorem stated in italics is an immediate deduction, and we may work back from this, by the principle of superposition, to Saint Venant's Principle."

4.15. Strain energy equations in terms of tension coefficients.—In some instances it is desirable to carry through a calculation in terms of tension coefficients rather than in actual loads. The equations can readily be recast into a suitable form, as follows :—

Let P_0 be the load in any member of length L and t_p the tension coefficient for this member, so that

$$P_0 = t_p L.$$

Let R_q be the load in any redundant member, t_q its tension coefficient and l_q its length, so that

$$R_q = t_q l_q.$$

Then, $P_0 = f(W) + at_1l_1 + bt_2l_2 + \ldots + qt_ql_q + \ldots + \text{etc.}$

where $f(W)$ is the contribution from the external load system.

Also $$\frac{\partial P_0}{\partial t_q} = ql_q$$

or $$\frac{L\partial t_p}{\partial t_q} = ql_q$$

so that $$\frac{\partial t_p}{\partial t_q} = \frac{ql_q}{L}.$$

Substituting these values in the expression

$$\frac{\partial u}{\partial R_q} = \frac{P_0 L}{AE} \cdot \frac{\partial P_0}{\partial R_q}$$

we have

$$\frac{\partial u}{\partial R_q} = \frac{t_p L^2}{AE} \cdot q$$

$$= \frac{t_p L^2}{AE} \cdot \frac{L\partial t_p}{l_q \partial t_q}$$

$$= \frac{t_p L^3}{AE}\left(\frac{1}{l_q}\right)\frac{\partial t_p}{\partial t_q}.$$

In the general case therefore the second theorem of Castigliano can be expressed in tension coefficients in the form,

$$\frac{\partial U}{\partial R_q} = \sum \frac{t_p L^3}{AE}\left(\frac{1}{l_q}\right)\frac{\partial t_p}{\partial t_q} = \lambda.$$

* *I.e.*, portions of which the *external* surfaces are free from load.

Since l_q is a divisor common to all terms we can, if λ is zero, *i.e.* if there is no self-straining, put the equation in the form

$$\sum \frac{t_p L^3 \partial t_p}{AE \partial t_q} = 0.$$

The summation extends to all members of the frame as in previous cases.

CHAPTER 5

DISPLACEMENTS OF ELASTIC BODIES

5.1. Displacement of the point of application of a single load.—If a body having a linear relationship between load and displacement is carried by supports which do no work when the body is loaded and bears a single load at any point, the displacement of that point can be calculated by a direct application of equation (2) of paragraph 4.5, which connects the strain energy with the external loads.

Thus, if W is the external load and Δ is its displacement in the line of action of W we have

$$\tfrac{1}{2}W\Delta = U$$

or

$$\Delta = \frac{2U}{W}$$

where U is the total strain energy of the body.

In the case of a framed structure $U = \sum \frac{\alpha^2 W^2 L}{2AE}$ where αW is the force in any member.

Then

$$\Delta = W \sum \frac{\alpha^2 L}{AE}.$$

As an example consider the steel frame shown in Fig. 5.1, which is pinned to a rigid support at A and D and carries a load of 20 tons

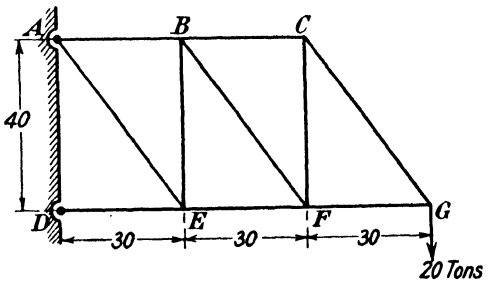

FIG. 5.1.

at G. It is desired to calculate the vertical movement of the point G.

The work should be set out as shown in Table 5.1, p. 65.

Columns 1, 2 and 3 are self-explanatory. In column 4 is entered the value of α. Since the load in any member is αW it is evident that α is the force in the member when W is made equal to unity. The required values of α may therefore be found by allowing unit load to act in the direction of W and determining the internal forces by any

TABLE 5.1.

1	2	3	4	5
Member	L ins.	A sq. ins.	α	$\frac{\alpha^2 L}{A}$
AB	30	4	$\frac{3}{4}$	$\frac{270}{16}$
BC	30	2	$\frac{3}{4}$	$\frac{135}{16}$
DE	30	6	$-\frac{3}{4}$	$\frac{405}{16}$
EF	30	4	$-\frac{3}{4}$	$\frac{270}{16}$
FG	30	2	$-\frac{3}{4}$	$\frac{135}{16}$
AE	50	5	$\frac{5}{4}$	$\frac{250}{16}$
BF	50	5	$\frac{5}{4}$	$\frac{250}{16}$
CG	50	5	$\frac{5}{4}$	$\frac{250}{16}$
BE	40	4	-1	$\frac{160}{16}$
CF	40	4	-1	$\frac{160}{16}$

of the methods described in Chapter 2. In the particular case under consideration they can be written down by inspection but in a more complicated example a stress diagram or tension coefficient analysis would probably be advisable.

Column 5 is completed from the earlier columns. Since E is the

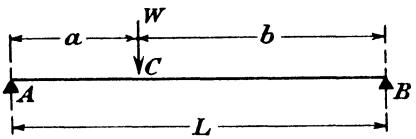

FIG. 5.2.

same for all members it has been omitted until the final calculation. If the material were not the same throughout the frame the correct value of E for each member would be entered in another column and column 5 would be $\frac{\alpha^2 L}{AE}$. Summing the results in column 5 we obtain $\Sigma\frac{\alpha^2 L}{A}=\frac{2,285}{16}$ and taking E as 13,000 tons per square inch,

$$\Sigma\frac{\alpha^2 L}{AE}=\frac{2,285}{16\times 13,000}.$$

Hence $$\Delta=\frac{20\times 2,285}{16\times 13,000}\text{ inch}=\cdot 22\text{ inch}.$$

As an example of the application of this method to a beam we will calculate the displacement of a load placed on a simply supported beam at a point C which is a distance *a* from one support and a distance *b* from the other as shown in Fig. 5.2.

The reaction at A is $\frac{b}{L}$W and in the length AC of the beam the bending

moment at a distance x from A is $\frac{Wbx}{L}$. Using the result of paragraph 4.6, we have for AC

$$U_{AC}=\frac{1}{2EI}\int_o^a M^2dx$$
$$=\frac{W^2b^2}{2EIL^2}\int_o^a x^2dx$$
$$=\frac{W^2b^2a^3}{6EIL^2}.$$

Similarly for the length BC, taking the origin at B, we have

$$U_{BC}=\frac{W^2a^2b^3}{6EIL^2}.$$

The total strain energy is therefore

$$U=\frac{W^2a^2b^2}{6EIL^2}(a+b)=\frac{W^2a^2b^2}{6EIL}$$

and so

$$\Delta=\frac{2U}{W}=\frac{Wa^2b^2}{3EIL},$$

which is a well known result obtainable by the methods of Chapter 3.

The method just described can only be used when a single load acts on the body. If more than one load is carried it is not applicable and deflections must be calculated by one or other of the methods now to be described.

5.2. Displacements by the first theorem of Castigliano.—If the displacements of a few points only are to be determined an application

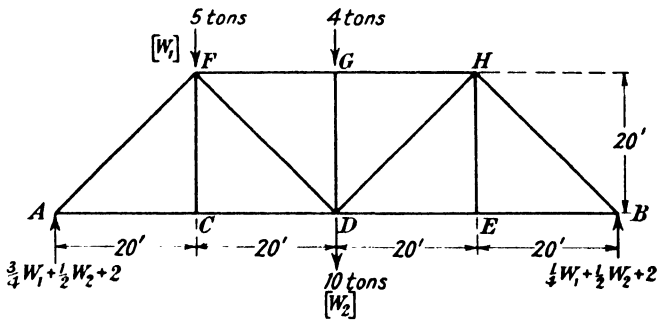

FIG. 5.3.

of the first theorem of Castigliano is probably the most satisfactory method of obtaining the result. An example will best explain the procedure and we will calculate the vertical deflection of points F and D of the steel truss shown in Fig. 5.3.

Since the strain energy of the frame has to be differentiated with respect to the external loads at the points F and D it is necessary first of all to denote those loads by algebraic symbols and they will

therefore be replaced by W_1 and W_2 respectively. The symbols will be given their numerical values only after the expressions for the deflections have been obtained. Since the movement of the point G is not required there is no need to denote the load there by a symbol.

The required deflections will then be

$$\Delta_F = \frac{\partial U}{\partial W_1} = \frac{1}{E}\sum \frac{P_0 L}{A}\frac{\partial P_0}{\partial W_1}$$

$$\Delta_D = \frac{\partial U}{\partial W_2} = \frac{1}{E}\sum \frac{P_0 L}{A}\frac{\partial P_0}{\partial W_2}.$$

As in all calculations of this type, the work should be systematised and Table 5.2 shows a suitable arrangement.

TABLE 5.2.

1	2	3	4			5			6		
Bar	L ins.	A ins.^{2}	P_0			$\frac{P_0 L}{A}\frac{\partial P_0}{\partial W_1}$			$\frac{P_0 L}{A}\frac{\partial P_0}{\partial W_2}$		
			W_1	W_2	Other Loads	W_1	W_2	Other Loads	W_1	W_2	Other Loads
AC	240	2	$\frac{3}{4}$	$\frac{1}{2}$	2	67·5	45	180	45	30	120
CD	240	4	$\frac{3}{4}$	$\frac{1}{2}$	2	33·75	22·5	90	22·5	15	60
DE	240	4	$\frac{1}{4}$	$\frac{1}{2}$	2	3·75	7·5	30	7·5	15	60
EB	240	2	$\frac{1}{4}$	$\frac{1}{2}$	2	7·5	15·0	60	15	30	120
FG	240	4	$-\frac{1}{2}$	-1	-4	15	30	120	30	60	240
GH	240	4	$-\frac{1}{2}$	-1	-4	15	30	120	30	60	240
AF	$240\sqrt{2}$	3	$-\frac{3\sqrt{2}}{4}$	$-\frac{\sqrt{2}}{2}$	$-2\sqrt{2}$	$90\sqrt{2}$	$60\sqrt{2}$	$240\sqrt{2}$	$60\sqrt{2}$	$40\sqrt{2}$	$160\sqrt{2}$
FC	240	2	—	—	—	—	—	—	—	—	—
FD	$240\sqrt{2}$	2	$-\frac{\sqrt{2}}{4}$	$\frac{\sqrt{2}}{2}$	$2\sqrt{2}$	$15\sqrt{2}$	$-30\sqrt{2}$	$-120\sqrt{2}$	$-30\sqrt{2}$	$60\sqrt{2}$	$240\sqrt{2}$
GD	240	2	—	—	-4	—	—	—	—	—	—
DH	$240\sqrt{2}$	2	$\frac{\sqrt{2}}{4}$	$\frac{\sqrt{2}}{2}$	$2\sqrt{2}$	$15\sqrt{2}$	$30\sqrt{2}$	$120\sqrt{2}$	$30\sqrt{2}$	$60\sqrt{2}$	$240\sqrt{2}$
HE	240	2	—	—	—	—	—	—	—	—	—
HB	$240\sqrt{2}$	3	$-\frac{\sqrt{2}}{4}$	$-\frac{\sqrt{2}}{2}$	$-2\sqrt{2}$	$10\sqrt{2}$	$20\sqrt{2}$	$80\sqrt{2}$	$20\sqrt{2}$	$40\sqrt{2}$	$160\sqrt{2}$

In the first place the force in every member must be calculated in terms of W_1, W_2 and the remaining loads, due regard being paid to signs: tensions are positive and compressions negative. If this is done graphically it will be necessary to draw three separate diagrams—one for W_1 acting alone, one for W_2 acting alone and the third for the remaining loads. These forces are entered in column 4; *e.g.* the force in GH is found by using the method of sections to be $P_0 = -\frac{1}{2}W_1 - W_2 - 4$ and the sub-divisions of column 4 are completed appropriately. It may be noted here that $\frac{\partial P_0}{\partial W_1}$ and $\frac{\partial P_0}{\partial W_2}$ for this bar are respectively $-\frac{1}{2}$ and

-1, *i.e.* the coefficients of W_1 and W_2 entered in the first two subdivisions of column 4.

Columns 1, 2 and 3 give particulars of the various bars.

In columns 5 and 6 respectively are entered the values of $\frac{P_0L}{A}\frac{\partial P_0}{\partial W_1}$ and $\frac{P_0L}{A}\frac{\partial P_0}{\partial W_2}$, calculated from the preceding columns. As an illustration, for bar AC, $\frac{L}{A}=120$ and $\frac{\partial P_0}{\partial W_1}=\frac{3}{4}$, so that $\frac{L}{A}\frac{\partial P_0}{\partial W_1}=90$. This is multiplied by P_0 which is tabulated in column 4 and the values entered in column 5 are obtained. Similarly $\frac{\partial P_0}{\partial W_2}=\frac{1}{2}$ and $\frac{L}{A}\frac{\partial P_0}{\partial W_2}=60$, which again multiplied by P_0 gives the figures entered in column 6.

The table is completed and columns 5 and 6 are summed to give $\Sigma\frac{P_0L}{A}\frac{\partial P_0}{\partial W_1}$ and $\Sigma\frac{P_0L}{A}\frac{\partial P_0}{\partial W_2}$.

These summations give

$$326W_1+263W_2+1{,}054$$

and $$263W_1+493W_2+1{,}971$$ respectively.

To obtain the deflection at points F and D these must be divided by E which is taken to be 13,000 tons per square inch.

Hence $$\Delta_F=\frac{1}{13{,}000}(326W_1+263W_2+1{,}054) \text{ inches,}$$

and $$\Delta_D=\frac{1}{13{,}000}(263W_1+493W_2+1{,}971) \text{ inches.}$$

The numerical values of W_1 and W_2, viz. 5 tons and 10 tons respectively, are now substituted and the actual deflections are found to be

$$\Delta_F=\cdot410 \text{ inch}$$

and $$\Delta_D=\cdot632 \text{ inch.}$$

5.3. Displacement of an unloaded point.—Since the expressions for Δ_F and Δ_D in the foregoing example are valid whatever the values of W_1 and W_2 a method is at once evident for determining the displacement of an unloaded point in a structure. Suppose for example that there were no load at F and it was required to calculate the vertical deflection at that point. A load W_F is placed at F and the previous procedure is followed, leading to the general expression for Δ_F as before. W_F is then put equal to zero and the vertical displacement of F is obtained.

5.4. Displacements in terms of stresses in the members.—Since $\frac{P_0}{A}=f$ is the stress in any bar the equation for the displacement of any point can be rewritten

$$\Delta=\Sigma\frac{fL}{E}\frac{\partial P_0}{\partial W}.$$

If then the stresses in the bars of a frame are specified it is unnecessary to calculate the areas; the displacement of any point can be found directly. If, for instance, in the previous example the frame is so designed that the stress in every loaded bar is 8 tons per square inch, the displacements of the points F and D respectively are

$$\Delta_F = \frac{1}{E}\Sigma f L \frac{\partial P_0}{\partial W_1}$$

and

$$\Delta_D = \frac{1}{E}\Sigma f L \frac{\partial P_0}{\partial W_2}.$$

The calculations should be set out as in Table 5.3.

TABLE 5.3.

1	2	3	4	5	6
Bar	L ins.	$\frac{\partial P_0}{\partial W_1}$	$\frac{\partial P_0}{\partial W_2}$	$L\frac{\partial P_0}{\partial W_1}$	$L\frac{\partial P_0}{\partial W_2}$
AC	240	$\frac{3}{4}$	$\frac{1}{2}$	180	120
CD	240	$\frac{3}{4}$	$\frac{1}{2}$	180	120
DE	240	$\frac{1}{4}$	$\frac{1}{2}$	60	120
EB	240	$\frac{1}{4}$	$\frac{1}{2}$	60	120
FG	240	$-\frac{1}{2}$	-1	-120	-240
GH	240	$-\frac{1}{2}$	-1	-120	-240
AF	$240\sqrt{2}$	$-\frac{3\sqrt{2}}{4}$	$-\frac{\sqrt{2}}{2}$	-360	-240
FD	$240\sqrt{2}$	$-\frac{\sqrt{2}}{4}$	$\frac{\sqrt{2}}{2}$	-120	240
DH	$240\sqrt{2}$	$\frac{\sqrt{2}}{4}$	$\frac{\sqrt{2}}{2}$	120	240
HB	$240\sqrt{2}$	$-\frac{\sqrt{2}}{4}$	$-\frac{\sqrt{2}}{2}$	-120	-240

It must be remembered that since f is $\frac{P_0}{A}$ it will have the same sign as P_0.

When the specified values of W_1 and W_2 are substituted in Table 5.2, it is found that the only bars in compression are FG, GH, AF and HB. The figures for these bars in columns 5 and 6 of Table 5.3 must therefore be multiplied by -8 tons per square inch and the remainder by $+8$ tons per square inch to obtain the values of $fL\frac{\partial P_0}{\partial W_0}$ and $fL\frac{\partial P_0}{\partial W_2}$.

The summation of these columns then gives

$$\Delta_F = \frac{1}{E}\Sigma f L \frac{\partial P_0}{\partial W_1} = \frac{9{,}600}{13{,}000} = \cdot 738 \text{ inch},$$

and $$\Delta_D=\frac{1}{E}\Sigma fL\frac{\partial P_0}{\partial W_2}=\frac{15{,}360}{13{,}000}=1.18 \text{ inches.}$$

If, as in paragraph 5.2, loads and not stresses are used, the question of sign is not so important. For example the force in FD can be expressed either as a tension of $-\frac{\sqrt{2}}{4}W_1+\frac{\sqrt{2}}{2}W_2+2\sqrt{2}$ or as a compression of $\frac{\sqrt{2}}{4}W_1-\frac{\sqrt{2}}{2}W_2-2\sqrt{2}$.

The terms which affect signs are $P_0\frac{\partial P_0}{\partial W_1}$ and $P_0\frac{\partial P_0}{\partial W_2}$ and it will be seen that whichever of the two values of P_0 are used the same final result is obtained, since in the second case the signs of P_0 and both differential coefficients are changed simultaneously, leaving the product unaffected.

5.5. Displacements of beams by strain energy methods.—The first theorem of Castigliano gives an alternative method for calculating the displacements of loaded beams to that described in Chapter 3 and in some cases the strain energy analysis has a decided advantage in simplicity.

The simple case of a beam carrying a single load has already been dealt with by the process of equating internal and external work and as a first example this same problem, illustrated in Fig. 5.2, will be solved by applying the first theorem of Castigliano. The vertical deflection of the point C is

$$\frac{dU}{dW}=\frac{1}{EI}\int M\frac{dM}{dW}dx.$$

At x from A, $$M_x=\frac{Wbx}{L}$$

$\therefore$ $$\frac{dM_x}{dW}=\frac{bx}{L},$$

and for the section AC of the beam,

$$\left[\frac{dU}{dW}\right]_{AC}=\frac{Wb^2}{EIL^2}\int_0^a x^2dx=\frac{Wa^3b^2}{3EIL^2}.$$

Similarly for the section BC,

$$\left[\frac{dU}{dW}\right]_{BC}=\frac{Wa^2}{EIL^2}\int_0^b x^2dx=\frac{Wa^2b^3}{3EIL^2}.$$

Hence

$$\Delta_C=\frac{dU}{dW}=\frac{Wa^2b^2}{3EIL^2}(a+b)=\frac{Wa^2b^2}{3EIL}.$$

As a second example, suppose the simply supported beam shown in Fig. 5.4 has a span L and carries loads W_1 and W_2 at distances L/3 and L/4 from the left- and right-hand supports respectively. It is

desired to calculate the vertical deflections at the loaded points. These will be

$$\Delta_C = \frac{\partial U}{\partial W_1} = \frac{1}{EI}\int M_x \frac{\partial M_x}{\partial W_1} dx$$

and

$$\Delta_D = \frac{\partial U}{\partial W_2} = \frac{1}{EI}\int M_x \frac{\partial M_x}{\partial W_2} dx.$$

In the first place the reactions at A and B are found to be

$$R_A = \frac{W_2}{4} + \frac{2W_1}{3}$$

and

$$R_B = \frac{3W_2}{4} + \frac{W_1}{3}.$$

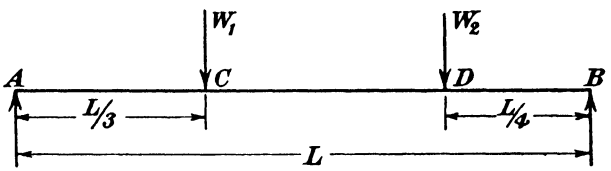

FIG. 5.4

Then, taking an origin at A, we have between A and C,

$$M_x = -R_A x = -x\left(\frac{W_2}{4} + \frac{2W_1}{3}\right),$$

so that

$$\frac{\partial M_x}{\partial W_1} = -\frac{2x}{3} \text{ and } \frac{\partial M_x}{\partial W_2} = -\frac{x}{4}.$$

Between C and D,

$$M_x = -R_A x + W_1(x - L/3) = -\frac{W_1}{3}(L-x) - \frac{W_2}{4}x,$$

and

$$\frac{\partial M_x}{\partial W_1} = -\frac{(L-x)}{3}; \quad \frac{\partial M_x}{\partial W_2} = -\frac{x}{4}.$$

For the section BD of the beam we take the origin at B and then

$$M_x = -R_B x = -x\left(\frac{3W_2}{4} + \frac{W_1}{3}\right),$$

so that

$$\frac{\partial M_x}{\partial W_1} = -\frac{x}{3} \text{ and } \frac{\partial M_x}{\partial W_2} = -\frac{3x}{4}.$$

We can now write the expressions for Δ_C and Δ_D,

$$\Delta_C = \frac{\partial U}{\partial W_1} = \frac{1}{EI}\left[\int_0^{L/3} \frac{2}{3}\left(\frac{W_2}{4} + \frac{2W_1}{3}\right)x^2 dx + \int_{L/3}^{3L/4} \left\{\frac{W_1}{9}(L-x)^2 + \frac{W_2}{12}x(L-x)\right\} dx + \int_0^{L/4} \left(\frac{3W_2}{4} + \frac{W_1}{3}\right)\frac{x^2}{3} dx\right]$$

and

$$\Delta_D=\frac{\partial U}{\partial W_2}=\frac{1}{EI}\left[\int_0^{L/3}\frac{1}{4}\left(\frac{W_2}{4}+\frac{2W_1}{3}\right)x^2dx + \int_{L/3}^{3L/4}\left\{\frac{W_1x}{12}(L-x)+\frac{W_2}{16}x^2\right\}dx+\int_0^{L/4}\frac{3}{4}\left(\frac{3W_2}{4}+\frac{W_1}{3}\right)x^2dx\right].$$

Upon integration these give

$$\Delta_C=\frac{L^3}{31104EI}(512W_1+357W_2)$$

and

$$\Delta_D=\frac{L^3}{20736EI}(238W_1+243W_2).$$

Any values may now be assigned to W_1 and W_2 and the deflections at C and D obtained.

As a final example of this method of calculation applied to simple

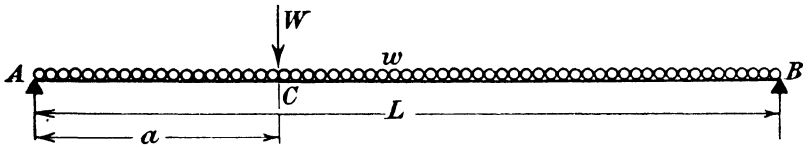

FIG. 5.5.

beams we will determine the curve of deflection for a uniformly loaded beam of span L, as shown in Fig. 5.5.

Assume that a concentrated load W is applied at any distance a from A. Then the deflection at the load W is

$$\frac{dU}{dW}=\frac{1}{EI}\int M_x\frac{dM_x}{dW}dx.$$

The reaction at A is $\frac{wL}{2}+\left(\frac{L-a}{L}\right)W$,

and at B is

$$\frac{wL}{2}+\frac{a}{L}W.$$

Consider first the section AC of the beam and take A as the origin. The bending moment at x from A is

$$M_x=-R_Ax+\frac{wx^2}{2}$$

$$=-\frac{wLx}{2}-\left(\frac{L-a}{L}\right)Wx+\frac{wx^2}{2},$$

so that

$$\frac{dM}{dW}=-\left(\frac{L-a}{L}\right)x$$

and

$$\left[\frac{dU}{dW}\right]_{AC}=-\frac{(L-a)}{LEI}\int_0^a\left\{\frac{w}{2}(x^3-Lx^2)-\left(\frac{L-a}{L}\right)Wx^2\right\}dx$$

$$=-\frac{(L-a)a^3}{LEI}\left\{\frac{w}{2}\left(\frac{a}{4}-\frac{L}{3}\right)-\left(\frac{L-a}{L}\right)\frac{W}{3}\right\}.$$

By replacing a and L—a by L—a and a respectively, we obtain

$$\left[\frac{dU}{dW}\right]_{BC}=-\frac{(L-a)^3a}{LEI}\left\{\frac{w}{2}\left(\frac{L-a}{4}-\frac{L}{3}\right)-\frac{aW}{3L}\right\}.$$

Then the deflection at C is

$$\left[\frac{dU}{dW}\right]_{AC}+\left[\frac{dU}{dW}\right]_{BC}$$

and if W is made zero the deflection at C due to the uniformly distributed load only is found to be

$$\Delta_C=-\frac{w(L-a)a}{2LEI}\left[\frac{a^3}{4}-\frac{a^2L}{3}+\frac{(L-a)^3}{4}-\frac{(L-a)^2L}{3}\right]$$

or
$$\Delta_C=\frac{wa(L-a)(L^2+aL-a^2)}{24EI}.$$

This is true for all values of a between 0 and L and is therefore the required curve of deflection for the uniformly loaded beam.

This method can be applied to any case of bending and further examples of its use will occur in later chapters.

5.6. Calculation of reactions in continuous beams and girders.—A knowledge of the actual magnitudes of the deflections of a beam or

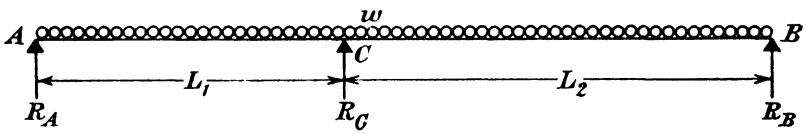

FIG. 5.6.

girder is not often required but the methods just described are useful for the calculation of reactive forces in continuous members.

Suppose, for example, that the beam ACB shown in Fig. 5.6 is continuous over the support C and carries a uniformly distributed load of intensity w over the whole length L_1+L_2. The reaction at C must be found before the bending moment and shearing force diagrams can be drawn.

Let the reaction be denoted by R_C. AB may then be considered as a simply supported beam of span L_1+L_2 loaded with a uniformly distributed downward load w and an upward concentrated load R_C.

The vertical displacement at C is $\frac{dU}{dR_C}$ but if the support is rigid this displacement will be zero and the condition which determines R_C is therefore

$$\frac{dU}{dR_C}=0.$$

Consider first the section AC of the beam and take the origin at A. The bending moment at any point is

$$M_x = -R_A x + \frac{wx^2}{2}$$

$$= -\frac{(L_1+L_2)wx}{2} + \frac{L_2 R_C x}{L_1+L_2} + \frac{wx^2}{2}$$

and $$\frac{dM_x}{dR_C} = \frac{L_2 x}{L_1+L_2}.$$

So, $$\left[\frac{dU}{dR_C}\right]_{AC} = \frac{L_2}{(L_1+L_2)EI}\int_0^{L_1}\left\{-\frac{(L_1+L_2)wx^2}{2} + \frac{L_2 R_C x^2}{L_1+L_2} + \frac{wx^3}{2}\right\}dx.$$

On integration and reduction this gives

$$\left[\frac{dU}{dR_C}\right]_{AC} = \frac{L_2}{24EI(L_1+L_2)^2}\{8R_C L_1^3 L_2 - w(L_1^5+5L_1^4L_2+4L_1^3L_2^2)\}.$$

Similarly we can write for the span CB

$$\left[\frac{dU}{dR_C}\right]_{BC} = \frac{L_1}{24EI(L_1+L_2)^2}\{8R_C L_2^3 L_1 - w(L_2^5+5L_2^4L_1+4L_2^3L_1^2)\}.$$

Adding these results we obtain

$$\frac{dU}{dR_C} = \frac{L_1 L_2}{24EI(L_1+L_2)}[8L_1L_2R_C - w(L_1+L_2)(L_1^2+3L_1L_2+L_2^2)]$$

and equating this result to zero we find

$$R_C = \frac{w(L_1+L_2)(L_1^2+3L_1L_2+L_2^2)}{8L_1L_2}$$

If $L_1=L_2$ this gives $R_C=\frac{5}{8}W$ where W is the total load on the beam, *i.e.* $w(L_1+L_2)$. This is a well-known result easily obtained by the methods of Chapter 3.

If the support at C instead of being fixed in position moves a certain distance, this can readily be taken into account. Suppose for example that C sinks a distance δ when the load is applied. The movement of R_C in its own line of action is then $-\delta$ and the condition to be satisfied for the determination of R_C is

$$\frac{dU}{dR_C} = -\delta.$$

If the support is moved upwards by an amount δ the condition is

$$\frac{dU}{dR_C} = \delta.$$

This method is applicable to beams with any number of supports, *e.g.* suppose a continuous girder supported at its ends A and B to have a number of intermediate supports, C, D . . . . Q. The reactive forces

at these supports are denoted by R_C, R_D . . . . R_Q. If the supports are fixed these forces can be evaluated by forming the equations

$$\frac{\partial U}{\partial R_C}=\frac{\partial U}{\partial R_D}= \ldots . =\frac{\partial U}{\partial R_Q}=0$$

and solving them simultaneously.

If any support moves under load the differential coefficient of the strain energy with respect to the force exerted there is equated to the movement of that support instead of to zero. Care must be observed in the sign ascribed to this movement as shown in the previous example.

The same principle may be applied to the calculation of reactive forces in a braced girder having more than two supports. For example, the bridge shown in Fig. 5.7 is supported at A, B and C and carries any

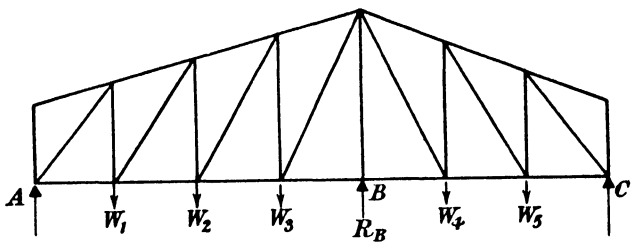

FIG. 5.7.

system of loads. The reactive force at B, denoted by R_B, may be determined from the condition

$$\frac{dU}{dR_B}=\delta$$

where δ is, as before, the movement of the support in the direction of action of R_B. If the support is rigid, δ is zero.

The structure is subjected to the known loads W_1, W_2, etc., and the unknown load R_B. The force P_0 in any member can be expressed in terms of these external loads and so

$$\frac{dU}{dR_B}=\Sigma\frac{P_0 L}{AE}\frac{dP_0}{dR_B}=\delta$$

which yields an equation to determine R_B.

5.7. Calculation of the angle of rotation.—In paragraph 4.13 it was shown that the angular movement of an external couple acting on an elastic body was given by the first differential coefficient of the strain energy with respect to the moment. As an example of the application of this theorem we will calculate the slope at all points on a cantilever of length L carrying a uniform load of intensity w; the procedure is as follows.

Apply a clockwise moment M_0 to the cantilever at a distance a from the free end as shown in Fig. 5.8.

Taking the origin at the free end of the cantilever the bending moment at any point is

$$M_x=\frac{wx^2}{2}+[M_0],$$

the second term appearing only when x is greater than a.

Then, $$\frac{dU}{dM_0}=\frac{1}{EI}\int M_x\frac{dM_x}{dM_0}dx=\frac{1}{EI}\int_a^L\left(\frac{wx^2}{2}+M_0\right)dx$$

since $\frac{dM_x}{dM_0}=0$ between $x=a$ and $x=0$.

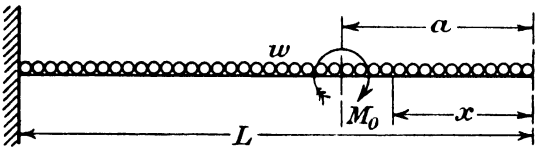

FIG. 5.8.

If M_0 is made zero, $\frac{dU}{dM_0}$ is the angle of rotation of the section at a from the end due to the load w.

Therefore $$\theta=\frac{1}{EI}\int_a^L\frac{wx^2}{2}dx,$$

or, $$\theta=\frac{w}{6EI}(L^3-a^3),$$

which is the curve of slopes for all values of a from 0 to L.

This result may be checked by a direct calculation thus

$$EI\frac{d^2y}{dx^2}=\frac{wx^2}{2}$$

$$EI\frac{dy}{dx}=\frac{wx^3}{6}+A$$

when $x=L$, $\frac{dy}{dx}=0$; therefore $A=-\frac{wL^3}{6}$,

and $$\theta=\frac{dy}{dx}=\frac{w}{6EI}(x^3-L^3).$$

This is the same result as by the former method, the negative sign corresponding to the same direction of slope as imposed by the clockwise moment M_0.

In this instance the second method is slightly more direct than the first but in many cases the application of the first theorem of Castigliano enables results to be obtained much more simply than by any other means.

5.8. Williot-Mohr displacement diagrams.—For many purposes it is convenient to determine the displacements of all points in a braced

frame and a graphical method then has advantages over those already described.

Let AC and BC in Fig. 5.9 represent two bars of a frame having internal forces which shorten the former by an amount Δ_1 and lengthen the latter by an amount Δ_2.

Corresponding to our convention of calling tensile stresses positive, increases in length will be treated as positive and decreases as negative.

The elastic straining of the frame will move the points A and B to new positions denoted by A′ and B′.

Suppose the bars AC and BC to be disconnected at C and let AC move to $A'C_1$ where $A'C_1$ is parallel to AC: similarly let BC move to $B'C_2$ where $B'C_2$ is parallel to BC. If we now take account of the strains of the bars, $A'C_1$ will shorten by Δ_1 to $A'C_1'$ while $B'C_2$ will lengthen by Δ_2 to $B'C'_2$.

The displaced position of C can be found by striking arcs from A′

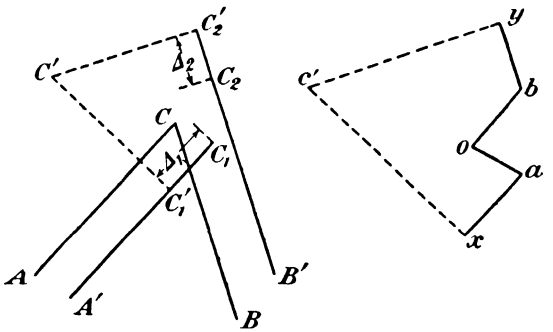

Fig. 5.9.

and B′ as centres with radii $A'C'_1$, and $B'C'_2$ respectively, the point of intersection being the required position.

Since however the strains are all small compared with the length of the bars the arcs may be replaced by lines C'_1C' and C'_2C' drawn perpendicular to $A'C'_1$ and $B'C'_2$ giving C′ as the displaced position of C.

Suppose now that *o* represents the original position of point C. Draw *oa*, *ob* parallel to CC_1 and CC_2 and proportional to these distances; the points *a* and *b* then represent C_1 and C_2.

From *a* draw *ax* parallel to CA and proportional to Δ_1 and from *b* draw *by* parallel to BC and proportional to Δ_2. Then *x* and *y* represent the points C'_1 and C'_2. Lines from *x* and *y* perpendicular to *ax* and *by* meet at *c′* and *oc′* is the displacement of the point C of the frame to the scale chosen.

Let Fig. 5.10 be any plane frame subjected to an external load system which causes alterations in the lengths of the bars of amounts Δ_1, Δ_2, etc., as shown in the figure. It is desired to determine the displacements of all points of the frame.

These displacements must be relative to some datum so we shall assume the point A to be fixed in space and the bar AB to be fixed in direction. This choice is quite arbitrary.

Let *a* represent the fixed point A. Draw *ab* parallel to AB and equal to Δ_1. Then *ab* represents the displacement of B relative to A. *ab* is drawn from *a* in the direction of movement of B.

Now C moves away from A by an amount Δ_3 so we draw *ac'* equal to Δ_3 and parallel to AC. Similarly C moves towards B so *bc''* is drawn from *b* equal to Δ_2 and parallel to BC. From *c'* and *c''* draw lines *c'c* and *c''c* perpendicular to *ac'* and *bc''* to meet at *c*. Then *c* is the displaced position of C relative to our datum point and direction.

To find the displacement of D the same procedure is followed. D moves towards C and away from A so *cd'* and *ad''* are drawn in the appropriate directions parallel to CD and AD and equal to Δ_5 and Δ_4 respectively. Perpendiculars *d'd* and *d''d* to *cd'* and *ad''* meet at *d* which is the displaced position of D.

The point *e* is found in the same way from the previously determined positions *c* and *d*.

Thus *ab*, *ac*, *ad*, *ae*, the displacements of B, C, D and E, are found

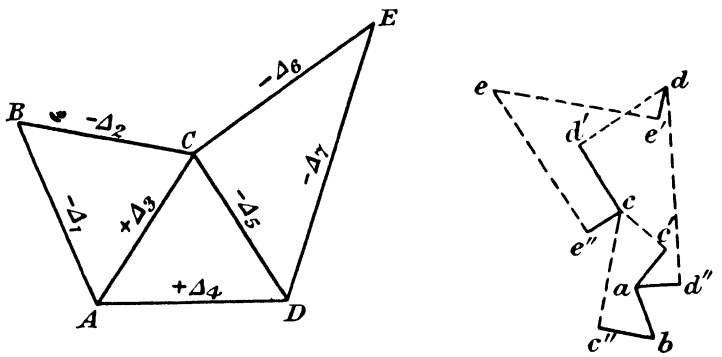

FIG. 5.10.

relative to the fixed point A and the fixed direction AB. The resulting diagram is known as a Williot diagram.

The fixed point and direction were, however, chosen arbitrarily and a diagram to be of general use must give absolute displacements. If A were actually fixed in space the true displacements of the various points could be determined by superimposing upon the relative ones found by the Williot diagram a suitable rigid body rotation to correct for the inaccuracy of the assumption that the direction of AB was unchanged. This correction is effected by means of the Mohr diagram now to be described.

Let ABCDEF in Fig. 5.11 be any frame which is supposed to rotate about an instantaneous centre P through an angle θ. Any point on the frame will then move in a direction perpendicular to the line joining the point to P. The amount of the movement will be $L\theta$ where L is the distance from P to the point. Hence the movements of all points will be proportional to their distances from P. Take any pole *o* and draw *oa*, *ob*, etc. parallel to the displacements of A, B, etc. and proportional in length to these displacements.

Join *abcdef* and consider the triangles PAB and *oab*. Since *oa* and *ob* are proportional to the displacements of A and B they are also proportional to PA and PB. Further, they are drawn parallel to the perpendiculars to PA and PB. Therefore the angle APB=*aob* and the triangles are similar. Hence *ab* is perpendicular to AB and bears the same ratio to it that *oa* does to PA.

This is true for all other corresponding lines of the two figures and so the Mohr diagram, *abcdef*, is similar to the frame diagram and is rotated relatively to it through a right angle.

If therefore two points on the Mohr diagram can be fixed the whole

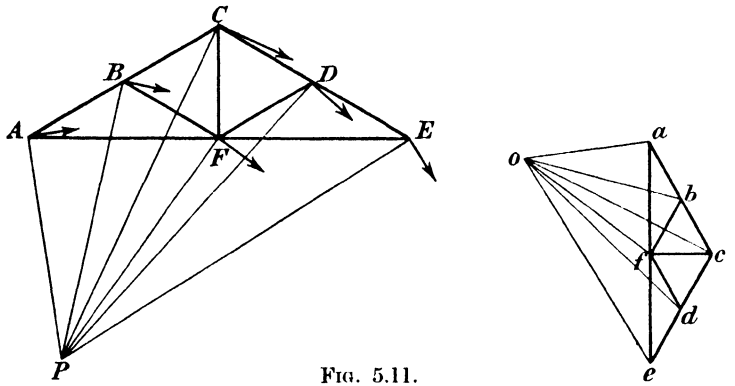

FIG. 5.11.

diagram may be drawn and can be superimposed on the Williot diagram to give absolute displacements of all points in the frame.

The method is best illustrated by an example and we will consider the king post truss shown in Fig. 5.12. This truss is assumed to be pinned at A and mounted on rollers at B so that any movement of B relative to A takes place along the line AB. The stress diagram is drawn for the load system for which the displacements are to be calculated and the elongations and shortenings of all members of the truss are calculated from a knowledge of their internal forces and sections. These are shown marked on the frame diagram of Fig. 5.12. It will be noticed that these strains are symmetrical but we shall proceed as would be necessary in the general case leaving until later the simplification which may be introduced due to this symmetry.

First, since A is fixed, we need only to assume a reference direction and for this purpose AD will be arbitrarily chosen. The Williot diagram is drawn exactly as described earlier and gives the vector *ab* as the displacement of B relative to A and AD. Actually the displacement of B relative to A is known to be horizontal and so a Mohr diagram must be superimposed on the Williot diagram to make the necessary correction.

The instantaneous centre of rotation will be the fixed pin A and a rigid rotation of the frame about A will cause a displacement of B perpendicular to AB.

From *a* draw a line perpendicular to AB and from *b* draw *bb'* horizontally to cut this line at *b'*.

Then ab' represents vectorially the displacement of B due to a rotation of the frame about A and the vector sum of $b'a$ and ab gives the

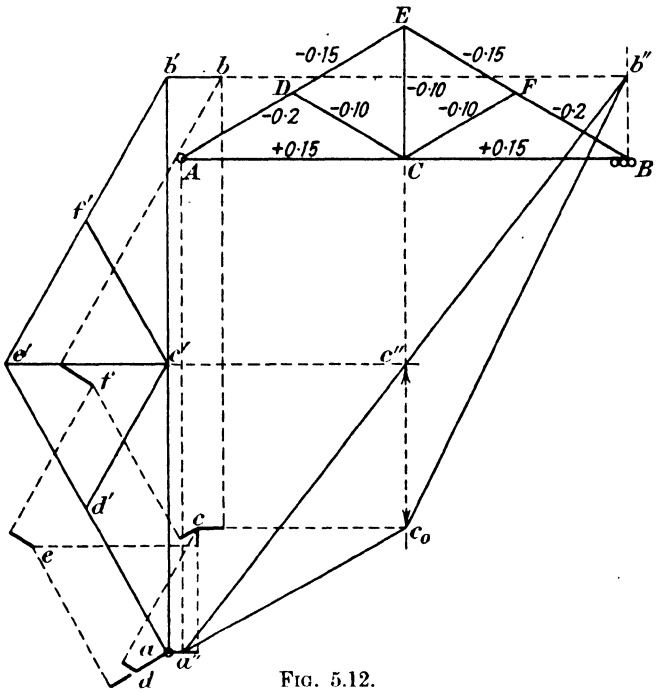

FIG. 5.12.

combined effects of the rotation and of the displacement obtained from the Williot diagram.

The vector sum of $b'a$ and ab is $b'b$ and this being horizontal complies with the necessary conditions that B must move along the line AB. Hence b' is fixed as a point on the Mohr diagram which is completed by drawing on ab' a figure similar to the frame diagram.

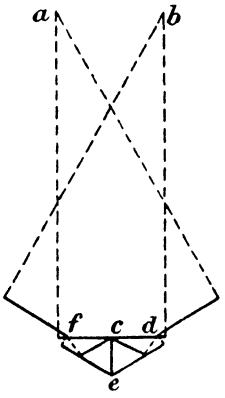

FIG. 5.13.

The true displacement of any point, *e.g.* E, is then the vector sum of ae, the elastic displacement and ac' the rotational displacement. This sum is $e'e$ and is measured from the point on the Mohr diagram to the corresponding one on the Williot diagram showing that E moves downwards.

Due to the symmetry of strains we could obtain the results much more easily as follows.

Take C as the fixed point and CE as the fixed direction and draw the Williot diagram as shown in Fig. 5.13. From the symmetry of the figure and of the strains it is clear that CE is actually fixed in direction and a Mohr diagram is not required. ac, ab, etc., give directly the true displacements of c, b, etc. relative to A.

In Fig. 5.12 project points A, C and B vertically to cut horizontal lines from a, c' and b' at the points a'', c'', b'' which will clearly lie on a straight line.

Also let horizontal projections of the points a, b, c cut the verticals through A, B and C at a'', b'', c_o.

Then $a''c_ob''$ is the displacement polygon for ACB and the vertical intercept of this polygon at any point gives the vertical displacement of that point, *e.g.* $c''c_o$ is the vertical displacement of point C.

This polygon is useful in dealing with certain problems in braced girders and will be referred to in later chapters.

EXERCISES

(*E for steel may be taken as* 13,000 *tons per square inch.*)

(1) A tripod is formed of steel tubes 2 inches outside diameter and ·056 inch thickness of metal. The feet of the tripod are at the apices of an equilateral triangle of 4 feet side in the horizontal plane and the tubes are each inclined at 60° to this plane.

Calculate the deflection of the top of the tripod under a load of 1 ton hanging there.

(*0·0055 in.*)

(2) A vertical steel mast of height L and flexural rigidity EI is firmly built into the ground and at its centre point a steel stay of cross-sectional area A is attached. This stay is led back at 45° to the mast and firmly attached to the ground.

A load W is applied horizontally to the top of the mast in the plane of the mast and stay.

If the stay is tightened so that its point of attachment is kept in the unloaded position calculate the tension in the stay and the deflection at the top of the mast.

$$\left(2{\cdot}5\sqrt{2}W,\ \frac{7WL^3}{96EI}\right)$$

(3) In the truss shown in diagram 5*a* all members are of steel and are stressed to 8 tons per square inch. Calculate the vertical deflection under the load. Check your answer by means of a Williot diagram.

(*1·04 ins.*)

(4) The steel frame shown in diagram 5*b* is so designed that the stress in all members is 8 tons per square inch.

Calculate the vertical deflection of the point D under a load of 10 tons.

(*0·540 in.*)

(5) Calculate the deflection of the point C in the steel frame shown at 5*c* if all members are 2 square inches in cross-sectional area. Verify the result by means of a Williot-Mohr diagram.

(*0·11 in.*)

(6) The frame shown at 5*d*, simply pinned at A and B, is so designed that every loaded member is stressed to 8 tons per square inch when 12 tons is carried at C.

Calculate the vertical deflection of C under this load.

(*1·108 ins.*)

(7) A rolled steel joist having a second moment of area of 300 inch units and a cross-sectional area of 12 square inches is firmly attached to a rigid base and is inclined at 60° to the horizontal. The length of the joist is 20 feet and from the free end a load of 1 ton is suspended. Calculate the vertical deflection of the load.

(*0·296 in.*)

(8) A steel beam of flexural rigidity EI and length L is pinned at one end to a wall. It is supported in a horizontal position by a steel wire of cross-sectional area A and modulus of elasticity E which is attached to the centre of the beam and to a point on the wall $\frac{L}{2}$ above the pinned end.

If a load is hung on the free end, calculate the deflection at the load.

$$\left[\frac{WL}{E}\left(\frac{L^2}{12I}+\frac{4\sqrt{2}}{A}\right)\right]$$

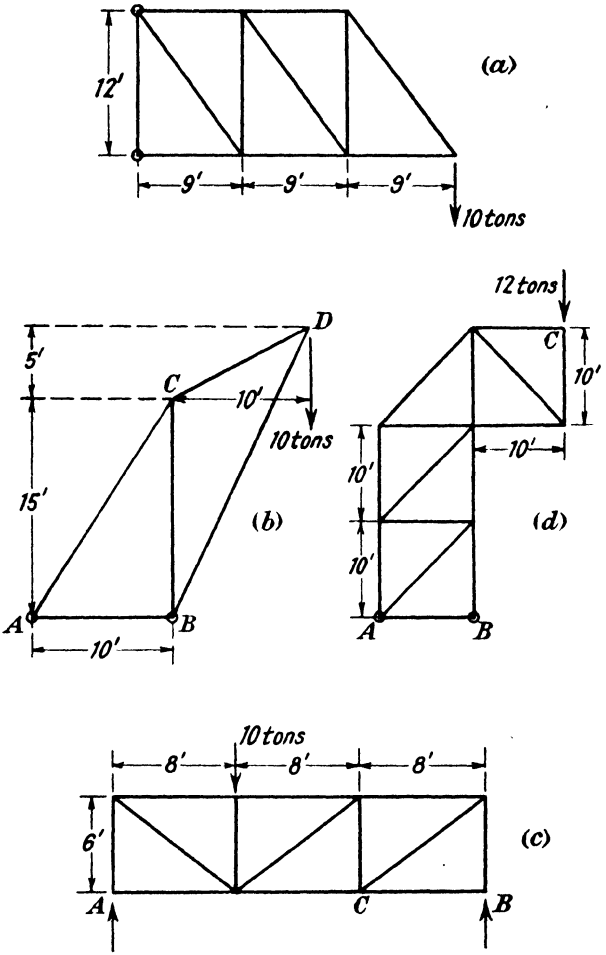

Diagram 5.

CHAPTER 6

STRESS ANALYSIS OF REDUNDANT FRAMES

6.1. Introduction.—Suppose as in Fig. 6.1 a weight W is suspended from two wires AD and BD which are attached to a rigid support AB. The forces in these two wires are calculable simply from a knowledge of the geometry of the arrangement and provided the wires are capable of carrying these loads it is immaterial what size they are made. The movement of the point D will, however, depend upon their elastic properties as well as upon the geometry. If a third wire CD be added to the suspension the problem of load distribution is considerably modified. If we denote the force in AD by T_1 we can determine the forces in DC and DB in terms of W and T_1, and since any value can be assigned to T_1 it is evident that there are an infinite number of solutions which will satisfy the conditions of static equilibrium of the point D, *i.e.* the condition of compatibility of stresses at D is not a sufficient criterion for the determination of the force distribution.

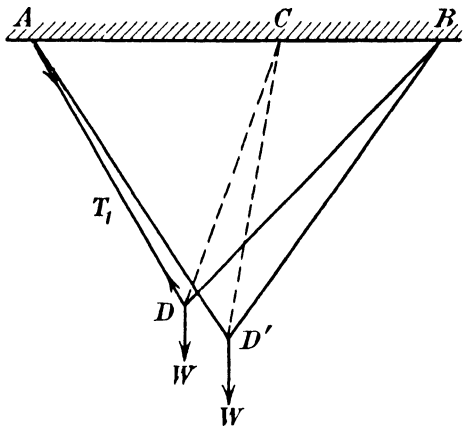

FIG. 6.1.

For any of these possible solutions the amounts by which the three wires will stretch due to the loads in them can be calculated.

If D′ is the displaced position of D, the strained lengths must be AD′, BD′ and CD′, *i.e.* arcs struck from A, C and B as centres and with radii equal to the respective strained lengths must intersect at a common point. This condition, which is known as that of compatibility of strains, enables the correct solution to be selected from the infinite number which satisfy the conditions of stress compatibility at D. The strains can only be calculated from a knowledge of the elastic properties of the wires and so the stress analysis of frameworks having redundant bracing members depends upon a knowledge of the elastic properties of all components of the structure. Several methods are available for making such an analysis, but they are essentially the same and differ only in application. The most widely used is probably the method of least work, *i.e.* an application of the second theorem

of Castigliano, which was given in paragraph 4.12 and the present chapter will be devoted to illustration of this method as well as others.

Objections have been made to this treatment on the ground that it does not allow the calculator to visualise the physical significance of his procedure at every step and that it is, in fact, something of a mechanical device for obtaining results. While the authors do not agree entirely with this view it is true that once the equations have been formed the arithmetical work is a matter of routine and many designers prefer to work by graphical methods. For this reason a treatment involving the direct comparison of displacements is used in some instances and a reference to it is therefore desirable at this stage.

6.2. Stress analysis by direct comparison of displacements.—Suppose a frame such as that shown in Fig. 6.2 (*a*) which has a single redundant

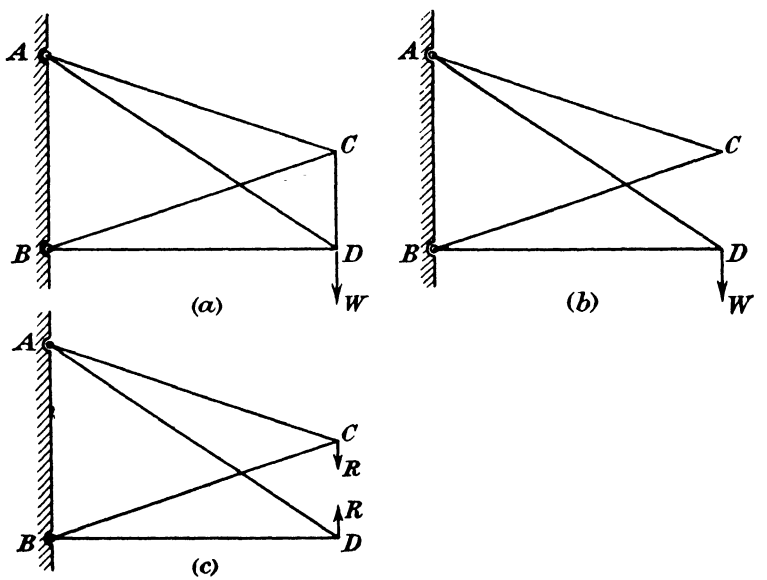

FIG. 6.2.

bar is to be analysed. In the first place any bar is chosen as the redundant member, provided that when this bar is removed from the frame the remaining or essential bars form a simply stiff structure.

In the present case it is convenient to treat CD as the redundancy and it is assumed to be removed, leaving the frame shown at (*b*).

A Williot-Mohr diagram is now drawn for this frame and the separation of the points C and D is obtained. Let this displacement be Δ.

If the force in the redundant member CD is denoted by R the effect of this bar will be to apply loads at C and D as shown at (*c*) and a second deflection diagram is drawn for this system and the approach of C and D is measured from it. Let this be $R\delta$.

The bar CD which applies the forces will itself stretch due to the tension in it by an amount $\frac{RL}{AE}$ where L is the length of CD, A is its cross-sectional area and E is the value of Young's modulus for the material.

The total separation of C and D will clearly be $\Delta - R\delta$ which must be equal to the stretch of the bar and so we obtain the relationship

$$\Delta - R\delta = \frac{RL}{AE}$$

from which

$$R = \frac{\Delta}{\left(\delta + \frac{L}{AE}\right)}$$

and can be calculated.

The method can readily be extended to cases in which there are more than one redundant member and it then involves the solution of as many simultaneous equations as there are redundancies. This method is developed further in Chapter 15 and no more need be said as to the details at this stage.

It should be noticed, however, that it involves the use of displacements, which are vector quantities, and signs are therefore of fundamental importance. Strain energy, on the other hand, is a scalar quantity and complications due to the sign of the quantities involved do not occur. In the case of a plane frame this is perhaps not a matter of serious importance, but in dealing with a space frame the consideration of signs is difficult and the method of least work has very considerable advantages over that just described.

6.3. Stresses in frames with one redundancy.—The application of strain energy analysis to frames will be illustrated by a number of examples and in the first place the simplest case involving a single redundant member will be taken. The three steel wires AB, CB and DB in Fig. 6.3 are attached to a rigid beam at A, C and D and carry a load of 5 tons at their junction B.

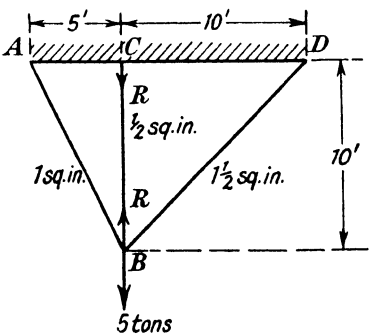

FIG. 6.3.

The dimensions of the frame and the wires are shown on the diagram and it is desired to know how the load is distributed between the wires.

There is clearly one redundant wire and it is convenient to treat CB as this element. The tensile load in CB is denoted by R.

In the first place it is necessary to find the forces in the two remaining wires in terms of W and R and this is best done by the use of tension coefficients. The equations for the point B are,

$$\left.\begin{aligned} -5t_{AB} + 10t_{BD} &= 0 \\ 10(t_{AB} + t_{BD}) &= 5 - R \end{aligned}\right\}$$

which give $t_{AB}=\frac{5-R}{15}$ and $t_{BD}=\frac{5-R}{30}$.

Multiplying these tension coefficients by the length of AB and BD respectively we have

$$T_{AB}=\frac{5-R}{15}\times\sqrt{25+100}=3{\cdot}725-{\cdot}745R$$

and

$$T_{BD}=\frac{5-R}{30}\times\sqrt{100+100}=2{\cdot}358-{\cdot}471R.$$

To determine the value of R we use the second theorem of Castigliano and put $\frac{dU}{dR}=0$.

Now

$$\frac{dU}{dR}=\sum\frac{P_0L}{AE}\frac{dP_0}{dR}$$

where P_0 is the load in any member, A is its area and L its length. The summation includes all members of the structure.

It is advisable in all calculations of this type, even in simple cases like the present, to arrange the work as in Table 6.1.

TABLE 6.1.

1	2	3	4	5	6
Member	L inches	A sq. inches	P_0 tons	$\frac{dP_0}{dR}$	$\frac{P_0L}{A}\frac{dP_0}{dR}$
AB	134·1	1	3·725 − ·745R	−·745	−372·5+74·5R
CB	120·0	0·5	R	1	240R
DB	169·6	1·5	2·358 − ·471R	−·471	−125·5+25·1R

This table is obtained as follows. In column 1 is entered the member and in column 2 its length. This is given in inches to keep the units consistent throughout, although in the present case it might have been given in feet since the final expression being equated to zero a constant multiplier does not affect the answer.

The area is entered in the third column, and in column 4 the force in the member in terms of R and the external load. Column 5 is the value of $\frac{dP_0}{dR}$ which is the coefficient of R in the expression in column 4. Column 6 is obtained by multiplication of the appropriate terms in the preceding columns. Since E is the same throughout and the final result is equated to zero it has been ignored.

Then, summing the three expressions in column 6 and equating to zero we have

$$\sum\frac{P_0L}{A}\frac{dP_0}{dR}=-498+339{\cdot}6R=0$$

i.e. $R=1{\cdot}466$ tons

and finally from column 4 of the table,

Force in AB=2·633 tons.
,, ,, CB=1·466 tons.
,, ,, DB=1·667 tons.

As a second example of this type of problem we will consider the case of a beam suspended by three rods as shown in Fig. 6.4 and loaded at any point. The dimensions are shown on the diagram. The beam is supposed to be so stiff that it may be considered to be rigid and therefore to store no energy due to bending while the rods are capable of taking either tensile or compressive loads.

There is one redundant support which we will assume to be BE.

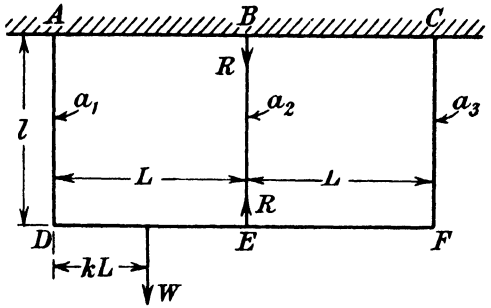

FIG. 6.4.

Let the tensile force in this member be R. By taking moments about D of the forces acting on the beam we obtain

$$2LT_{CF}+RL-kWL=0$$

or $$T_{CF}=\tfrac{1}{2}(kW-R)$$

and so $$T_{AD}=\tfrac{1}{2}\{W(2-k)-R\}.$$

To find the value of R we put $\frac{dU}{dR}=0$, and tabulating as before we obtain :—

TABLE 6.2.

Member	Length	A	P_0	$\frac{dP_0}{dR}$	$\frac{P_0L}{A}\frac{dP_0}{dR}$
AD	l	a_1	$\frac{1}{2}\{W(2-k)-R\}$	$-\frac{1}{2}$	$-\frac{l}{4a_1}\{W(2-k)-R\}$
BE	l	a_2	R	1	$\frac{l}{a_2}R$
CF	l	a_3	$\frac{1}{2}(kW-R)$	$-\frac{1}{2}$	$-\frac{l}{4a_3}(kW-R)$

Summing the last column we find

$$\frac{l}{4}\left\{R\left(\frac{1}{a_1}+\frac{4}{a_2}+\frac{1}{a_3}\right)-W\left(\frac{2-k}{a_1}+\frac{k}{a_3}\right)\right\}=0$$

or

$$R=\frac{W\left(\frac{2-k}{a_1}+\frac{k}{a_3}\right)}{\frac{1}{a_1}+\frac{4}{a_2}+\frac{1}{a_3}}$$

from which the loads in the other two rods may be found.

In both the cases just considered it has been assumed that the redundant member is exactly the right length to fit into its place so that no stresses are caused in the other members when it is inserted. The next example shows how stresses due to self-straining may be calculated.

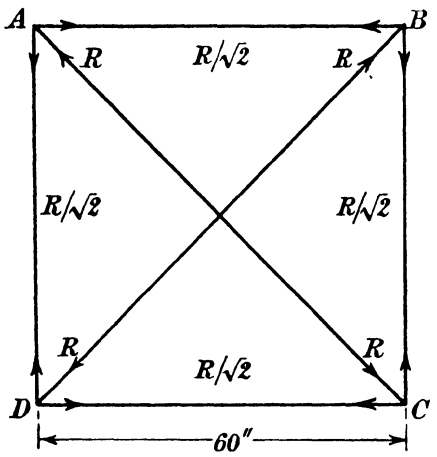

FIG. 6.5.

The square frame shown in Fig. 6.5 is formed of four pin-jointed steel bars each having a cross-sectional area of 2 square inches, braced diagonally by bars of the same material each having a cross-sectional area of 1 square inch. The diagonal AC was $\frac{1}{20}$ inch too long before it was forced into position and it is required to find the forces in all the bars of the frame due to this self-straining.

Since the bar AC was initially too long it will after insertion be in compression and so we assume that it *finally* carries a *compressive* force R. In order to determine the value of R we use the second theorem of Castigliano in its general form and evaluate

$$\frac{dU}{dR}=\frac{1}{20}\text{ inch}$$

where U is the total strain energy of the frame.

The forces in the other bars due to R acting at A and C are found by resolution at the joints and their values are shown on the diagram. The work is set out in Table 6.3, p. 89.

In this case since the value of $\frac{dU}{dR}$ is not equated to zero the modulus E must be included in the expression. The material being steel we shall take E as 13,000 tons per square inch. Then, summing the last column, we obtain

$$\sum\frac{P_0L}{AE}\frac{dP_0}{dR}=\frac{60R(1+2\sqrt{2})}{13{,}000}=\frac{1}{20}$$

or $$R = \frac{13{,}000}{20 \times 60(1+2\sqrt{2})} = 2{\cdot}83 \text{ tons.}$$

Thus, due simply to the lack of fit of the bar AC, the compressive force in each diagonal when it is inserted is 2·83 tons and the tensile

Member	L	A	P_0	$\frac{dP_0}{dR}$	$\frac{P_0 L}{A}\frac{dP_0}{dR}$
AB	60	2	$R/\sqrt{2}$	$1/\sqrt{2}$	15R
BC	,,	,,	,,	,,	,,
CD	,,	,,	,,	,,	,,
DA	,,	,,	,,	,,	,,
AC	$60\sqrt{2}$	1	$-R$	-1	$60\sqrt{2}R$
BD	,,	,,	,,	,,	

force in each side of the frame is 2 tons. These forces are additional to any caused by external loads which must be calculated either separately or at the same time as those due to self-straining.

Suppose, for example, that the same frame is simply supported on

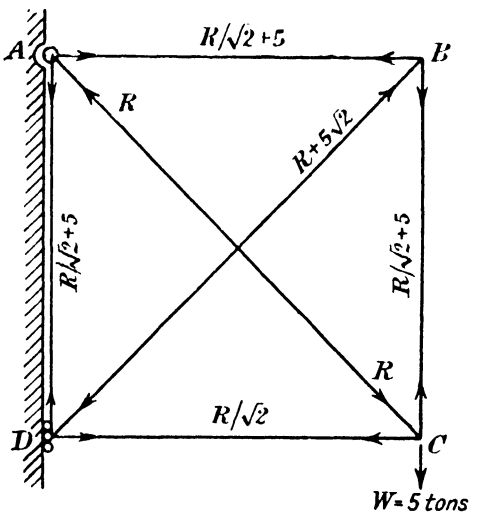

FIG. 6.6.

a pin at A and on rollers at D and that a load W=5 tons is suspended from C as shown in Fig. 6.6. Assume also the same lack of fit as before in AC. We may proceed in one of two ways. If the previous

calculation has already been made we can assume that we have an initially unstrained frame carrying the load W; call R the force in the redundant member AC and find the forces in all the bars of the frame due to W and R. Then, putting $\frac{dU}{dR}=0$ we find the value of R due to the load W alone and so the forces in all the other bars. These forces must then be added algebraically to those arising from the initial self-straining due to the lack of fit of AC and the sums will be the total forces. This result follows at once from the principle of superposition. Usually, however, it is unnecessary to make two separate calculations and the procedure is as follows. Fig. 6.6 shows the forces in the frame under the action of the vertical load of 5 tons, R as before being the force in AC, due now, however, *to the combined effects of the external load and of self-straining.* The work is set out in Table 6.4.

TABLE 6.4.

Member	L	A	P_0	$\frac{dP_0}{dR}$	$\frac{P_0 L}{A}\frac{dP_0}{dR}$
AB	60	2	$\frac{R}{\sqrt{2}}+5$	$\frac{1}{\sqrt{2}}$	$30\left(\frac{R}{2}+\frac{5}{\sqrt{2}}\right)$
BC	60	2	$\frac{R}{\sqrt{2}}+5$	$\frac{1}{\sqrt{2}}$	$30\left(\frac{R}{2}+\frac{5}{\sqrt{2}}\right)$
CD	60	2	$\frac{R}{\sqrt{2}}$	$\frac{1}{\sqrt{2}}$	15R
DA	60	2	$\frac{R}{\sqrt{2}}+5$	$\frac{1}{\sqrt{2}}$	$15R+\frac{150}{\sqrt{2}}$
BD	$60\sqrt{2}$	1	$-R-5\sqrt{2}$	-1	$60\sqrt{2}(R+5\sqrt{2})$
AC	$60\sqrt{2}$	1	$-R$	-1	$60\sqrt{2}R$

From the last column, after inserting E=13,000 tons per square inch as before, we have

$$\frac{dU}{dR}=\sum\frac{P_0 L}{AE}\frac{dP_0}{dR}=\frac{60R(1+2\sqrt{2})+918}{13{,}000}=\frac{1}{20}$$

or

$$R=\frac{\frac{13{,}000}{20}-918}{60(1+2\sqrt{2})}=-1{\cdot}166 \text{ tons}$$

i.e. there is a tension of 1·166 tons in AC under the combined effects of self-straining and the external load. An analysis of this result shows clearly the legitimacy of making the calculations in two parts as outlined earlier when it was stated that it could be done by calculating

the forces due to self-straining alone and superposing the forces due to the external load alone.

In the table just obtained, if we make the external load zero and equate $\frac{dU}{dR}$ to the lack of fit of AC, *i.e.* to $\frac{1}{20}$ inch, we obtain $R=\frac{13{,}000}{20}/60(1+2\sqrt{2})$, *i.e.* the first term in the expression for R, agreeing with the separate calculation of the previous example.

If we now assume R is due only to the external load system we obtain the same values in the last column but must equate the sum to zero; *i.e.* we get

$$\frac{60R(1+2\sqrt{2})+918}{13{,}000}=0$$

or $$R=-\frac{918}{60(1+2\sqrt{2})}.$$

This is the second term of our combined expression and the justification for superposing results is evident.

As a further example, consider the frame shown in Fig. 6.7, which has one correctly fitted redundant bar. This is taken to be BD and the load in it is assumed to be tensile and of magnitude R.

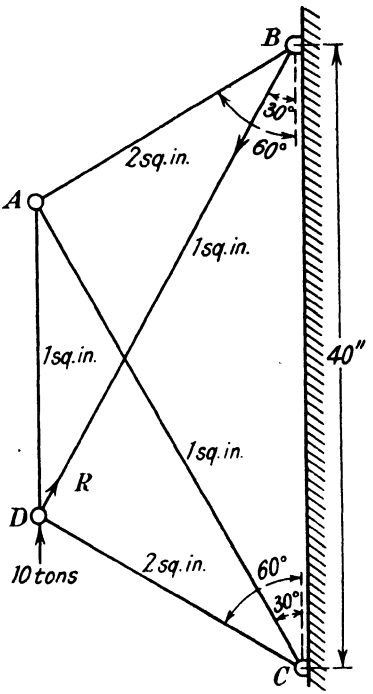

Fig. 6.7.

Proceeding as before, the loads in all bars of the frame are found in terms of R and the external force and the strain energy equations formed. The calculations are set out in tabular form below :

Table 6.5.

Member	L inches	A sq. in.	P_0	$\frac{dP_0}{dR}$	$\frac{P_0L}{A}\frac{dP_0}{dR}$	P_0
AB	20	2	$-5-\frac{R}{\sqrt{3}}$	$-\frac{1}{\sqrt{3}}$	$10\left(\frac{5}{\sqrt{3}}+\frac{R}{3}\right)$	−1·85
CD	20	2	$0-\frac{R}{\sqrt{3}}$	$-\frac{1}{\sqrt{3}}$	$10\left(0+\frac{R}{3}\right)$	+3·15
AD	20	1	$-10-\frac{2R}{\sqrt{3}}$	$-\frac{2}{\sqrt{3}}$	$20\left(\frac{20}{\sqrt{3}}+\frac{4}{3}R\right)$	−3·70
AC	$20\sqrt{3}$	1	$5\sqrt{3}+R$	+1	$20\sqrt{3}(5\sqrt{3}+R)$	+3·21
BD	$20\sqrt{3}$	1	0+R	+1	$20\sqrt{3}(0+R)$	−5·45

Summing the last column but one we obtain an equation in R which gives the value R=−5·45 tons. The forces in all bars of the frame are then entered in the last column of the table.

A slightly different type of problem which may be solved by strain energy methods is exemplified by the case of a number of columns supporting a roof. For example, suppose a rectangular flat roof 20 feet×30 feet, which may be considered to be rigid, is carried on four similar stanchions placed at the corners and is loaded by a concentrated weight of 2,400 lb. acting at 10 feet from a short side and 5 feet from a long side of the roof. The load in each stanchion is required. The arrangement is shown in Fig. 6.8. Denote the loads in the four stanchions by A, B, C and D. By taking moments about AB and CB in turn and equating vertical forces we obtain the following conditions for the static equilibrium of the system:

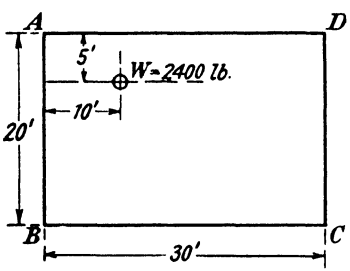

FIG. 6.8.

$$30(C+D)=10W \quad . \quad . \quad . \quad . \quad . \quad . \quad . \quad . \quad . \quad . \quad (1)$$

$$20(A+D)=15W \quad . \quad . \quad . \quad . \quad . \quad . \quad . \quad . \quad . \quad . \quad (2)$$

$$A+B+C+D=W \quad . \quad . \quad . \quad . \quad . \quad . \quad . \quad . \quad . \quad . \quad (3)$$

There is one redundant support and we will take this to be the stanchion at A so that the fourth equation necessary for the solution of the problem is

$$\frac{dU}{dA}=0.$$

Now $$U=\frac{L}{2aE}(A^2+B^2+C^2+D^2)$$

where a is the cross-sectional area and L is the length of each stanchion.

$$\therefore \quad \frac{dU}{dA}=\frac{L}{aE}\left(A+B\frac{dB}{dA}+C\frac{dC}{dA}+D\frac{dD}{dA}\right)=0. \quad . \quad . \quad . \quad . \quad (4)$$

From equation (1) we obtain $C=\frac{W}{3}-D$

and from equation (2) $D=\frac{3W}{4}-A$

$\therefore$ $C=A-\frac{5}{12}W$

and from equation (3) $B=\frac{2W}{3}-A.$

Hence $\frac{dB}{dA}=-1$, $\frac{dC}{dA}=1$ and $\frac{dD}{dA}=-1.$

So equation (4) becomes on substitution,

$$A+\left(A-\frac{2W}{3}\right)+\left(A-\frac{5W}{12}\right)+\left(A-\frac{3W}{4}\right)=0$$

or $$A=\tfrac{11}{24}W.$$

Putting in the value W=2,400 lb. the forces in the stanchions are found to be :

A=1,100 lb.
B= 500 lb.
C= 100 lb.
D= 700 lb.

As a final example of a structure with one redundant element we will analyse the king-posted beam shown in Fig. 6.9.

This consists of a continuous beam AB strengthened by a king post CD which is pinned to the centre of AB and braced by stays AD and BD. The beam is simply supported at A and B. Dimensions are as shown in the figure.

It is evident that if the beam consisted of two parts AC and CB

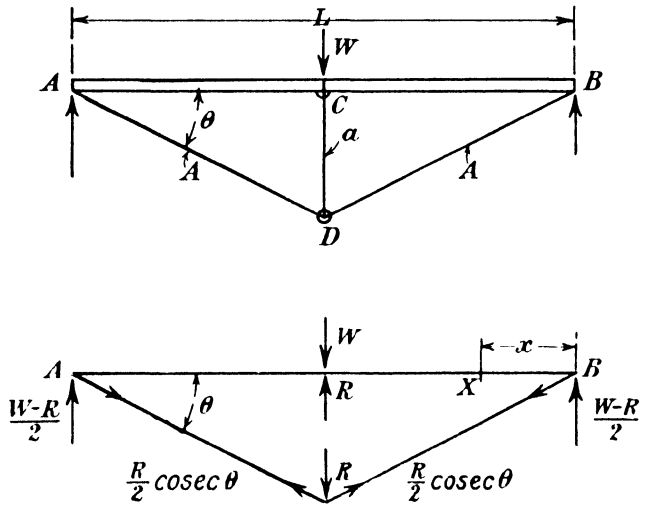

FIG. 6.9.

pinned together at C the structure would be a just-stiff frame and the loads in all the bars would be simple tensions or compressions. The continuity at C, however, introduces a redundancy and the member AB is subjected to bending moments as well as axial loads. This bending must be taken into account in the analysis and differentiates the treatment of this problem from the preceding ones.

It is convenient to take the compressive force in CD as the unknown to be determined and if this is denoted by R the axial forces in the bars are as given in Fig. 6.9. The shears at the ends of the beam are then each $\frac{W-R}{2}$ and at any point X in BC at a distance x from B the bending moment is

$$M_x=\left(\frac{W-R}{2}\right)x.$$

To determine R we have the relation $\frac{dU}{dR}=0$ where U is the total strain energy of the frame. If we neglect the strain energy due to the axial force in the beam we have for the beam

$$\left[\frac{dU}{dR}\right]_B=\frac{2}{E_BI}\int_0^{L/2}M_x\frac{dM_x}{dR}dx,$$

since it is symmetrical and symmetrically loaded.

I is the second moment of area of the cross-section of the beam and E_B its Young's modulus.

Since $$\frac{dM_x}{dR}=-\frac{x}{2}$$

$$\left[\frac{dU}{dR}\right]_B=-\frac{1}{2E_BI}\int_0^{L/2}(W-R)x^2dx$$

$$=-\frac{L^3}{48E_BI}(W-R).$$

For the member CD

$$\left[\frac{dU}{dR}\right]_S=\frac{P_0L'}{aE_S}\frac{dP_0}{dR}=\frac{R}{aE_S}\cdot\frac{L}{2}\tan\theta$$

or $$\left[\frac{dU}{dR}\right]_S=\frac{RL\tan\theta}{2aE_S}$$

where a and L′ are the cross-sectional area and length respectively of the strut CD and E_S its Young's modulus.

For each tie $$\left[\frac{dU}{dR}\right]_T=\frac{RL\,\mathrm{cosec}^2\theta\sec\theta}{8AE_T}.$$

So, for the two ties,

$$\left[\frac{dU}{dR}\right]_T=\frac{RL\,\mathrm{cosec}^2\theta\sec\theta}{4AE_T}.$$

Thus the total value of $\frac{dU}{dR}$ is

$$\frac{dU}{dR}=\frac{RL\,\mathrm{cosec}^2\theta\sec\theta}{4AE_T}+\frac{RL\tan\theta}{2aE_S}-\frac{WL^3}{48E_BI}+\frac{RL^3}{48E_BI}=0$$

which gives

$$R=\frac{\frac{WL^2}{48E_BI}}{\frac{\mathrm{cosec}^2\theta\sec\theta}{4AE_T}+\frac{\tan\theta}{2aE_S}+\frac{L^2}{48E_BI}}$$

Once this value has been determined the loads in all the bars can be found and the bending moment diagram for the beam can be plotted.

6.4. Strain energy analysis for frames with more than one redundant element.—When a frame has more than one redundant element the procedure is similar to that already explained but must be repeated for each redundancy. For example, if there are two redundant bars we denote the loads in them by R_1 and R_2 and determine the forces in the remainder of the bars in terms of R_1, R_2 and the external load system. Then U, the total strain energy, is a function of both these unknown forces and the external load and to evaluate R_1 and R_2 we have the two simultaneous equations

$$\frac{\partial U}{\partial R_1}=\sum\frac{P_0 L}{AE}\frac{\partial P_0}{\partial R_1}=\lambda_1$$

and

$$\frac{\partial U}{\partial R_2}=\sum\frac{P_0 L}{AE}\frac{\partial P_0}{\partial R_2}=\lambda_2$$

where λ_1 and λ_2 are the initial lack of fit in the two redundant bars.

As an illustration of the method of analysis the calculations for the airship fin rib having three redundant members shown in Fig. 6.10 are given in detail. The loading is quite arbitrary and the cross-sectional areas tabulated are those arrived at by a direct design method which will be explained later. These values have been chosen to serve as a check on the accuracy of that method. The calculation is arranged in tabular form as before. In the first four columns of the table are entered the reference to the bar, its length, cross-sectional area and value of Young's modulus respectively. It will be noticed that E is not the same throughout, some of the bars being of steel and the remainder of duralumin.

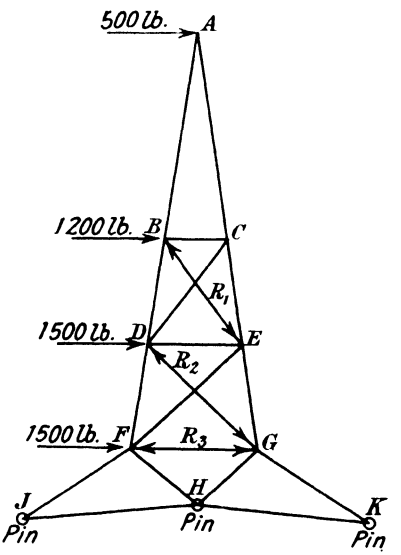

FIG. 6.10.

The forces in all bars are determined by resolution at the joints in terms of the external loading and the forces in the three redundant members which are taken to be R_1, R_2 and R_3 in BE, DG and FG respectively.

The force in any member can thus be expressed in the form

$$P_0=P+\alpha R_1+\beta R_2+\gamma R_3$$

where P is the force due to the external load and α, β and γ are numerical coefficients. The values of P, α, β and γ are entered for each member in the sub-columns of column 5.

TABLE 6.6.

1	2	3	4	5				6				7				8			
Member	L	A	E	P_0				$\frac{P_0L}{AE}\cdot\alpha\times10^6$				$\frac{P_0L}{AE}\cdot\beta\times10^6$				$\frac{P_0L}{AE}\cdot\gamma\times10^6$			
	Ins.	Sq. ins.	$\div10^6$	Lb.	R_1	R_2	R_3	Lb.	R_1	R_2	R_3	Lb.	R_1	R_2	R_3	Lb.	R_1	R_2	R_3
AB	118	·23	10·5	2,269	—	—	—	—	—	—	—	—	—	—	—	—	—	—	—
BD	64	·25	10·5	2,269	0·892	—	—	48.260	19·36	—	—	—	—	—	—	—	—	—	—
DF	73	·44	10·5	4,182	—	0·838	—	—	—	—	—	55,350	—	11·08	—	—	—	—	—
FJ	64	·72	10·5	8,030	—	−0·327	−0·712	—	—	—	—	22,200	—	·904	1·97	−48,400	—	1·97	4·29
AC	118	·23	10·5	−2,269	—	—	—	—	—	—	—	—	—	—	—	—	—	—	—
CE	64	·49	10·5	−4,182	0·892	—	—	− 46,350	9·88	—	—	—	—	—	—	—	—	—	—
EG	73	·92	10·5	−7,140	—	0·838	—	—	—	—	—	− 45,150	—	5·30	—	—	—	—	—
GK	64	·83	10·5	−5,815	—	−0·327	−0·712	—	—	—	—	13,940	—	·784	1·706	30,450	—	1·71	3·72
BC	26	·27	10·5	−1,200	0·559	—	—	− 6,132	2·85	—	—	—	—	—	—	—	—	—	—
DE	40·1	·51	10·5	−2,278	0·362	0·645	—	− 6,080	·98	1·744	—	− 10,980	1·745	3·11	—	—	—	—	—
FG	56·2	·50	10·5	—	—	—	−1·0	—	—	—	—	—	—	—	—	—	—	—	10·70
BE	71·7	·003	30	—	−1·0	—	—	—	797·0	—	—	—	—	—	—	—	—	—	—
CD	71·7	·024	30	2.146	−1·0	—	—	−213,600	99·6	—	—	—	—	—	—	—	—	—	—
DG	87·1	·003	30	—	—	−1·0	—	—	—	—	—	—	—	967	—	—	—	—	—
EF	87·1	·041	30	3.526	—	−1·0	—	—	—	—	—	−249,000	—	70·8	—	—	—	—	—
FH	39	·57	10·5	3,910	—	0·258	0·561	—	—	—	—	6,580	—	·43	·944	14,260	—	·942	2·046
HG	39	·56	10·5	−5,660	—	0·258	0·561	—	—	—	—	− 9,700	—	·44	·962	−21,020	—	·958	2·083

Now the equations to be formed are

$$\frac{\partial U}{\partial R_1}=\sum\frac{P_0L}{AE}\frac{\partial P_0}{\partial R_1}=\sum\frac{P_0L}{AE}\alpha=0,$$

$$\frac{\partial U}{\partial R_2}=\sum\frac{P_0L}{AE}\frac{\partial P_0}{\partial R_2}=\sum\frac{P_0L}{AE}\beta=0$$

and

$$\frac{\partial U}{\partial R_3}=\sum\frac{P_0L}{AE}\frac{\partial P_0}{\partial R_3}=\sum\frac{P_0L}{AE}\gamma=0.$$

In column 6, therefore, we enter the values of $\frac{P_0L}{AE}\alpha$ obtained by multiplying the term $\frac{P_0L}{AE}$ for each member by the coefficient of R_1 in P_0, *e.g.* for member BD by the value ·892.

Similarly, columns 7 and 8 are completed by multiplying the same terms $\frac{P_0L}{AE}$ by the coefficients of R_2 and R_3 respectively.

Columns 6, 7 and 8 are then severally summed to obtain $\sum\frac{P_0L}{AE}\alpha$, etc., and this results in the three equations :

$$\left.\begin{aligned}-223{,}900+930R_1+1{\cdot}75R_2 &=0\\ -261{,}160+1{\cdot}75R_1+1060R_2+5{\cdot}6R_3 &=0\\ -24{,}700+5{\cdot}61R_2+22{\cdot}8R_3 &=0\end{aligned}\right\}$$

The solution of these equations gives

$$R_1=R_2=240\text{ lb.}$$
$$R_3=1{,}030\text{ ,,}$$

6.5. Stresses due to changes in temperature. If a structure made of one material throughout, whether it be just stiff or redundant, experiences a uniform change of temperature, every bar is shortened or lengthened in the same proportion and no stresses are induced. The structure is geometrically similar to its original configuration but slightly smaller or larger.

If however a structure is made of more than one material which have different coefficients of expansion the effect of a temperature change depends upon whether the structure is just stiff or redundant. In the former case there will be no stresses induced since a just-stiff frame cannot be self-strained but there will be a slight change in the geometry of the structure. This, of course, is no more important than the small changes in configuration due to the unequal stressing of the component members when the structure is loaded but if the structure is redundant this tendency to distortion may induce stresses of considerable magnitude.

Suppose Fig. 6.11 (*a*) represents a rectangular frame in which all the members except AC are made of the same material having a coefficient of expansion α. AC is made of a different material, the coefficient of expansion being β.

If AC is removed the remaining bars form a just-stiff frame and if this frame has its temperature raised by $t°$ each member will be increased in length in the ratio $1+\alpha t : 1$. Thus the new lengths A'B', A'D', D'C', C'B' and D'B' shown at (*b*) will be $1+\alpha t$ times the lengths AB, etc., of those in (*a*) and the figure A'D'C'B' will be geometrically similar to ADCB.

Suppose now that the bar AC, of original length L, which was removed is heated to the same temperature as the remainder of the structure. Its new length will be $L(1+\beta t)$ and not $L(1+\alpha t)$ which would be necessary if it were to fit exactly into position in the heated just-stiff structure. It is in fact short of the correct length by an amount $\delta=L(\alpha-\beta)t$. If it is forced into position the stresses in the structure will be identical with those which would exist if the temperature of the original redundant frame were raised through $t°$.

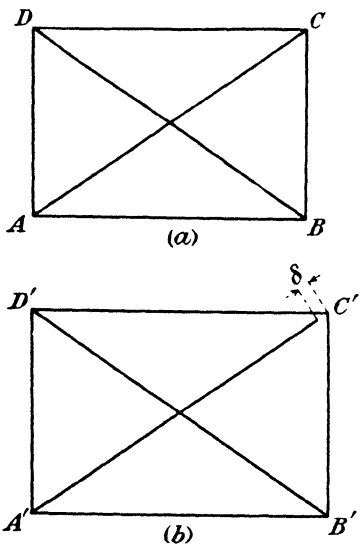

FIG. 6.11.

To calculate these stresses the procedure is exactly as for a redundant frame in which the redundant bar is initially too short. The tensile load in AC after heating is denoted by R : the forces in all bars of the frame are found in terms of R and then, if U is the strain energy, the value of R is found from the relation

$$\frac{dU}{dR}=L(\alpha-\beta)t.$$

Temperature stresses are induced not only if the structure is redundant by reason of its having more than the essential number of bars but also if the redundancy lies in the number of reactive forces. For example, if a just-stiff roof truss is supported on a pin at one end and on rollers at the other over a span L, a rise of temperature $t°$ will cause the free end to move over the rollers a distance $L\alpha t°$. If both ends are pinned, however, this movement cannot take place and forces which stress the truss are exerted by the pins.

To calculate these forces one end of the truss may be considered free and to move a distance $L\alpha t$. A load P is now supposed to act along the line joining the pins, this load being of such magnitude as to restore the freed support to its original position. P will then be the reactive force between the pin and the truss when movement due to the temperature rise is completely restricted. If U is the strain energy of the frame in terms of P we have, by the first theorem of Castigliano,

$$\text{movement of P in its own line of action}=\frac{dU}{dP}=L\alpha t$$

which enables P to be determined.

This question is of considerable importance in connection with metal arch ribs whose ends have to be fixed in position, and will be dealt with when considering the stresses in such structures.

6.6. Distribution methods of stress analysis applied to pin-jointed frames.—It will be seen that the methods of determining the forces in the members of a redundant structure outlined above involve the solution of as many simultaneous equations as there are redundancies. While the solution of simultaneous equations presents no difficulty mathematically the labour involved increases rapidly with the number of equations. Redundant structures requiring the solution of as many as fourteen equations have been analysed by strain energy methods but the resources of most calculating offices would be strained by such a task. When dealing with highly redundant structures, therefore, it is almost imperative to use other methods.

A process of successive approximation for determining the stresses in rigidly jointed frames which are highly redundant was described by Professor Hardy Cross in 1930 * and since then considerable attention has been given to such methods. Hardy Cross's original work will be discussed in a later section (paragraph 9.5), but it will be well here to outline an extension of it and another method, analogous to it, due to Professor Southwell, which are applicable to pin-jointed frames.

The first step taken in applying the strain energy method was to remove all the redundant bars and to determine the forces in the members of the resulting simple frame due to the external load system. The redundant bars were then re-inserted in the loaded frame and from energy considerations the forces arising in those bars were determined. The Hardy Cross method, on the other hand, leaves all the bars in place but it is assumed that before any external load is applied all the joints are held fixed ; that is to say, in a pin-jointed structure all the pins are held by external constraints so that they cannot move. The external loads are then applied to the joints and, since all the pins are fixed, no load can be transmitted to the members. One joint is now released by removing the constraint which fixed its pin in position. The external load applied to this joint then strains the members attached to it, the joint moves and easily calculable forces are induced in these members. The joint is now supposed to be fixed in its new equilibrium position and an adjacent joint is released. The out-of-balance forces acting on this second joint are the external loads applied to it and the force in the member connected to the first joint which was induced by the movement of the latter. The second joint moving into its equilibrium position induces, as a result, forces in the members connected to it. This procedure is repeated until all the joints have been released and fixed again sufficiently often to ensure that the modification in the forces brought about by further releases is small enough to be neglected. It will be seen that the method is one of successive approximation but it is not, in the ordinary sense of the term, an approxi-

* "Analysis of Continuous Frames by Distributing Fixed End Moments." H. Cross. Am. Soc. Civ. Eng., Proc. 1930. 56 (5), 919–28.

mate method since by repeating the process sufficiently often any desired degree of accuracy can be obtained.

The underlying principle and the detailed procedure will be most easily appreciated from the study of a worked example but before giving this example it will be useful to develop in general terms certain expressions which are required in the analysis.

It will be seen from the outline already given that the method requires a knowledge of the forces in such a group of members as is shown in Fig. 6.12, due to horizontal and vertical loads H and V applied at A. If under the action of these loads the joint A suffers horizontal and vertical displacements α_A and β_A then, since the other

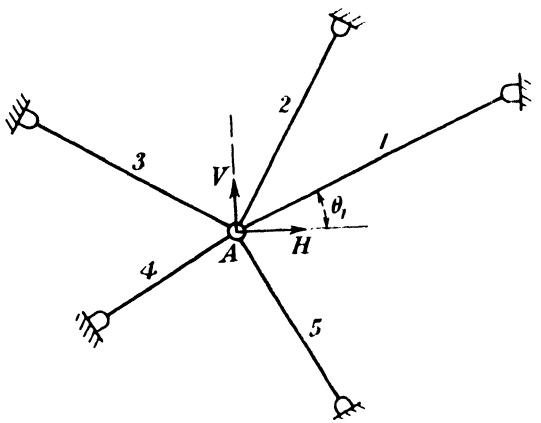

FIG. 6.12.

ends of the members are prevented from moving, the tension set up in member 1 will be, with the sign convention and notation used in earlier paragraphs,

$$F_1 = -\frac{EA_1}{L_1}(\alpha_A \cos\theta_1 + \beta_A \sin\theta_1) \quad . \quad . \quad . \quad . \quad . \quad . \quad (1)$$

and from a consideration of the equilibrium of joint A it follows that

$$H = \sum \frac{EA_1}{L_1}(\alpha_A \cos\theta_1 + \beta_A \sin\theta_1)\cos\theta_1 \quad . \quad . \quad . \quad . \quad (2)$$

and

$$V = \sum \frac{EA_1}{L_1}(\alpha_A \cos\theta_1 + \beta_A \sin\theta_1)\sin\theta_1 \quad . \quad . \quad . \quad . \quad (3)$$

the summation in each case extending to all the members.

By solving these two simultaneous equations the unknowns α_A and β_A may be evaluated in terms of H and V and equation (1) then enables the force in each member connected to A to be determined.

As an illustration of the procedure the stress analysis of the frame shown in Fig. 6.7, already treated by strain energy methods, will be given. The first step is to find, from equations (2), (3) and (1), or by other methods, the forces developed in members AB, AC and AD when the joints B, C and D are held fixed and loads are applied to the free

joint A ; also the forces developed in members DA, DB and DC when the joints A, B and C are held fixed and loads are applied to the free joint D. These forces are given in Table 6.7.

TABLE 6.7.

FORCES IN MEMBERS MEETING AT A JOINT.

	Horizontal load H at joint A	Vertical load V at joint A		Horizontal load H at joint D	Vertical load V at joint D
F_{AB}	−0·978 H	−0·206 V	F_{DC}	−0·978 H	+0·206 V
F_{AC}	−0·310 H	+0·357 V	F_{DB}	−0·310 H	−0·357 V
F_{AD}	−0·220 H	+0·588 V	F_{DA}	−0·220 H	−0·588 V

The analysis of the stresses in the complete framework may now be undertaken. It is advisable to adopt a tabular form for the calculations and a convenient arrangement is shown in Table 6.8, where the three upper columns refer to the three members meeting at the joint A and the three lower columns refer to those meeting at the joint D.

It is assumed initially that all joints are held fixed. The external vertical load+10 tons at D, is then applied. The joint D is now released, A still being fixed ; joints B and C are attached to a rigid abutment and therefore, in this particular example, are never released. Due to the external load acting at D, forces are developed in the members DA, DB and DC. Their magnitudes, read from the last column of Table 6.7, are entered in line *a'*, Table 6.8. The joint is now in equilibrium and to indicate this a full line is drawn below the entries so far made. It must not be forgotten that the member DA is attached to joint A and therefore the force—5·88 tons developed in it must be recorded also in the first of the upper columns, line *a*, where the forces in the members meeting at joint A are entered. Since joints B and C have not been released no forces have yet been developed in the members AC and AB and so in the second and third columns of line *a* the entries are zero. Joint D is now fixed in its new equilibrium position and joint A is released. Since there are no external loads at A the only force acting on the joint at its release is that due to the movement of D just recorded. Before A has moved into its equilibrium position, therefore, the unbalanced force acting on it is a vertical force of +5·88 tons and so the forces developed in the members AB, AC and AD as A moves are obtained by substituting this value of V in column 3 of Table 6.7. These forces are entered in line *b*, Table 6.8, and at the same time the force of +3·46 tons, developed in AD by this movement of joint A, is " carried over " to the other end of the member and entered in line *b'*. Joint A is now fixed in its new equilibrium position and joint D is once more released. This process of releasing and fixing joints is continued until the unbalanced force remaining at a joint is small enough to be neglected. In Table 6.8 the joints A and D have been released five and six times respectively and the unbalanced

TABLE 6.8.

FORCES (TONS) IN MEMBERS OF FRAMEWORK.

	AD	AC	AB
a	−5·88	0·00	0·00
b	+3·46	+2·10	−1·21
	−2·04	0·00	0·00
	+1·20	+0·73	−0·42
	−0·71	0·00	0·00
	+0·42	+0·25	−0·14
	−0·24	0·00	0·00
	+0·14	+0·09	−0·05
	−0·08	0·00	0·00
	+0·05	+0·03	−0·02
	−0·03	0·00	0·00

	DA	DB	DC
a'	−5·88	−3·57	+2·06
b'	+3·46	0·00	0·00
	−2·04	−1·23	+0·71
	+1·20	0·00	0·00
	−0·71	−0·43	+0·25
	+0·42	0·00	0·00
	−0·24	−0·15	+0·09
	+0·14	0·00	0·00
	−0·08	−0·05	+0·03
	+0·05	0·00	0·00
	−0·03	−0·02	+0·01

force is ·03 tons. The total forces in the members are the totals of the entries in the various columns and are :—

AD = −3·71 tons.
AB = −1·84 ,,
AC = +3·20 ,,
DB = −5·45 ,,
DC = +3·15 ,,

These values should be compared with those obtained by strain energy methods given on p. 91.

The forces in the members in this simple example were estimated to within ·01 tons of their true values after only eleven releases. The same degree of accuracy could not have been obtained so easily if the frame had been more complex as will be appreciated if the deformations suffered by the structure are considered. The percentage errors in the forces at any stage in the process are, in some degree, a measure of the difference between the shape of the frame at that stage and its final deflected form. If the frame can be so deformed before the balancing process at the joints is begun that its shape approximates to the final form fewer cycles will be necessary to obtain any desired degree of accuracy and, if the deformation is so chosen that the loads in the members produced by it are easily calculated, a considerable saving of labour will result. Fig. 6.13 illustrates one method of producing the deformation required. A two bay cantilever frame is shown

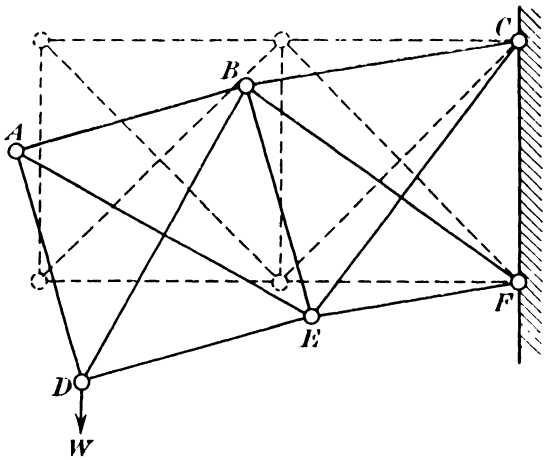

FIG. 6.13.

by broken lines in its unloaded position. When the external loads are applied, the joints of the frame are allowed to move, as shown by the full line diagram, but they are so constrained that those in the first bay, A, B, D and E, do not change their relative positions. Forces are therefore developed in the members of the second bay only and, an important point, their magnitudes are easily calculated. The joints are now held in these deformed positions and the process of releasing them one at a time, as described in the worked example, is begun. The equations for the determination of the forces developed in the members by this type of deformation are in no way complicated but for a complete discussion of the method reference should be made to a paper published by the Aeronautical Research Committee.*

6.7. Southwell's relaxation method.—A more elegant method than that described in the previous paragraph, due to Professor R. V.

* "A Distribution Method of Stress Analysis." J. F. Baker and A. J. Ockleston. R and M. No. 1667. H.M. Stationery Office.

Southwell, avoids all simultaneous equations and is concerned primarily with the determination of the deformations of the structure.

It follows from paragraphs 2.5 and 4.4 that the tension coefficient of any member PQ is

$$t_{PQ}=\frac{EA}{L^3}\{(x_Q-x_P)(\alpha_Q-\alpha_P)+(y_Q-y_P)(\beta_Q-\beta_P)+(z_Q-z_P)(\gamma_Q-\gamma_P)\} \quad . \quad (1)$$

where x_P, y_P, z_P and x_Q, y_Q, z_Q are the co-ordinates of P and Q in their initial positions and α_P, β_P, γ_P and α_Q, β_Q, γ_Q are the components of their displacements due to strain.

As in the previous method we shall be concerned with the displacements at one end of the member while the other end is held fixed in space though free to rotate on its pin.

If the end Q is held fixed the tension coefficient of the member may be written

$$t_{PQ}=-\frac{EA}{L^3}\{(x_Q-x_P)\alpha_P+(y_Q-y_P)\beta_P+(z_Q-z_P)\gamma_P\} \quad . \quad . \quad . \quad . \quad (2)$$

As a result of the tension in PQ the joint P will be subjected to a force having components :

$$\left.\begin{aligned} X_P&=t_{PQ}(x_Q-x_P)\\ Y_P&=t_{PQ}(y_Q-y_P)\\ Z_P&=t_{PQ}(z_Q-z_P) \end{aligned}\right\} \quad . \quad . \quad . \quad . \quad . \quad . \quad . \quad . \quad . \quad (3)$$

and the fixed joint Q will be subjected to forces equal and opposite to these.

If the joint P has a number of members connected to it, their remote ends being fixed as is Q, then when P is given a displacement α_P in the x-direction and no displacements in the directions of the other axes, the components of the total force developed on the joint P are :—

in the x-direction

$$\Sigma t_{PQ}(x_Q-x_P)=-\Sigma\frac{EA}{L^3}(x_Q-x_P)^2\alpha_P,$$

in the y-direction

$$\Sigma t_{PQ}(y_Q-y_P)=-\Sigma\frac{EA}{L^3}(x_Q-x_P)(y_Q-y_P)\alpha_P, \quad . \quad . \quad . \quad (4)$$

in the z-direction

$$\Sigma t_{PQ}(z_Q-z_P)=-\Sigma\frac{EA}{L^3}(x_Q-x_P)(z_Q-z_P)\alpha_P,$$

the summation including every member connected to P.

The forces developed by displacements β_P and γ_P may be found in the same way and no other preparatory calculations are needed.

The analysis of the stresses in a framework is made by giving each joint in turn that displacement in the direction of one of the co-ordinate axes which has most effect in reducing the resultant force on the joint. This process is continued until the resultant forces on the joints are small enough to be neglected. The total displacements given to the joints are then known and the forces in the members can be found

from equation (1). The method will be illustrated by applying it to the problem dealt with in the preceding paragraph, the framework concerned being shown in Fig. 6.7.

The first step is to evaluate the constant $\frac{EA}{L^3}$ for each member, the units of length and force adopted being inches and tons respectively and E being taken as 13,000 tons/sq. in. These constants are 3·250 for members AB and CD, 1·625 for AD and 0·312 for DB and AC.

The forces on the joints due to unit displacements must next be found. When joint D is given a unit displacement in the direction of the x-axis and no displacement in the direction of the y-axis, *i.e.* $\alpha_D=1$ and $\beta_D=0$, the forces exerted on the joint D by the member DC are, from equation (3),

$$X_D=t_{DC}(x_C-x_D)=-975$$

and

$$Y_D=t_{DC}(y_C-y_D)=+564.$$

Due to the same displacement, forces are exerted by the other members meeting at the joint and it will be found from equation (4) that the total forces on D are, in the x-direction −1,068 and in the y-direction +402. This information is set out in line 1 (*a*), Table 6.9, where it is also stated that X_A and Y_A, the forces on the joint A due to this displacement, $\alpha_D=1$, are zero.

In the same way the forces on the joints are calculated due to a unit displacement in the y-direction and no displacement in the x-direction, *i.e.* $\beta_D=1$ and $\alpha_D=0$. These forces are set out in line 2 (*a*), Table 6.9, and it will be seen that there is a force of +650 in the y-direction at joint A. This follows from equation (3) since, due to the displacements under consideration,

$$Y_A=t_{AD}(y_D-y_A)=\frac{EA}{L^3}\{(y_D-y_A)\beta_D\}(y_D-y_A)$$
$$=1{\cdot}625\{-20\times-20\}=+650.$$

It will be found a convenience in the later work if the largest force at a joint due to each displacement is reduced to 1,000. This has been done in Table 6.9 ; line 1 (*b*), for instance, being obtained from line 1 (*a*) by dividing throughout by 1·068.

The deformation of the framework as a whole can now be considered. All the joints in the framework are initially fixed in space and the external load is applied. Joint D will then be subjected to a force $Y_D=+10$. The joint must next be given a displacement, all other joints being held fixed, which will reduce this force as much as possible. A glance at Table 6.9 shows that a displacement of joint D in the y-direction is the most efficient for the purpose and that if its magnitude is one hundredth of the displacement recorded in line 2 (*b*), Table 6.9, the force on the joint in the y-direction will be reduced to zero.

Table 6.10 shows a convenient way of setting out these facts. The first line, p, in the table shows the conditions after the external load has been applied but before any joints have been displaced. Line q shows the forces developed at the joints A and D, which in this particular framework are the only ones to be given displacements, by a movement

TABLE 6.9.

FORCES (TONS) AT JOINTS DUE TO DISPLACEMENTS.

	Displacement	X_D	X_A	Y_D	Y_A
1 (*a*)	$\alpha_D=1$	−1,068	0	+ 402	0
1 (*b*)	$\alpha_D=0{\cdot}937$	−1,000	0	+ 377	0
2 (*a*)	$\beta_D=1$	+ 402	0	−1,256	+ 650
2 (*b*)	$\beta_D=0{\cdot}797$	+ 320	0	−1,000	+ 518
3 (*a*)	$\alpha_A=1$	0	−1,068	0	− 402
3 (*b*)	$\alpha_A=0{\cdot}937$	0	−1,000	0	− 377
4 (*a*)	$\beta_A=1$	0	− 402	+ 650	−1,256
4 (*b*)	$\beta_A=0{\cdot}797$	0	− 320	+ 518	−1,000

of joint D in the y-direction of magnitude 0·00797. The type and magnitude of this displacement are recorded in the first two columns of Table 6.10, the entry " 2 (*b*) " in the first column referring to line 2 (*b*) of Table 6.9. The forces at the joints after the displacement has been given to D are found by adding lines p and q; they are entered in line r. While the force Y_D has been reduced to zero it will be seen that forces X_D and Y_A, of magnitudes +3·20 and +5·18 respectively, have been induced by the displacement. Of these the latter is the greater and it will be seen from Table 6.9 that it can be made to disappear by giving joint A a displacement 0·00518 times that recorded in line 4 (*b*), Table 6.9. The forces at the joints induced by this displacement are entered in line s, Table 6.10, and those remaining after this second displacement has been completed, in line t. This process is repeated until the displacements become small enough to be neglected. In Table 6.10 a total of eighteen displacements have been made. The forces in the bars have now to be calculated. This is done by determining the total displacements given to the joints. It can be seen from columns 1 and 2, Table 6.10, that the total displacement in the x-direction suffered by joint D is

$$\alpha_D=0{\cdot}937(0{\cdot}00320+0{\cdot}00124+0{\cdot}00075+0{\cdot}00020)$$
$$=0{\cdot}937\times0{\cdot}00539.$$

The other displacements are

$$\beta_D=0{\cdot}797\times0{\cdot}01710$$
$$\alpha_A=-0{\cdot}937\times0{\cdot}00311$$
$$\beta_A=0{\cdot}797\times0{\cdot}01003$$

These displacements being known the tension coefficients can be calculated from equation (1), thus

$$t_{DA}=\frac{EA}{L^3}(y_A-y_D)(\beta_A-\beta_D)$$
$$=1{\cdot}625\times20\times0{\cdot}797(0{\cdot}01003-0{\cdot}01710)=-0{\cdot}183$$

and the force in member DA$=t_{DA}\times20=-3{\cdot}66$ tons.

TABLE 6.10.

Operation	Multiplier	X_D	X_A	Y_D	Y_A	
		0·00	0·00	+10·00	0·00	*p*
2 (*b*)	+0·01000	+3·20	0·00	−10·00	+5·18	*q*
		+3·20	0·00	0·00	+5·18	*r*
4 (*b*)	+0·00518	0·00	−1·65	+2·68	−5·18	*s*
		+3·20	−1·65	+2·68	0·00	*t*
1 (*b*)	+0·00320	−3·20	0·00	+1·20	0·00	
		0·00	−1·65	+3·88	0·00	
2 (*b*)	+0·00388	+1·24	0·00	−3·88	+2·01	
		+1·24	−1·65	0·00	+2·01	
4 (*b*)	+0·00201	0·00	−0·64	+1·04	−2·01	
		+1·24	−2·29	+1·04	0·00	
3 (*b*)	−0·00229	0·00	+2·29	0·00	+0·86	
		+1·24	0·00	+1·04	+0·86	
1 (*b*)	+0·00124	−1·24	0·00	+0·47	0·00	
		0·00	0·00	+1·51	+0·86	
2 (*b*)	+0·00151	+0·48	0·00	−1·51	+0·78	
		+0·48	0·00	0·00	+1·64	
4 (*b*)	+0·00164	0·00	−0·52	+0·85	−1·64	
		+0·48	−0·52	+0·85	0·00	
2 (*b*)	+0·00085	+0·27	0·00	−0·85	+0·44	
		+0·75	−0·52	0·00	+0·44	
1 (*b*)	+0·00075	−0·75	0·00	+0·28	0·00	
		0·00	−0·52	+0·28	+0·44	
3 (*b*)	−0·00052	0·00	+0·52	0·00	+0·20	
		0·00	0·00	+0·28	+0·64	
4 (*b*)	+0·00064	0·00	−0·20	+0·33	−0·64	
		0·00	−0·20	+0·61	0·00	
2 (*b*)	+0·00061	+0·20	0·00	−0·61	+0·32	
		+0·20	−0·20	0·00	+0·32	
4 (*b*)	+0·00032	0·00	−0·10	+0·17	−0·32	
		+0·20	−0·30	+0·17	0·00	
3 (*b*)	−0·00030	0·00	+0·30	0·00	+0·11	
		+0·20	0·00	+0·17	+0·11	
1 (*b*)	+0·00020	−0·20	0·00	+0·08	0·00	
		0·00	0·00	+0·25	+0·11	
2 (*b*)	+0·00025	+0·08	0·00	−0·25	+0·13	
		+0·08	0·00	0·00	+0·24	
4 (*b*)	+0·00024	0·00	+0·08	+0·17	−0·24	
		+0·08	+0·08	+0·17	0·00	

The forces in the other members are

AB = −1·92 tons.
AC = +3·14 ,,
DB = −5·36 ,,
DC = +3·17 ,,

It will be seen that these values differ appreciably from those obtained for the same framework in paragraphs 6.3 and 6.6. The reason for this is that the work in Table 6.10 has not been carried far enough.

In this method, as in the one described in paragraph 6.6, it will be found economical to deform the structure by " block " displacements and rotations before the process of displacing the joints one at a time is begun. A full account of the procedure is given in Professor Southwell's paper.*

6.8. Choice of method of stress analysis.—It is impossible to formulate general rules which will govern the method to be used in any particular case.

It is clear that less labour was involved in determining the forces in the members of the framework shown in Fig. 6.7 by strain energy methods than by either of the successive approximation methods and it is probably safe to say that when analysing the stresses in redundant structures having hinged ends the strain energy method will be found most economical in those cases where the number of redundancies does not exceed six.

There is little to choose between the two successive approximation methods except that in the second all simultaneous equations are avoided. It should be remembered, however, that in many cases it may be simpler to solve groups of two or three simultaneous equations as required by the first method than to obtain the same results by successive approximation.

6.9. Design of redundant frames.—Since the stress analysis of a redundant frame necessitates a knowledge of the cross-sectional areas of all the members it is evident that ordinary methods of design are not applicable to such a structure. The usual method is to guess sizes for all members, analyse the frame by means of strain-energy theorems, and if the stresses do not appear reasonable to make a second approximation to the sizes and go through the operation again. By this process of trial and error a suitable design can be achieved, but the procedure is laborious, especially if there are a number of redundancies, since each trial involves the solution of a number of simultaneous equations.

By a modification of the equations obtained from the second theorem of Castigliano, however, a method has been evolved which enables a much more direct approach to the problem to be made.† The results obtained by this method are not always of direct practical use and sizes obtained may have to be modified by conditions other than the stresses to be met, but it does give a structure which fulfils the conditions imposed by theoretical considerations and any necessary modifications are easily made.

* " Stress Calculations in Frameworks by the Method of Systematic Relaxation of Constraints," I and II. R. V. Southwell. Proc. Royal Soc., Series A, No. 872, Vol. 151.

† " On a Method for the Direct Design of Framed Structures having Redundant Bracing," A. J. S. Pippard, Reports and Memoranda, No. 793. Aeronautical Research Committee.

Suppose that the pin-jointed frame to be designed carries a number of external loads W_1, W_2 . . . W_N, and that it contains a number of redundant members the forces in which are R_1, R_2 . . . R_M. By drawing stress diagrams the loads in all members of the frame can be found and we can write

$$P_0 = aW_1 + bW_2 + \ldots + nW_N + \alpha R_1 + \beta R_2 \ldots + \mu R_M,$$

where P_0 is the load in any member and a, b . . . n, α, β . . . μ are numerical coefficients depending on the geometry of the frame.

The strain energy of the whole structure is

$$U = \tfrac{1}{2}\sum \frac{P_0^2 L}{AE}$$

and by the second theorem of Castigliano we can write

$$\frac{\partial U}{\partial R_1} = \frac{\partial U}{\partial R_2} = \ldots = \frac{\partial U}{\partial R_M} = 0.$$

Now

$$\frac{\partial U}{\partial R_1} = \sum \frac{\alpha P_0 L}{AE}$$

and P_0/A is the stress in the member $= f$.

Hence

$$\left.\begin{aligned} \frac{\partial U}{\partial R_1} &= \sum \frac{fL\alpha}{E} = 0 \\ \frac{\partial U}{\partial R_2} &= \sum \frac{fL\beta}{E} = 0 \\ &\ldots\ldots \\ \frac{\partial U}{\partial R_M} &= \sum \frac{fL\mu}{E} = 0. \end{aligned}\right\} \quad \ldots\ldots\ldots \quad (1)$$

If, as is common, E is the same throughout, these equations become

$$\Sigma fL\alpha = \Sigma fL\beta = \ldots = \Sigma fL\mu = 0 \quad \ldots\ldots \quad (2)$$

The procedure for design is as follows :—

Replace all redundant members in the structure by unknown forces R_1, R_2, etc., acting along the axes of these members. Since each member is connected to two joints of the frame, the force replacing it must be applied at both joints. The structure is now reduced to a just-stiff framework acted upon by R_1, R_2, etc., and W_1, W_2, etc. A stress diagram is drawn for the external load system, and this gives the sum of the terms

$$aW_1 + bW_2 + \ldots + nW_N$$

in the expression for P_0.

A stress diagram for the two equal forces R_1, acting on the structure, gives the values of α for all members of the frame, and similar diagrams for R_2 . . . R_M give values of β . . . μ. Since the values of L and E are known, the terms $L\alpha/E$, $L\beta/E$ . . . $L\mu/E$ are readily calculated for each member of the frame. The equations corresponding to (1) or (2) are now formed. There are the same number of equations as there are

redundant members, and each equation contains terms involving the stress in one of the redundant members and the stresses in those members of the truss affected by that particular redundancy: no other terms occur. Thus the equations connect the stresses in the various members of the structure and the next step is to select such stresses as will satisfy the equations.

It will be found convenient to begin with the equation which contains the smallest number of terms. The maximum permissible stress can be substituted for the majority of terms occurring, the remainder—which often need be no more than one—being adjusted to satisfy the equation. This is a very easy matter, since there are any number of possible variations, all correct, and it is not a question of determining a unique solution.

Certain stresses which are fixed in the first equation will occur in other equations and these values should be substituted. The remaining equations are then dealt with in the same way and all stresses determined.

The stresses thus fixed should be tabulated and among them will be the stresses in the redundant members. The next step is to fix the *load* in each redundancy by assigning suitable areas to these members. A study of the table of internal loads helps this decision, since it shows the effect of the load in the redundant member upon the loads in the other bars. Having fixed the sizes of the redundant members and so the loads in them, the loads in all the other members of the frame can be written down and by dividing these loads by the stresses already fixed the cross-sectional areas of all members are determined.

It should be noticed that this method eliminates the solution of simultaneous equations and further, that the stresses are controlled by the designer during the process of calculation. As an example the frame shown in Fig. 6.10 will be considered.*

The frame is fixed at J, H and K and assuming all diagonal braces to be operative there are three redundancies. These will be taken to be FG, BE and DG.

The force in FG will be denoted by $-R_3$, that in BE by $-R_1$, and in DG by $-R_2$.

The first step is to find the internal forces in all members of the frame in terms of the external load system and R_1, R_2 and R_3. This can be done by a stress diagram or by resolution at the joints. The values obtained by the latter method are given in Table 6.11. These loads and the length of each member having been tabulated, columns 4, 5 and 6 are obtained as follows :—

Since α, β and γ are the coefficients of R_1, R_2 and R_3 respectively, their values are known from column 3 and multiplying by the term L/E we get the numbers in the columns 4, 5 and 6. The structure is supposed to be made of duralumin, braced diagonally by steel, having values of E of $10{\cdot}5\times10^6$ lb. per square inch and 30×10^6 lb. per square inch respectively. Consider first column 4: this enables us to form

* This example is taken from "Report of Airship Stressing Panel," R. & M. 800, Appendix IX. Aeronautical Research Committee.

the equation $\sum \frac{fL\alpha}{E}=0$ and if we denote the stress in any member AB by AB we obtain

$$5{\cdot}43\,BD+5{\cdot}43\,CE+1{\cdot}38\,BC+1{\cdot}38\,DE-2{\cdot}39\,BE-2{\cdot}39\,CD=0, \quad . \quad (3)$$

where BD, CE, etc., are the members of the truss appearing in column 4.

Similarly, from columns 5 and 6, we obtain the equations

$$5{\cdot}82\,DF-1{\cdot}99\,FJ+5{\cdot}82\,EG-1{\cdot}99\,GK+2{\cdot}46\,DE$$
$$-2{\cdot}90\,DG-2{\cdot}90\,EF+0{\cdot}96\,FH+0{\cdot}96\,HG=0 \quad . \quad . \quad . \quad . \quad . \quad (4)$$
$$-4{\cdot}34\,FJ-4{\cdot}34\,GK-5{\cdot}35\,FG+2{\cdot}08\,FH+2{\cdot}08\,HG=0 \quad . \quad . \quad (5)$$

Since equation (5) contains the smallest number of terms, we begin with that and select any stresses to satisfy it.

Assuming that the stress in duralumin is limited to 10,000 lb. per square inch and in steel to 80,000 lb. per square inch, we put

$$FH=-GK=8{,}000 \text{ lb. per square inch.}$$
$$FJ=10{,}000 \quad ,, \quad ,,$$
$$FG=-2{,}000 \quad ,, \quad ,,$$

which gives
$$HG=-8{,}970 \quad ,, \quad ,,$$

It should be noted that any other stresses which satisfy equation (5) would be equally correct, but we have stressed four of these members fairly equally which is reasonable.

The values above are entered in column 7, and we turn next to equation (3). None of the stresses appearing here have been fixed from (5), so we again select suitable values.

$$-BE=CD=80{,}000 \text{ lb. per square inch.}$$
$$BD=10{,}000 \quad ,, \quad ,,$$
$$CE=-8{,}000 \quad ,, \quad ,,$$
$$BC=DE=-3{,}928 \quad ,, \quad ,,$$

and these are also entered in column 7.

Five stresses appearing in equation (4) have now been fixed and substituting them, we obtain the equation

$$5{\cdot}82\,DF+5{\cdot}82\,EG-2{\cdot}90\,DG-2{\cdot}90\,EF=14{,}602.$$

Put
$$DF=10{,}000 \text{ lb. per square inch.}$$
$$-DG=EF=80{,}000 \quad ,, \quad ,,$$

and then
$$EG=-7{,}495 \quad ,, \quad ,,$$

Since members AB and AC are unaffected by the redundancies, they do not enter into the equations, so that the stresses in them can be made anything we please. They are therefore put at the maximum allowable stress,

i.e. $$AB=-AC=10{,}000 \text{ lb. per square inch.}$$

We now fix the absolute values of the loads in the redundant members, and in doing so we consider the effect these members have upon the loads in the other members.

In this case, we take $R_1=R_2=$ 250 lb.
and $R_3=1{,}000$ lb.
and enter in column 8.

We now write down the load in every member from column 3 and these loads divided by the stresses in column 7 give the required areas tabulated in column 9.

It should be emphasised that this is only one of an infinite number of solutions of this particular problem, but we have by a direct process produced a design which we know will have the stresses of column 7 when loaded as shown in Fig. 6.10 and this design has not involved the solution of any simultaneous equations.

TABLE 6.11.

Italics denote negative values.

1	2	3				4	5	6	7	8	9
Member	Length	LOAD				$\frac{L\alpha}{E}\times10^6$	$\frac{L\beta}{E}\times10^6$	$\frac{L\gamma}{E}\times10^6$	Stress	Load	Area
	Ins.	Lb.	R_1	R_2	R_3				Lb./ sq. in.	Lb.	Sq. ins.
AB	118	2,269	—	—	—	—	—	—	10,000	2,269	0·23
BD	64	2,269	0·892	—	—	5·43	—	—	10,000	2,492	0·25
DF	73	4,182	—	0·838	—	—	5·82	—	10,000	4,392	0·44
FJ	64	8,030	—	*0·327*	*0·712*	—	*1·99*	*4·34*	10,000	7,236	0·72
AC	118	*2,269*	—	—	—	—	—	—	*10,000*	*2,269*	0·23
CE	64	*4,182*	0·892	—	—	5·43	—	—	*8,000*	*3,959*	0·49
EG	73	*7,140*	—	0·838	—	—	5·82	—	*7,495*	*6,931*	0·92
GK	64	*5,815*	—	*0·327*	*0·712*	—	*1·99*	*4·34*	*8,000*	*6,609*	0·83
BC	26	*1,200*	0·559	—	—	1·38	—	—	*3,928*	*1,060*	0·27
DE	40·1	*2,278*	0·362	0·645	—	1·38	2·46	—	*3,928*	*2,020*	0·51
FG	56·2	—	—	—	*1·0*	—	—	*5·35*	*2,000*	*1,000*	0·50
BE	71·7	—	*1·0*	—	—	*2·39*	—	—	*80,000*	*250*	0·003
CD	71·7	2,146	*1·0*	—	—	*2·39*	—	—	80,000	1,896	0·024
DG	87·1	—	—	*1·0*	—	—	*2·90*	—	*80,000*	*250*	0·003
EF	87·1	3,526	—	*1·0*	—	—	*2·90*	—	80,000	3,276	0·041
FH	39	3,910	—	0·258	0·561	—	0·96	2·08	8,000	4,536	0·57
HG	39	*5,660*	—	0·258	0·561	—	0·96	2·08	*8,970*	*5,034*	0·56

This example was used in paragraph 6.4 as an illustration of the method of stress analysis for a structure having more than one redundant member. The areas assumed in that analysis were those found by the present method and given in Table 6.11 above. The values of R_1, R_2 and R_3 were evaluated by an application of the method of least work. This meant the solution of three simultaneous equations which gave $R_1=R_2=240$ lb. and $R_3=1{,}030$ lb. These figures should of course have agreed with the values assigned to R_1, R_2 and R_3 above: the small error is due to the fact that only slide rule accuracy was aimed at in the calculations.

6.10. Effect of curved bars in a framework.—In some cases certain members of a framework are curved and not straight and if the structure is redundant special treatment of these members is necessary.*

* "The Effect of Curved Members upon the Elastic Properties of a Framework," A. J. S. Pippard, Phil. Mag., Vol. I., January, 1926, p. 254.

Let A and B in Fig. 6.14 be two nodes of a framework connected by a circular arc of radius R and subtending an angle 2ϕ at the centre. If the frame is pin-jointed, any force transmitted between A and B must act along the line AB. Let P be such a force.

Then if Δ is the amount by which the distance AB is shortened under the action of P,

$$\Delta = \frac{dU}{dP} \quad . \quad . \quad . \quad . \quad . \quad . \quad . \quad . \quad . \quad (1)$$

where U is the strain-energy of the bar.

If I is the relevant second moment of area of the bar,
A is the cross-sectional area of the bar,
E is the modulus of elasticity of the material,
N is the modulus of rigidity of the material,

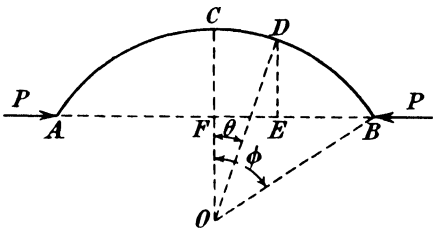

FIG. 6.14.

then at any point D on the arc where $\angle COD = \theta$ the resultant actions are :

an axial compression $= P \cos\theta$,
a radial shear $= P \sin\theta$,
a bending moment $= PR(\cos\theta - \cos\phi)$

and the total strain-energy of the bar is

$$U = \frac{P^2R}{EA}\int_0^{\phi} \cos^2\theta d\theta + \frac{P^2R^3}{EI}\int_0^{\phi} (\cos\theta - \cos\phi)^2 d\theta + \frac{P^2R}{AN}\int_0^{\phi} \sin^2\theta d\theta \quad . \quad (2)$$

where the first and second terms are the components due to axial load and bending respectively and the third term is an approximation to the unimportant component due to shear.

Differentiating and evaluating and giving N the value $\frac{2}{5}E$ we obtain

$$\Delta = \frac{PR}{AE}\left[\frac{7\phi}{2} - \frac{3\sin 2\phi}{4} + \frac{R^2}{k^2}\left(2\phi - \frac{3\sin 2\phi}{2} + \phi\cos 2\phi\right)\right] \quad . \quad . \quad (3)$$

where k is the radius of gyration of the cross-section.

If the curved bar were replaced by a straight member of the same cross-sectional dimensions, but with such a value of E that Δ remained the same, the elastic properties of the frame would be unaltered.

Let E′ be the modulus of elasticity of such a member. Then, under

the action of P its alteration in length would be $\frac{2PR \sin \phi}{AE'}$ and for this to be equal to Δ we must have

$$E' = E\left[\frac{2 \sin \phi}{\frac{7\phi}{2} - \frac{3 \sin 2\phi}{4} + \frac{R^2}{k^2}\left(2\phi - \frac{3 \sin 2\phi}{2} + \phi \cos 2\phi\right)}\right] \quad . \quad (4)$$

Any framework containing curved members can thus be simplified by replacing all such members by straight bars of the same cross-sections as the originals, but with modified values of E as given by equation (4). Such a simplified frame will be elastically equivalent to the original and the usual methods for calculating deflections and stresses can be employed.

The above formulas apply strictly only to circular arcs, but very little

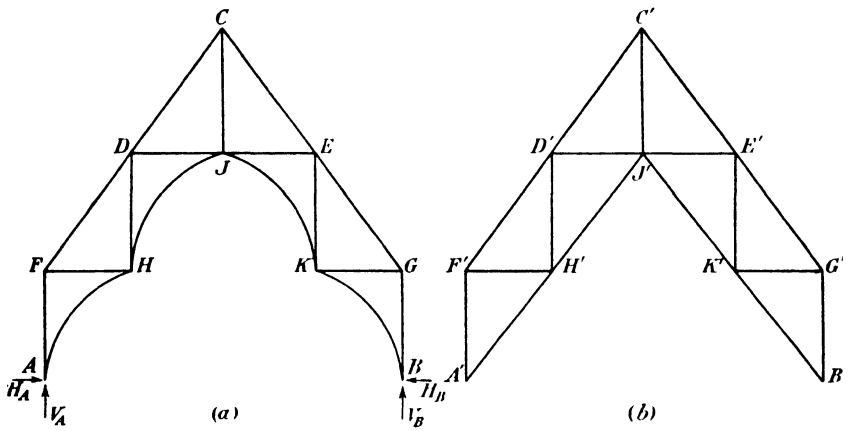

FIG. 6.15.

error is introduced if the arc is not circular provided the maximum bow is the same.

As an example we will consider the case shown in Fig. 6.15 (*a*) which represents a roof truss of the simple hammer-beam type supported at A and B on rigid walls. There are ten joints in the truss and seventeen members are required to make it just-stiff. This number is actually provided but since both the supports are formed by pins on rigid walls a redundant reaction is introduced. This may be conveniently taken as H_A. The loading, which is not shown, will consist of dead weights and wind forces.

To determine the value of H_A we must form the equation $\frac{dU}{dH_A} = 0$ and proceed as follows.

The curved members of the truss are replaced by straight bars as shown at (*b*) and the formula just deduced is used to calculate the equivalent values of E for these straight bars. The force P_0 in each member of the truss shown at (*b*) due to the external load system,

H_A and H_B, is found by any of the methods described in Chapter 2 and $\frac{P_0 L}{AE}\frac{dP_0}{dH_A}$ is calculated for each, using the equivalent value of E for the bars A'H', H'J', J'K' and K'B' and not the real value for the material. This work should be done in tabular form as shown in earlier examples and results in an expression for $\Sigma\frac{P_0 L}{AE}\frac{dP_0}{dH_A}$ in terms of H_A and the external loads. Equation of this expression to zero gives the value of H_A required, from which the forces in all the bars of the truss can be calculated.

Further and more detailed examples of analyses of this type of truss will be found in a paper published by the Department of Scientific and Industrial Research.*

6.11. Principle of superposition applied to redundant frameworks.— When a structure which has a number of redundant bars exhibits symmetry about a centre-line an application of the principle of superposition considerably reduces the work of analysis.

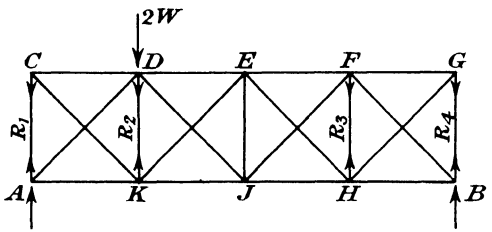

FIG. 6.16.

An example to illustrate this is shown in Fig. 6.16. It consists of a four-panel truss with counterbracing in each panel, so that there are four redundant bars. A load of 2W acts at joint D, and the bars CA, DK, FH and GB are conveniently chosen as the redundant members, the tensions in them being R_1, R_2, R_3, and R_4 respectively.

Using the second theorem of Castigliano, the conditions for the solution of the problem are

$$\frac{\partial U}{\partial R_1}=\frac{\partial U}{\partial R_2}=\frac{\partial U}{\partial R_3}=\frac{\partial U}{\partial R_4}=0.$$

The four resulting equations in the ordinary way must be solved simultaneously.

Suppose, however, that the load system is split into the two systems shown in Fig. 6.17. That shown in Fig. 6.17 (*a*) is symmetrical about EJ, the centre-line of the truss, and corresponding bars on either side of this axis must carry the same loads. It is only necessary, therefore, to assume two unknown tensions R'_1, and R'_2, as shown instead of four as in the case of unsymmetrical loading.

The second load system shown in (*b*) is skew-symmetrical, a load W acting downwards at D and an equal load acting upwards at F. The

* "Primary Stresses in Timber Roofs." A. J. S. Pippard and W. H. Glanville. Building Research Technical Paper No. 2. His Majesty's Stationery Office. 1928.

reactions are as shown, and corresponding bars on either side of the centre-line will carry equal but opposite loads. Thus. if CA has a

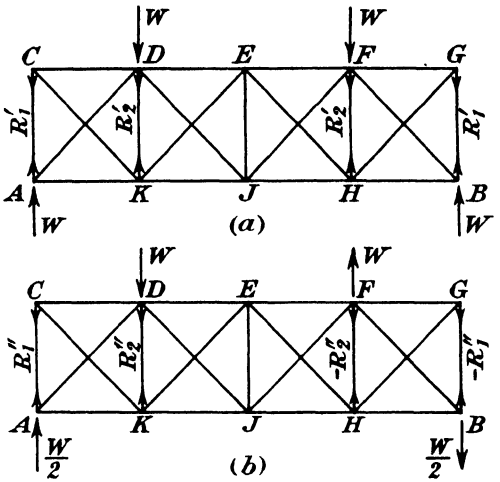

FIG. 6.17.

tension R''_1, GB will have a tension of $-R''_1$; that is, a compression of $+R''_1$. Here again the number of statically indeterminate forces is two instead of four. If the load systems shown at (*a*) and (*b*) are superposed the result is 2W acting at D as in Fig. 6.16, and the original problem is thus reduced to the solution of two pairs of two simultaneous equations instead of the solution of four simultaneous equations.

The saving in work is considerable even in the present simple case, but in a problem with a larger number of redundant bars the method enables solutions to be obtained which would otherwise be impracticable. For example, twelve simultaneous equations would generally involve a prohibitive amount of work, and it is only in very exceptional circumstances that a solution would be attempted; if, however, by the use of the principle of superposition they can be reduced to two independent sets of six each the problem, although still lengthy, is quite practicable.

The example shown in Fig. 6.16 has been solved both by the straightforward method and by using superposed load systems, and the working is given for comparison.

Numerical values have been reduced to the simplest terms to keep the arithmetical work as easy as possible.

In each case equations are formed of the type

$$\frac{\partial U}{\partial R}=\frac{P_0 L}{AE}\frac{\partial P_0}{\partial R}=0,$$

where the symbols have the same significance as previously in this chapter. The material is supposed to be the same throughout.

(1) First dealing with the problem straightforwardly, the necessary four simultaneous equations are formed, the work being set out in Table 6.12.

TABLE 6.12.

Bar	A	L	P_0					$\frac{P_0L}{A}\frac{\partial P_0}{\partial R_1}$					$\frac{P_0L}{A}\frac{\partial P_0}{\partial R_2}$					$\frac{P_0L}{A}\frac{\partial P_0}{\partial R_3}$					$\frac{P_0L}{A}\frac{\partial P_0}{\partial R_4}$				
			W	R_1	R_2	R_3	R_4	W	R_1	R_2	R_3	R_4	W	R_1	R_2	R_3	R_4	W	R_1	R_2	R_3	R_4	W	R_1	R_2	R_3	R_4
AC	2	1		1					$\frac{1}{2}$																		
KD	2	1			1										$\frac{1}{2}$												
JE	2	1		−1	1	1	−1		$\frac{1}{2}$	$-\frac{1}{2}$	$-\frac{1}{2}$	$\frac{1}{2}$		$-\frac{1}{2}$	$\frac{1}{2}$	$\frac{1}{2}$	$-\frac{1}{2}$		$-\frac{1}{2}$	$\frac{1}{2}$	$\frac{1}{2}$	$-\frac{1}{2}$		$\frac{1}{2}$	$-\frac{1}{2}$	$-\frac{1}{2}$	$\frac{1}{2}$
HF	2	1				1															$\frac{1}{2}$						
BG	2	1					1																				$\frac{1}{2}$
CD	4	1		1					$\frac{1}{4}$																		
DE	4	1	−1	−1	1			$\frac{1}{4}$	$\frac{1}{4}$	$-\frac{1}{4}$			$-\frac{1}{4}$	$-\frac{1}{4}$	$\frac{1}{4}$			$-\frac{1}{4}$			$\frac{1}{4}$	$-\frac{1}{4}$	$\frac{1}{4}$			$-\frac{1}{4}$	$\frac{1}{4}$
EF	4	1	−1			1	−1																				$\frac{1}{4}$
FG	4	1					1																				
AK	4	1	$\frac{3}{2}$	1				$\frac{3}{8}$	$\frac{1}{4}$																		
KJ	4	1	$\frac{3}{2}$	−1	1			$-\frac{3}{8}$	$\frac{1}{4}$	$-\frac{1}{4}$			$\frac{3}{8}$	$-\frac{1}{4}$	$\frac{1}{4}$			$\frac{1}{8}$			$\frac{1}{4}$	$-\frac{1}{4}$	$-\frac{1}{8}$			$-\frac{1}{4}$	$\frac{1}{4}$
JH	4	1	$\frac{1}{2}$			1	−1																	$\frac{1}{8}$			$\frac{1}{4}$
HB	4	1	$\frac{1}{2}$				1																				
CK	$\sqrt{2}$	$\sqrt{2}$		$-\sqrt{2}$					2																		
AD	$\sqrt{2}$	$\sqrt{2}$	$-\frac{3}{\sqrt{2}}$	$-\sqrt{2}$				3	2																		
DJ	$\sqrt{2}$	$\sqrt{2}$	$-\frac{1}{\sqrt{2}}$	$\sqrt{2}$	$-\sqrt{2}$			−1	2	−2			1	−2	2												
EK	$\sqrt{2}$	$\sqrt{2}$		$\sqrt{2}$	$-\sqrt{2}$				2	−2				−2	2												
EH	$\sqrt{2}$	$\sqrt{2}$				$-\sqrt{2}$	$\sqrt{2}$														2	−2				−2	2
FJ	$\sqrt{2}$	$\sqrt{2}$	$\frac{1}{\sqrt{2}}$			$-\sqrt{2}$	2											−1			2	−2	1			−2	2
FB	$\sqrt{2}$	$\sqrt{2}$	$-\frac{1}{\sqrt{2}}$				$-\sqrt{2}$																1				2
GH	$\sqrt{2}$	$\sqrt{2}$					$-\sqrt{2}$																				2

These equations are

$$\left.\begin{aligned} 9W+40R_1-20R_2-\ 2R_3+\ 2R_4&=0\\ 9W-40R_1+44R_2+\ 4R_3-\ 4R_4&=0\\ -9W-\ 4R_1+\ 4R_2+44R_3-40R_4&=0\\ 9W+\ 2R_1-\ 2R_2-20R_3+40R_4&=0. \end{aligned}\right\}$$

The solution is

$$\begin{aligned} R_1&=-0{\cdot}59799W\\ R_2&=-0{\cdot}77006W\\ R_3&=+0{\cdot}01434W\\ R_4&=-0{\cdot}22643W. \end{aligned}$$

The negative signs denote that the forces are compressive.

(2) Using the method of superposition, and dealing first with the case shown in Fig. 6.17 (*a*), the equations obtained are

$$\left.\begin{aligned} -9W-42R'_1+22R'_2&=0\\ 22R'_1-24R'_2&=0 \end{aligned}\right\}$$

which give

$$\left.\begin{aligned} R'_1&=-0{\cdot}41221W\\ R'_2&=-0{\cdot}37786W. \end{aligned}\right\}$$

The detailed work is set out in Table 6.13.

TABLE 6.13.

Bar	A	L	P_0			$\frac{P_0L}{A}\frac{\partial P_0}{\partial R'_1}$			$\frac{P_0L}{A}\frac{\partial P_0}{\partial R'_2}$		
			W	R'_1	R'_2	W	R'_1	R'_2	W	R'_1	R'
CA	2	1		1			$\frac{1}{2}$				
DK	2	1			1						$\frac{1}{2}$
CD	4	1		1			$\frac{1}{4}$				
DE	4	1	−1	−1	1	$\frac{1}{4}$	$\frac{1}{4}$	$-\frac{1}{4}$	$-\frac{1}{4}$	$-\frac{1}{4}$	$\frac{1}{4}$
AK	4	1	1	1		$\frac{1}{4}$	$\frac{1}{4}$				
KJ	4	1	1	−1	1	$-\frac{1}{4}$	$\frac{1}{4}$	$-\frac{1}{4}$	$\frac{1}{4}$	$-\frac{1}{4}$	$\frac{1}{4}$
CK	$\sqrt{2}$	$\sqrt{2}$		$-\sqrt{2}$			2				
DA	$\sqrt{2}$	$\sqrt{2}$	$-\sqrt{2}$	$-\sqrt{2}$		2	2				
DJ	$\sqrt{2}$	$\sqrt{2}$		2	$-\sqrt{2}$		2	−2		−2	2
KE	$\sqrt{2}$	$\sqrt{2}$		2	$-\sqrt{2}$		2	−2		−2	2
$\frac{1}{2}$ (EJ)	$\frac{1}{2}$ (2)	1		−1	1		1	−1		−1	1

The skew-symmetrical case shown in Fig. 6.17 (*b*) yields the equations

$$\left.\begin{aligned} 19R''_1-\ 9R''_2&=0\\ -9W+36R''_1-40R''_2&=0 \end{aligned}\right\}$$

the solution being

$$\left.\begin{aligned} R''_1&=-0{\cdot}18578W\\ R''_2&=-0{\cdot}39220W. \end{aligned}\right\}$$

The numerical work is given in Table 6.14.

The redundant forces under the original loading are then

$$R_1 = R'_1 + R''_1 = -(0{\cdot}41221 + 0{\cdot}18578)W = -0{\cdot}59799W$$
$$R_2 = R'_2 + R''_2 = -(0{\cdot}37786 + 0{\cdot}39220)W = -0{\cdot}77006W$$
$$R_3 = R'_2 - R''_2 = -(0{\cdot}37786 - 0{\cdot}39220)W = +0{\cdot}01434W$$
$$R_4 = R'_1 - R''_1 = -(0{\cdot}41221 - 0{\cdot}18578)W = -0{\cdot}22643W$$

TABLE 6.14.

Bar	A	L	P_0			$\frac{P_0 L}{A}\frac{\partial P_0}{\partial R''_1}$			$\frac{P_0 L}{A}\frac{\partial P_0}{\partial R''_2}$		
			W	R''_1	R''_2	W	R''_1	R''_2	W	R''_1	R''_2
CA	2	1		1			$\frac{1}{2}$				
DK	2	1			1						$\frac{1}{2}$
CD	4	1		1			$\frac{1}{4}$				
DE	4	1		−1	1		$\frac{1}{4}$	$-\frac{1}{4}$		$-\frac{1}{4}$	$\frac{1}{4}$
AK	4	1	$\frac{1}{2}$	1		$\frac{1}{8}$	$\frac{1}{4}$				
KJ	4	1	$\frac{1}{2}$	−1	1	$-\frac{1}{8}$	$\frac{1}{4}$	$-\frac{1}{4}$	$\frac{1}{8}$	$-\frac{1}{4}$	$\frac{1}{4}$
CK	$\sqrt{2}$	$\sqrt{2}$		$-\sqrt{2}$			2				
DA	$\sqrt{2}$	$\sqrt{2}$	$-\frac{1}{\sqrt{2}}$	$-\sqrt{2}$		1	2				
DJ	$\sqrt{2}$	$\sqrt{2}$	$-\frac{1}{\sqrt{2}}$	$\sqrt{2}$	$-\sqrt{2}$	−1	2	−2	1	−2	2
KE	$\sqrt{2}$	$\sqrt{2}$		$\sqrt{2}$	$-\sqrt{2}$		2	−2		−2	2

These results agree exactly with those obtained from the straightforward solution, but the work involved is considerably less.

It should be noted that the calculations are only required for one-half of the truss under each of the two component systems. In the case of skew-symmetrical loading the centre-post JE is unstressed and presents no difficulty; in the symmetrical loading, however, it is

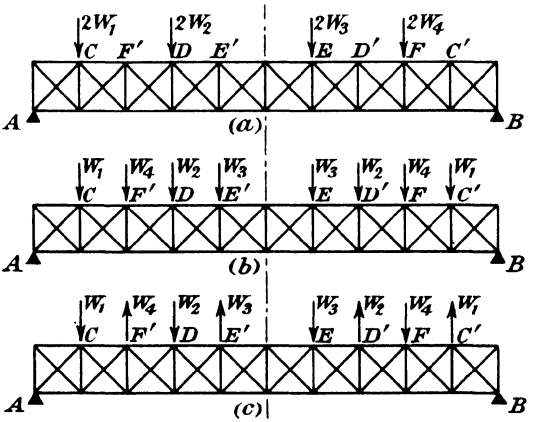

FIG. 6.18.

necessary to take a post of one-half the actual area carrying one-half the load when dealing with the half truss. This is indicated in Table 6.13 by the description ½ (EJ) in the first column.

In the foregoing case the truss carried only a single concentrated load. There is, however, no difficulty in applying the same method to any load system.

This is best illustrated by an example.

Suppose Fig. 6.18 (*a*) represents a structure carrying loads $2W_1$, $2W_2$, $2W_3$ and $2W_4$ at points C, D, E and F respectively. This system is to be replaced by symmetrical and skew-symmetrical systems which, when superposed, give the original system. Let C′, D′, E′ and F′ be the points corresponding to C, D, E and F on the other side of the centre-line of the truss.

Consider first the load $2W_1$. This is replaced by a pair of downward loads W_1 at C and C′ as shown in Fig. 6.18 (*b*), and by downward and upward loads W_1 at C and C′ respectively as shown in Fig. 6.18 (*c*). The other loads are dealt with similarly, and the two systems (*b*) and (*c*) result. The stress-analysis is then carried out as illustrated in the detailed case already given.

EXERCISES

(1) Three steel wires AB, CB, DB attached to points A, C and D on a rigid horizontal beam are connected at the point B which is 10 feet vertically below C. The distances AC and CD are each 10 feet.

If AB, CB and DB are respectively 1 square inch, ½ square inch and 1½ square inches in cross-sectional area, calculate what load each carries when a weight of 5 tons is hung at B.

(*AB=BD=+2·22 tons ; BC=+1·86 tons*)

(2) Four equal wires OA, OB, OC and OD of length L and cross-sectional area A support a weight W midway between two walls AD and BC which are $\sqrt{2}$L apart. The wires OD and OB are in the same straight line and at right angles to OA and OC. (See diagram 6*a*.)

If the wires are initially tensioned to remain taut under load find the deflection of O.

$\left(\frac{WL}{2AE}\right)$

(3) The rectangular space frame shown in diagram 6*b* is pinned to a rigid wall at the corners A, B, C and D, and a couple of 1,000 inch-lb. is applied to the face EFHG, which is rigid in its own plane.

Each panel is braced and counterbraced with steel wires each of 1/100 square inch cross-sectional area. These wires have no initial tension so that only one of each pair is operative.

All other members are of steel, having cross-sectional areas of 1/10 square inch.

Determine the loads in all the members.

(*DE=BH=35·2 lb.*
AF=CG=43·0 lb.
AE=CH=−28·1 lb.
BF=GD=−38·5 lb.)

(4) The pin-jointed structure shown in diagram 6*c* is simply supported at L and J and carries suspended loads of 4 tons and 2 tons as shown.

The members are unstressed when the loads are removed and have the following areas :—

EA = F′A = HA = 1·06 inch²
ED = EF = GH = 1·78 inch²
F′G = G′C = HB = FF′ = 2·09 inch²

Calculate the vertical deflection under each of the applied loads. (E = 13,000 tons/square inch.)

(*0·093 inch ; 0·071 inch*)

(5) The steel beam AB shown at 6*d* is strengthened by a steel king post CD which is pinned to C, the centre point of the beam. The point D is braced by steel rods to A and B which are simply supported.

Calculate the maximum central load which the beam can carry given the following data :—

Beam : I =250 inch units.
Depth= 12 inches.

Strut CD : Cross-sectional area=4 square inches.

Rods AD, BD : Cross-sectional area=1 square inch.

Permissible flexural stress in beam=8 tons per square inch.

(*36·3 tons*)

(6) The pin-jointed steel frame shown in diagram 6*e* is attached at A, B and C to a rigid wall.

AD and CF are each $\sqrt{2}$ square inches and each diagonal is 1 square inch in area. DE and EF are rigid. Calculate the loads in AD and CF when a load acts as shown.

(*AD=+2 tons ; CF=−2 tons*)

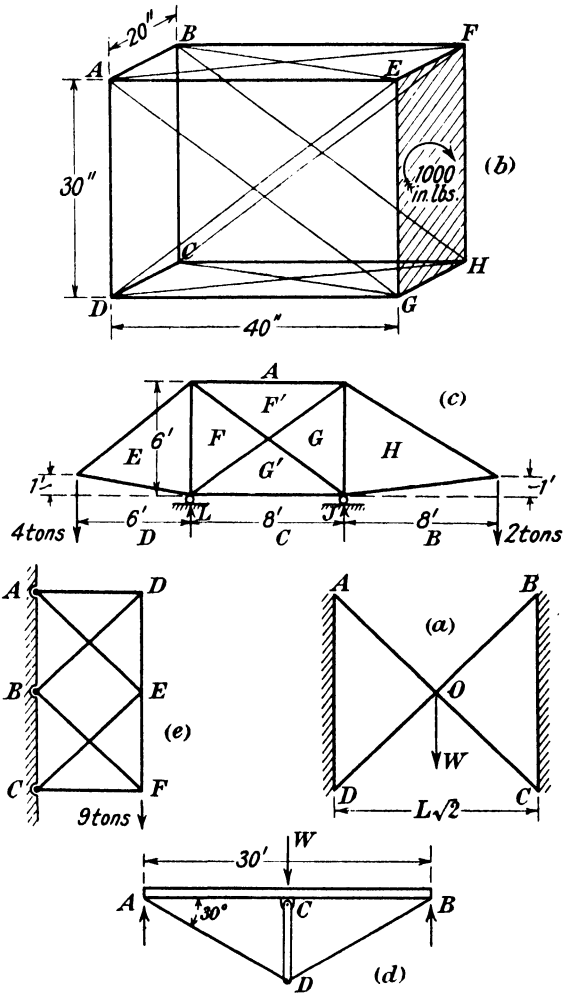

DIAGRAM 6

CHAPTER 7

STRUTS AND LATERALLY LOADED COLUMNS AND TIES

7.1. The behaviour of struts under load.—If a rod of perfectly uniform shape, perfectly straight and of homogeneous material throughout were loaded axially so that the point of application of the load coincided with the neutral axis of the rod, failure would occur by direct compression. In practice such an ideal set of conditions cannot occur. Small errors in workmanship, slight variations in the material and the practical impossibility of obtaining perfect test conditions all combine to give what is equivalent to an eccentricity of loading. This equivalent eccentricity, although small, exercises considerable influence upon the behaviour of the strut, and since it cannot in any individual case be measured, the problem of strut strength must of necessity be settled by the help of experimental data.

Before proceeding to a discussion of formulas suitable for design purposes it is necessary to consider further the behaviour of the ideal strut described above and this will depend upon the proportions of the strut, or the " slenderness ratio." This slenderness ratio is defined as the ratio of the length of the strut to the minimum radius of gyration (l/k) and appears in all rational strut formulas. The usual terms long and short struts are misleading, since absolute length has no bearing upon the behaviour of the member : a slender strut may be of any length and the important factor is the slenderness ratio. Struts will therefore be referred to as slender when the ratio l/k is large and stocky when this ratio is small.

Suppose that a stocky strut is subjected to an axial load. The axial strain will be elastic up to a certain value of the end stress, but when this stress reaches the yield point there will be a comparatively large permanent set and the strut will have failed. If the material is ductile a further increase of stress will cause flattening of the strut, but if it is brittle there will be an actual partition of the material along planes approximately at 45° to the direction of the load, due to the shear stresses induced along such planes.

If, on the other hand, a slender strut is subjected to an axial load a different state of affairs is obtained. Under relatively small loads the strut is in a stable state and if it is displaced by a small amount it will straighten itself when the disturbing force is removed. For a certain value of the axial force however, the strut is in a state of neutral equilibrium and will remain deflected after the removal of a disturbing force. A further increase in the axial load produces a state of unstable equilibrium and any disturbing force will start a deflection in the strut

which will increase in amount until the material is overstressed due to the increasing curvature of the member. If the axial force be removed before the fibre stress has reached the limit of proportionality, the strut will become perfectly straight again and show no signs of distress. The axial load which just induces this condition of elastic instability is known as the critical load, the buckling load or the Euler load, since Euler first investigated the problem. It should be noticed that in the absence of an external disturbing force all perfect struts, both slender and stocky, will fail by direct compression.

7.2. The critical load for slender struts.—In Fig. 7.1 let AB be a slender strut of length l, of uniform cross-section and of homogeneous material. It is pin-jointed at A and B and is subjected to an axial load P which just produces a state of neutral stability. The strut under this load is deflected a small amount a at the centre and the deflecting force is then removed. Since the strut is neutrally stable the deflection a remains.

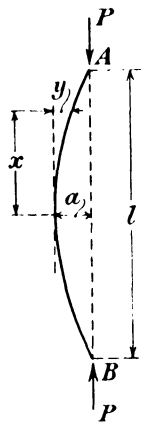

Fig. 7.1.

Take an origin at the centre of the deflected strut and measure x and y as shown in the figure. Then at any point

$$\frac{d^2y}{dx^2}=\frac{P}{EI}(a-y)$$

or writing $\mu^2=\frac{P}{EI}$, we have

$$\frac{d^2y}{dx^2}+\mu^2(y-a)=0.$$

The solution of this equation is

$$y=A\sin\mu x+B\cos\mu x+a$$

where A and B are constants of integration.

When $x=0$, $y=0$ so that $B=-a$.

When $x=0$, $\frac{dy}{dx}=0$ and on differentiating we obtain

$$\frac{dy}{dx}=\mu(A\cos\mu x-B\sin\mu x),$$

from which $A=0$.

Then $$y=a(1-\cos\mu x).$$

When $x=\frac{l}{2}$, $y=a$ and substitution in the above equation gives

$$a\cos\frac{\mu l}{2}=0.$$

Since by our hypothesis a cannot be zero, the solution required is

$$\cos\frac{\mu l}{2}=0.$$

The smallest value of $\mu l/2$ which satisfies this condition is $\pi/2$ and so for the critical load we have

$$\frac{\mu l}{2}=\frac{\pi}{2}$$

i.e.

$$\frac{Pl^2}{EI}=\pi^2$$

or

$$P=\frac{\pi^2 EI}{l^2}.$$

If instead of being pin-jointed the strut is encastré at both ends (Fig. 7.2), since the slopes at the ends and at the middle are zero, it is clear that there are points of inflection at the quarter points of the strut, D and E. The portion DE can be treated as a pin-jointed strut of length $l/2$, and for this method of fixing therefore the critical load for AC is

$$P=\frac{\pi^2 EI}{\left(\frac{l}{2}\right)^2}=\frac{4\pi^2 EI}{l^2}.$$

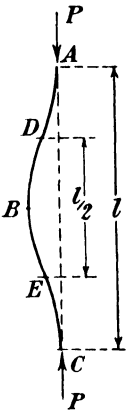

FIG. 7.2.

This case as well as others may be obtained directly by the same mathematical procedure as used for the pin-jointed strut.

The critical loads for the common cases are given in Table 7.1, the free condition in Case 3 means that the end of the strut is not constrained in any way, *i.e.* it is a mast carrying an axial load. The results in Case 4 are only approximate, but are sufficiently accurate for any practical purpose.

TABLE 7.1.

Case	Length of strut	End conditions		Critical load	Equivalent length
		1	2		
1	l	Pin	Pin	$\frac{\pi^2 EI}{l^2}$	l
2	l	Encastré	Encastré	$\frac{4\pi^2 EI}{l^2}$	$\frac{l}{2}$
3	l	Encastré	Free	$\frac{\pi^2 EI}{4l^2}$	$2l$
4	l	Pin	Encastré	$\frac{8 1 EI}{4l^2}$	$0{\cdot}7l$

7.3. Eccentrically loaded strut.—The case now to be considered is that of a strut pin-jointed at the ends and carrying a load at a specified distance from the neutral axis. For any value of the applied load the strut assumes a definite shape and the stresses in it can be calculated. We make no assumption as to slenderness but treat the problem

generally and so the result is applicable to members of any slenderness ratio. It will be shown however that when the strut is stocky the result can be simplified.

In Fig. 7.3, AB is a pin-jointed strut of length l having a load P acting at a distance e from the neutral axis.

It will be seen that for any value of P there will be a deflection of the strut, since there is now a bending moment which was absent in the axially loaded case.

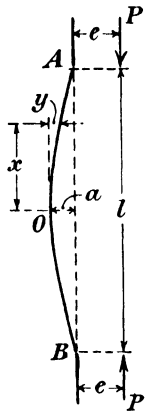

FIG. 7.3.

With the same notation as in paragraph 7.2, we have

$$\frac{d^2y}{dx^2}=\mu^2(a+e-y)$$

or

$$\frac{d^2y}{dx^2}+\mu^2(y-a-e)=0.$$

The solution of this is

$$y=(a+e)(1-\cos\mu x)$$

obtained in the same way as for the axially loaded strut.

Since $y=a$ when $x=\frac{l}{2}$, we have on substitution

$$a=e\left(\sec\frac{\mu l}{2}-1\right).$$

The maximum bending moment in the strut is at the centre and is $P(a+e)$

i.e.

$$M_0=Pe\sec\frac{l}{2}\sqrt{\frac{P}{EI}}.$$

If $I=Ak^2$ is the minimum second moment of area and h is the distance of the compressive fibre farthest from the neutral axis of the section, the maximum compressive stress in the strut is

$$p_f=\frac{P}{A}\left(1+\frac{eh}{k^2}\sec\frac{l}{2}\sqrt{\frac{P}{EI}}\right),$$

where k is the minimum radius of gyration and A is the area of the cross-section.

This formula is not convenient for design purposes since P occurs in the secant term and cannot be evaluated readily. The solution necessitates either a process of trial and error or a graphical method.

7.4. Stocky struts.—In the formula of the preceding paragraph the secant term can be written as $\sec\frac{l}{2k}\sqrt{\frac{P}{AE}}$ and when l/k approaches 0 its value approaches unity.

Hence for stocky columns the formula for maximum compressive stress becomes

$$p_f=\frac{P}{A}\left(1+\frac{eh}{k^2}\right)$$

and the maximum load which can be applied to a stocky column without permanent deformation is

$$P=\frac{p_y A}{\left(1+\frac{eh}{k^2}\right)},$$

where p_y is the yield stress in compression.

7.5. General strut formulas.—From the preceding work it is clear that neither the very slender nor the very stocky strut presents serious difficulty, but with few exceptions struts which are used in practice do not fall into either of these categories. They are intermediate and the real problem is to find a formula which will be sufficiently accurate to serve as a design basis for struts of any slenderness ratio.

Many such formulas for the axial load which a strut can carry have been proposed, one of the best-known being that due to Rankine:

$$P=\frac{p_y A}{1+a(l/k)^2}.$$

This is definitely an empirical formula, and the constant a should be determined experimentally. Its value for different materials is given in most books of engineering data.

If l/k is small the value of P approaches $p_y A$ as it should and by a suitable adjustment of a, P can be made to approach the Euler value as l/k approaches infinity.

Thus
$$a=\frac{p_y A k^2}{P l^2}-\frac{k^2}{l^2}.$$

When k/l approaches zero, P should approach $\pi^2 EI/l^2$

i.e.
$$a=\frac{p_y}{\pi^2 E}.$$

This value generally differs somewhat from the experimental one but in the absence of the more reliable figure it can be used for a rough approximation.

The Rankine formula can be written

$$p=\frac{p_y}{1+a(l/k)^2},$$

where p is the load per unit area on the end section of the strut.

It has already been shown in paragraph 7.4 that when a strut which is not slender is eccentrically loaded the ratio

$$\frac{p}{p_y}=\frac{1}{\left(1+\frac{eh}{k^2}\right)},$$

i.e. the allowable end loading is reduced by this amount due to eccentricity. If then a strut to which the Rankine formula is applied has an eccentricity of loading, an approximation to the allowable load is

$$P=\frac{p_y A}{\{1+a(l/k)^2\}\left(1+\frac{eh}{k^2}\right)}.$$

While the Rankine formula is still used to some extent it has largely been superseded by more rational formulas for which the essential empirical constants have been more accurately determined.

The Rankine formula makes no direct allowance for the eccentricity of loading due to slight imperfections in workmanship and material which have previously been mentioned although these would be dealt with to some extent by the empirical constant a. Later investigators however introduce such factors into their formulas and two methods have been adopted with success. In the first method the sum of all the departures from perfection is treated as an equivalent eccentricity of loading and appears in the formula as such.

The second method is to treat the sum of the imperfections as being equivalent to an initial curvature of the strut: this leads to a very useful strut formula of general applicability.

7.6. Modified Smith formula for pin-jointed struts.—If in the formula for an eccentrically loaded strut, as determined in paragraph 7.3, the specified eccentricity is replaced by an equivalent eccentricity to be found experimentally, a formula is obtained which is applicable to normally straight axially loaded members. This is the treatment of the problem adopted by Professor R. H. Smith and his formula was modified by Professor R. V. Southwell by the substitution of the yield stress, or more accurately the stress at the limit of proportionality, for the ultimate stress suggested by Smith.

The formula of paragraph 7.3 can be rewritten

$$p_v = p\left(1+\frac{eh}{k^2}\sec\frac{l}{2}\sqrt{\frac{p}{Ek^2}}\right),$$

or rewriting it in the more usual form, we obtain the modified Smith formula *

$$P = pA = \frac{p_v A}{1+\frac{h\delta}{k^2}\sec\frac{l}{2}\sqrt{\frac{p}{Ek^2}}},$$

where P=The limiting load.

p=The limiting average intensity of loading on the cross-section of the strut.

A=The area of the cross-section of the strut.

p_v=The yield point of the material.

h=The greatest distance of any point on the section from the centre line.

δ=The equivalent eccentricity of loading.

k=The minimum radius of gyration of the cross-section.

E=Young's modulus of the material.

l=Length of the strut.

A large number of measurements were made to determine the value of δ for tubes of circular cross-section used as aeroplane struts. As

* "Report on Materials of Construction used in Aircraft and Aircraft Engines," C. F. Jenkin, p. 53, H.M. Stationery Office, 1920.

a result of these measurements it was found that the equivalent eccentricity of loading is the sum of three terms—

(1) The crookedness of the tube, *i.e.* the maximum deflection of any point on the centre line of the tube from the line through the centres of the pin-joints.

In commercial tubes the crookedness need not exceed 0·02 inch per foot run of tube. With careful manufacture it may be made much less.

(2) A quantity representing the effect of the eccentricity of the bore of the tube. This may be taken as 0·025 times the bore of the tube, if the maximum eccentricity is due to a variation of thickness of the wall of the tube of ± 10 per cent. (Total difference between thickest and thinnest side=20 per cent. of mean thickness.)

(3) The radius of the friction circle of the pin-joint (*i.e.* the radius of the pin $\times$ coefficient of friction). This term may be omitted if the tube is pinned to attachments which do not rotate so as to assist the bending of the strut.

This formula cannot be used directly because p appears on both sides ; but curves may be drawn and the results read from them.

7.7. To construct a curve representing Smith's modified formula.— The co-ordinates chosen are p, the limiting average stress and l/k, the

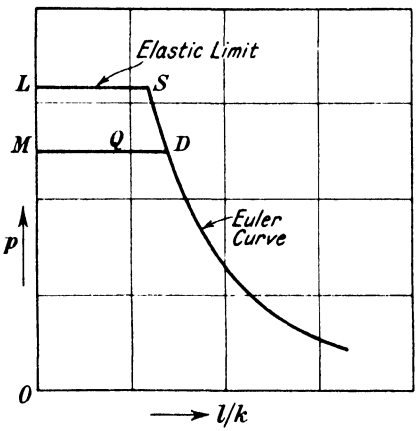

FIG. 7.4.

ratio of the length to the least radius of gyration of the cross-section of the strut.

First, draw Euler's curve given by the equation

$$p=\frac{\pi^2 E k^2}{l^2}$$

also the horizontal line p=elastic limit or yield point (LS, in Fig. 7.4). Next choose any value of $\lambda = \sec \frac{l}{2}\sqrt{\frac{p}{Ek^2}}$ with its corresponding value

of l/l' (l' given by $p=\frac{\pi^2 E k^2}{l'^2}$) from the following table, and mark off M so that

$$\frac{LM}{MO}=\lambda\frac{h\delta}{k^2}$$

and on the horizontal MD mark off Q so that

$$\frac{MQ}{MD}=\frac{l}{l'}.$$

Then Q is a point on the required curve. Any number of points may be found by selecting a series of values of λ and l/l' from Table 7.2.

TABLE 7.2.

VALUES OF λ CORRESPONDING TO DIFFERENT RATIOS l/l'.

l/l'	λ	l/l'	λ	l/l'	λ	l/l'	λ
0·0	1·000	0·25	1·082	0·50	1·414	0·75	2·613
0·05	1·003	0·30	1·122	0·55	1·540	0·80	3·236
0·10	1·012	0·35	1·173	0·60	1·701	0·85	4·284
0·15	1·028	0·40	1·236	0·65	1·914	0·90	6·329
0·20	1·051	0·45	1·315	0·70	2·203	0·95	12·745

It will be noticed that the curve constructed in this way depends on the values chosen for Young's modulus E, the elastic limit or yield point and the equivalent eccentricity δ. For a given quality of steel (or for tubes made in accordance with one specification) Young's modulus and the elastic limit or yield point may be assumed to be constant but the value of δ will generally depend on the length of the strut. The curve as drawn above is only correct for one value of δ.

If a series of curves be drawn for a series of values of δ, then the limiting stress may be read off one or other curve for any strut made of the steel (determined by E and the elastic limit or yield point) for which the curves are drawn.

If the value of δ be assumed to be a definite function of the dimensions of the tube, say, for commercial tubes—

$$\delta=\frac{\text{length}}{600}+\frac{\text{internal diameter}}{40},$$

then a new curve may be drawn for a reasonably straight tube of any selected size, giving the limiting stress for all lengths.

This method of expressing Smith's formula is due to Professor R. V. Southwell.

7.8. Deflection of a strut.—A strut of large slenderness ratio may have a large deflection under the limiting load; it is, therefore, desirable to calculate the deflection of such a strut.

The deflection due to the limiting load is given by the expression

$$\Delta = \frac{2k^2}{d} \times \frac{AB}{BC} - \delta.$$

If the strut is initially crooked the total deflection will be the sum of the initial deflection and the deflection due to the limiting load.

In the above expression AB and BC are to be measured off the

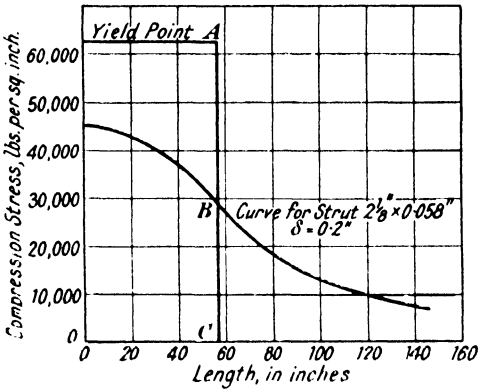

FIG. 7.5.

strength curve corresponding to the strut. For example, suppose that the curve in Fig. 7.5 corresponds with the tube in question, and let

OC=The length of the strut (56 inches).
CA=The yield point (28 tons per square inch).
CB=The ordinate to the curve at point B, *i.e.* the limiting stress (13·1 tons per square inch).
δ=The equivalent eccentricity of loading (0·2 inch).
d=The outside diameter of the strut ($2\frac{1}{8}$ inches).
k=The radius of gyration of the cross-section (0·73 inch).

Then $$\frac{AB}{BC} = 1{\cdot}13$$

and $$\frac{2k^2}{d} = 0{\cdot}501 \text{ inch.}$$

Therefore the deflection due to the limiting load=0·367 inch. The figure shows clearly how the deflection increases with the length, by the increase in the ratio $\frac{AB}{BC}$.

7.9. Perry strut formula.—Professor Perry's formula is based on the assumption that the effect of imperfections in material and workmanship, unavoidable eccentricity of loading etc., can be represented by a hypothetical initial curvature of the strut. The exact initial shape which is assumed for the strut does not seriously affect the final results and for ease of manipulation a cosine curve was used, as this leads to simple equations.

Let AB (Fig. 7.6) be a pin-jointed strut of length l. Take an origin at O and measure x and y as shown. The initial shape of the strut is assumed to be given by the equation

$$y_0 = c_o \cos \frac{\pi x}{l},$$

where c_o is the initial departure from straightness at the centre.

Under a load P the deflection at x is increased by y so that

$$EI\frac{d^2y}{dx^2} = -P\left(y + c_o \cos \frac{\pi x}{l}\right)$$

i.e.

$$\frac{d^2y}{dx^2} + \mu^2\left(y + c_o \cos \frac{\pi x}{l}\right) = 0,$$

where

$$\mu^2 = \frac{P}{EI}.$$

The solution of this equation is

$$y = A \sin \mu x + B \cos \mu x + \frac{\mu^2 c_o \cos \dfrac{\pi x}{l}}{\dfrac{\pi^2}{l^2} - \mu^2},$$

where A and B are constants of integration.

When

$$x = \pm\frac{l}{2}, \quad y = 0 \quad \text{and so} \quad A = B = 0,$$

hence

$$y = \frac{Pc_o \cos \dfrac{\pi x}{l}}{Q - P},$$

where

$$Q = \frac{\pi^2 EI}{l^2}.$$

If A is the cross-sectional area of the strut,

put

$$\frac{P}{A} = p \quad \text{and} \quad \frac{Q}{A} = p_e.$$

Then

$$y = \frac{p}{p_e - p} c_o \cos \frac{\pi x}{l}$$

and the total deflection at any point is

$$(y + y_0) = \left(\frac{p}{p_e - p} + 1\right) c_o \cos \frac{\pi x}{l}$$

$$= \frac{p_e}{p_e - p} c_o \cos \frac{\pi x}{l}.$$

The maximum deflection occurs at the centre where $x = 0$, and its value is

$$y_{max} = \frac{p_e c_o}{p_e - p},$$

while the maximum bending moment is

$$M_{max}=Pc_o\left(\frac{p_e}{p_e-p}\right).$$

The maximum compressive stress occurs on the concave side of the strut and is

$$p_1=\frac{Pc_o\left(\frac{p_e}{p_e-p}\right)a_1}{I}+\frac{P}{A},$$

where a_1 is the distance of the most stressed compressive fibre from the neutral axis.

If we put $\frac{c_o a_1}{k^2}=\eta$ we obtain

$$p_1=p\left(\frac{\eta p_e}{p_e-p}+1\right).$$

Putting $p_1=p_y$, the yield stress in compression, and solving for p we find

$$p=\frac{p_y+(\eta+1)p_e}{2}-\sqrt{\left\{\frac{p_y+(\eta+1)p_e}{2}\right\}^2-p_y p_e}$$

which is the Perry formula for the intensity of end loading which will cause the fibre stress to reach the yield point.

In a brittle material failure may occur on the tension side of the strut and following the same procedure we obtain for this case

$$p'=\frac{(1-\eta')p_e-p'_y}{2}+\sqrt{\left\{\frac{(1-\eta')p_e-p'_y}{2}\right\}^2+p'_y p_e},$$

where p' is the intensity of end loading which will cause the fibre stress to reach p'_y the yield point in tension and $\eta'=\frac{c_o a_2}{k^2}$, where a_2 is the distance of the most stressed tension fibre from the neutral axis.

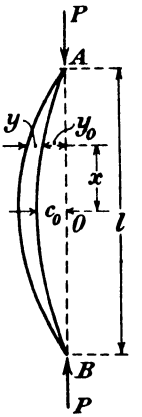

FIG. 7.6.

This formula, with others, has been subjected to a critical examination by Professor Andrew Robertson, who has made an exhaustive series of carefully controlled tests upon struts of various materials. As a result of these and tests made by other experimenters, he has stated his conclusion * that for all materials having a real yield the Perry formula gives good results for pin ended struts if η be taken as $\cdot 001\, l/k$ for an average value, and $\cdot 003\, l/k$ for a lower limit. For materials with considerable ductility but no real yield phenomena, as defined by a drop of stress, the value of p_y should be taken at the point in the stress-strain diagram where the

* "The Strength of Struts," Andrew Robertson, Inst. C.E. Selected Engineering Paper, No. 28.

slope is three times that in the elastic region. η is then the same as for materials with a real yield.

For materials having no yield (at any rate for cast iron) it is sufficient to take the ultimate stress in compression as the value of p_y and η as $\cdot 015\ l/k$. In the particular case of cast iron this curve is slightly below the one representing tensile failure. If the strut has end conditions other than free these values of η require modification and Robertson makes the necessary corrections by working on an equivalent length of strut. The values he suggests for practical struts are given in Table 7.3.

TABLE 7.3.

Case	End conditions	Equivalent length	η	
			Ductile	Brittle
1	Free	l	$\cdot 003\frac{l}{k}$	$\cdot 015\frac{l}{k}$
2	Flat	$\cdot 5l$	$\cdot 006\times\frac{\cdot 5l}{k}$	$\cdot 03\times\frac{\cdot 5l}{k}$
3	Fixed	$\cdot 5l$	$\cdot 006\times\frac{\cdot 5l}{k}$	$\cdot 03\times\frac{\cdot 5l}{k}$

It will be noticed that the numerical values of η are the same for flat and fixed ends as for free ends. The correction on the results is introduced by the fact that the Euler crippling stress p_e is calculated for a strut of only half the length, *i.e.* p_e has four times the value in Cases 2 and 3 that it has in Case 1.

If a strut has a real eccentricity of loading, e_o, it may be allowed for in the way suggested by Ayrton and Perry by replacing the term c_o, *i.e.* the initial departure from the straight, by a term $c_1=c_o+\frac{6}{5}e_o$.

Let η' be the value of the constant for this case.

Then, since $$\eta'=\frac{a_1c_1}{k^2}$$

we have $$\eta'=\frac{a_1}{k^2}(c_o+\tfrac{6}{5}e_o)$$

or $$\eta'=\eta+\frac{6a_1e_o}{5k^2},$$

where η is the value for the strut when there is no deliberate eccentricity of loading.

The most satisfactory way of using the formula is to plot a curve of p against l/k for the material to be used, from which the ultimate end loading of the member can be read directly.

A load factor can be incorporated in this formula by writing Np instead of p and in this form its use was recommended by the Steel Structures Research Committee,* who suggested that the following

* "First Report of the Steel Structures Research Committee." H.M. Stationery Office, 1931, p. 271.

values of the various terms should be used when dealing with members made of Quality A steel (British Standard Specification No. 15):

Yield stress =18 tons per square inch.
Young's modulus=13,000 tons per square inch.
N=2·36.
η=0·003 l/k.

Table 7.4, taken from the Report of the Committee, gives the values of p, the permissible end load in tons per square inch of cross-sectional area or working stress for different values of l/k when the above figures are used.

TABLE 7.4.

l/k	p	l/k	p
20	7·2	130	2·6
30	6·9	140	2·3
40	6·6	150	2·0
50	6·3	160	1·8
60	5·9	170	1·6
70	5·4	180	1·5
80	4·9	190	1·3
90	4·3	200	1·2
100	3·8	210	1·1
110	3·3	220	1·0
120	2·9	230	0·9
		240	0·9

The curve plotted from this table is shown in Fig. 7.7, p. 130.

In Chapter 1 two methods of strength specification by means of a load factor and a factor of safety respectively were briefly mentioned and the formula now under discussion serves as a useful illustration of the fundamental difference between them.

The formula as used for design is

$$\mathrm{N}p_c=\frac{p_y+(\eta+1)p_e}{2}-\sqrt{\left\{\frac{p_y+(\eta+1)p_e}{2}\right\}^2-p_yp_e}$$

Since $\mathrm{N}p_c$ is the intensity of end loading which will cause the maximum fibre stress to reach the yield stress p_y, N is a load factor.

The formula can be rewritten in the form

$$p_1=p_c\left(1+\frac{\eta p_e}{p_e-p_c}\right)$$

where p_1 is the maximum fibre stress produced by an axial compressive load per unit area p_c.

Substituting the adopted value of η=·003 l/k this becomes

$$p_1=p_c\left\{1+\frac{\cdot 003\ l/k}{1-\frac{p_c}{\pi^2\mathrm{E}}\left(\frac{l}{k}\right)^2}\right\}$$

The table quoted above gives values of p_c for different values of l/k and on substituting these values in the formula just obtained the actual working fibre stress in the material is obtained.

The factor of safety is then p_v/p_1 and Fig. 7.8 shows its relation to l/k. Thus, with a constant load factor the factor of safety varies greatly and the result emphasizes in a striking manner the difference between the two methods of specifying strength.

If the design of struts were based on a constant factor of safety

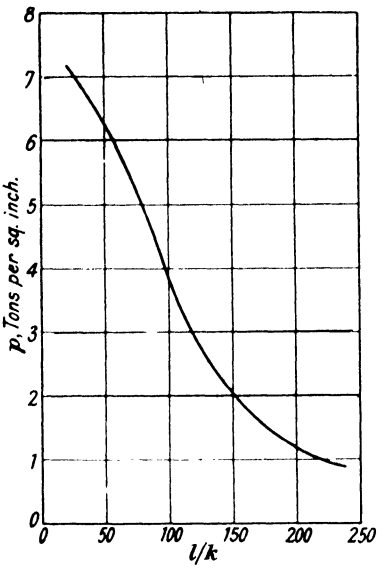

FIG. 7.7.

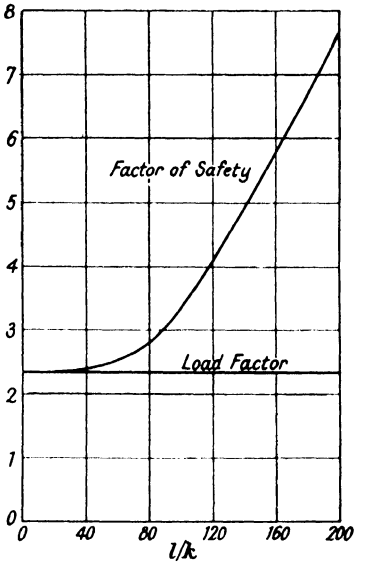

FIG. 7.8.

instead of a constant load factor very different design curves would be used. Fig. 7.9 shows the present standard curve with a constant load factor of 2·36 and curves plotted from the same formula when the factor of safety is kept constant. Two such curves are given, the factors of safety corresponding to those in actual struts designed as at present with ratios of 20 and 200 respectively.

7.10. Members with combined loads.—Any member carrying a lateral load will deflect under such load, the amount depending upon the magnitude of the load and the flexural rigidity of the member. If in addition an axial thrust is applied to the member, it is in the condition of a strut having an initial curvature and the bending moment due to the axial load will still further increase the deflection. In cases where the flexural rigidity is large compared with the loads it is often sufficiently accurate to determine the deflection Δ due to lateral loads and to add to the bending moment produced by such loads a term $P\Delta$ where P is the axial load. The stress is then found from the net bending moment in the usual way.

In some cases however, notably in aircraft construction, the members

are so flexible that determination of the stress in this way would result in serious error and more accurate treatment is necessary. The

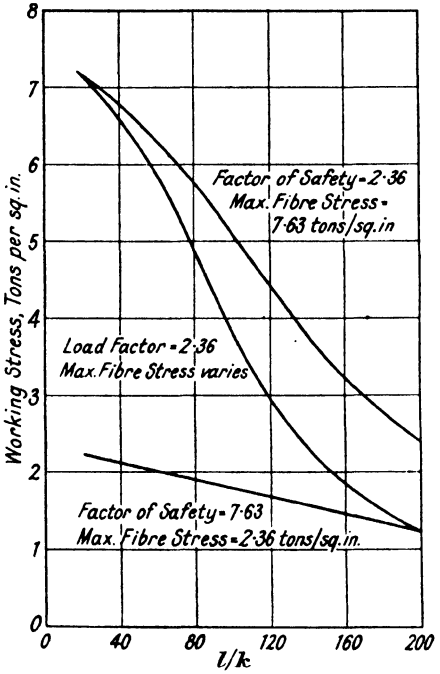

FIG. 7.9.

methods of dealing with such cases will be described in the succeeding paragraphs.

7.11. The pin-jointed strut with a uniform lateral load.—Let AB in Fig. 7.10 be a pin-jointed member carrying an axial load P and a uniformly distributed lateral load of intensity w. Take an origin at O,

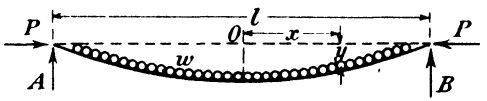

FIG. 7.10.

the centre of the undeflected strut and measure x and y as shown in the diagram.

Then $$M = EI\frac{d^2y}{dx^2} = -Py - \frac{w}{2}\left(\frac{l^2}{4} - x^2\right),$$

or $$M + Py = \frac{w}{2}\left(x^2 - \frac{l^2}{4}\right),$$

i.e. $$\frac{d^2M}{dx^2} + P\frac{d^2y}{dx^2} = w.$$

As before, putting $\mu^2=\frac{P}{EI}$, this becomes

$$\frac{d^2M}{dx^2}+\mu^2M=w$$

and the solution is

$$M=A\sin\mu x+B\cos\mu x+\frac{w}{\mu^2}.$$

When $x=\pm\frac{l}{2}$, $M=0$,

therefore $$A\sin\frac{\mu l}{2}+B\cos\frac{\mu l}{2}+\frac{w}{\mu^2}=0$$

and $$-A\sin\frac{\mu l}{2}+B\cos\frac{\mu l}{2}+\frac{w}{\mu^2}=0.$$

From these equations $A=0$; $B=-\frac{w}{\mu^2}\sec\frac{\mu l}{2}$

and so $$M=\frac{w}{\mu^2}\left(1-\cos\mu x\sec\frac{\mu l}{2}\right).$$

The maximum value of the bending moment occurs when $x=0$ and is

$$M_{max}=\frac{w}{\mu^2}\left(1-\sec\frac{\mu l}{2}\right).$$

Substituting for μ^2 and putting $\frac{\pi^2EI}{l^2}=Q$, the Euler critical load, this reduces to

$$M_{max}=\frac{8M_0}{\pi^2}\frac{Q}{P}\left(1-\sec\frac{\pi}{2}\sqrt{\frac{P}{Q}}\right)$$

where M_0 is the bending moment at the centre due to the lateral loads only, *i.e.* $wl^2/8$.

The maximum stress, at the centre of the member, is then

$$p_f=\frac{8p_bp_e}{\pi^2p}\left(1-\sec\frac{\pi}{2}\sqrt{\frac{p}{p_e}}\right)+p$$

where p_b, p_e and p represent the stress due to lateral bending loads alone, the Euler stress and the intensity of end loading respectively.

A very general problem which arises in aeroplane design is that of calculating the load factor of a given member of this sort when the unit loadings are known. For example, in normal flight a wing spar may carry a distributed load of intensity w and an axial load P. It is required to know by what factor these loads must be increased so as to stress the material to its allowable limit.

If we call this load factor N, then p_b and p will be increased to Np_b and Np; p_f will be the yield stress p_y, and p_e which is only dependent on the size and material of the spar will remain unaltered.

The equation above can then be rewritten

$$p_v=\frac{8p_bp_e}{\pi^2p}\left(1-\sec\frac{\pi}{2}\sqrt{\frac{Np}{p_e}}\right)+Np$$

This can only be solved for N by a process of trial and error and is very inconvenient for calculations of the type under discussion. To overcome this difficulty an approximate formula due to Professor Perry is generally used which will be discussed in a later paragraph.

If we write $\theta=\frac{\pi}{2}\sqrt{\frac{P}{Q}}$ and expand, the maximum bending moment can be written as the series

$$M_{max}=-\frac{8M_0}{\pi^2}\frac{Q}{P}\left(\frac{\theta^2}{|2}+\frac{5\theta^4}{|4}+\frac{61\theta^6}{|6}+\ldots\right),$$

or

$$M_{max}=-\frac{8M_0}{\pi^2}\frac{Q}{P}\left(\frac{\pi^2P}{8Q}+\frac{5\pi^4P^2}{384Q^2}+\ldots\right),$$

i.e.

$$M_{max}=-\left(M_0+\frac{5}{384}\frac{wl^4P}{EI}+\ldots\right)$$

The first term in this series is the bending moment due to lateral loads alone and the second is the deflection at the centre due to these lateral loads multiplied by P. It will be seen therefore that the method indicated in paragraph 7.10, which is often used for stiff members, consists of taking two terms of an infinite series. If P is small compared with Q the third term is very small and can be justifiably neglected, but in most aeroplane work this is not the case, the factored load NP often being a big fraction of the value of Q.

7.12. Pin-jointed strut with a concentrated lateral load.—Let AB

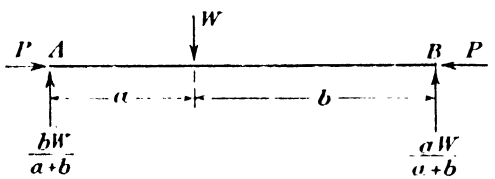

FIG. 7.11.

be a pin-jointed strut under an end load P and a concentrated lateral load W.

Let the dimensions be as in Fig. 7.11.

If the origin be taken at A we have for any point from $x=0$ to $x=a$

$$EI\frac{d^2y}{dx^2}+Py=-\left(\frac{b}{a+b}\right)xW.$$

The solution of this is

$$y=A_1\sin\mu x+B_1\cos\mu x-\frac{W}{P}\left(\frac{b}{a+b}\right)x,$$

where $\mu^2=\dfrac{P}{EI}$.

Since $y=0$ when $x=0$, $B_1=0$.

At $x=a$ we have

$$y_W=A_1 \sin \mu a-\frac{W}{P}\frac{ab}{a+b}.$$

By taking the origin at B we have when $x=b$, $y_W=$ a similar expression with a and b interchanged, derived from the second span,

therefore $$A_1 \sin \mu a-\frac{W}{P}\frac{b}{a+b}a=A_2 \sin \mu b-\frac{W}{P}\frac{a}{a+b}b \quad . \quad . \quad . \quad (1)$$

The two values of $\dfrac{dy}{dx}$ are equal and opposite since W is approached from opposite sides and so

$$\mu A_1 \cos \mu a-\frac{W}{P}\frac{b}{a+b}=-\left\{\mu A_2 \cos \mu b-\frac{W}{P}\frac{a}{a+b}\right\} \quad . \quad . \quad (2)$$

Hence, from (1) and (2)

$$\frac{A_1}{\sin \mu b}=\frac{A_2}{\sin \mu a}=\frac{W/P}{\mu \sin \mu(a+b)};$$

from $x=0$ to $x=a$

$$y=\frac{W}{P}\frac{\sin \mu b}{\mu \sin \mu(a+b)} \sin \mu x-\frac{W}{P}\left(\frac{b}{a+b}\right)x,$$

$$\frac{d^2y}{dx^2}=-\mu^2\frac{W}{P}\frac{\sin \mu b}{\mu \sin \mu(a+b)} \sin \mu x$$

and $$M=EI\frac{d^2y}{dx^2}=-\frac{W \sin \mu b}{\mu \sin \mu(a+b)} \sin \mu x.$$

At $x=a$ $$M=-\frac{W \sin \mu a \sin \mu b}{\mu \sin \mu(a+b)}.$$

In the special case when the load is placed at the centre of the member this becomes

$$M_{max}=-\frac{W}{2\mu} \tan \frac{\mu l}{2}$$

since $a=b=\dfrac{l}{2}$.

Substituting for μ this reduces to the well-known result

$$M_{max}=-\frac{W}{2}\sqrt{\frac{EI}{P}} \tan \frac{l}{2}\sqrt{\frac{P}{EI}}.$$

As before, putting M_0 for the bending moment due to the lateral load alone, *i.e.* $Wl/4$ and Q for the Euler crippling load of the member, the equation can be written

$$M_{max}=-\frac{2M_0}{\pi}\sqrt{\frac{Q}{P}} \tan \frac{\pi}{2}\sqrt{\frac{P}{Q}},$$

or using the same symbols for stress as before,

$$p_f=\frac{2p_b}{\pi}\sqrt{\frac{\bar{p}_e}{p}}\tan\frac{\pi}{2}\sqrt{\frac{\bar{p}}{p_e}}+p.$$

7.13. Strut with end couples.—In Fig. 7.12 AB is a pin-jointed strut with terminal couples $-M_A$ and $-M_B$ as shown. Taking the origin at A we have

$$M+Py+M_A+\frac{x}{l}(M_B-M_A)=0$$

or

$$\frac{d^2M}{dx^2}+\mu^2M=0.$$

The solution of this is

$$M=A\sin\mu x+B\cos\mu x.$$

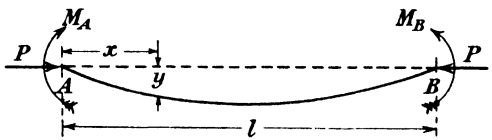

FIG. 7.12.

When $x=0$ and l, M is $-M_A$ and $-M_B$ respectively. Substituting these values we obtain

$$A=M_A\cot\mu l-M_B\operatorname{cosec}\mu l,$$
$$B=-M_A.$$

For the maximum bending moment $\frac{dM}{dx}=0$,

i.e.

$$\tan\mu x_0=\frac{A}{B}=\frac{M_B\operatorname{cosec}\mu l-M_A\cot\mu l}{M_A},$$

where x_0 is the position of the maximum bending moment.

Then $M_{max}=(M_A\cot\mu l-M_B\operatorname{cosec}\mu l)\sin\mu x_0-M_A\cos\mu x_0$

i.e. $M_{max}=-M_A(\tan\mu x_0\sin\mu x_0+\cos\mu x_0)$

$=-M_A\sec\mu x_0.$

Now $\sec^2\mu x_0=1+\tan^2\mu x_0=1+\left(\frac{M_B\operatorname{cosec}\mu l-M_A\cot\mu l}{M_A}\right)^2,$

from which

$$M_{max}=-M_A\sec\mu x_0=-\sqrt{(M_A^2+M_B^2)\operatorname{cosec}^2\mu l-2M_AM_B\operatorname{cosec}\mu l\cot\mu l}$$

When $M_A=M_B=M_0$ this becomes

$$M_{max}=-M_0\sec\frac{\mu l}{2}.$$

7.14. Pin-jointed strut with two lateral loads.—In testing beams it is convenient to adopt the four-point system shown in Fig. 7.13 for the application of lateral loads.

The member AB is a pin-jointed bar of length $2l$ subjected to an axial load P and having two lateral loads, each of magnitude W, symmetrically applied about the centre of AB and separated by a distance $2kl$.

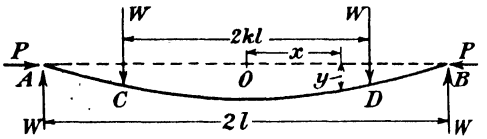

FIG. 7.13.

Taking an origin at the centre of the undeflected bar and measuring x and y as shown, we have :—

For the central part of the bar between O and D,

$$EI\frac{d^2y}{dx^2}+Py=-Wl(1-k)$$

or
$$\frac{d^2y}{dx^2}+\mu^2y=-\frac{Wl(1-k)}{EI}.$$

The solution of this is

$$y=A\sin\mu x+B\cos\mu x-\frac{Wl(1-k)}{P}$$

and so
$$\frac{dy}{dx}=\mu(A\cos\mu x-B\sin\mu x). \quad . \quad . \quad . \quad . \quad . \quad . \quad . \quad (1)$$

When $x=0$, $\frac{dy}{dx}=0$ and so $A=0$;

then
$$M=EI\frac{d^2y}{dx^2}=-EI\mu^2B\cos\mu x=-PB\cos\mu x. \quad . \quad . \quad . \quad (2)$$

Between D and B

$$EI\frac{d^2y}{dx^2}+Py=-W(l-x)$$

or
$$\frac{d^3y}{dx^3}+\mu^2\frac{dy}{dx}=\frac{W}{EI}.$$

The solution of this is

$$\frac{dy}{dx}=C\sin\mu x+D\cos\mu x+\frac{W}{P} \quad . \quad . \quad . \quad . \quad . \quad (3)$$

or
$$M=EI\frac{d^2y}{dx^2}=\mu EI(C\cos\mu x-D\sin\mu x). \quad . \quad . \quad . \quad . \quad (4)$$

When $x=l$, $M=0$ and so $C=D\tan\mu l$.

Since the slope at D is continuous we have, from (1) and (3),

$$-\mu B\sin\mu kl=D(\tan\mu l\sin\mu kl+\cos\mu kl)+\frac{W}{P}$$

or
$$-\mu B=D(\tan\mu l+\cot\mu kl)+\frac{W}{P}\operatorname{cosec}\mu kl. \quad . \quad . \quad (5)$$

Again, the bending moments at D are the same, hence from (2) and (4)

$$-\mu B \cos \mu kl = D(\tan \mu l \cos \mu kl - \sin \mu kl),$$

i.e.

$$-\mu B = D(\tan \mu l - \tan \mu kl). \quad . \quad . \quad . \quad . \quad . \quad . \quad . \quad (6)$$

From (5) and (6)

$$D = -\frac{W}{P} \cos \mu kl.$$

The maximum bending moment is at O and is $-\mu^2 EIB$ and from (6) we obtain

$$M_{max} = \frac{W}{\mu}\left[\tan \frac{\pi}{2}\sqrt{\frac{P}{Q}} - \tan \frac{k\pi}{2}\sqrt{\frac{P}{Q}}\right]\cos \frac{k\pi}{2}\sqrt{\frac{P}{Q}}.$$

Since the bending moment at the centre due to lateral loads alone is

$$M_0 = -Wl(1-k)$$

we can write

$$M_{max} = \frac{-M_0}{(1-k)\frac{\pi}{2}\sqrt{\frac{P}{Q}}}\left[\tan \frac{\pi}{2}\sqrt{\frac{P}{Q}} - \tan \frac{k\pi}{2}\sqrt{\frac{P}{Q}}\right]\cos \frac{k\pi}{2}\sqrt{\frac{P}{Q}}. \quad . \quad . \quad (7)$$

7.15. Encastré strut with a uniform lateral load.—When the ends of the member are completely restrained in direction we have, with the same notation as in paragraph 7.11 and Fig. 7.10,

$$M + Py = \frac{w}{2}\left(x^2 - \frac{l^2}{4}\right) + M',$$

where M′ is the fixing moment at the ends,

so

$$\frac{d^2M}{dx^2} + \mu^2 M = w,$$

the solution of which is

$$M = A \sin \mu x + B \cos \mu x + \frac{w}{\mu^2}.$$

When

$$x = \pm\frac{l}{2}, \quad M = M'$$

and these conditions give

$$A = 0 \quad \text{and} \quad B = \left(M' - \frac{w}{\mu^2}\right)\sec \frac{\mu l}{2};$$

therefore

$$M = \left(M' - \frac{w}{\mu^2}\right)\sec \frac{\mu l}{2} \cos \mu x + \frac{w}{\mu^2}.$$

The shearing force at any point is

$$\frac{dM}{dx} = -\mu\left(M' - \frac{w}{\mu^2}\right)\sec \frac{\mu l}{2} \sin \mu x$$

which is $\frac{wl}{2}$ when $x = \frac{l}{2}$.

Hence

$$M' = \frac{w}{\mu^2} - \frac{wl}{2\mu} \cot \frac{\mu l}{2}.$$

At the centre the maximum bending moment is

$$M_{max}=B+\frac{w}{\mu^2}$$
$$=\frac{wEI}{P}-\frac{wl}{2\mu}\operatorname{cosec}\frac{\mu l}{2},$$

which can be written

$$M_{max}=M_0\left\{\frac{24}{\pi^2}\frac{Q}{P}-\frac{12}{\pi}\sqrt{\frac{Q}{P}}\operatorname{cosec}\frac{\pi}{2}\sqrt{\frac{P}{Q}}\right\}.$$

7.16. Encastré strut with a central lateral load.—With the notation of paragraph 7.12 and Fig. 7.11, when $a=b=l/2$ we have, taking the origin at the centre,

$$EI\frac{d^2y}{dx^2}+Py=M'-\frac{W}{2}\left(\frac{l}{2}-x\right)$$

or

$$\frac{d^2y}{dx^2}+\mu^2y=\frac{M'}{EI}-\frac{W}{2EI}\left(\frac{l}{2}-x\right).$$

The solution of this is

$$y=A\sin\mu x+B\cos\mu x+\frac{1}{P}\left\{M'-\frac{W}{2}\left(\frac{l}{2}-x\right)\right\}$$

and

$$\frac{dy}{dx}=\mu(A\cos\mu x-B\sin\mu x)+\frac{W}{2P}.$$

When $x=0$, $\frac{dy}{dx}=0$ and so $A=-\frac{W}{2\mu P}$;

when $x=\frac{l}{2}$, $\frac{dy}{dx}=0$ and so $B=\frac{W}{2\mu P}\left(\operatorname{cosec}\frac{\mu l}{2}-\cot\frac{\mu l}{2}\right)$;

when $x=\frac{l}{2}$, $y=0$,

so

$$0=-\frac{W}{2\mu P}\left(\operatorname{cosec}\frac{\mu l}{2}-\cot\frac{\mu l}{2}\right)+\frac{M'}{P},$$

or

$$M'=\frac{W}{2\mu}\left(\operatorname{cosec}\frac{\mu l}{2}-\cot\frac{\mu l}{2}\right)=\frac{W}{2\mu}\tan\frac{\mu l}{4}.$$

The bending moment at the centre is

$$-Py+M'-\frac{Wl}{4}$$

which is

$$-PB \text{ or } -\frac{W}{2\mu}\tan\frac{\mu l}{4}.$$

Hence the bending moment has the same numerical value at the ends and the centre and

$$M_{max}=\pm\frac{W}{2\mu}\tan\frac{\mu l}{4}$$
$$=M_0\left\{\frac{4}{\pi}\sqrt{\frac{Q}{P}}\tan\frac{\pi}{4}\sqrt{\frac{P}{Q}}\right\}.$$

It should be noted that M_0 is $Wl/8$ for an encastré beam with a central lateral load. Q as before $=\frac{\pi^2 EI}{l^2}$.

7.17. Perry's approximation for a pin-jointed strut with uniform lateral load.—The secant formula given in paragraph 7.11 is an inconvenient one if it is desired to calculate the load factor from a knowledge of unit loads and the following approximation due to Professor Perry is much easier to apply. The results given by it are very close to the exact results of the secant formula except when the end compression approaches the Euler critical load for the member; this case will be considered later. It is assumed that the deflected form of the member is a cosine curve, so that if the central deflection is c we may write

$$y=c\cos\frac{\pi x}{l}, \quad \ldots\ldots\ldots \quad (1)$$

where x, y, etc., are as in Fig. 7.10.

Then
$$M_x=EI\frac{d^2y}{dx^2}=M'_x-Py, \quad \ldots\ldots\ldots \quad (2)$$

where M'_x is the bending moment at x due to the lateral load alone.

Substituting for d^2y/dx^2 from (1) we have

$$-\frac{EI\pi^2}{l^2}c\cos\frac{\pi x}{l}=M'_x-Py$$

or
$$-Qy=M'_x-Py \quad \text{where} \quad Q=\pi^2EI/l^2;$$

so
$$y=\frac{M'_x}{P-Q}.$$

Then in (2)

$$M_x=M'_x+\left(\frac{P}{Q-P}\right)M'_x=\left(\frac{Q}{Q-P}\right)M'_x.$$

The maximum bending moment at the centre of the member is

$$M_{max}=M_0\left(\frac{Q}{Q-P}\right), \quad \ldots\ldots\ldots \quad (3)$$

where M_0 is the central moment due to the lateral load alone $=\frac{wl^2}{8}$.

The maximum fibre stress is then

$$p_f=\frac{wl^2h}{8I}\left(\frac{Q}{Q-P}\right)+\frac{P}{A},$$

where A is the cross-sectional area of the strut and h is the distance from the neutral axis of the section to the outside compressive fibre. If we write p_b for the bending stress due to the lateral load alone, p for the end load per unit area and p_e for the Euler stress as before, we can, if the material is to be stressed to the yield point p_y, express the formula as

$$p_y=p_b\left(\frac{p_e}{p_e-p}\right)+p.$$

In general, if w and P represent unit loads carried by the member, the load factor N which will cause a stress p_v in the material is found from the equation

$$p_v = \frac{Nwl^2}{8}\frac{h}{I}\left(\frac{Q}{Q-NP}\right)+\frac{NP}{A}. \quad \ldots\ldots\ldots \quad (4)$$

This is a simple quadratic which is readily solved and the Perry equation is therefore always to be preferred to the secant formula for this class of calculation.

7.18. Approximate formulas for laterally loaded struts.—It has been shown that an approximate formula for the laterally loaded strut when the load is uniformly distributed can be obtained in the form

$$M_{max} = M_0\left(\frac{Q}{Q-P}\right).$$

If we modify this equation by the introduction of a constant C so that we have

$$M_{max} = M_0\left(\frac{Q}{Q-CP}\right)$$

it is possible by a suitable choice of constants to obtain very good approximations to other cases of lateral loads acting upon struts.* Table 7.5 gives the values of C and the errors involved by the use of these values.

TABLE 7.5.

Ends	Lateral load	C	Range of values Q/P examined	Maximum error per cent.	Remarks
Pin	Uniform	1·000	—	—	Perry formula, para. 7.17
Pin	Central	0·894	2·0–9·0	1·0	When $\frac{Q}{P}=1{\cdot}5$, error = 6 per cent.
Pin	Constant B.M.	1·110	2·0–9·0	2·1	—
Encastré	Uniform	0·276	1·0–9·0	1·0	Centre of bay
		0·172	1·0–9·0	1·0	Fixing moment
Encastré	Central	0·212	1·0–9·0	0·3	Centre and fixing moments
Pin	Two equal loads spaced symmetrically	1·064	2·0–9·0	1·0	$k=\frac{1}{3}$ in para. 7.14
		1·030	2·0–9·0	1·0	$k=\frac{1}{5}$
		1·000	2·0–9·0	1·0	$k=\frac{1}{4}$

7.19. Members with combined bending and end tensions.—In the case of a member subjected to bending and axial tension the maximum deflection at the centre is less than would be produced by the lateral loads alone and the approximation referred to in paragraph 7.10 would overestimate the stress.

* "Some Approximate Solutions for Laterally Loaded Struts," A. J. S. Pippard, "Aircraft Engineering," May, 1920, p. 149.

In the exact solution of these problems the sign of P in the differential equation is reversed and the solution appears in terms of hyperbolic instead of trigonometrical functions. As an example, consider the case of a pin-jointed bar with a lateral uniform load and an end tension P. Then as in paragraph 7.11 we obtain

$$\frac{d^2\mathrm{M}}{dx^2}-\mathrm{P}\frac{d^2y}{dx^2}=w$$

and the solution of this is

$$\mathrm{M}=\mathrm{A}\sinh\mu x+\mathrm{B}\cosh\mu x-\frac{w}{\mu^2}.$$

When $$x=\pm\frac{l}{2},\quad \mathrm{M}=0.$$

$\therefore$ $$\mathrm{A}\sinh\frac{\mu l}{2}+\mathrm{B}\cosh\frac{\mu l}{2}-\frac{w}{\mu^2}=0,$$

and $$-\mathrm{A}\sinh\frac{\mu l}{2}+\mathrm{B}\cosh\frac{\mu l}{2}-\frac{w}{\mu^2}=0.$$

From these equations $\mathrm{A}=0$ and $\mathrm{B}=\frac{w}{\mu^2}\operatorname{sech}\frac{\mu l}{2}$.

The bending moment is

$$\mathrm{M}=\frac{w}{\mu^2}\left(\operatorname{sech}\frac{\mu l}{2}\cosh\mu x-1\right).$$

This is a maximum when $x=0$ and its value is

$$\mathrm{M}_{\max}=\frac{w}{\mu^2}\left(\operatorname{sech}\frac{\mu l}{2}-1\right).$$

Other cases of laterally loaded ties can be solved in the same way.

7.20. Initially curved strut with end couples.—In the practical design of compression members allowance must be made for imper-

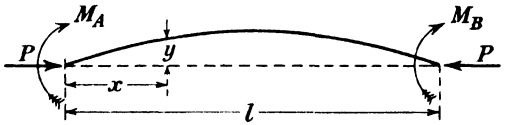

FIG. 7.14.

fections in material and workmanship which may be expected to exist in the finished structure. It was pointed out in paragraph 7.9, where the safe axial loads for pin-ended struts are tabulated, that these imperfections can be represented by an initial curvature of the axis of the member. In actual structures very few members satisfy the requirement that the ends shall be free from restraint and it is necessary, therefore, to consider the case of the initially curved strut subjected to end couples.

Suppose a strut, of uniform cross-section as shown in Fig. 7.14, to

have ends which are fixed in position and to have an initial curvature defined by the equation

$$y'=\epsilon \sin \frac{\pi x}{l}. \quad \ldots\ldots\ldots \quad (1)$$

It is acted on by an axial compressive load P and clockwise end couples M_A and M_B in the same plane as the curvature. The bending moment at any point at a distance x from the origin is

$$M_x=M_A-(M_A+M_B)\frac{x}{l}-Py$$

or

$$EI\frac{d^2(y-y')}{dx^2}=M_A-(M_A+M_B)\frac{x}{l}-Py \quad \ldots\ldots\ldots \quad (2)$$

where I is the relevant second moment of area of the strut.

The solution of this equation is

$$y=\frac{M_A}{P}\left\{\frac{l-x}{l}-\frac{\sin \mu(l-x)}{\sin \mu l}\right\}+\frac{M_B}{P}\left\{\frac{\sin \mu x}{\sin \mu l}-\frac{x}{l}\right\}+\frac{\epsilon\pi^2}{\pi^2-\mu^2l^2}\sin\frac{\pi x}{l} \quad (3)$$

where

$$\mu^2=\frac{P}{EI}.$$

Upon differentiating this expression the slope at any point is found to be

$$\frac{dy}{dx}=\frac{M_A}{Pl}\left\{\frac{2\alpha\cos 2\alpha\left(1-\frac{x}{l}\right)}{\sin 2\alpha}-1\right\}+\frac{M_B}{Pl}\left\{\frac{2\alpha\cos\frac{2\alpha x}{l}}{\sin 2\alpha}-1\right\}+\frac{\epsilon\pi^3}{l(\pi^2-4\alpha^2)}\cos\frac{\pi x}{l} \quad (4)$$

where

$$2\alpha=\mu l.$$

Adopting the sign convention that clockwise rotations are positive, the *changes* of slope, θ_A and θ_B at the ends of the strut are given by

$$\theta_A=-\frac{M_A}{Pl}(2\alpha\cot 2\alpha-1)-\frac{M_B}{Pl}(2\alpha\operatorname{cosec}2\alpha-1)-\frac{4\alpha^2\epsilon\pi}{l(\pi^2-4\alpha^2)},$$

$$\theta_B=-\frac{M_A}{Pl}(2\alpha\operatorname{cosec}2\alpha-1)-\frac{M_B}{Pl}(2\alpha\cot 2\alpha-1)+\frac{4\alpha^2\epsilon\pi}{l(\pi^2-4\alpha^2)}.$$

Making use of the Berry functions * $f(\alpha)$ and $\phi(\alpha)$ these expressions can be written in the form

$$\theta_A=\frac{M_Al}{3EI}\phi(\alpha)-\frac{M_Bl}{6EI}f(\alpha)-\frac{4\alpha^2\epsilon\pi}{l(\pi^2-4\alpha^2)} \quad \ldots\ldots \quad (5)$$

and

$$\theta_B=-\frac{M_Al}{6EI}f(\alpha)+\frac{M_Bl}{3EI}\phi(\alpha)+\frac{4\alpha^2\epsilon\pi}{l(\pi^2-4\alpha^2)} \quad \ldots\ldots \quad (6)$$

where

$$f(\alpha)=\frac{6(2\alpha\operatorname{cosec}2\alpha-1)}{4\alpha^2} \quad \text{and} \quad \phi(\alpha)=\frac{3(1-2\alpha\cot 2\alpha)}{4\alpha^2}.$$

* See Paragraph 8.5.

The solution of equations (5) and (6) gives

$$M_A=\frac{6EI}{l}(2Y\theta_A+X\theta_B-Z) \quad . \quad . \quad . \quad . \quad . \quad . \quad (7)$$

and

$$M_B=\frac{6EI}{l}(X\theta_A+2Y\theta_B+Z), \quad . \quad . \quad . \quad . \quad . \quad . \quad (8)$$

where

$$X=\frac{f(\alpha)}{4\phi^2(\alpha)-f^2(\alpha)},$$

$$Y=\frac{\phi(\alpha)}{4\phi^2(\alpha)-f^2(\alpha)}$$

and

$$Z=\frac{4\alpha^2\epsilon\pi}{l(\pi^2-4\alpha^2)}(X-2Y).$$

These expressions, which are more general forms of the slope deflection equations derived in paragraph 3.13, will be used later in the stress analysis of frames having members which cannot be considered perfectly straight and where the axial loads are sufficiently great to affect appreciably the flexure of the members.

This stress analysis will enable the magnitudes of the end couples and of the axial loads acting on the members of the frame to be determined. The next step in design procedure is the determination of the maximum total stress developed in each member. For this, the distribution of bending stress in an initially curved strut subjected to axial load and end couples must be studied.

From equations (2) and (3) the bending moment, and therefore the bending stress, at any section of such a member may be obtained and, as in paragraph 7.13, the maximum values determined. A slight variation on this method has however been found useful.

It has been convenient so far to assume the initial shape of the axis of the member, which represents its imperfections, to be a sine curve. There is, however, nothing axiomatic about that curve and the stresses in the member would not be seriously affected by a slight change in its initial shape so long as the versed sine remained the same.

In calculating the safe axial loads for pin-ended struts in paragraph 7.9, the initial shape was taken to be a cosine curve. If we transfer the origin of co-ordinates from the centre of the member to one end to agree with the work of the present paragraph and substitute for the value of c_o given in paragraph 7.9 we can write the equation of initial curvature in the form

$$y=0{\cdot}003\frac{lk}{a}\sin\frac{\pi x}{l}. \quad . \quad . \quad . \quad . \quad . \quad . \quad . \quad (9)$$

This is compared, in Table 7.6, with the shape taken by an originally straight member when subjected to a uniform moment M′ such that

$$M'=0{\cdot}024\frac{kEI}{al}. \quad . \quad . \quad . \quad . \quad . \quad . \quad . \quad (10)$$

TABLE 7.6.

COMPARISON OF SHAPES FOR INITIAL CURVATURE OF STRUT

x		$\frac{ya}{lk}$	
		Sine curve, equation (9)	Beam under uniform moment, equation (10)
0	l	0	0
$l/8$	$7l/8$	0·00115	0·00131
$l/4$	$3l/4$	0·00212	0·00225
$3l/8$	$5l/8$	0·00280	0·00282
$\frac{l}{2}$		0·00300	0·00300

It is clear that no serious differences in the final results will arise if the latter shape instead of the sine curve is assumed to represent the imperfections in the member.

The shape of the initially curved strut under examination when subjected to an axial end load P and end couples M_A and M_B tending to increase the curvature of the member as in Fig. 7.15 will therefore

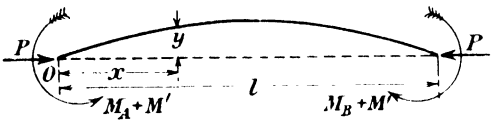

FIG. 7.15.

be, for all practical purposes, indistinguishable from that of an originally straight member of the same cross-section, subjected to the same axial end load P and to end couples M_A+M' and M_B+M' as in Fig. 7.15. The bending moment in the latter at a section a distance x from the origin is, from equations (2) and (3),

$$M'_x=(M_A+M')\frac{\sin \mu(l-x)}{\sin \mu l}+(M_B+M')\frac{\sin \mu x}{\sin \mu l}$$

and the bending moment at the corresponding section of the initially curved member is

$$M_x=(M_A+M')\frac{\sin \mu(l-x)}{\sin \mu l}+(M_B+M')\frac{\sin \mu x}{\sin \mu l}-M', \quad . \quad . \quad . \quad (11)$$

since it was actually unstressed before the application of the axial end load P and end couples M_A and M_B. If the maximum bending moment in the initially curved member occurs at the section x

$$(M_A+M')\cos\mu(l-x)-(M_B+M')\cos\mu x=0$$

or
$$\tan\mu x=\operatorname{cosec}\mu l\left(\frac{M_B+M'}{M_A+M'}-\cos\mu l\right) \quad . \quad . \quad . \quad . \quad . \quad (12)$$

Dividing equation (11) throughout by the relevant modulus of section of the strut we obtain

$$\frac{f_x+f'}{f_A+f'}=\frac{\sin\mu x}{\sin\mu l}\frac{f_B+f'}{f_A+f'}+\frac{\sin\mu(l-x)}{\sin\mu l} \quad . \quad . \quad . \quad . \quad . \quad (13)$$

where f_x, f', f_A, etc., are the extreme fibre stresses developed in the section by the moments M_x, M', M_A, etc.

In designing a member it is essential that the maximum total stress should not rise above a certain limit p'. If the compressive axial load per unit area is $p=\frac{P}{A}$ where A is the cross-sectional area of the member

$$p+f_x\not> p'.$$

When the maximum total stress reaches the limit it follows from equation (13) that

$$\frac{p'-p+f'}{f_A+f'}=\sin\mu x\operatorname{cosec}\mu l\left(\frac{f_B+f'}{f_A+f'}+\sin\mu l\cot\mu x-\cos\mu l\right) \quad . \quad (14)$$

For any ratio $\frac{f_B+f'}{f_A+f'}$ it is possible to calculate from equations (12) and (14) the value of the maximum end bending stress f_A which can be applied to a strut of any slenderness ratio carrying any axial load without raising the maximum stress at any point beyond a predetermined value p'.

These equations are much too complex for use in design, but it is a simple matter to present the results obtained from them in the form of families of curves. If M_A is always taken as the numerically greater end couple the ratio f_B/f_A must always lie within the limits ±1. In Fig. 7.16 are plotted the values of f_A, calculated from these equations, which cause a maximum total stress of 8 tons per square inch for any ratio of f_B/f_A and for a number of values of the slenderness ratio l/k when the axial load is 6 tons per square inch and the imperfections of the members are represented by an initial curvature having a versed sine of $0{\cdot}0015\frac{lk}{a}$. A more convenient way of setting out the information for design purposes is shown in Fig. 7.17. If a compression member in a structure is subjected to an axial load of 6 tons per square inch and to anti-clockwise end couples, one being 0·6 times the other, then the ratio $\frac{f_B}{f_A}=-0{\cdot}6$ and Fig. 7.17 shows that, if the slenderness ratio of the member is 90, the maximum total stress will not rise above 8 tons per square inch so long as f_A, the end bending stress due to the greater end couple, does not rise above 1·33 tons per square inch. It must not be concluded that the result in this example would have been

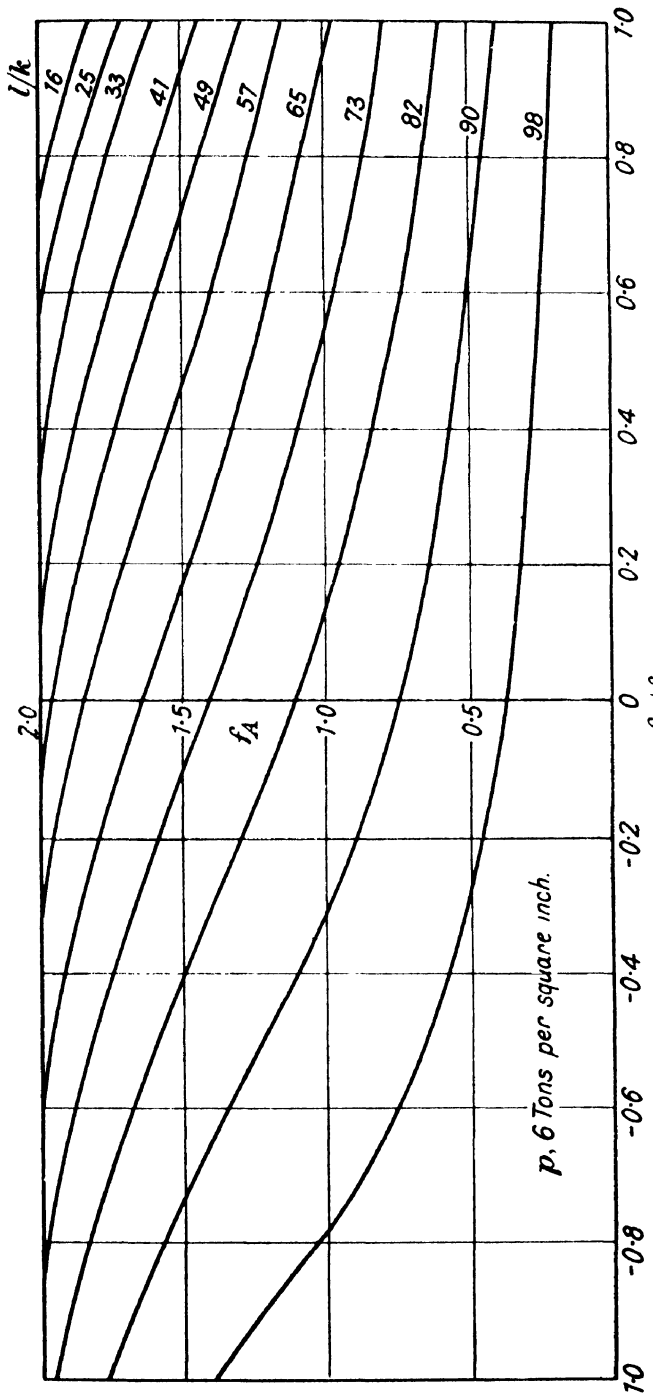
l/k
16
25
33
41
49
57
65
73
82
90
98
2·0
1·5
1·0
0·5
f_A
p, 6 Tons per square inch.
1·0
0·8
0·6
0·4
0·2
0
-0·2
-0·4
-0·6
-0·8
-1·0
f_B/f_A

FIG. 7.16.

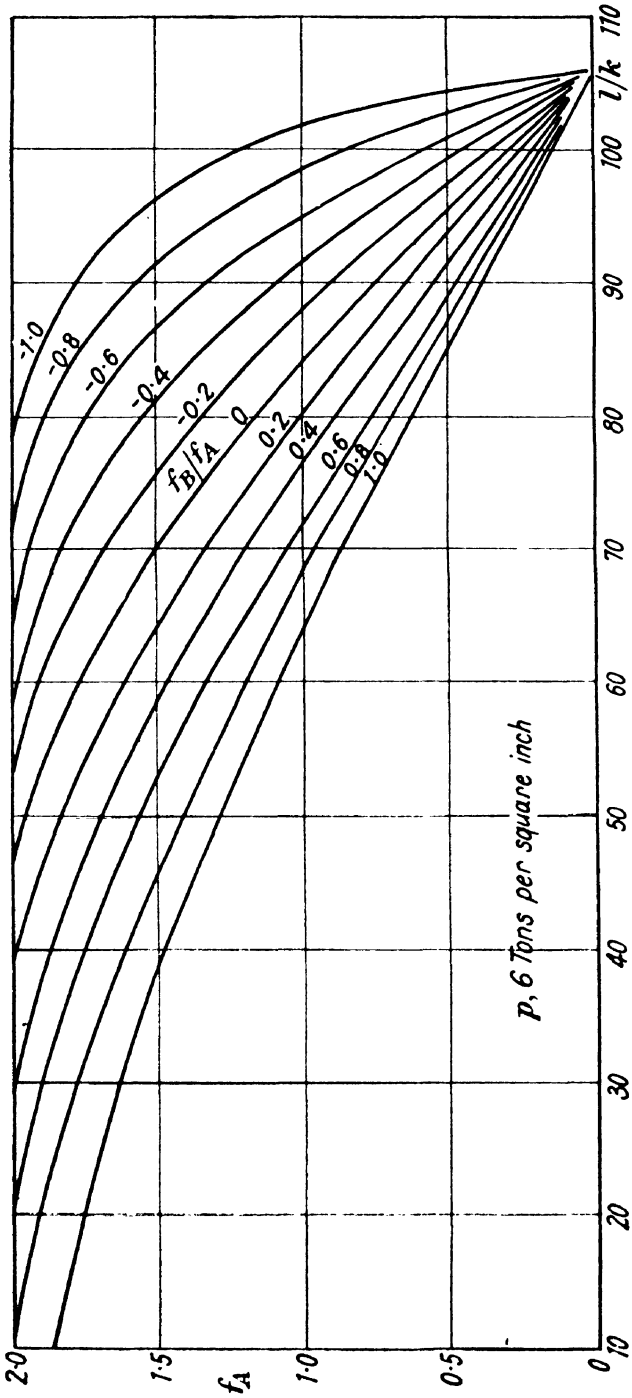
2·0
1·5
1·0
0·5
0
f_A
10
20
30
40
50
60
70
80
90
100
110
l/k
P, 6 Tons per square inch
f_B/f_A
-1·0
-0·8
-0·6
-0·4
-0·2
0
0·2
0·4
0·6
0·8
1·0

Fig. 7.17.

different if both end couples, M_A and M_B, had acted in a clockwise direction. The designer is unaware of the nature of the imperfections which will be found in the member and he must, therefore, assume that they are such as to give rise to the worst stress conditions. This assumption is automatically made in the method outlined above.

7.21. Polar diagrams for beams with end thrusts.—Many problems of the type we have dealt with in this chapter can be solved very neatly by the aid of a polar diagram originally due to J. Ratzersdorfer * but discovered independently by H. B. Howard.†

The differential equation for any laterally loaded strut is

$$EI\frac{d^2y}{dx^2}=M=-Py+M', \quad \ldots\ldots\ldots \quad (1)$$

where M′ is the bending moment due to the lateral loads and end moments.

Differentiating this equation twice and putting $\mu^2=\frac{P}{EI}$ as before, we get for a uniformly distributed lateral load of intensity w

$$\frac{d^2M}{dx^2}+\mu^2M=w.$$

The solution of this can be written either as the sum of a cosine and a sine term as hitherto in this chapter or in the form

$$M=C\cos(\mu x-\epsilon)+\frac{w}{\mu^2}, \quad \ldots\ldots\ldots \quad (2)$$

where C and ϵ are constants of integration replacing the A and B of the former analysis, or

$$m=M-\frac{w}{\mu^2}=C\cos(\mu x-\epsilon) \quad \ldots\ldots\ldots \quad (3)$$

The shearing force S is given by dM/dx so that we have

$$S=-\mu C\sin(\mu x-\epsilon), \quad \ldots\ldots\ldots \quad (4)$$

or in another form by differentiating (1)

$$S=-Pi+S', \quad \ldots\ldots\ldots \quad (5)$$

where i is the slope at the point under consideration and S′ is the apparent shear due to lateral loads and end moments alone.

Since x is a distance, μx is an angle measured in radians and lengths upon the beam can therefore be represented by angles in a polar diagram. In Fig. 7.18 let OZ be any base line and O a pole on it. Draw OX=C

* "The Investigation of Structural Members under Combined Axial and Transverse Loads." Julius Ratzersdorfer. Zeitschrift für Flugtechnik und Motorluftschiffahrt. Heft 7/8. 1930.

† "The Graphical and Analytical Determination of Stresses in Single Span and Continuous Beams under End Compression and Lateral Load with Variation in Shear, Distributed Load and Moment of Inertia." R. & M., No. 1233. Aeronautical Research Committee. H.M.S.O.

at an angle ZOX=ϵ and on OX as diameter describe the circle OAXB. Let ON be any chord of this circle, and let angle ZON=μx.

Then ON=OX cos $\widehat{XON}$=C cos ($\mu x-\epsilon$). Hence ON represents m to the scale to which OX represents C, and if the angles ZOA and ZOB are respectively made equal to μx_1 and μx_2, AXNBO represents the polar diagram for m between the two values of x_1 and x_2.

Again $$XN=C \sin (\mu x-\epsilon)$$

and so XN represents $-S/\mu$ from equation (4). X is termed the apex of the diagram. Positive values of μx will be measured in a clockwise direction from OZ. Positive values of m will be measured into the angle ZOB, *e.g.* OA, ON are positive. Negative values would appear from O outwards from the angle. This will be clear from some of the examples.

If we look along a radius vector in the positive direction, shearing

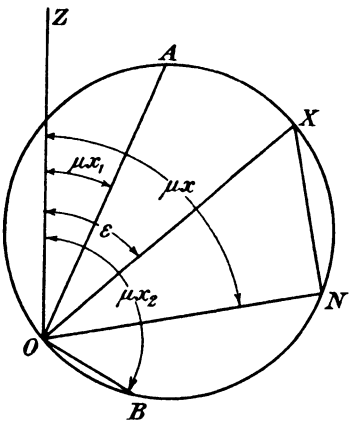

FIG. 7.18.

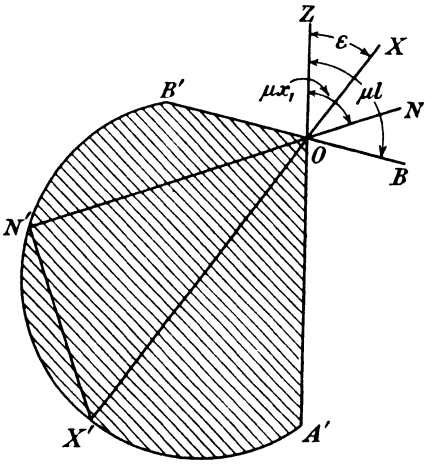

FIG. 7.19.

forces will be positive if measured to the right and negative if measured to the left. Thus the shearing force at x is μ(NX) and looking along ON it is on the left and so is negative.

A few examples will make the method of using these diagrams clear.

Case 1. *Initially straight strut with end couples.*—In the first place consider the case of a strut with end couples as described in paragraph 7.13 and shown in Fig. 7.12. Here, since there are no distributed lateral loads

$$M=C \cos (\mu x-\epsilon);$$

when $\mu x=0$, $M=-M_A$,

and when $\mu x=\mu l$, $M=-M_B$.

In Fig. 7.19 make angle ZOB=μl and mark off OA′ and OB′ equal to M_A and M_B. Since these moments are negative they are measured outwards from the angle ZOB.

Through B′, O and A′ draw a circle of which OX′ is a diameter. Then B′X′A′ is the polar diagram for this case.

The maximum bending moment is OX′ which is negative and angle ZOX$=\epsilon$.

Suppose it is required to know the bending moment and shearing force at a point x_1 from the origin, we make angle ZON$=\mu x_1$ and produce NO to meet the circle at N′. Then the bending moment at x_1 is given by ON′ and the shearing force by μ(N′X′).

The bending moment is negative, since ON′ is in the negative direction: the shearing force is positive since, looking along N′O, *i.e.* the positive direction for moments, the line N′X′ is to the right.

Case 2. *Uniformly loaded beam with positive end couples.*—This case is similar to that shown in Fig. 7.10 but positive end moments M_A and M_B are applied at A and B respectively. Two diagrams are shown in

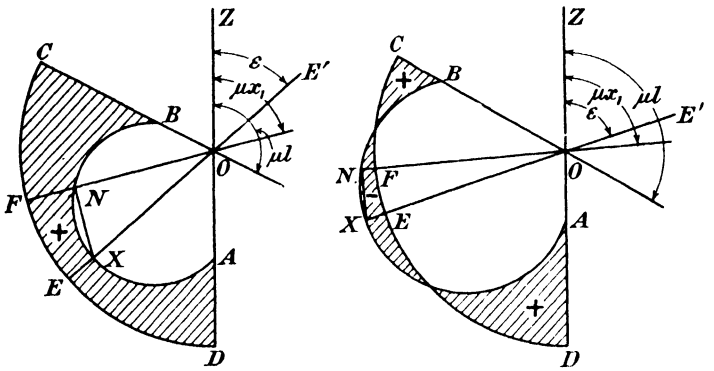

FIG. 7.20.

Fig. 7.20 to illustrate the effect of varying the size of the end moments; the description applies to both.

Here $m=M-\frac{w}{\mu^2}=C\cos(\mu x-\epsilon)$.

Since the term in w is negative, we draw an arc CD in the negative sector with centre at O and of radius w/μ^2.

When $\mu x=0$, $\quad m_A=M_A-\frac{w}{\mu^2}$

and when $\mu x=\mu l$, $\quad m_B=M_B-\frac{w}{\mu^2}$.

Therefore if we set off DA in the positive direction equal to M_A and CB in the positive direction equal to M_B we have

$$OA=M_A-\frac{w}{\mu^2}=m_A$$

and

$$OB=M_B-\frac{w}{\mu^2}=m_B$$

Hence, a circle drawn through B, O and A is the polar diagram for m.

Draw E'OXE through the centre of this circle: OX is then C and angle ZOE' is ϵ. The position of the mathematical maximum or minimum value of M is defined by $\mu x = \epsilon$ and the value of the moment here is EX, which is positive in the first diagram and negative in the second.

Draw any other radius vector ONF whose position is defined by the angle μx_1. Then the bending moment in the beam at a distance x_1 from the origin is FN and the shearing force is $+\mu$(NX). The bending moment is positive in the first diagram and negative in the second; the shearing force is positive in both, since if we look along the positive direction of the vector NX is drawn to the right.

Case 3. *A uniformly loaded beam with a negative fixing couple at one end and a positive fixing couple at the other.*—This case is similar to the last, but the fixing couple at A is now in the opposite direction, *i.e.* it is $-M_A$. That at B is still M_B.

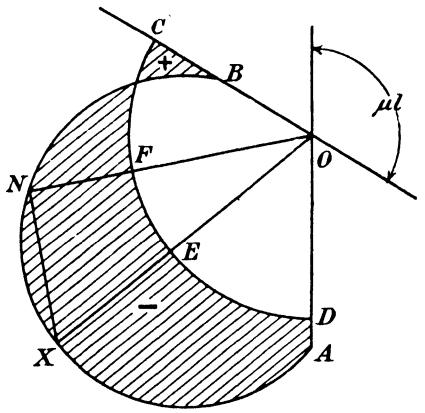

FIG. 7.21.

As in the previous case, the arc CD in Fig. 7.21 is drawn with centre at O and radius w/μ^2.

DA is set off in the negative direction equal to M_A and CB in the positive direction equal to M_B. A circle drawn through AOB completes the diagram as shown. X is the apex, and XE the maximum negative bending moment in the beam.

Case 4. *Beam with a single concentrated load, axial thrust and terminal couples.*—The case is that shown in Fig. 7.11 with the addition of positive terminal couples M_A and M_B at the two supports A and B respectively.

Here $M = C \cos(\mu x - \epsilon)$ with different values of the constants C and ϵ in the two sections into which the beam is divided by the load.

To construct the diagram, mark off OA and OB equal to M_A and M_B along the radii drawn at $\mu x = 0$ and $\mu x = \mu l$ (Fig. 7.22).

From A and B draw AC and BD perpendicular to the radii OA and OB.

Draw the line Y'OY at the angle μa to OZ to represent the position of W on the beam.

On BD take any point h and draw hk perpendicular to OY and of length $\frac{W}{\mu}$.

From k draw a line kX_1 parallel to hB cutting AC in X_1 and from X_1 draw X_1X_2 parallel to hk and cutting BD in X_2.

Then X_1 and X_2 will be the apices of the polar diagrams for the two sections of the beam.

Join OX_1 and OX_2 and describe circles on these lines as diameters, completing the diagram as shown in Fig. 7.22.

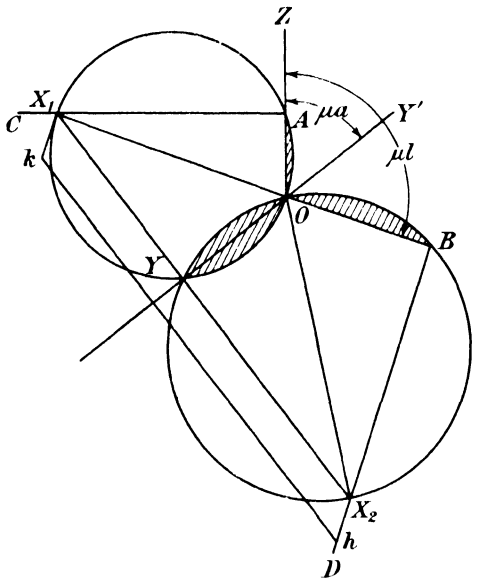

FIG. 7.22.

The circle AOY with apex X_1 relates to the left-hand section of the beam and the circle BOY with apex X_2 relates to the right-hand section.

The conditions at the load point which must be satisfied are:

(1) The bending moment is the same on either side of the load point.
(2) The slope of the beam is the same on either side.
(3) The deflection of the beam is the same whether considered from the left or from the right of the load point.

It will now be shown that the construction given above satisfies these conditions.

In the first place, since OYX_1 and OYX_2 are right-angled triangles, circles drawn on OX_1 and OX_2 as diameters must intersect at Y.

But OY represents the bending moment at the load point whether it be considered from the left-hand or the right-hand section of the beam and so the first condition is satisfied.

Again, it is evident from the construction that

$$X_1X_2=hk=\frac{W}{\mu}.$$

The true shearing force to the left of the load

$$S_L=-(X_1Y)\mu$$

and to the right of the load

$$S_R=+(X_2Y)\mu$$

therefore $$S_R-S_L=\mu(X_2Y+X_1Y)=W.$$

From equation (5) we have

$$S_L+Pi_a=S'_L,$$
$$S_R+Pi'_a=S'_R,$$

where i_a and i'_a are the slopes to left and right of the load,

therefore $$S_R-S_L+P(i'_a-i_a)=S'_R-S'_L.$$

But $S'_R-S'_L$ is the difference of the apparent shearing force in passing through the point and is W. Hence, since

$$S_R-S_L=W,$$
$$i'_a=i_a$$

and the condition of equality of slopes is satisfied.

From equation (1), $$M-M'=-Py$$

and, since neither M nor M′ changes in passing through the load point, the deflection of the beam is the same whether considered to the left or right of the load.

Hence, all conditions are satisfied and the diagram is proved correct.

Case 5. *Initially curved strut with end couples.*—The initially curved strut considered in paragraph 7.20 can be dealt with conveniently by means of a polar diagram.

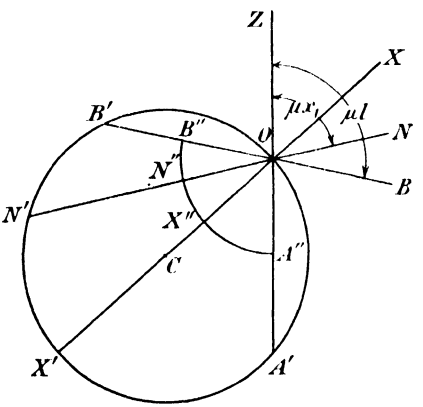

FIG. 7.23.

If the strut is initially curved with a versed sine of $\cdot 003\frac{lk}{a}$ the approximate bending moment at any point due to the application of end couples M_A and M_B and of an axial compressive load P can be found as follows. In Fig. 7.23 mark off OA′ and OB′ equal to M_A+M' and M_B+M' where $M'=\cdot 024kEI/al$ is the uniform moment necessary to produce the initial curvature in the strut. The circle A′X′B′O gives the moment in an originally straight member subjected to end couples M_A+M' and M_B+M'; the bending moment required in the initially curved strut is this moment less the moment M′. Thus the required moment at a point x_1 from the origin is given by the intercept

N'N'' of ON between the circle A'X'B'O and the circle A''X''B'' which is drawn with centre O and radius M'.

If OX' is a diameter of the circle A'X'B'O the maximum bending moment in the initially curved strut will be given by the length of the intercept X'X''. It will be seen that when the centre C of this circle lies on OA' or on OB' or anywhere on the opposite sides of those lines from the position shown in Fig. 7.23 the maximum bending moment will be found at one or other end of the strut. When this occurs the end couples will have completely masked the strut action and there is no reason why the working stress in the strut should be cut down below the value allowed for beams subjected to flexure. The critical values of the end couples which make C lie on OA' or on OB' are therefore of importance.

They are given by the equation

$$\frac{M_B+M'}{M_A+M'}=\cos \mu l.$$

The maximum bending moment in a practical strut will, therefore, occur at the end where the greater couple is applied when the end couples have values defined by this equation or when the greater end couple is equal to M_A and the smaller is less than M_B or when the smaller end couple is equal to M_B and the greater exceeds M_A.

The use of polar diagrams has been extended to the case of continuous girders and to various types of loading. For details of these extensions the reader should consult the paper by Howard referred to at the beginning of this paragraph.

7.22. Derivation of strut formulas from polar diagrams.—The polar diagram provides a useful method for the derivation of formulas for laterally loaded struts geometrically instead of by the more usual methods of the earlier paragraphs in this chapter. This use of the diagram does not need accurate drawing, as when numerical problems are solved graphically; sketches are quite sufficient. The following examples will illustrate the method.

Case 1. *The pin-jointed strut with an eccentric thrust.*—This case is dealt with in paragraph 7.3 and shown in Fig. 7.3. For the present

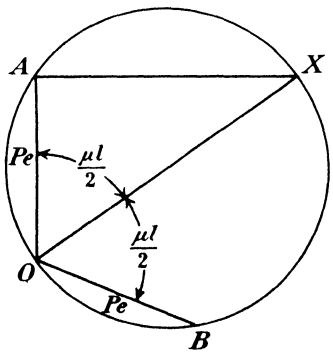

FIG. 7.24.

analysis, however, the origin will be taken at A and not at the centre of the strut as shown in that figure. Since there is no distributed load, $M=m$.

So, at $x=0$ and at $x=L$ the value of m is Pe, and the polar diagram is shown in Fig. 7.24 where $OA=OB=Pe$, and angles AOX and XOB are each equal to $\frac{\mu l}{2}$.

Then $$M_{max}=m_{max}=Pe \sec \frac{\mu l}{2}.$$

Also, from equation (1) of paragraph 7.21.

$$M_{max}=-Py_{max}+Pe,$$

and so at the centre of the bar $y_{max}=e\left(1-\sec \frac{\mu l}{2}\right)$.

Case 2. Strut with an axial thrust and a uniformly distributed load.— This is dealt with in paragraph 7.11 and illustrated in Fig. 7.10. Again however the origin will be taken at A and not at the centre. From equation (3) of paragraph 7.21.

$$m=M-\frac{w}{\mu^2}.$$

At A and B, since there are no applied end couples, $m=-\frac{w}{\mu^2}$, so OA and OB in Fig. 7.25 are set off in the negative direction to represent $\frac{w}{\mu^2}$. The m-circle is then drawn through O, A and B, and m_{max} is seen to be $-OX$ or $-\frac{w}{\mu^2}\sec \frac{\mu l}{2}$.

Hence, $$M_{max}=m_{max}+\frac{w}{\mu^2}=-\frac{w}{\mu^2}\sec \frac{\mu l}{2}+\frac{w}{\mu^2}.$$

or $$M_{max}=\left(1-\sec \frac{\mu l}{2}\right)\frac{w}{\mu^2},$$

as in paragraph 7.11.

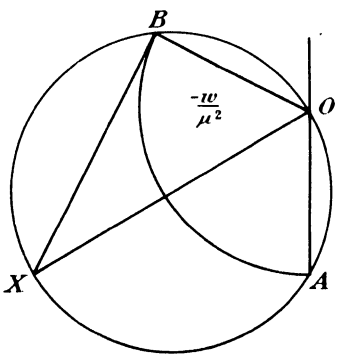

FIG. 7.25.

Case 3. *Strut with an axial thrust and a concentrated load.*—This case is dealt with in paragraph 7.12 and illustrated in Fig. 7.11. We shall write $a+b=l$.

The polar diagram is shown in Fig. 7.26 and is generally similar to Fig. 7.22, but since there are no end couples, the circles must not cut the lines ZOZ′ and KOK′, so these lines will be tangents to the appropriate circles at O. The centre of the circle for sector ZOD will therefore lie on OX_1, which is perpendicular to ZO, and the centre of the other circle will lie on OX_2, which is perpendicular to KO. The maximum value of m and therefore of M occurs at the load point and is given by OY.

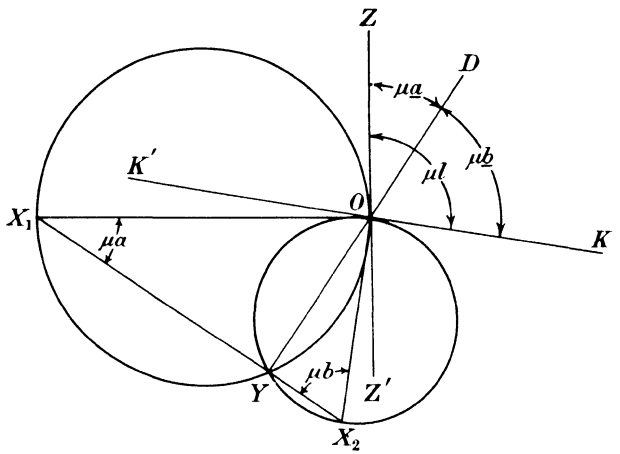

FIG. 7.26.

Then in the diagram, since OX_1 and X_1Y are respectively perpendicular to OZ and OY, the angle $OX_1Y=\mu a$, and similarly the angle $OX_2Y=\mu b$.

Hence, $$X_1OX_2=\pi-\mu l.$$

Now, $$OY=OX_1 \sin \mu a.$$

Also, $$\frac{OX_1}{\sin \mu b}=\frac{X_1X_2}{\sin \mu l},$$

and so, $$OX_1=\frac{X_1X_2 \sin \mu b}{\sin \mu l}=\frac{W \sin \mu b}{\mu \sin \mu l}.$$

Therefore,

$$M_{max}=m_{max}=-OY=-\frac{W}{\mu}\frac{\sin \mu a \sin \mu b}{\sin \mu l}.$$

If the load is central, $a=b=\frac{l}{2}$ and

$$M_{max}=-\left(\frac{W}{2\mu}\right)\tan \frac{\mu l}{2}.$$

These results are the same as those already found in paragraph 7.12.

Case 4. *Pin-jointed strut with specified end couples.*—This is dealt with in paragraph 7.13 and shown in Fig. 7.12. The m-circle is shown in Fig. 7.27, but is drawn as though the end couples were positive and not negative as shown in Fig. 7.12. OX is the maximum value of m and therefore of M.

From the diagram,

$$\mathrm{OX}=\mathrm{M_A}\sec\mu x_0=\mathrm{M_B}\sec(\mu l-\mu x_0),$$

where $\mu x_0=\epsilon$ is the position of maximum bending moment in the bar.

This gives $$\tan\mu x_0=\left(\frac{\mathrm{M_B}}{\mathrm{M_A}}\right)\operatorname{cosec}\mu l-\cot\mu l,$$

Then, $$\mathrm{OX}^2=\mathrm{M}^2{}_{\mathrm{A}}(1+\tan^2\mu x_0),$$

and substituting the value of $\tan\mu x_0$, already found, we have

$$m_{\max}=\mathrm{M_{max}}=\sqrt{\{(\mathrm{M}^2{}_{\mathrm{A}}+\mathrm{M_B}^2)\operatorname{cosec}^2\mu l-2\mathrm{M_A}\mathrm{M_B}\operatorname{cosec}\mu l\cot\mu l\}},$$

as in paragraph 7.13.

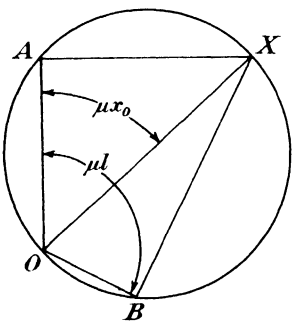

FIG. 7.27.

Case 5. *Encastré strut with axial thrust and uniformly distributed load.*—This case is treated in paragraph 7.15. The end couples are unknown and must be determined in addition to the bending moment at the centre.

From equation (5), since the slope of the bar at the end is zero, the true shearing force is the same as the apparent shearing force, *i.e.* $\frac{1}{2}wl$. The diagram is as shown in Fig. 7.28, where AX is now known to be $\frac{wl}{2\mu}$.

Hence, $$m_{\max}=-\mathrm{OX}=-\left(\frac{wl}{2\mu}\right)\operatorname{cosec}\frac{\mu l}{2},$$

and $$\mathrm{M_{max}}=m_{\max}+\frac{w}{\mu^2}=-\frac{wl}{2\mu}\operatorname{cosec}\frac{\mu l}{2}+\frac{w}{\mu^2}.$$

The value of m at the support is

$$-\mathrm{OA}=-\mathrm{AX}\cot\frac{\mu l}{2}=-\left(\frac{wl}{2\mu}\right)\cot\frac{\mu l}{2}.$$

The end fixing moment is therefore

$$M_A = -\left(\frac{wl}{2\mu}\right)\cot\frac{\mu l}{2} + \frac{w}{\mu^2}.$$

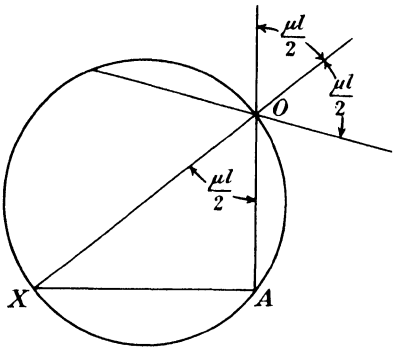

FIG. 7.28.

Case 6. *Encastré strut with axial thrust and central load.*—This case is dealt with in paragraph 7.16. The *m*-diagram will consist of two equal circles interesecting at the point Y in Fig. 7.29. As in the preceding case, we do not know the value of the end fixing moments, but the real and apparent shearing forces at the supports are both $\frac{1}{2}W$. So $AX = \frac{W}{2\mu}$. By the same reasoning, the true shearing force to the left of the load is also $\frac{1}{2}W$, and so $XY = \frac{W}{2\mu}$. The triangles OAX and OYX are therefore similar, and

$$AO = OY = \left(\frac{W}{2\mu}\right)\tan\frac{\mu l}{4}.$$

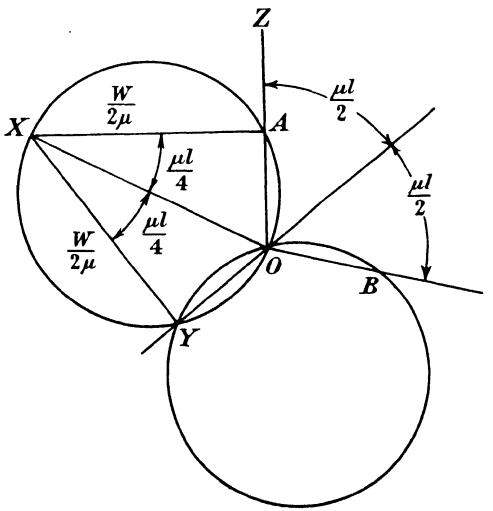

FIG. 7.29.

Since $m=M$, this is the value both of the bending moment at the centre and at the supports, the former being negative and the latter positive.

Other cases can be solved in a similar way and can be found in a paper in the *Mathematical Gazette* of July, 1942.

EXERCISES

(1) Compare the Perry and Rankine formulas for struts by plotting curves of axial loading against L/k for a wide range of values. Take the yield stress in the Perry formula and the constant p_y in the Rankine formula to be 18 tons per square inch; $a=\frac{1}{7,500}$ and $\eta=\cdot 003L/k$.

(2) Express the secant formula for a laterally-loaded pin-jointed strut and the Perry approximation to this formula in terms of the two ratios M_0/M' and P/Q where M_0 is the maximum bending moment due to the lateral load alone and M' the maximum bending moment due to the lateral load and end thrust P. Compare these formulas by plotting curves of M_0/M' against P/Q.

(3) Use Smith's modified formula to calculate the strength of a circular steel tube 100 inches long, $2\frac{1}{8}$ inches outside diameter and 0·058 inches thick when used as a pin-jointed strut.

The equivalent eccentricity of loading may be taken to be $\frac{\text{length}}{600}+\frac{\text{internal diameter}}{40}$, the yield stress to be 28 tons per square inch and $E=13,600$ tons per square inch. *(5,000 lb.)*

(4) A pin-jointed rectangular wooden beam 6 inches deep by 3 inches wide and 100 inches long carries an axial thrust of 10,000 lb. and a uniform lateral load of 3 lb. per inch over its whole length.

Calculate the factor of safety under this loading and the load factor of the member if the yield stress of the material is 5,000 lb. per square inch and $E=1\cdot 6\times 10^6$ lb. per square inch.

(6·3 ; 4·8)

(5) A uniform bar of length L and flexural rigidity EI is encastré at one end and pin-jointed at the other. At the pinned end it carries a compressive load P and a moment M.

Show that the position of the maximum bending moment is given by

$$\tan \mu x=\frac{1-\mu L \sin \mu L-\cos \mu L}{\sin \mu L-\mu L \cos \mu L}$$

where $\mu^2=P/EI$ and x is measured from the pin-joint along the original central line of the bar.

(6) A steel tube 60 inches long, 1 inch outside diameter and ·056 inch thick is pinned at the ends and carries an axial load of 500 lb.

Calculate what lateral load, uniformly distributed, is required to produce a stress of 8 tons per square inch in the material. $E=13,600$ tons per square inch.

(0·83 lb. per inch)

(7) The strut in the last question without lateral load has bending moments applied to its ends of 650 and 300 inch-lb. respectively.

Use a graphical method to determine the position and magnitude of the maximum bending moment in the strut, and the bending moment and shearing force at the centre.

(748 inch-lb. at 17·6 inches from larger end moment ; 700 inch-lb. ; −6·77 lb.)

(8) A circular steel bar 10 feet long and 2 inches diameter is pinned at the ends and carries an axial compression equal to one quarter of the Euler critical load. In addition it carries a uniformly distributed load of 10 lb. per foot and has

terminal couples of 2,400 inch-lb. and −2,400 inch-lb. at the right- and left-hand supports respectively.

Determine graphically—

(a) the position and magnitude of the maximum bending moment;
(b) the bending moment and shearing force at the midpoint of the span.

[(a) *−234 foot-lb. at 1·89 feet from end*
(*b*) *−164 foot-lb.; 46·5 lb.*]

CHAPTER 8

CONTINUOUS BEAMS AND COLUMNS

8.1. The general problem of the continuous beam.—We have seen in a previous chapter that a beam requires three reactive forces to ensure equilibrium under any loading conditions which may occur; if we assume that the beam is horizontal and that there are no horizontal forces acting upon it, two vertical reactions only are needed. If more than the essential number are provided the resultant actions at any point are statically indeterminate and a solution depends upon a knowledge of the elastic properties of the beam and its supports.

A common case is that of a continuous beam supported at a number of points along its length. The beam may be of the same section throughout or may vary from span to span. The loads may be all normal to the longitudinal axis or there may be component forces acting along this axis. The first is the usual type of loading on girders in building frames and the second occurs in the main plane spars of a biplane where the flying wires impose axial compressions or tensions which vary from bay to bay. The problem may be still further complicated by the supports which may either be rigid, in which case the beam does not deflect at the supported points when loaded, or they may be elastic, thus allowing such movement to occur. Also the beam may be simply pinned to the supporting points or be so attached that the joints between the supports and the beam are rigid. It will be realised that any problem of this type can be analysed by making use of strain energy methods, but these are not always the most convenient for the purpose and a number of other methods have been developed which will be described in the present chapter.

It will be assumed unless otherwise stated that the beams are continuous but are simply pinned to their supports. Before proceeding to a discussion of the methods available it is desirable to examine the problem generally.

Suppose a horizontal beam such as specified above and subjected to vertical loads only, rests on n supports. Two of these supports only are essential for equilibrium and the vertical reactions exerted by the remaining $n-2$ may be considered as redundant. If we denote these $n-2$ unknown forces by R_2, R_3 . . . R_{n-1} and the essential reactive forces by R_1 and R_n the values of R_1 and R_n can be expressed in terms of the external loads and of the unknowns R_2 . . . R_{n-1} by making use of the equations of static equilibrium for the beam as a whole. If the redundant supports are known to sink by amounts δ_2,

$\delta_3 \ldots \delta_{n-1}$ below the level of the line joining R_1 and R_n an application of the first theorem of Castigliano yields the equations

$$\frac{\partial U}{\partial R_2} = -\delta_2,$$

$$\frac{\partial U}{\partial R_3} = -\delta_3,$$

. . . . .

and

$$\frac{\partial U}{\partial R_{n-1}} = -\delta_{n-1}.$$

These, together with the equations of static equilibrium, enable all the reactive forces to be calculated.

When they have been found the beam can be treated as a simple one subjected to a known load system and the bending moment and shearing force diagrams can be plotted.

The reactive forces in general act in the opposite direction to the applied loads and the bending moments produced by them are thus of opposite sign to those due to the loads. One effect of continuity is therefore to reduce the bending moments which would occur if the member had consisted of a number of separate beams.

8.2. Wilson's method.—If a continuous beam is of constant section throughout its length a method of analysis due to Dr. George Wilson is often convenient. This is in principle the same as that given in the previous paragraph in so far that the deflections of the beam at the points of support are equated to zero in the case of rigid supports or to known values in the case of elastic supports. It differs from it however in the method of obtaining expressions for the deflections of these points. Wilson finds these by making use of the equation of the elastic line of the beam. The unknown reactive forces are treated as loads acting in the opposite direction to the applied load system and the bending moment at any point is conveniently found by Macaulay's method ; this will of course involve the unknown reactions. A double integration of the bending moment equation gives expressions for the deflections at the support points and these when equated to the known movements of such points yield, with the equations of static equilibrium, the necessary equations for a complete solution of the problem.

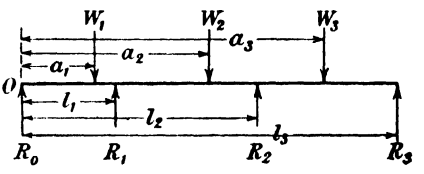

FIG. 8.1.

For example, suppose a beam of uniform cross-section and of length l_3 as in Fig. 8.1 to be simply supported at its ends and to rest on two intermediate supports at distances l_1 and l_2 from the left-hand support O, while applied loads W_1, W_2 and W_3 act at distances a_1, a_2 and a_3 respectively from O.

The bending moment at a section which is x from O is

$$EI\frac{d^2y}{dx^2}=-R_0x+W_1[x-a_1]-R_1[x-l_1]+W_2[x-a_2]-R_2[x-l_2]+W_3[x-a_3],$$

so, $$EI\frac{dy}{dx}=-R_0\frac{x^2}{2}+\frac{W_1}{2}[x-a_1]^2-\frac{R_1}{2}[x-l_1]^2+\frac{W_2}{2}[x-a_2]^2-\frac{R_2}{2}[x-l_2]^2+\frac{W_3}{2}[x-a_3]^2+A$$

and $$EIy=-\frac{R_0x^3}{6}+\frac{W_1}{6}[x-a_1]^3-\frac{R_1}{6}[x-l_1]^3+\frac{W_2}{6}[x-a_2]^3-\frac{R_2}{6}[x-l_2]^3+\frac{W_3}{6}[x-a_3]^3+Ax+B,$$

where R_0, R_1 and R_2 are the reactive forces supplied by the supports and A and B are constants of integration.

If there is no sinking of the supports when the external loads are applied, four equations result from the conditions that $y=0$ when $x=0$, l_1, l_2 and l_3 respectively. If the supports sink by specified amounts these values of y are used instead. There are six unknowns and the remaining equations necessary for their evaluation come from a consideration of the equilibrium of the beam as a whole.

Thus, resolving vertically we have the equation

$$R_0+R_1+R_2+R_3=W_1+W_2+W_3,$$

and taking moments about O we have

$$R_1l_1+R_2l_2+R_3l_3=W_1a_1+W_2a_2+W_3a_3.$$

These six equations enable the four reactive forces to be determined and the bending moment and shearing force at any section can then be calculated.

8.3. The theorem of three moments.—Wilson's method is useful if the beam is of constant section throughout its length but when it varies from bay to bay the equations become cumbersome. A more general method, which can be used in all cases, was originally given by Clapeyron and is known as the theorem of three moments. In the first place the general form of this theorem will be proved for any system of transverse loads; special cases and extensions to cover the case when axial loads occur will follow.

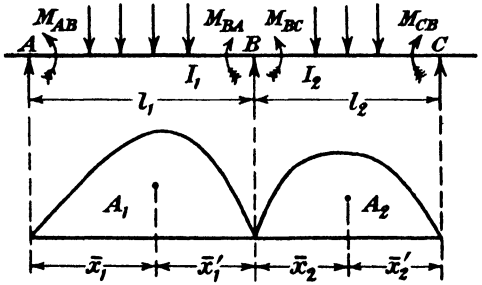

FIG. 8.2.

A continuous beam may be considered to consist of a number of single span beams subjected to known external load systems and to end moments such as M_{AB} and M_{BA} (Fig. 8.2) which are the restraints

supplied by the neighbouring spans. The magnitude of these end restraining moments are such that the beams are made continuous over each support; that is to say, considering the support B, the slope at the end B of the beam AB is the same as the slope at the end B of the beam BC.

This condition for continuity can be readily expressed in general terms from equations (8) and (9) of paragraph 3.13 which give the slopes at the ends of a simply supported beam subjected to transverse loads and end couples.

Suppose that the area of the bending moment diagram due to the external load system alone on the span AB, considered as a simply supported beam, is A_1 and that the distance of the centroid of this area from the end A is $\bar{x}_1$ then, from equation (8) of paragraph 3.13, the slope at the end B of AB is

$$\theta_{BA}=\frac{l_1}{6EI_1}\left[M_{AB}+2M_{BA}+\frac{6A_1\bar{x}_1}{l_1^2}\right]+\frac{\delta_B-\delta_A}{l_1} \quad . \quad . \quad . \quad . \quad . \quad (1)$$

where l_1 and I_1 are the length of AB and the relevant second moment of area of the section of the beam respectively and δ_A and δ_B are the deflections of the ends A and B when the external load system is applied to the continuous beam.

Similarly if A_2 is the area of the bending moment diagram due to the external load system alone on the span BC considered as simply supported, and $\bar{x}_2'$ is the distance of the centroid of this area from the end C, then the slope at the end B of BC is

$$\theta_{BC}=-\frac{l_2}{6EI_2}\left[M_{CB}+2M_{BC}+\frac{6A_2\bar{x}_2'}{l_2^2}\right]+\frac{\delta_C-\delta_B}{l_2} \quad . \quad . \quad . \quad . \quad (2)$$

Since the beam is continuous at B the slopes given by expressions (1) and (2) must be the same. Equating them we have

$$\frac{l_1}{I_1}M_{AB}+\frac{2l_1}{I_1}M_{BA}+\frac{2l_2}{I_2}M_{BC}+\frac{l_2}{I_2}M_{CB}+\frac{6A_1\bar{x}_1}{l_1I_1}+\frac{6A_2\bar{x}_2'}{l_2I_2}$$
$$=\frac{6E(\delta_A-\delta_B)}{l_1}+\frac{6E(\delta_C-\delta_B)}{l_2}. \quad . \quad . \quad . \quad . \quad . \quad . \quad (3)$$

A consideration of the equilibrium of the short length of beam immediately above the support B shows that when no external couple is applied to the beam at B

$$M_{BA}=M_{BC}. \quad . \quad . \quad . \quad . \quad . \quad . \quad . \quad . \quad . \quad (4)$$

When, as part of the external load system, a clockwise couple M is applied to the beam at B

$$M_{BA}=M+M_{BC}. \quad . \quad . \quad . \quad . \quad . \quad . \quad . \quad . \quad . \quad (5)$$

For a continuous beam of n spans there will be $2n$ unknown end restraining moments. From a consideration of the slope and equilibrium of the beam at the intermediate supports, $n-1$ equations of type (3) and $n-1$ equations of type (5) may be obtained. The remaining two equations necessary for the complete determination of the end moments are obtained from a consideration of the conditions at the

end supports. The moment at an end support may be known. If, for instance, the left-hand end A of the beam is simply supported $M_{AB}=0$. The change of slope of the beam at an end support may be known, in which case the required equation can be written down immediately from one of the expressions (1) or (2). If, for instance, the end C is encastré and there is no sinking of the supports, we have from (1)

$$M_{BC}+2M_{CB}+\frac{6A_2\bar{x}_2}{l_2^2}=0. \quad \ldots\ldots\ldots (6)$$

When the end restraining moments at the supports have been evaluated the reactions at the supports may be calculated by taking the moments of internal and external forces about the various supports or by adding the shears on each side of the support algebraically.

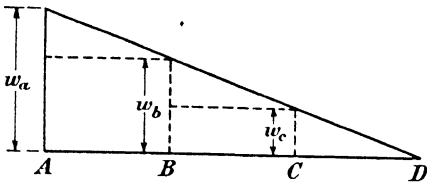

FIG. 8.3.

As a particular application of the general theorem consider the beam ABCD of uniform section shown in Fig. 8.3 under a triangular distribution of load acting upwards. Let w_a, w_b, w_c be the intensities of loading at the supports A, B and C which remain collinear.

The B.M. due to the load on BC can be divided into two parts—

(1) Due to a uniform distributed load w_c.

(2) Due to a distributed load varying from 0 to w_b-w_c.

The moment of the free B.M. diagram about C is the sum of the moments of (1) and (2).

The moment of (1) is $\frac{2}{3}l_2 \cdot \frac{w_c l_2^2}{8} \cdot \frac{l_2}{2} = \frac{w_c l_2^4}{24}$

To find the moment of (2) let $w_b-w_c=w_0$, then the B.M. at a distance x from C is

$$-\frac{w_0}{6}\left(\frac{x^3}{l_2}-l_2x\right)$$

and the moment of the B.M diagram is $-\frac{w_0}{6}\int_0^{l_2}\left(\frac{x^3}{l_2}-l_2x\right)x\,dx=\frac{w_0 l_2^4}{45}$.

Therefore the total moment of moment is

$$\frac{w_c l_2^4}{24}+\frac{(w_b-w_c)l_2^4}{45}=\frac{l_2^4}{360}(7w_c+8w_b).$$

Bay AB.—To find the moment of the B.M. diagram due to (2). The area of the B.M. diagram

$$=-\frac{w'_0}{6}\int_0^{l_1}\left(\frac{x^3}{l_1}-l_1x\right)dx$$

$$=\frac{w_0'l_1^3}{24},$$

where $w_0'=w_a-w_b$.

$$\text{The moment about B} = \frac{w_0' l_1^4}{45},$$

$$\text{therefore the distance of the C.G. from B} = \frac{w_0' l_1^4}{45} \cdot \frac{24}{w_0' l_1^3} = \frac{24 l_1}{45}$$

$$\text{and the distance of the C.G. from A} = \frac{21}{45} l_1 = \frac{7 l_1}{15}.$$

$$\text{The moment about A} = \frac{7 l_1}{15} \cdot \frac{w_0' l_1^3}{24}$$

$$= \frac{7 w_0' l_1^4}{360}$$

The total moment of the area about A

$$= \frac{7 w_0' l_1^4}{360} + \frac{w_b l_1^4}{24}$$

$$= \frac{l_1^4}{360}(7 w_a + 8 w_b).$$

Substituting in the general equation (3) we obtain the result

$$\frac{7}{60} w_a l_1^3 + \frac{8}{60} w_b (l_1^3 + l_2^3) + \frac{7}{60} w_c l_2^3 + M_A l_1 + 2 M_B (l_1 + l_2) + M_C l_2 = 0.$$

A similar equation is found for the bays BC and CD to connect M_B, M_C and M_D. The other two necessary equations are given by the conditions of support at A and D and all fixing moments can then be evaluated.

When the spans of a continuous beam carry uniformly distributed downward loads only, no external couples being applied at the supports, the general equation (3) takes the simple form of the three moment equation.

$$\frac{l_1}{I_1} M_A + 2\left(\frac{l_1}{I_1} + \frac{l_2}{I_2}\right) M_B + \frac{l_2}{I_2} M_C - \frac{w_1 l_1^3}{4 I_1} - \frac{w_2 l_2^3}{4 I_2} = \frac{6E(\delta_A - \delta_B)}{l_1} + \frac{6E(\delta_C - \delta_B)}{l_2} \quad \ldots \ldots \quad (7)$$

It must be remembered when using the general equation that the areas A_1 and A_2 were of bending moment diagrams in which hogging bending moments were taken as positive.

As an example of the use of equation (7) consider the four span continuous beam ABCDE shown in Fig. 8.4. It is of uniform cross-section throughout and carries a uniformly distributed load of intensity w. The supports remain at the same level and the length of each span is l.

Since the beam is simply supported at A and E

$$M_A = M_E = 0 \quad \ldots \ldots \quad (8)$$

From considerations of symmetry

$$M_B = M_D \quad \ldots \ldots \quad (9)$$

The three moment equation for ABC is

$$M_A+4M_B+M_C-\frac{wl^2}{4}-\frac{wl^2}{4}=0$$

and for BCD it is

$$M_B+4M_C+M_D-\frac{wl^2}{4}-\frac{wl^2}{4}=0.$$

Making use of (8) and (9) these equations may be written

$$4M_B+M_C=\frac{wl^2}{2} \quad \ldots\ldots\ldots \quad (10)$$

and

$$2M_B+4M_C=\frac{wl^2}{2} \quad \ldots\ldots\ldots \quad (11)$$

from which

$$M_B=M_D=\frac{3wl^2}{28}$$

and

$$M_C=\frac{wl^2}{14}.$$

The reactions at A may be found by considering the equilibrium of AB. Taking moments about B, we have

$$R_A l-\frac{wl^2}{2}+M_B=0$$

or

$$R_A=\frac{11wl}{28}.$$

In the same way the reaction at B is found by considering the length AC. Taking moments about C we have

$$2R_A l+R_B l-2wl^2+M_C=0$$

or

$$R_B=\frac{8wl}{7}.$$

For R_C, considering the whole beam and resolving vertically, we have

$$2R_A+2R_B+R_C=4wl$$

or

$$R_C=\frac{13wl}{14}.$$

These reactions could have been found rather more elegantly by writing down the shears on each side of each support. Thus

the shear to the left of B is $R_{BL}=\frac{wl}{2}+\frac{M_B-M_A}{l}$

and that to the right of B is $R_{BR}=\frac{wl}{2}+\frac{M_B-M_C}{l}$

so that the reaction at B is

$$R_B=\frac{wl}{2}+\frac{M_B-M_A}{l}+\frac{wl}{2}+\frac{M_B-M_C}{l}=\frac{8wl}{7}$$

The shearing force diagram for the continuous beam is shown in Fig. 8.4. The bending moment diagram can be drawn in the usual way by

calculating at every section the algebraic sum of the moments of all the applied forces, including the reactions, on one side of the section, but it is usually simpler to follow the method adopted in Fig. 8.4 and to consider each span separately. Span BC, for instance, may be considered as subjected to two load systems, the first being a uniformly distributed load of intensity w and the second consisting of end couples M_B and M_C. The bending moment diagrams for these separate systems, a parabola and a trapezium respectively, are easily drawn and the net bending moment diagram for the span forming part of the continuous beam is the algebraic sum of these diagrams. As the uniformly distributed load causes a sagging bending moment at each section of BC and the end couples cause a hogging bending moment, the net diagram is formed by subtracting the trapezium from the parabola as

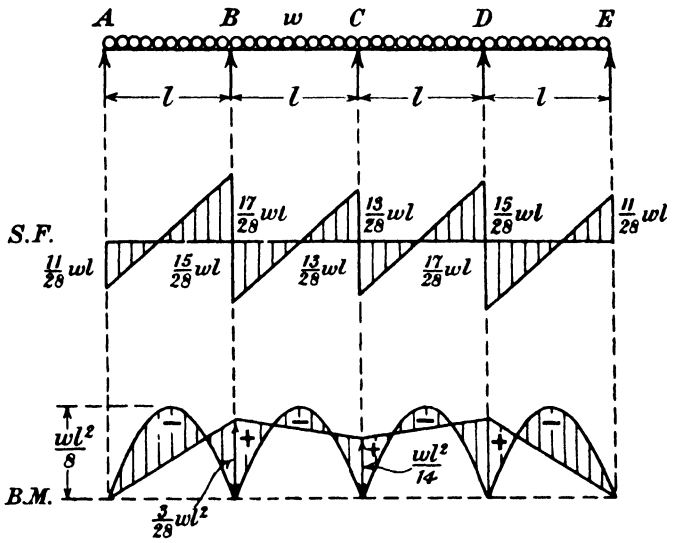

FIG. 8.4.

in Fig. 8.4. The positions of the points of contraflexure, *i.e.* where the bending moment changes sign, can be seen in the completed bending moment diagram.

8.4. Moment distribution method.—The two methods given above involve the solution of simultaneous equations and though this is not usually an arduous matter in continuous beam problems it is sometimes an advantage to avoid it. This can be done by applying the moment distribution method to which reference has already been made in paragraph 6.6.

In the three moment method, paragraph 8.3, it was imagined that the continuous beam was made up of a number of simply supported beams to which the external load system and unknown end couples were applied; the magnitudes of these end couples which would so rotate the ends of the simply supported beams as to make one continuous beam were then found. In the moment distribution

method the beam is kept continuous throughout but before the external loads are applied it is clamped at each support so that it cannot change its slope there. When the loads are applied the continuous beam behaves as if it were a number of single span encastré beams. The clamps are therefore subjected to moments equal and opposite to the fixing moments on the beams and in general an external moment has to be applied at each support to maintain the clamping action. At one support this external moment is removed, that is to say the beam is freed. It immediately moves into a new position of equilibrium and in so doing modifies the end moments. The beam is clamped again in its new equilibrium position and is freed at another support. This procedure is repeated until the resulting modifications in the end moments are small enough to be ignored.

Before illustrating the method by a worked example it will be useful to develop in general terms certain expressions which are required in the analysis. As in paragraph 8.3 we will confine our attention to beams having a uniform cross-section between supports though the method can be applied more generally.

As the ends of each span are clamped before the load is applied, the fixed end moment which the clamp exerts on the beam is the same as the restraining moment at the end of a similarly loaded encastré beam. Expressions for this have been given in equations (1) and (2) of paragraph 3.14.

When the external moment at a support is removed the loaded beam behaves exactly as the same beam would if subjected to no other action than a moment at the support equal and opposite to the external moment. This behaviour is easily followed with the help of the slope deflection equations. As it is necessary to adopt here a new sign convention in which all end moments acting on a beam are positive when clockwise it will be well to restate the slope deflection equations.

If θ_{AB} and θ_{BA} are the changes of slope at the ends of a member of uniform cross-section due to the application of positive (clockwise) end moments M_{AB} and M_{BA} then if there is no relative deflection of the ends we have from equations (6) and (7) of paragraph 3.13,

$$\theta_{BA}=\frac{l}{6EI}(-M_{AB}+2M_{BA}) \quad . \quad . \quad . \quad . \quad . \quad . \quad (1)$$

and

$$\theta_{AB}=\frac{l}{6EI}(2M_{AB}-M_{BA}). \quad . \quad . \quad . \quad . \quad . \quad . \quad . \quad (2)$$

Solving (1) and (2) we obtain

$$M_{AB}=\frac{2EI}{l}(2\theta_{AB}+\theta_{BA}) \quad . \quad . \quad . \quad . \quad . \quad . \quad . \quad (3)$$

and

$$M_{BA}=\frac{2EI}{l}(\theta_{AB}+2\theta_{BA}). \quad . \quad . \quad . \quad . \quad . \quad . \quad . \quad (4)$$

The beam subjected to a moment at the support is shown in Fig. 8.5. It is encastré at A and C and freely supported at B. A moment $\bar{M}$ is applied at B and under its action the beam moves into a new position

of equilibrium rotating through an angle θ_B at B. In moving, moments M_{BA} and M_{BC} as shown are induced at the ends of BA and BC. It is often convenient in using the moment distribution method to think of the members as being joined, not directly to one another but each to a "joint" which in this case would be the small length of beam containing the support B. Thus the moment $\bar{M}$ is applied to this "joint" and M_{BA} and M_{BC} are the moments applied by the "joint" to the ends of the members. From a consideration of the equilibrium of the "joint"

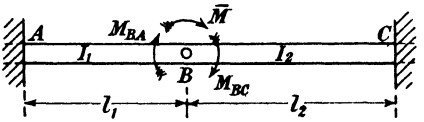

FIG. 8.5.

$$M_{BA}+M_{BC}=\bar{M} \quad \ldots\ldots\ldots \quad (5)$$

From equation (4) since the end A of AB is encastré and the end B turns through an angle θ_B we have

$$M_{BA}=\frac{4EI_1}{l_1}\theta_B \quad \ldots\ldots\ldots \quad (6)$$

Similarly

$$M_{BC}=\frac{4EI_2}{l_2}\theta_B \quad \ldots\ldots\ldots \quad (7)$$

so that

$$\bar{M}=4E\left(\frac{I_1}{l_1}+\frac{I_2}{l_2}\right)\theta_B$$

from (6) and (7)

$$M_{BA}=\frac{\frac{I_1}{l_1}\bar{M}}{\frac{I_1}{l_1}+\frac{I_2}{l_2}}$$

and

$$M_{BC}=\frac{\frac{I_2}{l_2}\bar{M}}{\frac{I_1}{l_1}+\frac{I_2}{l_2}} \quad \ldots\ldots\ldots \quad (8)$$

The moments induced at the ends B of AB and BC are thus proportional to the stiffnesses of AB and BC, the stiffness of a member being defined as its second moment of area divided by its length.

When the beam moves into its new position of equilibrium, moments are, of course, induced at the encastré ends A and C also. They can most conveniently be evaluated from a consideration of such a member as PQ, Fig. 8.6, which has the end Q encastré and the end P, to which a moment M_{PQ} is applied, fixed in position.

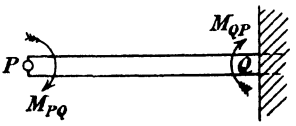

FIG. 8.6.

Suppose that under this moment the end P turns through an angle θ_P and that the restraining moment developed at Q is M_{QP}, then from equation (3)

$$M_{PQ}=\frac{2EI}{l}(2\theta_P)$$

and from equation (4)

$$M_{QP}=\frac{2EI}{l}(\theta_P)=\tfrac{1}{2}M_{PQ}, \quad \ldots\ldots\ldots \quad (9)$$

so that the restraining moment induced at the encastré end of such a member as PQ is one-half the moment applied at the other end P.

By means of these expressions (8) and (9) together with those for the fixed end moments at the ends of an encastré beam, equations (1) and (2) of paragraph 3.14, the bending moments in continuous beams can be found with ease.

Consider the beam ABC of uniform cross-section in Fig. 8.7 which is to carry a uniformly distributed load of 12 tons per foot on AB. The ends A and C are encastré and B, the mid-point of AC, is simply supported. In this and in all other examples it will be assumed, unless otherwise stated, that there is no sinking of the supports.

Before the load is applied, clamp the beam at B so that it cannot change its slope there. Apply the load. AB will then behave as an

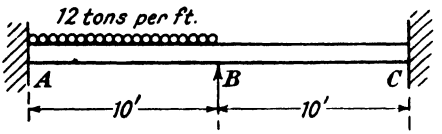

FIG. 8.7.

encastré beam and restraining moments will act upon it, the magnitudes of these being -100 tons-feet $\left(=\frac{wl^2}{12}\right)$ at A and $+100$ tons-feet at B. The latter is supplied by the clamp and no bending moment exists anywhere in BC. Now free B by removing the clamp; the beam at B will be no longer in equilibrium, since the external clockwise moment of 100 tons-feet has been removed, and will immediately accommodate itself to the new conditions, changing its slope at B until it is once more in equilibrium. This change of slope is that experienced by the beam ABC on the removal of the external moment $+100$ tons-feet, and is, therefore, the same as that produced by the application of an external moment of -100 tons-feet. The moments induced in the beam at B by this change of slope can be found by substituting $\overline{M}=-100$ tons-feet in expression (8). Since, in this particular case, $I_1/l_1=I_2/l_2$

$$M_{BA}=M_{BC}=-50 \text{ tons-feet.}$$

The moments, -25 tons-feet, induced at A and C are found from expression (9). The modifications in all the end moments are therefore known. Since A and C are encastré and cannot be released the beam has, by this one movement, reached its final deflected form and the exact values of the bending moments are obtained. The end moment at A was in the first, or fixed end, stage -100 tons-feet and due to the movement of B, on the removal of the clamp, an additional moment -25 tons-feet was induced at A so that $M_{AB}=-100-25=-125$ tons-feet.

At the end B of BA the fixed end moment was +100 tons-feet and on the release of the clamp the moment induced was −50 tons-feet so that

$$M_{BA} = 100 - 50 = +50 \text{ tons-feet.}$$

In the same way $M_{BC} = 0 - 50 = -50$ tons-feet

and $M_{CB} = 0 - 25 = -25$ tons-feet.

The end moments being known, the bending moment diagram for ABC can be drawn.

The process will perhaps be more easily followed from another example in which the end moments are tabulated. Fig. 8.8 shows a three span beam ABCD of uniform cross-section throughout which is

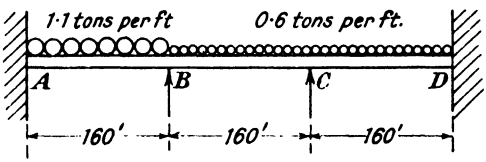

FIG. 8.8.

encastré at A and D and supported at B and C. A load of 1·1 tons per foot is distributed over AB and 0·6 ton per foot over BD. Each span is 160 feet long.

TABLE 8.1.

END MOMENTS (TONS-FEET).

	A	B		C		D	
	−2,346·6	+2,346·6	−1,280·0	+1,280·0	−1,280·0	+1,280·0	*a*
	− 266·6	− 533·3	− 533·3	− 266·6	0·0	0·0	*b*
	0·0	0·0	+ 66·6	+ 133·3	+ 133·3	+ 66·6	*c*
	− 16·6	− 33·3	− 33·3	− 16·6	0·0	0·0	*d*
	0·0	0·0	+ 4·2	+ 8·3	+ 8·3	+ 4·2	*e*
	− 1·0	− 2·1	− 2·1	− 1·0	0·0	0·0	*f*
Totals .	−2,630·8	+1,777·9	−1,777·9	+1,137·4	−1,138·4	+1,350·8	

Clamp the beam at B and C and apply all the loads: the fixed end moments induced at the ends of the spans will be as entered in line *a*, Table 8.1. Release B; the out of balance moment acting on the joint at B is −(2,346·6−1,280) or −1,066·6 tons-feet at the instant of release. The balancing moments induced at the ends B of AB and BC as B rotates into its new equilibrium position will be therefore from (8) −533·3 tons-feet. The moments carried over to the ends A and C will be, from (9), −266·6 tons-feet. These end moments, induced by the movement of B, are entered in line *b*. The entries in columns 5 and 6 are zero because, C remaining clamped, no moments can be induced at the ends of the span CD by the movement of B.

B is now clamped in its new equilibrium position and C is released. The out of balance moment on the joint at C is $-(1{,}280{\cdot}0-1{,}280{\cdot}0-266{\cdot}6)$ or $+266{\cdot}6$ tons-feet. The balancing moments at C will then be $+133{\cdot}3$ tons-feet and the carry-over moments at B and D $+66{\cdot}6$ tons-feet. These are entered in line *c* Table 8.1. C is now clamped in its new equilibrium position and B is once more released. The balance of B has been upset by the moment carried over as a result of C's movement, so that at the instant of release the out of balance moment on joint B is $-66{\cdot}6$ tons-feet. As B moves once more into a new equilibrium position the balancing moments induced are $-33{\cdot}3$ tons-feet and the carry-over moments $-16{\cdot}6$ tons-feet; these are entered in line *d*. B is clamped again and so the process is continued until the modifications in the end moments brought about by further releases are small enough to be neglected. Two further releases have been made in Table 8.1. The total values of the end moments are obtained by adding the entries in each column and we find

$$M_{AB}=-2{,}630{\cdot}8,\ M_{BA}=+1{,}777{\cdot}9,\ M_{BC}=-1{,}777{\cdot}9.$$
$$M_{CB}=+1{,}137{\cdot}4,\ M_{CD}=-1{,}138{\cdot}4,\ M_{DC}=+1{,}350{\cdot}8.$$

In both these examples the ends of the continuous beam were built in or encastré. Considerably more work is entailed if the ends are simply supported.

TABLE 8.2.

END MOMENTS (TONS-FEET).

A	B		C	
−100	+100	0	0	*a*
+100	− 50	−50	0	*b*
− 25	+ 50	0	−25	*c*
+ 25	− 25	−25	+25	*d*
− 12·5	+ 12·5	+12·5	−12·5	*e*
+ 12·5	− 12·5	−12·5	+12·5	
− 6·25	+ 6·25	+ 6·25	− 6·25	

Suppose the beam of Fig. 8.7 is simply supported at A and C. The procedure is exactly as before. All joints are clamped and the load is applied, the fixed end moments being as shown in line *a* Table 8.2. The joints have now to be released. The lay-out of Table 8.2 is slightly different from that of Table 8.1. Instead of releasing each joint separately and inserting in one line of the table the balancing and carry-over moments induced by that release, all joints are released at the same instant and the balancing moments at all the joints are entered in one line of the table while in the line below are put the carry-over moments induced by all these releases. Thus in Table 8.2, line *b* the entries are the balancing moments +100, −50, −50

and 0. A line is drawn below these entries to show that the joints are balanced. In line *c* are the carry-over moments −25, +50, 0 and −25 tons-feet induced by the balancing moments. These carry-over moments upset the balance at the joints so that when they are once again released the balancing moments of line *d* come into operation and as a result the carry-over moments of line *e*. It can be seen from Table 8.2 that the total end moments will be 0, +75, −75 and 0 respectively. The physical significance of the steps shown in Table 8.2 may not be seen immediately but if the calculations are set out in the same way as those in Table 8.1, each joint in turn being released, there will be no difficulty in realising that the steps are justified. By releasing all joints together a more concise table can be formed.

When the continuous beam has a simply supported end A it is worth while to calculate a special set of distribution factors to be used in finding the balancing moments when the support next to A is released. This can be done by considering the beam ABC in Fig. 8.9

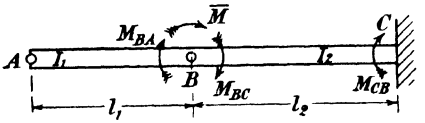

FIG. 8.9.

which is simply supported at A and B and is encastré at C. If, when an external moment M is applied at B the changes of slope at A and B are θ_A and θ_B respectively then, since the end A is simply supported and C is encastré, it follows from equations (3) and (4) that

$$0=\frac{2EI_1}{l_1}(2\theta_A+\theta_B),$$

$$M_{BA}=\frac{2EI_1}{l_1}(\theta_A+2\theta_B)$$

and

$$M_{BC}=\frac{2EI_2}{l_2}(2\theta_B).$$

From a consideration of the equilibrium of the joint B

$$M_{BA}+M_{BC}=\bar{M}$$

so that

$$M_{BA}=\frac{\frac{3I_1}{l_1}}{\frac{3I_1}{l_1}+\frac{4I_2}{l_2}}\bar{M}$$

and

$$M_{BC}=\frac{\frac{4I_2}{l_2}}{\frac{3I_1}{l_1}+\frac{4I_2}{l_2}}\bar{M} \qquad \ldots\ldots\ldots (10)$$

The convenience of these expressions can be gauged from Table 8.3,

which gives the calculation of the end moments in the continuous beam shown in Fig. 8.10 resting on the supports A, B, C and D.

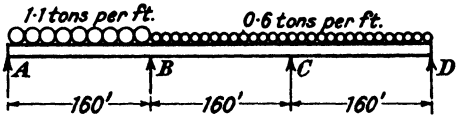

Fig. 8.10.

Table 8.3.

End Moments (tons-feet).

A	B	C	D	
−2,346·6	+2,346·6	−1,280·0	+1,280·0	−1,280·0	+1,280·0	*a*
+2,346·6	0·0	0·0	0·0	0·0	−1,280·0	*b*
0·0	+1,173·3	0·0	0·0	− 640·0	0·0	*c*
0·0	− 960·0	−1,280·0	+ 366·0	+ 274·0	0·0	*d*
0·0	0·0	+ 183·0	− 640·0	0·0	0·0	*e*
0·0	− 78·0	− 105·0	+ 366·0	+ 274·0	0·0	
0·0	0·0	+ 183·0	− 52·5	0·0	0·0	
0·0	− 78·0	− 105·0	+ 30·0	+ 22·5	0·0	
0·0	0·0	+ 15·0	− 52·5	0·0	0·0	
0·0	− 6·4	− 8·6	+ 30·0	+ 22·5	0·0	
0·0	0·0	+ 15·0	− 4·3	0·0	0·0	
0·0	− 6·4	− 8·6	+ 2·6	+ 1·7	0·0	

To avoid the calculation of special fixed-end moments for the end spans the beam is considered to be clamped initially at all the supports. When the load is applied the fixed-end moments produced are those shown in line *a* Table 8.3. When the ends A and D are released, the resulting balancing and carry-over moments are those shown in lines *b* and *c* respectively. A and D are not clamped again but a e kept free for the remainder of the process. The distribution factors by which an out of balance moment at B or C is to be multiplied to give the balancing moments in the beam must therefore be calculated from expressions (10). Since the spans are of equal stiffnesses these factors are 3/7 and 4/7. That is to say, if the out of balance moment on joint B is $\bar{M}$, when the beam moves into its equilibrium position the moments induced in it will be

$$M_{BA}=\frac{3}{7}\bar{M} \text{ and } M_{BC}=\frac{4}{7}\bar{M}.$$

When B is released the out of balance moment is −(2,346·6−1,280·0 +1,173·3) or −2,239·9 tons-feet so that the balancing moments are −960 and −1,280 tons-feet approximately. These are entered in line *d* together with those resulting from the release of C. The carry-

over moments are entered in line *e*. The entries in columns 1 and 2, line *e* are zero since A is a free support and therefore no moment is developed there when B is released, and as no balancing moment was applied at A line *d* there is no corresponding carry-over moment to be entered at B. The process is continued as shown in the Table. The total moments after five balances are $M_{AB}=0$; $M_{BA}=2,391{\cdot}1 =-M_{BC}$; $M_{CB}=1,325{\cdot}3=-M_{CD}$ and $M_{DC}=0$.

The moment distribution method can be used with advantage for the case in which the supports of the beam sink a known distance under load. It is most convenient to assume that the deflection of the supports takes place when the load is first applied, while the beam is still clamped, that is to say so restrained as to remain horizontal at the supports. The fixed-end moments are calculated from expressions (1) and (2) of paragraph 3.14 in which a term appears giving the modification in the moments due to the relative deflection of the ends. The beam is then released and the balancing and carry-over moments are found as before, the initial sinking of the supports having no effect on these processes.

As an example, consider a uniform beam whose relevant second moment of area is 90 (ins.)^4, carried on supports A, B, C and D. When three concentrated loads as shown in Fig. 8.11 are applied to the beam the support B sinks a distance of $\frac{1}{10}$ inch. To find the resulting bending moments imagine the beam clamped at the supports so that when the loads are applied the support B sinks $\frac{1}{10}$ inch but the beam there and at A, C and D remains horizontal. The fixed-end moments induced under these conditions are found from paragraph 3.14, taking E=13,000 tons per square inch, to be

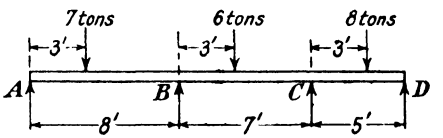

FIG. 8.11.

$M_{AB}=-14{\cdot}65$ tons-feet. $M_{BA}=-1{\cdot}54$ tons-feet. $M_{BC}=2{\cdot}40$ tons-feet.
$M_{CB}=12{\cdot}69$ tons-feet. $M_{CD}=-3{\cdot}84$ tons-feet. $M_{DC}=5{\cdot}76$ tons-feet.

TABLE 8.4.

END MOMENTS (TONS-FEET).

A		B	C		D
−14·65	−1·54	+2·40	+12·69	−3·84	+5·76
+14·65	0·00	0·00	0·00	0·00	−5·76
0·00	+7·33	0·00	0·00	−2·88	0·00
0·00	−3·25	−4·94	− 2·91	−3·06	0·00
0·00	0·00	−1·45	− 2·47	0·00	0·00
0·00	+0·57	+0·88	+ 1·20	+1·27	0·00
0·00	0·00	+0·60	+ 0·44	0·00	0·00
0·00	−0·24	−0·36	− 0·21	−0·23	0·00
0·00	0·00	−0·10	− 0·18	0·00	0·00
0·00	+0·04	+0·06	+ 0·09	+0·09	0·00

These moments are entered in the first line of Table 8.4. The beam is now released at the supports the procedure being exactly as that described for Table 8.3 and the calculation of the end moments is completed.

8.5. The generalised theorem of three moments.—The top spars of a biplane in normal flight are subjected to a distributed load from the air reaction on the wing and to compressive forces produced by the horizontal components of the loads in the flying wires. In the bottom spars the end load is tensile as will be evident from Fig. 8.12, which shows the half elevation of a typical biplane truss. Application of the ordinary theorem of three moments described in paragraph 8.3, which neglects the effects of end loads in the bays of the spar, leads in many cases to insufficiently accurate results and a more complete analysis is necessary.

The complete solution of the problem of a continuous beam under a distributed transverse load and axial end loads was given by H. Booth and H. Bolas in 1915.* The solution was in too cumbersome a form for general use, but in the following year Arthur Berry published † a simplification of the method.

This treatment will be followed here.

We shall consider the top spar ABC . . . of a biplane, A being the outermost support (Fig. 8.12). As in the notation used elsewhere in

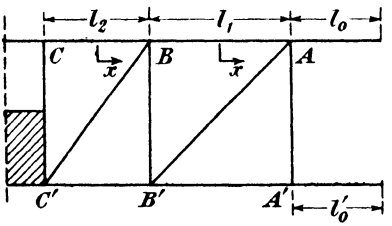

FIG. 8.12.

this chapter M_A, M_B, M_C . . . will denote the fixing moments at A, B, C . . . considered positive when they tend to produce convexity upwards. The deflection at any point is denoted by y, the intensity of loading by w. Dimensions are as in Fig. 8.12. The distance of any point in a member is measured from the centre point of the span and is counted positive in the direction B to A or C to B.

As before $\mu=\sqrt{\frac{P}{EI}}$, where P is the compressive end load in the span under consideration and E and I have their usual significance; also $\alpha=\frac{\mu l}{2}$, α being measured in radians.

* "Some Contributions to the Theory of Engineering Structures with Special Reference to the Problem of the Aeroplane," by H. Booth and H. Bolas. Issued by the Air Department, Admiralty, April, 1915.

† "The Calculation of Stresses in Aeroplane Wing Spars," A. Berry, *Transactions of Royal Aeronautical Society*, No. 1.

Suffixes are used to denote the particular span under consideration, though where there is no risk of confusion these are dropped.

The bending moment at any point is

$$M=EI\frac{d^2y}{dx^2}.$$

Taking moments about any point in AB we obtain the equation

$$EI\frac{d^2y}{dx^2}+Py=\frac{w}{2}\left(\frac{l}{2}-x\right)^2+S_A\left(x-\frac{l}{2}\right)+M_A,$$

where S_A is the shear at A.

Differentiating this equation twice we get

$$\frac{d^2M}{dx^2}+\mu^2M=w. \quad . \quad . \quad . \quad . \quad . \quad . \quad . \quad . \quad (1)$$

The solution of this equation is

$$M=A\sin\mu x+B\cos\mu x+\frac{w}{\mu^2}, \quad . \quad . \quad . \quad . \quad . \quad . \quad (2)$$

where A and B are constants of integration.

When $x=\frac{l}{2}$, $M=M_A$

and when $x=-\frac{l}{2}$, $M=M_B$.

Therefore $M_A=A\sin\alpha+B\cos\alpha+\frac{w}{\mu^2}$,

$$M_B=-A\sin\alpha+B\cos\alpha+\frac{w}{\mu^2}.$$

These give $A=\frac{M_A-M_B}{2\sin\alpha}$

and $B=\frac{M_A+M_B}{2\cos\alpha}-\frac{w}{\mu^2\cos\alpha}$.

Substituting for A and B in (2) we have

$$M=\frac{M_A-M_B}{2}\frac{\sin\mu x}{\sin\alpha}+\frac{M_A+M_B}{2}\frac{\cos\mu x}{\cos\alpha}+\frac{w}{\mu^2}\left(1-\frac{\cos\mu x}{\cos\alpha}\right) \quad . \quad . \quad . \quad (3)$$

and integrating this equation twice we have

$$EIy=-\frac{M_A-M_B}{2}\frac{\sin\mu x}{\mu^2\sin\alpha}-\frac{M_A+M_B}{2}\frac{\cos\mu x}{\mu^2\cos\alpha}+\frac{w\cos\mu x}{\mu^4\cos\alpha}$$

$$-\frac{w}{2\mu^2}\left(\frac{l^2}{4}-x^2\right)+A_1\left(x+\frac{l}{2}\right)+B_1\left(x-\frac{l}{2}\right), \quad . \quad . \quad . \quad (4)$$

where A_1 and B_1 are constants of integration.

Now $y=0$ when $x=\pm\frac{l}{2}$,

therefore $$0=-\frac{M_A}{\mu^2}+\frac{w}{\mu^4}+A_1 l$$

and $$0=-\frac{M_B}{\mu^2}+\frac{w}{\mu^4}-B_1 l.$$

Substituting in (4) we obtain

$$EIy=-\frac{M_A-M_B}{2}\frac{\sin\mu x}{\mu^2\sin\alpha}-\frac{M_A+M_B}{2}\frac{\cos\mu x}{\mu^2\cos\alpha}+\frac{w}{\mu^4}\left(\frac{\cos\mu x}{\cos\alpha}-1\right)$$
$$-\frac{w}{2\mu^2}\left(\frac{l^2}{4}-x^2\right)+(M_A-M_B)\frac{x}{l\mu^2}+\frac{M_A+M_B}{2\mu^2} \quad . \quad . \quad . \quad . \quad (5)$$

Differentiation of this gives

$$EI\frac{dy}{dx}=-\frac{M_A-M_B}{2}\frac{\cos\mu x}{\mu\sin\alpha}+\frac{M_A+M_B}{2}\frac{\sin\mu x}{\mu\cos\alpha}$$
$$-\frac{w}{\mu^3}\frac{\sin\mu x}{\cos\alpha}+\frac{wx}{\mu^2}+\frac{M_A-M_B}{l\mu^2} \quad . \quad (6)$$

The slope at B is the same whether we consider it from the point of view of the span AB or the span BC and so by using equation (6) for both spans in turn and equating the slopes when $x=-\frac{l_1}{2}$ and $x=+\frac{l_2}{2}$, we have

$$\frac{1}{I_1}\left(\frac{M_A-M_B}{2}\cot\alpha_1-\frac{M_A+M_B}{2}\frac{\tan\alpha_1}{\mu_1}+\frac{w_1}{\mu_1{}^3}\tan\alpha_1-\frac{w_1 l_1}{2\mu_1{}^2}+\frac{M_A-M_B}{l_1\mu_1{}^2}\right)$$
$$=\frac{1}{I_2}\left(-\frac{M_B-M_C}{2}\cot\alpha_2+\frac{M_B+M_C}{2}\frac{\tan\alpha_2}{\mu_2}-\frac{w_2}{\mu_2{}^3}\tan\alpha_2+\frac{w_2 l_2}{2\mu_2{}^2}+\frac{M_B-M_C}{l_2\mu_2{}^2}\right).$$

This equation, on rearranging, can be written

$$\frac{l_1 M_A}{I_1}\left(\frac{3}{2}\cdot\frac{2\alpha_1\operatorname{cosec}2\alpha_1-1}{\alpha_1{}^2}\right)+\frac{l_2 M_C}{I_2}\left(\frac{3}{2}\cdot\frac{2\alpha_2\operatorname{cosec}2\alpha_2-1}{\alpha_2{}^2}\right)$$
$$+\frac{2l_1 M_B}{I_1}\cdot\frac{3}{4}\cdot\frac{1-2\alpha_1\cot 2\alpha_1}{\alpha_1{}^2}+\frac{2l_2 M_B}{I_2}\cdot\frac{3}{4}\cdot\frac{1-2\alpha_2\cot 2\alpha_2}{\alpha_2{}^2}$$
$$=\frac{w_1 l_1{}^3}{4I_1}\cdot 3\cdot\frac{\tan\alpha_1-\alpha_1}{\alpha_1{}^3}+\frac{w_2 l_2{}^3}{4I_2}\cdot 3\cdot\frac{\tan\alpha_2-\alpha_2}{\alpha_2{}^3},$$

or writing

$$f(\alpha)=\frac{3}{2}\cdot\frac{2\alpha\operatorname{cosec}2\alpha-1}{\alpha^2},$$

$$\phi(\alpha)=\frac{3}{4}\cdot\frac{1-2\alpha\cot 2\alpha}{\alpha^2},$$

$$\psi(\alpha)=3\cdot\frac{\tan\alpha-\alpha}{\alpha^3},$$

we get

$$\frac{l_1}{I_1}M_A f(\alpha_1)+\frac{l_2}{I_2}M_C f(\alpha_2)+2M_B\left\{\frac{l_1}{I_1}\phi(\alpha_1)+\frac{l_2}{I_2}\phi(\alpha_2)\right\}$$
$$=\frac{w_1 l_1^3}{4I_1}\psi(\alpha_1)+\frac{w_2 l_2^3}{4I_2}\psi(\alpha_2). \quad . \quad (7)$$

This is the most general form of the equation of three moments for a continuous beam.

If instead of compressions in the spars there are tensions, (7) becomes

$$\frac{l_1}{I_1}M_A F(\alpha_1)+\frac{l_2}{I_2}M_C F(\alpha_2)+2M_B\left\{\frac{l_1}{I_1}\Phi(\alpha_1)+\frac{l_2}{I_2}\Phi(\alpha_2)\right\}$$
$$=\frac{w_1 l_1^3}{4I_1}\Psi(\alpha_1)+\frac{w_2 l_2^3}{4I_2}\Psi(\alpha_2), \quad . \quad (8)$$

where

$$F(\alpha)=\frac{3}{2}\cdot\frac{1-2\alpha\ \text{cosech}\ 2\alpha}{\alpha^2},$$

$$\Phi(\alpha)=\frac{3}{4}\cdot\frac{2\alpha\coth 2\alpha-1}{\alpha^2},$$

$$\Psi(\alpha)=3\cdot\frac{\alpha-\tanh\alpha}{\alpha^3}.$$

If $\alpha=0$ the corresponding functions are unity and the ordinary equation of three moments is at once deduced from (7) by putting $P_1=P_2=0$. If one span is in tension and the other in compression the corresponding series of functions must be used. Suppose for example AB is in tension and BC in compression. Then (7) becomes

$$\frac{l_1}{I_1}M_A F(\alpha_1)+\frac{l_2}{I_2}M_C f(\alpha_2)+2M_B\left\{\frac{l_1}{I_1}\Phi(\alpha_1)+\frac{l_2}{I_2}\phi(\alpha_2)\right\}=\frac{w_1 l_1^3}{4I_1}\Psi(\alpha_1)+\frac{w_2 l_2}{4I_2}\psi(\alpha_2).$$

The functions $f(\alpha)$, etc., were tabulated by Berry, to whom the result in (7) is due, and the Tables are given in an Appendix to this book.

Maximum Bending Moment.—From equation (3), on putting $\mu=\frac{2\alpha}{l}$ and rearranging, we find that the bending moment at any point in AB is given by

$$M=\frac{wl^2}{4\alpha^2}-\left(\frac{wl^2}{4\alpha^2}-\frac{M_A+M_B}{2}\right)\frac{\cos\mu x}{\cos\alpha}+\frac{M_A-M_B}{2}\frac{\sin\mu x}{\sin\alpha}.$$

It is easy to show that M is a numerical maximum when

$$\tan\mu x=-\frac{\frac{M_A-M}{2}}{\frac{wl^2}{4\alpha^2}-\frac{M_A+M_B}{2}}\cot\alpha, \quad . \quad . \quad . \quad . \quad . \quad (9)$$

which gives the distance from the middle of the span of the point where the bending moment is greatest.

If μx obtained from this equation is numerically greater than α there is no maximum, the bending moment increasing steadily from M_A to M_B. But if μx is less than α,

$$M_{max}=\frac{wl^2}{4\alpha^2}-\frac{\frac{wl^2}{4\alpha^2}-\frac{M_A+M_B}{2}}{\cos \mu x \cos \alpha} \quad . \quad . \quad . \quad . \quad . \quad . \quad . \quad (10)$$

The corresponding formulas for a member under tension are

$$\tanh \mu x = -\frac{\frac{M_A+M_B}{2}}{\frac{wl^2}{4\alpha^2}+\frac{M_A+M_B}{2}} \coth \alpha$$

and

$$M_{max}=-\frac{wl^2}{4\alpha^2}+\frac{\frac{wl^2}{4\alpha^2}+\frac{M_A+M_B}{2}}{\cosh \mu x \cosh \alpha},$$

while for a spar subjected to neither compression nor tension we obtain the result

$$M=\frac{w}{2}\left(x^2-\frac{l^2}{4}\right)+\frac{M_A+M_B}{2}+(M_A-M_B)\frac{x}{l}.$$

In this case M_{max} occurs where $x=-\frac{M_A-M_B}{wl}$

and its value is $M_{max}=-\frac{wl^2}{8}+\frac{M_A+M_B}{2}-\frac{(M_A-M_B)^2}{2wl^2}$.

8.6. The Continuous Column.—A particular case, to which equations similar to those derived in the last paragraph are applicable, is that of the compression member continuous through a number of storeys or panels. If such a member has imperfections represented by an initial curvature of the axis the end moments in each length may be determined from the three moment equations derived from expressions similar to (5) and (6) of paragraph 7.20.

Such equations would apply to a member connected to the other parts of the structure by perfectly free joints and subjected to axial loads only. These conditions are rarely found in practice. The connection between the members will usually have some rigidity so that any change of slope of the compression member will be resisted, restraining moments being induced at the ends of each length where connection is made to the other members in the structure. A discussion of such a case is outside the scope of this chapter, but a number of examples will be found in a paper published in the Second Report of the Steel Structures Research Committee.* In many structures such as building frames the continuous column is subjected to large moments in addition to axial loads, arising from the applications of load to the other members of the structure. This case is dealt with in Chapters 9 and 19.

* "A Note on the Effective Length of a Pillar forming part of a Continuous Member in a Building Frame." J. F. Baker, 2nd Report Steel Structures Research Committee. H.M. Stationery Office, 1934.

EXERCISES

(These exercises should be solved by all of the methods described in this Chapter.)

(1) A girder ABCD is continuous over the supports B and C and freely supported at A and D. The spans are AB = 10 feet; BC = 12 feet; CD = 15 feet. AB carries a uniformly distributed load of 1 ton per foot, BC 0·8 ton per foot, and CD 0·5 ton per foot.

Sketch neatly the bending moment and shearing force diagrams for the beam, indicating the principal values on your diagrams.

(M_B = 10·3 tons-feet; M_C = 11·9 tons-feet.
R_{AR} = 3·97 tons; R_{BR} = 4·67 tons; R_{CR} = 4·55 tons;
R_{BL} = 6·03 tons; R_{CL} = 4·93 tons; R_{DL} = 2·95 tons.)

(2) A continuous girder rests on four supports A, B, C and D at the same level, and carries a uniform load of 1 ton per foot run. The spans are AB = 15 feet; BC = 20 feet and CD = 12 feet.

Determine the bending moments at the supports and the reactions on the supports.

(M_B = 32·7 tons-feet; M_C = 27·8 tons-feet.
R_A = 5·32 tons; R_B = 19·92 tons; R_C = 18·06 tons; R_D = 3·70 tons.)

(3) A beam AB which is 23 feet long is encastré at A and supported at points C and D, which are 8 feet and 20 feet respectively from A. The beam carries a load of 10 tons at a point 4 feet from A, 2 tons at B and a uniformly distributed load of 1 ton per foot between C and D.

Sketch the bending moment and shearing force diagrams.

CHAPTER 9

FRAMES WITH STIFF JOINTS

9.1. Stiff joints.—In earlier chapters we have dealt with the stress analysis of braced frameworks upon the assumption that the bars forming them were pinned together at the ends. Such a joint as this is unable, theoretically, to transmit a bending moment so that when a pin-jointed frame is loaded at the nodes the forces in the component members are pure tensions or compressions. In practice it is very seldom that even an attempt is made to obtain pin joints in a frame; connections are usually made by rivetted or bolted joints which restrain the free movement of the ends of the members. A joint between two components of a structure which can transmit a bending moment will be called a stiff joint and the degree of stiffness will depend upon the type of joint. A practical pinned joint will have some stiffness due to the friction between the pin and the bearing on the member, and

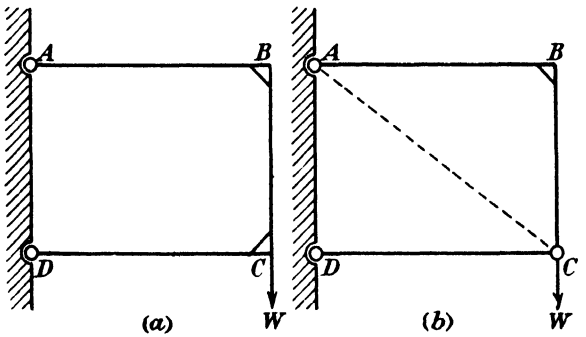

FIG. 9.1.

between this degree of stiffness and that of perfect rigidity there are infinite possibilities. A convenient measure of stiffness is obtained by specifying the change of angle between two members connected by the joint under a unit moment applied to the members. When the joint is pinned the change of angle will be a maximum; when it is infinitely stiff the change will be zero. This method of measuring the degree of stiffness will be defined more precisely at a later stage; at the moment it is only necessary to realise the importance of stiffness as affecting stress distribution. For the present, joints will be considered to be rigid; the modifications to methods of analysis when they are only partially fixed will be considered later.

To understand the effect of a stiff joint upon a frame, consider the simplest case of a quadrilateral frame as shown in Fig. 9.1.

If the joints at B and C are to be connected to the pins A and D by a skeleton frame it is necessary to use the four members AB, AC, BC and CD. The joints at B and C may be frictionless pins and the result is a just-stiff structure. If, however, we make the joint at B stiff, as shown at (*b*) in the same figure, the members AB and BC may be considered to be a single cranked bar and joint C is braced to A and D by this bar and DC. The diagonal member AC can be omitted and if it is present it constitutes a redundant element. Each rigid joint is thus equivalent to a member and the frame at (*a*) has one redundancy.

As another example, consider the frame shown in Fig. 9.2 in which A, F and E are pinned supports to which the joints B, C and D are to be braced. For the construction of a just-stiff frame six members are required and so, if joints B, C and D are all pins the arrangement is incomplete since only five bars are provided. If, however, joint B is made rigid, we have the equivalent of six members, *i.e.* five bars and one stiff joint, and the structure is just stiff. Thus, C is braced by the cranked bar ABC and FC, while D is braced to C and E by

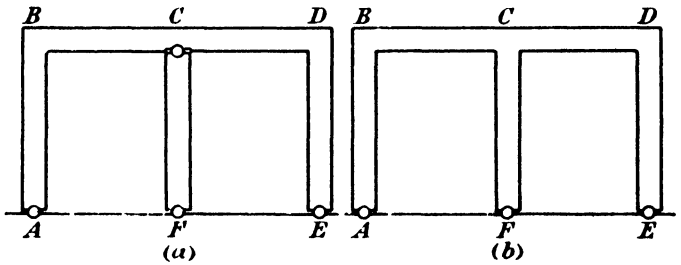

FIG. 9.2.

the bars CD and ED. Any stiff connections additional to that at B will introduce redundancies. Thus, the frame shown at (*a*) in Fig. 9.2 consists of the continuous member BCD to which the end verticals AB and ED are rigidly attached. The remaining bar FC is connected to it by a pinned joint and the equivalent number of members actually provided is made up as follows.

Five bars, AB, BC, CD, FC and ED.
Two stiff joints at B and D respectively.
One stiff joint at C due to the continuity of BC and CD.

This gives eight equivalent members and since only six are essential the frame has two redundant elements. If the vertical member FC is connected to the continuous member BCD by a rigid joint as shown at (*b*) in Fig. 9.2 instead of by a pin, this will introduce an extra redundancy. Later examples will indicate which members are most conveniently taken as redundancies for the purposes of analysis.

It will be realised that frames of this type are very common in engineering construction—the framed building is perhaps the best example of the use of stiff joints to replace diagonal bracing members but they are found in many other structures. It is therefore important

to examine methods of analysis and we shall discuss the treatment of this type of structure by the three methods of strain energy, slope deflection and moment distribution.

9.2. Strain energy analysis of stiff-jointed frames.—The general theory of this method has already been developed in earlier chapters and examples of its application in special cases will now be given. In the first place consider the portal shown in Fig. 9.3 which consists of a frame ACDB having rigid joints at C and D and pinned to A and B. The dimensions are shown on the figure and a single load W is carried in the position indicated on the top member. All members of the frame are supposed to be of the same section. As already shown in the previous paragraph this frame has one redundancy. If the joint B, instead of being pinned, simply rested on a frictionless support,

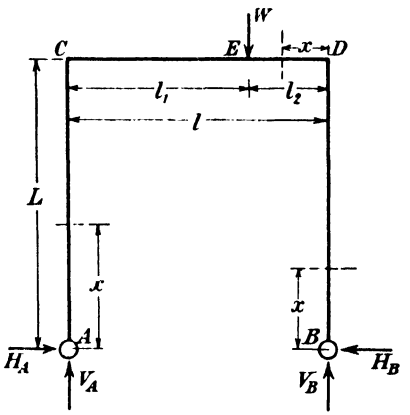

FIG. 9.3.

ACDB would be a cranked beam and the bending moment diagram could be plotted without difficulty. Since B is fixed in position however, a horizontal force H_B can be exerted by the pin and it is convenient to take this force as the redundant element.

Then, by the second theorem of Castigliano we have

$$\frac{dU}{dH_B}=0$$

where U is the total strain-energy of the frame.

The strain-energy consists of that due to bending in all members of the frame and that due to axial compression and shear. The last two are in most practical cases negligible compared with the former and we shall ignore them in the present example.

Then
$$\frac{dU}{dH_B}=\frac{1}{EI}\int M_x\frac{dM_x}{dH_B}dx=0$$

where M_x is the bending moment at any point and the integration extends round the whole frame.

The conditions for static equilibrium of the frame are expressed by the following equations :—

$$V_A + V_B = W$$
$$H_A = H_B$$
$$V_B l = W l_1$$

which give

$$V_B = \frac{W l_1}{l} \text{ and } V_A = \frac{W l_2}{l}.$$

We shall put $H_A = H_B = H$.

Then for the member BD, measuring x from B, we have

$$M_x = Hx$$

and

$$\frac{dM_x}{dH} = x$$

$$\therefore \quad \left[\frac{dU}{dH}\right]_{BD} = \frac{1}{EI}\int_0^L Hx^2 dx = \frac{HL^3}{3EI}.$$

For the section DE of the top beam, measuring x from D, we have

$$M_x = HL - V_B x$$
$$= HL - \frac{W l_1 x}{l}$$

and

$$\frac{dM_x}{dH} = L$$

$$\therefore \quad \left[\frac{dU}{dH}\right]_{DE} = \frac{L}{EI}\int_0^{l_2}\left(HL - \frac{W l_1 x}{l}\right)dx$$
$$= \frac{L l_2}{EI}\left(HL - \frac{W l_1 l_2}{2l}\right).$$

Similarly for AC and CE, measuring x from A and C respectively we have

$$\left[\frac{dU}{dH}\right]_{AC} = \frac{HL^3}{3EI}$$
$$\left[\frac{dU}{dH}\right]_{CE} = \frac{L l_1}{EI}\left(HL - \frac{W l_1 l_2}{2l}\right).$$

Adding the components we obtain for the whole frame, since EI is the same throughout,

$$EI\frac{dU}{dH} = \frac{2HL^3}{3} + Ll\left(HL - \frac{W l_1 l_2}{2l}\right) = 0$$

and so

$$H = \frac{3 l_1 l_2 W}{2L(2L + 3l)}.$$

If L=20 feet, l_1=6 feet and l_2=4 feet we have

$$H = \frac{18W}{700}$$

and the bending moment diagram for the portal is as shown in Fig. 9.4 which is plotted from the equations for M_x used in the analysis.

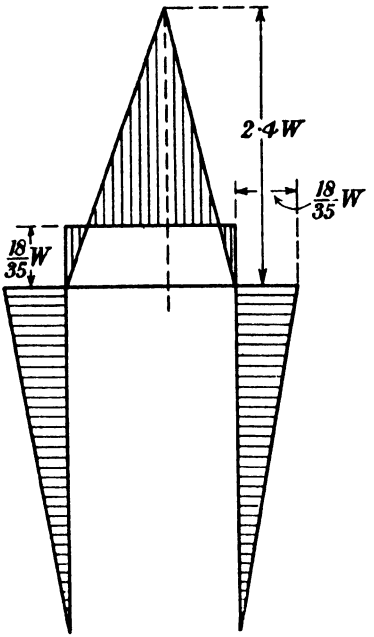

FIG. 9.4.

If the load had been placed midway along CD it would only have been necessary to consider one-half the structure.

As the next example we shall consider the portal shown in Fig. 9.5

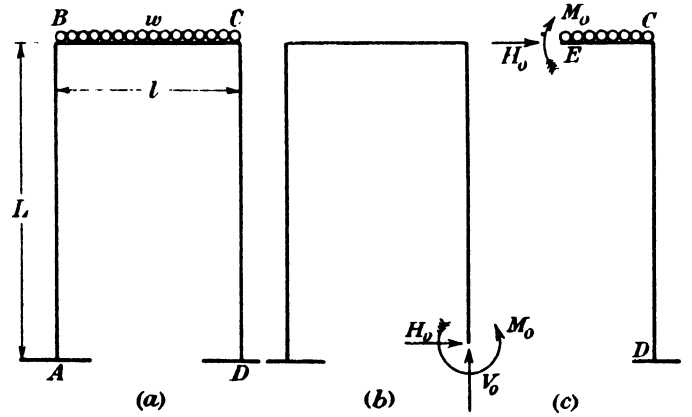

FIG. 9.5.

which has a uniformly distributed load on the top member. The feet of the vertical members are assumed to be rigidly fixed.

If the vertical member CD were cut through at D the frame would

be statically determinate, consisting simply of a double cranked cantilever built in at A and free at D. In order to restore the conditions existing before the cut was made it is necessary to impose at D a bending moment M_0, a vertical reaction V_0 and a horizontal reaction H_0. These resultant actions must be of such magnitude as to prevent the section at D from any movement either of translation or rotation and the conditions for this requirement to be satisfied are, using the first theorem of Castigliano,

movement of D in a vertical direction $=\dfrac{\partial U}{\partial V_0}=0,$

movement of D in a horizontal direction $=\dfrac{\partial U}{\partial H_0}=0,$

rotation of D $=\dfrac{\partial U}{\partial M_0}=0.$

The solution of these equations determines the values of the resultant actions at D in the original state of the frame.

This would be the method adopted in the general case of the problem now under consideration, *e.g.* if the load were not symmetrically placed on the structure or if the second moments of area of the vertical members were not equal. In the present instance, however, we are assuming symmetry both of structure and of loading and the solution may be simplified. Suppose the top member to be cut at E on the axis of symmetry of the frame as shown at (*c*) in the figure and the resultant action there to be replaced by an external moment M_0 and a horizontal force H_0. From the symmetry of the frame there can be no shearing force at E and we reduce the number of unknowns by one.

Then, since the section at E neither rotates nor moves laterally, M_0 and H_0 must satisfy the conditions

$$\frac{\partial U}{\partial M_0}=0\,;\quad \frac{\partial U}{\partial H_0}=0.$$

As in the previous example we shall neglect all terms in the energy expression except that due to bending and we have

$$\frac{\partial U}{\partial M_0}=\frac{1}{EI}\int M_x\frac{\partial M_x}{\partial M_0}dx=0$$

and

$$\frac{\partial U}{\partial H_0}=\frac{1}{EI}\int M_x\frac{\partial M_x}{\partial H_0}dx=0.$$

For the section EC, when x is measured from E we have

$$M_x=-M_0+\frac{wx^2}{2}$$

so

$$\frac{\partial M_x}{\partial M_0}=-1 \text{ and } \frac{\partial M_x}{\partial H_0}=0$$

$$\left[\frac{\partial U}{\partial M_0}\right]_{EC}=\frac{1}{EI}\int_0^{l/2}\left(M_0-\frac{wx^2}{2}\right)dx$$

$$=\frac{1}{EI}\left[\frac{M_0 l}{2}-\frac{wl^3}{48}\right]$$

For the section CD, measuring x from C, we have

$$M_x = -M_0 + \frac{wl^2}{8} - H_0 x$$

so $$\frac{\partial M_x}{\partial M_0} = -1 \text{ and } \frac{\partial M_x}{\partial H_0} = -x$$

$$\therefore \quad \left[\frac{\partial U}{\partial M_0}\right]_{CD} = \frac{1}{EI}\int_0^L \left(M_0 - \frac{wl^2}{8} + H_0 x\right) dx = \frac{1}{EI}\left[M_0 L - \frac{wl^2 L}{8} + \frac{H_0 L^2}{2}\right]$$

and $$\left[\frac{\partial U}{\partial H_0}\right]_{CD} = \frac{1}{EI}\int_0^L \left(M_0 - \frac{wl^2}{8} + H_0 x\right) x\,dx = \frac{1}{EI}\left[\frac{M_0 L^2}{2} - \frac{wl^2 L^2}{16} + \frac{H_0 L^3}{3}\right].$$

Hence, adding the appropriate terms for the half frame we obtain

$$\left.\begin{aligned} M_0\left(L + \frac{l}{2}\right) - \frac{wl^2}{8}\left(L + \frac{l}{6}\right) + \frac{H_0 L^2}{2} &= 0 \\ \frac{M_0 L}{2} - \frac{wl^2 L}{16} + \frac{H_0 L^2}{3} &= 0 \end{aligned}\right\}$$

and the solution of these equations is

$$H_0 = \frac{wl^3}{4L(L + 2l)}$$

$$M_0 = \frac{wl^2}{24}\left(\frac{3L + 2l}{L + 2l}\right)$$

while from symmetry the vertical reaction at D is $\frac{wl}{2}$.

The bending moment diagram for one half of this frame is shown in Fig. 9.6 when $L = 1{\cdot}5l$.

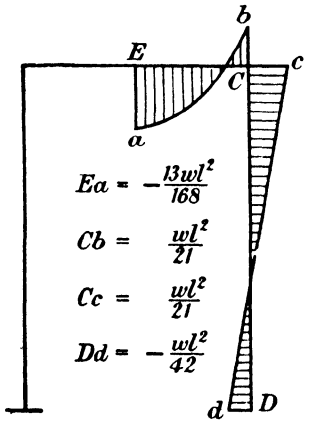

FIG. 9.6.

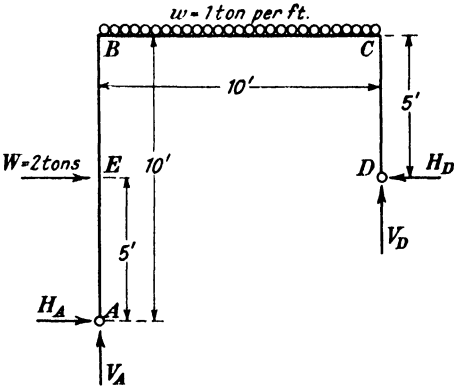

FIG. 9.7.

As a final example of structures of this type we will analyse that shown in Fig. 9.7 in which the pinned supports of the vertical members are not at the same level. As in the first example the redundant element will be taken to be H_A.

In the first place the conditions for static equilibrium give the equations

$$H_D = H_A + 2$$
$$V_A + V_D = 10$$
$$10V_D - 5W + 5H_D - 50w = 0, \text{ by moments about A.}$$

Substituting for W and w and solving we obtain the result

$$V_A = 5 + 0{\cdot}5H_A$$
$$H_D = 2 + H_A$$
$$V_D = 5 - 0{\cdot}5H_A.$$

For the determination of H_A we have the condition

$$\frac{dU}{dH_A} = \frac{1}{EI}\int M_x \frac{dM_x}{dH_A}dx = 0.$$

For AE, measuring x from A, we have

$$M_x = H_A x.$$

$$\therefore \quad \frac{dM_x}{dH_A} = x$$

and

$$\left[\frac{dU}{dH_A}\right]_{AE} = \frac{1}{EI}\int_0^5 H_A x^2 dx = \frac{125H_A}{3EI}$$

For EB, measuring x from A, we have

$$M_x = H_A x + 2(x-5)$$

and again

$$\frac{dM_x}{dH_A} = x$$

$$\therefore \quad \left[\frac{dU}{dH_A}\right]_{EB} = \frac{1}{EI}\int_5^{10}(H_A x^2 + 2x^2 - 10x)dx = \frac{1}{EI}\left[\frac{875H_A}{3} + \frac{625}{3}\right]$$

For the length BC, measuring x from B, we have

$$M_x = 10H_A + 10 - V_A x + \frac{x^2}{2}$$

and substituting for V_A in terms of H_A this gives

$$M_x = H_A(10 - 0{\cdot}5x) + 10 - 5x + \frac{x^2}{2}.$$

This is an important point—since V_A is a function of H_A it is essential to substitute its value before differentiating the expression or a wrong value of $\frac{dM_x}{dH_A}$ will be found.

Thus

$$\frac{dM_x}{dH_A} = 10 - 0{\cdot}5x$$

and

$$\left[\frac{dU}{dH_A}\right]_{BC} = \frac{1}{EI}\int_0^{10}\Big\{H_A(10-0{\cdot}5x)^2 + (100-5x) - 5x(10-0{\cdot}5x) + \frac{x^2}{2}(10-0{\cdot}5x)\Big\}dx$$

$$= \frac{1}{EI}\int_0^{10}\{H_A(10-0{\cdot}5x)^2 + 100 - 55x + 7{\cdot}5x^2 - 0{\cdot}25x^3\}dx$$

i.e.

$$\left[\frac{dU}{dH_A}\right]_{BC} = \frac{1}{EI}\left[\frac{1750}{3}H_A + 125\right].$$

For the length CD it is convenient to measure x from D,

then $$M_x = H_D x$$
$$= (H_A + 2)x$$

and $$\frac{dM_x}{dH_A} = x$$

$$\therefore \quad \left[\frac{dU}{dH_A}\right]_{CD} = \frac{1}{EI}\int_0^5 (H_A+2)x^2 dx = \frac{1}{EI}\left[\frac{125}{3}H_A + \frac{250}{3}\right]$$

Adding the components we have

$$\frac{dU}{dH_A} = \frac{1}{3EI}(2875H_A + 1250) = 0$$

from which we determine

$$\left.\begin{aligned} H_A &= -0{\cdot}4 \text{ tons} \\ V_A &= \ \ 4{\cdot}8 \text{ tons} \\ H_D &= \ \ 1{\cdot}6 \text{ tons} \\ V_D &= \ \ 5{\cdot}2 \text{ tons} \end{aligned}\right\}$$

The bending moment diagram is therefore as shown in Fig. 9.8.

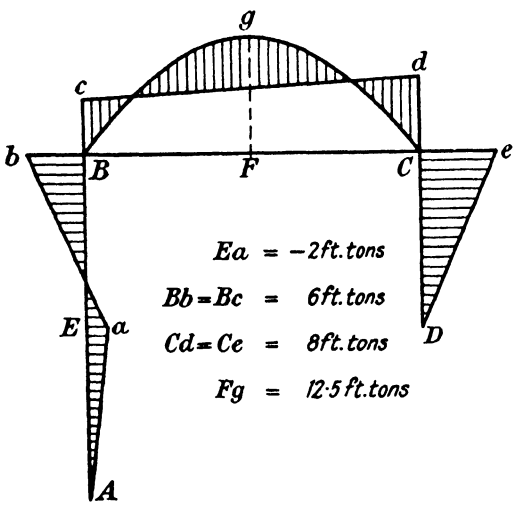

FIG. 9.8.

The strain energy method of analysis illustrated in the foregoing examples is very useful for simple portals but is complicated for more elaborate structures. If, for example, the structure shown at (*b*) in Fig. 9.2 were rigidly fixed at A, F and E it would have six redundant elements. This is apparent by an application of the method described for determining the number of redundancies in such a frame and is also obvious if we imagine the verticals to be cut at F and E. The remaining structure is a doubly cranked cantilever ABDE held at A with a free arm CF attached. By making these cuts we have destroyed a moment, a vertical force and a horizontal force at both F and E and these six resultant actions may be taken as the redundant elements in

an analysis. For a solution of this problem therefore we have to form and solve the six simultaneous equations

$$\frac{\partial U}{\partial M_F}=\frac{\partial U}{\partial V_F}=\frac{\partial U}{\partial H_F}=\frac{\partial U}{\partial M_E}=\frac{\partial U}{\partial V_E}=\frac{\partial U}{\partial H_E}=0.$$

This is a possible but laborious task. If, however, the number of bays is increased beyond two the work involved is prohibitive. Approximate methods are therefore necessary in such cases and will be discussed in a later Chapter dealing with the design of steel framed buildings.

9.3. Slope deflection analysis of rigidly jointed frames.—Another method of determining the stresses in the members of a framework with stiff joints makes use of the slope deflection expressions already set out in paragraph 3.13.

Equations are derived in much the same way as were the three moment equations for a continuous beam. In general, each member of a framework is subjected, in addition to the external loads, to restraining moments at its ends transmitted through the stiff joints. These moments can be expressed in terms of the unknown slopes and deflections at the ends of the members. By considering the equilibrium of each joint in the frame and of the frame as a whole, a sufficient number of equations can be obtained to enable all the slopes and deflections to be evaluated. The restraining moments and the stresses at any point in the frame can then be found without difficulty.

Though the method is capable of dealing with any type of frame, complication will be avoided here by confining attention to members of uniform cross-section carrying uniformly distributed or point loads. The usual assumption will be made that deformations due to shear and to direct stress, and also the effect of the direct thrust on the flexure of a member, are negligible.

When an initially straight horizontal member AB of uniform cross-section and length l is subjected to a uniformly distributed load of

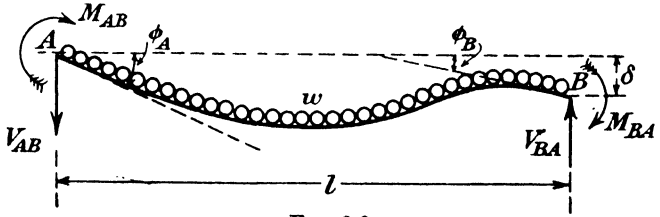

FIG. 9.9.

intensity w and to clockwise end couples M_{AB} and M_{BA} as shown in Fig. 9.9, where all the loads and reactions applied to the member and all changes of slope and deflection suffered by it are shown in positive directions, ϕ_A and ϕ_B the changes of slope at A and B, are given by

$$\phi_A=\frac{l}{6EI}\left[2M_{AB}-M_{BA}+\frac{wl^2}{4}\right]+\frac{\delta}{l} \quad . \quad . \quad . \quad . \quad . \quad (1)$$

and

$$\phi_B=-\frac{l}{6EI}\left[M_{AB}-2M_{BA}+\frac{wl^2}{4}\right]+\frac{\delta}{l} \quad . \quad . \quad . \quad . \quad (2)$$

The solution of these gives

$$M_{AB}=\frac{2EI}{l}\left[2\phi_A+\phi_B-\frac{3\delta}{l}\right]-\frac{wl^2}{12} \quad . \quad . \quad . \quad . \quad . \quad . \quad . \quad (3)$$

and

$$M_{BA}=\frac{2EI}{l}\left[\phi_A+2\phi_B-\frac{3\delta}{l}\right]+\frac{wl^2}{12} \quad . \quad . \quad . \quad . \quad . \quad . \quad . \quad (4)$$

By taking moments about A and B the reactions are found to be

$$V_{AB}=-\frac{wl}{2}+\frac{6EI}{l^2}\left[\phi_A+\phi_B-\frac{2\delta}{l}\right] \quad . \quad . \quad . \quad . \quad . \quad . \quad . \quad (5)$$

and

$$V_{BA}=+\frac{wl}{2}+\frac{6EI}{l^2}\left[\phi_A+\phi_B-\frac{2\delta}{l}\right] \quad . \quad . \quad . \quad . \quad . \quad . \quad . \quad (6)$$

The use of these equations can be illustrated by considering a symmetrical portal of the type illustrated in Fig. 9.5. When the uniformly distributed load is applied to the beam it bends, changing

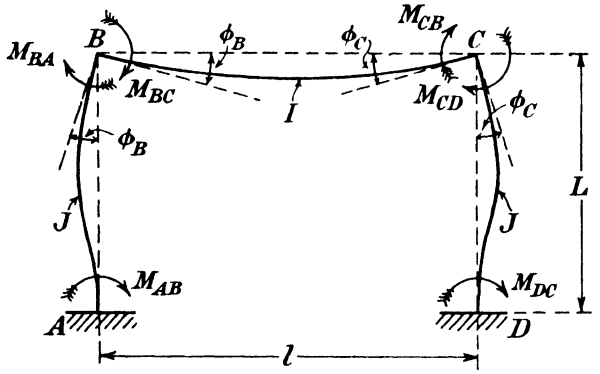

FIG. 9.10.

its slope at the ends. Since the joints of the portal are perfectly rigid the tops of the stanchions must suffer the same changes of slope as the ends of the beam to which they are attached, as shown in Fig. 9.10. It follows from a consideration of symmetry that $\phi_C=-\phi_B$ and that B and C have neither horizontal nor, since deformation due to direct stresses are negligible, vertical movement. It is now possible to write down relations between the changes of slope and the restraining moments applied to the ends of the members by the joints shown, Fig. 9.10, in their positive (clockwise) directions. From equation (3)

$$M_{BC}=\frac{2EI}{l}\phi_B-\frac{wl^2}{12} \quad . \quad . \quad . \quad . \quad . \quad . \quad . \quad . \quad (7)$$

also, since $\phi_A=0$, the foot of the stanchion being rigidly fixed,

$$M_{BA}=\frac{2EJ}{L}[2\phi_B] \quad . \quad . \quad . \quad . \quad . \quad . \quad . \quad . \quad (8)$$

where J and L are the second moment of area and height of the stanchion respectively.

From the equilibrium of the joint B, neglecting the widths of the members, it follows that

$$M_{BA}+M_{BC}=0 \quad . \quad . \quad . \quad . \quad . \quad . \quad . \quad . \quad . \quad . \quad (9)$$

so that $$\frac{2EJ}{L}[2\phi_B]+\frac{2EI}{l}[\phi_B]-\frac{wl^2}{12}=0$$

or $$\phi_B=\frac{wl^2}{24\left(\frac{2J}{L}+\frac{I}{l}\right)E}.$$

Substituting in equations (7) and (8) we obtain

$$M_{BA}=-M_{BC}=\frac{\frac{J}{L}}{\left[\frac{2J}{L}+\frac{I}{l}\right]}\frac{wl^2}{6}$$

and from equation (3)

$$M_{AB}=\frac{2EJ}{L}[\phi_B]=\tfrac{1}{2}M_{BA}.$$

All the end moments are now known and the bending moment diagram for the frame may be drawn. It will be seen that for the frame of Fig. 9.5 in which the second moment of area was the same throughout,

$$M_{BC}=-\frac{l}{L+2l}\frac{wl^2}{6}$$

so that the bending moment at the centre of the beam is

$$M_0=\frac{wl^2}{8}-\frac{l}{L+2l}\frac{wl^2}{6}=\frac{wl^2}{24}\left(\frac{3L+2l}{L+2l}\right)$$

If a comparison is made with paragraph 9.2 it will be seen that for this particular portal the slope deflection method is more direct than the strain energy analysis since, due to symmetry and the fact that the feet of the stanchions are rigidly fixed, one change of slope is sufficient to define the shape of the loaded frame completely while two reactions have to be found by strain energy. Had the portal been unsymmetrically loaded both slopes at the ends of the beam and the horizontal movement of the beam would have to be found by slope deflection methods. This would necessitate the derivation and solution of three equations, the same number as required in the strain energy analysis so that there would be little to choose between the two methods. When the foot of a stanchion is hinged, strain energy usually has the advantage as it means one less redundancy, the fixing moment, but one more slope. For a single bay, single storey frame therefore, one or other of the methods may have the advantage but as the number of bays and storeys increases it will be found that the slope deflection method soon becomes the more economical. This will be appreciated if the two bay frame shown in Fig. 9.11 is examined. When the load is unsymmetrically placed, six redundant reactions would have to be found by strain energy whereas only four slopes and deflections need

to be evaluated to give the shape of the loaded frame, and therefore the reactions, completely.

Suppose both beams of the frame have the same span l and the same second moment of area I, the stanchions being identical having a second moment of area J and a height h. A load of intensity w is applied to PR. At P, from equation (3),

$$M_{PR}=\frac{2EI}{l}[2\phi_P+\phi_R]-\frac{wl^2}{12} \quad . \quad . \quad . \quad . \quad . \quad . \quad (10)$$

also

$$M_{PQ}=\frac{2EJ}{h}\left[2\phi_P-\frac{3\delta}{h}\right] \quad . \quad . \quad . \quad . \quad . \quad . \quad . \quad . \quad (11)$$

Where δ, the horizontal movement of P relative to Q, is the sway which will take place due to the lack of symmetry in the frame.

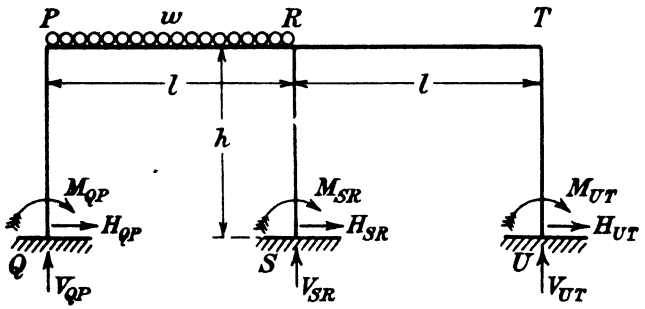

FIG. 9.11.

From a consideration of the equilibrium of joint P

$$M_{PR}+M_{PQ}=0$$

or

$$2EK_B[2\phi_P+\phi_R]+2EK_S\left[2\phi_P-\frac{3\delta}{h}\right]=\frac{wl^2}{12} \quad . \quad . \quad . \quad . \quad (12)$$

where K_B and K_S are written for $\frac{I}{l}$ and $\frac{J}{h}$ respectively.

Similarly at R, expressions for M_{RP} and M_{RT} can be written down and

$$M_{RS}=\frac{2EJ}{h}\left[2\phi_R-\frac{3\delta}{h}\right] \quad . \quad . \quad . \quad . \quad . \quad . \quad (13)$$

since, owing to the assumption that deformations due to direct stress are negligible, the horizontal movement of R with respect to S must be the same as the " δ " of equation (11).

From a consideration of the equilibrium of joint R which gives

$$M_{RP}+M_{RS}+M_{RT}=0$$

it follows that

$$2EK_B[\phi_P+2\phi_R]+\frac{wl^2}{12}+2EK_B[2\phi_R+\phi_T]+2EK_S\left[2\phi_R-\frac{3\delta}{h}\right]=0 \quad . \quad . \quad (14)$$

also from the joint T

$$2EK_B[\phi_R+2\phi_T]+2EK_S\left[2\phi_T-\frac{3\delta}{h}\right]=0 \quad . \quad . \quad . \quad . \quad (15)$$

An additional equation is needed before the unknowns ϕ_P, ϕ_R, ϕ_T and δ can be evaluated and this is obtained from a consideration of the equilibrium of the frame as a whole.

In Fig. 9.11 the reactions imposed on the ends of the members by the foundations are shown and the frame is in equilibrium under these reactions and the external applied load on PR.

Taking moments about U, the foot of the right-hand stanchion, we have

$$V_{QP}2l+V_{SR}l+M_{QP}+M_{SR}+M_{UT}=wl\,.\,\frac{3l}{2} \quad . \quad . \quad . \quad . \quad (16)$$

As the feet of the stanchions are at the same level the horizontal reactions do not appear in this equation. The reactions V_{QP} and V_{SR} are the same as those imposed on the beams at P and R and can be evaluated from equations (5) and (6). They are

$$V_{QP}=\frac{wl}{2}-\frac{6EI}{l^2}[\phi_P+\phi_R]$$

and

$$V_{SR}=\frac{wl}{2}+\frac{6EI}{l^2}[\phi_P+\phi_R]-\frac{6EI}{l^2}[\phi_R+\phi_T].$$

Substituting these expressions and those for the moments in equation (16) we have

$$-6EK_B[\phi_P+2\phi_R+\phi_T]+2EK_S\left[\phi_P+\phi_R+\phi_T-\frac{9\delta}{h}\right]=0 \quad . \quad . \quad (17)$$

The unknown slopes and deflection can be found from equations (12), (14), (15) and (17). All the end moments then follow from equations (3) and (4) and the bending moment diagram can be drawn.

Had the feet of the stanchions not been at the same level (see Fig. 9.7) the horizontal reactions H_{QP} etc. would have appeared in equation (16). These reactions can be expressed in terms of the slopes and deflections from equations (5) and (6) so that the form of equation (17) would not have been altered.

It is now possible to set out general equations for the rigidly jointed frame which carries the loads in a framed building. The structure considered is two dimensional and consists of a line of vertical stanchions, rigidly fixed at the base, connected by horizontal beams as shown in Fig. 9.12. The assumptions and sign conventions already given will be used. The notation is as shown in Fig. 9 12 and as follows :—

B_r is the joint where stanchion B is crossed by the rth floor.

h_r is the rth storey height, that is the height between the neutral axis of the $(r-1)$th and the rth floors.

l_{2r}=the length of the beam in the second bay of the rth floor.

d_{Br}=the distance of the faces of the stanchion from the neutral axis at B_r.

f_{Br}=the distance of the upper and lower surfaces of the beam from the neutral axis at B_r.

I_{2r}=the second moment of area of the beam in the second bay of the rth floor.

I_{Br}=the second moment of area of stanchion B in the rth storey, that is between $B_{(r-1)}$ and B_r.

θ_{Br}=the slope of the stanchion at B_r.

ϕ=the slope at the end of a beam.

δ_r=the deflection of a stanchion in the rth storey height, that is the horizontal deflection of the rth relative to the $(r-1)$th joint in a stanchion.

$R_r=\frac{\delta_r}{h_r}$.

M^r_{BC}=the bending moment at the end B of the beam BC in the rth floor.

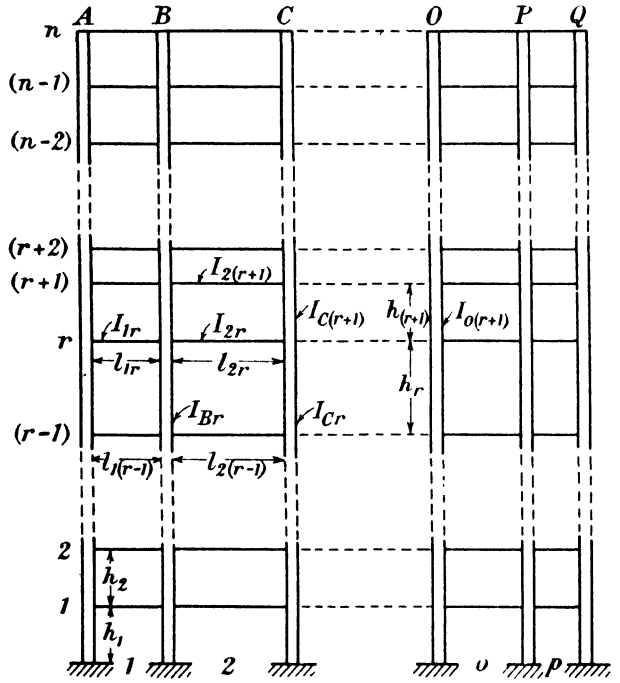

FIG. 9.12.

$M^B_{r(r+1)}$=the bending moment at the end B_r of the length of stanchion $B_rB_{(r+1)}$.

V=a vertical reaction.

H=a horizontal reaction.

$K_{1r}=\frac{I_{1r}}{l_{1r}}$; $K_{Br}=\frac{I_{Br}}{h_r}$.

w_{2r}=load per unit length on the beam in the second bay of the rth floor.

It will be evident from the two bay portal example, which has been treated in detail above, that there will be as many unknowns as there

are joints and storeys in the structure. When any load is applied each joint will rotate and each line of beams at a floor level will suffer horizontal displacement in the plane of the frame. The equations needed for the evaluation of these slopes and displacements are derived from a consideration of the equilibrium of each joint and each storey in the frame.

Fig. 9.13 shows a typical joint with the reactions applied to it by the members. It will be assumed that the shaded portion enclosed by the beams and stanchions suffers no distortion. This is quite well justified in any practical frame. In fact the error produced by neglecting the widths of the members is usually small when the joints

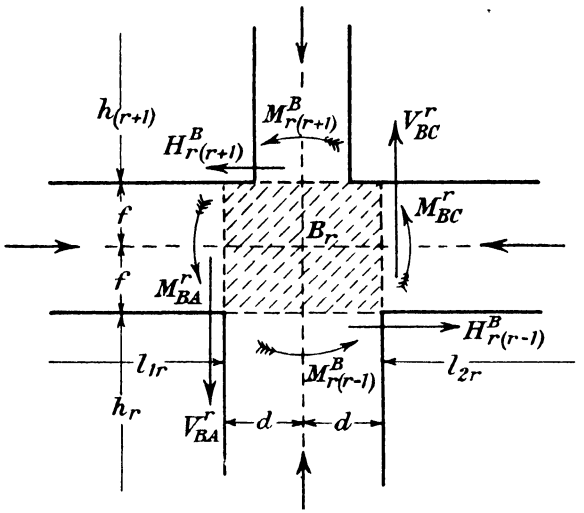

FIG. 9.13.

are rigid but it is considered worth while to include them here as they do not complicate the analysis seriously.

From the equilibrium of this joint it follows that

$$M^r_{BA}+M^B_{r(r-1)}+M^r_{BC}+M^B_{r(r+1)}+d(V^r_{BA}+V^r_{BC}) +f(H^B_{r(r+1)}+H^B_{r(r-1)})=0 \quad . \quad . \quad . \quad (18)$$

and expressing these moments and reactions in terms of the slopes and deflections, equations (3)-(6), we have

$$\begin{aligned}
&K_{1r}\left(1+\frac{3d}{l_{1r}}\right)\theta_{Ar}+K_{Br}\left(1+\frac{3f}{h_r}\right)\theta_{B(r-1)}\\
&+\left[K_{1r}\left(2+\frac{3d}{l_{1r}}\right)+K_{2r}\left(2+\frac{3d}{l_{2r}}\right)+K_{Br}\left(2+\frac{3f}{h_r}\right)+K_{B(r+1)}\left(2+\frac{3f}{h_{(r+1)}}\right)\right]\theta_{Br}\\
&+K_{B(r+1)}\left(1+\frac{3f}{h_{(r+1)}}\right)\theta_{B(r+1)}+K_{2r}\left(1+\frac{3d}{l_{2r}}\right)\theta_{Cr}\\
&-3K_{Br}\left(1+\frac{2f}{h_r}\right)R_r-3K_{B(r+1)}\left(1+\frac{2f}{h_{(r+1)}}\right)R_{(r+1)}\\
&+\frac{l_{1r}}{4E}\left(d+\frac{l_{1r}}{6}\right)w_{1r}-\frac{l_{2r}}{4E}\left(d+\frac{l_{2r}}{6}\right)w_{2r}=0 \quad . \quad . \quad . \quad . \quad . \quad . \quad . \quad . \quad . \quad . \quad (19)
\end{aligned}$$

A similar equation can be written down for each joint in the frame. The other type of general equation can be derived by considering the equilibrium of all the stanchions in a storey but it will probably be clearer if approached in the following way.

Fig. 9.14 represents the rth storey in the frame. Imagine it cut first at XX just below the rth floor. The reactions shown at XX are those applied by the upper ends of the stanchions in the rth storey to the joints in the rth floor. That part of the frame above XX is therefore

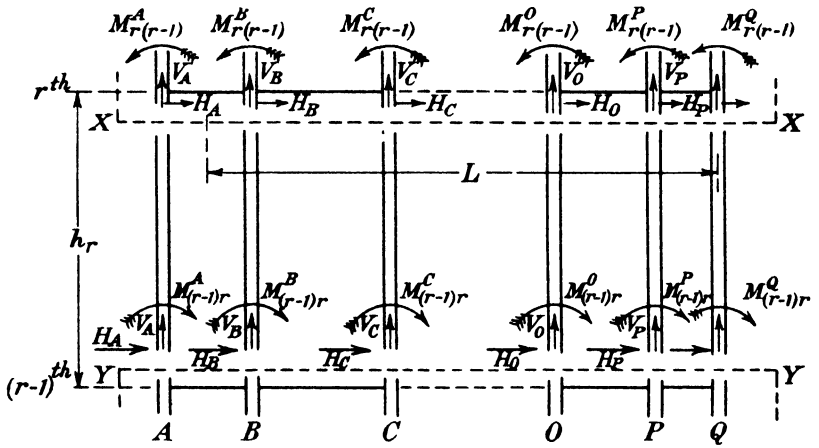

FIG. 9.14.

in equilibrium under these reactions and the external loads. Taking moments about the cut section in stanchion Q we obtain

$$V_A \sum_1^p l + V_B \sum_2^p l + \ldots - \sum_A^Q M_{r(r-1)} = \sum_r^n \sum_1^p wl \,.\, L \quad . \quad . \quad . \quad (20)$$

where L is the horizontal distance from the centre of a beam to stanchion Q.

Now imagine the cuts at XX repaired and others made at YY just above the $(r-1)$th floor (Fig. 9.14). The reactions shown there are those applied to the lower ends of the stanchions by the joints in the $(r-1)$th floor. The whole of the frame above YY is therefore in equilibrium under these reactions and the external loads. Taking moments about the cut section in stanchion Q we have

$$V_A \sum_1^p l + V_B \sum_2^p l + \ldots + \sum_A^Q M_{(r-1)r} = \sum_r^n \sum_1^p wl \,.\, L \quad . \quad . \quad . \quad (21)$$

Subtracting equation (20) from (21) gives

$$\sum_A^Q (M_{r(r-1)} + M_{(r-1)r}) = 0,$$

or from equations (3) and (4)

$$\sum_A^Q EK_{Ar}(\theta_{Ar} + \theta_{A(r-1)} - 2R_r) = 0. \quad . \quad . \quad . \quad . \quad . \quad (22)$$

A similar equation can be obtained for each storey in the frame so that with those of type (19) there are sufficient for the evaluation of all the unknown slopes and deflections from which the bending moments anywhere can be calculated.

Equations (19) and (22) have been derived for vertical floor loads only but it is not difficult to deduce from them the corresponding equations for the equally important case of horizontal wind loads.

If horizontal loads W_1, W_2 . . . W_n alone act from left to right at the levels of the first, second, etc. floors so that each produces a clockwise overturning moment on the structure, equation (19) will be unchanged except that the terms in w_{1r} and w_{2r} will disappear since these loads no longer act on the structure. Equation (22) becomes

$$\sum_{A}^{Q} 6EK_{Ar}(\theta_{Ar}+\theta_{A(r-1)}-2R_r)+h_r\sum_{r}^{n} W=0. \quad . \quad . \quad . \quad . \quad (23)$$

It has so far been assumed in this analysis that the effect of the direct thrust on the flexure of a member is negligible. While, as will be shown in Chapter 19, this is justifiable for the purposes of design of steel frames and, in all probability, of reinforced concrete structures it is useful to derive expressions which enable an estimate of the effect to be made.

In a symmetrical single bay frame supporting uniformly distributed floor loads it is not difficult to examine the effect of the flexure of the stanchions since the reactions at the ends of the beams are independent of the end moments.

If it is assumed that the stanchions are initially straight it will be seen from equations (7) and (8) of paragraph 7.20 that the moments at the ends of a stanchion length A_rA_{r-1} may be expressed as

$$M^A_{r(r-1)}=6EK_{Ar}(2Y_r\theta_{Ar}+X_r\theta_{A(r-1)})$$

and

$$M^A_{(r-1)r}=6EK_{Ar}(X_r\theta_{Ar}+2Y_r\theta_{A(r-1)})$$

where X_r and Y_r are coefficients depending on the axial load in the stanchion length, having the values

$$X_r=\frac{f(\alpha)}{4\phi^2(\alpha)-f^2(\alpha)} \text{ and } Y_r=\frac{\phi(\alpha)}{4\phi^2(\alpha)-f^2(\alpha)}.$$

$f(\alpha)$ and $\phi(\alpha)$ are the Berry functions referred to in paragraph 8.5, and tabulated in the Appendix, the axial compressive load in the member to be used in evaluating them being $P=\sum_{r}^{n}\frac{w_rl}{2}$.

For a single bay frame when rigid joints are assumed and if the widths of the members are neglected we have from the equilibrium of joint A_r

$$M^A_{r(r-1)}+M^A_{r(r+1)}+M^r_{AB}=0$$

or

$$3J_rX_r\theta_{A(r-1)}+(1+6J_rY_r+6L_rY_{(r+1)})\theta_{Ar}+3L_rX_{(r+1)}\theta_{A(r+1)}=W_r. \quad . \quad . \quad . \quad . \quad . \quad . \quad . \quad (24)$$

where

$$J_r=\frac{K_{Ar}}{K_{1r}},\ L_r=\frac{K_{A(r+1)}}{K_{1r}} \text{ and } W_r=\frac{w_rl^2}{24EK_{1r}}.$$

From this and the similar equations derived from a consideration of the other joints in the frame the complete solution can be obtained. By comparing the results with those found when the effect of flexure is neglected an estimate of the errors involved may be made.

9.4. Slope deflection analysis of frames with semi-rigid joints.—In many framed structures, particularly those of steel in which bolts or rivets are used in fabrication, the joints are far from rigid. A detailed examination of the behaviour of certain riveted beam-to-stanchion connections is made in Chapter 11. It is shown there that when a moment is transmitted through such connections an appreciable relative rotation occurs between the members joined. The relation between the moment transmitted and the relative rotation is often far from linear but as stated in Chapter 11 the only practicable method of stress analysis, for all but the simplest frames, is to assume that a linear relation does hold and to substitute for the curve connecting

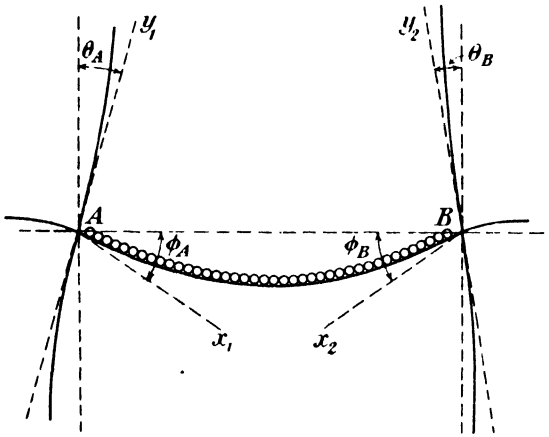

FIG. 9.15.

moment and relative rotation an arrangement of its chords. It will be well, therefore, to expand the slope deflection equations derived in the previous paragraph to cover the condition of semi-rigidity of beam-to-stanchion connections.

Part of a loaded frame, the beam-to-stanchion connections of which are semi-rigid, is shown in Fig. 9.15.

Ay_1 is the tangent to the stanchion at A and θ_A is its change of slope under load.

Ax_1 is the tangent to the beam AB at A and ϕ_A is its change of slope under load.

By_2 is the tangent to the stanchion at B and θ_B is its change of slope under load.

Bx_2 is the tangent to the beam AB at B and ϕ_B is its change of slope under load.

Since a linear relation is assumed between the relative rotation of

the members at a connection and the moment transmitted through the connection we may write

$$\theta_A-\phi_A=\gamma_L M_{AB} \quad . \quad . \quad . \quad . \quad . \quad . \quad . \quad . \quad (1)$$

and

$$\theta_B-\phi_B=\gamma_R M_{BA} \quad . \quad . \quad . \quad . \quad . \quad . \quad . \quad . \quad (2)$$

where γ_L and γ_R are constants depending on the connections at A and B.

From equations (3) and (4), paragraph 9.3, the moments M_{AB} and M_{BA} may be expressed in terms of ϕ_A and ϕ_B and the external load applied to AB, thus enabling equations (1) and (2) to be solved for ϕ_A and ϕ_B.

Writing α and β for $\frac{2EI\gamma_L}{l}$ and $\frac{2EI\gamma_R}{l}$ respectively we obtain

$$\phi_A=\frac{1}{(3\alpha\beta+2\alpha+2\beta+1)}\left[(2\beta+1)\theta_A-\alpha\theta_B+\alpha(3\beta+1)\frac{wl^3}{24EI}\right] \quad . \quad . \quad (3)$$

and

$$\phi_B=\frac{1}{(3\alpha\beta+2\alpha+2\beta+1)}\left[-\beta\theta_A+(2\alpha+1)\theta_B-\beta(3\alpha+1)\frac{wl^3}{24EI}\right] \quad . \quad (4)$$

The moments and reactions at the ends of the beam may be written in the form

$$M_{AB}=\frac{2EI}{l}\frac{1}{(3\alpha\beta+2\alpha+2\beta+1)}\left[(3\beta+2)\theta_A+\theta_B-(3\beta+1)\frac{wl^3}{24EI}\right], \quad . \quad (5)$$

$$M_{BA}=\frac{2EI}{l}\frac{1}{(3\alpha\beta+2\alpha+2\beta+1)}\left[\theta_A+(3\alpha+2)\theta_B+(3\alpha+1)\frac{wl^3}{24EI}\right], \quad . \quad (6)$$

$$V_A=\frac{6EI}{l^2}\frac{1}{(3\alpha\beta+2\alpha+2\beta+1)}\left[(\beta+1)\theta_A+(\alpha+1)\theta_B-(6\alpha\beta+3\alpha+5\beta+2)\frac{wl^3}{24EI}\right], \quad . \quad . \quad . \quad . \quad (7)$$

$$V_B=\frac{6EI}{l^2}\frac{1}{(3\alpha\beta+2\alpha+2\beta+1)}\left[(\beta+1)\theta_A+(\alpha+1)\theta_B+(6\alpha\beta+5\alpha+3\beta+2)\frac{wl^3}{24EI}\right] \quad . \quad . \quad . \quad . \quad (8)$$

It is most usual in steel framed buildings for the stanchion to be a continuous member, the beams being connected to it as shown in Fig. 9.16. From a consideration of the equilibrium of this joint, neglecting the depth of the beam, we have

$$M^r_{BA}+M^B_{r(r-1)}+M^r_{BC}+M^B_{r(r+1)}+V^r_{BA}d_{Br}+V^r_{BC}e_{Br}=0, \quad . \quad (9)$$

or substituting the values given in expressions (5)—(8) we have

$$\frac{2EK_{1r}}{(3\alpha_{1r}\beta_{1r}+2\alpha_{1r}+2\beta_{1r}+1)}\left[1+\frac{3d_{Br}}{l_{1r}}(\beta_{1r}+1)\right]\theta_{Ar}+2EK_{Br}\theta_{B(r-1)}$$
$$+\left[\frac{2EK_{1r}}{(3\alpha_{1r}\beta_{1r}+2\alpha_{1r}+2\beta_{1r}+1)}\left\{(3\alpha_{1r}+2)+\frac{3d_{Br}}{l_{1r}}(\alpha_{1r}+1)\right\}\right.$$
$$+\frac{2EK_{2r}}{(3\alpha_{2r}\beta_{2r}+2\alpha_{2r}+2\beta_{2r}+1)}\left\{(3\beta_{2r}+2)+\frac{3e_{Br}}{l_{2r}}(\beta_{2r}+1)\right\}$$
$$\left.+4EK_{Br}+4EK_{B(r+1)}\right]\theta_{Br}$$

$$+2EK_{B(r+1)}\theta_{B(r+1)}+\frac{2EK_{2r}}{(3\alpha_{2r}\beta_{2r}+2\alpha_{2r}+2\beta_{2r}+1)}\left[1+\frac{3e_{Br}}{l_{2r}}(\alpha_{2r}+1)\right]\theta_{Cr}$$
$$-6EK_{Br}R_r-6EK_{B(r+1)}R_{(r+1)}$$
$$+\frac{l^2_{1r}}{(3\alpha_{1r}\beta_{1r}+2\alpha_{1r}+2\beta_{1r}+1)}\left[\frac{1}{12}(3\alpha_{1r}+1)+\frac{d_{Br}}{4l_{1r}}(6\alpha_{1r}\beta_{1r}+5\alpha_{1r}+3\beta_{1r}+2)\right]w_{1r}$$
$$-\frac{l^2_{2r}}{(3\alpha_{2r}\beta_{2r}+2\alpha_{2r}+2\beta_{2r}+1)}\left[\frac{1}{12}(3\beta_{2r}+1)\right.$$
$$\left.+\frac{e_{Br}}{4l_{2r}}(6\alpha_{2r}\beta_{2r}+3\alpha_{2r}+5\beta_{2r}+2)\right]w_{2r}=0. \quad . \quad . \quad . \quad (10)$$

This is exactly the same form as equation (19), paragraph 9.3, and will be found to reduce to it when the connections are made rigid, *i.e.*

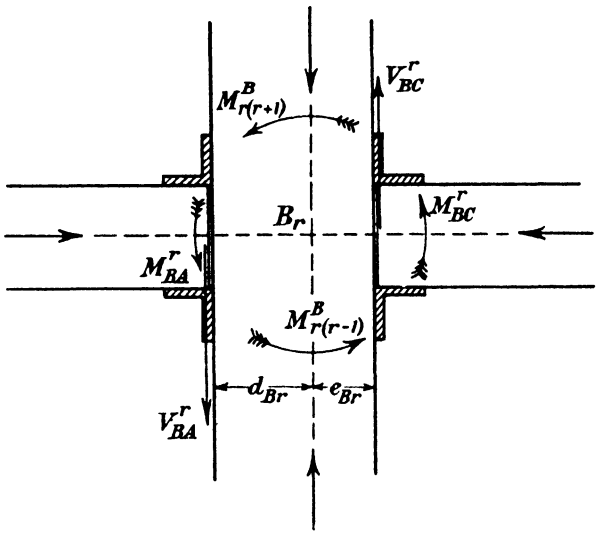

FIG. 9.16.

when $\alpha=\beta=0$, $d_{Br}=e_{Br}$, and when the width of the beam is neglected, *i.e.* when $f=0$. An equation similar to (10) may be written down for each joint in the frame. The other set of equations needed for the evaluation of the unknown slopes comes, as before, from a consideration of the equilibrium of the stanchions in each storey. The general equations are identical with those already found for the rigid frame, that is to say for the rth storey

$$\sum_{A}^{Q} K_{Ar}(\theta_{Ar}+\theta_{A(r-1)}-2R_r)=0 \quad . \quad . \quad . \quad . \quad . \quad (11)$$

There are as many equations of type (10) as there are joints and of type (11) as there are storeys in the frame. A sufficient number of equations are thus provided for the evaluation of the unknown slopes θ_{A1} . . . θ_{Qn} and the deflections R_1 . . . R_n. When these are known, the moments and reactions can be found from equations (3)–(6), paragraph 9.3, and (5)–(8) above and the stresses in the frame follow.

When horizontal wind loads alone act the same procedure is followed. This results in the equation found from a consideration of the equilibrium of a joint being identical with equation (10) except that the last two terms disappear while equation (23) paragraph 9.3 appears in place of equation (11).

9.5. Moment distribution method.—The slope deflection method in common with the strain energy method of analysis suffers from the handicap that a large number of simultaneous equations have to be solved before the stresses in a multi-storey, multi-bay frame can be evaluated. A three storey three bay frame, giving rise to fifteen equations marks the practical limit of the method in one direction. Though the slope deflection method is of great value in special cases, giving general expressions for slopes and moments from which tabular data may be prepared as shown in Chapter 19, the stresses in a frame can very often be found much more easily by the distribution method to which reference has already been made (paragraph 6.6).

It was to the rigidly jointed frame that Professor Hardy Cross first applied the moment distribution method. In the long and instructive discussion,* to which the original paper gave rise, Prof. H. E. Wessman gives the following description.

" Other methods usually begin by making the structure simple ; in other words, by theoretically cutting restrained ends or inserting temporary hinges. End moments are then obtained by solving simultaneous equations which are functions of the angles through which the cut or pinned ends must be rotated to make the structure continuous again. The Cross method, on the other hand, starts by making the structure rigidly fixed at every joint or support and then finding fixed-end moments for any loading conditions under consideration. One joint at a time is then released and the fixed-end moments are modified to secure equilibrium at the released joint. This joint is temporarily fixed again until all other joints have been released and fixed in their new positions. Then the procedure is repeated again and again until the desired degree of accuracy is obtained."

The application of the method to the continuous beam has been described in considerable detail (paragraph 8.4) ; the procedure is the same when the moments in a frame with perfectly rigid joints are to be determined and therefore the general expressions will not be set down again. As an illustration of the application of the method to a frame, a simple case will be worked out.

Fig. 9.17 shows a simple symmetrical portal with rigid joints and encastré feet, the bending moments in which, due to a central concentrated load of 80 lb., are to be determined. The members are all of the same length (100 inches), of the same uniform cross-section, and of the same material. If all the joints are held so that they can neither rotate nor have any lateral movement, then, on the application of the load, the bending moments at the ends of the beam BC will be the same as those for a similar beam with

* Procs. Amer. Soc. of Civ. Engrs., Sept. 1930–April 1932.

encastré ends, and there will be no bending moments at the ends of the stanchions. These moments, called by Cross the fixed-end moments, are ±1,000 lb.-in. at the ends of the beams, shown at *a* in Fig. 9.17 and zero at the ends of the stanchions, shown at *b*. The joint B is now released so that it is free to rotate; before rotation the unbalanced moment on the joint was 1,000 lb.-in., on release the joint will rotate to an equilibrium position in which there will be no unbalanced moment on the joint. The next step is, therefore, the distribution of the unbalanced moment between the members meeting at the joint in the ratio of the stiffnesses (I/l) of the members (see equation (8), paragraph 8.4). This step is shown at *c*; since the stiffnesses of the members are equal, the balancing moment applied to

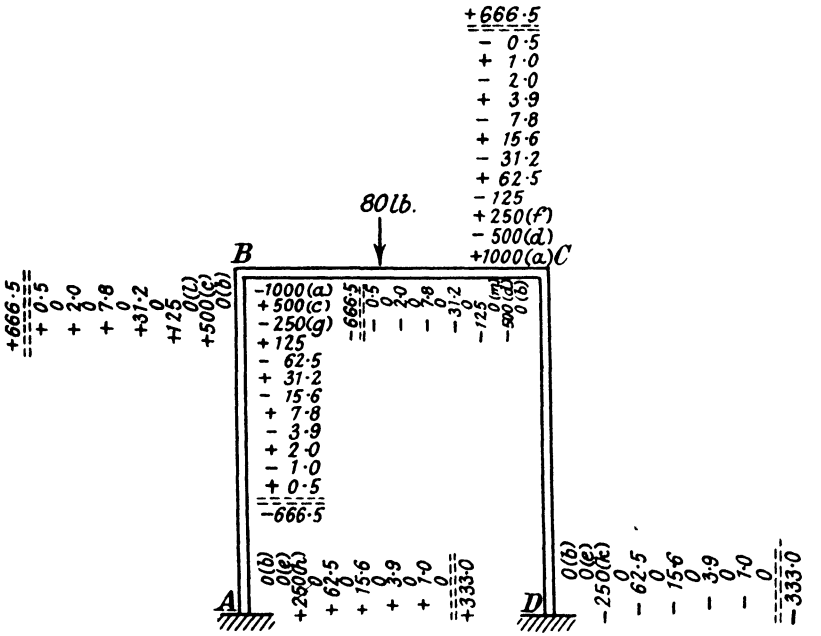

FIG. 9.17.

each member at the joint is +500 lb.-in. The same process is carried out at joint C (step *d*). Since the feet, A and D, of the stanchions are encastré they are not released and so no balancing moments are applied there (step *e*). When a joint such as B is released and takes up its new equilibrium position, moments are induced at the other ends of the members meeting at B; these moments must next be inserted. For a straight member of uniform cross-section the carry-over factor is $\frac{1}{2}$, that is to say, the moment induced at one end of the member when a moment M is applied at the other is $\frac{1}{2}$M as shown in equation (9) of paragraph 8.4. Thus the moment carried over to the end C of the member BC due to the balancing moment +500 lb.-in. applied at B is +250 lb.-in.; this is shown as step *f*, Fig. 9.17. Similarly, a moment

of −250 lb.-in. is carried over from C to B (step *g*). In the stanchions, moments of ±250 lb.-in. are carried over from B and C to A and D (steps *h* and *k*), but since no balancing moments were applied at the encastré feet the carry-over moments from A and D to B and C are zero (steps *l* and *m*).

The first full cycle of the process has been described. It will be seen that at the end of it there is no longer balance at the joints; for instance at B the out-of-balance moment is 250 lb.-in. The same steps are therefore repeated again and again until the moments for distribution are small enough to be neglected. In Fig. 9.17 four cycles are shown and the total values of the end moments, found by adding the figures in each column, are at B and C, 666·5 lb.-in. and at A and D, 333·0 lb.-in. The corresponding values calculated from the slope deflection equations are 666·6 and 333·3 lb.-in.

This example has been worked out and presented in the way suggested by Cross. The column of figures giving the moment in a member has been written at right angles to the member concerned and therefore each time a figure relating to a stanchion is entered the diagram has to be turned through a right angle. Though this may appear to be a small matter it leads to considerable confusion when a complicated frame is being stressed and before the method can be used for analysing complicated frames a more convenient arrangement is essential.

In Fig. 9.18 is shown a double portal with rigid joints and encastré feet carrying a concentrated load of 80 lb. at the centre of the beam PR.

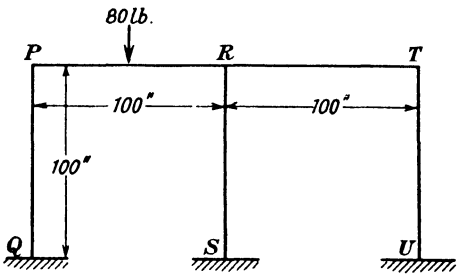

FIG. 9.18.

As in the previous example the members are assumed to be of the same length (100 ins.) and of the same uniform cross-section and material. The calculations of the moments in the members are given in Table 9.1; the upper part of the first column contains the figures relating to the end P of stanchion PQ, the lower part of this column containing the figures relating to the end Q; columns 2 and 3 deal with the ends P and R of the beam PR and so on.

In the first step, *a*, the fixed-end moments ±1,000 lb.-in. are entered in the second and third columns; at the ends of all other members the fixed-end moments are zero. In step *b* the joints are released and balanced; it has been found convenient, as shown in Table 9.1, to draw a line across the columns at each balance. There should be no difficulty in seeing that the balancing moment at the end of each

TABLE 9.1.

CALCULATION OF END MOMENTS (LB.-IN.)
DOUBLE PORTAL. RIGID JOINTS. VERTICAL LOAD.

1	2	3	4	5	6	7	(Step)
P	P	R	R	R	T	T	
0	−1000	+1000	0	0	0	0	*a*
+ 500	+ 500	− 334	− 333	− 333	0	0	*b*
0	− 167	+ 250	0	0	− 167	0	*c*
+ 83	+ 84	− 84	− 83	− 83	+ 84	+ 83	*d*
0	− 42	+ 42	0	+ 42	− 42	0	*e*
+ 21	+ 21	− 28	− 28	− 28	+ 21	+ 21	*f*
0	− 14	+ 11	0	+ 11	− 14	0	
+ 7	+ 7	− 7	− 7	− 7	+ 7	+ 7	
0	− 4	+ 4	0	+ 4	− 4	0	
+ 2	+ 2	− 3	− 3	− 3	+ 2	+ 2	
0	− 2	+ 1	0	+ 1	− 2	0	
+ 1	+ 1	− 1	− 1	− 1	+ 1	+ 1	*g*
− 68	0	0	− 69	0	0	68	*h*
+ 34	+ 34	− 23	+ 23	+ 23	− 34	34	*k*
0	+ 12	+ 17	0	+ 17	− 12	0	*l*
− 23	0	0	− 23	0	0	23	*m*
+ 6	+ 5	− 4	− 4	− 4	+ 5	− 6	
0	− 2	+ 3	0	+ 3	− 2	0	
− 2	0	0	− 2	0	0	2	
+ 2	+ 2	− 1	1	1	+ 2	+ 2	*n*

Q	S	U	
0	0	0	*a*
0	0	0	*b*
+ 250	167	0	*c*
0	0	0	*d*
+ 42	− 42	+ 12	*e*
0	0	0	*f*
+ 11	− 14	+ 11	
0	0	0	
+ 4	− 4	+ 4	
0	0	0	
+ 1	− 2	+ 1	
0	0	0	*g*
− 68	69	68	*h*
0	0	0	*k*
+ 17	+ 12	+ 17	*l*
− 23	− 23	23	*m*
0	0	0	
+ 3	− 2	+ 3	
− 2	− 2	− 2	
0	0	0	*n*

member meeting at R is $-\frac{1,000}{3}$ lb.-in. Extending equations (5)–(8), paragraph 8.4, to the case of any number of members connected rigidly together at one joint, their far ends being encastré, we can write down the balancing moment in any one of the members having a stiffness I/l due to the application of a moment M to the joint as $\frac{\frac{I}{l}M}{\sum\frac{I}{l}}$ where $\sum\frac{I}{l}$ is the sum of the stiffnesses of all the members meeting at the joint.

Next, step *c*, the moment resulting from the balance is carried over to the opposite end of each member, thus, in column 3 the carry-over moment is +250 lb.-in. resulting from the balancing moment of +500 lb.-in. applied at P (column 2, step *b*). With the calculations arranged in this way the out-of-balance moment at a joint can be seen at a glance and the risk of omitting any part of a step is reduced to a minimum. After the first carry over, step *c*, the moment to be balanced at joint R is +250 lb.-in., made up of +250 lb.-in. in column 3 and zero moments in columns 4 and 5; after the second, step *e*, it is +84 lb.-in. made up of +42 lb.-in. in column 3, zero in column 4 and +42 lb.-in. in column 5; since the stiffnesses of the members are equal this last joint is balanced, step *f*, by applying the moments of −28 lb.-in. shown in columns 3, 4 and 5.

The process is continued until the necessary accuracy is obtained. In this particular example six balances were made before, at step *g*, the balancing moment dropped to 1 lb.-in. The total moments at the ends of the members, given in column 2 of Table 9.2, may be obtained by adding up each column of figures in Table 9.1.

It will be seen that while the balance at the joints is satisfactory the frame as a whole is not in equilibrium; this is due to the fact that, though each joint was allowed to rotate until its equilibrium position was reached, complete freedom was not given to the structure as a whole and it was thus prevented from swaying.

Since vertical load only is applied to the frame under consideration the sum of the moments at the top and bottom of all the stanchions must, in the final state, be zero from equation (22) paragraph 9.3. It will be seen from Table 9.2, column 2, that, at the stage represented by step *g*, Table 9.1, a residual moment of +410 lb.-in. exists. This means that, in preventing sway, an external horizontal force of 1.10 lb., acting from right to left at the level of the beam has been imposed on the frame. The next step is the removal of this force so as to allow the frame to deflect horizontally.

The moments induced at the ends of the members when the frame is allowed to deflect horizontally can be calculated most easily if the ends of the members are prevented from rotating while the sway takes place. It will be convenient at this stage to obtain general expressions for these moments.

TABLE 9.2.

BENDING MOMENTS (LB.-IN.) IN MEMBERS OF DOUBLE PORTAL FRAME. RIGID JOINTS.

(Vertical load)

1	2	3	4	5	6
Moment	Cross method (sway neglected)	Cross method (complete solution)	Slope deflection equations	Percentage difference between 4 and 3	Percentage difference between 4 and 2
QP . .	+308	+235	+234·4	0·3	31·4
PQ . .	+614	+563	+562·5	0·1	9·2
SR . .	−229	−313	−312·5	0·2	26·7
RS . .	−455	−531	−531·2	0·0	14·3
UT . .	+ 58	− 15	− 15·6	3·9	471·0
TU . .	+114	+ 63	+ 62·5	0·8	82·5
PR . .	−614	−563	−562·5	0·1	9·2
RP . .	+851	+889	+890·6	0·2	4·4
RT . .	−397	−359	−359·3	0·1	10·5
TR . .	−114	− 63	− 62·5	0·8	82·5

Consider the behaviour of the rth storey in a frame in which all rotation of joints is prevented. Suppose a horizontal shear P acts from left to right at the level of the rth floor causing a horizontal deflection δ of that floor relative to the $(r-1)$th. Then, from equations (3) and (4) paragraph 9.3, the end moments induced in any stanchion length will be

$$M_{r(r-1)}=M_{(r-1)r}=-\frac{6EJ\delta}{h^2},$$

while from equation (23) of the same paragraph

$$12E\delta\Sigma\frac{J}{h^2}=Ph,$$

the summation extending over all the stanchions in the storey.

It follows, therefore, that the magnitudes of the moments at the ends of a stanchion length are

$$M_{r(r-1)}=M_{(r-1)r}=-\tfrac{1}{2}P\frac{\left(\frac{J}{h^2}\right)}{\Sigma\frac{J}{h^3}} \quad . \quad . \quad . \quad . \quad . \quad . \quad (1)$$

In the example under consideration the moments induced when the restraining force is removed will be the same as those arising from the application to the otherwise unloaded frame of a force +4·10 lb. at the level of the beams acting from left to right. Since all the stanchions are identical the moments at their ends are of the same magnitude, viz. −410/6 lb.-in. These values are inserted in their respective columns, step h, in Table 9.1; the entries in the beam columns 2, 3, 5 and 6 being zero as no rotations of the joints were allowed. The

TABLE 9.3.

CALCULATION OF END MOMENTS (LB.-IN.).

DOUBLE PORTAL. RIGID JOINTS. HORIZONTAL LOAD.

1	2	3	4	5	6	7
P	P	R	R	R	T	T
−5000	0	0	−5000	0	0	−5000
+2500	+2500	+1666	+1668	+1666	+2500	+2500
0	+ 833	+1250	0	+1250	+ 833	0
−1667	0	0	−1667	0	0	−1667
+ 417	+ 417	− 278	− 278	− 278	+ 417	+ 417
0	− 139	+ 209	0	+ 209	− 139	0
− 140	0	0	− 140	0	0	− 140
+ 140	+ 140	− 93	− 93	− 93	+ 140	+ 140
0	− 46	+ 70	0	+ 70	− 46	0
− 46	0	0	− 46	0	0	− 46
+ 46	+ 46	− 31	− 31	− 31	+ 46	+ 46
0	− 16	+ 23	0	+ 23	− 16	0
− 16	0	0	− 16	0	0	− 16
+ 16	+ 16	− 10	− 10	− 10	+ 16	+ 16
0	− 5	+ 8	0	+ 8	− 5	0
− 5	0	0	− 5	0	0	− 5
+ 5	+ 5	− 4	− 4	− 4	+ 5	+ 5
0	− 2	+ 2	0	+ 2	− 2	0
− 2	0	0	− 2	0	0	− 2
+ 2	+ 2	− 1	− 1	− 1	+ 2	+ 2

Q	S	U
−5000	−5000	−5000
0	0	0
+1250	+ 834	+1250
−1667	−1667	−1667
0	0	0
+ 209	− 139	+ 209
− 140	− 140	− 140
0	0	0
+ 70	− 46	+ 70
− 46	− 46	− 46
0	0	0
+ 23	− 16	+ 23
− 16	− 16	− 16
0	0	0
+ 8	− 5	+ 8
− 5	− 5	− 5
0	0	0
+ 2	− 2	+ 2
− 2	− 2	− 2
0	0	0

joints must now be released and allowed to rotate; the balancing moments are entered at step *k* and the carry-over moments at step *l*. It will be found at this point that the sum of the moments at the ends of the stanchions again shows a residual moment, now reduced to +137 lb.-in. This is dealt with as before, a correcting moment of −23 lb.-in. being entered at the ends of the stanchions (step *m*). These last three steps, the balancing of the joints, the insertion of the carry-over moments and the correction of the residual moments, are then repeated until the necessary accuracy is obtained. The final total moments at the ends of the members found by adding up each column of figures from step *a* to step *n*, are tabulated in column 3, Table 9.2. In column 4 of this Table the moments calculated from the usual slope deflection equations are given; the excellent agreement between these values and those calculated by the Cross method, taking sway into account, will be seen from column 5. Column 6 shows that the neglect of the sway corrections leads to very appreciable inaccuracies.

The stressing of a frame subjected to a horizontal wind load is carried out in the way described above from step *h* to step *n*. The moments in the members of the same double portal Fig. 9.18 due to a horizontal load of 300 lb. acting from left to right at the joint P are determined in Table 9.3. In this case a horizontal shear is applied to the frame. In the first step, therefore, the joints are held so that they cannot rotate but the whole frame is allowed to sway. The moments induced at the ends of each stanchion length by this movement are found from equation (1) to be

$$M_{10}=M_{01}=-\tfrac{1}{2}\times 300\times 100/3=-5{,}000 \text{ lb.-in.}$$

These are entered in the first line of the table. The joints are then released and the calculation continued as before. In Table 9.3 seven balances have been carried out, giving the values of the end moments collected in Table 9.4, column 3. In practice only half this work

TABLE 9.4.

BENDING MOMENTS (LB.-IN.) IN MEMBERS OF DOUBLE PORTAL FRAME.

(Horizontal Load).

1	2	3
Moment	Cross method (after 4 balances)	Cross method (after 7 balances)
QP	−5,324·0	−5,314·0
PQ	−3,750·0	−3,750·0
SR	−6,204·0	−6,250·0
RS	−5,588·0	−5,626·0
UT	−5,324·0	−5,314·0
TU	−3,750·0	3,750·0
PR	+3,750·0	+3,750·0
RP	+2,793·0	+2,811·0
RT	+2,793·0	+2,811·0
TR	+3,750·0	+3,750·0

would be necessary since, as a comparison of columns 2 and 3 Table 9.4 shows, sufficient accuracy is obtained after only four balances.

The same method can be applied to the case where the feet of the stanchions are at different levels, Fig. 9.19. Following the same steps

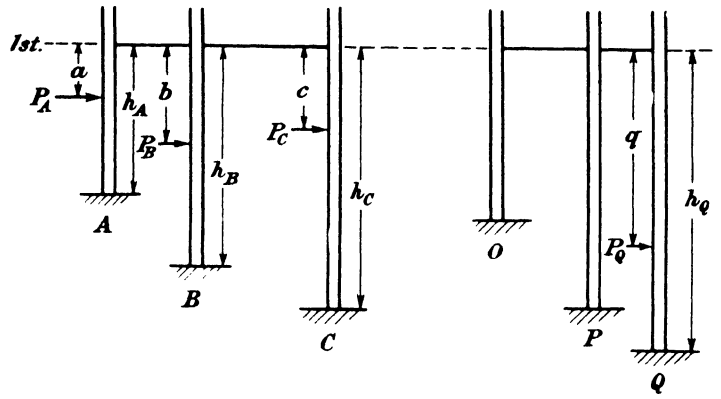

FIG. 9.19.

as were used in dealing with the rth storey of the frame shown in Fig. 9.14, a general equation can be derived, by considering the equilibrium of all the stanchions in the bottom storey, as follows :

$$\sum_{A}^{Q}\frac{1}{h_A}(M^A{}_{10}+M^A{}_{01})+\sum_{1}^{n}W+\sum_{A}^{Q}\frac{P_A}{h_A}(h_A-a)=0$$

or

$$\sum_{A}^{Q}\frac{1}{h_A}(M^A{}_{10}+M^A{}_{01})+\sum_{1}^{n}W+\sum_{A}^{Q}P'_A=0 \quad . \quad . \quad . \quad (1\ (a))$$

where $\sum_{1}^{n}W$ is the total horizontal load acting from left to right at and above the first floor

and

$$P'_A=\frac{P_A}{h_A}(h_A-a).$$

This equation is used in making the sway correction as were equations (22) and (23) paragraph 9.3 in the examples already worked out.

Fig. 9.20 shows a double portal frame with rigid joints and encastré feet, not at the same level, subjected to a concentrated horizontal load of 80 lb. half way up the centre stanchion. The members of the frame are of the same uniform cross-section and material. The calculations of the moments in the members are given in Table 9.5. By step (a) all joints have been released and balanced but no sway of the frame has been allowed. At this stage it will be found by substituting the moments at the ends of the stanchions (see Table 9.6) in the left-hand side of equation 1 (a), that, in preventing sway, an external horizontal force of 38.9 lb. acting from right to left at the level of the beam has been imposed on the frame. The next step is the removal of this force so as to allow sway to take place but, as in the earlier examples, without

TABLE 9.5.

CALCULATION OF END MOMENTS.

DOUBLE PORTAL. FEET NOT AT SAME LEVEL. RIGID JOINTS. HORIZONTAL LOAD.

1	2	3	4	5	6	7	(Step)
P	P	R	R	R	T	T	
0	0	0	+1000	0	0	0	
0	0	− 333	− 333	− 333	0	0	
0	− 167	0	0	0	− 167	0	
+ 111	+ 56	0	0	0	+ 100	+ 67	
0	0	+ 28	0	+ 50	0	0	
0	0	− 26	− 26	− 26	0	0	
0	− 13	0	0	0	− 13	0	
+ 9	+ 4	0	0	0	+ 8	+ 5	
0	0	+ 2	0	+ 4	0	0	
0	0	− 2	− 2	− 2	0	0	*a*
− 837	0	0	− 209	0	0	− 93	*b*
+ 558	+ 279	+ 70	+ 70	+ 70	+ 56	+ 37	
0	+ 35	+ 139	0	+ 28	+ 35	0	
− 23	− 12	− 56	− 56	− 56	− 21	− 14	
0	− 28	− 6	0	− 10	− 28	0	
+ 19	+ 9	+ 5	+ 5	+ 5	+ 17	+ 11	
0	+ 2	+ 4	0	+ 8	+ 2	0	
− 1	− 1	− 4	− 4	− 4	− 1	− 1	*c*

Q	S	U	
0	−1000	0	
0	0	0	
0	− 167	0	
0	0	0	
+ 55	0	+ 33	
0	0	0	
0	− 13	0	
0	0	0	
+ 5	0	+ 3	
0	0	0	*a*
− 837	− 209	− 93	*b*
0	0	0	
+ 279	+ 35	+ 18	
0	0	0	
− 11	− 28	− 7	
0	0	0	
+ 10	+ 3	+ 5	
0	0	0	*c*

allowing the joints to rotate. The moments induced at the ends of the stanchions by this movement are calculated from equation (1), § 9.5, and are entered in Table 9.5 as step (*b*). The joints must now be released and allowed to rotate, further sway being prevented. When the joints are once more balanced, step (*c*), it will be found, by substituting in equation 1 (*a*), that the horizontal force preventing sway is 17·2 lb. This must be removed, as before, and sway allowed. The whole process between steps (*b*) and (*c*) need not be repeated since we already know the moments induced at the ends of the members by the removal of the horizontal force 38·9 lb. and the subsequent balance of the joints which introduced again a restraining force of 17·2 lb. If, therefore, these moments, Column (4), Table 9.6, are multiplied by $\frac{17{\cdot}2}{(38{\cdot}9-17{\cdot}2)}$ the additional moments to produce final balance result. These are entered in Table 9.6 as step (*d*).

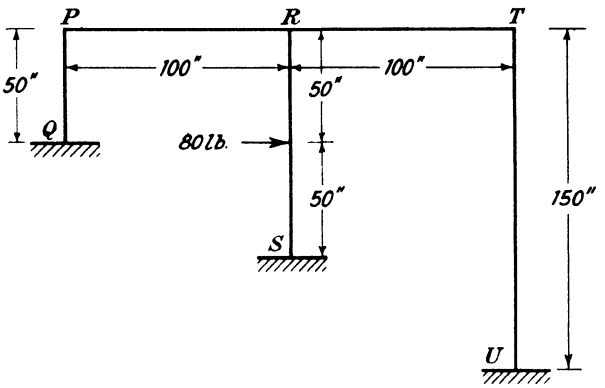

FIG. 9.20.

There is no difficulty in extending the moment distribution method to include frames with semi-rigid beam-to-stanchion connections. Fig. 9.21 represents part of such a frame. It will be found most convenient to consider the parts of the stanchions at the levels of the beams, shown cross-hatched at B_1, etc., as the joints which are in turn fixed and released. The assumption will be made in the first place that the widths of the members may be neglected without giving rise to serious errors. The fixed-end moments, distribution and carry-over factors can then be deduced directly from the general expressions given in paragraph 9.4.

When a uniformly distributed load w per unit length is applied to a beam of uniform cross-section, such as A_1B_1, Fig. 9.21, the fixed-end moments are

$$M_{AB}=\frac{-(3\beta+1)wl^2}{12(3\alpha\beta+2\alpha+2\beta+1)}$$

and

$$M_{BA}=\frac{(3\alpha+1)wl^2}{12(3\alpha\beta+2\alpha+2\beta+1)}$$

} Fixed-end moments.

where α and β are the constants for the connections at the ends A and B, and l is the length of the beam. These expressions are derived from equations (5) and (6) paragraph 9.4 by making $\theta_A=\theta_B=0$.

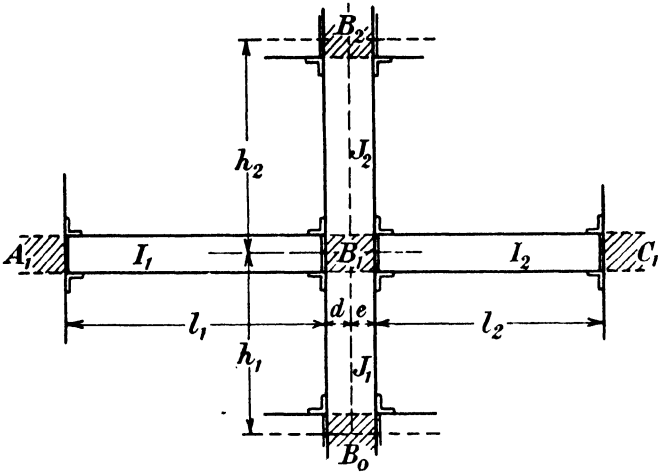

FIG. 9.21.

The carry-over factors can be found quite simply. Suppose a moment M_{AB} is applied to the end A of a beam AB, the other end B being attached by a semi-rigid connection to a stanchion which is clamped so that it cannot rotate.

From equation (4) paragraph 9.3 we have

$$M_{BA}=\frac{2EI}{l}[\phi_A+2\phi_B]. \quad . \quad . \quad . \quad . \quad . \quad . \quad . \quad . \quad (2)$$

TABLE 9.6.

BENDING MOMENTS (LB.-IN.) IN MEMBERS OF PORTAL, SHOWN IN FIG. 9.20, AT VARIOUS STAGES IN THE CALCULATION.

1	2	3	4	5	6
Moment	At step (*a*)	At step (*c*)	Induced between steps (*a*) and (*c*) [Col. (3) − Col. (2)]	Added at step (*d*)	Total [Col. (3) + Col. (5)]
QP . . .	+ 60	− 499	−559	−443	− 942
PQ . . .	+ 120	− 164	−284	−225	− 389
PR . . .	− 120	+ 164	+284	+225	+ 389
RP . . .	− 331	− 179	+152	+120	− 59
RS . . .	+ 639	+ 445	−194	−154	+ 291
SR . . .	−1180	−1379	−199	−158	−1537
RT . . .	− 307	− 266	+ 41	+ 33	− 233
TR . . .	− 72	− 12	+ 60	+ 48	+ 36
TU . . .	+ 72	+ 12	− 60	− 48	− 36
UT . . .	+ 36	− 41	− 77	− 61	− 102

Since the stanchion does not rotate we obtain, from equation (2) paragraph 9.4,

$$\phi_B = -\frac{\beta l}{2EI} M_{BA} \quad \ldots\ldots\ldots \quad (3)$$

and from (2) and (3) above

$$\frac{2EI}{l}\phi_A = (1+2\beta)M_{BA}. \quad \ldots\ldots\ldots \quad (4)$$

But, from equation (3) paragraph 9.3

$$M_{AB} = \frac{2EI}{l}[2\phi_A + \phi_B]$$

or, from (3) and (4) above

$$M_{AB} = (2+3\beta)M_{BA},$$

so that if a moment M_{AB} is applied to one end A of a beam the moment induced at the other end B is $M_{AB}/(2+3\beta)$. It can be shown in the same way that if a moment M_{BA} is applied to the end B the moment induced at the other end A attached to a rigid support by a semi-rigid connection is $M_{BA}/(2+3\alpha)$.

We may say, therefore, that from the end A to the end B

the carry-over factor is $\dfrac{1}{(2+3\beta)}$

and from the end B to the end A

the carry-over factor is $\dfrac{1}{(2+3\alpha)}$

} Carry-over factors.

where α and β are the constants for the connections at the ends A and B of the beam.

For all stanchion lengths the carry-over factor will be $\frac{1}{2}$, as before.

The distribution factors may be obtained from a consideration of Fig. 9.21. If the joint B_1 is rotated through an angle θ while the neighbouring joints A_1, B_2, C_1 and B_0 are kept fixed the total moment acting on the joint B_1 will be, when the widths of the members are neglected,

$$M^1_{BA} + M^B_{12} + M^1_{BC} + M^B_{10}$$

$$= \left[\frac{2EI_1(3\alpha_1+2)}{l_1(3\alpha_1\beta_1+2\alpha_1+2\beta_1+1)} + \frac{4EJ_2}{h_2} + \frac{2EI_2(3\beta_2+2)}{l_2(3\alpha_2\beta_2+2\alpha_2+2\beta_2+1)} + \frac{4EJ_1}{h_1}\right]\theta$$

$$= 2EY\theta \text{ (say). (See equation (10) paragraph 9.4.)}$$

The distribution factors by which an unbalanced moment at B_1 must be multiplied to give the balancing moments at the ends of the members meeting at the joint are therefore,

for B_1A_1 .. $\dfrac{I_1}{l_1 Y}\dfrac{(3\alpha_1+2)}{(3\alpha_1\beta_1+2\alpha_1+2\beta_1+1)}$

for B_1B_2 .. $\dfrac{2J_2}{h_2 Y}$

for B_1C_1 .. $\dfrac{I_2}{l_2 Y}\dfrac{(3\beta_2+2)}{(3\alpha_2\beta_2+2\alpha_2+2\beta_2+1)}$

for B_1B_0 .. $\dfrac{2J_1}{h_1 Y}$

} Distribution factors.

The various factors for any particular case of a frame with semi-rigid beam connections may be evaluated from these general expressions. Once they are obtained, exactly the same procedure is adopted as that already described for the rigid frames.

Table 9.7 gives the detailed calculations of the bending moments in a three storey, single bay frame carrying a central concentrated load W on the middle beam. The dimensions of the frame and the values of the constants of the beam connections are given in Fig. 9.22 where

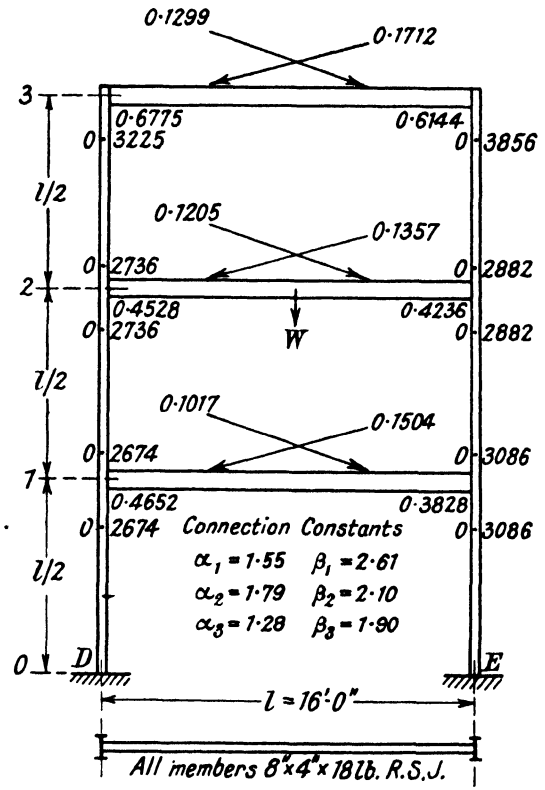

FIG. 9.22.

will also be found the distribution factors grouped around each joint and the carry-over factors placed above each beam.

The only difference between the procedure adopted in Table 9.7 and that given for the rigid frame in Table 9.1 is that in the former the sway correction is not made separately at the end of the calculation but is included in each cycle as in the wind load case of Table 9.3. Thus, each time the joints are balanced and the carry-over moments inserted, the residual moment in the stanchions is determined and the necessary correction made.

The total moments from Table 9.7 and those calculated by the slope deflection equations are given in Table 9.8.

TABLE 9.7.

CALCULATION OF END MOMENTS. THREE STOREY, SINGLE BAY FRAME. SEMI-RIGID CONNECTIONS. VERTICAL LOAD.

0 0		0 0	0 0	0 0	
+0·00623 −0·00038 −0·00189		0 0 −0·00396	0 0 +0·00375	−0·00572 −0·00038 +0·00235	
+0·00042 −0·00030 −0·00025		+0·00064 0 −0·00051	−0·00051 0 +0·00065	−0·00025 −0·00030 +0·00041	
+0·00033 −0·00012 −0·00010		+0·00011 0 −0·00022	−0·00007 0 +0·00027	−0·00025 −0·00012 +0·00017	
+0·00007 −0·00005 −0·00002		+0·00005 0 −0·00005	−0·00003 0 +0·00007	−0·00004 −0·00005 +0·00005	
0 +0·01245	0 +0·01245	−0·04549 +0·02059	+0·03969 −0·01681	0 −0·01144	0 −0·01144
0 −0·00038 +0·00083	0 −0·00038 +0·00083	−0·00228 0 +0·00138	+0·00248 0 −0·00072	0 −0·00038 −0·00050	0 −0·00038 −0·00050
−0·00095 −0·00030 +0·00065	−0·00078 −0·00024 +0·00065	−0·00010 0 +0·00107	+0·00017 0 −0·00074	+0·00118 −0·00030 −0·00050	+0·00094 −0·00024 −0·00050
−0·00013 −0·00012 +0·00014	−0·00006 −0·00012 +0·00014	−0·00010 0 +0·00024	+0·00013 0 −0·00010	+0·00021 −0·00012 −0·00007	+0·00014 −0·00012 −0·00007
−0·00005 −0·00005 +0·00005	−0·00003 −0·00006 +0·00005	−0·00001 0 +0·00010	+0·00003 0 −0·00003	+0·00009 −0·00005 −0·00002	+0·00007 −0·00006 −0·00002
0 0	0 0	0 0	0 0	0 0	0 0
0 0 −0·00156	+0·00623 −0·00038 −0·00156	0 0 −0·00272	0 0 +0·00234	0 0 +0·00188	−0·00572 −0·00038 +0·00188
0 −0·00012 −0·00011	+0·00042 −0·00024 −0·00011	+0·00035 0 −0·00019	−0·00028 0 +0·00034	0 −0·00012 +0·00027	−0·00025 −0·00024 +0·00027
0 −0·00006 −0·00005	+0·00033 −0·00012 −0·00005	+0·00005 0 −0·00009	−0·00002 0 +0·00017	0 −0·00006 +0·00014	−0·00025 −0·00012 +0·00014
0 −0·00003 0	+0·00007 −0·00006 0	+0·00003 0 0	−0·00001 0 +0·00005	0 −0·00003 +0·00004	−0·00004 −0·00006 +0·00004
0 0				0 0	
0 0 0				0 0 0	
−0·00078 −0·00012 0	*[All entries to be multiplied by Wl where W is the concentrated load and l is the length of the beam.]*			+0·00094 −0·00012 0	
−0·00006 −0·00006 0				+0·00014 −0·00006 0	
−0·00003 −0·00003 0				+0·00007 −0·00003 0	

TABLE 9.8.

BENDING MOMENTS IN MEMBERS OF THREE STOREY FRAME, SEMI-RIGID CONNECTIONS.

(Vertical Load.)

Moment	Cross	Slope deflection	Percentage difference
D_0D_1	$-0{\cdot}00094\ Wl$	$-0{\cdot}00092\ Wl$	2·2
D_1D_0	$-0{\cdot}00212\ Wl$	$-0{\cdot}00209\ Wl$	1·4
D_1D_2	$+0{\cdot}00473\ Wl$	$+0{\cdot}00478\ Wl$	1·0
D_2D_1	$+0{\cdot}01218\ Wl$	$+0{\cdot}01222\ Wl$	0·3
D_2D_3	$+0{\cdot}01190\ Wl$	$+0{\cdot}01191\ Wl$	0·1
D_3D_2	$+0{\cdot}00413\ Wl$	$+0{\cdot}00417\ Wl$	1·0
E_0E_1	$+0{\cdot}00108\ Wl$	$+0{\cdot}00109\ Wl$	1·0
E_1E_0	$+0{\cdot}00193\ Wl$	$+0{\cdot}00192\ Wl$	0·5
E_1E_2	$-0{\cdot}00453\ Wl$	$0{\cdot}00453\ Wl$	0·0
E_2E_1	$-0{\cdot}01245\ Wl$	$-0{\cdot}01243\ Wl$	0·2
E_2E_3	$-0{\cdot}01214\ Wl$	$-0{\cdot}01213\ Wl$	0·1
E_3E_2	$-0{\cdot}00394\ Wl$	$-0{\cdot}00393\ Wl$	0·3

In certain cases frequently found in practice to-day, where the beams are attached to the flanges of the stanchions by connections which are far from rigid, appreciable errors arise when the members are assumed for purposes of calculation to be represented by their neutral axes. The moment distribution method can, however, be expanded to take into account the widths of the stanchions and so give accurate results for such cases without adding any serious complication to the work.

A new set of distribution factors must first be obtained. If the joint B_1, Fig. 9.21, is rotated through an angle θ while the neighbouring joints are fixed, the total moment acting on the joint B_1 will be, when the widths of the stanchions are not neglected,

$$M^1{}_{BA}+M^B{}_{12}+M^1{}_{BC}+M^B{}_{10}+dV^1{}_{BA}+eV^1{}_{BC}$$

where d and e are the distances of the left- and right-hand faces of the stanchion from the neutral axis at B_1, or

$$\left[\frac{2EI_1}{l_1}\frac{(3\alpha_1+2)}{(3\alpha_1\beta_1+2\alpha_1+2\beta_1+1)}+\frac{4EJ_2}{h_2}\right.$$
$$+\frac{2EI_2}{l_2}\frac{(3\beta_2+2)}{(3\alpha_2\beta_2+2\alpha_2+2\beta_2+1)}+\frac{4EJ_1}{h_1}$$
$$+\frac{6EI_1d}{l_1{}^2}\frac{(\alpha_1+1)}{(3\alpha_1\beta_1+2\alpha_1+2\beta_1+1)}$$
$$\left.+\frac{6EI_2e}{l_2{}^2}\frac{(\beta_2+1)}{(3\alpha_2\beta_2+2\alpha_2+2\beta_2+1)}\right]\theta.$$
$$=2EZ\theta \text{ (say). (See equation (10) paragraph 9.4.)}$$

The distribution factors by which an unbalanced moment at B_1 must be multiplied to give the balancing moments and reactions at the ends of the members meeting at the joint are therefore

for moment on B_1A_1, $\dfrac{I_1}{l_1Z}\dfrac{(3\alpha_1+2)}{(3\alpha_1\beta_1+2\alpha_1+2\beta_1+1)}$

for moment on B_1B_2, $\dfrac{2J_2}{h_2Z}$

for moment on B_1C_1, $\dfrac{I_2}{l_2Z}\dfrac{(3\beta_2+2)}{(3\alpha_2\beta_2+2\alpha_2+2\beta_2+1)}$

for moment on B_1B_0, $\dfrac{2J_1}{h_1Z}$

for reaction on B_1A_1, $\dfrac{3I_1}{l_1^2Z}\dfrac{(\alpha_1+1)}{(3\alpha_1\beta_1+2\alpha_1+2\beta_1+1)}$

for reaction on B_1C_1, $\dfrac{3I_2}{l_2^2Z}\dfrac{(\beta_2+1)}{(3\alpha_2\beta_2+2\alpha_2+2\beta_2+1)}$

} Distribution Factors.

It should be noted that the last two of these factors give the reactions at the ends of the beams, while the first four give moments.

For all stanchion lengths the carry-over factor will be $\frac{1}{2}$, as usual.

The fixed-end moments

$$M_{AB}=\frac{-(3\beta+1)wl^2}{12(3\alpha\beta+2\alpha+2\beta+1)}$$

and

$$M_{BA}=\frac{(3\alpha+1)wl^2}{12(3\alpha\beta+2\alpha+2\beta+1)}$$

} Fixed-end Moments.

are unchanged.

In addition, fixed-end reactions must now be set down. They are

$$V_{AB}=\frac{-(6\alpha\beta+3\alpha+5\beta+2)wl}{4(3\alpha\beta+2\alpha+2\beta+1)}$$

and

$$V_{BA}=\frac{(6\alpha\beta+5\alpha+3\beta+2)wl}{4(3\alpha\beta+2\alpha+2\beta+1)}$$

} Fixed-end Reactions.

derived from equations (7) and (8) paragraph 9.4 by making $\theta_A=\theta_B=0$.

Since the reactions as well as the moments at the ends of the beams are to be calculated, there is now no necessity to derive general expressions for carry-over factors. If a balancing moment $+M$ and a balancing reaction $+V$ are applied to one end of a beam of length l, then a moment $-(M-Vl)$ and a reaction $+V$ must be carried over to the other end.

A simple example will make the process clear. A single storey two bay semi-rigid frame with stanchions 10 in. wide is shown in Fig. 9.23. The distribution factors are entered around each joint. It will be seen from Table 9.9 where the detailed calculations are given that four more columns are used than in the similar case worked out in Table 9.1.

Table 9.9.

Calculation of End Moments and Beam Reactions. Double Portal. Semi-Rigid Connections. Vertical Load.

	1	2	3	4	5	6	7	8	9	10	11
	A	A	A	C	C	C	C	C	E	E	E
a	0	−450·0	−40·0	+40·0	+450·0	0	0	0	0	0	0
b	+474·3	+164·7	+ 2·196	− 1·729	−129·7	−373·4	−129·7	−1·729	0	0	0
c	0	− 25·9	− 1·729	+ 2·196	+ 33·0	0	0	0	−1·729	−25·9	0
d	− 25·2	0	0	0	0	− 25·2	0	0	0	0	−25·2
	+ 43·6	+ 15·1	+ 0·202	− 0·050	− 3·8	− 10·8	− 3·8	−0·050	+0·202	+15·1	+43·6
	0	− 0·7	− 0·050	+ 0·202	+ 3·1	0	+ 3·1	+0·202	−0·050	− 0·7	0
	− 19·1	0	0	0	0	− 19·1	0	0	0	0	−19·1
	+ 14·7	+ 5·1	+ 0·068	+ 0·029	+ 2·2	+ 6·3	+ 2·2	+0·029	+0·068	+ 5·1	+14·7
	0	+ 0·4	+ 0·029	+ 0·068	+ 1·0	0	+ 1·0	+0·068	+0·029	+ 0·4	0
	− 8·9	0	0	0	0	− 8·9	0	0	0	0	− 8·9
	+ 6·1	+ 2·1	+ 0·028	+ 0·016	+ 1·2	+ 3·6	+ 1·2	+0·016	+0·028	+ 2·1	+ 6·1
	0	+ 0·3	+ 0·016	+ 0·028	+ 0·5	0	+ 0·5	+0·028	+0·016	+ 0·3	0
	− 4·0	0	0	0	0	− 4·0	0	0	0	0	− 4·0
	+ 2·6	+ 0·9	+ 0·012	+ 0·007	+ 0·5	+ 1·6	+ 0·5	+0·007	+0·012	+ 0·9	+ 2·6
	B					D					F
	0					0					0
	0					0					0
	+237·2					−186·7					0
	− 25·2					− 25·2					−25·2
	0					0					0
	+ 21·8					− 5·4					+21·8
	− 19·1					− 19·1					−19·1
	0					0					0
	+ 7·4					+ 3·2					+ 7·4
	− 8·9					− 8·9					− 8·9
	0					0					0
	+ 3·1					+ 1·8					+ 3·1
	− 4·0					− 4·0					− 4·0
	0					0					0

These columns, 3, 4, 8 and 9, contain the reactions at the ends of the beams.

The usual procedure is adopted. All joints are, in the first place, held fixed. The central load of 80 lb. applied to beam AC then gives rise to fixed-end moments of ∓ 450 lb.-in. and fixed-end reactions of ∓ 40 lb. at A and C, entered in columns 2, 5, 3 and 4, step *a*.

The joints are next released and allowed to take up new equilibrium positions. The out-of-balance moment acting at joint A, on release, is made up of the moment -450 lb.-in., column 2, at the end of the beam and the moment -40×5 lb.-in. due to the eccentric beam reaction, column 3. The total out-of-balance moment is, therefore, 650 lb.-in. and it is distributed in step *b*, on the joint taking up its new equilibrium position, into three balancing moments $+474{\cdot}3$ lb.-in. (column 1) on AB, $+164{\cdot}7$ lb.-in. (column 2) on AC and $+11{\cdot}0$ lb.-in. arising from the balancing reaction $+2{\cdot}196$ lb. (column 3). These values inserted in step *b* are, of course, found directly by multiplying

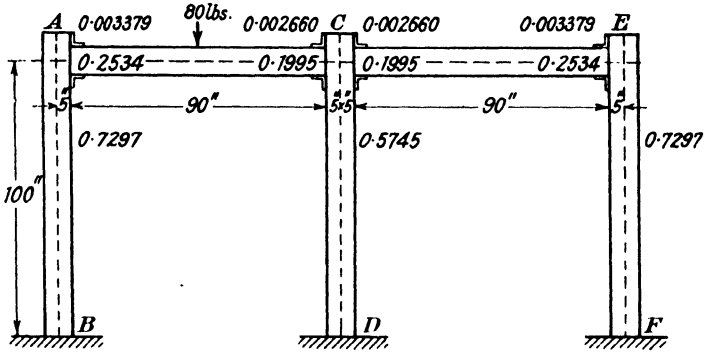

FIG. 9.23.

All members of same section throughout.
All beam connections similar. $a_{11}=\beta_{11}=a_{21}=\beta_{21}=1$.

the appropriate distribution factors by 650. In the same way, balancing moments and reactions are found for joint C and entered in columns 4 to 8.

The carry-over moments and reactions are next inserted, step *c*. The reaction and moment at the end A of AC arising from the balancing reaction $-1{\cdot}729$ lb. and the balancing moment $-129{\cdot}7$ lb.-in. applied at the end C are $-1{\cdot}729$ lb. and $-(-129{\cdot}7+90\times 1{\cdot}729)$ lb.-in. or $-25{\cdot}9$ lb.-in. respectively; these will be found in columns 3 and 2, step *c*. Similarly, the reaction and moment carried over to the end C of AC are $+2{\cdot}196$ lb. and $-(164{\cdot}7-90\times 2{\cdot}196)$ lb.-in. or $+33{\cdot}0$ lb.-in. When the sway correction, step *d*, has been applied as described in earlier cases, the first cycle of operations is complete.

The moments at the ends of the members resulting from the five cycles shown in Table 9.9 are collected in Table 9.10, together with the values calculated from the slope deflection equations and those found when the widths of the stanchions are neglected and all members are represented by their neutral axes.

TABLE 9.10.

BENDING MOMENTS (LB.-IN.) IN STANCHIONS OF TWO BAY SEMI-RIGID FRAME WITH STANCHIONS OF FINITE WIDTH.

Moment	Stanchions of finite width		Members represented by N.A.'s
	Cross	Slope deflection	Cross
BA	+212·3	+211·4	+170·0
AB	+484·1	+483·1	+384·0
DC	−244·3	−245·9	−193·0
CD	−429·9	−431·6	−342·5
FE	− 24·9	− 25·7	− 20·5
EF	+ 9·8	+ 8·8	+ 2·8

A comparison of the second and fourth columns shows the appreciable errors, of the order of 20 per cent. in the larger moments, arising from a neglect of the true width of the stanchions.

This is rather an extreme case since the stanchions have considerable width and the connections are far from rigid but it shows that the assumptions must be chosen with care if accurate results are to be obtained. It is, unfortunately, impossible to give a complete guide but it can be said that in general when joints are rigid the width of the members can be safely neglected in the collection of design data. For instance, in single bay frames of one, two, three and four storeys made up of 8 in.×6 in. **I** stanchions, storey height 8 feet and 12 in.×5 in. **I** beams, span between stanchion faces 15 feet 3 inches, the error in the bending moments produced by assuming the members were represented by their neutral axes was found to vary between 2·27 and 3·45 per cent.

In all building frames of practical proportions with rigid or semi-rigid connections the deformations due to direct stress and shear can be neglected. The effect of these deformations on frames built up of 8 in.×6 in. **I** stanchions and 12 in.×5 in. **I** beams was found to be less than 1 per cent. The effect of the direct thrust in the member on the flexure may be slightly more pronounced but as far as design data are concerned it can usually be neglected, as shown in Chapter 19.

EXERCISES

(These exercises should be solved by the various methods described in the Chapter.)

(1) Plot the bending moment diagram for the bent shown in diagram 9*a*. A and D are pinned joints, B and C are rigid.

The flexural rigidity is constant throughout the bent.

(2) The frame ABCD shown at 9*b* has rigid corners at B and C and is pinned to supports at A and D. It carries a load W in the position shown. If the cross-

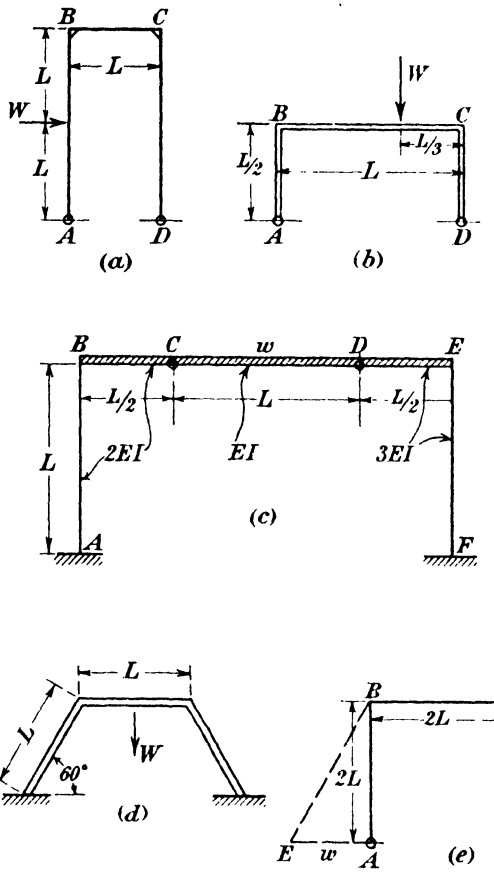

DIAGRAM 9.

section of the members is the same throughout, plot the bending moment diagram for the whole structure.

(3) The frame shown at 9*c* is built in at A and F: the joints at B and E are rigid and at C and D are pinned.

A uniform load of intensity w is carried on BE.

Calculate the deflection of the mid-point of BE below its original position. The flexural rigidity of the frame varies as shown in the diagram.

$$\left(\frac{205wL_4}{4{,}608EI}\right)$$

(4) The stiff-jointed trestle of constant flexural rigidity shown at 9*d* is encastré at both supports. Plot the bending moment diagram when a concentrated load is placed at the centre of the horizontal member.

(5) A stiff-jointed portal ABCD of constant flexural rigidity is encastré at A and D and carries a uniform load of intensity w on BC. The length AB=CD=L and BC=2L.

Find the fixing moments at A and D.

$$\left(\frac{2wL^2}{15}\right)$$

(6) Diagram 9*e* represents a stiff-jointed frame of constant flexural rigidity pinned at A and D. A load is distributed along AB which varies as shown from an intensity w at A to nothing at B.

Calculate the thrust on the support pin D.

$$\left(\frac{104wL}{345}\right)$$

(7) A horizontal force of 10 lb. is applied at the level of the top beam of a three storey single bay frame similar to that shown in Fig. 9.20, but having semi-rigid beam-to-stanchion connections defined by the constants

$$\alpha_1 = 2{\cdot}20 \qquad \beta_1 = 1{\cdot}78$$
$$\alpha_2 = 1{\cdot}46 \qquad \beta_2 = 1{\cdot}77$$
$$\alpha_3 = 1{\cdot}82 \qquad \beta_3 = 1{\cdot}49.$$

Show that the magnitudes of the bending moments at the feet of the stanchions are 295 and 305 lb.-ins.

CHAPTER 10

SECONDARY STRESSES IN FRAMED STRUCTURES

10.1. Secondary stresses. Slope deflection method of analysis.—In paragraph 1.7 primary stresses were defined as the axial forces in the bars of a framework, assumed to have perfectly free pin joints, under loads applied to the nodes. The extra stresses induced by the stiffness of the joints, where they are not in fact perfect hinges, are known as secondary stresses. Other stresses, additional to the primary system, found in actual structures due to such causes as the weight of the members themselves, eccentricity in the joints and, in certain aeronautical structures, to the true distribution of external load differing from the distribution assumed in the calculation of the primary stresses may have a claim to be included in the term secondary stresses, but it is with those arising from the stiffness of joints that we shall be concerned in this chapter.

When a pin-jointed framework is loaded at the nodes the internal forces set up in the bars are simple tensions or compressions under the action of which the bars elongate or shorten so that the geometry of the framework is altered, the angles between the bars increasing or decreasing. If, as is most usual in practice, the joints are not pinned but are made stiff, *e.g.* in a steelwork truss where the bars are riveted to a gusset plate, the angles between the bars cannot change. The result is that, as external loads are applied and the geometry of the framework is altered, restraining moments are set up at the ends of the members and give rise to secondary bending stresses with which we are concerned in this chapter.

It will be realised from the illustrative examples in Chapter 9 that if the problem were attacked in the direct way set out there the labour involved in the determination of all the stresses in such a stiff-jointed truss as that shown in Fig. 10.1 (*a*) would be very considerable though, if one of the methods given in the paper referred to in the footnote on page 103 or in a later paper by Prof. Southwell,* is followed, it is not impossible. Fortunately, in most braced frameworks where an examination of the secondary stresses has to be made, the effect of the stiffness of the joints, while giving rise to appreciable local secondary bending stresses, is not sufficient to modify the axial forces in the members seriously. The positions of the nodes of the actual stiff-jointed framework, therefore, are very nearly the same as those which

* "Stress Calculation in Frameworks by the Method of Systematic Relaxation of Constraints III." R. V. Southwell. Proc. Roy. Soc., Series A, No. 878, Vol. 153, December, 1935.

would have been observed had the joints been pinned. This being so the secondary stresses can be considered as due to the bending of the members which takes place when the nodes of the stiff-jointed framework are forced into the positions which the nodes of the pin-jointed framework would have taken up under the external load system. In moving into these positions the stiff joints would, of course, rotate and

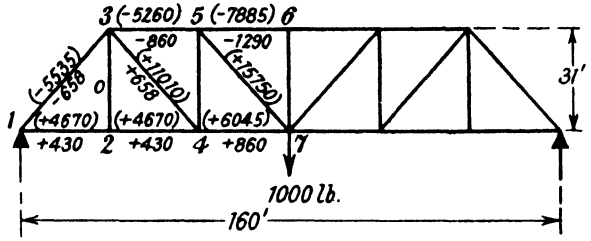

(a)

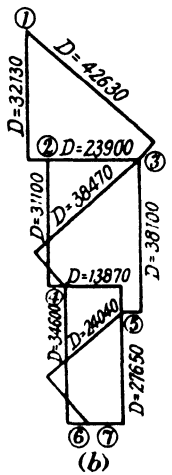

(b)

Member	Cross Sectional Area (sq. in)
1-2	29·44
1-3	58·49
2-3	16·00
2-4	29·44
3-4	29·42
3-5	52·35
4-5	26·48
4-7	45·48
5-7	20·58
5-6	52·35
6-7	14·70

FIG. 10.1.

the magnitudes of these rotations must be found before the bending stresses can be evaluated.

It is not difficult, with the help of the slope deflection expressions, to write down equations in terms of the unknown rotations. Fig. 10.2 shows a section of a rigid-jointed frame in which the secondary stresses due to a given arrangement of external loads at the nodes are to be determined. The deflections δ_{CB}, δ_{EB}, etc., of the neighbouring joints, C, E, etc., relative to B are shown. These deflections, according to our assumption, are the same as those which would have been observed had the given arrangement of external loads been applied to the nodes of the framework having pinned instead of rigid joints. They can be found without difficulty by means of the Williot-Mohr deflection diagram (paragraph 5.8). Suppose the joints of the framework, Fig. 10.2, rotate through angles θ_A, θ_B, θ_C, etc. when they are forced

into their deflected positions. It follows from equation (3) of paragraph 9.3 that the bending moments developed at the end B of the bar BC and at the end B of the bar BE are respectively

$$\left.\begin{aligned} M_{BC} &= \frac{2EI_{BC}}{l_{BC}}\left[2\theta_B+\theta_C-\frac{3\delta_{BC}}{l_{BC}}\right] \\ \text{and}\quad M_{BE} &= \frac{2EI_{BE}}{l_{BE}}\left[2\theta_B+\theta_E-\frac{3\delta_{BE}}{l_{BE}}\right] \end{aligned}\right\} \quad . \quad . \quad . \quad . \quad . \quad (1)$$

Similar expressions may be written down for the moments at the ends

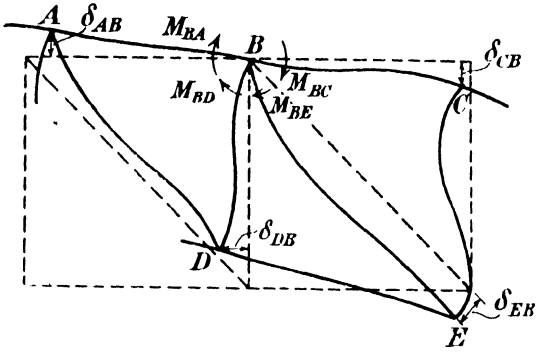

FIG. 10.2.

of the other bars and since the joint B is in equilibrium we may write, neglecting the dimensions of the gusset plate,

$$\sum \frac{2EI_{BC}}{l_{BC}}\left[2\theta_B+\theta_C-\frac{3\delta_{BC}}{l_{BC}}\right]=0 \quad . \quad . \quad . \quad . \quad . \quad . \quad (2)$$

the summation extending over all the bars meeting at B.

An equation similar to (2) can be written down from a consideration of the equilibrium of each joint in the framework so that as many equations are forthcoming as there are joints in the frame and therefore, as many as there are unknowns θ_A, θ_B, θ_C, etc. The slopes can then, in theory, be evaluated and the end bending moments and the secondary bending stresses calculated. In most practical trusses the number of equations makes an exact solution impracticable and it is usual to advocate the use of an approximate method for the solution of the equations. It will be found, however, that much tedious computation is still involved and it is not proposed to explore this method further. The reason for this is that other means are now available for attacking the problem. As the reader will in all probability have realized, the moment distribution method is ideally suited for the determination of secondary stresses. Once it is appreciated the older methods will fall into disuse and there is no object, therefore, in elaborating them.

10.2. Moment distribution method of analysis. In his original paper, Cross suggested the application of the moment distribution

method to the determination of secondary stresses and the first worked example appears to be due to Thompson and Cutler.* We cannot do better than set out their calculations. The truss considered is that shown in Fig. 10.1 (*a*), which has been treated by the orthodox methods in "Modern Framed Structures," Part II, Johnson, Bryan and Turneaure, where an exhaustive discussion of secondary stresses is given. As in the method already outlined in the present chapter the deflections of the nodes of the pin-jointed frame must first be found. The Williot diagram, giving these deflections, is shown in Fig. 10.1 (*b*) in which D is the displacement δ multiplied by E, the Young's modulus of the material of the truss. The figures in brackets on the line diagram of the truss are the deformations of the members multiplied by E while the other figures are the axial forces in the members in pounds.

The nodes of the actual rigid-jointed frame are first moved into the deflected positions given by the Williot diagram but are not allowed to rotate. Fixed end moments will, therefore, be developed in the members. These can be calculated from equations (1), etc. by putting $\theta_B=\theta_C=0$ and substituting for I, l and D, the values which are collected in Table 10.1. The sign convention is that used in earlier examples and the arrangement of the calculations, Table 10.2, should be clear from the examples which are given in Chapter 9.

Consider the member 5–6. It will be seen from the Williot diagram that this member rotates in a clockwise direction and that D=27,650, so that from equation (1) the fixed end moment M_{56} has the value

$$M_{56}=-\frac{6ID}{l^2}=-6\times\frac{3,978}{(320)^2}\times 27,650=-6,440 \text{ lb.-in.}$$

This is entered in the first line of the appropriate column (*a*). In the same way all the other fixed end moments are calculated and entered. The joints of the truss will not be in equilibrium under these fixed end moments; it will be seen for instance that the out-of-balance moment acting on joint (5) is +15,986. When a joint is released, therefore, it will rotate until it reaches a position of equilibrium and balancing moments proportional to their stiffnesses will be developed at the ends of the members. As in the later examples of Chapter 9 all the joints are released together and the balancing moments are entered in the second line of each column, Table 10.2. The carry-over moments, entered in the third line, throw the joints once more out of balance; they must therefore be released and balanced again. The procedure is exactly the same as that described in paragraph 9.5. Five cycles have been carried out in Table 10.2, and the end moments, found by summing up each column, are entered in column 6, Table 10.1, where a comparison is made (column 7) with the moments calculated by a more exact method (column 5). It will be seen that the moments at the ends of members 2–1 and 2–4 show errors of 12 and 21 per cent. respectively. If greater accuracy is required further cycles of the moment distribution process can be carried out. Had only one more been completed these particular errors would have dropped to 3 and

* Transactions, American Society of Civil Engineers, Vol. 96, p. 108, 1932.

6 per cent. respectively. From the end moments the end bending stresses, which are the secondary stresses required, are calculated. Thus in member 3–4, which is made up of two 15-inch channels back to back having a total relevant second moment of area of 805 (in.)^4 the maximum bending stress in the member, due to the end moment −301 lb.-in. (Table 10.1, column 6) is of magnitude $\frac{301 \times 7{\cdot}5}{805} = 2{\cdot}81$ lb. per square inch. The primary stress in this member due to the particular arrangement of external load considered is 22·43 lb. per square inch so that the secondary stress is 12·6 per cent. of the primary.

TABLE 10.1.

1	2	3	4	5	6	7
Member	l (inches)	I (inches)^4	D	End moments (lb.-in.)		
				More exact method	Cross method	
					Five cycles	Percentage difference between column 6 and column 5
1–2	320·0	1,218	32,130	+ 230	+ 240	4
2–1	—	—	—	+ 135	+ 151	12
1–3	490·7	4,490	42,630	− 230	− 240	4
3–1	—	—	—	− 527	− 507	4
2–3	372·0	95	23,900	− 53	− 54	2
3–2	—	—	—	− 55	− 56	2
2–4	320·0	1,218	31,100	− 80	− 97	21
4–2	—	—	—	− 141	− 133	6
3–4	490·7	805	38,470	− 307	− 295	4
4–3	—	—	—	− 320	− 301	6
3–5	320·0	3,978	38,100	+ 900	+ 858	5
5–3	—	—	—	+ 495	+ 523	6
4–5	372·0	750	13,870	− 875	− 880	0·5
5–4	—	—	—	− 924	− 927	0
4–7	320·0	1,907	34,600	+1,342	+1,314	2
7–4	—	—	—	+2,602	+2,625	1
5–7	490·7	358	24,040	− 130	− 133	2
7–5	—	—	—	+ 42	+ 45	7
5–6	320·0	3,978	27,650	+ 562	+ 537	4
6–5	—	—	—	+3,544	+3,563	0·5
6–7	372·0	288	0	0	0	0

Though it is an effect that can usually be neglected, the end moments do modify the axial forces in the members. If great accuracy is required

Table 10.2.

3			
−4,768	− 98	−700	−8,880
+5,640·3	+157·2	+986·3	+7,662·0
+2,493·4	+ 74·7	+432·3	+3,598·3
−2,576 3	− 71·8	−450·5	−3,499·9
−1,389·5	− 34·7	−131·0	− 985·1
+ 991·8	+ 27·6	+173·4	+1,347·4
+ 638·0	+ 15·0	+ 54·0	+ 431·1
− 444·4	− 12·4	− 77·7	− 603·7
− 254·1	− 6·6	− 22·8	− 166·9
+ 175·9	+ 4·9	+ 30·8	+ 238 9

5			*a*
−8,880	− 452	−214	−6,440
+7,196·6	+1,169·5	+423·2	+7,196·6
+3,831·0	+ 545·7	0	0
−1,970·3	− 320 2	−115·9	−1,970·3
−1,749·9	− 165·4	0	0
+ 862·2	+ 140·1	+ 50·7	+ 862·2
+ 673·7	+ 68·1	0	0
− 333·9	− 34·3	− 19·6	− 333·9
− 301·8	− 28·8	0	0
+ 148·8	+ 24·2	+ 8·8	+ 148·8

6		
−6,440	0	+6,440
0		0
+3,598·3		−3,598·3
0		0
− 985·1		+ 985·1
0		0
+ 431·1		− 431·1
0		0
− 166·9		+ 166·9
0		0

1	
− 4,768	−2,290
4,986·9	+2,071·1
+2,820·1	+1,113·1
−2,779·1	−1,154·1
−1,288·1	− 517·8
+1,276·0	+ 529·9
+ 495·9	+ 223·5
− 508·3	− 211·1
− 222·2	− 98·4
+ 226·5	+ 94·1

2		
−2,290	− 98 0	−2,214
+2,226·3	+143·4	+2,226·3
+1,035·5	+ 78·6	+1,026·7
−1,035·6	− 69·5	−1,035·6
− 577·0	− 35·9	− 311·1
+ 447·1	+ 30·0	+ 447·1
+ 264·9	+ 13·8	+ 128·2
− 196·8	− 13·2	− 196·8
− 105·5	− 6·2	− 54·1
+ 80·2	+ 5·4	+ 80·2

4			
−2,214	−700	− 452	−3,864
+2,053·4	+864·6	+1,091·5	+3,220·5
+1,113·1	+493·1	+ 584·7	0
− 622·2	−262·0	− 330·8	− 975·9
− 517·8	−225·2	− 160·1	0
+ 256·5	+108·0	+ 136·3	+ 402·3
+ 223·5	+ 87·7	+ 70·0	0
− 108·3	− 45·6	− 57·6	− 169·8
− 98·4	− 38·8	− 27·1	0
+ 46 7	+ 19·6	+ 24·8	+ 73·2

7				
−3,864	−214	0	+214	+3,864
0	0		0	0
+1,610·2	+211·6		−211·6	−1,610·2
0	0		0	0
− 487·9	− 57·9		+ 57·9	+ 487·9
0	0		0	0
+ 201·1	+ 25·3		− 25·3	− 201·1
0	0		0	0
− 84·9	− 9·8		+ 9·8	+ 84·9
0	0		0	0

in the calculation allowance can be made for the modification by the moment distribution method. The change in the position of the nodes due to the alterations in the axial forces brought about by the end moments is determined and the process of moving the rigid joints into the new positions, determining the fixed end moments, releasing the joints and balancing is again carried out.

The moment distribution method also enables the other secondary effects mentioned at the beginning of the chapter to be evaluated without difficulty. If the weights of the members are to be taken into account the bars are considered as beams carrying a distributed load equal to their own weight. The fixed end moments are then found from the expressions

$$M_{BC} = -\frac{6ID}{l^2} - \frac{wl^2}{12}$$

and

$$M_{CB} = -\frac{6ID}{l^2} + \frac{wl^2}{12}$$

where w is the intensity of the transverse load representing the weight of the bar. These moments are entered in the first lines of the table of calculations and the releasing and balancing of the joints is carried out as before.

When there is eccentricity in a joint due to the axes of the members not intersecting at one point the stresses arising can be determined by

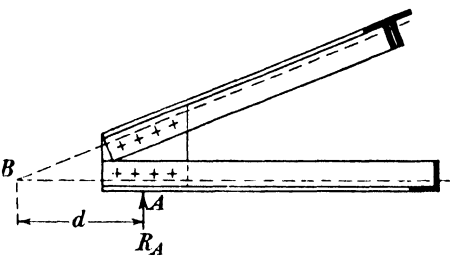

FIG. 10.3.

introducing into the analysis an external moment at the joint equal to the moment produced by the axial primary forces in the bars meeting there. An example of this type of eccentricity is commonly found at one end of light roof trusses and is shown diagrammatically in Fig. 10.3. The axes of the members meet at the point B which is a distance d from the support A. The theoretical joint where the axes meet is therefore subjected to an external moment of magnitude $-d.R_A$ and this must be included in the first balance of the joint. Suppose the truss illustrated in Fig. 10.1 (a) was supported, not at the intersection of the members 1–3 and 1–2 but at a point 6 inches nearer to joint 2. As far as the development of stresses is concerned this is equivalent to the provision of a support at the point of intersection of the members together with an anti-clockwise moment of magnitude 3,000 lb.-in. acting on the joint. It will be seen from the first two columns of Table 10.2 that the fixed end moments applied by joint (1) to the

members meeting at it are −4,768 and −2,290. The total out of balance moment on the joint at the instant when it is released is therefore +4,058 lb.-in. made up of −3,000 arising from the eccentricity of the support together with +4,768 and +2,290 lb.-in., the moments applied by the members. As the joint moves into its equilibrium position this out-of-balance moment is divided between the members in proportion to their stiffnesses so that the first two lines of the appropriate columns of Table 10.2 will appear as in Table 10.3.

TABLE 10.3.

−4,768	−2,290
+2,863	+1,195

The entries in the first two lines of the other columns are unchanged and the subsequent procedure is the same as before.

When, as frequently happens, one end of a truss is firmly fixed to its support so that it cannot rotate, the procedure in the calculations is the same as that used in the case of a continuous beam having one end encastré. If the joint (1) of the truss which has been considered above is firmly bolted to its abutment then the fixed end moments will be as before, Table 10·2, but since the joint cannot rotate no balancing moments appear in the second line of Table 10.4. The subsequent procedure is the same as before except that joint (1) is never released.

TABLE 10.4.

−4,768	−2,290
0	0

Little more remains to be said upon the determination of secondary stresses. The moment distribution method provides the most efficient tool for the work and the principles underlying the method have been described so fully in earlier chapters that the reader should be in a position to attack any particular case of secondary stress determination without the help of further illustrative examples. The assumptions used have been set out clearly. They are adequate for most practical problems but, as has been emphasised more than once already, it is impossible to define the limits beyond which they need amplification. Experience alone can define these. One assumption made so far in this chapter is that the effect of the axial force on the flexure of a member is negligible. Manderla, to whom is due the first satisfactory treatment of secondary stresses, gave in 1880 equations which take into account the effect of the axial force. These equations are derived just as equation (2) and state the fact that the sum of the end moments in the members meeting at a joint is zero. The expressions

for the end moments to be substituted in these equations are, however, not the simple slope deflection expressions but the more elaborate equations of which those for a member, initially curved, carrying a compressive force have been written down in full, equations (7) and (8) paragraph 7.20. Those for a member carrying a tensile force can be derived from the expressions of paragraph 8.5. The labour of solving these equations makes the method impracticable for most practical trusses and use must again be made of distribution methods which, though exceedingly laborious in this case, are possible.

CHAPTER 11

THE BEHAVIOUR OF CONNECTIONS IN STEEL FRAMES

11.1. General description of the behaviour of connections.—The stress distribution in a framework may be considerably influenced by the behaviour of the connections between the members. The modification in the stresses in a truss effected by the substitution of rigid for pinned joints was examined in the last chapter; in other types of frames, where the influence on the stresses is even more marked, the

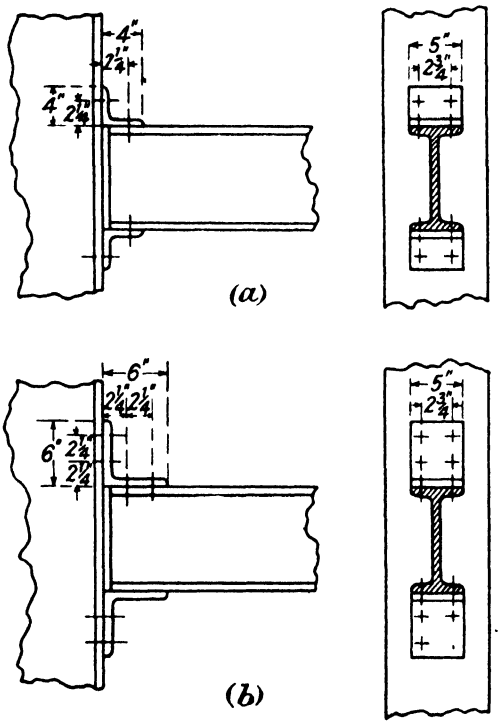

FIG. 11.1.

connections cannot be divided into the extreme classes of pinned and rigid. Before detailed design is begun or any accurate estimate of the stresses is attempted in such cases the behaviour of the connections must be understood.

Observations made on the steel frames of actual buildings have shown that when a beam having end connections of the simple bottom bracket and top cleat type of Fig. 11.1 is loaded, a curve similar to

OAB, Fig. 11.2, represents the relation between M, the moment transmitted through a connection, and $\theta - \phi$, the relative rotation of the members joined by the connection. It may be well to point out here that if the members had been joined by a frictionless pin the curve would have coincided with the axis OX, while if they had been rigidly connected it would have coincided with the axis OY. When load is removed from the beam the relationship between moment and rotation is as shown by BCDE. The moment has dropped to zero at D before the whole of the load has been removed from the beam and as the remainder of the load is removed a reversed moment comes into operation (D to E). When the load has been completely removed (E) there remains an end moment OM tending to cause sagging of the

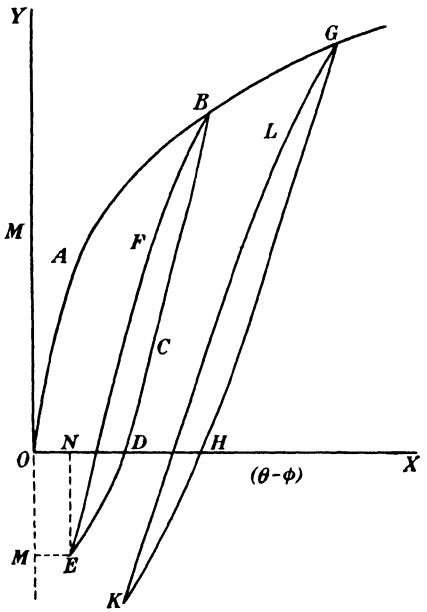

FIG. 11.2.

beam and a residual relative rotation, ON. On reloading, the curve traced out will be EFB, the point B being reached under the same load as before. If still more load is now added the first loading curve OAB will be continued to G.

It will be seen from these curves that the connection does not behave elastically. This fact may have an important bearing on the frame as a whole and some knowledge of the cause of the deformations suffered by the connection is essential to the designer. A complete analysis of the behaviour of a connection is difficult and no attempt will be made here to give more than a descriptive treatment.

When, due to the application of load to the beam, a small moment is transmitted through the connection, the legs of the bottom bracket and top cleat forming the connection will bend as if they were beams clamped firmly to the members at the rows of rivets nearest the roots

of the angles. If the vertical leg of the bottom bracket were perfectly fitted to the face of the stanchion it would be unable to bend. It is always found in practice, however, that the fitting is not good and under small transmitted moments the bottom bracket bends as freely as the top cleat so that the end of the beam rotates about its centre of depth. In these circumstances the relation between rotation and transmitted moment is the straight line OA (Fig. 11.3). As the transmitted moment increases, the pull in the rivets connecting the vertical leg of the cleat to the stanchion also increases. These rivets clamp the cleat efficiently until the pull in them exceeds their initial tension when they begin to extend elastically, increasing the flexibility of the connection and giving the relation represented by the line AB in Fig. 11.3. This continues until, as the moment increases further, the distortion of the top cleat is such that yield occurs in it ; the flexibility then increases

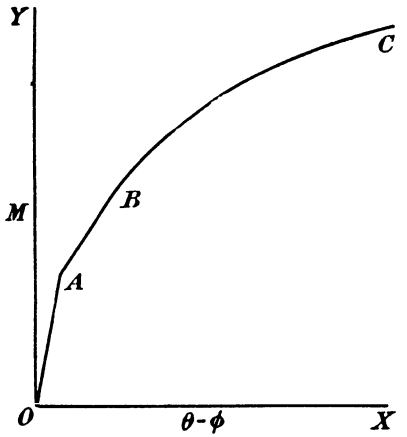

FIG. 11.3.

still more as shown by BC. This is the inelastic range during which the rate of change of moment decreases in a pronounced manner.

Actually the behaviour is much more complex than this description indicates. Over no part of the range does there appear to be a true linear relation between moment and rotation ; some inelastic deformation occurs under the smallest moment. Other influences affecting the behaviour are the closing in of the vertical leg of the bottom bracket and the relative movement between the horizontal leg of the cleat and the beam. As the vertical leg of the bracket bends it comes sooner or later into contact with the face of the stanchion and is restrained. Thus after a certain, and generally small, transmitted moment has been reached, the centre of rotation of the end of the beam moves down from the axis of the beam until eventually, when the whole of the vertical leg of the bracket is in close contact with the stanchion, it is at the level of the bottom flange of the beam. This change in the position of the centre of rotation tends to increase the rigidity of the connection. Relative movement between the horizontal leg of the

cleat and the top flange of the beam may also occur. Sometimes, more particularly when bolts are used, this " slip " is sudden, the relative rotation increasing considerably for a very small increase in transmitted moment.

So far only the deformations in the cleats and rivets or bolts have been considered but the local deformations in the members to which they are attached may also be of considerable importance. The action on the stanchion of a bracket and cleat type of connection may be taken to be the same as that of two equal and opposite horizontal forces applied in the neighbourhood of the rivets through the vertical legs of the bracket and cleat. The strains and stresses in the stanchion due to those forces can be estimated approximately. It will be found, when the connection of the beam is to the flange of a stanchion, that the strains, which always tend to increase the flexibility of the connection, are too small to have any appreciable influence on the stress distribution in the member at sections remote from the connections. The local stresses may, however, be considerable. When the connections are heavy the stresses developed in the web of the stanchion may be so large as to call for the introduction of web stiffeners and when a beam is connected to the web of the stanchion and is not balanced by a beam on the other side the local deformations of the web may be comparable to those of the connection itself. The overall flexibility may thus be considerably increased and the effect on the stresses in the frame marked.

The part of the curve OAB in Fig. 11.2, produced by the first application of the load, has now been considered in some detail. When load is removed the sequence of events is much the same, the deformations which occur first being similar to the elastic deformations produced on loading, so that the slope of the portion BC is not very different from that of OA. As more load is removed the beam, in straightening, deforms the bracket and cleat still more and the slope of the curve decreases as shown from C to D. At D no moment is being transmitted through the connection but, since the inelastic deformation produced by the first loading has not been removed, there is still an appreciable relative rotation of the members and there must consequently be some load still remaining on the beam. As this is removed the beam in straightening transmits a moment through the connection of the opposite sense from that so far produced and further deformation of the connection occurs until at the point E when all load has been removed the reverse moment is a maximum and there is some residual relative rotation. The magnitude of the reverse moment may be very much greater than that shown in the figure. On reloading, the curve traced out is EFB, a closed loop being formed which is retraced almost exactly as further unloading and loading is carried out. If, after B has been reached, load is added to the beam the first loading curve OAB will be continued to some point G. If the load is again removed then the path followed will be GHK and on reloading another loop will be formed by the curve KLG. It is not difficult to see from this that the stress distribution in a frame having

connections of the type under discussion will depend not only on the loads borne at the moment but also on the history of the frame. This is illustrated by the example given in paragraph 11.2.

A number of first loading curves for bracket and top cleat (flange cleat) connections are shown in Fig. 11.4, each curve being marked with the size of angle used for the cleats. In all cases the connections were 5 inches long, the beam 12 inches deep and the rivets $\frac{3}{4}$ inch diameter.

Another form of steelwork connection consists of a pair of angles connecting the web of the beam to the stanchion. Such a web cleat connection behaves in much the same way as the flange cleat type

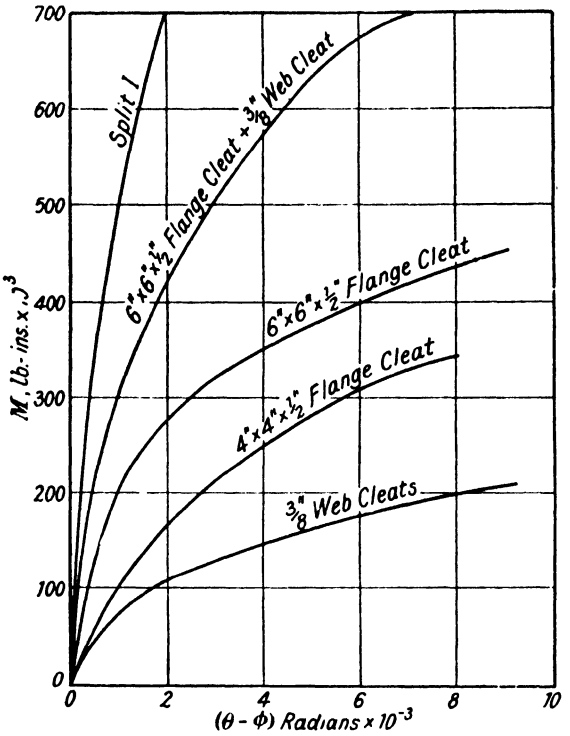

FIG. 11.4.

discussed above but is more flexible. A typical curve for a web cleat connection made up of $6 \times 3\frac{1}{2} \times \frac{3}{8}$ inch angles 9 inches long joined to a 12-inch deep beam and to a stanchion by $\frac{3}{4}$-inch rivets is shown in Fig. 11.4.

Though the web cleat connection alone is very flexible the addition of angles connecting the web of a beam to a stanchion already joined by flange cleats increases the rigidity of the connection considerably above that for the flange cleats alone. This is shown in Fig. 11.4 by the curve for a connection made up of $6 \times 6 \times \frac{1}{2}$-inch flange cleats and $\frac{3}{8}$-inch web cleats to a 12-inch deep beam.

A type of connection sometimes used when heavy moments have

to be transmitted is the split I connection (Fig. 11.5) Two large T's made by cutting one flange from a length of I section join the top and bottom flanges of the beam to the stanchion. It will be seen that this type of connection is likely to be more rigid than that made up of flange or web cleats. Until the moment transmitted is considerable the only deformation which can take place is that due to stretch of the rivets through the flange of the split I and the small amount of flexure of this flange. A typical curve for such a connection made with T's cut from a 15 in.$\times$6 in.$\times$45-lb. R.S.J. $7\frac{3}{4}$ inches long and fitted with $\frac{7}{8}$-inch rivets (Fig. 11.5) is shown in Fig. 11.4. It will be seen that the relation between moment and relative rotation is almost linear; this continues until a moment of 9×10^5 lb.-in. is reached. Above this the rate of increase of moment decreases, due probably to slip between the web of the split I and the flange of the beam.

Steelwork connections differ in one important respect from the rest of the structure of which they form part. They are, under normal

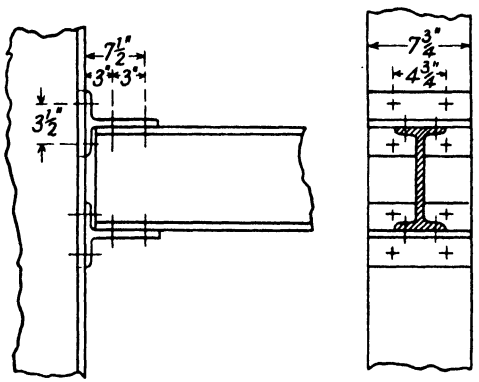

FIG. 11.5.

loading conditions, overstrained; that is to say the yield point of the material has been passed. This is not a source of danger when the material used is as ductile as structural steel since tests have shown that the relative rotation needed to cause fracture is many times greater than that which can occur under normal circumstances in a steel frame.

The curves shown in Fig. 11.4 are for bare connections. In many frames the connections are encased in concrete. Tests on buildings have shown that when the casing is of unreinforced concrete, such as that formed by the pouring of the floor slab, the rigidity of the connection under working loads is increased to such an extent that in certain cases the connection has behaved very nearly as a perfectly rigid joint. Laboratory tests on encased connections show that the flexibility is reduced to a very small value until a moment is transmitted which cracks the concrete. Under greater moments the curve is similar to that for the uncased connection. It seems probable that the addition of a small percentage of reinforcement running just above

the top flange of the beam and hooked around the stanchion would ensure the increased rigidity under all working conditions.

Though almost all the beam-to-stanchion connections made to-day in this country are bolted or riveted the use of welded connections cannot be long delayed. Connections with the flexibility of those already described could be made by welding but if one can judge from the designs used in other countries the tendency will be to produce almost perfectly rigid connections. If this is done the designer will need to estimate accurately the moments transmitted. Recent research has shown that these moments may be very large and the joint will have to be designed to transmit them.

11.2. Effect of the behaviour of connections on the design of a frame. —It will be seen from the curves of Fig. 11.4 that the relation between

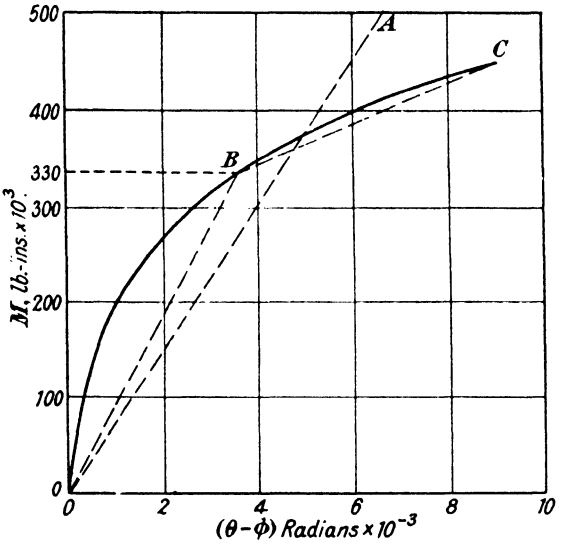

FIG. 11.6.

the moment transmitted by a connection and the relative rotation between the members is not linear and this complicates the analysis of the stresses in the framework. It means that no exact analysis can be obtained by the method given in paragraph 9.4 where the assumption is made that such a linear relation exists. Fortunately the stresses can be calculated accurately enough for many practical purposes if the curves are replaced by a straight line. For example it is clear from Fig. 11.4 that a straight line passing through the origin can be chosen which will represent the curve for the split I connection without serious error. For the more flexible connections a suitable substitute line can be plotted if an approximate preliminary estimate of the moment transmitted through the connection can be made. If the connection is made up of $6\times6\times\frac{1}{2}$-inch flange cleats the line OA, Fig. 11.6, will lead to a fairly accurate analysis of the stresses so long as the moment through the connection lies within the range $3{\cdot}5\times10^5$ to 4×10^5 lb.-in.

Where a more accurate analysis is required the curve for the connection can be replaced by its chords. Thus for the $6\times6\times\frac{1}{2}$-inch flange cleats great accuracy will result from the use of the chords OB, BC. The analysis would be carried out by the method of paragraph 9.4 for a connection having a flexibility defined by OB and the portion of the applied load which would produce a transmitted moment of $3{\cdot}3\times10^5$ lb.-in. is calculated together with the stresses due to this load. The stresses arising from the application of the remainder of the load, the connection having a flexibility defined by the slope of BC, are then found.

This method will be illustrated by a consideration of the symmetrical single storey single bay portal of span 8 feet and height 18 feet shown

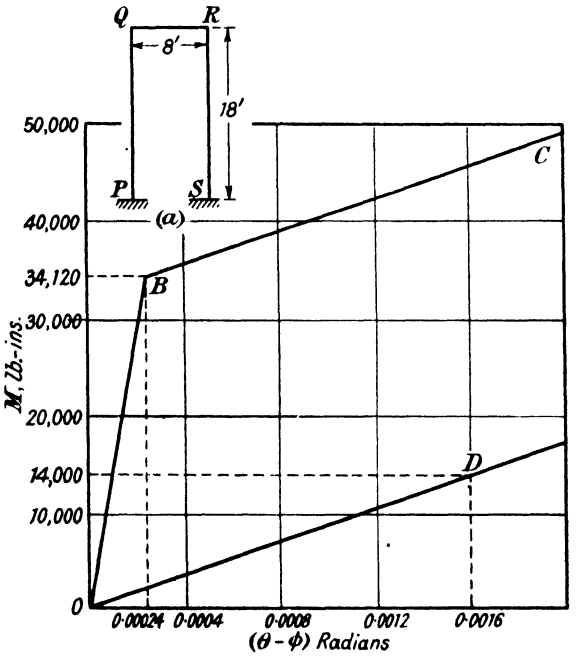

FIG. 11.7.

in Fig. 11.7 (*a*). The feet of the stanchions are rigidly fixed to the ground, the beam to stanchion connections are identical and their characteristics are shown by the M. $(\theta-\phi)$ curve of Fig. 11.7. The stanchions and beams are of the same cross-section, uniform throughout and have a depth D of 8 inches. The portal is to carry a uniformly distributed load of 200 lb. per inch run on the beam. In the first place the portal is considered to be a frame having semi-rigid connections with a flexibility defined by the line OB. From the equations of paragraph 9.4, or by means of the moment distribution method, the restraining moments produced at the ends of the beam are found when a load of unit intensity is applied. From this it is possible to deduce the load necessary to produce a moment of 34,120 lb.-in. which, as can

be seen from Fig. 11.7, is the value at the point B where the slope of the curve changes. It is found that the load necessary is 100 lb. per inch and so a further 100 lb. per inch has to be added before the beam is fully loaded. While this extra load is being added the moments at the ends of the beam continue to increase, but as the relation between M and $\theta-\phi$ is represented by the line BC for all transmitted moments greater than 34,120 lb.-in., a further calculation must be performed. For this purpose the portal is considered to have a flexibility defined by the line OD, where OD is parallel to BC, and a calculation is made of the moments at the ends of the beam produced by the application of a load of unit intensity. It will be found for this portal that when a load of 100 lb. per inch is applied to the beam the restraining moment developed is 12,800 lb.-in. Therefore when the full load of 200 lb. per inch run is applied to the beam of the original portal the restraining moments at the ends of the beam, which are equal to those at the tops of the stanchions, will be 46,920 lb.-in. Since the portal is symmetrical it follows from the slope deflection equations that the moments at the feet of the stanchions have a magnitude one-half that at the upper ends or 23,460 lb.-in. The bending moment diagram for the portal can then be drawn and the bending stress at any point determined.

It is interesting to consider the behaviour of this portal when a horizontal load, which might be produced by wind, acts at the level of the beam. Such a load acting from left to right will tend to decrease the moment, due to vertical load on the beam, transmitted through joint Q and to increase that through joint R. From the discussion of the behaviour of semi-rigid connections given in the preceding paragraph it will be seen that as the transmitted moment tends to decrease, the flexibility of the connection will return very nearly to the value it had originally under small moments (see BC, approximately parallel to AO in Fig. 11.2) while as the transmitted moment continues to increase the flexibility will continue as it was (see BG, Fig. 11.2). The curves of Fig. 11.8 relate to the connections at the ends Q and R of the beam in the portal. The lines 01, 12 represent their behaviour under the vertical load of 200 lb. per inch applied to the beam. As the first 100 lb. per inch was added the transmitted moment increased along 0–1, while as the second 100 lb. per inch was added it increased from the point 1 until the point 2 was reached. If a horizontal load is now applied from left to right the flexibility of the connection Q will be represented by OB (Fig. 11.7), since the transmitted moment decreases, while that of the connection R will continue to be represented by OD as the moment continues to increase. In determining the moments developed by the horizontal load, therefore, the portal must be considered as unsymmetrical, having connections of different flexibilities. There is no difficulty in analysing the stresses in such a frame and it will be found that under a horizontal load of 200 lb. the decrease in moment through joint Q is 9,960 lb.-in. while the increase through R is only 3,736 lb.-in. The curves traced out while the horizontal load is being applied are, therefore, the portions 2–3 in Fig. 11.8. If the horizontal load is now removed the moment transmitted through joint

Q will tend to increase while that through R will decrease. Both connections will therefore have flexibilities represented closely by the line OB, Fig. 11.7 (see EF and GH approximately parallel to OA in Fig. 11.2) so that the portal may be considered once more as a symmetrical frame having connections with flexibilities represented by OB. Under a horizontal load of 200 lb. acting from right to left the moments developed at Q and R in this portal are 7,312 lb.-in. so that the curves traced out while the original horizontal load is being removed are the portions 3–4, in Fig. 11.8. The points 4 do not coincide with the points 2 and it will be seen that the application and removal of the horizontal load have resulted in a decrease in the restraining moments at Q and R of 2,648 and 3,576 lb.-in. respectively.

In certain simple cases the stresses in beams fitted with flexible connections can be found more exactly by a construction due to

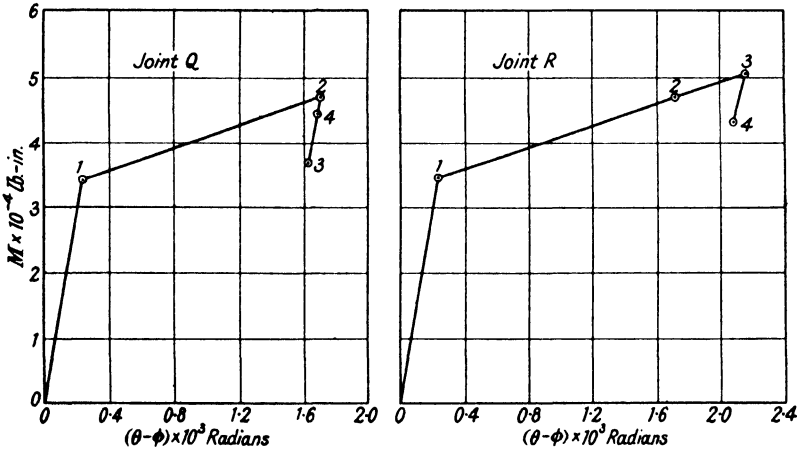

FIG. 11.8.

Professor C. Batho, to whom we owe much of our detailed knowledge of the behaviour of connections.*

Suppose a beam of uniform cross-section and length l carries a uniformly distributed load of intensity w per unit length and is connected to rigid abutments by identical connections having a flexibility defined by the curve OPQ in Fig. 11.9.

If ϕ is the change of slope and M is the moment at the end of the beam then from equation (3) of paragraph 9.3 the relation between the end moment and the end rotation is

$$M=\frac{2EI}{l}[\phi]-\frac{wl^2}{12}.$$

This is a straight line and can be drawn as AB in Fig. 11.9. The curve OPQ showing the relation between transmitted moment and angular rotation for the connection is already plotted so that P, the

* "Beam and Stanchion Connections." C. Batho, 2nd Report, Steel Structures Research Committee. H.M. Stationery Office, 1934.

intersection of AB and OPQ, gives the moment present at the end of the beam. The bending moment and the bending stress at any point in the beam can then be determined.

It is much more usual for a beam to be connected at its end to a stanchion which is flexible and will therefore change its slope when a moment is applied to it. Suppose the beam considered in the last example is connected at its ends to identical stanchions the flexibility of which is known, so that on Fig. 11.9 it is possible to plot the line ON showing the change of slope of a stanchion at the level where the beam is attached, due to any moment applied to it at that level. If, as before, the curve OPQ defines the flexibility of the beam-to-stanchion connection the change of slope suffered by the end of the beam when any moment M is transmitted from it through the connection to the

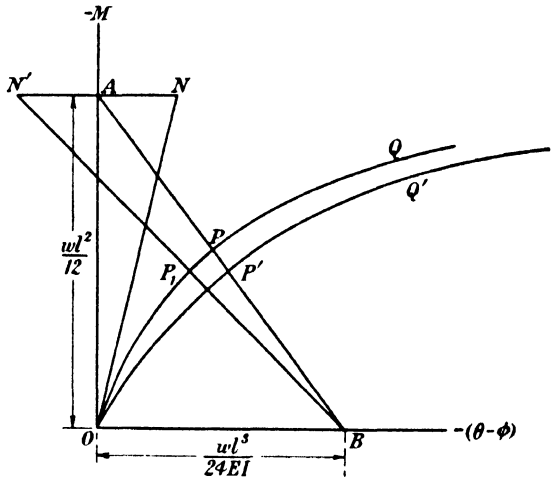

FIG. 11.9.

stanchion is given by the sum of the abscissæ of ON and OPQ corresponding to M. The curve representing this sum is OP'Q' and, as in the first example, the moment at the end of the beam when a uniformly distributed load of intensity w is applied is given by the intersection of OP'Q' with the beam line AB.

The curve OP'Q' need not be drawn if the following construction is used. Join B to N' a point on NA produced such that N'A=AN. Then P_1, the point where N'B cuts the curve OPQ gives the end moment on the beam.

This graphical method has been extended to cover unsymmetrical arrangements of load and structure. A description will be found in Professor Batho's original paper.*

* "The Analysis and Design of Beams under Given End Restraints." C. Batho, Final Report, Steel Structures Research Committee. H.M. Stationery Office, 1936.

CHAPTER 12

ELASTIC ARCHES AND RINGS

12.1. Action of the arch.—It has been shown that the essential reactive forces for the equilibration of any system of loads acting upon a plane frame are provided if the structure is supported on a pin at one point and on a frictionless bearing at another; the reactive forces are then determinate from the equations of static equilibrium for the system. Thus, the curved beam shown in Fig. 12.1 which is pinned to a support at A and rests on rollers at B can carry any system of loads and the reactions will consist of vertical forces at A and B and

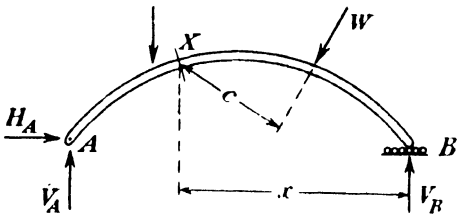

FIG. 12.1.

a horizontal force at A. The elastic straining of the beam will cause the end B to move slightly in a horizontal direction.

The resultant actions at a section of the beam, such as X, normal to its centre line will be :—

(*a*) A thrust equal to the algebraic sum of the forces to the right of X resolved in a direction normal to the section.

(*b*) A shearing force equal to the algebraic sum of the forces to the right of X resolved in a direction parallel to the section.

(*c*) A bending moment $M = Wc - V_B x$.

If the free movement of the end B is restricted by the introduction of a horizontal force at B the resultant actions at any section are not modified in type but their magnitude will be altered, the amount of this alteration being dependent upon the extent to which the point B is restrained. The most important change will be in the magnitude of the bending moment, which may be reduced considerably. The action of the horizontal restraining force upon the structure is known as arch action and its effects are very important since it may considerably reduce the size of a member required to carry a specified load system and so allow spans to be bridged which might otherwise be impossible.

It is usual to restrict the movement of the end completely and the

term arch is generally applied to a curved structure in which both supports are fixed in position, although not necessarily in direction.

Arches are constructed of a variety of materials. Steel is commonly used for the purpose and the arch may be either a rolled or plated section when it is termed an arch rib, or a braced structure such as the Sydney Harbour Bridge. Concrete, either plain or reinforced, is also frequently used in similar structures. Both steel and concrete arches are characterised by a homogeneity of structure: they may be considered as units made of a single material and in this respect differ from arches of brickwork or masonry where small units, bricks or voussoirs, are held together by cement or mortar joints. From the standpoint of theoretical treatment the distinction is of some importance since a homogeneous structure may reasonably be expected to behave elastically within the limits set by the material of which it is made, whereas the same assumption becomes questionable in the case of a structure made of composite material.

There is, however, good experimental evidence that masonry and brickwork arches behave elastically and obey Hooke's Law. This will be dealt with in Chapter 23.

12.2. General types.—The simplest type of arch theoretically is that known as the three-pinned arch and shown in Fig. 12.2. It consists

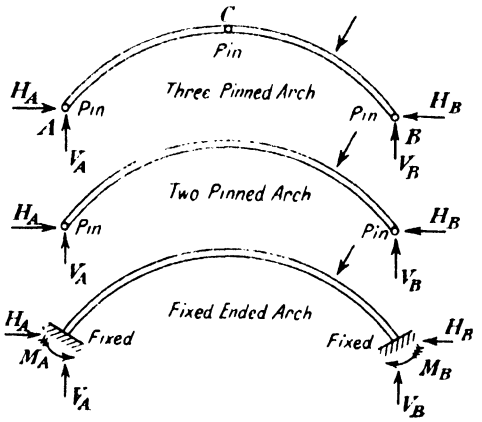

FIG. 12.2.

of two sections pinned together at the crown C and to pins at A and B so that its ends are fixed in position but not in direction.

If the central pin is omitted and the member is made continuous between supports it becomes a two-pinned arch. In both these types the reactive forces consist of vertical and horizontal components at A and B.

The ends of the arch may be restrained not only in position but also in direction in a manner analogous to that of an encastré beam: the arch is then of the fixed-end type and the reactions consist of vertical and horizontal forces and fixing moments at each support. Arches of

any of these types may be either ribs or braced structures and the stress analysis of the various forms will now be considered.

12.3. The three-pinned arch.—Fig. 12.3 represents a three-pinned arch of span L, the third pin being midway between A and B. A load having vertical and horizontal components Y and X is carried at a horizontal distance x from the centre, y being the rise of the arch at this point.

AC and BC are essentially two bars connecting the point C to the

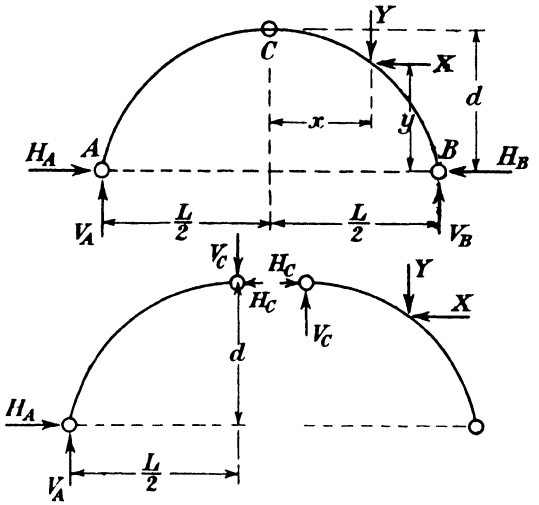

FIG. 12.3.

two fixed points A and B, and the frame is just stiff: the arch is therefore statically determinate.

Let the vertical and horizontal forces at A be V_A and H_A, and at B, V_B and H_B.

The equation of the vertical and horizontal forces on the structure and the equation of moments about A gives:—

$$V_A+V_B-Y=0 \quad . \quad . \quad . \quad . \quad . \quad . \quad . \quad . \quad (1)$$

$$H_A-H_B-X=0 \quad . \quad . \quad . \quad . \quad . \quad . \quad . \quad . \quad (2)$$

$$Y\left(\frac{L}{2}+x\right)-Xy-V_BL=0. \quad . \quad . \quad . \quad . \quad . \quad . \quad . \quad . \quad (3)$$

If the arch be separated at the crown pin, as shown in the figure, the internal reactions which it provided must be replaced by external forces H_C and V_C for equilibrium of each half to be restored. The equations of equilibrium for the left-hand section are then

$$V_A-V_C=0 \quad . \quad . \quad . \quad . \quad . \quad . \quad . \quad . \quad (4)$$

$$H_A-H_C=0 \quad . \quad . \quad . \quad . \quad . \quad . \quad . \quad . \quad (5)$$

$$H_Cd-V_C\frac{L}{2}=0. \quad . \quad . \quad . \quad . \quad . \quad . \quad . \quad . \quad (6)$$

These equations, together with the three above, enable the values H_A, H_B, H_C, V_A, V_B and V_C to be found in any particular case.

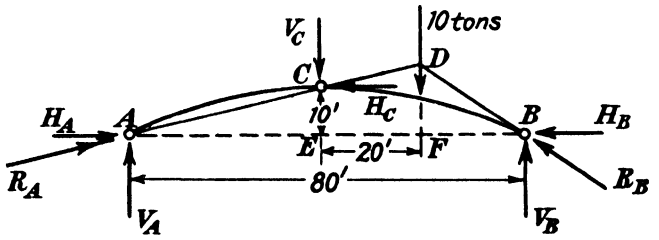

FIG. 12.4.

As an example suppose an arch of 80 feet span and 10 feet rise carries a load of 10 tons at the quarter span as shown in Fig. 12.4 and it is desired to calculate the reactions. From a consideration of the equilibrium of the whole arch the following equations are obtained :—

$$V_A+V_B-10=0$$
$$H_A-H_B=0$$
$$600-80V_B=0$$

which give $V_B=7{\cdot}5$ tons,
$V_A=2{\cdot}5$ tons,
and $H_A=H_B$.

For equilibrium of the left-hand section of the arch the following equations must be satisfied :—

$$V_A-V_C=0$$
$$H_A-H_C=0$$
$$10H_C-40V_C=0,$$

from which $H_C=4V_C=4V_A$
$H_A=H_C$
and so $V_A=2{\cdot}5$ tons
$V_B=7{\cdot}5$ tons
$H_A=H_B=10$ tons.

In many cases of three-pinned arches the results can be obtained in a simpler manner. In the example just worked, for instance, it should be noticed that since C is a pin-joint there can be no bending moment there and the line of action of the resultant of all the forces on the left-hand section must, therefore, pass through it. Hence, if AC in Fig. 12.4 be joined, the reaction at A is directed along AC. Also, since the reaction at A, the reaction at B and the external load are in equilibrium their lines of action must meet at a point. If AC be produced to meet the load line at D therefore, the resultant of the forces at B must act along the line BD. Hence the directions of the reactions at A and B are known and their components are readily obtained. Thus, R_A is directed along AC, and CE and AE represent the values of V_A and H_A to the same scale that AC represents R_A.

Therefore $H_A=4V_A$.

Similarly R_B is directed along BD and so BF and FD represent to scale the values of H_B and V_B.
Since FD=15 and FB=20

$$H_B=\tfrac{4}{3}V_B.$$

By taking moments about A, V_B is found to be 7·5 tons and V_A to be 2·5 tons and so

$$H_A=H_B=10 \text{ tons as before.}$$

12.4. Bending moments in a three-pinned arch.—Having found the horizontal thrust, the bending moment at any point is readily calculated.

In Fig. 12.5 if K is any point on an arch carrying vertical loads only, the bending moment at K is

$$M_K=\Sigma Wc-V_Bx+H_By$$

where the summation sign denotes that all loads to the right of the section must be included.

Since V_B is unaffected by horizontal forces acting at A and B its

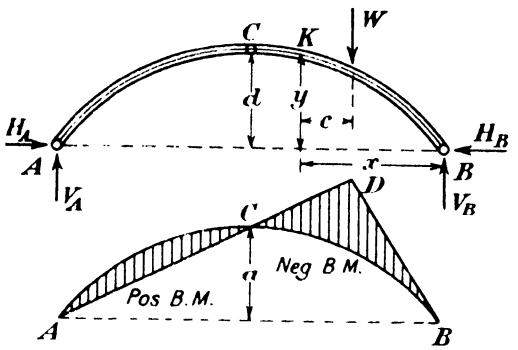

FIG. 12.5.

value would be unaltered if AB were spanned by a horizontal beam instead of by an arch. The terms $\Sigma Wc-V_Bx$ give the bending moment at any point for the hypothetical beam AB and the bending moment for this is readily plotted. As there are no horizontal loads on the arch $H_A=H_B=H$ say, and the term Hy can be represented for all values of x by the line of the arch itself. Remembering that there can be no bending moment at the pin C the complete bending moment diagram is readily drawn as follows. The curve of the arch is first set out. If the rise is actually represented by a inches on the diagram this dimension represents Hd foot-tons, the value of Hy at the centre. The bending moments represented by this line are positive and the values of the " beam " bending moment which are essentially negative must be deducted to obtain the true moments. The bending moment diagram for the beam in the case shown is a triangle with its apex on the line of action of the load. Hence, if the line ACD is drawn to meet the load line at D, and D and B are joined, ADB is the beam diagram and the bending moment at any point on the arch is the intercept between the two diagrams.

It will be seen that whatever is the shape of the arch, the centre line will always represent the Hy term of the bending moment to an appropriate scale and the beam bending moment diagram has then only to be drawn to pass through the points A, B and C in order to complete the construction. If the arch carries horizontal as well as vertical loads the diagram cannot be plotted quite so simply. H_A will not then be equal to H_B and the curve of the arch no longer represents Hy. There is, however, no difficulty since the reactive forces can be calculated with no more trouble than in the case described. In the special case of a three-pinned arch carrying a uniformly-distributed load of intensity w over its whole span the bending moment diagram for the pin-jointed beam of the same span is a parabola. If the centre line of the arch is also a parabola the Hy curve and the load curve coincide at all points and there is no bending moment anywhere in the rib.

12.5. The two-pinned arch.—The curved beam of Fig. 12.1 is a statically determinate structure: the provision of the restraint at B which transforms it from a beam into an arch introduces a redundant reaction and so a two-pinned arch cannot be analysed simply by the application of the laws of statics, but must be treated by one or other of the methods which take account of its elastic properties. Whatever method of solution is adopted the object is the same—to determine the magnitude of the horizontal reactive force. Once this has been found, the bending moments, normal thrusts and transverse shearing forces can be calculated for all points on the arch.

12.6. Two-pinned segmental arch rib. Strain energy analysis.—As an example of the strain energy method of analysing an arch rib, a

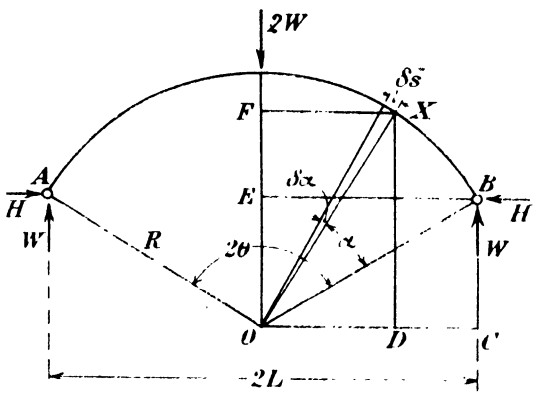

Fig. 12.6.

segmental arch with a central load will be considered in detail. Fig. 12.6 illustrates the case. The angle subtended at the centre of the segment is 2θ and the span of the arch is 2L; the central load 2W produces a vertical reactive force W at each support. The horizontal reactive force H, which is the same at both supports, will be chosen as the redundant element.

At any point X on the rib at an angular distance α from B the resultant actions are a thrust normal to the section, a shearing force tangential to the section and a bending moment. The effect of the first two is small compared with the third and will be neglected.

If U is the total strain energy due to bending in the rib, the value of H will be such as to make U a minimum.

i.e. $$\frac{dU}{dH}=0,$$

or $$\frac{2}{EI}\int_{\alpha=0}^{\alpha=\theta} M_x\frac{dM_x}{dH}ds=0$$ where M_x is the bending moment at X.

Since $ds=Rd\alpha$, where R is the radius of curvature of the rib,

we have $$\int_0^{\theta} M_x\frac{dM_x}{dH}d\alpha=0.$$

Now
$$\begin{aligned}M_x&=-W\,.\,CD+H\,.\,EF\\&=-W(OC-OD)+H(FO-EO)\\&=-WR\{\sin\theta-\sin(\theta-\alpha)\}+HR\{\cos(\theta-\alpha)-\cos\theta\}\end{aligned}$$

and $$\frac{dM_x}{dH}=R\{\cos(\theta-\alpha)-\cos\theta\}.$$

$$\therefore\int_0^{\theta}[H\{\cos(\theta-\alpha)-\cos\theta\}^2+W\{\sin\theta-\sin(\theta-\alpha)\}\{\cos\theta-\cos(\theta-\alpha)\}]d\alpha=0.$$

Upon integrating, this gives

$$H\left[\frac{\alpha}{2}-\tfrac{1}{4}\sin 2(\theta-\alpha)+2\cos\theta\sin(\theta-\alpha)+\alpha\cos^2\theta\right]_0^{\theta}$$
$$=-W\left[\frac{\alpha\sin 2\theta}{2}+\sin\theta\sin(\theta-\alpha)-\cos\theta\cos(\theta-\alpha)+\frac{\cos 2(\theta-\alpha)}{4}\right]_0^{\theta}$$

or
$$H[2\theta-3\sin 2\theta+4\theta\cos^2\theta]$$
$$=-W[2\theta\sin 2\theta+3\cos 2\theta+1-4\cos\theta]$$

so that
$$H=\frac{(4\cos\theta-1-2\theta\sin 2\theta-3\cos 2\theta)W}{4\theta-3\sin 2\theta+2\theta\cos 2\theta}.$$

In the particular case when $\theta=90°$
$$H=\frac{2W}{\pi}.$$

As another example of this method the segmental arch with a load not at the centre will be considered. As before, taking a span 2L, radius R and load 2W we will assume 2θ to be 120° and the load to act at 30° from OB, as in Fig. 12.7. As before H_B will be taken as the redundant element.

From the conditions of static equilibrium
$$H_A=H_B=H \text{ say}$$
$$V_A+V_B=2W$$
$$2V_BL=2W(L+R\sin 30°),$$

which give

$$V_B=\frac{W}{L}\left(L+\frac{R}{2}\right)=W\left(\frac{\sqrt{3}+1}{\sqrt{3}}\right),$$
$$V_A=\frac{W}{L}\left(L-\frac{R}{2}\right)=W\left(\frac{\sqrt{3}-1}{\sqrt{3}}\right).$$

At any point X on the rib between B and C such that $\overset{\frown}{BOX}=\alpha$ we have

$$M_x=HR\{\cos(\theta-\alpha)-\cos\theta\}+V_BR\{\sin(\theta-\alpha)-\sin\theta\},$$
$$\frac{dM_x}{dH}=R\{\cos(\theta-\alpha)-\cos\theta\}$$

and

$$\left[\frac{dU}{dH}\right]_{BC}=\frac{R^3}{EI}\int_0^{\frac{\pi}{6}}[H\{\cos(\theta-\alpha)-\cos\theta\}^2+V_B\{\sin(\theta-\alpha)-\sin\theta\}\{\cos(\theta-\alpha)-\cos\theta\}]d\alpha.$$

Between C and A,

$$M_x=HR\{\cos(\theta-\alpha)-\cos\theta\}+V_BR\{\sin(\theta-\alpha)-\sin\theta\}+2WR\{\tfrac{1}{2}-\sin(\theta-\alpha)\}$$

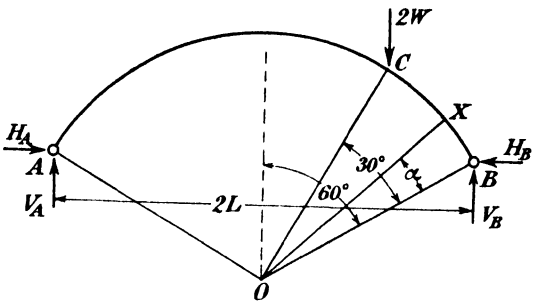

FIG. 12.7.

and

$$\left[\frac{dU}{dH}\right]_{CA}=\frac{R^3}{EI}\int_{\frac{\pi}{6}}^{\frac{2\pi}{3}}[H\{\cos(\theta-\alpha)-\cos\theta\}^2+V_B\{\sin(\theta-\alpha)-\sin\theta\}\{\cos(\theta-\alpha)-\cos\theta\}]d\alpha$$
$$+\frac{2WR^3}{EI}\int_{\frac{\pi}{6}}^{\frac{2\pi}{3}}\{\tfrac{1}{2}-\sin(\theta-\alpha)\}\{\cos(\theta-\alpha)-\cos\theta\}d\alpha.$$

The complete equation $\frac{dU}{dH}=0$ is therefore

$$\int_0^{\frac{2\pi}{3}}[H\{\cos(\theta-\alpha)-\cos\theta\}^2+V_B\{\sin(\theta-\alpha)-\sin\theta\}\{\cos(\theta-\alpha)-\cos\theta\}]d\alpha$$
$$+2W\int_{\frac{\pi}{6}}^{\frac{2\pi}{3}}\{\tfrac{1}{2}-\sin(\theta-\alpha)\}\{\cos(\theta-\alpha)-\cos\theta\}d\alpha=0$$

or
$$H\left(\frac{\pi}{2}-\frac{3\sqrt{3}}{4}\right)+V_B\left(\frac{\pi}{2\sqrt{3}}-\frac{3}{2}\right)+2W\left(\frac{6-\pi}{8}\right)=0.$$

Substituting the value of V_B this gives

$$\frac{H}{2W}=\cdot 406.$$

The calculation of the thrust in the case of a two-pinned symmetrical arch carrying a load not at the centre can be simplified by a device now to be explained. Suppose such an arch, which will be taken for purposes of illustration to be segmental, has a central angle of 2θ and a span of 2L as before. It carries a load 2W at an angle ψ from the centre line OC as shown at (*a*) in Fig. 12.8. If a second load, also equal to 2W, acts at a point in CB which is an angular distance ψ from OC the horizontal thrust due to it will be equal to that caused by the first

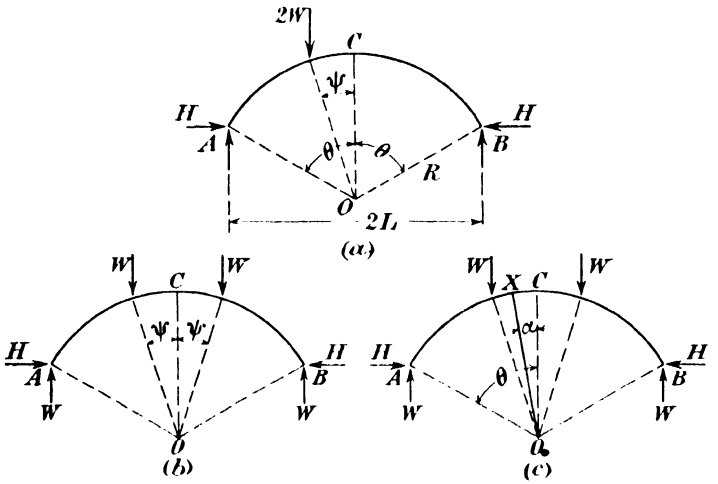

FIG. 12.8.

load and the total thrust under the two loads acting together will be twice that due to the single load 2W. Hence, if the loading shown at (*a*) in Fig. 12.8 be replaced by that shown at (*b*) the horizontal thrust in the two cases will be the same and since the case (*b*) is a symmetrical one it is much easier to solve. The vertical reaction at each support is W and we let H be the horizontal thrust.

If X is any point on the rib at an angular distance α from OC as shown at (*c*) in Fig. 12.8 the bending moment at X is,

$$M_x=-WR(\sin\theta-\sin\alpha)+HR(\cos\alpha-\cos\theta)+WR(\sin\psi-\sin\alpha),$$

the last term only appearing when α is less than ψ.

Since the arch is symmetrical about OC it is only necessary to consider the strain energy of one half and we have

$$\frac{dU}{dH}=\frac{R}{EI}\int_0^{\theta}M_x\frac{dM_x}{dH}d\alpha=0.$$

Substituting for the value of $\frac{dM_x}{dH}$ this becomes,

$$-W\int_0^\theta(\sin\theta-\sin\alpha)(\cos\alpha-\cos\theta)d\alpha+H\int_0^\theta(\cos\alpha-\cos\theta)^2d\alpha$$
$$+W\int_0^\psi(\sin\psi-\sin\alpha)(\cos\alpha-\cos\theta)d\alpha=0.$$

Upon integrating and reducing, the value of H is found to be

$$H=\frac{2W[2\cos\theta\cos\psi+2\psi\sin\psi\cos\theta+\frac{1}{2}\cos 2\psi-\theta\sin 2\theta-1-\frac{3}{2}\cos 2\theta]}{4\theta-3\sin 2\theta+2\theta\cos 2\theta}$$

which is a general expression for the horizontal thrust in any segmental arch with a single load 2W acting at an angular distance ψ from the axis of symmetry of the arch.

12.7. Two-pinned parabolic arch.—In the case of the parabolic arch cartesian co-ordinates must be used in place of the polar co-ordinates of the previous paragraph.

Fig. 12.9 shows a parabolic arch rib carrying a central load of 2W.

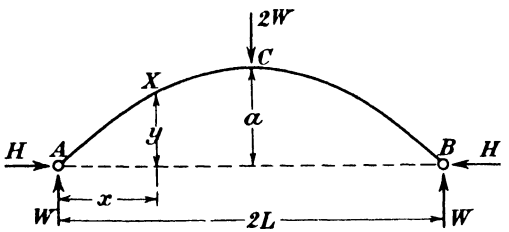

FIG. 12.9.

Taking the origin of co-ordinates at A the equation for the rib can be written

$$y=\frac{ax(2L-x)}{L^2}.$$

The bending moment at any point X on the rib between A and C is

$$M_x=Hy-Wx$$

and

$$\frac{dM_x}{dH}=y.$$

The value of H is given by the solution of the equation

$$\frac{dU}{dH}=2\int_0^L\frac{M_x}{EI}\frac{dM_x}{dH}ds=0$$

where EI is the flexural rigidity of the rib. The value of $\frac{dU}{dH}$ is the same between A and C as between B and C due to the symmetry of loading and the integral is therefore taken as twice that between $x=0$ and $x=L$.

Now $\frac{ds}{dx}=\left\{1+\left(\frac{dy}{dx}\right)^2\right\}^{\frac{1}{2}}$ and if this be substituted, the resultant

integral is a difficult one. Suppose however, taking a special case, that the section of the rib varies in such a way that

$$I_x = I_0 \sec \alpha$$

where I_x is the second moment of area about the axis of bending at the point X,

I_0 is the second moment of area at the crown

and α is the angle of slope of the rib to the axis of x at X.

Then
$$\sec \alpha = \frac{ds}{dx},$$

$$I_x = I_0 \frac{ds}{dx}$$

and the equation

$$\frac{1}{E}\int_0^L \frac{M_x}{I_x}\frac{dM_x}{dH}ds = 0$$

becomes
$$\frac{1}{E}\int_0^L \frac{M_x}{I_0}\frac{dM_x}{dH}dx = 0$$

or
$$\int_0^L M_x \frac{dM_x}{dH}dx = 0,$$

i.e.
$$\int_0^L \left[H\left\{\frac{ax(2L-x)}{L^2}\right\} - Wx\right]\frac{ax(2L-x)}{L^2}dx = 0$$

or
$$\frac{Ha^2}{L^4}\int_0^L x^2(2L-x)^2dx = \frac{Wa}{L^2}\int_0^L x^2(2L-x)dx.$$

Upon integration this leads to

$$\frac{8}{15}aL^3H = \frac{5}{12}L^4W$$

or
$$\frac{H}{2W} = \frac{25}{128}\left(\frac{2L}{a}\right)$$

i.e. the horizontal thrust is $\frac{25}{128}\left(\frac{\text{span}}{\text{rise}}\right)$ times the centre load.

If the rise is small the assumption that the second moment of area varies as the slope does not yield a very different result from that of a uniform rib and this assumption is therefore often made to render the calculations manageable.

The same method can be used for any loading other than the central concentrated weight: the integration becomes correspondingly more lengthy as in the parallel case of the segmental arch given in the last paragraph, but presents no particular difficulty in obtaining the value of H.

12.8. Two-pinned arch; graphical solution of equations.—If the arch is of such a shape that the equations cannot readily be integrated, a graphical treatment is of general applicability. Suppose the arch

shown in Fig. 12.10 is subjected to any system of loads indicated by W_1, W_2 and W_3 which act at distances a, b and c respectively from A. Let X be any point on the arch rib at a horizontal distance x from A and let the rise of the arch at this point be y.

Then, as before, the condition for the determination of H is

$$\frac{dU}{dH}=\frac{1}{E}\int\frac{M_x\,dM_x}{I_x\,dH}ds=0$$

where I_x is the second moment of area about the axis of bending at X and M_x is the bending moment at X.

Then $M_x=Hy-V_Ax+W_1(x-a)+W_2(x-b)+W_3(x-c)$, where the terms in brackets are only included if they are positive.

Also $$\frac{dM_x}{dH}=y$$

and the equation for H takes the form

$$\int\left\{\frac{Hy^2}{I_x}-\frac{V_Axy}{I_x}+\frac{W_1(x-a)y}{I_x}+\frac{W_2(x-b)y}{I_x}+\frac{W_3(x-c)y}{I_x}\right\}ds=0$$

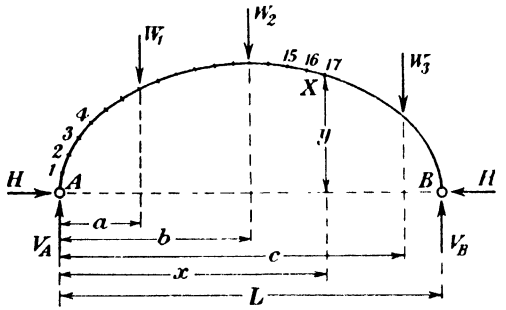

FIG. 12.10.

the limits of integration being from $x=0$ to $x=L$ for the terms in H and V_A and from $x=a$, b and c to $x=L$ for W_1, W_2 and W_3 respectively. Unless $\frac{ds}{dx}$ can be expressed simply the integration will be impossible mathematically and we proceed as follows.

Divide the centre line of the rib into a number of parts; it is preferable but not essential to make these equal. The greater the number the more accurate will be the final result. Let the length of each part be δs.

At each point obtained by this division, numbered 1, 2, etc., in the figure, measure the values of I_x, x and y and calculate the terms $\frac{y^2}{I_x}$, $\frac{xy}{I_x}$, $\frac{(x-a)y}{I_x}$, $\frac{(x-b)y}{I_x}$ and $\frac{(x-c)y}{I_x}$. Plot these values upon a base representing s at the appropriate distances from the origin. The area of the resulting curves will give the coefficients of H, V_A, W_1, W_2 and W_3 in the equation for H and if these areas are denoted by A_1, A_2 . . . A_5, the equation is

$$HA_1-V_AA_2+W_1A_3+W_2A_4+W_3A_5=0.$$

Since V_A can be calculated from the moment equation about B the equation is soluble for H.

As an example this method will be applied to the segmental arch of Fig. 12.7, which has already been solved analytically.

Fig. 12.11 shows the centre line of the rib divided into 13 equal parts,

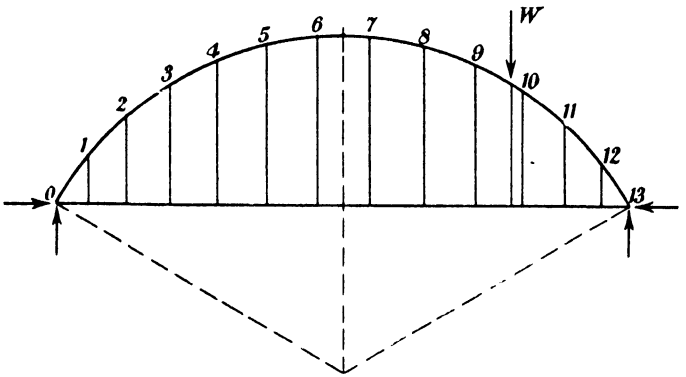

Fig. 12.11.

the load acting between points 9 and 10. Since the second moment of area of the rib is constant it can be omitted from the equation.

The values of x and y for each point and the terms calculated from them are given in Table 12.1. The scales used are immaterial provided they are the same throughout.

Table 12.1.

Point	x	y	y^2	xy	$(x-a)y$
0	0	0	0	0	—
1	7·2	11·2	123	80·5	—
2	17·0	21·0	441	357	—
3	28·0	29·0	841	812	—
4	40·0	35·5	1,260	1,420	—
5	52·5	40·0	1,600	2,100	—
6	66·0	42·0	1,764	2,772	—
7	79·5	42·0	1,764	3,340	—
8	92·6	40·0	1,600	3,704	—
9	105·6	35·5	1,260	3,750	—
9·78	115·0	31·0	961	3,565	0
10	117·5	29·0	841	3,410	72·5
11	128·6	21·0	441	2,700	286·0
12	138·0	11·2	123	1,530	257·5
13	146·0	0	0	0	0

The load does not come exactly at one of the divisions but at the point $x=115$, $y=31$. This is entered in the Table as 9·78, *i.e.* it is $9{\cdot}78\delta s$ from the origin.

The curves of y^2, xy and $(x-a)y$ are plotted on a base s in Fig. 12.12 and the proportional areas of these curves as measured are

$$A_1=\int y^2 ds \quad = 6{\cdot}12.$$
$$A_2=\int xy ds \quad =13{\cdot}36.$$
$$A_3=\int (x-a)y ds = 0{\cdot}35.$$

Hence

$$6{\cdot}12H-13{\cdot}36V_A+{\cdot}35W=0$$

and by taking moments about B we find

$$146V_A=31W$$

or

$$V_A={\cdot}212W$$

$\therefore$

$$6{\cdot}12H-2{\cdot}84W+{\cdot}35W=0$$

and

$$\frac{H}{W}={\cdot}406$$

which agrees with the value found previously since the load in this example is represented by W instead of 2W as in the analytical case.

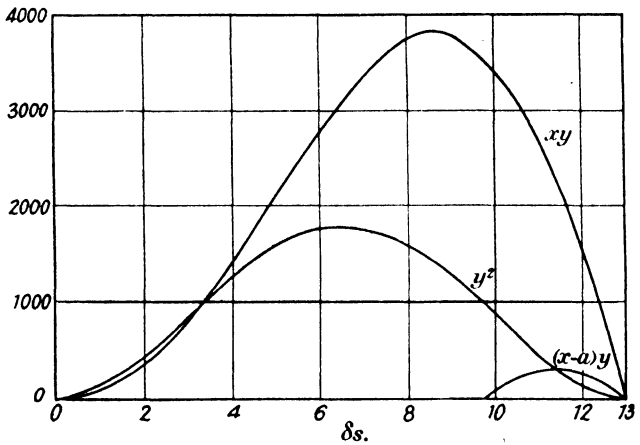

FIG. 12.12.

12.9. Analysis of two-pinned arch from strain equations.—Suppose Fig. 12.13 represents the centre line of a curved bar subjected to any system of bending moments. Let the bending on a small element of length δs at C turn this element through a small angle δi and cause the chord CB to move to CD.

If CF is the perpendicular from C to the chord AB

$$BCF=BDE=\alpha$$

where BE and ED are the component movements of B normal and parallel to AB.

Then

$$DE=BD\cos\alpha=\delta i BC\cos\alpha=y\delta i.$$

Also, applying the theory of bending for initially straight beams which is sufficiently accurate for the case of the arch rib,

$$\frac{\delta i}{\delta s}=\frac{M}{EI}$$

where M is the bending moment at C and EI is the flexural rigidity of the element δs.

Hence $$DE = y\delta i = \frac{M}{EI} y\delta s$$

or, in the limit when δs is made infinitesimal, the total horizontal movement of B due to the bending of AB is

$$\int_A^B \frac{M}{EI} y ds.$$

In the two-pinned arch the total movement of B along AB is zero and so

$$\int \frac{My}{EI} ds = 0.$$

But y is $\frac{dM}{dH}$ and the equation is identical with that obtained from considerations of strain energy.

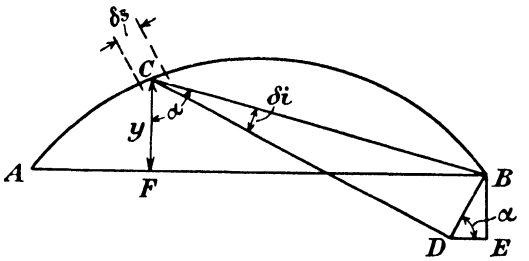

FIG. 12.13.

12.10. Resultant actions in two-pinned arch.—Having calculated the value of the horizontal thrust as shown in previous paragraphs, the bending moment, normal thrust and transverse shearing force can be found for all points on the arch rib.

Fig. 12.14 represents a two-pinned arch carrying loads W_1 and W_2 tons at points C and D which are at distances a and b respectively from A.

The bending moment at X, which is x from A is

$$M_x = Hy - \{V_A x - W_1(x-a) - W_2(x-b)\}$$

where the terms $(x-a)$, $(x-b)$ only appear when $x>a$ and $x>b$ respectively.

Hy represents the bending moment due to H and the remainder of the expression that upon a beam of span AB loaded identically with the rib. The curve of Hy is, to an appropriate scale, the centre line of the rib : thus, if the true rise of the arch at the centre is d inches and the scale of the drawing of the rib is $\frac{1}{n}$ then Hd inch-tons is represented by $\frac{d}{n}$ inches and the drawing of the rib is the Hy curve to a scale of 1 inch$=Hn$ inch-tons. The " beam " bending moment diagram *acdb* is plotted to the same scale, as shown in Fig. 12.14 and the bending

moment at any point on the rib is then given by the intercept between the two curves.

If the arch had been made in the shape of the beam bending moment diagram, in this case if the centre line had followed the line *acdb*, there would clearly be no bending moment at any point in the arch. *acdb* is known as the linear arch.

The normal thrust and transverse shearing force at any point in the rib may be found by resolving the forces to the right or left of the

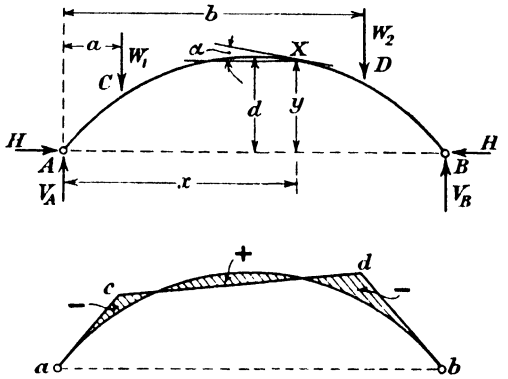

FIG. 12.14.

section in directions along and normal to the tangent to the rib at that point. Thus, at X, in Fig. 12.14, if the tangent makes an angle α to the horizontal,

the resultant vertical shearing force at X $= V_B - W_2$
and the resultant horizontal force $= H$.
Resolving along and normal to the tangent we obtain
normal thrust at X $= (V_B - W_2) \sin \alpha + H \cos \alpha$
and transverse shearing force $= (V_B - W_2) \cos \alpha - H \sin \alpha$.

The linear arch may be considered from another point of view. If the loads on the arch were reversed in direction and carried on a flexible cable, this cable would take the form of the linear arch provided the constant horizontal tension in it were equal to H. Such a cable would be stable since every section would be in tension. Theoretically therefore when the loads act in their original directions, struts *ac*, *cd* and *db* pinned together at their ends would support the loads; the resulting arrangement would however obviously be unstable. For every load system there is an unlimited number of possible linear arches depending on the polar distance used in drawing the funicular polygon, *i.e.* on the value of H. The correct linear arch is that having the true value of H for the real arch. Having obtained the correct linear arch we know the direction, point of application and magnitude of the thrust at any section of the true arch. Its distance from the centre line of the real arch is the eccentricity of loading at that section and the bending moment there is the product of this eccentricity and the thrust.

The linear arch, or line of thrust as it is often called, is much used in the design and analysis of masonry arches: this is dealt with in Chapter 23.

12.11. Arched rib with fixed ends.—Fig. 12.15 (*a*) shows a curved cantilever rigidly fixed at A and it is clear that this constitutes a

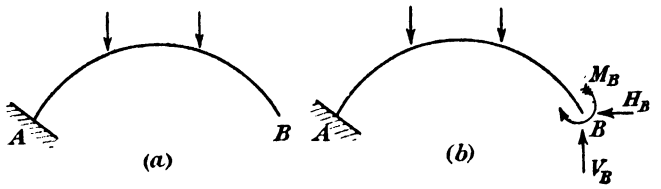

FIG. 12.15.

perfectly sound theoretical structure for carrying any system of loads. These loads may consist of weights acting as at (*a*) or of a combination of weights and terminal actions as at (*b*).

Suppose the terminal actions as shown at (*b*) are so proportioned that they keep B completely fixed in position and direction: it is evident that they will then be the same actions as would be induced if the end B were rigidly fixed in the same way as A. Such end actions consist of a vertical force V_B to prevent vertical movement, a horizontal force H_B to prevent horizontal movement, and a couple M_B to prevent rotation and since these three actions are not required for the static equilibrium of the member AB, the arch with completely fixed ends has three degrees of redundancy. It is convenient to take the terminal reactions as the redundant elements. The bending moment at any point X on the fixed end arch rib shown in Fig. 12.16 is

$$M_x = M_B + H_B y - V_B x + W_1(x-a) + W_2(x-b) + W_3(x-c),$$

the terms in brackets only being taken into the equation when they are positive.

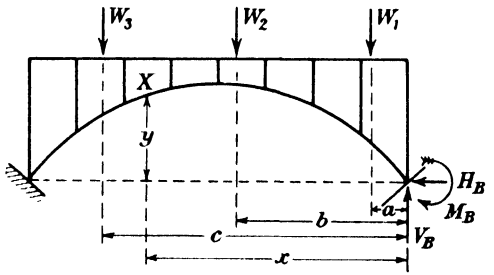

FIG. 12.16.

The unknown reactions may then be found by an application of the principle of minimum strain energy, the conditions being that

$$\frac{\partial U}{\partial H_B} = 0,$$

$$\frac{\partial U}{\partial V_B} = 0$$

and

$$\frac{\partial U}{\partial M_B} = 0.$$

As before, the bending strain energy is the only portion that need be considered since that due to normal thrust and transverse shearing force is very small in comparison. Hence, the equations can be written

$$\int \frac{M_x}{I_x} y ds = 0.$$

$$\int \frac{M_x}{I_x} x ds = 0.$$

$$\int \frac{M_x}{I_x} ds = 0.$$

Just as in the case of the two-pinned rib these equations can be solved either by direct integration or by graphical methods. In the case of the parabolic rib the assumption that $I_x = I_0 \sec \alpha$ will make the equations integrable as shown in paragraph 12.7.

Consideration of the problem from the strain conditions for the rib leads to the same equations. It has already been shown in paragraph 12.9 that the condition that there shall be no horizontal movement of B is

$$\int \frac{M_x}{I_x} y ds = 0.$$

Reference to Fig. 12.13 shows that the vertical movement of B due to the rotation of a small element δs is

$$BE = BD \sin \alpha = \delta i BC \sin \alpha = x \delta i$$

and the argument follows exactly as for the horizontal component leading to the equation

$$\int \frac{M_x}{I_x} x ds = 0.$$

The third condition to be satisfied is that the change of slope at B must be zero.

The change of slope at B due to the rotation of the element δs is δi.

But $$\delta i = \frac{M_x}{EI_x} \delta s$$

Therefore the total change of slope $= \int \frac{M_x}{EI_x} ds$

and since this is zero, we obtain our third equation

$$\int \frac{M_x}{I_x} ds = 0.$$

These are the same equations as obtained by an application of the strain energy method.

As an example consider the case of the semi-circular arch rib shown in Fig. 12.17 carrying a load W at an angular distance of 45° from OB. The radius of the arch is R and its constant flexural rigidity is EI.

At any point X on the rib situated at α from OB

$$M_x = M_B + H_B R \sin\alpha - V_B R(1-\cos\alpha) + WR(\cos\tfrac{\pi}{4} - \cos\alpha)$$

where the term in W only occurs between $\alpha = \frac{\pi}{4}$ and $\alpha = \pi$.

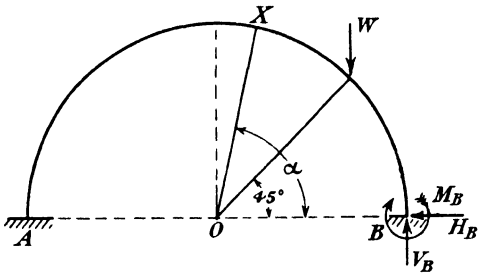

FIG. 12.17.

Since $\dfrac{\partial M_x}{\partial M_B} = 1,$

$$\frac{\partial M_x}{\partial H_B} = R\sin\alpha$$

and $$\frac{\partial M_x}{\partial V_B} = -R(1-\cos\alpha),$$

the equations for $\dfrac{\partial U}{\partial M_B}$, $\dfrac{\partial U}{\partial H_B}$ and $\dfrac{\partial U}{\partial V_B}$ are

$$\frac{1}{EI}\int_0^\pi \{M_B + H_B R\sin\alpha - V_B R(1-\cos\alpha)\}ds + \frac{1}{EI}\int_{\frac{\pi}{4}}^\pi WR(\cos\tfrac{\pi}{4} - \cos\alpha)ds = 0,$$

$$\frac{R}{EI}\int_0^\pi \{M_B + H_B R\sin\alpha - V_B R(1-\cos\alpha)\}\sin\alpha ds + \frac{R}{EI}\int_{\frac{\pi}{4}}^\pi WR(\cos\tfrac{\pi}{4} - \cos\alpha)\sin\alpha ds = 0,$$

$$-\frac{R}{EI}\int_0^\pi \{M_B + H_B R\sin\alpha - V_B R(1-\cos\alpha)\}(1-\cos\alpha)ds - \frac{R}{EI}\int_{\frac{\pi}{4}}^\pi WR(\cos\tfrac{\pi}{4} - \cos\alpha)(1-\cos\alpha)ds = 0,$$

or, putting $ds = Rd\alpha$ and removing constant divisors these become

$$\int_0^\pi \{M_B + H_B R\sin\alpha - V_B R(1-\cos\alpha)\}d\alpha + WR\int_{\frac{\pi}{4}}^\pi \left(\cos\tfrac{\pi}{4} - \cos\alpha\right)d\alpha = 0,$$

$$\int_0^\pi \{M_B + H_B R\sin\alpha - V_B R(1-\cos\alpha)\}\sin\alpha d\alpha + WR\int_{\frac{\pi}{4}}^\pi \left(\cos\tfrac{\pi}{4} - \cos\alpha\right)\sin\alpha d\alpha = 0,$$

$$\int_0^{\pi}\{M_B+H_BR\sin\alpha-V_BR(1-\cos\alpha)\}(1-\cos\alpha)d\alpha$$
$$+WR\int_{\frac{\pi}{4}}^{\pi}\left(\cos\frac{\pi}{4}-\cos\alpha\right)(1-\cos\alpha)d\alpha=0.$$

Upon integration and reduction these give

$$\pi M_B+2RH_B-\pi RV_B+\frac{RW}{\sqrt{2}}\left(\frac{3\pi}{4}+1\right)=0,$$

$$2M_B+\frac{\pi}{2}RH_B-2RV_B+RW\left(\frac{2\sqrt{2}+3}{4}\right)=0,$$

$$\frac{\pi}{2}RV_B-RW\left(\frac{2+3\pi}{8}\right)=0.$$

The solution is

$V_B=\cdot91\ W$
$H_B=\cdot18\ W$
$M_B=\cdot04\ WR.$

12.12. Symmetrically loaded arch rib fixed at ends.—If the arch rib is symmetrical and symmetrically loaded about its vertical axis the work is somewhat simplified since $V_A=V_B$ and can be calculated from the loads direct: the bending moments at A and B being equal do not cause a redistribution of the shearing forces and the vertical reactions are the same as if the arch were pinned.

Hence the equation for $\frac{\partial U}{\partial V_B}$ is unnecessary and only two equations have to be solved instead of three, as with the unsymmetrically-loaded rib.

If the rib is subjected to a central load only, a further simplification is possible since the integrations need only be done for one half of the rib and the terms of the previous paragraph relating directly to W do not appear. Thus, if the load of the previous example were at the centre instead of at 45° from OB we should have, following the method of that paragraph, $V_B=\frac{W}{2}$ and the first two equations would become

$$\int_0^{\pi}\left\{M_B+H_BR\sin\alpha-\frac{WR}{2}(1-\cos\alpha)\right\}d\alpha+WR\int_{\frac{\pi}{2}}^{\pi}-\cos\alpha d\alpha=0,$$

$$\int_0^{\pi}\left\{M_B+H_BR\sin\alpha-\frac{WR}{2}(1-\cos\alpha)\right\}\sin\alpha d\alpha+WR\int_{\frac{\pi}{2}}^{\pi}-\cos\alpha\sin\alpha d\alpha=0.$$

If, however, we integrate for one half of the rib only we get for $\frac{\partial U}{\partial M_B}=0$ and $\frac{\partial U}{\partial H_B}=0$ the equations

$$2\int_0^{\frac{\pi}{2}}\left\{M_B+H_BR\sin\alpha-\frac{WR}{2}(1-\cos\alpha)\right\}d\alpha=0$$

$$2\int_0^{\frac{\pi}{2}}\left\{M_B+H_BR\sin\alpha-\frac{WR}{2}(1-\cos\alpha)\right\}\sin\alpha d\alpha=0.$$

Integrating these expressions we obtain in either case,

$$\pi M_B+2RH_B+RW\left(1-\frac{\pi}{2}\right)=0,$$

$$2M_B+\frac{\pi}{2}RH_B-\frac{RW}{2}=0,$$

which give

$$H_B=\cdot459W$$
$$M_B=-\cdot111WR.$$

12.13. Application of principle of superposition to fixed arches.—A solution in general terms of the equations of paragraph 12.11 is very laborious if the arch is unsymmetrically loaded, but by an application of the principle of superposition a considerable simplification is effected.

Consider the arch shown at (*a*) in Fig. 12.18 which is fixed at A and B and carries a load 2W at an angle ψ from the axis of symmetry OC. The reactions at A are V_A, H and M_A and at B they are V_B, H and M_B. The load system is exactly equivalent to the sum of the two systems shown at (*b*) and (*c*) so that the results obtained from (*b*) and (*c*), treated separately, may be added to find the corresponding results for (*a*).

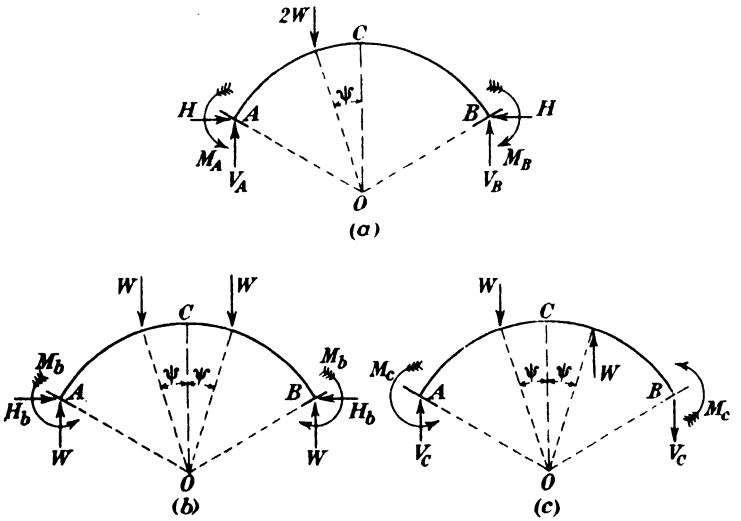

FIG. 12.18.

The reactions at A and B under the symmetrical system shown at (*b*) consist of equal vertical reactions W, a thrust H_b and equal fixing moments M_b. Under the skew-symmetrical load system shown at (*c*) there will be no thrust, the vertical reactions will be equal and opposite of magnitude V_c and the fixing moments will be equal and opposite of magnitude M_c.

Since in case (*b*) the loading is symmetrical we only need to consider

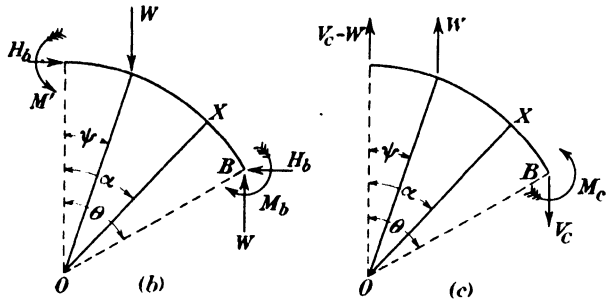

FIG. 12.19.

one half of the arch and with the notation shown in Fig. 12.19 (*b*) we have, for the bending moment at any point X,

$$M_x = M' - H_b R(1 - \cos\alpha) + WR(\sin\alpha - \sin\psi),$$

where M′ is the bending moment at the crown and the last term only occurs when α is greater than ψ. Treating M′ and H_b as the redundant elements the conditions to be satisfied are

$$\frac{\partial U}{\partial M'} = 0 \quad \text{and} \quad \frac{\partial U}{\partial H_b} = 0.$$

Now

$$\frac{\partial M_x}{\partial M'} = 1 \quad \text{and} \quad \frac{\partial M_x}{\partial H_b} = -R(1 - \cos\alpha)$$

and the equations are therefore

$$\int M_x d\alpha = 0 \quad \text{and} \quad \int M_x (1 - \cos\alpha) d\alpha = 0.$$

But

$$\int M_x (1 - \cos\alpha) d\alpha = \int M_x d\alpha - \int M_x \cos\alpha d\alpha$$
$$= 0 - \int M_x \cos\alpha d\alpha.$$

The equations to be solved for the redundant elements are therefore

$$\int_0^\theta \{M' - H_b R(1 - \cos\alpha)\} d\alpha + WR \int_\psi^\theta (\sin\alpha - \sin\psi) d\alpha = 0$$

$$\int_0^\theta \{M' - H_b R(1 - \cos\alpha)\} \cos\alpha d\alpha + WR \int_\psi^\theta (\sin\alpha - \sin\psi) \cos\alpha d\alpha = 0.$$

Upon integrating and reducing these we obtain

$$M'\theta - H_b R(\theta - \sin\theta) + WR\{\cos\psi - \cos\theta - (\theta - \psi)\sin\psi\} = 0$$

$$4M' \sin\theta - H_b R(4\sin\theta - 2\theta - \sin 2\theta) + WR\{\cos 2\psi - \cos 2\theta - 4\sin\psi(\sin\theta - \sin\psi)\} = 0$$

and these give

$$H_b = W \frac{\theta(\cos 2\psi + \cos 2\theta - 2) + 4\sin\theta(\cos\psi - \cos\theta + \psi\sin\psi)}{2\theta^2 + \theta\sin 2\theta + 2\cos 2\theta - 2} \quad . \quad . \quad . \quad (1)$$

By taking moments about B we have

$$M_b = M' - H_b R(1 - \cos\theta) + WR(\sin\theta - \sin\psi)$$

and substituting for M′ in terms of H_b from the first equation we obtain

$$M_b=\frac{R}{\theta}[H_b(\theta\cos\theta-\sin\theta)-W\{(\cos\psi+\psi\sin\psi)-(\cos\theta+\theta\sin\theta)\}] \quad . \quad (2)$$

Now consider the skew symmetrical case shown in Fig. 12.18 (*c*). From the symmetry there can be no bending moment at C and since the strain energy of both halves of the arch will be equal, we can again deal with one half only as shown in Fig. 12.19 (*c*).

The bending moment at X is,

$$M_x=(V_c-W)R\sin\alpha+WR(\sin\alpha-\sin\psi),$$

the second term only appearing when α is greater than ψ.

The only redundant element is V_c so

$$\frac{dU}{dV_c}=0$$

Since $\frac{dM_x}{dV_c}=R\sin\alpha$ this condition gives the equation

$$(V_c-W)R\int_0^\theta \sin^2\alpha d\alpha+WR\int_\psi^\theta(\sin^2\alpha-\sin\alpha\sin\psi)d\alpha=0.$$

Upon integrating this and reducing we have

$$\left.\begin{aligned} V_c&=\frac{W(2\psi+\sin 2\psi-4\cos\theta\sin\psi)}{2\theta-\sin 2\theta}\\ \text{and}\qquad M_c&=\frac{WR\{2\psi\sin\theta-\sin\psi(2\theta+\sin 2\theta)+\sin 2\psi\sin\theta\}}{2\theta-\sin 2\theta}\end{aligned}\right\} \quad (3)$$

Superposing the two sets of results, we obtain as the complete solution

$$\left.\begin{aligned} H&=W\frac{\theta(\cos 2\psi+\cos 2\theta-2)+4\sin\theta(\cos\psi-\cos\theta+\psi\sin\psi)}{2\theta^2+\theta\sin 2\theta+2\cos 2\theta-2}\\ V_A&=W\left\{1+\frac{2\psi+\sin 2\psi-4\cos\theta\sin\psi}{2\theta-\sin 2\theta}\right\}\\ V_B&=W\left\{1-\frac{2\psi+\sin 2\psi-4\cos\theta\sin\psi}{2\theta-\sin 2\theta}\right\}\\ M_A&=M_b+M_c\\ M_B&=M_b-M_c.\end{aligned}\right\} \quad (4)$$

It will be noticed that although there are still three redundancies to be evaluated, two in case (*b*) and one in case (*c*), this involves only two simultaneous equations, which occur in case (*b*). If the problem were attacked directly there would be three simultaneous equations to be solved. In addition, the number of terms would be considerably greater and the whole process very much more involved.

As another example this method will be applied to the case of a parabolic arch rib encastré at both ends and to simplify the integration it will be assumed as before that the second moment of area at any point is given by $I_0\sec\alpha$ where I_0 is the value at the crown and α is the slope of the rib at the point.

Taking the origin of co-ordinate axes at the centre of the line joining the ends A and B of the rib we have for the shape of the arch

$$y=d\left(1-\frac{4x^2}{L^2}\right)$$

where d is the central rise and L is the span. If a load 2W acts at a distance $-a$ from the origin its effect can be replaced by two load systems as in the case of the segmental arch. The first of these is a symmetrical system consisting of equal downward loads W at distances $\pm a$ from the origin and the second a skew symmetrical system W downwards at $-a$ and W upwards at $+a$.

Taking the first of these we have

$$M_x=M_b+Hd\left(1-\frac{4x^2}{L^2}\right)-W\left(\frac{L}{2}-x\right)+W[(a-x)]$$

where M_b is the clockwise moment at the support and the term in square brackets only appears when positive.

As before we need only consider one half of the arch and the equations $\frac{\partial U}{\partial M_b}=0$ and $\frac{\partial U}{\partial H}=0$ lead to

$$12M_b+8Hd-3WL(1-4\alpha^2)=0$$
$$80M_b+64Hd-WL(25-120\alpha^2+80\alpha^4)=0$$

where α is written for a/L.

The solution of these gives

$$\left.\begin{aligned} M_b&=WL\left(-\frac{1}{16}+\frac{3\alpha^2}{2}-5\alpha^4\right)\\ \text{and}\quad H&=\frac{15WL}{32d}(1-8\alpha^2+16\alpha^4)\end{aligned}\right\} \quad \ldots\ldots\ldots (5)$$

In dealing with the skew symmetrical case we may proceed as for the segmental arch or take M_c, the fixing moment at B, as the redundancy. It is clear that this fixing moment will be counter-clockwise and we shall take it so. The vertical reaction at B is then $\frac{2}{L}(M_c+aW)$ downwards and the bending moment at X is

$$M_x=\frac{2}{L}(M_c+aW)\left(\frac{L}{2}-x\right)-M_c-W[(a-x)].$$

There is no horizontal reaction and the equation derived from the condition $\frac{dU}{dM_c}=0$ gives

$$M_c=-\frac{WL\alpha}{2}(1-4\alpha^2).$$

The complete solution is therefore

$$\left.\begin{aligned} H &= \frac{15WL}{32d}(1-8\alpha^2+16\alpha^4) \\ M_A &= M_b+M_c = -WL\left(\frac{1}{16}-\frac{\alpha}{2}-\frac{3\alpha^2}{2}+2\alpha^3+5\alpha^4\right) \\ M_B &= M_b-M_c = -WL\left(\frac{1}{16}+\frac{\alpha}{2}-\frac{3\alpha^2}{2}-2\alpha^3+5\alpha^4\right) \\ V_A &= W+\frac{2}{L}(M_c+aW) = W(1+3\alpha-4\alpha^3) \\ V_B &= W-\frac{2}{L}(M_c+aW) = W(1-3\alpha+4\alpha^3) \end{aligned}\right\} \quad . \quad . \quad . \quad (6)$$

12.14. The braced arch.—The arches considered so far have been of the rib type, but most large arches are braced. They may be three-pinned, two-pinned or built in.

The three-pinned arch such as shown in Fig. 12.20 is statically determinate as regards reactive forces and can be dealt with in the way described for the arch rib. Thus, for a load W acting as shown, the reactions can be found by joining BC and producing the line to cut the line of action of W at D and then drawing DA. The vertical components of the reactions at A and B are known from the equation of moments

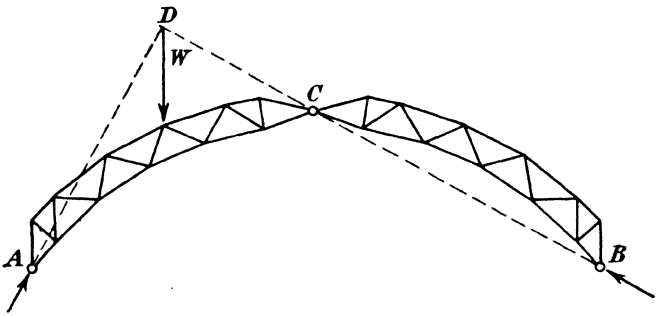

FIG. 12.20.

about A, and since AD and BC give the lines of their action, R_A and R_B are readily calculated from the geometry of the figure as in paragraph 12.3.

The arch can now be treated like any other framed structure and the forces in all the bars found by means of a stress diagram, by the method of sections or by means of tension coefficients.

The two-pinned braced arch has one degree of redundancy due to its method of support; the redundant element may conveniently be taken to be the horizontal thrust at one pin.

In Fig. 12.21 is shown a two-pinned spandrel braced arch. If the pin at B were replaced by a frictionless bearing the structure would be a just-stiff braced girder and could be analysed for any system of loads by the usual methods. The introduction of the pin at B, however, gives a horizontal constraint H_B and the stress analysis requires strain-

energy or other equivalent methods. H_B may be considered either as an internal redundancy, in which case the method of minimum strain

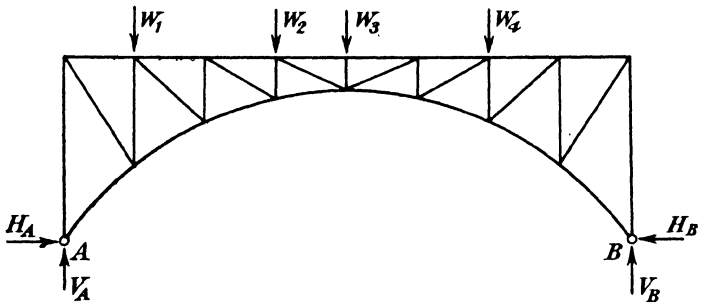

FIG. 12.21.

energy demands that $\frac{dU}{dH_B}=0$, or as an external force which prevents movement of the pin in a horizontal direction: the first theorem of Castigliano then gives the same equation.

The forces in all the bars of the arch must first be found in terms of the known external loads $W_1 \ldots W_4$ and the unknown H_B.

This is best done by drawing one stress diagram for the external load system and another for H_B.

The force in any member is then of the form

$$P_0=f(W)+\alpha H_B$$

where $f(W)$ is the force arising from the loads $W_1 \ldots W_4$ and αH_B is that from H_B.

Then
$$\frac{du}{dH_B}=\frac{P_0 L}{AE}\frac{dP_0}{dH_B}$$

where L is the length of the bar and A its cross-sectional area,

and
$$\frac{dU}{dH_B}=\sum\frac{P_0 L}{AE}\frac{dP_0}{dH_B}=0.$$

The various terms in this equation should be tabulated as previously explained in Chapter 6 and the resulting equation solved for H_B. Substitution of the value of H_B in the expressions for P_0 then gives the stresses in all members of the arch.

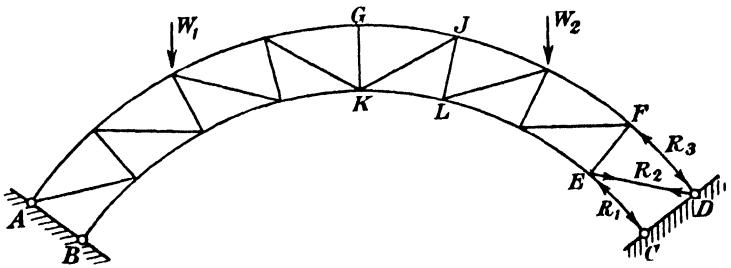

FIG. 12.22.

Fig. 12.22 shows a braced arch which is fixed to pins at A, B, C and D.

If the bars EC, ED and FD are removed the structure remaining is a cantilever which can be analysed without difficulty.

If the forces in the three bars specified above are denoted by R_1, R_2 and R_3 respectively the following conditions must be satisfied :—

$$\frac{\partial U}{\partial R_1}=\sum\frac{P_0 L}{AE}\frac{\partial P_0}{\partial R_1}=0$$

$$\frac{\partial U}{\partial R_2}=\sum\frac{P_0 L}{AE}\frac{\partial P_0}{\partial R_2}=0$$

$$\frac{\partial U}{\partial R_3}=\sum\frac{P_0 L}{AE}\frac{\partial P_0}{\partial R_3}=0.$$

A stress diagram is drawn for the external loads acting together, and one for each of the redundancies R_1, R_2 and R_3 acting separately. The equations derived from the above conditions can then be formed and their simultaneous solution gives the values of R_1, R_2 and R_3.

If it is more convenient, any three members such as GJ, JK and KL may be treated as redundancies ; the arch is then divided into two cantilever portions and each requires the separate diagrams for external loads, R_1, R_2 and R_3 to be drawn. The three equations corresponding to the above conditions are then formed as before.

12.15. Temperature stresses in an arch.—The effect of a change of temperature upon any structure is to cause alterations in the lengths of the members composing it. If the structure, even if redundant, is made of the same material throughout and has just the essential number of reactive forces, such changes in length result only in a slight change in the geometry of the truss without the introduction of extra stresses. If, however, the structure has redundant reactive forces which restrain free movement the temperature change causes extra stresses in the bars of the truss.

Consider, for example, the effect of a rise in temperature on a curved beam pinned at one end and resting on a frictionless roller at the other. The dimensions of the member increase and since it is free to move on the roller the result is merely a proportional increase in all dimensions of the beam. If, however, it is fixed to pins at both ends movement is prevented and the resulting thrust from the pins induces stresses throughout the member.

The result is the same as if free movement were allowed and the end of the rib was then forced back into its original position by a horizontal force.

Suppose a two-pinned arch rib of span L is subjected to a temperature rise $t°$.

Then, if it were free to expand, the new span would be $L(1+\beta t)$ where β is the coefficient of expansion of the material. Now assume that a horizontal force H is applied to the free end of sufficient amount to force it back through the distance $L\beta t$.

The first theorem of Castigliano gives

$$\text{movement of H horizontally}=\frac{dU}{dH}=L\beta t$$

or, if we neglect all effects except bending of the rib,

$$\int \frac{M}{EI}\frac{dM}{dH}ds = L\beta t.$$

But $M = Hy$ with the usual symbols :

hence $$\int \frac{Hy^2}{EI}ds = L\beta t,$$

the integration extending round the whole rib.

This equation can be solved by one of the methods already described and H evaluated.

Example.—In a two-pinned parabolic arch rib the second moment of area at any section is $I_0 \sec \alpha$ where I_0 is the value at the crown and α is the slope of the rib at the section. Find the increase in the horizontal thrust per degree rise of temperature.

Let span $=L$.
,, rise of rib at centre $=d$.
,, coefficient of expansion $=\beta$.

If one pin were released the increase in span due to a unit rise of temperature would be $L\beta$.

If the origin be taken at the centre of the span the rise of the arch at x from the origin is

$$y = d\left(1 - \frac{4x^2}{L^2}\right)$$

and $$M_x = Hd\left(1 - \frac{4x^2}{L^2}\right)$$

also $$\frac{dM_x}{dH} = d\left(1 - \frac{4x^2}{L^2}\right)$$

$$\therefore \quad \frac{dU}{dH} = \frac{2}{E}\int_{x=0}^{x=\frac{L}{2}} \frac{Hd^2}{I_x}\left(1 - \frac{4x^2}{L^2}\right)^2 ds = L\beta.$$

But $$I_x = I_0 \frac{ds}{dx}$$

$$\therefore \quad \frac{2Hd^2}{EI_0}\int_0^{\frac{L}{2}} \left(1 - \frac{4x^2}{L^2}\right)^2 dx = L\beta$$

which gives $$H = \frac{15EI_0\beta}{8d^2}.$$

12.16. The circular ring.—Closely allied to the problem of the arch rib is that of the circular ring subjected to a system of forces in equilibrium. The ring may be a simple link in a chain, when it will be subjected to a diametral pull, or it may be a section of a culvert in which case it will be loaded by earth pressure varying in intensity around its circumference. The general method of treatment is the same whatever the loading may be although it may be advisable, if complicated load systems are applied, to use graphical methods of integration for certain terms in the equations.

In the first place the case of a ring under a load system symmetrical about one axis will be considered. In Fig. 12.23 (*a*) two radial loads each of magnitude P act at angular distances θ from the vertical OA. They are balanced by the single radial load $Q=2P\cos(\pi-\theta)$ acting at A.

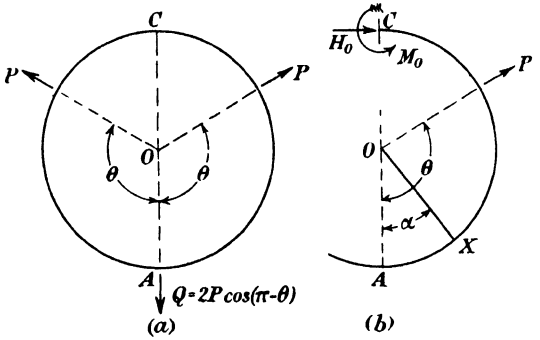

FIG. 12.23.

If the ring were cut at the top section as shown in (*b*) it would be necessary, if the original conditions were to be restored, to apply external actions to the cut section equal to the internal actions originally provided by the continuity of the ring at that section.

These actions are a bending moment and a tangential force represented by M_0 and H_0 respectively. It is clear from the symmetry of the system that there is no radial shearing force on the section.

It is only necessary to deal with one half of the ring which will be considered to be held at A. The symmetry of the loading shows that in the uncut ring there can be neither angular rotation nor horizontal movement of the section at C.

Hence, if U be the total strain energy of the half ring

$$\frac{\partial U}{\partial M_0}=\text{angular movement of C}=0$$

$$\frac{\partial U}{\partial H_0}=\text{horizontal movement of C}=0.$$

As before, we shall neglect the strain energy due to axial and shearing forces since the effect is small compared with that due to bending.

Then
$$U=\frac{1}{2EI}\int M_x^2 ds$$

where EI is the flexural rigidity of the section of the ring.

And the conditions for the determination of M_0 and H_0 are

$$\int M_x\frac{\partial M_x}{\partial M_0}ds=0$$

$$\int M_x\frac{\partial M_x}{\partial H_0}ds=0.$$

Let X be any point on the ring at an angular distance α from OA.

Then
$$M_x=M_0-H_0R(1+\cos\alpha)-PR\sin(\theta-\alpha)$$

where the term in P appears only between $\alpha=0$ and $\alpha=\theta$.

Now $$\frac{\partial M_x}{\partial M_0}=1$$

and $$\frac{\partial M_x}{\partial H_0}=-R(1+\cos\alpha).$$

Also $ds=Rd\alpha$ and the equations above are

$$\int_0^{\pi}\{M_0-H_0R(1+\cos\alpha)\}d\alpha-\int_0^{\theta}PR\sin(\theta-\alpha)d\alpha=0$$

$$\int_0^{\pi}\{M_0-H_0R(1+\cos\alpha)\}(1+\cos\alpha)d\alpha-\int_0^{\theta}\{PR\sin(\theta-\alpha)\}(1+\cos\alpha)d\alpha=0.$$

Integrating and reducing these we get

$$\pi M_0-\pi H_0R-PR(1-\cos\theta)=0$$

$$\pi M_0-\tfrac{3}{2}\pi H_0R-PR\left(1-\cos\theta+\frac{\theta\sin\theta}{2}\right)=0.$$

The solution of these gives

$$H_0=-\frac{P}{\pi}\theta\sin\theta$$

$$M_0=\frac{PR}{\pi}(1-\cos\theta-\theta\sin\theta).$$

If θ be made equal to π the result is a link with a diam pull of 2P and the values given above reduce to

$$H_0=0$$

$$M_0=\frac{2PR}{\pi}.$$

The values of H_0 and M_0 can be substituted in the equation for M_x and the bending moment diagram for the ring can be plotted.

In calculating the stresses it should be remembered that if the dimensions of the ring are large compared with the radius of curvature, it is necessary to use the equation for a curved bar : failure to do so will result in serious error.

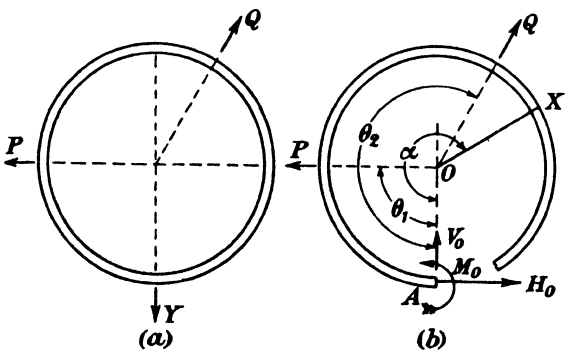

FIG. 12.24.

The method just described can be applied to any symmetrical load

system but the less frequent case where the loading has no axis of symmetry requires slightly different treatment. Fig. 12.24 (*a*) represents such a case where the ring is loaded with three radial forces P, Q and Y which are in equilibrium. The ring is supposed to be cut to the left of the force Y and the necessary resultant actions applied to the cut section. These are M_0 and H_0 as in the symmetrical case but in addition a radial shearing force V_0 is required. Treating M_0, V_0 and H_0 as redundant internal actions we have

$$\frac{\partial U}{\partial M_0}=0$$

$$\frac{\partial U}{\partial H_0}=0$$

$$\frac{\partial U}{\partial V_0}=0,$$

or

$$\int M_x\frac{\partial M_x}{\partial M_0}d\alpha=\int M_x\frac{\partial M_x}{\partial H_0}d\alpha=\int M_x\frac{\partial M_x}{\partial V_0}d\alpha=0.$$

If P and Q are at angular distances θ_1 and θ_2 respectively from OA and X is any point at α from OA.

$$M_x=M_0+V_0R\sin\alpha+H_0R(1-\cos\alpha)-PR\sin(\alpha-\theta_1)-QR\sin(\alpha-\theta_2)$$

where the terms in P and Q only appear when $\alpha>\theta_1$ and $\alpha>\theta_2$ respectively.

Then

$$\frac{\partial M_x}{\partial M_0}=1$$

$$\frac{\partial M_x}{\partial H_0}=R(1-\cos\alpha)$$

$$\frac{\partial M_x}{\partial V_0}=R\sin\alpha$$

and the equations can be formed as before. In this case, however, the integration must extend around the whole circumference of the ring. The equations are more unwieldy than those obtained when the load system is symmetrical but present no other feature of difficulty.

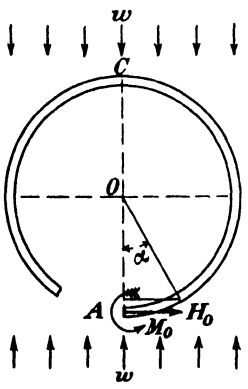

FIG. 12.25.

As an example of the analysis for a distributed load system the case shown in Fig. 12.25 will be considered. This represents an idealised loading on a circular culvert the earth pressure being assumed to give a uniform weight of w per unit projected length of diameter. Taking the origin at A as before the culvert is assumed to be cut at A and the internal reactions replaced by M_0 and H_0.

Then

$$M_x=M_0+H_0R(1-\cos\alpha)-\frac{w}{2}R^2\sin^2\alpha.$$

and the conditions $\frac{\partial U}{\partial M_0}=\frac{\partial U}{\partial H_0}=0$ give

$$\int_0^{\pi}\left(M_0+H_0R(1-\cos\alpha)-\frac{wR^2}{2}\sin^2\alpha\right)dx=0$$

$$\int_0^{\pi}\left\{M_0+H_0R(1-\cos\alpha)-\frac{wR^2}{2}\sin^2\alpha\right\}(1-\cos\alpha)d\alpha=0.$$

These lead to the result

$$H_0=0$$

$$M_0=\frac{wR^2}{4}.$$

A ring which is not circular can be dealt with in the same way, but in general the equations are not directly integrable. Graphical methods similar to those described in paragraph 12.8 must then be used.

12.17. Stresses in a braced ring.—In certain forms of airship construction braced rings have been used as the transverse members of the main framework of the hull. This problem may be one of great difficulty and no attempt will be made here to treat the general case.

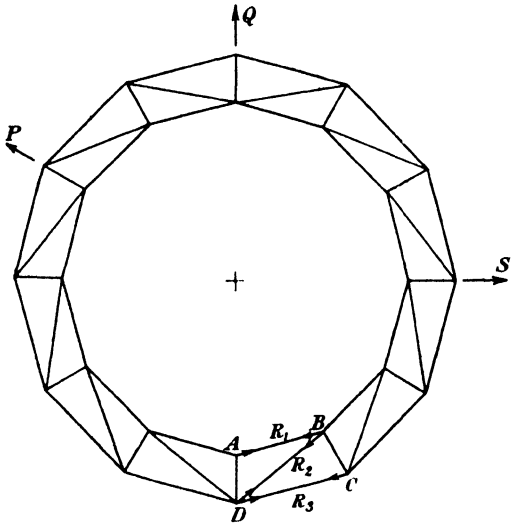

FIG. 12.26.

The ring in such a structure is actually a polygon and the bracing may be of a variety of types. Fig. 12.26 shows a simple form of braced polygon carrying three loads P, Q and S which are in equilibrium. This frame has three degrees of redundancy and presents no difficulty in solution. If any three members such as AB, BD and CD are replaced by unknown forces R_1, R_2 and R_3 the frame can be considered to be held at points A and D and the forces in all the bars determined as functions of R_1, R_2, R_3, P, Q and S just as in the case of the braced

arch described in paragraph 12.14.

Then by the method of minimum strain energy,

$$\frac{\partial U}{\partial R_1}=\frac{\partial U}{\partial R_2}=\frac{\partial U}{\partial R_3}=0$$

where U is the total strain energy of the ring including that in the three members AB, BD and CD. These equations enable the unknown forces to be determined and hence the forces in all members of the structure. Many rings of this type, however, may have redundant bars in addition to the three due to the continuity of the ring, *e.g.* the one shown in Fig. 12.26 might have been provided with counterbracing members in each panel. Each such redundancy introduces an extra equation and the problem, although theoretically soluble, may present such arithmetical complexity that an exact solution will be impracticable.

Should the panels have counterbracing wires, not stressed initially, those which would be called upon by the load system to carry compression will become slack. A difficulty arises then in determining which are the operative wires and several solutions may have to be obtained before the correct one is found.

EXERCISES

(1) An arch span is 50 feet, its centre line being the segment of a circle subtending 120° at the centre. It is pinned at the supports and at the crown, and carries a load of 10 tons at 12 feet 6 inches measured horizontally from the left-hand support. Calculate the magnitude and direction of the reactions at the supports and the force on the central pin.

(*Left support : $5\sqrt{3}$ tons at 60° to horizontal.*
Right support : 5 tons at 30° to horizontal.
Centre pin : Shear $= 2\frac{1}{2}$ tons ; thrust $= \frac{5\sqrt{3}}{2}$ tons.)

(2) A semi-circular arch of 40 feet span is pinned at the supports and at the crown. It carries a uniform load of 2 tons per foot (horizontal projection) over the left-hand half of the span. Calculate the magnitudes and directions of the reactions on the end pins and sketch carefully the bending moment diagram for the arch.

(*Left-hand pin : 31·62 tons at $\tan^{-1}3$ to horizontal.*
Right-hand pin : 14·14 tons at 45° to horizontal.)

(3) A parabolic arch rib of uniform section with pinned ends is 80 feet span and has a rise of 10 feet at the centre. It carries a concentrated load of 10 tons at the crown.

Plot the approximate bending moment diagram for the rib.

(4) A rolled steel joist $24 \times 7\frac{1}{2}$ inches having a second moment of area of 2,200-inch units is used to make a two-pinned segmental arch of 40 feet span and 5 feet rise.

Calculate what central load this arch can carry if the bending stress in the material is limited to 8 tons per square inch.

(*53·5 tons.*)

(5) A two-hinged segmental arch rib of 120 feet span and 12 feet rise experiences a change of temperature of 50° F.

Calculate the alteration which this makes in the horizontal thrust.

E = 13,000 tons per square inch.

I = 90 inch units.

Coefficient of expansion for steel $= 6 \times 10^{-6}$ per 1° F.

(*0·035 tons.*)

(6) Find the value of the horizontal force and end-fixing moment for an encastré segmental arch of radius R carrying a central load W, when the ratio of rise to span is 1 to 4.

(*$H = 0{\cdot}926\ W$; $M = 0{\cdot}059\ WR$.*)

(7) A stiff-jointed frame in the form of a regular hexagon with a length of side L carries two equal and opposite loads of W applied radially at opposite corners.

Calculate the bending moments at the loaded points.

$\left(\frac{WL}{2\sqrt{3}}\right)$

(8) A steel ring made of 1-inch square material is 8 inches mean diameter. A steel rod 0·1 square inches in cross-sectional area connects two points at the ends of a diameter and the ring is compressed by equal and opposite loads W acting at right angles to the rod. Calculate the tension in the rod.

(*0·54 W.*)

(9) A ring of radius R and flexural rigidity EI is radially braced by three equally-spaced spokes of cross-sectional area a and Young's modulus E which are pinned to a small centre hub and to the ring. If the hub, which is rigid, is held fixed show that the loads in the spokes when a load W acts radially inwards at a spoke point are

$$\frac{W}{3}\left(\frac{I}{I + \cdot 016R^2a}\right); \quad \frac{W}{3}\left(\frac{I}{I + \cdot 016R^2a}\right); \quad -\frac{2W}{3}\left(\frac{I + \cdot 024R^2a}{I + \cdot 016R^2a}\right).$$

CHAPTER 13

THEORY OF COMPOSITE STRUCTURES AND REINFORCED CONCRETE.

13.1. Simple composite members.—A structural member may be made of more than one material, the parts being so rigidly connected that when the member is loaded there is no relative movement between them. This is termed a composite member and in modern engineering practice the use of such a method of construction is confined almost entirely to reinforced concrete. It is of interest, however, as an approach to this branch of the theory of structures to consider some simpler cases, although at the present day these may be of little more than academic importance.

The most elementary example of a composite member is that of a tension member made up of two different metals. Suppose, for example, that a tube of one metal is shrunk on to a bar of another metal, as shown in Fig. 13.1, so that there is a firm connection between the two. Let this composite member carry an axial tensile load W.

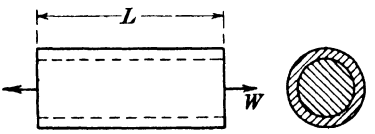

FIG. 13.1.

Let A_1 be the cross-sectional area of the tube,
A_2, the cross-sectional area of the rod,
L, the length of the composite member,
f_1, the stress in the tube,
f_2, the stress in the rod,
E_1, the value of Young's modulus for the tube,
E_2, the value of Young's modulus for the rod.

Since the two parts of the member are rigidly connected the elastic strains in the tube and rod will be equal, *i.e.*,

$$\frac{f_1}{E_1}=\frac{f_2}{E_2} \quad \ldots\ldots\ldots\ldots \quad (1)$$

The total load carried by the tube and rod is W, so

$$f_1A_1+f_2A_2=W. \quad \ldots\ldots\ldots\ldots \quad (2)$$

Substituting the value of f_2 from equation (1) in this we obtain

$$f_1\left(A_1+\frac{E_2A_2}{E_1}\right)=W$$

or
$$f_1=\frac{WE_1}{E_1A_1+E_2A_2}$$

and
$$f_2=\frac{WE_2}{E_1A_1+E_2A_2} \quad \ldots\ldots\ldots\ldots \quad (3)$$

The extension of the bar under load is given either by $\frac{f_1 L}{E_1}$ or $\frac{f_2 L}{E_2}$,

i.e. $$\text{Extension} = \frac{WL}{E_1A_1 + E_2A_2} \quad . \quad . \quad . \quad . \quad . \quad . \quad . \quad . \quad (4)$$

Another simple case of a composite member is afforded by the flitched beam shown in cross-section in Fig. 13.2, which consists of a piece of steel plate bolted firmly between two cheeks of wood. This type of beam was in common use before the introduction of rolled steel joists but is now obsolete.

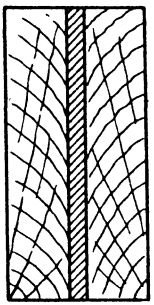

FIG. 13.2.

Suppose such a beam, simply supported over a span L, to be bent under the action of a central load W. The strains in the wood and the steel at any point are equal and so at the centre we have

radius of curvature of wood
=radius of curvature of steel

or $$\frac{M_w}{E_wI_w} = \frac{M_s}{E_sI_s} \quad . \quad . \quad . \quad . \quad . \quad . \quad . \quad (5)$$

where M_w is the bending moment resisted by the wood,
M_s is the bending moment resisted by the steel,
E_w, E_s are the values of Young's modulus for wood and steel respectively
and I_w, I_s are the second moments of area of the wood and steel sections respectively.

Also $$M_w + M_s = \frac{WL}{4} \quad . \quad . \quad . \quad . \quad . \quad . \quad . \quad . \quad (6)$$

From (5) $$M_w = \frac{E_wI_w}{E_sI_s} M_s$$

and so from (6) $$M_s\left(\frac{E_wI_w + E_sI_s}{E_sI_s}\right) = \frac{WL}{4} \quad . \quad . \quad . \quad . \quad . \quad . \quad . \quad (7)$$

which gives the value of the bending moment carried by the steel.

The stress in the steel is then

$$f_s = \frac{M_s d}{2I_s}$$

where d is the depth of the beam.

M_w can be determined from equation (6) and the stress in the wood calculated.

13.2. General principles of reinforced concrete.—By far the most useful composite structure in modern engineering is reinforced concrete and the uses to which it has been put are innumerable. Concrete consists of a mixture of cement, sand and graded stone or aggregate, which sets after the addition of water into a solid mass which has considerable compressive strength but very little resistance to tension. In this form, therefore, it is very useful for such purposes as foundations, where the loads to be carried are wholly compressive, but

it is useless for the construction of members subjected to bending since failure would occur at very low loads in regions where tension is developed. This limitation of the material can, however, be overcome and the necessary resistance to tensile stresses can be provided by the insertion of steel rods at appropriate places; this composite structure is known as reinforced concrete. Such a combination is made practicable by two fortunate circumstances. Steel and concrete have almost identical coefficients of expansion, so that no serious internal stresses are set up by temperature changes, and when concrete sets in air it contracts so that if a steel bar is embedded in a mass of wet concrete it is found to be firmly gripped after set has occurred. The bond between the steel and the concrete is so good that the loads are shared between the two materials in the ideal manner we have assumed in earlier paragraphs for other composite members. In order that calculation of strength can be made it is necessary to know the physical properties of the component materials, *i.e.* the concrete and the steel. For the present it will be assumed that the necessary information is available and the general theory will be developed; in later paragraphs the values of the constants to be taken for design purposes will be discussed. The following general assumptions are made in all calculations on reinforced concrete :—

(*a*) Both the concrete and the steel reinforcement are assumed to behave elastically and to follow a linear stress-strain law. This assumption entails a constant relationship between the moduli of elasticity of the two materials and the constant ratio is known as the modular ratio.

(*b*) The concrete is assumed to be incapable of taking any tensile stress.

(*c*) Sections of the members which were plane before straining actions were applied are supposed to remain plane under such actions.

These assumptions are open to criticism and none of them is strictly true. They may be considered as simplifications introduced to make possible a practical theory of the behaviour of reinforced concrete which can be used for design purposes. The justification for accepting them is to be found in the reasonable agreement in most cases between the calculated and experimental strengths of members designed by their application.

Accepting them as being sufficiently accurate for their purpose the design of reinforced concrete members is reduced to very simple terms. These may be stated as follows and cover all cases :

(1) When steel is embedded in concrete the strains produced at any point by forces acting on the combination are the same in both materials.

(2) At any section of a structural member the sum of the forces in the steel and concrete in any direction is equal to the resultant action of the external forces at that section in the same direction.

(3) At any section the total moment of the forces in the steel and concrete, *i.e.* the moment of resistance of the section, is equal to the applied bending moment at that section.

The expression of these in algebraic form leads to very simple formulas. These simple results can, however, be cast into various forms which, although more complicated, serve a useful purpose when considerable design work has to be done since they form the basis of curves which, once plotted, can be used very rapidly. The re-casting of the fundamental formulas does not however contribute anything to the basic theory and the subject will be considered in the simplest terms.

13.3. The rectangular reinforced concrete beam with tension reinforcement.—The first case to be considered is that of a rectangular beam which is reinforced on the tension side only. This is not a complete system of reinforcement, since if a shearing force acts at any section of the beam the shearing stresses caused thereby are accompanied by tensile and compressive stresses at angles of 45° to the shear and failure is just as liable to occur on these tension planes as on any others.

Further, in modern reinforced concrete practice it is usual to provide not only tension steel but reinforcement against compressive stresses. For the present, however, both these points will be ignored and the effect of longitudinal tension reinforcement alone considered. Fig. 13.3 represents a rectangular beam of width b and depth d from the top of the concrete to the centre of the reinforcing bars. It is subjected to a pure couple.

Since it is assumed that plane sections in the unstrained beam remain plane when the beam is bent, *efohg* in the figure is a strain diagram, *ef* representing the maximum compressive strain in the concrete, *gh* the strain of the reinforcement and *o* the position of the neutral axis NA.

Let NA be a distance n below the top of the beam.

Also let t be the tensile stress in the steel,

c, the maximum compressive stress in the concrete,

E_s, the modulus of elasticity of the steel,

E_c, the modulus of elasticity of the concrete,

m, the modular ratio, E_s/E_c,

and A, the total cross-sectional area of steel in the reinforcement.

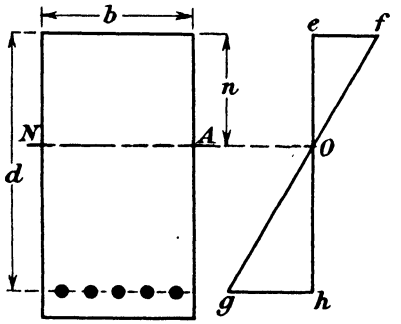

FIG. 13.3.

Then, the maximum strain in the concrete : strain in the steel : : *oe* : *oh*

i.e.

$$\frac{c}{E_c} : \frac{t}{E_s} :: n : d-n$$

or $$\frac{t}{c}=\left(\frac{d-n}{n}\right)m \quad \ldots\ldots\ldots \quad (1)$$

Again, there is no resultant axial load on the beam and so the total compression in the concrete must be equal to the total tension in the steel. Since the average compressive stress in the concrete is $c/2$ we have

$$\frac{bnc}{2}=At$$

or $$\frac{t}{c}=\frac{bn}{2A} \quad \ldots\ldots\ldots\ldots \quad (2)$$

The total compressive force in the concrete at any cross-section is $\frac{bnc}{2}$ and this acts at the centre of compression. Since the strain, and therefore the stress distribution, is linear the centre of compression is $n/3$ from the top of the beam. The total tensile force is At acting at the centre of the reinforcement and these equal and opposite forces acting at a distance apart $a=d-n/3$ form a couple which is the moment of resistance of the cross-section.

Hence

$$M_R=\frac{bnc}{2}\left(d-\frac{n}{3}\right)=At\left(d-\frac{n}{3}\right) \quad \ldots\ldots \quad (3)$$

and the applied bending moment must not exceed the value given by this expression when either t or c reaches the prescribed limiting value.

If t/c is eliminated from equations (1) and (2) it is seen that the value of n for a beam of given dimensions depends only on m and the area of the reinforcement. Therefore, if these are specified the ratio of the stresses developed in the steel and concrete is determined by equation (2). Conversely, if the stress ratio is specified the values of A and n are determined.

The value of A which causes the stresses in both steel and concrete to reach their allowable limits simultaneously is known as the economic area, and the ratio $100A/bd$ is called the economic percentage.

To illustrate the work of this paragraph we will consider a reinforced concrete beam 12 inches wide and $22\frac{1}{2}$ inches deep to the centre of the reinforcement in which the stresses in the concrete and steel are limited to 600 lb. per square inch and 16,000 lb. per square inch respectively. It is required to determine the area of steel needed and what uniformly distributed load the beam can carry over a freely supported span of 20 feet.

$$\frac{\text{The strain in the steel}}{\text{Max. strain in the concrete}}=\frac{t/E_s}{c/E_c}=\frac{d-n}{n}$$

i.e. $$\frac{16{,}000}{600\times 15}=\frac{22{\cdot}5-n}{n},$$

from which $n=8{\cdot}1$ inches.

Also the total compression in the concrete=total tension in the steel,

or $$\frac{bnc}{2}=At$$

i.e. $$A=\frac{bnc}{2t}=\frac{12\times 8\cdot 1\times 600}{32{,}000}=1\cdot 822 \text{ square inches.}$$

The moment of resistance = total tension × arm of couple
$$=At(d-n/3)$$
$$=1\cdot 822\times 16{,}000\times 19\cdot 8=578{,}000 \text{ in.-lb.}$$

Let w be the intensity of loading on the beam in lb. per foot so that the total load is $20w$ lb.

The maximum bending moment is then $\frac{20w\times 240}{8}$ inch-lb.

Equating this to the moment of resistance we have

$$600w=578{,}000$$

or $$w=963\cdot 3 \text{ lb. per foot.}$$

This includes the weight of the beam itself which, assuming reinforced concrete to weigh 140 lb. per cubic foot, is $\frac{12\times 24\times 140}{144}$ lb. per foot, *i.e.* 280 lb. per foot. The extra $1\frac{1}{2}$ inches is added to the effective depth to provide cover for the steel bars.

The additional load which the beam can carry is therefore 683 lb. per foot.

As another example of calculation we will assume that the beam just considered has 2·5 square inches of reinforcing steel and determine the alteration this makes in the strength.

From the equation for the proportionality of strain we now obtain,

$$\frac{t}{600\times 15}=\frac{22\cdot 5-n}{n}$$

i.e. $$t=\frac{9{,}000(22\cdot 5-n)}{n}.$$

From the equation of total compression and tension we have

$$\frac{12\times n\times 600}{2}=2\cdot 5t$$

or $$t=1{,}440n.$$

Equating these two values of t we obtain

$$1{,}440n^2=9{,}000(22\cdot 5-n)$$

or $$n^2+6\cdot 25n-140\cdot 6=0,$$

which gives $$n=9\cdot 125 \text{ inches}$$

and so $t=1{,}400\times 9\cdot 125=13{,}140$ lb. per square inch.

The safe load on this beam is therefore governed by the stress in the concrete.

The moment of resistance $=2\cdot 5\times 13{,}140\times 19\cdot 41$
$$=638{,}000 \text{ inch-lb.}$$

Equating this to the bending moment as found in the previous example, we have

$$w=\frac{638{,}000}{600}=1{,}063{\cdot}3 \text{ lb. per foot.}$$

Deducting the weight of the beam itself this gives 783 lb. per foot as the safe distributed load on the beam.

13.4. The reinforced concrete T-beam with tension reinforcement.—In a floor made of joists and planks the latter do not contribute to the

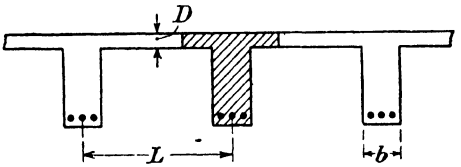

FIG. 13.4.

strength of the structure and the whole load must be carried by the joists. In reinforced concrete construction, however, the floor consists of a slab which is integral with the beams, as shown diagrammatically in Fig. 13·4. It will be seen that the beam member is actually of T section, as shown shaded, but the great difficulty in dealing with this form of construction is to know what width of the floor slab may be safely assumed to act as the compression flange of the beam. In the Code of Practice recommended by the Reinforced Concrete Structures Committee of the Building Research Board * it is laid down that the breadth of slab taken into account in calculation shall be not greater than the least of the following :—

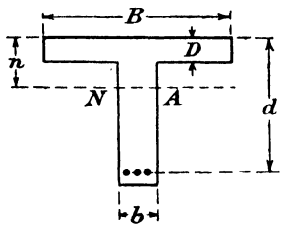

FIG. 13.5.

(*a*) One-third of the effective span of the T-beam,

(*b*) The distance between the centres of the ribs of the T-beam, L,

(*c*) The breadth of the rib plus twelve times the thickness of the slab, D.

Suppose Fig. 13.5 represents such a T-beam and that the dimensions are as shown. It will be assumed that the neutral axis is below the bottom of the slab. The principles involved in design are exactly the same as for the rectangular beam, but the formulas become more elaborate.

Thus, as before,

maximum strain in concrete : strain in steel : : $n : d-n$,

or $$c/E_c : t/E_s : : n : d-n$$

and so $$\frac{t}{c}=\left(\frac{d-n}{n}\right)m, \quad \ldots\ldots\ldots \quad (1)$$

* "Recommendations for a Code of Practice for the use of Reinforced Concrete in Buildings." H.M.S.O., January, 1934. See also, "Explanatory Handbook on the Code of Practice for Reinforced Concrete." W. L. Scott and W. H. Glanville. Concrete Publications, Ltd.

as in equation (1) of the last paragraph.

Since the stresses are proportional to the distances from the neutral axis the stress at the underside of the slab is

$$\left(\frac{n-D}{n}\right)c$$

The mean stress over the slab is therefore $\frac{c}{2}\left(\frac{2n-D}{n}\right)$ and over the portion of the rib above the neutral axis it is $\frac{c}{2}\left(\frac{n-D}{n}\right)$.

Hence the total compressive force on the section is

$$\frac{BDc}{2}\left(\frac{2n-D}{n}\right)+\frac{b(n-D)c}{2}\left(\frac{n-D}{n}\right),$$

or

$$\frac{c}{2n}\{BD(2n-D)+b(n-D)^2\}.$$

This must be equal to the total tensile force in the steel, so that

$$\frac{c}{2n}\{BD(2n-D)+b(n-D)^2\}=At$$

or

$$\frac{t}{c}=\frac{BD(2n-D)+b(n-D)^2}{2nA} \quad \ldots\ldots\ldots \quad (2)$$

The remainder of the work closely follows that for a rectangular beam and it is unnecessary to derive the rather cumbersome equations since any particular case is more easily solved arithmetically than by substitution in an algebraic equation.

Moreover, the solution is of rather an academic character which it is unnecessary to use in most actual cases.

Suppose Fig. 13.6 represents the cross-section of a rectangular beam, the neutral axis, determined in the way already explained, being NA.

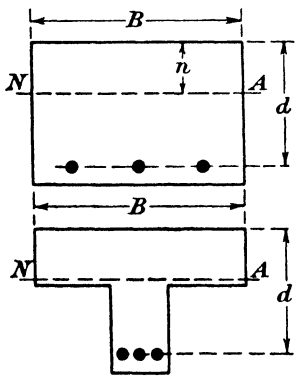

FIG. 13.6.

The concrete below NA has been assumed to take no stress and so, as long as sufficient is left to form a proper cover for the steel the remainder can be removed without affecting the strength of the beam. This is shown in the figure and the result is a T-beam. It is thus evident that any T-beam in which the neutral axis is not below the bottom of the slab can be treated exactly as a rectangular beam of breadth B and effective depth *d*. Even in the case where the neutral axis is below the bottom of the slab the error involved by designing on the assumption of a rectangular section is usually very small. In Fig. 13.7, for example, (*a*) is the cross-section of a T-beam, the neutral axis being calculated for the rectangular section shown dotted to be at NA. The stress at any point in the compression area

is given by the diagram (*b*) and if this stress is multiplied by the appropriate width over which it acts a load intensity curve such as that shown at (*c*) is obtained. The sudden break is due to the change of width from B to *b*. The area of the triangle *efk* represents the total compression in the rectangular beam and the area *efjhk* that in the

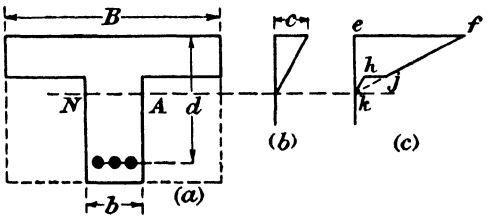

FIG. 13.7.

T-beam. The difference between these areas, *khj*, is a measure of the error involved and if NA is not much below the bottom of the slab this error is negligible. This calculation of the error is not exact since the real position of the neutral axis for the T-section would be displaced slightly from that for the rectangular section but it indicates, in view of the approximate nature of the design data which are generally available, especially with regard to the value to be assigned to B, that for most T-beams the rather elaborate formulas derived from exact consideration of the geometry need not be used.

13.5. Rectangular beam with compression reinforcement.—Since steel is much stronger in compression than concrete it is usual, especially when it is required to keep the overall size of beams as small as possible, to reinforce the compression as well as the tension area. Fig. 13.8 shows a rectangular section beam which has, in addition to the usual tension reinforcement, a total cross-sectional area of steel A′ in compression at a distance *d′* from the top of the beam. Other symbols used will be the same as in paragraph 13.3.

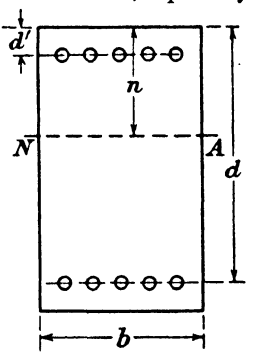

FIG. 13.8.

Since the same assumptions as to the planarity of sections is made as in the beam with single reinforcement, equation (1) of paragraph 13.3 is valid for this case.

Also,

$$\text{the maximum compressive strain in the concrete} : \text{compressive strain in steel} :: n : n-d'$$

or
$$\frac{mc}{f} = \frac{n}{n-d'}$$

so that
$$f = \frac{m(n-d')c}{n} \quad \ldots\ldots\ldots \quad (1)$$

where f is the stress in the compression steel.

The total area of concrete in compression is $bn-A'$ and the total compressive force in it is $c\left\{\frac{bn}{2}-A'\left(\frac{n-d'}{n}\right)\right\}$.

The compressive force in the steel is $A'f=\frac{A'm(n-d')c}{n}$.

Hence, equating the total compressive force on the cross-section to the total tensile force, we obtain

$$c\left\{\frac{bn}{2}+\frac{A'(m-1)(n-d')}{n}\right\}=At$$

or

$$\frac{t}{c}=\frac{1}{A}\left\{\frac{bn}{2}+\frac{A'(m-1)(n-d')}{n}\right\} \quad . \quad . \quad . \quad . \quad . \quad (2)$$

To calculate the moment of resistance of a beam reinforced in this way it is necessary to determine the centre of resistance of the compressive force.

It is clear from equation (1) that the compressive force in the steel is $\frac{A'm(n-d')c}{n}$ which can be written as

$$\frac{A'(n-d')c}{n}+\frac{A'(m-1)(n-d')c}{n}.$$

The first term is the amount which would be contributed by the area A' if the compression area contained no steel and the second term is the extra amount due to the substitution of steel for concrete on that area.

The moment of resistance of the beam is therefore

$$\frac{bnc}{2}\left(\frac{2n}{3}\right)+\frac{A'(m-1)(n-d')c}{n}(n-d')+At(d-n)$$

i.e.

$$M_R=c\left\{\frac{bn^2}{3}+\frac{A'(m-1)(n-d')^2}{n}\right\}+At(d-n). \quad . \quad . \quad . \quad (3)$$

The arm of the moment of resistance is

$$a=\frac{M_R}{At} \quad . \quad . \quad . \quad . \quad . \quad . \quad . \quad . \quad . \quad . \quad (4)$$

Equations (1), (2), (3) and (4) together with equation (1) of paragraph 13.3 are sufficient for the solution of any problem connected with doubly reinforced rectangular beams as will be evident from an example.

Suppose a rectangular beam 10 inches wide and 20 inches deep to the centre of tension reinforcement has 1 square inch of compression steel at a distance of 1 inch from the top of the beam. If the maximum stresses in the concrete and steel are limited to 600 lb. per square inch and 18,000 lb. per square inch respectively, determine the area of tension steel required and the moment of resistance of the beam.

From equation (1) of paragraph 13.3, taking $m=18$ we have

$$30=\frac{(20-n)}{n}18$$

or $$n=7{\cdot}5 \text{ inches.}$$

Then from equation (1) of the present paragraph

$$f=\frac{18(7{\cdot}5-1)\times 600}{7{\cdot}5},$$

and the stress in the compression steel is 9,360 lb. per square inch.

From equation (2)

$$30=\frac{1}{A}\left(\frac{10\times 7{\cdot}5}{2}+\frac{17\times 6{\cdot}5}{7{\cdot}5}\right)$$

and the area of tension steel required is 1·74 square inches.

The moment of resistance is then, from equation (3)

$$M_R=600\left(\frac{10\times 7{\cdot}5^2}{3}+\frac{17\times 6{\cdot}5^2}{7{\cdot}5}\right)+(1{\cdot}74\times 18{,}000)12{\cdot}5$$

or $$M_R=561{,}000 \text{ inch-lb}$$

The arm of this moment is

$$\frac{561{,}000}{1{\cdot}74\times 18{,}000}=18 \text{ inches.}$$

13.6. Adhesion and bond.—It was indicated in an earlier paragraph that reinforced concrete construction was made possible by the fact that the steel was so firmly gripped by the concrete that the strains in the steel of a composite member under load were equal to those in the concrete immediately in contact with it. The resistance which is offered by a rod to withdrawal from a block of concrete in which it is embedded is known as adhesion and the stress between the surface of the steel and the concrete in contact with it is the bond stress. It is clearly vital that the bond stress shall at no point in a structure be so great as to overcome the adhesion. When concrete sets it contracts and the force exerted on the steel is sufficient to ensure a good adhesion even on plain bars.

Suppose that a singly reinforced concrete beam is loaded in any manner so that the bending moments at two sections separated by a small distance δx are M and M+δM respectively.

Let the distance between the centre of action of the compressive force in the concrete and the centre of the reinforcement be $a=d-n/3$. The total tensions in the steel at the sections we are considering are, therefore,

$$\frac{M}{a} \text{ and } \frac{M+\delta M}{a}.$$

There is consequently a change in the tension, in the distance δx, of $\frac{\delta M}{a}$.

This change in tension is transmitted to the concrete and if rupture is to be avoided it must be less than the adhesion.

If the reinforcement consists of n bars each of diameter d the total

surface of steel in contact with the concrete is $n\pi d\delta x$ and if the mean bond stress over the short distance δx is s_b we have, for equilibrium,

$$s_b n\pi d\delta x = \frac{\delta M}{a}$$

or

$$s_b = \frac{\delta M}{\delta x}\frac{1}{an\pi d}.$$

In the limit when δx is infinitely small $\frac{\delta M}{\delta x}$ becomes $\frac{dM}{dx}$, which is the shearing force S at the section considered and if the total perimeter of the bars $n\pi d$ be denoted by o the bond stress at any point is

$$s_b = \frac{S}{ao} \quad \ldots\ldots\ldots\ldots \quad (1)$$

The allowable values for s_b are given in Tables 13.2–13.4 ; they vary from 100 to 150 lb. per square inch.

If a bar is embedded in concrete as shown in Fig. 13.9 and subjected to a tensile load, it will be pulled out unless l is made sufficient to ensure that the adhesion is not overcome. Such a case occurs where reinforcing bars are not in one length but have to be lapped, *e.g.* in a circular water tank.

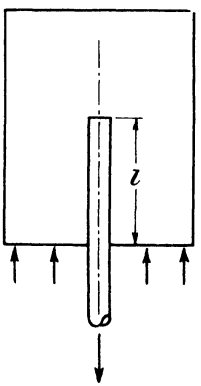

FIG. 13.9.

The usual criterion is to make l such that the adhesion calculated on a safe bond stress is at least equal to the tensile force in the bar. This length l is known as the grip length and is calculated as follows.

The safe tensile strength of one bar of diameter d is $\frac{t\pi d^2}{4}$ and the safe adhesive force, assuming a uniform distribution along l, is $s_b\pi dl$.

Equating these we have

$$\frac{t\pi d^2}{4} = s_b\pi dl$$

or

$$l = \frac{td}{4s_b} \quad \ldots\ldots\ldots\ldots \quad (2)$$

If t be taken as 18,000 lb. per square inch and s_b as 100 lb. per square

inch this gives

$$l=45d.$$

Dr. Oscar Faber* recommends a value of $l=48d$ wherever possible. It is not usual, however, to rely solely on the adhesion of a plain rod for anchorage. Bars are generally hooked at their ends and if these hooks are properly proportioned the bond is greatly improved.

13.7. Distribution of shear stress in a reinforced concrete beam.—The distribution of shearing stress across the section of a reinforced concrete beam can be approximately determined in the same way as for a homogeneous section.

Fig. 13.10 shows a singly reinforced beam and we consider two sections at a small distance δx apart on which the bending moments are respectively M and M+δM.

Equating the bending moment at any section to the moment of resistance, we have

$$M=aAt=\frac{abnc}{2}$$

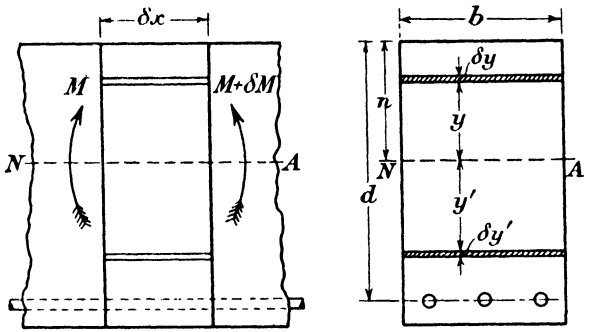

Fig. 13.10.

where t and c are the actual stresses developed in the steel and concrete and a is the moment arm $d-n/3$.

We shall consider first the compressive portion of the beam, *i.e.* the part above the neutral axis. The maximum compressive stresses developed at the top of the beam at the two sections considered are respectively

$$c_1=\frac{2M}{abn} \quad \text{and} \quad c_2=\frac{2(M+\delta M)}{abn}.$$

On any lamina which is y above NA the stresses at these sections are y/n times the maximum, *i.e.*

$$\frac{2My}{abn^2} \quad \text{and} \quad \frac{2(M+\delta M)y}{abn^2}.$$

If the thickness of the lamina is δy the compressive forces on the

* "Reinforced Concrete Design." Faber and Bowie. Arnold. 1919.

area $b\delta y$ at the two sections are respectively

$$\frac{2My\delta y}{an^2} \quad \text{and} \quad \frac{2(M+\delta M)y\delta y}{an^2}.$$

Hence, the difference in force on the lamina between the two ends of the length δx is

$$\frac{2\delta My\delta y}{an^2}$$

and the total difference of force on a section of the beam between $y=y_1$ and $y=n$ is

$$\frac{2\delta M}{an^2}\int_{y_1}^{n} y\,dy=\frac{\delta M}{an^2}(n^2-y_1^2).$$

This difference in force is balanced by the shearing force on the horizontal plane of area $b\delta x$ at y_1 above NA so that the average shearing stress is

$$s=\frac{\delta M}{\delta x}\frac{(n^2-y_1^2)}{abn^2}.$$

In the limit when δx is infinitely small $\frac{\delta M}{\delta x}$ is the shearing force at the section of beam at which the bending moment is M and so

$$s=\frac{S(n^2-y_1^2)}{abn^2}.$$

This is a parabola having a maximum value of $\frac{S}{ab}$ when $y_1=0$, *i.e.* at the neutral axis of the beam and a zero value when $y_1=n$, *i.e.* at the top of the beam.

We shall now consider the portion of the beam below the neutral axis. Since it is assumed that the concrete takes no tension there is no difference of load between the ends of a lamina in the concrete such as that shown at y' in the figure and the shearing stress has the constant value $\frac{S}{ab}$ until it is balanced by an equal and opposite shearing stress set up by the steel. The difference in tensile stress in the steel between the two ends of the length δx is $\frac{\delta M}{aA}$ and the difference in tension is therefore $-\frac{\delta M}{a}$ since it is in the opposite direction to the difference in compressions. This may be assumed to be transmitted uniformly to the concrete and the average shearing stress is therefore

$$s=-\frac{\delta M}{\delta x}\frac{1}{ab}=-\frac{S}{ab}$$

and this balances the constant shearing stress transmitted downwards through the concrete from the neutral axis.

The shearing stress distribution curve is therefore as shown in Fig. 13.11.

In a beam having double reinforcement the distribution of the shearing stress is modified. It is convenient to treat the total compression as being composed of that upon an area of concrete bn and an extra amount due to the substitution of concrete by steel over the area A′.

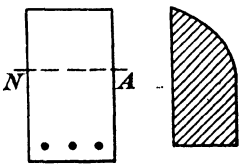

FIG. 13.11.

The shearing stress distribution over the concrete area is parabolic as before, but the stress due to the additional term has to be superimposed. This is of constant magnitude and only occurs between the level of the compression steel and the neutral axis; there is in consequence a discontinuity in the distribution curve at the compression steel.

The additional stress on the area A′ due to the substitution of steel for concrete is, as shown in paragraph 13.5,

$$\frac{(m-1)(n-d')c}{n}.$$

Also the total compression is

$$c\left\{\frac{bn}{2}+\frac{A'(m-1)(n-d')}{n}\right\}=cA_0.$$

If c_1 and c_2 are the maximum concrete stresses at the ends of the length δx the change in the total compression over this length is $(c_2-c_1)A_0$.

But this change is also $\frac{\delta M}{a}$ where a is the moment arm.

Hence, the change in the additional compression on the area A′ over the length δx is

$$\frac{A'(m-1)(n-d')}{n}\frac{\delta M}{aA_0}.$$

Assuming this to be uniformly distributed over the area the additional shear stress due to steel is

$$s'=\frac{A'}{A_0}\frac{(m-1)(n-d')}{n}\frac{S}{ab}.$$

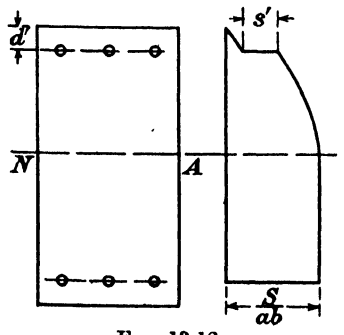

FIG. 13.12.

Since the change of total compression over the length δx is $\frac{\delta M}{a}$ the shearing stress at the neutral axis is $\frac{\delta M}{ab\delta x}=\frac{S}{ab}$ and the diagram of distribution is then as shown in Fig. 13.12.

The value of a may be calculated from equation (6) of paragraph 13.5.

13.8. Shear reinforcement in beams.—At any point in a beam there is a system of complex stress consisting of the direct tension or compression due

to the bending of the beam and complementary shearing stresses calculated as described in the last paragraph. The principal planes through the point will be subjected to pure tensions and compressions and at the neutral axis where there are no bending stresses these principal planes will be at 45° to the direction of shearing stresses and the principal stresses will be of the same intensity as the shearing stresses. Shearing stress is, therefore, accompanied by tension and, in consequence, concrete in shear needs reinforcement. Although in calculations for the main reinforcement of the beam it has been assumed that the tensile stresses must all be taken by steel, concrete is in fact capable of resisting some tension and in calculations for shearing resistance it is customary to take this into account. If the shearing stress calculated by the formula $s=\frac{S}{ab}$ of the last paragraph does not exceed a specified value, which varies with the quality of concrete from 150 to 75 lbs. per square inch, shear reinforcement may be omitted. If it exceeds such a value, however, sufficient reinforcement should be provided to carry the whole of the shear, *i.e.*, the assumption that there must be no tension in the concrete is again adopted. The Code of Practice previously referred to also lays down that in no case must the shearing stress calculated from the formula $\frac{S}{ab}$ exceed four times the permissible shear stress for plain concrete.

Shear reinforcement is provided in one of three ways or by combination of these. In regions where the bending moment is small and the shearing force is large, some of the longitudinal reinforcing bars are bent to cross the beam diagonally, as shown in Fig. 13.13.

Fig. 13.13.

The ends of these bars are carried well into the compression concrete and must be firmly anchored by hooks or otherwise.

The second method of reinforcing against shear is by means of inclined stirrups, as shown in Fig. 13.14. These stirrups are firmly attached to the tension reinforcing bars, carried well into the compression concrete and anchored. If compression steel is provided they should be connected to it to give the necessary anchorage; if it is not, the ends should be bent.

In the third type of shear reinforcement the inclined stirrups are

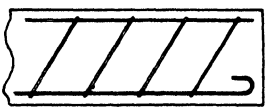

Fig. 13.14.

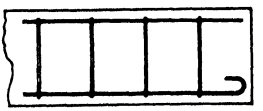

Fig. 13.15.

replaced by vertical stirrups as in Fig. 13.15, the same attention being

paid to the question of anchorage.

To understand the action of the inclined rods and stirrups in resisting the shearing force it is convenient to imagine a braced girder in which all the compression members are concrete and all the tension members are steel. A truss of this type can be constructed in two ways shown in Fig. 13.16. Concrete members are shown section-lined and steel members as single lines. Fig. 13.16 (*a*) shows a concrete top boom and steel rod bottom boom connected by vertical concrete struts. The panels thus formed are braced diagonally by steel members. A is a point of support and when loads are carried on the top boom it is clear

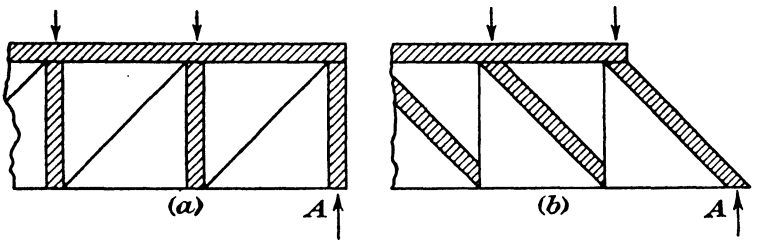

FIG. 13.16.

that all the steel is in tension and all the concrete is in compression. An alternative is shown at (*b*) in which steel vertical members are used and the panels braced by concrete bars across the opposite diagonals to those at (*a*). This structure also fulfils the condition that the concrete and steel are in compression and tension respectively. Provided the joints are suitable either of these trusses is a sound theoretical structure and the spaces between the members may be supposed to be filled in with useless concrete. The result is then reinforced concrete beams with inclined and vertical stirrups respectively. The stress distribution is, of course, affected by the filling in process and the analogy of the reinforced concrete beam with the trussed girder must not be pushed too far. It does give, however, an idea of the way in which stirrups can resist shearing forces and offers one basis of design.

The application of this method to determine the adequacy of shear reinforcement gives results which are too conservative and another method is more generally used.

On the assumption that the concrete takes no tensile stress the shearing stress between the neutral axis and the tension reinforcement has been shown to be constant and there is no direct stress in this region. The state of stress is therefore one of pure shear which induces a principal tensile stress of the same intensity on planes inclined at 45° to the axis of the beam. Hence if rods are turned through 45° or inclined stirrups are placed at the same angle they will be in the best position to resist this tensile stress. In Fig. 13.17 let AD be the level of the centre of compression and EB the tension reinforcement, so that the distance BD is a, the arm of the moment of resistance. The shear reinforcement is provided by stirrups inclined at 45° and spaced a distance p apart along the line EB.

Consider a length of the beam EB equal to a and let the shearing

force transmitted from BD to EA be S.

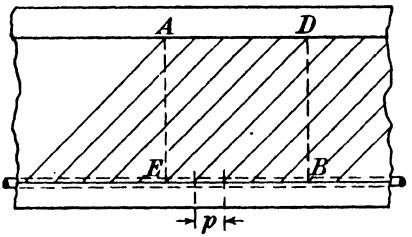

FIG. 13.17.

Since the tensile stress on AB is of the same intensity as the shearing stress on BD, the total pull on AB is $S\sqrt{2}$.

The number of stirrups cut by AB is $\frac{2a}{p}$.

Hence the load taken by each stirrup is $\frac{pS\sqrt{2}}{2a} = \frac{pS}{a\sqrt{2}}$.

Let A_w be the cross-sectional area of a stirrup and t_w the permissible tensile stress in the material.

Then the maximum shearing force which can be resisted is given when

$$\frac{pS}{a\sqrt{2}} = t_w A_w$$

or
$$S = \frac{t_w A_w a\sqrt{2}}{p} \quad \ldots\ldots\ldots\ldots \quad (1)$$

If the stirrups are vertical, as in Fig. 13.18, the tensile force on AB which is $S\sqrt{2}$ as before is resisted by a/p stirrups. The vertical component of the force on AB is S and so the load in each stirrup is $\frac{Sp}{a}$.

Then, as before, the maximum shearing resistance of the stirrups is given when

$$\frac{Sp}{a} = t_w A_w$$

i.e.
$$S = \frac{t_w A_w a}{p} \quad \ldots\ldots\ldots\ldots \quad (2)$$

This formula is recommended for design purposes in the Code of Practice.

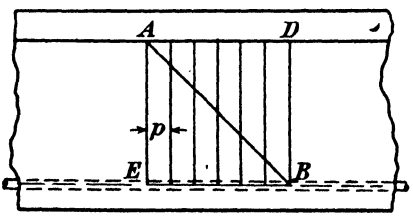

FIG. 13.18.

13.9. Flexural stiffness of reinforced concrete members.—The second moment of area or, as it is usually but erroneously called, the moment of inertia of the cross-section appears in many calculations for homogeneous members and this seems to have led to a confusion of ideas in connection with reinforced concrete structures. The second moment of area is a purely geometrical conception and has no reference whatever to the material of which a member is made. For example, in calculations of strength for a steel and a wooden beam of the same cross-section the same value of I would be used in both cases. It is therefore somewhat disconcerting to find methods given by many authorities for calculating the "moment of inertia" which make allowance for the reinforcement. The confusion has arisen between the second moment of area, I, and the flexural rigidity, EI, and it is only this latter term which has a real significance in calculation.

In the case of a beam with single reinforcement such as shown in Fig. 13.3 we have seen that the moment of resistance is either

$$\frac{bnc}{2}\left(d-\frac{n}{3}\right) \quad \text{or} \quad At\left(d-\frac{n}{3}\right).$$

Also, from the ordinary theory of bending for homogeneous bars,

$$M=\frac{fI}{y}$$

where f is the stress at a distance y from the neutral axis and I is the second moment of area.

or
$$I=\frac{My}{f}.$$

Applying this to the reinforced concrete beam we obtain two different values for I depending upon whether we consider the concrete or the steel. Thus,

$$I_c=\frac{\frac{bnc}{2}\left(d-\frac{n}{3}\right)n}{c}=\frac{bn^2}{2}\left(d-\frac{n}{3}\right)$$

or
$$I_s=\frac{At(d-n/3)(d-n)}{t}=A\left(d-\frac{n}{3}\right)(d-n)$$

And from the work of paragraph 13.3.

$$\frac{I_c}{I_s}=\frac{bn^2}{2A(d-n)}=\frac{t}{c}\cdot\frac{n}{d-n}=m.$$

Thus, $I_c=mI_s$ showing that the term "moment of inertia" is misleading in connection with composite sections.

Substituting for m, however, we have

$$E_cI_c=E_sI_s$$

and we see that the flexural rigidity is the same whether we consider it in terms of concrete or steel.

In most calculations the flexural rigidity is required but if the term I is isolated considerable ambiguity arises and great care is necessary. For example, in column formulas containing the term l/k, *i.e.* the ratio of length to the radius of gyration, it is imperative to know exactly how this term was measured in the experiments upon which the formulas are based.

13.10. The axially loaded reinforced concrete column.—The simplest form of reinforcement in a column consists of a number of rods running the whole length of the column and sharing the compression with the concrete. Such simple reinforcement is, however, not sufficient by itself to develop the full strength of the combination since the long rods tend to buckle under load and premature failure occurs. It is necessary, therefore, to tie the longitudinal reinforcement together transversely to stabilise it against this tendency. The ties may be either separate link pieces spaced at intervals of from 6 to 12 inches throughout the column, or a continuous spiral reinforcement may encircle the main bars. The spirals should be evenly spaced and the ends must be properly anchored. The pitch of the spirals should be not more than 3 inches or one-sixth of the diameter of the core of concrete included in the spiral, whichever is the smaller, and should be not less than one inch or three times the diameter of the bar of which the spiral is made, whichever is the greater.

Columns with spiral reinforcement should have at least six longitudinal bars and other types of column one bar near each angle of the cross-section.

Spiral reinforcement restricts the lateral expansion of the core when the column is loaded and thus enables the concrete to be more highly stressed. This extra strength is recognised by an allowance in practical design formulas.

The theoretical strength of a short axially loaded column is easily obtained as follows :—

Let A_c be the area of the concrete in the cross-section,
A, the cross-sectional area of steel in longitudinal bars,
c, the stress developed in the concrete,
t, the compressive stress developed in the steel,
and m, the modular ratio.

Then if the steel and concrete are assumed to strain together, we have

$$\text{strain in concrete} = \text{strain in steel}$$

or $$c/E_c = t/E_s$$

i.e. $$t = mc$$

Also, if the total axial load which the column can carry is P,

$$P = cA_c + tA$$

or $$= c(A_c + mA) \quad . \quad . \quad . \quad . \quad . \quad . \quad . \quad . \quad . \quad (1)$$

Actual tests of columns indicate that this simple theory gives low results and the formula specified in the Code is

$$P = cA_c + tA \quad . \quad . \quad . \quad . \quad . \quad . \quad . \quad . \quad . \quad (2)$$

where c and t in this case are stresses which are actually allowable in the concrete and steel respectively; they are not related by the expression $t=mc$ derived from the equation of strains.

When spiral reinforcement encircles the longitudinal bars it encloses a core of concrete.

Let the total volume of spiral reinforcement in a column of length l be denoted by V and let the radius of the concrete core be r.

If we suppose the whole of the spiral reinforcement to be replaced by a steel tube enclosing the core, the cross-sectional area of this tube is

$$A_b=V/l.$$

Also let A_k=the area of concrete core$=\pi r^2$,

t =permissible stress in longitudinal reinforcement,

and t_b=permissible stress in the spiral steel, 13,500 or 15,000 lb. per square inch, depending on the quality.

When a compressive load is applied to the column the spiral does more than bind the longitudinal reinforcement; it decreases the lateral expansion of the concrete in the core which would accompany the shortening of the column and enables the concrete to resist greater longitudinal stresses. The steel in the spiral, which is thrown into tension, is found to be approximately twice as effective in strengthening the column as an equal amount used as additional longitudinal reinforcement. The formula suggested for design purposes is based on this and the load which the column can carry is expressed as

$$P=cA_k+tA+2{\cdot}0t_bA_b \quad . \quad . \quad . \quad . \quad . \quad . \quad . \quad (3)$$

The greater of the two values of P obtained from (2) and (3) may be used.

If the columns are long the loads calculated from the above formulas must be reduced to allow for the effect of buckling and Table 13.1 taken from the Code gives suitable correcting coefficients. These have been calculated from the formulas

$$C_r=1{\cdot}5-\frac{l}{30d}$$

and

$$C_r=1{\cdot}5-\frac{l}{100k}$$

where C_r is the buckling coefficient,

l is the effective length,

d is the least lateral dimension of the column

and k is stated to be the radius of gyration of the column.

As explained in the last paragraph, this term has no significance unless k is more specifically defined. This is not done in the Code, but it appears to be

$$\sqrt{\frac{\text{Flexural rigidity}}{E_cA_c}}.$$

In spirally reinforced columns dimensions refer to the core of the column.

TABLE 13.1.

Ratio of effective length to least lateral dimension of column	Ratio of effective length to least "radius of gyration"	Coefficient
15	50	1·0
18	60	0·9
21	70	0·8
24	80	0·7
27	90	0·6
30	100	0·5
33	110	·0·4
36	120	0·3
39	130	0·2
42	140	0·1
45	150	0

The effective length of a column depends upon the type of end fixing and its assessment is very largely a matter of judgment; typical cases are given in the Code. The design of columns is based on experimental tests and the equations quoted above are subject to certain restrictions. Such points of practical design are outside the scope of this book and the reader is referred to the Code itself or to the Handbook * on the Code for information upon this and other details.

13.11. Reinforced concrete members subjected to combined bending and axial load.—In most cases the beams attached to columns impose a moment as well as an axial load and the stress distribution under such conditions must now be considered.

Let the singly reinforced member shown in Fig. 13.19 carry a load P acting through the neutral axis and a bending moment M.

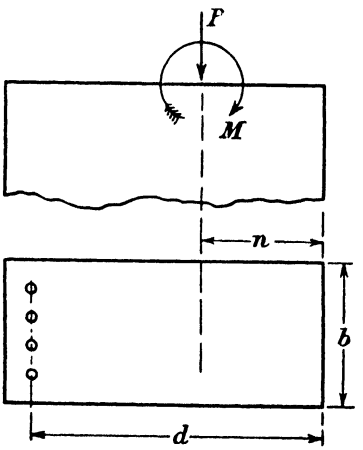

FIG. 13.19.

* Loc. cit., p. 2

The condition of strain proportionality has to be satisfied as in paragraph 13.3 and equation (1) of that paragraph is valid.

In this case, however, there is a resultant axial thrust on the member and so

$$\frac{bnc}{2} - At = P \quad . \quad . \quad . \quad . \quad . \quad . \quad . \quad . \quad . \quad (1)$$

In addition the moment of resistance of the cross-section must be equal to the applied moment M, so that

$$M = \left(\frac{bnc}{2} \times \frac{2n}{3}\right) + At(d-n) \quad . \quad . \quad . \quad . \quad . \quad . \quad (2)$$

These two equations and equation (1) of paragraph 13.3 are sufficient for the calculation of the strength of any member of this type. Generally, however, members liable to combined thrust and bending have compression as well as tension reinforcement and the equations must be correspondingly modified.

Equation (1) of paragraph 13.3 and equations (1) and (3) of paragraph 13·5 are all valid for this case and using the notation of the latter paragraph we have in addition, equating forces on the section,

$$c\left\{\frac{bn}{2} + \frac{A'(m-1)(n-d')}{n}\right\} - At = P \quad . \quad . \quad . \quad . \quad . \quad (3)$$

It will be observed that the only difference between these equations and those previously used for beams arises from the introduction of the load P ; the total compressive force must now exceed the tensile force by the amount P to obtain equilibrium of the section. The calculations are similar to those already illustrated but slightly more elaborate.

13.12. Strength of materials and allowable stresses.—The Reinforced Concrete Code recognises three grades of concrete which are known as ordinary grade, high grade, and special grade. These must comply with certain requirements of which the most important is a laboratory test of compressive strength. The allowable stresses in bending, direct compression, shear and bond are based on the value thus obtained and the quality of the material is checked by simpler tests carried out at frequent intervals on the works where the concrete is in use. Full details of the tests are given in the Code, to which references should be made, and the test requirements and allowable stresses are given in Tables 13.2, 13.3 and 13.4.

The stresses allowed in the steel reinforcement are given in Table 13.5.

TABLE 13.2.—ORDINARY GRADE CONCRETE.

Nominal mix	Proportions. Cubic feet of aggregate per 112-lb. bag of cement		Minimum cube strength requirements at 28 days. Lb. per sq. in.		Modular ratio	Permissible concrete stresses. Lb. per sq. in.			
	Fine	Coarse	Preliminary tests	Works tests		Bending	Direct	Shear	Bond
			$4{\cdot}5x$	$3x$	$\frac{40{,}000}{3x}$	x	$0{\cdot}8x$	$0{\cdot}1x$	$0{\cdot}1x+25$
1 : 1 : 2 . . .	$1\frac{1}{4}$	$2\frac{1}{2}$	4,388	2,925	14	975	780	98	123
1 : 1·2 : 2·4 . .	$1\frac{1}{2}$	3	4,163	2,775	14	925	740	93	118
1 : 1·5 : 3 . .	$1\frac{7}{8}$	$3\frac{3}{4}$	3,825	2,550	16	850	680	85	110
1 : 2 : 4 . . .	$2\frac{1}{2}$	5	3,375	2,250	18	750	600	75	100

TABLE 13.3.—HIGH GRADE CONCRETE.

Nominal mix	Proportions. Cubic feet of aggregate per 112-lb. bag of cement		Minimum cube strength requirements at 28 days. Lb. per sq. in.		Modular ratio	Permissible concrete stresses. Lb. per sq. in.			
	Fine	Coarse	Preliminary tests	Works tests		Bending	Direct	Shear	Bond
			$4{\cdot}5x$	$3x$	$\frac{40{,}000}{3x}$	x	$0{\cdot}8x$	$0{\cdot}1x$	$0{\cdot}1x+25$
1 : 1 : 2 . . .	$1\frac{1}{4}$	$2\frac{1}{2}$	5,625	3,750	11	1,250	1,000	125	150
1 : 1·2 : 2·4 . .	$1\frac{1}{2}$	3	5,400	3,600	11	1,200	960	120	145
1 : 1·5 : 3. . .	$1\frac{7}{8}$	$3\frac{3}{4}$	4,950	3,300	12	1,100	880	110	135
1 : 2 : 4 . . .	$2\frac{1}{2}$	5	4,275	2,850	14	950	760	95	120

TABLE 13.4.—SPECIAL GRADE CONCRETE (LIMITING VALUES).

Nominal mix	Proportions. Cubic feet of aggregate per 112-lb. bag of cement		Minimum cube strength requirements at 28 days. Lb. per sq. in.		Modular ratio	Permissible concrete stresses. Lb. per sq. in.			
	Fine	Coarse	Preliminary tests	Works tests		Bending	Direct	Shear	Bond
			$5x$	$3x$	$\frac{40{,}000}{3x}$	x	$0{\cdot}8x$	$0{\cdot}1x$ but not greater than 150	$0{\cdot}1x+25$ but not greater than 150
1 : 1 : 2 . . .	$1\frac{1}{4}$	$2\frac{1}{2}$	Strength requirements, modular ratios and permissible stresses to be calculated from above factors and to be based on preliminary test results. The values for the permissible stresses shall not exceed those for similar mixes of High Grade concrete (Table 13.3) by more than 25 per cent. Shear and bond stresses also shall not exceed 150 lb. per square inch. Modular ratios may be taken to the nearest whole number.						
1 : 1·2 : 2·4 . .	$1\frac{1}{2}$	3							
1 : 1·5 : 3 . .	$1\frac{7}{8}$	$3\frac{3}{4}$							
1 : 2 : 4 . . .	$2\frac{1}{2}$	5							

TABLE 13.5.

	Permissible stress, lb. per sq. in.	
	(1) Mild steel complying with B.S.S. No. 15	(2) Mild steel complying with B.S.S. No. 15 and with a yield point stress of not less than 44,000 lb. per sq. in.
BENDING.		
Tension in longitudinal steel in beams, slabs or columns subject to bending	18,000	20,000
Compression in longitudinal steel in beams, slabs or columns subject to bending where the compressive resistance of the concrete is taken into account	The compression stress in the surrounding concrete multiplied by the modular ratio.	
Compression in longitudinal steel in beams where the compressive resistance of the concrete is not taken into account	18,000	20,000
DIRECT COMPRESSION.		
Compression in longitudinal steel in axially loaded columns	13,500	15,000
Tension in spiral reinforcement	13,500	15,000
SHEAR.		
Tension in web reinforcement	18,000	18,000

EXERCISES

(1) A flitched beam is made of two timber joists each 4 inches wide and 12 inches deep with a $12 \times \frac{1}{2}$-inch steel plate firmly fastened between them.

If the stress in the timber is limited to 1,000 lb. per square inch and that in the steel to 10,000 lb. per square inch, calculate the safe uniformly distributed load which the beam can carry when freely supported on a span of 20 feet.

E for steel $= 30 \times 10^6$ lb. per square inch.

E for timber $= 1{\cdot}5 \times 10^6$ lb. per square inch.

(7,200 lbs.)

(2) A reinforced concrete beam is 10 inches wide and 12 inches deep to the centre of reinforcement which consists of a total area of 1 square inch of steel. Calculate the position of the neutral axis of the beam and the stress in the steel when that in the concrete is 600 lb. per square inch. $m = 15$.

($n = 4{\cdot}68$ inches; $t = 14{,}040$ lb. per square inch)

(3) A reinforced concrete floor slab is $4\frac{1}{2}$ inches deep to the centre of reinforcement and is carried on secondary beams 8 feet apart. If a concrete stress of

600 lb. per square inch and a steel stress of 18,000 lb. per square inch are developed simultaneously, calculate the area of steel required per foot width of slab and the load per square foot the floor can carry. $m=15$.

(0·30 square inches ; 225 lb. per square foot)

(4) A reinforced concrete T-beam 40 inches wide and 6 inches deep at the top has 5 square inches of reinforcement at a depth of 20 inches where the width of the beam is 12 inches.

Calculate the uniformly distributed load it can carry on a freely supported span of 20 feet, inclusive of its own weight, if the stresses in the concrete and steel are limited to 600 and 16,000 lb. per square inch respectively.

The modular ratio may be taken as 15.

(1·05 tons per foot)

(5) Take the overall sizes of the beam specified in the last question and calculate the percentage error involved in the moment of resistance determined by the approximate method when the slab thickness is 4 inches.

(3·6 per cent.)

(6) A reinforced concrete beam, rectangular in cross-section, is 8 inches wide and 18 inches effective depth to the centre of the tension reinforcement. It is reinforced on both the tension and compression sides by two $\frac{3}{4}$-inch diameter rods and subjected to a pure bending moment. The compression steel is centred at 1 inch from the top of the beam.

Calculate the position of the neutral axis and the stresses in the steel when the maximum concrete stress is 600 lb. per square inch. $m=15$.

(5·35 inches ; 7,310 lb. per square inch in compression ; 21,350 lb. per square inch in tension)

(7) The moment of resistance of an economically designed reinforced concrete beam may be expressed by the formula

$$M=Rbd^2$$

where M is the moment of resistance, b the breadth of the beam and d the depth to the reinforcement, R being a constant depending on the allowable concrete and steel stresses and the modular ratio.

If the allowable stresses in the concrete and steel are 750 lbs. per square inch and 18,000 lb. per square inch respectively and the value of the modular ratio is 18, determine the value of R. Also calculate the economic percentage of steel.

(137·7 ; 0·893 per cent.)

(8) Derive a shear stress distribution curve for a concrete beam of rectangular section reinforced on the tension side only.

A beam of this description is 10 inches wide, 12 inches deep to the centre of reinforcement and 4·8 inches deep to the neutral axis. It is subjected to a maximum shear force of 7,500 lbs. Calculate the maximum shear stress in the concrete.

(72 lb. per square inch)

CHAPTER 14

INFLUENCE LINES FOR STATICALLY DETERMINATE STRUCTURES

14.1. Definition.—A diagram which represents the variation of any resultant action, force, deflection or slope at a particular point in a structure as a unit load rolls across the structure is known as an influence line. Thus the influence line of bending moment for any point A on a beam shows how the bending moment at A changes as a load of unity traverses the beam : the ordinate to the curve at any point B is the bending moment at A when the unit load is at B. Influence lines are of considerable value in studying the effect of rolling loads on structures and in the present chapter their use in the case of statically determinate beams and trusses will be described.

14.2. Influence lines for a simply supported beam.—Let AB in Fig. 14.1 represent a simply supported beam which is traversed by a

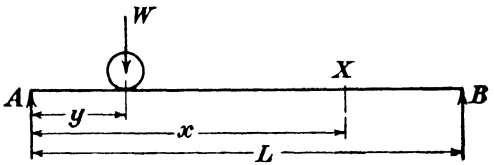

FIG. 14.1.

rolling load W, At any instant let W be at a distance y from A. It is desired to draw a diagram which will represent the variation of bending moment at a fixed point X, which is at a distance x from A, as the load rolls from A to B.

The bending moment at X is

$$M_x = -R_B(L-x)+[W(y-x)]$$

where R_B is the reaction at B and the term in square brackets only appears when it is positive, *i.e.* when $y>x$.

Since $$R_B=\frac{yW}{L},$$

$$M_x=W\left\{-\frac{y(L-x)}{L}+[y-x]\right\}.$$

This represents two straight lines covering the ranges A—X and X—B respectively.

When $y=0$, $M_x=0$,

when $y=x$, $M_x=-\dfrac{Wx(L-x)}{L}$,

when $y=L$, $M_x=0$.

If we now make W=unity, the influence line of bending moments for X is as shown in Fig. 14.2. The bending moment at X when the unit load is at C is given by the ordinate CD.

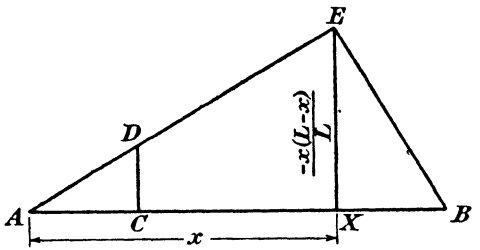

FIG. 14.2.

Again, the shearing force at X is

$$S_x=+R_B-[W]$$

the second term only occurring when $y>x$.

i.e. $$S_x=W\left\{\frac{y}{L}-[1]\right\}.$$

This again represents two straight lines covering the ranges A—X and X—B respectively.

When $y=0$ or L, $S_x=0$,

when $y=x$, $S_x=\dfrac{Wx}{L}$ or $-\dfrac{W}{L}(L-x)$

according as the point is immediately to the left or immediately to the right of X.

The influence line of shearing force for X is therefore as shown in Fig. 14.3, when W is made unity. Since XE : XF : : AX : XB, the

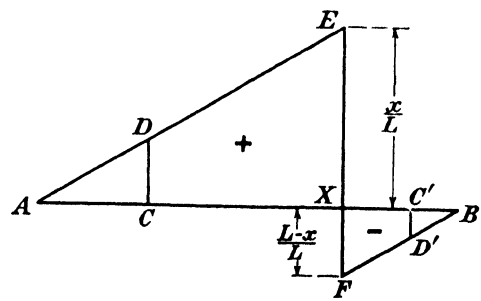

FIG. 14.3.

lines AE and BF are parallel. When the unit load is between A and X the shearing force at X is positive; when it is between X and B the

shearing force at X is negative. It is in either case represented by ordinates such as CD or C'D' drawn to the influence line from the load point.

From these influence lines the bending moment or shearing force at X can be found for any system of loads upon the beam. For example, let loads W_1, W_2 . . . W_n act at points 1, 2, . . . n, and let the ordinates to the influence lines of bending moment and shearing force at these points be m_1, m_2 . . . m_n and s_1, s_2 . . . s_n respectively. Then the bending moment and shearing force at X due to this loading are

$$\left.\begin{aligned} M_x &= W_1m_1 + W_2m_2 + \ldots + W_nm_n \\ \text{and} \quad S_x &= W_1s_1 + W_2s_2 + \ldots + W_ns_n \end{aligned}\right\} \quad \ldots\ldots \quad (1)$$

The bending moment and shearing force at the point X due to a uniformly distributed load on any section of the beam can be found readily from the influence lines. Suppose a load of intensity w covers a length c as indicated on the influence diagram for shearing force drawn in Fig. 14.4. The load on a small element of length δx at D

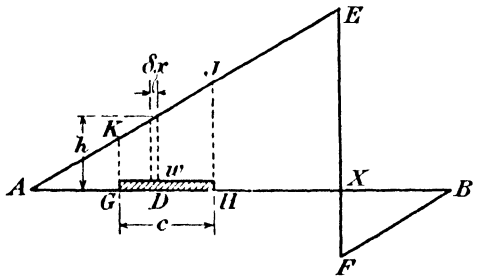

FIG. 14.4.

is $w\delta x$ and if the ordinate at D is h the shearing force at X due to this element of load is $hw\delta x$. Hence the total shearing force at X due to the whole load cw is $w\int hdx$.

But $\int hdx$ is the area between the length c and the influence line, *i.e.* GHJK, and the shearing force at X is therefore $w\times$(area of the influence diagram covered by the load). The same argument is applicable to bending moments or any other property for which the influence line is known.

Influence lines will now be used to find the curves of maximum bending moment and shearing force in a beam when certain systems of rolling loads cross it.

14.3. Single rolling load on a simply supported beam.—Reference to Fig. 14.2 shows that the maximum bending moment at X as a load rolls from A to B occurs when it reaches X, its value then being

$$M_{max} = -\frac{Wx(L-x)}{L}$$

Since x can have any value between 0 and L the curve of maximum

bending moment for any point on the beam is given by this expression which represents a parabola with a maximum ordinate $\frac{WL}{4}$ at the centre of the span. This maximum bending moment diagram is shown in Fig. 14.5.

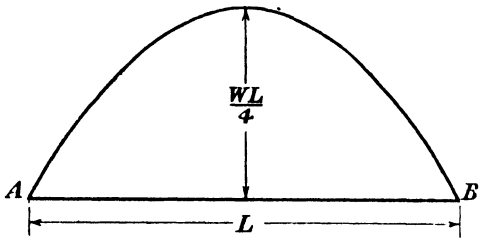

FIG. 14.5.

The influence line for shearing force in Fig. 14.3 shows that the maximum positive shearing force at X occurs when the load reaches X from the left but has not crossed that section. Its value is

$$S_{max}=\frac{Wx}{L}.$$

Similarly the maximum negative shearing force at X occurs when the load has just crossed the section X, its value being

$$S'_{max}=-\frac{W(L-x)}{L}.$$

These expressions both represent straight lines and are true for all values of x between 0 and L. Hence the curves of maximum positive and negative shearing forces at all points of the beam are given by the diagrams of Fig. 14.6.

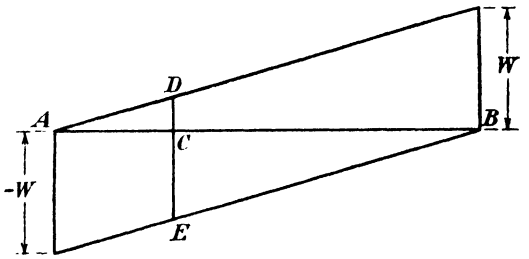

FIG. 14.6.

The two values at any point occur under different load conditions: at C for example the shearing force when the load just reaches C is represented by CD. As the load crosses the section C it changes from CD to CE which is the maximum negative value at C and occurs when the load acts immediately to the right of that point.

14.4. Distributed rolling load on simply supported beam.—Two cases arise here, first when the distance covered by the load is greater than the span of the beam and secondly when it is less than that span.

Case 1. *Load covering a greater length than the span.*—Since the bending moment at X, Fig. 14.2, is represented by the area between the load and the influence line, it is clear that the maximum bending moment will occur when the whole span is covered since then the area over the load has the greatest possible value

$$M_{max}=-\frac{wL}{2}\times\frac{x(L-x)}{L}=-\frac{wx(L-x)}{2}.$$

This represents the value of the maximum bending moment for any value of x between 0 and L and is a parabola with a maximum ordinate $\frac{wL^2}{8}$ at the centre, as shown in Fig. 14.7.

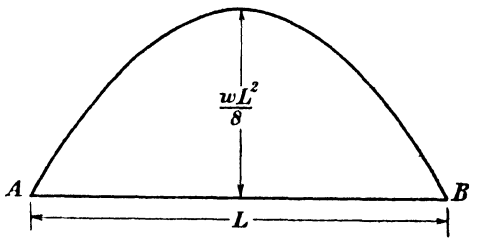

FIG. 14.7.

From Fig. 14.3 it is clear that the maximum positive and negative shearing force at X occur when AX and XB respectively are covered by the load, since the positive and negative areas are then the greatest possible.

Hence $$S_{max}=\frac{wx}{2}\cdot\frac{x}{L}=\frac{wx^2}{2L},$$

and $$S'_{max}=-\frac{w(L-x)}{2}\cdot\frac{(L-x)}{L}=-\frac{w(L-x)^2}{2L}.$$

These equations hold for all values of x and are parabolas with maximum ordinates of $\frac{wL}{2}$ and $-\frac{wL}{2}$ when $x=L$ and $x=0$ respectively. The curves are shown in Fig. 14.8.

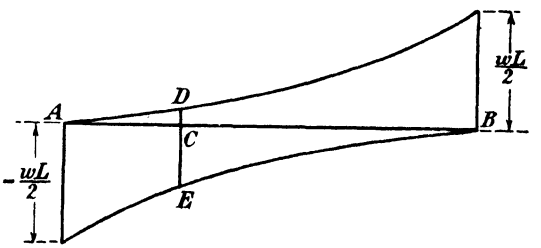

FIG. 14.8.

The two values of the maximum shearing force at C, represented by CD and CE occur when AC and CB respectively are covered by the load.

Case 2. *Load covering a shorter length than the span.*—Let a rolling load of uniform intensity w cover a distance c which is less than L.

It is clear from the influence line that the maximum bending moment at X will occur when the load covers a length FG, part of which lies to the left and part to the right of X as in Fig. 14.9. The area FCEHG will then have the greatest possible value.

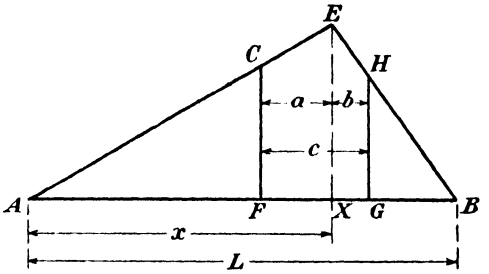

FIG. 14.9.

Suppose XF$=a$ and XG$=b$ so that $a+b=c$.

The mean ordinate between F and X is $\frac{(2x-a)(L-x)}{2L}$ and that between G and X is $\frac{\{2(L-x)-b\}x}{2L}$.

The area FCEHG=area FCEX+area GHEX,

or
$$A=\frac{(2x-a)(L-x)a}{2L}+\frac{(2L-2x-b)xb}{2L},$$
$$=\frac{1}{2L}\{(2xL-2x^2)c-a^2(L-x)-(c-a)^2x\}.$$

For this to be a maximum $\frac{dA}{da}=0$.

Therefore
$$-2a(L-x)+2(c-a)x=0,$$

or
$$\frac{x}{L-x}=\frac{a}{c-a}$$

i.e.
$$\frac{x}{L}=\frac{a}{c},$$

so the bending moment at X is a maximum when the point X divides the load and the span in the same ratio.

The bending moment is then wA and, putting a equal to $\frac{cx}{L}$ in the above expression for A, we obtain

$$M_x=\frac{cwx(L-x)}{L}\left(1-\frac{c}{2L}\right).$$

This is a parabola having the maximum ordinate $\frac{cwL}{4}\left(1-\frac{c}{2L}\right)$ at the centre.

From Fig. 14.3 it is clear that the maximum positive shearing force at X occurs when the load is on the part AX of the beam and the right-hand end of it is at X.

The ordinate at the mid-part of the load is then

$$\frac{x-\frac{c}{2}}{x}\times\frac{x}{\mathrm{L}}=\frac{2x-c}{2\mathrm{L}}$$

and the maximum positive shearing force is

$$\mathrm{S}_{\max}=\frac{cw(2x-c)}{2\mathrm{L}}.$$

This is a straight line in x but it only holds as long as the whole load is on the beam, *i.e.* when $x\gtrless c$.

For values of x less than c the curve will be the parabola of Case 1 (Fig. 14.8).

To plot the complete curve it is convenient to draw the straight line defined by the points

$$x=\left(\mathrm{L}+\frac{c}{2}\right),\quad \mathrm{S}=cw.$$

$$x=\frac{c}{2},\qquad \mathrm{S}=0.$$

This gives the maximum positive shearing force between $x=c$ and $x=\mathrm{L}$. The diagram is completed by drawing the parabola of Fig. 14.8 between $x=0$ and $x=c$ as shown in Fig. 14.10.

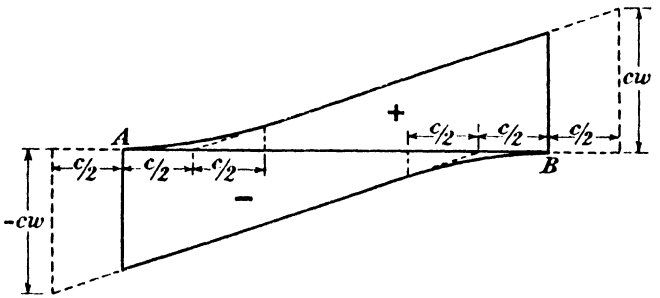

FIG. 14.10.

The maximum negative shearing force at X occurs when the load is on the section XB of the beam (Fig. 14.3) with the left-hand end of the load at X.

The ordinate at the mid-point of the load is

$$\frac{\mathrm{L}-x-\frac{c}{2}}{\mathrm{L}-x}\times\frac{\mathrm{L}-x}{\mathrm{L}}=\frac{2\mathrm{L}-2x-c}{2\mathrm{L}}$$

and the maximum negative shearing force is

$$\mathrm{S}'_{\max}=-\frac{cw(2\mathrm{L}-2x-c)}{2\mathrm{L}}.$$

This is a straight line between $x=0$ and $x=L-c$ and a parabola between $x=L-c$ and $x=L$. Convenient points on the straight line for plotting the diagram are

$$x=\left(L-\frac{c}{2}\right), \quad S'=0.$$

$$x=-\frac{c}{2}, \qquad S'=-cw.$$

The complete maximum shearing force diagram for this case is then as shown in Fig. 14.10.

14.5. Two concentrated loads on a simply supported beam.—Let two loads W_1 and W_2 separated by a distance a, as in Fig. 14.11, roll across a simply supported beam. Let P, the resultant of these loads, act at c from W_1 and b from W_2 so that $P=W_1+W_2$ and $a=c+b$.

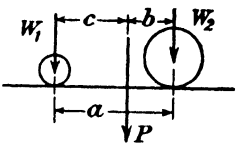

FIG. 14.11.

From a consideration of the bending moment diagram for the loads in any position on the beam it is clear that the maximum value of the bending moment will occur under one of the loads. Hence the maximum value of the bending moment at a point X will occur when one of the loads is at this point.

In the first place suppose W_2 is at X. The total bending moment at X due to the two loads is then, from the influence line of Fig. 14.2,

$$M_2=-\frac{W_2x(L-x)}{L}-\frac{W_1(x-a)(L-x)}{L}$$

$$=-\frac{(L-x)}{L}\{W_2x+W_1(x-a)\}.$$

The term in brackets is the moment of the loads about the left-hand support of the beam and is therefore equal to the moment of their resultant about the same point.

i.e.

$$M_2=-\frac{P(L-x)(x-b)}{L}.$$

Now suppose W_1 to be at X. The bending moment at X due to the load system is

$$M_1=-\frac{W_1x(L-x)}{L}-\frac{W_2x(L-x-a)}{L}$$

$$=-\frac{x}{L}\{W_1(L-x)+W_2(L-x-a)\}.$$

Substituting for the term in brackets the moment of P about the right-hand support of the beam we have

$$M_1=-\frac{Px(L-x-c)}{L}.$$

M_2 will be numerically greater than M_1 if

$$(L-x)(x-b)>x(L-x-c)$$

i.e. if $$Lx-Lb-x^2+bx>Lx-x^2-cx$$

or $$-Lb>-(b+c)x.$$

Substituting $a=b+c$, this leads to

$$ax>Lb.$$

Hence M_2 will be numerically greater than M_1 if $\frac{x}{L}>\frac{b}{a}$,

i.e. if $$\frac{x}{L}>\frac{W_1}{W_1+W_2}.$$

To plot the diagram of maximum bending moments on the beam it is convenient to draw the curves for M_1 and M_2 separately and then use the appropriate one.

Thus $$M_2=-\frac{P}{L}(L-x)(x-b)$$

and this is a parabola having its maximum ordinate at the point where

$$L-x=x-b,$$

i.e. at $$x=\tfrac{1}{2}(L+b).$$

The value of this maximum ordinate is $\frac{P(L-b)^2}{4L}$.

The value of M_2 is zero at $x=L$ and $x=b$ and the parabola is shown in Fig. 14.12.

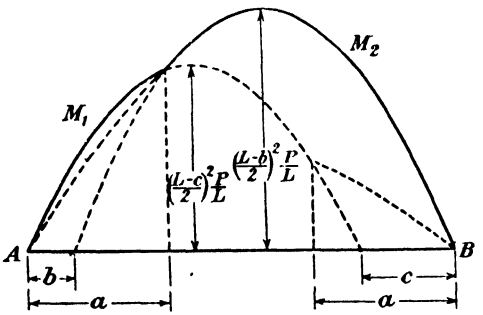

FIG. 14.12.

Again $$M_1=-\frac{Px}{L}(L-x-c)$$

which is another parabola with its maximum ordinate at $x=\frac{1}{2}(L-c)$, the value of the bending moment at this point being $\frac{P(L-c)^2}{4L}$.

Zero values occur at $x=0$ and at $x=L-c$ and the parabola is plotted in Fig. 14.12.

The parabolas are correct only as long as both the loads are on the beam, *i.e.* M_1 holds from $x=0$ to $x=L-a$ and M_2 from $x=a$ to $x=L$. Between $x=L-a$ and $x=L$, M_1 must be drawn for the single load W_1

on the beam and between $x=0$ and $x=a$, M_2 must be drawn for the single load W_2 on the beam. These curves are both parts of parabolas and are shown in the diagram. The curve of maximum bending moment for the beam is indicated by a full line: the point of intersection of the parabolas occurs at $x=\frac{W_1 L}{W_1+W_2}$ which in Fig. 14.12 coincides accidentally with $x=a$.

Now consider the shearing force on the beam: reference to the influence line of Fig. 14.3 shows that the maximum positive and negative values occur when W_2 and W_1 are respectively at X. The values of these maximum shearing forces are obtained directly from the influence line. Thus the maximum positive value is

$$S_{max}=\frac{xW_2}{L}+\left(\frac{x-a}{x}\right)\frac{xW_1}{L}$$
$$=\frac{1}{L}\{W_2x+W_1(x-a)\}$$

or, substituting as in the case of the bending moment,

$$S_{max}=\frac{P}{L}(x-b).$$

Similarly, the maximum negative value is

$$S'_{max}=\left(\frac{L-x}{L}\right)W_1+\left(\frac{L-x-a}{L-x}\right)\left(\frac{L-x}{L}\right)W_2$$
$$=\frac{P}{L}(L-x-c).$$

The expression for S_{max} is a straight line which holds between $x=a$ and $x=L$. When x is less than a, W_2 only is on the beam and the curve is the appropriate one for a single load, *i.e.* a straight line, as shown in Fig. 14.6.

It should be noticed that the formula above gives $S_{max}=0$ when $x=b$ and $S_{max}=P$ when $x=L+b$. The straight line representing

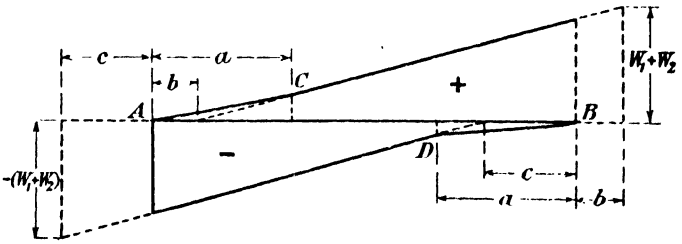

FIG. 14.13.

S_{max} is conveniently plotted from these two points as shown in Fig. 14.13. The diagram is completed by joining AC to represent the effect of the single load W_2 between $x=0$ and $x=a$.

Similarly, S'_{max} is plotted from the two points,

$x=L-c$, $S'_{max}=0$.
$x=-c$, $S'_{max}=P$.

Then BD, completing the diagram, represents the effect of the single load W_1 between $x=L-a$ and $x=L$.

14.6. Any number of loads on a beam.—When a train of loads crosses a simply supported beam the construction of the maximum bending moment and shearing force diagrams is considerably more difficult than in the cases already considered. At any point on the beam the maximum bending moment will occur when one of the loads is over that point, but the particular load will depend upon the position of the point. A criterion to determine which load will produce the required result may be obtained as follows.

Fig. 14.14 represents a train of loads which passes over a span L,

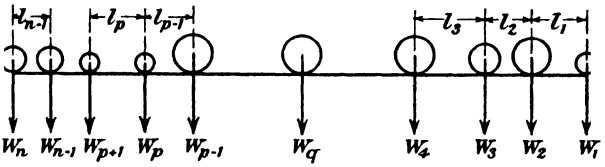

FIG. 14.14.

and we shall consider the bending moment at a point X, which is x from A, as shown in Fig. 14.1.

When the load W_p is at X, the negative bending moment at X is, from the influence line,

$$M_p=\frac{L-x}{L}[W_p x+W_{p+1}(x-l_p)+W_{p+2}(x-l_p-l_{p+1})+ \ldots +W_n(x-l_p-l_{p+1}- \ldots -l_{n-1})]$$
$$+\frac{x}{L}[W_{p-1}(L-x-l_{p-1})+W_{p-2}(L-x-l_{p-1}-l_{p-2})+ \ldots +W_1(L-x-l_{p-1}-l_{p-2}- \ldots -l_1)]$$

Similarly when W_{p+1} is at X, the negative bending moment at X is

$$M_{p+1}=\frac{L-x}{L}[W_{p+1}x+W_{p+2}(x-l_{p+1})+ \ldots +W_n(x-l_{p+1}-l_{p+2}- \ldots -l_{n-1})]$$
$$+\frac{x}{L}[W_p(L-x-l_p)+W_{p-1}(L-x-l_p-l_{p-1})+ \ldots +W_1(L-x-l_p-l_{p-1}- \ldots -l_1)]$$

M_{p+1} will be greater than M_p if

$$M_{p+1}-M_p>0.$$

Subtracting the expressions just obtained for these bending moments, collecting terms and eliminating constant multipliers, we obtain the condition

$$M_{p+1}>M_p$$

if $(L-x)[W_{p+1}+W_{p+2}+ \ldots +W_n]-x[W_p+W_{p-1}+ \ldots +W_1]>0.$

i.e. if $L[W_{p+1}+W_{p+2}+ \ldots +W_n]-x[W_1+W_2+ \ldots +W_n]>0.$

or if $$\frac{\text{Sum of loads to left of X}}{\text{Total load}}>\frac{x}{L} \quad \ldots \ldots \quad (1)$$

Suppose for example a particular load of the train, say W_q, is crossing X. Just before W_q reaches X the sum of the loads to the left of X is $W_q + \ldots + W_n$ and just after W_q has passed X the sum of the loads to the left of X is $W_{q+1} + \ldots + W_n$.

If
$$\frac{W_q + \ldots + W_n}{\sum_1^n W} > \frac{x}{L}$$

but
$$\frac{W_{q+1} + \ldots + W_n}{\sum_1^n W} < \frac{x}{L}$$

the maximum bending moment at X occurs when W_q is at X.

To illustrate this suppose the train of loads shown in Fig. 14.15 crosses a girder.

The maximum bending moment at a point one-third of the span from

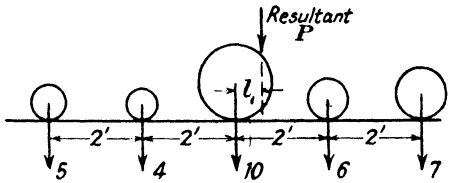

FIG. 14.15.

the left-hand support will occur when the 10-ton load is at the point, since
$$\frac{10+4+5}{32} > \frac{1}{3}$$

and
$$\frac{4+5}{32} < \frac{1}{3}.$$

The maximum bending moment at a point two-thirds of the span from the left-hand support will occur when the 6-ton load is at that point, since
$$\frac{6+10+4+5}{32} > \frac{2}{3}$$

and
$$\frac{10+4+5}{32} < \frac{2}{3}$$

In the foregoing analysis it is assumed that all the loads are on the beam. At points where this is not the case only those loads which are acting should be considered, *e.g.* when the 7-ton load has passed the right-hand support the criterion should be applied for the remaining four loads only.

The maximum bending moment which can occur under any particular load as the train crosses the girder can be determined as follows. Let AB in Fig. 14.16 represent a beam which is traversed by a train of loads and let W_p, the load we are considering, have just reached the point X. The total load is P, which acts through the centre of gravity of the system, a distance l_1 from X. Let P_L be the resultant of all the

loads on the section AX of the beam, acting at a distance l_2 from X. The bending moment at X is then

$$M_x = -R_A x + P_L l_2$$
$$= -\frac{Px}{L}(L - x + l_1) + P_L l_2.$$

This will reach a maximum value at the point where

$$\frac{dM_x}{dx} = 0,$$

i.e. when $L - 2x + l_1 = 0,$

or
$$x = \frac{L}{2} + \frac{l_1}{2} \quad \ldots\ldots\ldots \quad (2)$$

Thus, the maximum bending moment under any load occurs when the centre of the beam C bisects the distance between the centre of gravity of the load system and the load under consideration.

Once the position of the load is determined the bending moment at X can be calculated. The maximum possible bending moment on the

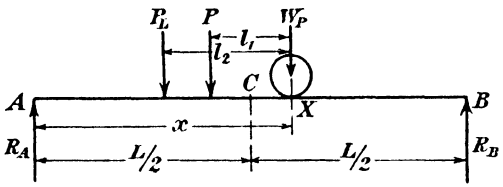

FIG. 14.16.

beam will occur under one of the loads and by applying the criterion just obtained to all loads in turn and calculating the maximum bending moment under each, the absolute maximum can be found. This is, however, a lengthy process if there are a number of loads and it is generally possible by the help of the criterion given in equation (1) to deduce the load under which the absolute maximum will occur, remembering that such maximum will be almost invariably near the centre of the span.

As an example, consider the train of loads shown in Fig. 14.15. The load of 10 tons in crossing any section changes the ratio of loads to the left of the section to the total load from $\frac{19}{32}$ to $\frac{9}{32}$. Hence from equation (1) it is evident that between points $\frac{9}{32}$ and $\frac{19}{32}$ of the span of the beam measured from the left-hand support the maximum bending moment will occur under the 10-ton load. Since this range covers the centre of the beam, it may be deduced that the absolute maximum occurs under this load, and from (2) its position will be such that P, the resultant load and the 10-ton load are each a distance $l_1/2$ from the centre of the beam. Should this disposition in any particular case place the 10-ton load outside the range over which it governs the position of maximum bending moment, the same procedure should be applied to the load on the other side of the resultant.

Maximum shearing force.—When a train of loads crosses a beam

the maximum shearing force at any point X will occur when $\Sigma W s$ in equation (1) of para. 14.2 is a maximum. In general, therefore, as will be seen from the influence line in Fig. 14.3, the maximum positive shearing force will occur when the load at one end of the train is at X and all the other loads are on the section AX. Similarly, the maximum negative shearing force will occur when the other end load is at X and all the other loads are on the section XB. This, while generally the case, is not however invariably true and conditions may arise in which the maximum occurs when part of the load has crossed X. An instance of this is afforded if the end load is small compared with the next or is separated from it by a considerable distance. It is therefore useful to determine a criterion for load position giving maximum values.

Consider the train of loads represented in Fig. 14.14 and suppose the load W_p has just reached X. Then the loads $W_p \ldots W_n$ contribute positive shearing forces and the loads $W_{p-1} \ldots W_1$ contribute negative shearing forces to the total at X.

The total shearing force at X is then, from the influence line,

$$S_p=\left[\frac{W_p x}{L}+\frac{W_{p+1}(x-l_p)}{L}+\frac{W_{p+2}(x-l_p-l_{p+1})}{L}+ \ldots + \frac{W_n(x-l_p- \ldots -l_{n-1})}{L}\right] - \left[\frac{W_{p-1}(L-x-l_{p-1})}{L}+\frac{W_{p-2}(L-x-l_{p-1}-l_{p-2})}{L}+ \ldots + \frac{W_1(L-x-l_{p-1}-l_{p-2} \ldots -l_1)}{L}\right]$$

or

$$S_p=\frac{1}{L}\left[x\sum_1^n W-\{W_{p+1}l_p+W_{p+2}(l_p+l_{p+1})+ \ldots +W_n(l_p+l_{p+1}+ \ldots +l_{n-1})\}-\{W_{p-1}(L-l_{p-1})+W_{p-2}(L-l_{p-1}-l_{p-2})+ \ldots +W_1(L-l_{p-1}-l_{p-2} \ldots -l_1)\}\right].$$

Now suppose the train to have moved forward so that W_{p+1} is at X. The shearing force at X is then

$$S_{p+1}=\frac{1}{L}\left[x\sum_1^n W-\{W_{p+2}l_{p+1}+W_{p+3}(l_{p+1}+l_{p+2})+ \ldots +W_n(l_{p+1}+l_{p+2} \ldots +l_{n-1})\}-\{W_p(L-l_p)+W_{p-1}(L-l_p-l_{p+1}) + \ldots +W_1(L-l_p-l_{p-1} \ldots -l_1)\}\right].$$

S_p will be greater than S_{p+1} if

$$S_p-S_{p+1}>0.$$

Subtracting the above expressions and simplifying the result we have

$$S_p>S_{p+1}$$

if

$$W_pL-l_p\sum_1^n W>0$$

i.e. if

$$\frac{W_p}{l_p}>\frac{\sum_1^n W}{L} \quad \ldots \ldots \ldots \quad (3)$$

In the above analysis the load W_p is supposed to have just reached X and to contribute a positive shearing force to the total at X.

If it had just passed X its contribution would be negative and the results for S_p and S_{p+1} would be modified by deducting W_p and W_{p+1} respectively.

The criterion would then become

$$S_p > S_{p+1}$$

if

$$\frac{W_{p+1}}{l_p} > \frac{\overset{n}{\Sigma} W}{L} \quad \ldots\ldots\ldots\ldots \quad (4)$$

In the consideration of maximum positive shearing forces equation (3) must be used: in considering maximum negative shearing forces, equation (4).

The two results can be combined in a single criterion by an assumption as to the direction in which the loads are moving across the girder.

It will be assumed when considering positive shearing forces that the load system moves from left to right and when considering negative shearing forces that it moves from right to left.

Let w'_q be the intensity of loading obtained by uniformly distributing any load W_q of the train over the distance between that load and the following load, and let w be the intensity of loading obtained by similarly distributing the total load over the span of the girder.

Then if $w'_q > w$, the shearing force when the leading load is at any point is *numerically* greater than when the following load is that point. If $w'_q = w$ it signifies that the shearing force at the section will be the same whether the leading or the following load is placed there.

If the section of the beam under consideration is so close to the support that some of the loads are not on the beam, w must be calculated from the total operative load and not from the total of the train of loads.

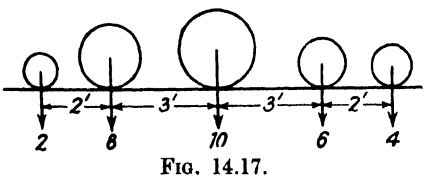

FIG. 14.17.

As an example, the train of loads shown in Fig. 14.17 will be assumed to cross beams of different spans.

In the first case let the span be 60 feet. Since the total load is 30 tons, $w = \frac{1}{2}$ ton per foot. For positive shearing forces the load is considered to move from left to right, *i.e.* the 4-ton load leads.

Then for the 4-ton load

$$w'_4 = \tfrac{4}{2} = 2 \text{ tons per foot.}$$

Similarly

$$w'_6 = \tfrac{6}{3} = 2 \text{ tons per foot,}$$
$$w'_{10} = \tfrac{10}{3} = 3{\cdot}33 \text{ tons per foot}$$

and

$$w'_8 = \tfrac{8}{2} = 4 \text{ tons per foot.}$$

Since these are all greater than w we have

$$S_4 > S_6 > S_{10} > S_8$$

and the maximum positive shearing force at any section occurs when the 4-ton load is at that section.

For negative shearing forces the train is supposed to move over the beam in the opposite direction, *i.e.* with the 2-ton load leading.

Then, $w'_2 = \frac{2}{2} = 1$ ton per foot,
$w'_8 = \frac{8}{3} = 2{\cdot}67$ tons per foot,
$w'_{10} = \frac{10}{3} = 3{\cdot}33$ tons per foot,
and $w'_6 = \frac{6}{2} = 3{\cdot}0$ tons per foot.

Here also, since all of these are greater than w, the maximum negative shearing force at any section occurs when the 2-ton load is at that section.

Suppose now that the span of the beam is 30 feet, so that $w=1$ ton per foot. As in the previous case the maximum positive shear will occur when the 4-ton load is at any section, but since for negative shearing forces $w'_2=w$, the shearing force at any section will be the same whether the 2-ton load or the 8-ton load be placed at that section.

This can be verified by considering any section and as an example, the mid-section of the beam will be taken. When the 2-ton load just reaches this section the negative shearing force there will be the left-hand reaction R_A, *i.e.* $-\frac{14}{15}$ tons, and when the 8-ton load reaches the section the shearing force there will be $-R_A+2$ or $-\frac{14}{15}$ tons.

As a final case let the span of the beam be 24 feet, so that $w=1{\cdot}25$.

For negative shearing forces, w'_2 is less than w and the greatest negative shearing force at any section will occur when the 8-ton load is at that section.

Again verifying this by reference to the mid-section of the beam, the respective shearing forces when the 2-ton and 8-ton loads reach that section are $-\frac{103}{12}$ tons and $-\frac{109}{12}$ tons.

14.7. Influence lines for framed structures.—Influence lines may be drawn to show changes of the force in any member of a framed structure as a load rolls across the truss. Such lines are of considerable importance

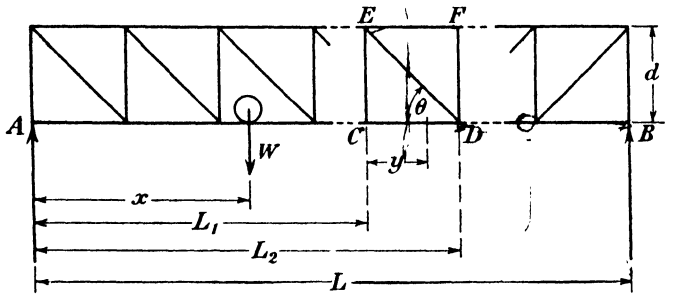

FIG. 14.18.

in bridge design and the method of drawing them is best illustrated by examples. In the first place we shall consider the truss shown in Fig. 14.18 and find the influence line for the force in a diagonal bracing member as a load rolls along the bottom chord. Let the total span of

the truss be L, and the distances of any adjacent panel points C and D from A be L_1 and L_2 respectively.

Suppose a load W to be at a distance x from A. Then if x is less than L_1, the vertical shearing force across the panel ED is

$$S_{ED}=\frac{xW}{L}$$

and the force in the member ED is

$$F_{ED}=-\frac{xW}{L}\operatorname{cosec}\theta, \quad \ldots\ldots\ldots \quad (1)$$

the negative sign denoting a compression.

If x is greater than L_2

$$S_{ED}=-\left(\frac{L-x}{L}\right)W$$

and

$$F_{ED}=\left(\frac{L-x}{L}\right)W\operatorname{cosec}\theta \quad \ldots\ldots\ldots \quad (2)$$

When the load is between two panel points the chord between these points acts as a beam and distributes the load to them. It is generally assumed that the truss is pin-jointed so that the load is divided in the inverse ratio of its distances from the panel points. If the load is between A and C or between D and B the total shear, and so the force in ED, is unaffected whether we assume this distribution to have taken place or not. If, however, the load is on the length CD the distribution affects the shearing force.

Suppose then the load to be at y from C, *i.e.* at L_1+y from A where y is less than L_2-L_1. The proportion of the load transferred to D is $\frac{yW}{L_2-L_1}$ and the shearing force across the panel ED is $R_B-\frac{yW}{L_2-L_1}$

or

$$S_{ED}=\left(\frac{L_1+y}{L}-\frac{y}{L_2-L_1}\right)W$$

and

$$F_{ED}=-\left(\frac{L_1+y}{L}-\frac{y}{L_2-L_1}\right)W\operatorname{cosec}\theta. \quad \ldots\ldots \quad (3)$$

Equations (1), (2) and (3) all represent straight lines in x or y and if W is made equal to unity they define the complete influence line for the force in ED.

When the load is at C, x in (1) is L_1 and y in (3) is zero and both equations give $F_{ED}=-\frac{L_1}{L}\operatorname{cosec}\theta$.

Similarly, when the load is at D, x in (2) is L_2 and y in (3) is L_2-L_1. Both equations then give $F_{ED}=-\frac{L-L_2}{L}\operatorname{cosec}\theta$. The influence diagram is thus seen to consist of three straight lines and this is the general case in a pin-jointed truss. Sometimes, as will be seen later, two of these lines merge into one.

To plot the diagram the two lines of equations (1) and (2) are first drawn. These are defined by the co-ordinates (0, 0), (L, $-\operatorname{cosec}\theta$)

and (0, cosec θ), (L, 0) respectively. They are parallel and are shown at AG and BJ in Fig. 14.19. Then if C and D represent any two adjacent panel points, CK and DM are drawn perpendicular to AB to cut AG and BJ at K and M. These ordinates are the values of F_{ED} at C and D respectively and if K and M are joined by a straight line this represents equation (3). The influence line of force in ED is therefore AKMB.

The lines AG and BJ are common to all influence lines for diagonal members of the truss; differences in diagrams depend only on the position of the panel under consideration. In the case shown in Fig. 14.19 the left side of the diagram is negative, indicating a compression in the diagonal member when the load is on that section of the truss. The sign depends on the direction of the diagonal: if the panel ED had been braced across the opposite diagonal the force in the bracing member would have been reversed, *i.e.* tensile when the load

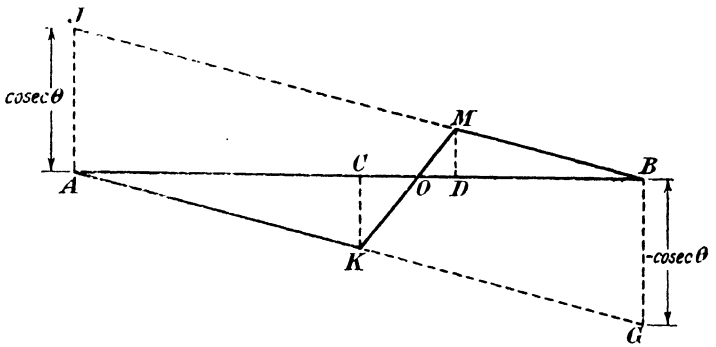

FIG. 14.19.

was on the left-hand portion of the truss and compressive when it was on the right-hand side.

The influence line for the force in a chord member, say EF, will now be drawn.

To find a general expression for the force in this member the method of sections may be used: thus by taking moments about point D we have, when $x < L_2$,

$$F_{EF} = -\frac{R_B(L-L_2)}{d} = -\frac{x(L-L_2)W}{Ld} \quad . \quad . \quad . \quad . \quad (4)$$

and when $x > L_2$,

$$F_{EF} = -\frac{x(L-L_2)W}{Ld} + \frac{(x-L_2)W}{d} = -\frac{WL_2}{Ld}(L-x) \quad . \quad . \quad . \quad (5)$$

the negative sign as before denoting that the force is compressive.

When the load is between C and D the portion transferred to D has no moment about that point and equations (4) and (5) are sufficient for the influence diagram, which consists of two straight lines instead of three as in the previous case. Making W equal to unity, convenient co-ordinates for plotting equation (4) are (0, 0) and $\left(L, -\frac{L-L_2}{d}\right)$

and for plotting equation (5) $\left(0, -\frac{L_2}{d}\right)$ and (L, 0). These lines are shown at AG and BJ in Fig. 14.20. It is evident from the geometry

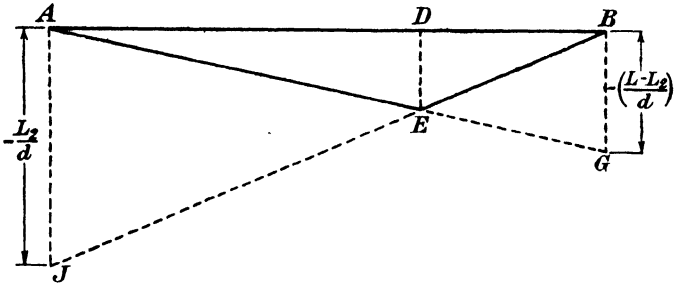

FIG. 14.20.

of the figure that they intersect at E vertically below D and the influence line is AEB.

In a similar way the influence line may be drawn for a member of the bottom chord. For this particular truss the influence lines for any member are the same whether the load be considered to roll across the top or the bottom chord but in many structures this is not the case.

As another example the Warren truss shown in Fig. 14.21 will be

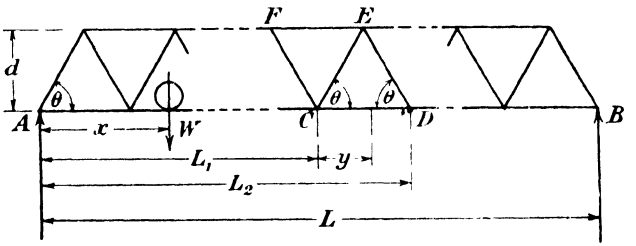

FIG. 14.21.

considered and in the first place the bottom chord will be assumed to be loaded.

When $x < L_1$

the shearing force across CE is $\frac{x}{L}W$

and
$$F_{CE} = \frac{x}{L} W \operatorname{cosec} \theta. \quad \ldots \ldots \quad (6)$$

When $x > L_2$,
$$F_{CE} = -\left(\frac{L-x}{L}\right) W \operatorname{cosec} \theta. \quad \ldots \ldots \quad (7)$$

When W is between L_1 and L_2 so that $x = L_1 + y$
$$F_{CE} = \left\{\left(\frac{L_1+y}{L}\right) - \left(\frac{y}{L_2-L_1}\right)\right\} W \operatorname{cosec} \theta \quad \ldots \ldots \quad (8)$$

As before, these equations represent three straight lines and the influence diagram is as shown in Fig. 14.22, which is obtained in exactly the same way as that in the previous case.

The force in CD can be found by the method of sections for any position of the load and since the distances of E from A and B are

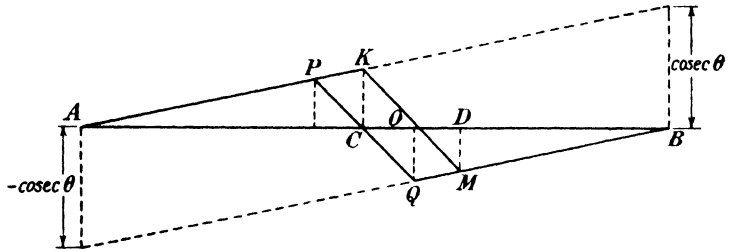

FIG. 14.22.

respectively $\frac{1}{2}(L_1+L_2)$ and $\frac{1}{2}(2L-L_1-L_2)$ the following results are obtained.

When $x<L_1$ $$F_{CD}=\frac{R_B(2L-L_1-L_2)}{2d}$$
$$=\frac{W}{2Ld}x(2L-L_1-L_2). \quad \ldots\ldots\ldots \quad (9)$$

This is a linear relationship and gives values for F_{CD} of 0 and $\frac{WL_1}{2Ld}(2L-L_1-L_2)$ when x is 0 and L_1 respectively.

When $x>L_2$, $$F_{CD}=\frac{R_A(L_1+L_2)}{2d}$$
$$=\frac{W}{2Ld}(L-x)(L_1+L_2) \quad \ldots\ldots\ldots \quad (10)$$

which is also a straight line, F_{CD} being $\frac{W}{2Ld}(L-L_2)(L_1+L_2)$ and 0 when x is L_2 and L respectively.

When x lies between L_1 and L_2,

$$F_{CD}=\frac{R_B}{2d}(2L-L_1-L_2)-\left(\frac{x-L_1}{L_2-L_1}\right)\left(\frac{L_2-L_1}{2}\right)\frac{W}{d}$$
$$=\frac{W}{2Ld}\{x(L-L_1-L_2)+LL_1\} \quad \ldots\ldots\ldots \quad (11)$$

This is a straight line, the values of F_{CD} when x is L_1 and L_2 being $\frac{WL_1}{2Ld}(2L-L_1-L_2)$ and $\frac{W}{2Ld}(L-L_2)(L_1+L_2)$ as obtained for the same points from equations (9) and (10).

If W is made equal to unity these three lines complete the influence diagram. Those represented by the first two equations may be plotted from the co-ordinates (0, 0), $\left(L, \frac{2L-L_1-L_2}{2d}\right)$ and $\left(0, \frac{L_1+L_2}{2d}\right)$, (L, 0) respectively and are shown in Fig. 14.23. If from C and D

perpendiculars are drawn to cut these lines at G and H and points G, H are joined the complete influence diagram is AGHB.

When the top chord is loaded the diagrams obtained will be of the same general shape but since the nodes of the top chord are not vertically above those of the bottom chord the three lines forming the diagrams will not terminate at the same points as when the bottom chord is loaded, *e.g.* the influence diagram for the force in CE will be APQB in Fig. 14.22 instead of AKMB as before.

From these diagrams it is easy to determine the worst position of a uniformly distributed load for any particular member. From Fig. 14.20 or 14.23, for example, it is clear that the worst load in any chord member will occur when the whole truss is loaded. If the load is of such length that the whole span cannot be covered by it, it must be arranged in such a way that the area of the diagram over the load is a maximum. In the case of a truss in which the influence diagram is formed of two lines, as in Fig. 14.20, this is done exactly as in para-

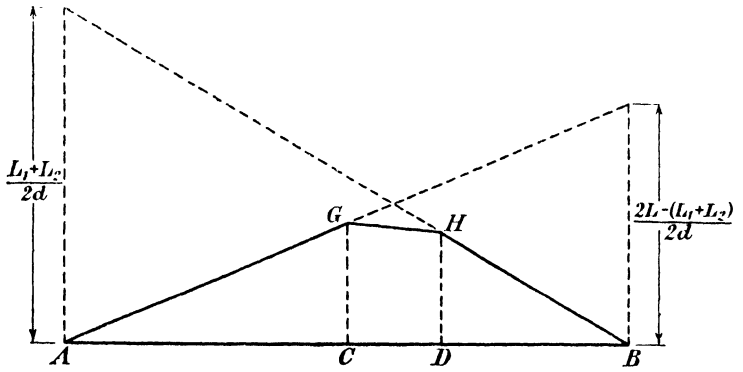

Fig. 14.23.

graph 14.4, the result obtained there being directly applicable. When the diagram consists of three lines as in Fig. 14.23, the disposition of load will depend on its length relative to a bay of the truss and a general solution is cumbersome.

The maximum load in a diagonal member will occur either when AO or OB (Fig. 14.19) is completely covered. In the first case the load will be the maximum compression and in the second the maximum tension. The position of O is found thus :—

From the similar triangles OCK and ODM,

$$\frac{OC}{OD} = \frac{CK}{MD}$$

Since BJ and AG are parallel the triangles AKC, BMD are similar and

$$\frac{CK}{MD} = \frac{AC}{BD}$$

Hence

$$\frac{OC}{OD} = \frac{AC}{BD} = \frac{L_1}{L-L_2}.$$

If the load is of insufficient extent to cover these lengths the positions for the maximum areas to be enclosed may be found as in paragraph 14.4.

14.8. Influence lines for three-pinned arch.—Let ACB in Fig. 14.24 be a three-hinged arch of any shape.

The load W is at y from A where y is less than L_1. The line of action of the resultant reaction at B must pass through C and the sides BO,

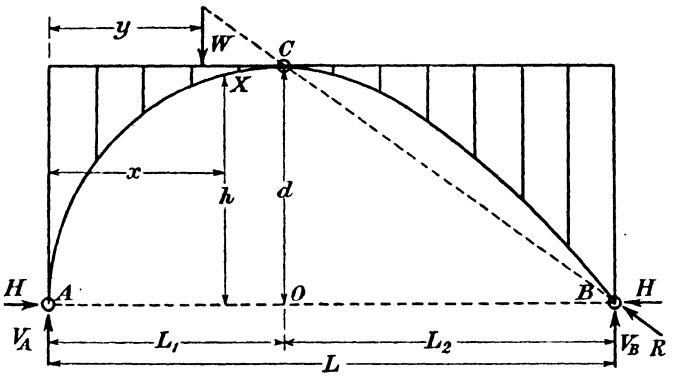

FIG. 14.24.

OC and BC of the triangle BOC represent to scale the forces H, V_B and R.

Then
$$H=\left(\frac{OB}{OC}\right)V_B$$
$$=\frac{L_2yW}{Ld} \quad \ldots\ldots\ldots\ldots \quad (1)$$

where $L=L_1+L_2$.

This is a straight line and is the influence line for H for positions of the load between A and C.

When $y=L_1$,
$$H=\frac{L_1L_2W}{Ld}$$

which is the maximum value of H.

A corresponding line is obtained for the load between B and C, taking the origin at B and measuring y to the left.

The influence diagram is then ADB in Fig. 14.25, the two lines being plotted from the co-ordinates (0, 0), $\left(L, \frac{L_2}{d}\right)$ and $\left(0, \frac{L_1}{d}\right)$, (L, 0).

To obtain the influence line of bending moments it is necessary to consider the load in three regions.

If X is any point between A and C at a distance x from A we have when $y<x$,

$$M_x=Hh-V_B(L-x)$$
$$=\frac{L_2yWh}{Ld}-\frac{yW}{L}(L-x)$$
$$=\frac{Wy}{L}\left\{\frac{L_2h}{d}-(L-x)\right\}. \quad \ldots\ldots\ldots \quad (2)$$

When y lies between x and L_1

$$M_x = Hh - V_A x,$$

$$= \frac{L_2 y W h}{Ld} - \frac{x(L-y)W}{L}$$

$$= \frac{W}{L}\left\{\frac{L_2 h y}{d} - x(L-y)\right\}. \quad \ldots\ldots\ldots \quad (3)$$

When $y > L_1$,

$$H = \frac{L_1(L-y)W}{Ld} \qquad \text{by analogy with (1)}$$

and

$$M_x = Hh - V_A x$$

$$= \frac{L_1(L-y)Wh}{Ld} - \frac{x(L-y)W}{L}$$

$$= \frac{W(L-y)}{L}\left\{\frac{L_1 h}{d} - x\right\}. \quad \ldots\ldots\ldots \quad (4)$$

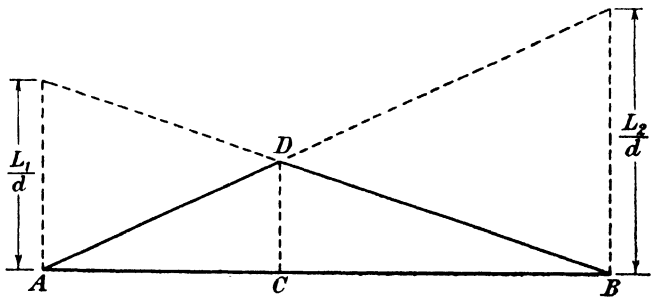

FIG. 14.25.

These three linear equations define the influence diagram of bending moments.

When $y = x$, (2) and (3) give

$$M_x = \frac{Wx}{L}\left\{\frac{L_2 h}{d} - (L-x)\right\}. \quad \ldots\ldots\ldots \quad (5)$$

When $y = L_1$, (3) and (4) give

$$M_x = \frac{WL_2}{L}\left\{\frac{L_1 h}{d} - x\right\}. \quad \ldots\ldots\ldots \quad (6)$$

When $y = 0$ and L, $M_x = 0$ from (2) and (4) respectively.

The result obtained from equation (5) will always be negative and that from equation (6) will be positive. The bending moment at X when the load is at X will be numerically greater than when it is at C if

$$\frac{Wx}{L}\left\{\frac{L_2 h}{d} - (L-x)\right\} + \frac{WL_2}{L}\left\{\frac{L_1 h}{d} - x\right\} \qquad \text{is negative,}$$

i.e. if

$$\frac{xL_2 h}{d} - x(L-x) + \left(\frac{L_1 L_2 h}{d} - xL_2\right) < 0,$$

or $$\frac{L_2 h}{d}(x+L_1)-x(L_2+L-x)<0,$$

i.e. if $$\left(\frac{L_2 h}{d}+x\right)(x+L_1)<2xL.$$

This condition is not always satisfied and the maximum bending moment at X may occur either when the load is at X or at C. The influence diagram is shown in Fig. 14.26. The curve of maximum

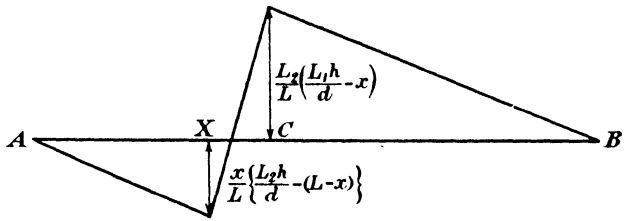

FIG. 14.26.

negative bending moments can now be found from (5) by giving x all values from 0 to L_1 and as a particular case we will take that of a semi-circular arch with a centre pin.

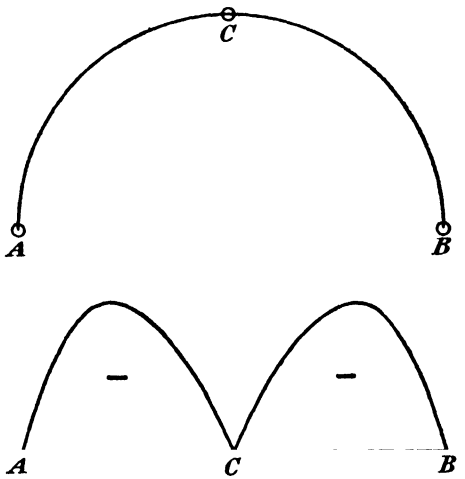

FIG. 14.27.

Then $$L_1=L_2=L/2,$$

$$\frac{h}{d}=\frac{2\sqrt{x(L-x)}}{L}$$

and $$M_x=\frac{Wx}{L}\{\sqrt{x(L-x)}-(L-x)\}.$$

This is zero at $x=0$ and at $x=\frac{L}{2}$, and the curve of maximum negative bending moments is shown in Fig. 14.27.

14.9. Conventional load systems.—The exact calculation of the maximum bending moments and shearing forces at all sections of a bridge as a train of loads passes across it is very laborious and the uncertainties introduced by the dynamic effects of the system travelling at high speed are such that extreme accuracy in calculation is not justified. It is usual therefore in design to adopt conventional systems of load to simplify the procedure.

One method assumes that the effect of a train of wheels can be reproduced by an equivalent uniformly distributed load. It has already been shown that when a single load traverses a girder the curve of maximum bending moments is a parabola having a maximum ordinate $\frac{WL}{4}$ at the centre of the span: if the concentrated load be supposed to be replaced by a uniformly distributed load of intensity w it is necessary, if the maximum bending moments are to be the same, to make

$$\frac{wL^2}{8} = \frac{WL}{4}$$

i.e.

$$w = \frac{2W}{L}.$$

The bending moments at all points when this equivalent load w covers the span will be the same as those under the concentrated load W as it traverses the girder. The maximum shearing forces caused by both systems will also be the same at the ends of the beam but for no other points, since in the case of the concentrated load the curves of maximum shearing force are straight lines whilst in the case of the uniformly distributed load they are parabolas.

When the train consists of a number of concentrated loads the curve of maximum bending moments can be enveloped by a curve which approximates to a parabola but which is rather flatter at midspan and steeper at the ends than a true parabola. It is thus impossible to obtain exact agreement at all points when a uniformly distributed load is substituted for the train. If a parabola is drawn which has the same area as the true curve the ordinates of the two curves are equal at about the quarter-point of the span and one approximate method of determining the effect of a train of loads is to calculate the maximum bending moment they produce at the quarter-point and to make the equivalent uniformly distributed load of such magnitude that it gives the same value at that point.

The bending moment at the quarter-point of the span under a uniformly distributed load of intensity w is $\frac{3wL^2}{32}$ and if the calculated maximum bending moment at the same point due to the actual load system is M′ the equivalent load is

$$w = \frac{32M'}{3L^2}.$$

This equivalent load gives a bending moment at the centre of the

span rather greater and near the end rather less than the correct values. Agreement between the true bending moment and that due to a uniformly distributed load may be obtained for any point other than the quarter span by using a different value of w and if a number of bridges have to be designed for the same rolling load system it is worth while to determine the values of w appropriate to a number of points along the span. Once tables or curves embodying these data have been obtained they can be applied very simply to the design of any bridge subjected to the particular load system, but unless the number to be designed is considerable the time involved in obtaining the data will not be justified.

In general, if M′ is the true bending moment caused at the $\frac{1}{n}$-th point of the bridge by the actual load system and w the equivalent distributed load which produces the same bending moment at this point we make

$$M' = \frac{w}{2}\left(\frac{n-1}{n^2}\right)L^2$$

or

$$w = \frac{2n^2M'}{(n-1)L^2}.$$

In American railway practice use is made of a number of conventional load systems proposed by Mr. Theodore Cooper in 1894. These are so designed that any two of them are connected by a constant multiplier. The system consists of two engines followed by a train. An

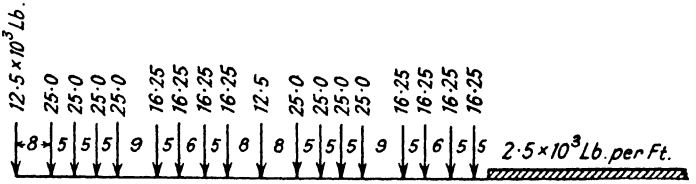

Loads are those on one rail.

FIG. 14.28.

example which represents the E.50 loading on one line of rail is shown in Fig. 14.28.

When a system of this type is in general use the method of calculation by the use of equivalent distributed loads varying for different points on the span is very satisfactory since curves giving these equivalent loads can be standardised.*

The shearing force across a panel cannot be calculated directly from the equivalent loads for bending moments but a simple device enables the same data to be used for this purpose.

Fig. 14.29 shows a truss and the influence line of shearing force for the panel CD. The panels are of equal length l. Suppose that any system of loads is placed on the section AO of the truss and let P_L

* Such curves for E.50 loading are given in "Modern Framed Structures," by Johnson, Bryan and Turneaure. 9th edition. Vol. I, p. 251.

and P_R be the resultants of the loads to the left and right of C respectively.

These resultants act at a distance a from A and b from C. It is evident from the geometry of the diagram that

$$OC=\frac{nl}{N-1}\ ;\quad AO=\frac{Nnl}{N-1}$$

and C is the $\frac{1}{N}$th point of the length OA.

Suppose the length AO to be a simply supported beam, then the bending moment at C, due to the load system, is

$$M_C=-R_0\,.\,CO+P_R\,.\,b$$

where R_0 is the reaction at O.

i.e.
$$M_C=-CO\left\{\frac{aP_L}{AO}+\left(\frac{AC+b}{AO}\right)P_R\right\}+P_Rb.$$

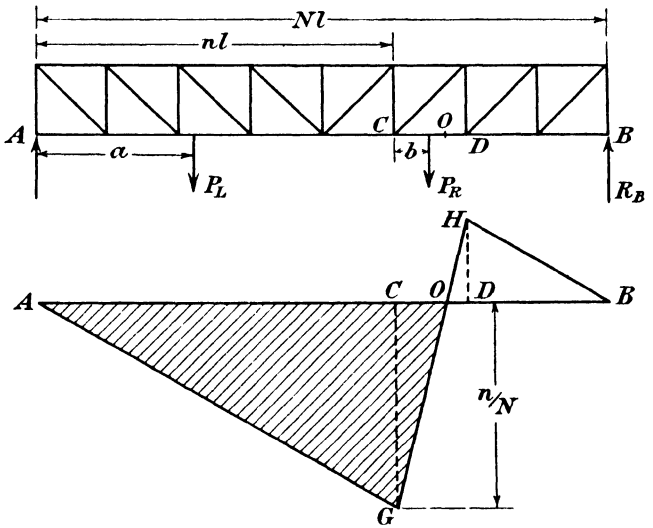

FIG. 14.29.

On substituting for the lengths this becomes

$$M_C=-\frac{1}{N}\{aP_L+(nl+b)P_R-NbP_R\}.$$

Now consider the complete span AB.

The shearing force across the panel CD is

$$S_{CD}=R_B-\frac{b}{l}P_R$$

which gives, on substitution for R_B,

$$S_{CD}=\frac{1}{Nl}\{aP_L+(nl+b)P_R-NbP_R\},$$

i.e. for any system of loads on AO,

$$M_C=lS_{CD}\text{ numerically}\quad\ldots\ldots\quad(1)$$

Now let w_s be the uniformly distributed load which will give the same maximum shearing force across the panel CD as the actual load system considered. This will occur when the length AO is covered and then

$$S_{CD}=w_s(\text{area AOG})$$

$$=w_s\times\frac{n}{N}\times\frac{Nnl}{2(N-1)}$$

or

$$S_{CD}=\frac{w_s n^2 l}{2(N-1)}.$$

Hence the true bending moment at C on a span of length AO is, from equation (1),

$$M_C=\frac{w_s n^2 l^2}{2(N-1)}. \quad \ldots\ldots\ldots \quad (2)$$

Now the influence line of bending moments for point C on the span AO is a triangle similar to AOG, the ordinate CG being given by $\frac{AC\,.\,CO}{AO}$ *i.e.* by $\frac{nl}{N}$.

From the tables or curves of equivalent loading already prepared we determine the value appropriate to the $\frac{1}{N}$th point on a span of length AO. If this is w, the correct bending moment at C is, from the influence line,

$$\frac{w}{2}\times AO\times\frac{nl}{N}$$

or

$$M_C=\frac{wn^2l^2}{2(N-1)}.$$

Equating this to the value given in (2) we obtain

$$w_s=w. \quad \ldots\ldots\ldots \quad (3)$$

Hence, to determine the true value of the shearing force across the panel CD, we assume AO to carry the uniform load which produces the correct bending moment at the $\frac{1}{N}$th point on a span AO.

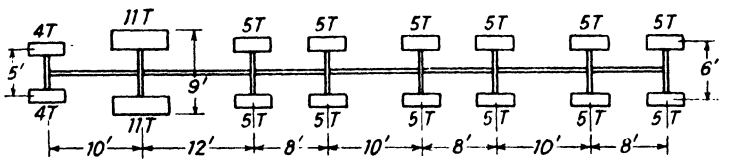

FIG. 14.30.

Another method of conventional design may be illustrated by reference to the requirements of the Ministry of Transport for Highway bridges. Fig. 14.30 shows the standard train of loads which is assumed

to cross the bridge and for calculation purposes this is reduced to an equivalent distributed load, which varies with the loaded length of the bridge as shown in Fig. 14.31, and a single concentrated load. The equivalent load is plotted from the values in Table 14.1.

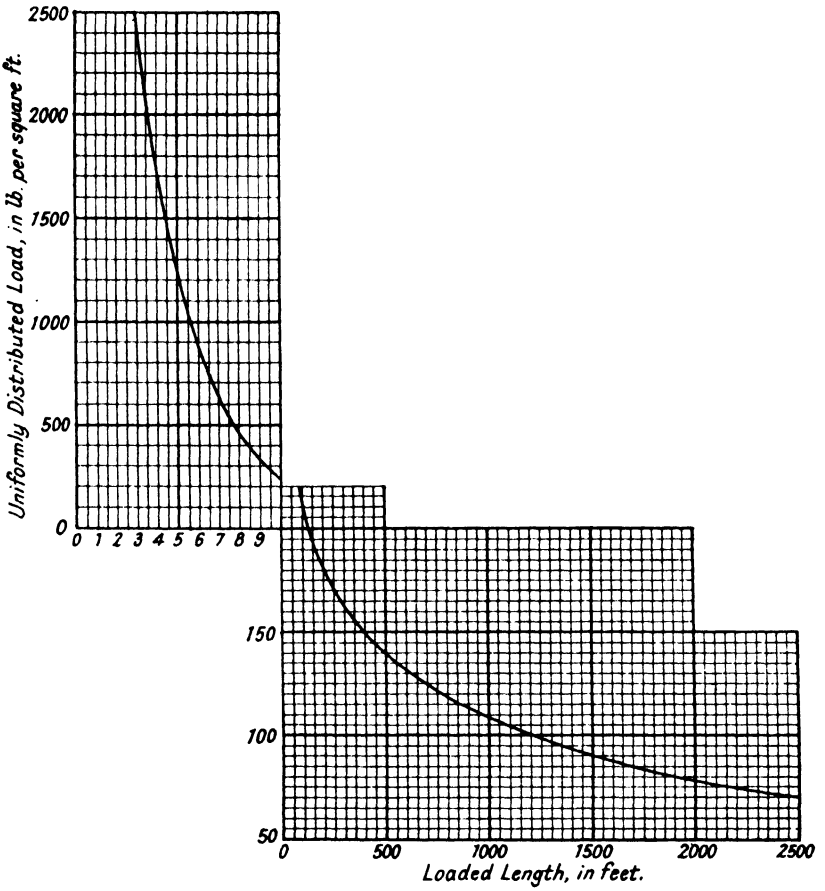

FIG. 14.31.

The " loaded length " is that length of the bridge which when loaded produces the worst effect at any particular section and in general it is found from the influence diagram. In a freely supported girder the " loaded length " is the full span for the calculation of bending moments and the portion between one support and the section under consideration for the calculation of shearing forces.

In addition to the effect of the uniformly distributed load a concentrated load of 2,700 lb. per foot width of the bridge is assumed to act at that section where it will produce the most effect, *e.g.* for the bending moment at midspan it would be placed at the midspan point and for shearing force it would be placed at the section for which the calculation is made.

TABLE 14.1.

Loaded length		lb./sq. ft.	Loaded length	lb./sq. ft.	Loaded length	lb./sq. ft.
feet	inches		feet		feet	
3	0	2,420	100	208	1,200	100
3	6	2,020	150	192	1,300	97
4	0	1,700	200	180	1,400	94
4	6	1,445	250	170	1,500	90
5	0	1,225	300	163	1,600	88
5	6	1,033	350	156	1,700	85
6	0	872	400	150	1,800	82
6	6	735	450	145	1,900	79
7	0	625	500	140	2,000	77
7	6	525	600	132	2,100	76
8	0	444	700	125	2,200	74
8	6	374	800	119	2,300	73
9	0	314	900	114	2,400	72
9	6	265	1,000	108	2,500 and over	70
10 to 75	0 to 0	220	1,100	104	—	—

14.10. Dynamical loads on bridges.—It has long been recognised that the stresses in a bridge are not due simply to the static effects of the loads which traverse it: dynamical effects play a very important part and a structure designed without due consideration of these would have an actual carrying capacity very much below that estimated.

The customary method of dealing with this problem prior to 1928 was by the introduction of an impact factor: the live loads were multiplied by this factor and the stresses obtained on the assumption that these increased loads actually traversed the bridge. The impact factor was usually calculated from an empirical formula, the most widely used up to 1920 being the Pencoyd formula, according to which the actual loads were multiplied by the term $\left(1+\frac{300}{300+l}\right)$, where l was the span of the bridge in feet: in 1920 this formula was modified by the Ministry of Transport to $\left(1+\frac{120}{90+1{\cdot}5l}\right)$. The impact factor was thus assumed to be merely a function of the span and this assumption was common to the many other formulas proposed for the purpose of calculating impact allowances.

In 1923 a Committee of the Department of Scientific and Industrial Research, under the Chairmanship of the late Sir Alfred Ewing, was set up to investigate the whole problem of impact on railway bridges and a comprehensive report was published in 1928.* This report was

* "Report of the Bridge Stress Committee." H.M. Stationery Office, 1928.

amplified by Professor C. E. Inglis, F.R.S., in a paper to the Institution of Civil Engineers * and later in a book dealing with the mathematical treatment of vibrations in railway bridges.† These three publications have placed a difficult problem upon a scientific basis and very close approximations to the dynamical effects of a train upon a bridge can now be made.

When a train crosses a bridge there is a certain amount of vibration due to the sudden application of the load; irregularities in the track and the presence of rail joints also cause impact effects which are irregular and incalculable. These, however, were found by the Committee to be completely overwhelmed by another cause of vibration. The driving-wheels of a locomotive are balanced for the inertia effects of the reciprocating parts and the centrifugal effect of these revolving balance weights causes the pressure of the wheel on the rail to undergo a periodic variation; this effect is known as hammer-blow and the peak value of the pressure which occurs at intervals of distance equal to the circumference of the driving-wheel may be very high. This hammer-blow is the main cause of the vibrations set up in a bridge and since it occurs periodically the effect can be investigated mathematically. The considerable amount of experimental data obtained by the Bridge Stress Committee from tests on actual bridges have shown that applications of the mathematical analysis lead to very accurate estimates of the true values of the stresses produced by vibration.

The analysis is too long to be reproduced here and Professor Inglis' book should be consulted, but the general principles underlying the problem must be mentioned.

A locomotive is supported on springs and the effect of these is considerable: if it crosses a bridge at low speeds the vibrations set up are so small that the springs do not come into operation and the locomotive acts as if it were non-spring-borne. At higher speeds, since the hammer-blow varies in intensity as the square of the speed, the vibrations are greater and may reach an amplitude which brings the springs into action. This results in a damping of the oscillations, since the spring-borne part of the mass is out of phase with the non-spring-borne portion. The two cases corresponding to non-spring-borne and spring-borne loads both produce distinct resonance; the second being that which must be considered in bridges of moderate span.

In its unloaded state any bridge has a natural frequency which is decreased by the addition of a mass at any point; as the locomotive passes across it, therefore, the natural frequency of the loaded bridge changes. This natural frequency depends on whether the loads are spring-borne or not; if they are, the frequency may even be raised above that for the unloaded bridge.

This variation of natural frequency tends to increase safety, for, unless the speed of the locomotive is so adjusted that the peak values

* "Impact on Railway Bridges." C. E. Inglis. Proc. Inst. C.E., Vol. 234, 1931–2.

† "A Mathematical Treatise on Vibrations in Railway Bridges." C. E. Inglis. Camb. Univ. Press, 1934.

of the hammer-blow synchronise with the natural frequency at every point, the dangers of resonance are reduced.

Other factors which limit the cumulative effects of hammer-blow are the restriction imposed by the length of span upon the number of impulses given to the bridge and the damping exercised by the imperfect elasticity of the bridge, ballast, piers, etc.

In view of what has been said it is evident that it is impossible to specify a single critical speed for a given engine on a given bridge. Since, however, the worst effect will be produced when the centre of gravity of the engine is at the centre of the bridge in its most heavily loaded state the Committee defined critical speed as that engine speed at which the frequency of the hammer-blow coincides with the natural frequency of the loaded structure at the instant when the load is over the middle of the bridge.

The frequency of a long bridge is less than that of a short one and the Committee classified bridges according to the following scheme :—

Long spans.—In these the maximum effects occur at speeds such that the locomotive can be considered as non-spring-borne, *i.e.* at the lower critical speed.

Medium spans.—In these the maximum effects are produced at the higher critical speed, *i.e.* when the oscillations are sufficient to bring the springs of the locomotive into action.

Short spans.—In these the frequency is so great that no attainable frequency of hammer-blow can produce resonance.

This classification cannot be interpreted merely in terms of the actual length of a bridge, since the frequency is affected both by the depth of the girders through the influence of this term on the second moment of area of the cross-section and also by the mass of the structure.

When a bridge oscillates due to the passage of a locomotive the stresses caused in the members arise from three separate causes as follows :—

(1) From the statical effects of the mass of the locomotive.
(2) From the hammer-blow which varies periodically as the locomotive crosses the span.
(3) From the forces due to the acceleration of the masses composing the bridge as it oscillates.

Professor Inglis has shown that for long and medium span bridges the last can be represented by additional loads on the bridge and that little error is caused if these are assumed to include the effect under (2).

The practical way to allow for impact effects on a bridge is therefore to superimpose the effects of equivalent loads upon those caused by the statical loads of the train as it crosses the bridge. The methods of calculating these equivalent loads will be considered in the next paragraph.

14.11. Calculation of impact allowance on railway bridges.—In the following treatment, due to Professor Inglis, it is assumed that the bridge is of uniform section and mass freely supported at the ends and

that the locomotive consists of a mass which is spring supported on a single pair of wheels and axle. In an actual bridge the section and mass vary along the span but little error is introduced by assuming an idealised uniform bridge having a constant second moment of area equal to that at the mid cross-section and the average mass per unit length.

Let M_G be the total mass of the bridge in tons,
l, the span in feet,
m, the mass per unit length,
I, the second moment of area of the cross-section in feet units,
M, the total mass of the locomotive (excluding tender) in tons,
M_S, the spring-borne mass of the locomotive,
M_U, the non-spring-borne mass of the locomotive,
n_s, the frequency for free vertical oscillations of M_S on its springs,
F, the total frictional force resisting spring movement,
N, the revolutions per second of the driving wheels,
v, the speed of the locomotive,
$n=\frac{v}{2l}$,
P sin $2\pi Nt$, the hammer-blow at N revolutions per second in tons,
$P_1N^2=P$, the intensity of the hammer-blow at N revolutions per second,
and E, the modulus of elasticity of the material of the bridge in tons-inch units.

These constitute the data for a solution of the problem and are supposed to be known or calculable with sufficient accuracy. Then the fundamental frequency of the unloaded bridge is given by

$$n_0=10{\cdot}83\frac{\pi^2}{l^2}\sqrt{\frac{EIl}{M_G}} \quad . \quad . \quad . \quad . \quad . \quad . \quad . \quad . \quad (1)$$

where M_G, I and l are in tons and feet units and E is in tons per square inch.

If the bridge carries extra masses M_1, M_2 . . . etc., at distances of a_1, a_2 . . . etc., from one end of the span, this frequency is reduced to

$$n_0\sqrt{\frac{M_G}{M_G+2\left(M_1\sin^2\frac{\pi a_1}{l}+M_2\sin^2\frac{\pi a_2}{l}+\ldots\right)}} \quad . \quad . \quad . \quad . \quad (2)$$

The central deflection of the bridge in feet under a static load of P tons at the centre of the span is

$$D_P=\frac{Pg}{2\pi^2n_0^2M_G} \quad . \quad . \quad . \quad . \quad . \quad . \quad . \quad . \quad (3)$$

For an alternating force of P sin $2\pi Nt$ acting at a section which is a distance a from the end of the span the central deflection is

$$D_P \frac{\sin(2\pi Nt-\alpha)\sin\frac{\pi a}{l}}{\left\{\left(1-\frac{N^2}{n_0^2}\right)^2+\left(\frac{2Nn_b}{n_0^2}\right)^2\right\}^{\frac{1}{2}}}, \quad \ldots\ldots\ldots (4)$$

where $$\tan\alpha=\frac{2Nn_b}{n_0^2-N^2}$$

and n_b is the damping coefficient of the bridge, the ratio of successive deflections of the bridge when the oscillating force is removed being $l^{-2\pi\frac{n_b}{n}}$. A formula for n_b for spans between 80 and 300 feet has been deduced from the experimental results obtained by the Bridge Stress Committee as follows:

$$n_b=\frac{l}{M_G}\left(0{\cdot}12+\frac{0{\cdot}63\times10^6}{l^3}\right). \quad \ldots\ldots\ldots (5)$$

The magnitude of the hammer-blow varies considerably: in the Report of the Bridge Stress Committee data are given relating to 173 engines and an analysis of this list shows that its magnitude was as follows:

In 27 cases it lay between the values					0	and $\cdot138N^2$ tons.
,, 44	,,	,,	,,	,,	$\cdot138N^2$	and $\cdot278N^2$,,
,, 59	,,	,,	,,	,,	$\cdot278N^2$	and $\cdot417N^2$,,
,, 31	,,	,,	,,	,,	$\cdot417N^2$	and $\cdot556N^2$,,
,, 8	,,	,,	,	,,	$\cdot556N^2$	and $\cdot694N^2$,,
,, 4	,,	,,	,,	,,	$\cdot694N^2$	and $\cdot833N^2$,,

Since the bridge is affected so vitally by this factor it is evident that exact data relating to the particular classes of locomotives which will use it should be obtained prior to design: otherwise a very large value must of necessity be assumed to ensure the safety of the structure.

The cases of long, medium and short span bridges must be dealt with separately, since the conditions controlling their oscillations are different, as explained in the previous paragraph. The oscillations are greatest when the locomotive is not followed by a train, the presence of which tends to damp them, and four separate cases of loading are considered as follows:

Case (1). Single locomotive on a single track bridge.

Case (2). Two similar locomotives separated by a distance d on a single track bridge.

Case (3). Two similar locomotives arriving simultaneously at the centre of a double track bridge.

Case (4). Two similar locomotives as in Case (2) on each track of a double track bridge.

Long span bridges.—In this class are included all bridges in which the oscillations are not sufficient to overcome the friction of the springs on the locomotive. If $\delta \sin 2\pi Nt$ is the maximum vertical displacement of the wheels the springs will remain locked if

$$\delta<\frac{Fg}{4\pi^2N^2M_S} \quad \ldots\ldots\ldots (6)$$

TABLE 14.2.

FORMULAS FOR LONG SPAN BRIDGES.

1			2	3	4	5	6
Case			N/n_0	n_b'/n_b	Dynamic increment of central deflection. δ_0 feet	Uniformly distributed load for dynamic bending moments. Tons	Allowance for dynamic shear at a from far end of span. Tons
No.	No. of tracks	No. of locos.					
1	One.	One.	$\sqrt{\frac{M_G}{M_G+2M}}$	$\left(\frac{N}{n_0}\right)^2$	$\frac{D_P}{2}\frac{N}{\sqrt{n^2+n_b'^2}}$	$\left(M_G+\frac{\pi^2 M}{4}\right)\delta_0 N^2$	$\frac{\pi}{8}\left[-M_G\cos\frac{\pi a}{l}+M\frac{\pi a}{l}\sin\frac{\pi a}{l}\right]\delta_0 N^2$
2	One.	Two. Separated by distance d.	$\sqrt{\frac{M_G}{M_G+4M\cos^2\frac{\pi d}{2l}}}$	$\left(\frac{N}{n_0}\right)^2$	$D_P\cos\frac{\pi d}{2l}\frac{N}{\sqrt{n^2+n_b'^2}}$	$\left(M_G+\frac{\pi^2 M}{2}\frac{(l-d)}{l}\cos\frac{\pi d}{2l}\right)\delta_0 N^2$	$\frac{\pi}{8}\left[-M_G\cos\frac{\pi a}{l}+M\frac{\pi a}{l}\sin\frac{\pi a}{l}+M\frac{\pi(a-d)}{l}\sin\frac{\pi(a-d)}{l}\right]\delta_0 N^2$
3	Two.	One on each track, reaching centre of span simultaneously.	$\sqrt{\frac{M_G}{M_G+4M}}$	$\left(\frac{N}{n_0}\right)^2$	$D_P\frac{N}{\sqrt{n^2+n_b'^2}}$	$\left(M_G+\frac{\pi^2 M}{2}\right)\delta_0 N^2$	$\frac{\pi}{8}\left[-M_G\cos\frac{\pi a}{l}+2M\frac{\pi a}{l}\sin\frac{\pi a}{l}\right]\delta_0 N^2$
4	Two.	Two. Separated by distance d on each track.	$\sqrt{\frac{M_G}{M_G+8M\cos^2\frac{\pi d}{2l}}}$	$\left(\frac{N}{n_0}\right)^2$	$2D_P\cos\frac{\pi d}{2l}\frac{N}{\sqrt{n^2+n_b'^2}}$	$\left(M_G+\frac{\pi^2 M}{l}\frac{(l-d)}{l}\cos\frac{\pi d}{2l}\right)\delta_0 N^2$	$\frac{\pi}{8}\left[-M_G\cos\frac{\pi a}{l}+2M\frac{\pi a}{l}\sin\frac{\pi a}{l}+2M\frac{\pi(a-d)}{l}\sin\frac{\pi(a-d)}{l}\right]\delta_0 N^2$

and this is the criterion as to whether a particular bridge falls into the category of long span.

The formulas for use in calculating the impact allowance for long span bridges are given in Table 14.2 and the procedure is as follows. First determine n_0 from equation (1) or (2): N, the speed of the driving wheels which produces the maximum dynamical deflection is then found from the formula in column 2 of the table.

The coefficient of damping, n_b, is calculated from equation (5) and column 3 enables n_b' to be found.

The dynamic increment of central deflection, δ_0, is then obtainable from the formula in column 4 and on substituting this in the formula of column 5 we find the total load which must be distributed uniformly along the span to allow for the extra bending moments produced by the oscillation of the bridge. The allowance for dynamic shearing force is calculated from the formula in column 6 which gives the maximum shearing force produced at a distance a from the farther end of the span.

Medium span bridges.—The greatest dynamical effect on bridges in this category is found by considering the locomotive to be stationary at the centre of the bridge while its wheels skid at a constant speed N. If there are two locomotives they are spaced equally about the centre. The first step, as in the case of long span bridges, is to calculate the fundamental frequency n_0 from equation (1) or (2). This done, the value of N for which the bridge oscillations are greatest is found from the equation

$$N^4 - N^2 n_1^2 \left(1 + \frac{n_s^2}{n_2^2}\right) + n_1^2 n_s^2 = 0. \quad . \quad . \quad . \quad . \quad . \quad (7)$$

This is solved as a quadratic in N^2, the greatest of the two roots being that required.

The values of n_1^2 and n_2^2 are given in Table 14.3.

TABLE 14.3.

Case	$\frac{n_1^2}{n_0^2}$	$\frac{n_2^2}{n_0^2}$
1	$\frac{M_G}{M_G+2M_U}$	$\frac{M_G}{M_G+2M}$
2	$\frac{M_G}{M_G+4M_U \cos^2 \frac{\pi d}{2l}}$	$\frac{M_G}{M_G+4M \cos^2 \frac{\pi d}{2l}}$
3	$\frac{M_G}{M_G+4M_U}$	$\frac{M_G}{M_G+4M}$
4	$\frac{M_G}{M_G+8M_U \cos^2 \frac{\pi d}{2l}}$	$\frac{M_G}{M_G+8M \cos^2 \frac{\pi d}{2l}}$

The value of n_s is given approximately by the formula

$$n_s = \frac{1}{2\pi}\sqrt{\frac{\mu_1+\mu_2+\ldots+\mu_n}{M_S}g} \quad \ldots\ldots\ldots (8)$$

in which $\mu_1 \ldots \mu_n$ are the stiffnesses of the different axle springs of the locomotive, *i.e.* the loads required to produce unit deflections measured in tons per foot. This formula assumes that the values of μ for all the axle springs are appreciably the same, so that if a load were applied to the centre of gravity of the spring-borne mass of the locomotive this mass would sink without any angular movement. An average value for n_s found by the Bridge Stress Committee was 3.

The value of N found from equation (7) which will be denoted by N_2 may be greater than the permissible speed, which may be taken as 6. The subsequent calculation will depend on whether N_2 is less than or greater than this limiting value.

If it is less than the limiting value the formulas in Table 4.14, column 2, are used to determine the central dynamic deflection δ_0: if greater, the appropriate equation of column 4 is first solved for n_d the functions of N in these equations being,

$$\phi(N) = \frac{N^4}{n_1^2} - N^2\left(1+\frac{4n_b n_d}{n_0^2}+\frac{n_s^2}{n_2^2}\right)+n_s^2,$$

and

$$\psi(N) = 2N\left(n_d\frac{n_2^2-N^2}{n_2^2}+n_b\frac{n_s^2-N^2}{n_0^2}\right)$$

n_1^2 and n_2^2 are given in Table 14.3.

The formulas in column 3 of Table 14.4 then enable the value of δ_0 to be calculated.

The formulas giving the allowances for dynamic bending moment are given in column 2 of Table 14.5: as in the case of long span bridges the load obtained in this way is assumed to be distributed uniformly over the span.

To calculate the maximum dynamic shearing forces at a distance a from the farther end of the bridge the values of S_1 and S_2 are found from the formulas of columns 3 and 4 in Table 14.5. The shearing force required is then $(S_1^2+S_2^2)^{\frac{1}{2}}$ but this may, near the centre of the span, fall below a minimum permissible value given by the formulas of column 5, in which case the value obtained from column 5 should be used. In this formula N_F is the frequency at which spring friction just breaks down calculated from equation (6) and $P_1N_F^2$ is the hammer-blow at this frequency.

Short span bridges.—In short span bridges the period of vibration is too rapid for resonance to occur.

The value of the hammer-blows should be calculated for the maximum permissible speed and treated as statical loads added to the corresponding axle loads.

14.12. Influence lines of deflection.—So far in this chapter the use of influence lines has been confined to the representation of bending moments and shearing forces. Influence lines can, however, be drawn

TABLE 14.4.

1	2	3	4
Case	N_2<Limiting Value	N_2=Limiting Value	
	Central dynamical deflection, δ_0 feet	Central dynamical deflection, δ_0 feet	Equation to determine n_d
1	$D_P \frac{n_0^2}{2N_2 n_b}\left[1-\frac{4F}{\pi P}\frac{N_2^2}{N_2^2-n_s^2}\right]$	$D_P \frac{F}{\pi P}\frac{M_G}{M_S}\frac{n_0^2\{(N^2-n_s^2)^2+(2Nn_d)^2\}^{\frac{1}{2}}}{N^3 n_d}$	$\left[\frac{2\pi^3 N^3 M_S D_P}{Fg}\right]^2 n_d^2=[\phi(N)]^2+[\psi(N)]^2$
2	$2D_P \cos\frac{\pi d}{2l}\frac{n_0^2}{2N_2 n_b}\left[1-\frac{4F}{\pi P}\frac{N_2^2}{N_2^2-n_s^2}\right]$	$D_P \frac{F}{\pi P \cos\frac{\pi d}{2l}}\frac{M_G}{M_S}\frac{n_0^2\{(N^2-n_s^2)^2+(2Nn_d)^2\}^{\frac{1}{2}}}{N^3 n_d}$	$\left[\frac{4\pi^3 N^3 M_S D_P \cos^2\frac{\pi d}{2l}}{Fg}\right]^2 n_d^2=[\phi(N)]^2+[\psi(N)]^2$
3	Twice the value for Case 1	As for Case 1	$\left[\frac{4\pi^3 N^3 M_S D_P}{Fg}\right]^2 n_d^2=[\phi(N)]^2+[\psi(N)]^2$
4	Twice the value for Case 2	As for Case 2	$\left[\frac{8\pi^3 N^3 M_S D_P \cos^2\frac{\pi d}{2l}}{Fg}\right]^2 n_d^2=[\phi(N)]^2+[\psi(N)]^2$

TABLE 14.5.

1	2	3	4	5
Case	Allowance for dynamic bending moment. Total load uniformly distributed. Tons	Maximum dynamic shearing force $=(S_1^2+S_2^2)^{\frac{1}{2}}$		Minimum permissible shearing force near centre
		S_1	S_2	
1	$M_G\left[N_2^2+\frac{\pi^2}{8}(n_0^2-N_2^2)\right]\delta_0$	$\frac{\pi M_G\delta_0}{32}\left[-4N_2^2\cos\frac{\pi a}{l}+\pi(n_0^2-N_2^2)\right]$	$\frac{\pi M_G\delta_0}{32}2N_2n_b\left(4\cos\frac{\pi a}{l}+\pi\right)$	$\frac{1}{2}\left(P_1N_F^2+\frac{M}{M_S}F\right)$
2	$M_G\left[N_2^2+\frac{\pi^2}{8}\frac{l-d}{l}\frac{1}{\cos\frac{\pi d}{2l}}(n_0^2-N_2^2)\right]\delta_0$	$\frac{\pi M_G\delta_0}{32}\left[-4N_2^2\cos\frac{\pi a}{l}+\frac{\pi}{\cos\frac{\pi d}{2l}}(n_0^2-N_2^2)\right]$	$\frac{\pi M_G\delta_0}{32}2N_2n_t\left(4\cos\frac{\pi a}{l}+\frac{\pi}{\cos\frac{\pi d}{2l}}\right)$	Twice the value for Case 1.
3	As in Case 1	As in Case 1	As in Case 1	Twice the value for Case 1.
4	As in Case 2	As in Case 2	As in Case 2	Four times the value for Case 1.

to represent the way in which the deflection at any point on a girder or braced structure changes during the passage of a unit load and such diagrams are used extensively in the analysis of redundant structures. In the present chapter statically determinate structures alone will be dealt with, leaving the consideration of redundant structures to a later stage.

The simplest method of drawing an influence line of deflection for a beam is by the use of Clerk Maxwell's reciprocal theorem (paragraph 4.10). For example, to take a very elementary case, suppose that the influence line of deflections is required for A, the free end of the cantilever AB shown in Fig. 14.32. If a unit load be placed at any point C

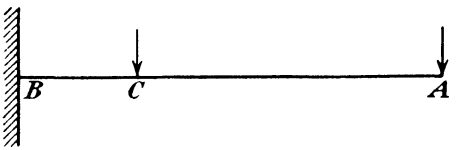

FIG. 14.32.

on the cantilever, we know from the reciprocal theorem that the vertical deflection at A when the load is at C is the same as the vertical deflection at C when the load is at A. The deflection at A when the load is at C gives a point on the influence diagram and therefore the influence diagram will be the same as the deflection curve for the cantilever AB when the load of unity is placed at A. Hence, for a beam, the influence diagram of deflections for any point is found by placing a unit load at that point and determining the deflected form of the beam. This curve is the influence line required.

This is equally true for a frame, but usually it is not so easy to obtain the deflected form of such a structure as it is for a beam. The simplest method is by the use of the Williot-Mohr diagram. An example will make the procedure clear: Fig. 14.33 shows a Pratt truss with 6 equal bays and we shall determine the influence line for the point L as a unit load traverses the top boom of the girder. As before, when the load is at any point such as J, the deflection at L will be the same as the deflection at J when the load is placed at L and so we must determine the deflection polygon for the top chord of the girder under the action of a unit load at L. The table given in Fig. 14.33 shows the alteration in length of the various members when a unit load is placed at L. Since the structure is assumed to be symmetrical about the centre line we take L as the reference point and LE as the datum line and avoid the necessity for drawing a Mohr diagram, since this line will not rotate. The Williot diagram for one half of the truss, drawn as described in paragraph 5.8, is shown in the figure. The point A is fixed and so the vertical distances below A of the various joints taken from the Williot diagram give the true vertical deflections. If a is projected horizontally as shown and the line HJKLM is set out to represent the top boom of the girder, the deflections of the various joints on this top boom are obtained by projecting h, j, k and l as shown in the diagram. The

deflection polygon for the top chord is thus found and is the influence line of deflections for the point L as a load traverses the top boom.

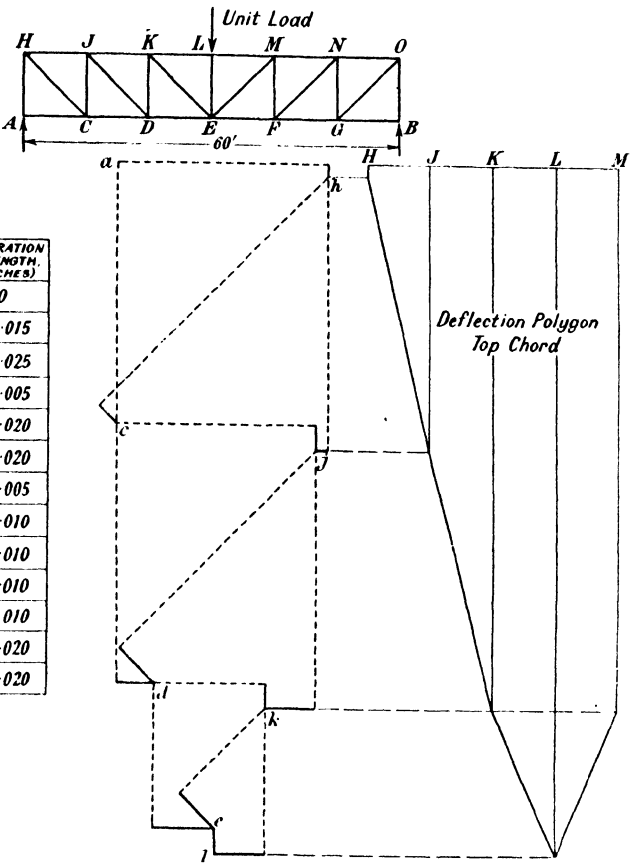

MEMBER	ALTERATION IN LENGTH. (INCHES)
AC, BG	0
CD, FG	+0·015
DE, EF	+0·025
HJ, NO	-0·005
JK, MN	-0·020
KL, LM	-0·020
HA, OB	-0·005
JC, NG	-0·010
KD, MF	-0·010
LE	-0·010
HC, GO	+0·010
JD, NF	+0·020
KE, ME	+0·020

FIG. 14.33.

EXERCISES

(1) A bridge of 56 feet span has simply supported ends. It is crossed by a four-wheeled lorry which imposes a load of 2 tons through the two front wheels and a load of 3 tons through the two rear wheels. The wheel base of the lorry is 14 feet.

Draw the bending moment and shearing force diagrams for the mid-point of the bridge for all positions of the load. (*These may be plotted directly from the influence lines for the mid-point of the bridge.*)

(2) A bridge truss of 150 feet span is crossed by a uniformly distributed load of $\frac{1}{2}$ ton per foot and of length 40 feet. Plot the diagrams of maximum bending moment and shearing force for the truss.

(3) A span of 300 feet is crossed from left to right by a train of six loads, A, B, C, D, E and F, their magnitudes being 10, 15, 15, 25, 15, and 10 tons respectively. The distances between them are AB=6 feet, BC=8 feet, CD=8 feet, DE=10 feet, and EF=12 feet. A is the leading load.

Calculate the maximum bending moment and shearing forces for a point 100 feet

from the left-hand support and the magnitude and position of the maximum bending moment.

(5,560 tons-feet ; 52·7 tons
6,280 tons-feet when D is 151·17 feet from right-hand support)

(4) A Pratt (N) truss has a span of 200 feet, a depth of 16 feet and is divided into ten equal panels. Draw the influence lines for the loads in the top boom of the eighth panel from the left-hand support and for the diagonal in the sixth panel from the same support when the bottom chord is loaded.

(5) A five-panel Warren truss is formed of equilateral triangles and is loaded on the bottom chord.

Draw the influence lines for the diagonal member and the top chord member immediately to the left of the centre point of the truss.

(6) A three-pinned segmental arch in which the rise is one quarter of the span is crossed by a rolling load. Plot the influence lines of horizontal thrust and also the influence line of bending moment at a quarter-span point.

(7) A beam ABC is pinned to supports A and B a distance 15 feet apart. The overhang BC is 5 feet.

Draw the influence line of deflection for the mid-point of AB.

CHAPTER 15

INFLUENCE LINES FOR STATICALLY INDETERMINATE STRUCTURES

15.1. Use of influence lines.—It was shown in the concluding paragraph of the last chapter that the curve of deflection for any structure under a unit load placed at any point is the influence line of deflection for that point. In the case of beams this curve is easily found by the methods described in Chapter 3 and in the case of trusses by means of a Williot-Mohr diagram and deflection polygon for the loaded chord as described in paragraph 5.8.

Influence lines of deflection are not often needed in the case of statically determinate structures, since, except in special circumstances, knowledge of the deflected form of the girder or truss is not an essential step in the design. When the structure is redundant, however, whether the redundancy is due either to the provision of more than the essential number of reactive forces or of more internal members than are statically necessary, the stress analysis involves the elastic properties of the structure. Calculations of deflections in some form or another thus become imperative and in many cases the use of deflection influence lines enables the analysis of the structure to be made with the minimum of labour. This chapter therefore will deal with some of the applications of influence lines to problems connected with statically indeterminate structures. The simpler cases only are considered; others will be found in a later chapter, but reference should be made to specialised works for more elaborate extensions of these principles.

15.2. Müller-Breslau's theorem.– A simple theorem due to Müller-Breslau enables the influence line of deflections to be used for the calculation of redundant reactions in a beam or truss.

The truss shown in Fig. 15.1 is supported at the three points A, D and F and these supports are assumed to be rigid. Let the support D be removed: the structure is now statically soluble and if a unit load acts vertically downwards at D the deflection polygon for the bottom chord can be drawn by means of a Williot-Mohr diagram. This diagram, *abcdef*, is also the influence line of deflection for the point D on the simply supported truss AF and so, if a unit load acts vertically at any panel point of the bottom chord the ordinate to the polygon represents the deflection produced at D; a unit load at C, for example, will produce a deflection δ_{CD} at D.

In order to move the point D through a distance δ_{DD} it is necessary to apply a unit force at D and, since the structure is assumed to follow

a linear load-displacement law, to move the same point through a distance δ_{CD} a force of $\frac{\delta_{CD}}{\delta_{DD}}$ must be applied at D. If the support D were in position, therefore, the reaction upon it due to the application of a unit force at C would be $\frac{\delta_{CD}}{\delta_{DD}}$ and similarly for a load at any other panel point. Thus, if the ordinates of the polygon be divided by the ordinate δ_{DD} the resulting diagram is the influence line of reactions at the support D.

In general terms the ordinates of the influence line for the force in any redundant element of a structure are equal to those of the deflection curve drawn for the structure when a unit load replaces the redundancy, the scale being so chosen that the deflection at the point of application of the unit load represents unity.

This is Müller-Breslau's theorem. It may also be deduced by an application of the first theorem of Castigliano, for if D is replaced by a

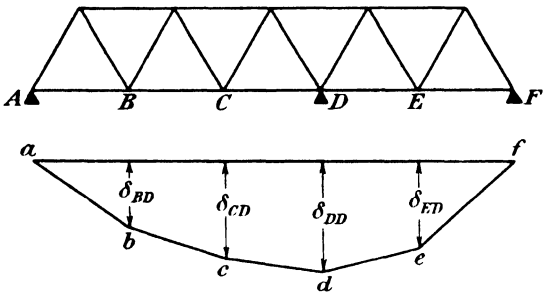

FIG. 15.1.

downward load Q and another load P acts at E, the load in any member of the truss can be expressed in the form

$$P_0=\alpha Q+\beta P.$$

The deflection of D is

$$\Delta_D=\frac{\partial U}{\partial Q}=\sum\frac{\alpha(\alpha Q+\beta P)L}{AE}$$

and the deflection of E is

$$\Delta_E=\frac{\partial U}{\partial P}=\sum\frac{\beta(\alpha Q+\beta P)L}{AE}.$$

If P is now made equal to zero and Q equal to unity, the deflection of D is

$$\Delta'_D=\sum\frac{\alpha^2 L}{AE}$$

and the deflection of E is

$$\Delta'_E=\sum\frac{\alpha\beta L}{AE}.$$

If P is made equal to unity and a force R is applied upwards to the

point D, R being sufficient to maintain the support at its original level, the load in any member is $-\alpha R+\beta$ and

$$\frac{\partial U}{\partial R}=\sum\frac{\alpha(\alpha R-\beta)L}{AE}=0.$$

This equation gives the reaction at D when a unit load acts at E.

Hence $$R\sum\frac{\alpha^2 L}{AE}=\sum\frac{\alpha\beta L}{AE}$$

or $$R\Delta'_D=\Delta'_E$$

i.e. $$R=\frac{\text{deflection at E when a unit load acts at D}}{\text{deflection at D when a unit load acts at D}},$$

which proves the theorem.

The theorem applies to any elastic body and can be used either for beams or trusses: when dealing with the former the deflected shape can be found by the usual methods and this will be considered in the next paragraph.

15.3. Influence lines of reaction for continuous girders.—The problem of influence lines for continuous girders has been discussed at considerable length by Professor F. C. Lea * and in the first instance his treatment will be given.

Let Fig. 15.2 represent a girder resting on supports A and C and continuous over the third support B. The spans AB and BC are L_1

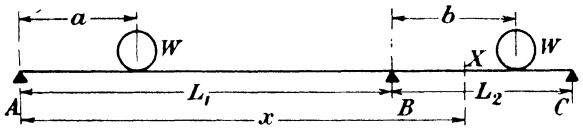

FIG. 15.2.

and L_2 respectively and the variation of the reactions as a load W rolls across the girder is to be found.

Suppose the load W to be on the span AB at a distance a from A and let X be any point on the girder at a distance x from A. Then the bending moment at X is

$$EI\frac{d^2y}{dx^2}=-R_A x+W[x-a]-R_B[x-L_1]$$

where the terms in brackets are ignored if they are negative.

Integrating this expression twice we obtain

$$EI\frac{dy}{dx}=-\frac{R_A x^2}{2}+\frac{W}{2}[x-a]^2-\frac{R_B}{2}[x-L_1]^2+A$$

and $$EIy=-\frac{R_A x^3}{6}+\frac{W}{6}[x-a]^3-\frac{R_B}{6}[x-L_1]^3+Ax+B,$$

where A and B are constants of integration.

* "Influence Lines for Continuous Girders." F. C. Lea. Proc. Inst. C.E. Vol. 185, 1910–11, p. 277.

Since $y=0$ when $x=0$, B=0, and since $y=0$ when $x=L_1$

$$A=\frac{R_A L_1^2}{6}-\frac{W(L_1-a)^3}{6L_1}.$$

Putting $y=0$ when $x=L_1+L_2$ we obtain

$$R_A L_2(L_1+L_2)(2L_1+L_2)-W\left[(L_1+L_2-a)^3-\frac{(L_1-a)^3(L_1+L_2)}{L_1}\right]+R_B L_2^3=0. \quad . \quad . \quad . \quad . \quad (1)$$

We also have

$$R_A+R_B+R_C=W \quad . \quad . \quad . \quad . \quad . \quad . \quad . \quad . \quad (2)$$

and by taking moments about B,

$$R_C L_2+W(L_1-a)-R_A L_1=0. \quad . \quad . \quad . \quad . \quad . \quad (3)$$

The solution of these three equations gives, when W is made equal to unity, the result

$$R_A=\frac{L_1^2+L_1L_2-aL_2-\frac{3}{2}aL_1+\frac{a^3}{2L_1}}{L_1(L_1+L_2)} \quad . \quad . \quad . \quad . \quad . \quad (4)$$

When the load is on the span BC the general equations for slope and deflection are the same but the term L_1-a is negative and the value of the constant A is modified. Putting $y=0$ when $x=L_1$ we now have

$$A=\frac{R_A L_1^2}{6}.$$

When $x=L_1+L_2$, $y=0$ and equation (1) becomes

$$R_A L_2(L_1+L_2)(2L_1+L_2)-W(L_1+L_2-a)^3+R_B L_2^3=0.$$

The result is simplified by measuring the distance of the load from the support B so we shall put $a=L_1+b$. The above equation then becomes

$$R_A L_2(L_1+L_2)(2L_1+L_2)-W(L_2-b)^3+R_B L_2^3=0 \quad . \quad . \quad . \quad (5)$$

Equation (2) is unaltered but equation (3) becomes

$$R_C L_2-Wb-R_A L_1=0. \quad . \quad . \quad . \quad . \quad . \quad . \quad . \quad (6)$$

Solving equations (2), (5) and (6) and putting W equal to unity we then find

$$R_A=-\frac{bL_2-\frac{3b^2}{2}+\frac{b^3}{2L_2}}{L_1(L_1+L_2)} \quad . \quad . \quad . \quad . \quad . \quad . \quad . \quad (7)$$

Equations (4) and (7) are the equations of the influence line of reaction at A and they may be plotted in the following manner.

In Fig. 15.3, ABC represents the beam as before. From B draw a line BD perpendicular to AC representing the product L_1L_2 to some convenient scale. Join CD and produce CD to meet the perpendicular from A at E.

Then $AE=L_1(L_1+L_2)$, the slope of ED is $-L_1$ and the equation of the line ED is

$$y=L_1^2+L_1L_2-aL_1.$$

A curve plotted from the equation

$$y=\frac{1}{2}aL_1+aL_2-\frac{a^3}{2L_1}$$

will pass through the points A and D; let it cut the ordinate from a at the point d. Then

$$dc=(L_1^2+L_1L_2-aL_1)-\left(\frac{1}{2}aL_1+aL_2-\frac{a^3}{2L_1}\right)$$

$$=L_1^2+L_1L_2-aL_2-\frac{3}{2}aL_1+\frac{a^3}{2L_1}$$

i.e. dc represents the numerator of R_A in equation (4) and since AE is the denominator of this equation to the same scale, the value of R_A

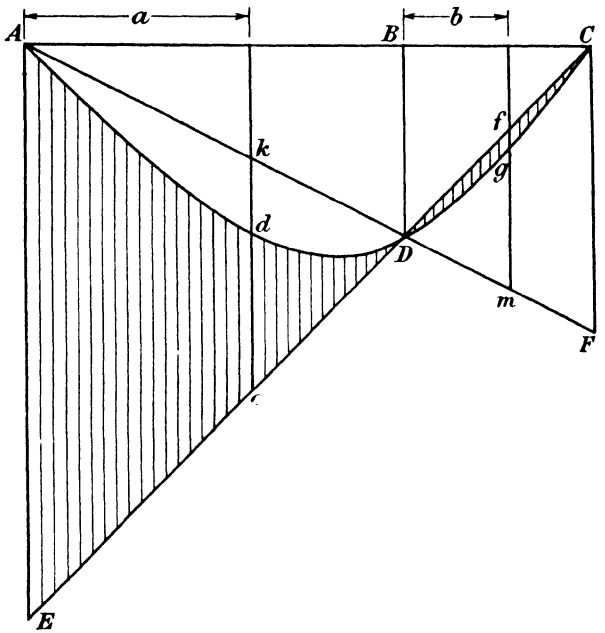

FIG. 15.3.

is given by the ordinate dc if AE be taken to be unity. AED is thus the influence diagram for R_A for all positions of the load between A and B.

The numerator of equation (7) can be written in the form

$$-\left(bL_2-\frac{3b^2}{2}+\frac{b^3}{2L_2}+L_1L_2-bL_1\right)+(L_1L_2-bL_1).$$

The second term is the ordinate to the line CE when $a=L_1+b$ and the first term represents a curve DgC passing through the points D and C. Hence, when the load is at any point between B and C the reaction at A is measured by the distance gf to the scale for which AE is unity. gf is negative and so for a load between A and B the reaction at A is

positive while for a load between B and C it is negative. The complete influence diagram for R_A is therefore as shown shaded in Fig. 15.3.

From equation (3)

$$R_C=\frac{1}{L_2}\{R_AL_1-W(L_1-a)\}$$

and substituting the value of R_A from equation (4) we obtain

$$R_C=-\frac{\left(\frac{1}{2}aL_1-\frac{a^3}{2L_1}+aL_2\right)-aL_2}{L_2(L_1+L_2)}.$$

The first term in the numerator is the equation of the curve A*d*D and the second is that of the straight line ADF. Hence for loads between A and B the distance *kd* represents the reaction at C to the scale for which CF is unity. Similarly, *gm* represents the reaction at C for load positions between B and C and so the complete influence diagram for R_C is obtained.

The foregoing results may also be obtained by an application of the theorem of paragraph 15.2. Suppose the support at A to be removed and a load W applied downwards at that point. The reaction at B is found by taking moments about C to be

$$R_B=\frac{W(L_1+L_2)}{L_2}$$

and we have

$$EI\frac{d^2y}{dx^2}=Wx-\frac{W(L_1+L_2)}{L_2}[x-L_1],$$

the term in square brackets only occurring when it is positive.

Integrating twice we find

$$EI\frac{dy}{dx}=\frac{Wx^2}{2}-\frac{W(L_1+L_2)}{2L_2}[x-L_1]^2+A$$

and

$$EIy=\frac{Wx^3}{6}-\frac{W(L_1+L_2)}{6L_2}[x-L_1]^3+Ax+B.$$

The two conditions to determine the constants A and B are $y=0$ when $x=L_1$ and $x=L_1+L_2$ respectively.

Substitution of these in the above expression gives

$$A=-\frac{WL_1}{6}(3L_1+2L_2)$$

and

$$B=\frac{WL_1^2}{3}(L_1+L_2).$$

The curve of deflections for the span AB is then

$$y=\frac{W}{6EI}\{x^3-3L_1^2x-2L_1L_2x+2L_1^3+2L_1^2L_2\},$$

while the deflection of the point A is,

$$y_A=\frac{WL_1^2}{3EI}(L_1+L_2).$$

Hence the influence line of reactions at A is from Müller-Breslau's theorem,

$$\frac{y}{y_A}=\frac{1}{L_1(L_1+L_2)}\left\{\frac{x^3}{2L_1}-\frac{3}{2}L_1x-L_2x+L_1^2+L_1L_2\right\}. \quad . \quad . \quad (8)$$

which is the same result as given in equation (4) when a is written instead of x.

For the span BC, putting $x=L_1+b$, we find,

$$y=\frac{W}{6EI}\frac{L_1}{L_2}\{-2bL_2^2-b^3+3b^2L_2\}$$

and

$$\frac{y}{y_A}=-\frac{1}{L_1(L_1+L_2)}\left\{bL_2-\frac{3}{2}b^2+\frac{b^3}{2L_2}\right\}, \quad . \quad . \quad . \quad . \quad . \quad (9)$$

which is the result given in equation (7).

The influence line for the centre reaction may be found from equation (2) since expressions for R_A and R_C have been determined, but as a further example of the use of Müller-Breslau's theorem we will obtain it directly. The support at B is removed and an upward load W placed at that point. Then, if x be measured from A, we have

$$EI\frac{d^2y}{dx^2}=W\left(\frac{L_2}{L_1+L_2}\right)x-W[x-L_1]$$

the term in square brackets only occurring when it is positive.

Integrating twice we obtain

$$EI\frac{dy}{dx}=\frac{W}{2}\left(\frac{L_2}{L_1+L_2}\right)x^2-\frac{W}{2}[x-L_1]^2+A$$

and

$$EIy=\frac{W}{6}\left(\frac{L_2}{L_1+L_2}\right)x^3-\frac{W}{6}[x-L_1]^3+Ax+B.$$

y is zero for the two conditions $x=0$ and $x=L_1+L_2$ and so

$$B=0$$

and

$$A=-\frac{WL_1L_2(L_1+2L_2)}{6(L_1+L_2)}.$$

Between the points A and B the substitution of these values gives

$$y=\frac{WL_2x}{6EI(L_1+L_2)}\{x^2-L_1(L_1+2L_2)\}$$

and under the load

$$y_B=-\frac{2WL_1^2L_2^2}{6EI(L_1+L_2)}.$$

Hence the equation of the influence line for R_B is

$$R_B=\frac{y}{y_B}=-\frac{x}{2L_1^2L_2}\{x^2-L_1(L_1+2L_2)\}. \quad . \quad . \quad . \quad . \quad (10)$$

When the load is between B and C, similar methods lead to the equation

$$R_B=\frac{y}{y_B}=-\frac{L_2-b}{2L_1L_2^2}\{(L_2-b)^2-L_2(L_2+2L_1)\} \quad . \quad . \quad . \quad (11)$$

where b is measured from B as before.

In the particular case when $L_1=L_2=L$ these equations respectively reduce to

$$R_B=\frac{x(3L^2-x^2)}{2L^3} \quad \ldots\ldots\ldots \quad (12)$$

and

$$R_B=\frac{(L-b)\{3L^2-(L-b)^2\}}{2L^3} \quad \ldots\ldots \quad (13)$$

The influence line is shown in Fig. 15.4.

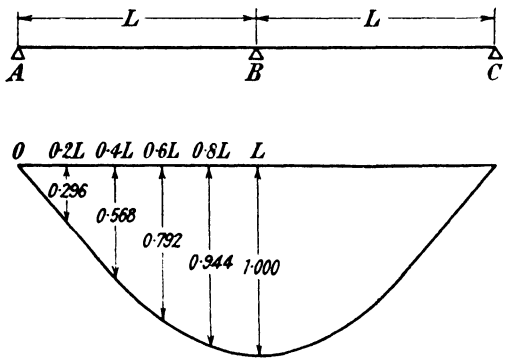

FIG. 15.4.

15.4. Influence line of shearing force for a continuous girder.—Let AEDC in Fig. 15.5 be the influence line of reaction at the support A of a continuous girder ABC, found as in the previous paragraph and let X be any point on the girder between A and B.

If a load W is at G, between A and X, the shearing force at X is

$$F=-R_A+W$$
$$=W(1-bc)$$

or, if W is made equal to unity,

$$F=1-bc.$$

If from A a line AK is drawn parallel to EC and cG is produced to meet it at e,

$$ec=AE=1$$

and

$$eb=1-bc.$$

The intercept eb between the line AK and the curve ADC thus represents the shearing force at X for a unit load between A and X and AKM is the influence diagram for this section of the girder.

When the load is at any point H between X and B,

$$F=-R_A=-fy$$

and the influence diagram for this section of the girder is MND.

When the load has passed B and is at a point J between B and C, the shearing force at X is again

$$F=-R_A=+hj.$$

The influence diagram of shearing force for the span BC is therefore D*j*C and the complete diagram is as shown shaded in Fig. 15.5.

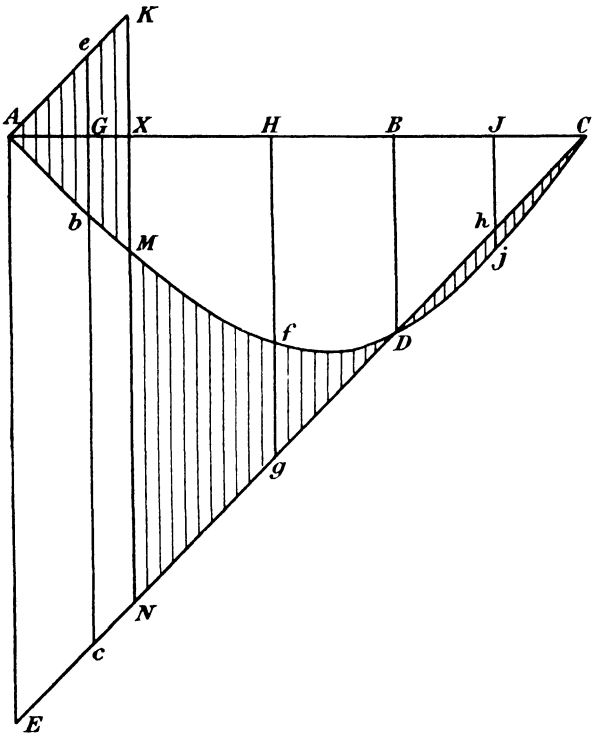

FIG. 15.5.

15.5. Influence line of bending moment for a continuous girder.—Considering the case dealt with in previous paragraphs, let AEDC in Fig. 15.6 be the influence line of reaction at A and X any point on the span AB at a distance x from A. If a load W is placed at the point G, lying between A and X where the distance AG is a, the bending moment at X is

$$M_x = -R_A x + W(x-a)$$

or

$$\frac{M_x}{x} = -R_A + W\left(\frac{x-a}{x}\right).$$

If W is made equal to unity

$$\frac{M_x}{x} = -bc + \frac{x-a}{x}.$$

If a perpendicular to AC be dropped from X to cut EC in H and HA be drawn

$$\frac{dc}{AE} = \frac{x-a}{x}$$

and since AE represents unity on the influence diagram,

$$dc = \frac{x-a}{x}.$$

Therefore $$\frac{M_x}{x} = dc - bc = -bd.$$

When the load is at a point H lying between X and B,

$$\frac{M_x}{x} = -R_A = -ef$$

and when it is at any point J on the span BC,

$$\frac{M_x}{x} = -R_A = +hj.$$

Thus the influence diagram for the bending moment at X is as shown shaded in Fig. 15.6.

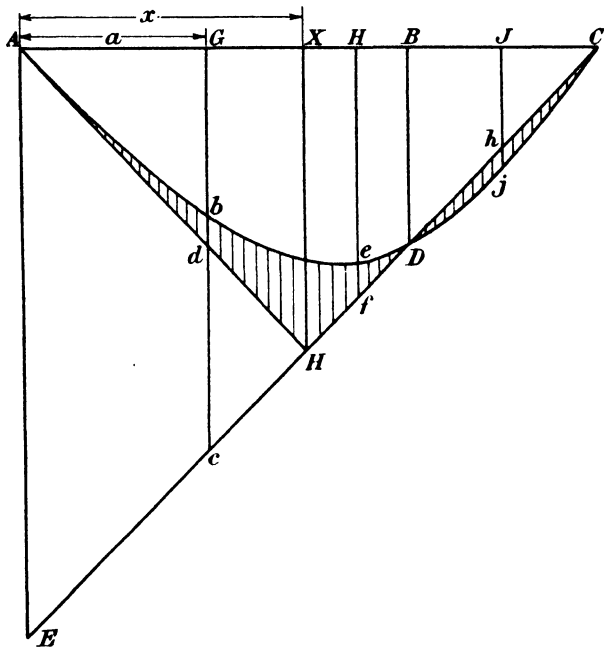

Fig. 15.6.

15.6. Influence lines of reactions for a continuous truss.—In paragraph 15.2 it was shown how the influence line of reaction for a single redundant support in a continuous truss might be obtained. The method will now be extended to the case of two redundant reactions. The truss shown in Fig. 15.7 is simply supported at A and B and is continuous over supports at C and D. The influence lines of reactions at the points C and D are to be found. The load will be supposed to travel along the top chord of the truss.

In the first place both the supports C and D are supposed to be removed and a unit load acting downwards is applied at C. A Williot-Mohr diagram is drawn as explained in paragraph 5.8 for the simply supported truss AB and from it the deflection polygon for the top chord is obtained. A similar polygon is drawn for a unit load acting down-

wards at D. These polygons are also the influence lines for the deflections at C and D respectively and from them we can measure

δ_C, the deflection of point C under a unit load at any panel point M on the top chord

and δ_D, the deflection of point D under a unit load at the same point M.

From the Williot-Mohr diagrams the following data are found :—

Δ_C, the vertical movement of the point C for a unit load at C,

Δ'_C, the vertical movement of the point C for a unit load at D,

Δ_D, the vertical movement of the point D for a unit load at D,

and Δ'_D, the vertical movement of the point D for a unit load at C.

Let R_C and R_D be the reactions at C and D when the supports are in position and a unit load acts at M and suppose these forces are applied upward to the truss deflected by the load at M.

Under the action of such forces alone the movement of C would be $R_C\Delta_C+R_D\Delta'_C$ and the movement of D would be $R_C\Delta'_D+R_D\Delta_D$.

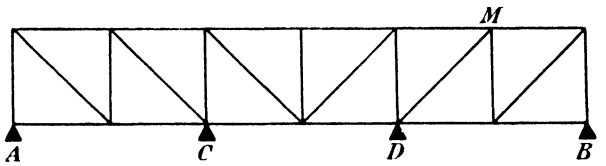

FIG. 15.7.

Since it is assumed that in the actual truss the points C and D do not move, these movements must be respectively equal to δ_C and δ_D, *i.e.*

$$\delta_C=R_C\Delta_C+R_D\Delta'_C$$

and

$$\delta_D=R_C\Delta'_D+R_D\Delta_D.$$

The solution of these simultaneous equations gives the values of R_C and R_D.

The terms Δ_C, Δ'_C, Δ_D and Δ'_D are constants for a given truss and are found once and for all from the Williot-Mohr diagrams while the terms δ_C and δ_D are measured directly from the influence diagrams. The above equations can therefore be formed quickly for all panel points on the top chord and the values of R_C and R_D thus determined enable the influence lines of reaction at C and D to be drawn. This method is very considerably quicker than if a process of calculation by strain energy methods were adopted entailing lengthy computation for the load at each panel point.

The process described above can be extended to the case of any number of redundant supports ; each redundancy needs the construction of a Williot-Mohr diagram and an influence line of deflection, and if there are n such redundancies there will be n simultaneous equations to be solved for each load position.

15.7. Influence line of force in a continuous truss.—In the paper previously quoted Lea makes the tacit assumption that the reactions in a continuous parallel chord truss are the same as those in a continuous girder similarly supported and loaded and uses the results for

the girder to obtain influence lines of force for a truss such as that shown in Fig. 15.8.

The load is assumed to travel along the bottom chord of the truss and in the first place we shall consider the force in a diagonal member such as GE.

If the shearing force across the panel GE is F, the force in GE is F cosec θ.

As long as the load is between A and Q or between E and C the

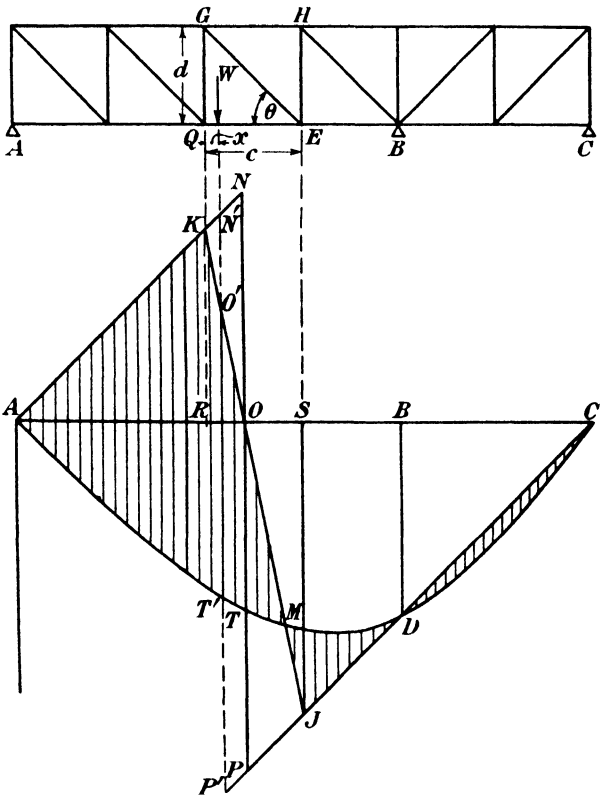

FIG. 15.8.

shearing force across the panel is the same as that for a girder, and the influence line of shearing force is drawn exactly as shown in paragraph 15.4. When it is between Q and E some modification is necessary.

Project points Q and E to cut AN and CP at K and J respectively and AC at R and S. Join KJ and let this line cut AC at O. Through O draw NOP perpendicular to AC.

Then
$$\frac{ON}{OP}=\frac{KN}{PJ}=\frac{OR}{OS}$$

and so
$$\frac{ON}{NP}=\frac{OR}{RS}=\frac{OR}{c}.$$

Since NP represents unity on the influence diagram we obtain

$$ON=\frac{OR}{c}.$$

If the load acts at x from Q and its line of action cuts the diagram at N'O'T'P', we have

$$\begin{aligned} O'T' &= N'P'-O'N'-T'P' \\ &= 1-\frac{x}{c}-R_A \\ &= -R_A+\frac{c-x}{c}. \end{aligned}$$

But $\frac{c-x}{c}$ is the proportion of the load transferred to Q by the beam action of QE and so O'T' represents the shearing force across the panel GE. The influence diagram for F is therefore as shown shaded in Fig. 15.8 and the ordinates to this when multiplied by cosec θ give the force in GE for all load positions.

The force in the chord member QE is, by the method of sections, equal to

$$\frac{\text{Moment about G}}{d}.$$

The moments about G are the same as for a continuous girder and so if the influence line of bending moments for G is drawn as explained in paragraph 15.5 the ordinates of this diagram when divided by d give the ordinates of the required influence line of force in QE.

The assumption underlying this method imposes severe restrictions and it must be used with caution. For a truss having a large number of panels and chord members of constant area the results obtained would be very nearly correct, but in most cases the conditions are such that it is safer to use the more exact method of the previous paragraph.

15.8. Forces in redundant bars by influence diagrams.—The construction of influence lines enables the calculation of the forces in redundant bars of a truss to be made quickly for any position of the load. Let Fig. 15.9 represent a truss supported at A and B and having one redundant member PQ for which the force influence line is required when the bottom chord is loaded. Suppose the bar PQ to be removed and unit loads to act at P and Q as shown. The forces in all the members of the resulting just-stiff frame can then be found and their changes of length calculated. A Williot-Mohr diagram and a deflection polygon for the bottom chord is then constructed as explained in paragraph 5.8. The ordinate δ_m to this deflection polygon at any panel point M on the bottom chord is the vertical displacement of this point under unit loads at P and Q and by Clerk Maxwell's theorem it is therefore the amount by which the points P and Q separate when a unit load acts vertically at M. The polygon is therefore the influence line of separation of P and Q when the member PQ is removed.

The free separation of P and Q can also be obtained from the Williot-Mohr diagram ; let this be Δ.

When the redundant member is in position and a unit load acts at M let R be the force in PQ. This force will cause the member to stretch by an amount $\frac{RL}{AE}$ where L is its length, A is its cross-sectional area and E is Young's modulus for the material, and the force R will pull

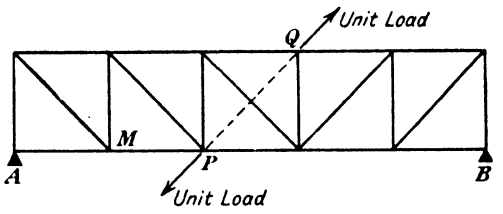

Fig. 15.9.

the points P and Q together by an amount $R\Delta$. The total separation of the two points in the absence of the member PQ is δ_m and so

$$R\Delta+\frac{RL}{AE}=\delta_m$$

or

$$R=\frac{\delta_m}{\Delta+\frac{L}{AE}}.$$

Hence, if the ordinates of the deflection polygon for the bottom chord under unit loads at P and Q are divided by the term $\Delta+\frac{L}{AE}$ the deflection polygon represents the influence line for the force in PQ.

If the truss has two redundant members PQ and ST as shown in

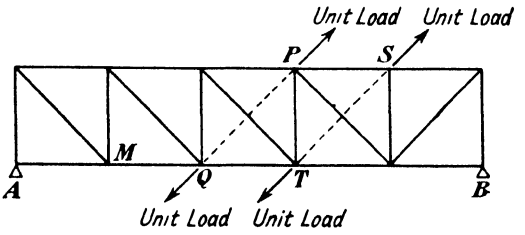

Fig. 15.10.

Fig. 15.10 the following method may be used to determine the forces in them as a load crosses the truss.

PQ and ST are assumed to be removed and unit loads placed at P and Q. The stresses in the remaining bars are calculated, the alterations in their lengths determined and a Williot-Mohr diagram is drawn from which the deflection polygon for the loaded chord is obtained. This polygon is also the influence line representing the separation of points P and Q. Thus, if a load of unity is placed at any panel point

M on the lower chord the ordinate to the influence line at M is the amount by which P and Q separate. Call this ${}_1\delta_m$. From the Williot-Mohr diagram are also obtained Δ_1 the amount by which P and Q separate under unit loads at P and Q, and Δ'_1 the amount by which S and T separate under the action of the same loads.

Similar diagrams are drawn for unit loads acting at S and T and from them are obtained ${}_2\delta_m$ the separation of S and T for a unit load at M; Δ_2 and Δ'_2 the separations of S and T and of P and Q respectively under unit loads at S and T.

The redundant bars PQ and ST are now supposed to be in position, the forces in them when a unit load is placed at M being R_1 and R_2 respectively.

Due to the force R_1 acting at P and Q,
P and Q approach by an amount $R_1\Delta_1$
and S and T approach by an amount $R_1\Delta'_1$.
Due to the force R_2 acting at S and T,
P and Q approach by an amount $R_2\Delta'_2$
and S and T approach by an amount $R_2\Delta_2$.
Hence due to R_1 and R_2 acting together,
P and Q approach by an amount $R_1\Delta_1+R_2\Delta'_2$
while S and T approach by an amount $R_1\Delta'_1+R_2\Delta_2$.

The lengths of the bars PQ and ST are increased by amounts $\frac{R_1L_1}{A_1E}$ and $\frac{R_2L_2}{A_2E}$ due to the loads in them and so we have

$${}_1\delta_m=R_1\Delta_1+R_2\Delta'_2+\frac{R_1L_1}{A_1E}$$

and

$${}_2\delta_m=R_1\Delta'_1+R_2\Delta_2+\frac{R_2L_2}{A_2E}.$$

These simultaneous equations enable the values of R_1 and R_2 to be found.

It will be noticed that Δ_1 Δ'_1 Δ_2 and Δ'_2 are constant values for the frame whatever the position of the load on the bottom chord, while ${}_1\delta_m$ and ${}_2\delta_m$ are found from the respective deflection polygons. By this method therefore the forces in the two redundant bars for any position of the load can be calculated by the solution of two simple simultaneous equations once the influence lines have been drawn. Here again, as in the case of paragraph 15.6, application of strain energy methods would entail a lengthy calculation for each load position and the advantage to be gained by the use of influence lines is considerable.

15.9. Influence line of thrust for a two-pinned arch.—Since a two-pinned arch is a statically indeterminate structure the calculation of the thrust involves the application of strain energy or similar methods of analysis. Examples of this calculation have already been given in paragraph 12.6 and the same treatment will be now used to obtain a general expression for the value of the thrust when a load acts at any point on a segmental rib.

Such a rib is shown in Fig. 15.11, the radius being R and the angle subtended at the centre being 2θ. A load W is placed at the point D, the angle AOD being ϕ and X any point on the rib at an angular distance α from AO.

The general expression for the thrust can be obtained at once from the equation of paragraph 12.6 by substituting $\theta-\phi$ for ψ and W for 2W in that equation. This gives

$$H=\frac{\left\{\begin{array}{l}\sin 2\theta \sin\phi(1+\cos\phi)-(1+\cos 2\theta+\theta \sin 2\theta)(1-\cos\phi)\\ \qquad\qquad -\cos 2\theta \sin^2\phi\\ -\sin 2\theta(\phi\cos\phi)-(1+\cos 2\theta)\theta\sin\phi+(1+\cos 2\theta)\phi\sin\phi\end{array}\right\}}{4\theta-3\sin 2\theta+2\theta\cos 2\theta}W. \quad (1)$$

and this is the equation for the H line, as it is called for convenience, for any two-pinned segmental arch.

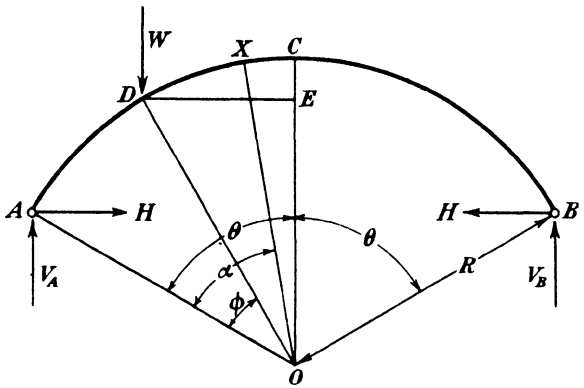

Fig. 15.11.

As an example, if the subtended angle 2θ is taken to be 120° and W is made equal to unity the equation reduces to,

$$\cdot 544H=\cdot 866\sin\phi(1+\cos\phi)-1\cdot 406(1-\cos\phi)+\tfrac{1}{2}\sin^2\phi-\cdot 866\phi\cos\phi$$
$$-\cdot 524\sin\phi+\frac{\phi}{2}\sin\phi$$

and the following values are obtained :—

ϕ	0°	15°	30°	45°	60°
H	0	·197	·408	·57	·634

The influence line for this case is shown in Fig. 15.12.

If, instead of being segmental, the arch is parabolic in form the work is very much simplified by the assumption, explained in paragraph 12.7, that the second moment of area at any section is proportional to the secant of the angle of slope of the arch, *i.e.* $I=I_0\frac{ds}{dx}$ where I_0 is the

second moment of area at the crown. If such a rib having a span L and a central rise d carries a load of unity at a distance a from one support the expression for the horizontal thrust is found, as in paragraph 12.7, to be

$$H=\frac{5}{8L^3d}a(L-a)(L^2+aL-a^2) \quad . \quad . \quad . \quad . \quad . \quad (2)$$

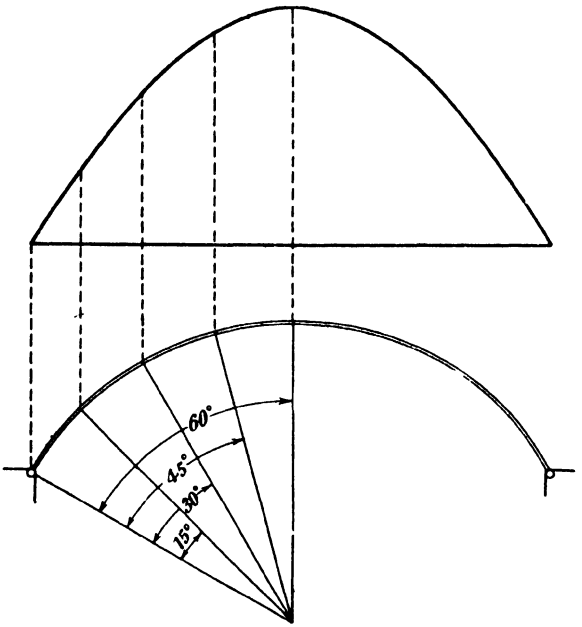

FIG. 15.12.

The ordinates to the H line for different values of $\frac{a}{L}$ are given below :—

$\frac{a}{L}$	0	0·1	0·2	0·3	0·4	0·5
H	0	$\cdot0613\frac{L}{d}$	$\cdot1160\frac{L}{d}$	$\cdot1588\frac{L}{d}$	$\cdot1860\frac{L}{d}$	$\cdot1953\frac{L}{d}$

From this table the H line can be plotted for any ratio L/d. If the arch is, in fact, of uniform section throughout there will be an error on account of the assumption as to the variation of the second moment of area, but unless L/d is small this will not be serious and for most practical cases it may be neglected.

The same method may be used for an arch of any shape but if it is of such form that the equations cannot be readily integrated the work involved in estimating H may be considerable since graphical integration will be necessary.

15.10. Influence line of bending moment for a two-pinned arch.— The bending moment at a point X on a two-pinned arch such as shown in Fig. 15.13 is

$$M = H\bar{y} - V_A\bar{x} + Wx'$$

where $\bar{x}$ and $\bar{y}$ are the co-ordinates of the point X taking A as the origin and x' is the distance of the load from X. The last term only occurs

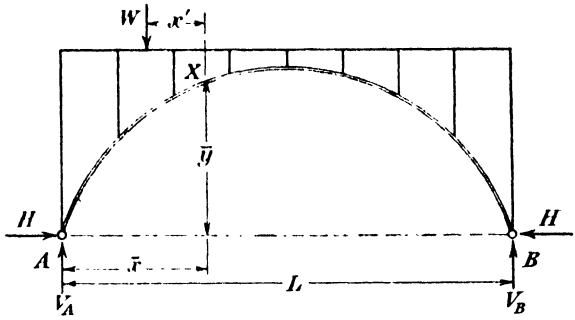

FIG. 15.13.

when W is between A and X. Now the equation to the influence line of bending moments at X on a beam of span AB is

$$M' = -V_A\bar{x} + Wx'$$

and the equation of the influence line of moment at X due to the thrust alone is

$$M'' = H\bar{y}.$$

The complete influence line for M is therefore the sum of the two separate influence lines for M′ and M″. The first of these is readily plotted as in paragraph 14.2, but the second is rather more troublesome since the ordinates of the H line have to be multiplied by a different value of $\bar{y}$ for each position of X. If, however, we divide the equation for M throughout by $\bar{y}$ we have

$$\frac{M}{\bar{y}} = H + \frac{M'}{\bar{y}}$$

and this is a more convenient form for plotting, since the H line is the same for all positions of X. As an example we will take the case of a segmental arch rib having a central angle of 120°. The H line is plotted from the data given in the last paragraph and is shown in Fig. 15.14.

The M′ line is a triangle with its apex at $\bar{x}$ from A, the ordinate at that point being $\frac{\bar{x}(L-\bar{x})}{L}$ and so, if XD is made equal to $\frac{\bar{x}(L-\bar{x})}{L\bar{y}}$ the triangle ADB is the $\frac{M'}{\bar{y}}$ line and the shaded figure is the influence diagram of $\frac{M}{\bar{y}}$ for the point X. If a load W acts at a point which is a distance x from A the bending moment in the rib at X is $W\bar{y} \times$ (ordinate

FG). If the influence line is required for any other position on the rib it is only necessary to calculate the new value of the ordinate corresponding to XD and to complete the diagram, keeping the same curve

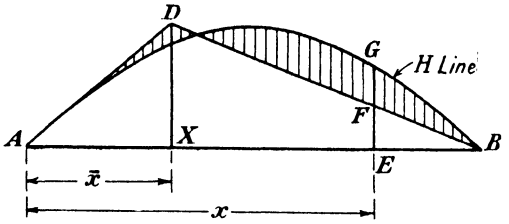

FIG. 15.14.

for H. The advantages of plotting $M/\bar{y}$ instead of M are thus seen to be considerable.

15.11. Influence lines for a fixed arch.—A general solution for the fixed arch carrying a vertical load at any point was given in paragraph 12.13 and the formulas quoted there can be used to plot the influence lines. The load was taken as 2W so we must put $W=\frac{1}{2}$ to obtain the results in the correct form for the influence diagrams

As an example we will consider the case of an arch in which the rise is one quarter of the span. This gives a central angle $2\theta=106°\ 16'$ and upon substituting the trigonometrical functions for θ and putting $W=\frac{1}{2}$ the formulas of paragraph 12.13 reduce to

$$H=9{\cdot}273\cos 2\psi+32\cos\psi+32\psi\sin\psi-40{\cdot}34$$

$$\frac{M_b}{R}=\frac{1}{{\cdot}9273}\{-{\cdot}2436H+{\cdot}6709-\tfrac{1}{2}(\cos\psi+\psi\sin\psi)\}$$

$$V_c=\frac{\psi-\sin\psi(1{\cdot}2-\cos\psi)}{{\cdot}8946}$$

$$\frac{M_c}{R}=\frac{0{\cdot}8\psi-\sin\psi(1{\cdot}4073-0{\cdot}8\cos\psi)}{{\cdot}8946}$$

$\psi°$	H	V_A	V_B	$\frac{M_A}{R}$	$\frac{M_B}{R}$
0	·93	0·5	·5	−·059	−·059
5	·91	0·577	·423	−·037	−·074
15	·75	0·725	·275	+·019	−·082
25	·52	0·849	·152	+·067	−·069
35	·25	0·940	·061	+·091	−·037
45	·05	0·989	·012	+·065	−·009
53° 8′	0	1·000	0	0	0

The values calculated from these equations enable those for V_A, V_B, M_A and M_B, also given in paragraph 12.13, to be tabulated (p. 364).

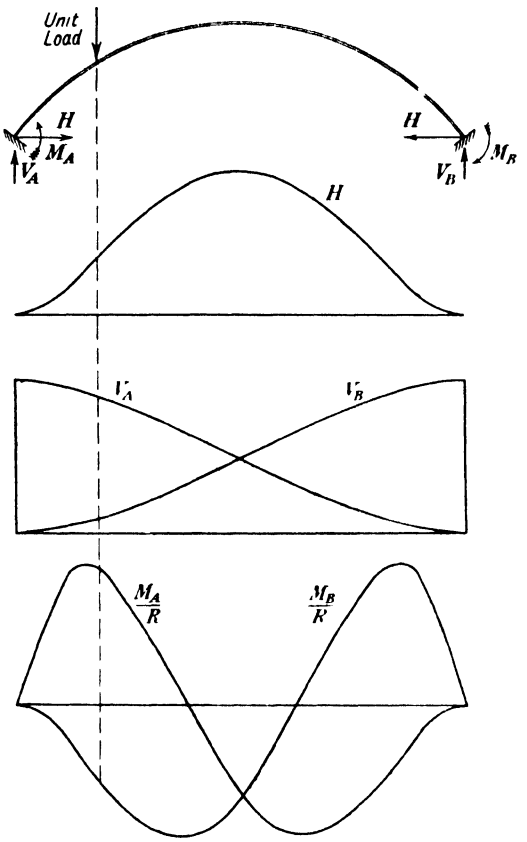

FIG. 15.15.

The influence lines are plotted in Fig. 15.15 on a base representing the span of the arch.

15.12. Choice of redundant elements to simplify calculations.—A judicious choice of redundancies enables calculations in many instances to be considerably simplified and this is particularly the case when the redundant elements can be taken to act at the same section of the structure. The method to be described is due to Müller-Breslau.

Suppose the structure shown in Fig. 15.16 is supported by pins at the points A, B and C. If the pin C were removed the frame would be statically determinate and so, when supported as shown, there are two redundant elements. These are usually taken to consist of a vertical and a horizontal reaction at C, but there is no reason why these particular directions should be chosen and we can in fact assume the two forces at C to act in any directions chosen arbitrarily.

Suppose then we take component reactive forces at C acting in the

direction shown by R_1 and R_2, these being inclined at any angle to each other.

To draw the influence diagrams for these forces we proceed as explained in previous examples. A unit load is applied to C in the line of R_1,

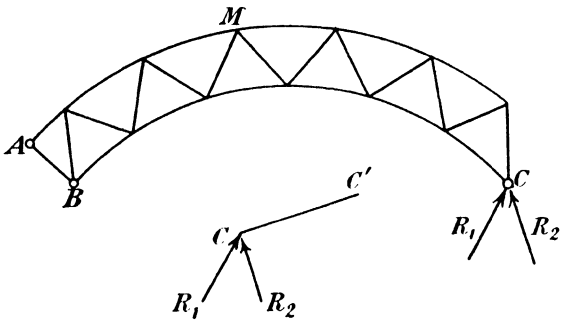

FIG. 15.16.

but in the opposite direction and a Williot diagram is drawn. From this diagram the following data are measured:

The vertical deflection of a point M $=\delta_1$
The movement of C in the line of $R_1=\Delta_1$
The movement of C in the line of $R_2=\Delta_1'$.

A second diagram is now drawn for a unit load acting in the line of R_2, but in the opposite direction and corresponding data are obtained as follows:

The vertical deflection of M $=\delta_2$
The movement of C in the line of $R_2=\Delta_2$
The movement of C in the line of $R_1=\Delta_2'$.

If a unit load acts vertically at M when the support C is removed the movements of C in the lines of R_1 and R_2 are δ_1 and δ_2 respectively. If the support is kept in position by reactive forces R_1 and R_2 the following equations must be satisfied:

$$R_1\Delta_1+R_2\Delta_2'=\delta_1$$

and,

$$R_1\Delta_1'+R_2\Delta_2=\delta_2.$$

δ_1 and δ_2 can be obtained from the Williot diagrams for all panel points and these equations can be solved and the R_1 and R_2 lines plotted.

This is a general result irrespective of the direction assumed for R_1 and R_2. Suppose, however, that from the Williot diagram for a unit load acting in the line of R_1 we find that point C moves to C'. If the line of action of R_2 is then made perpendicular to CC' there will be no movement of C in the line of R_2 under the action of the unit load in the line of R_1, *i.e.* $\Delta_1'=0$. But, by Clerk Maxwell's theorem $\Delta_2'=\Delta_1'$ and the equations above reduce to the simple results

$$R_1=\frac{\delta_1}{\Delta_1}$$

and

$$R_2=\frac{\delta_2}{\Delta_2}.$$

A similar procedure can be followed in the case of three redundant elements.

Fig. 15.17 represents a braced arch supported at the four points A, B, C and D by pins. The redundancies introduced by the pins at C and D can be represented by two forces acting in arbitrary directions as in the last example and by a couple applied to the section CD.

In the first place assume that a unit couple acts at the section CD, represented by two forces $\frac{1}{d}$ at a distance apart d as shown in the Figure. From the Williot diagram the displaced position of CD is found to be C'D'. Lines perpendicular to CC' and DD' are drawn from the centre

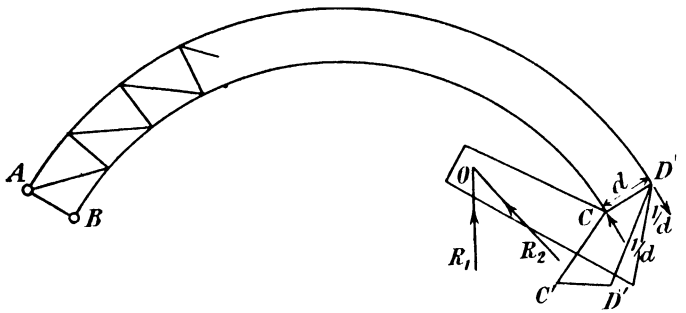

FIG. 15.17.

points of these lines to intersect at O, the instantaneous centre of rotation of CD. Imagine points C, D and O to be connected by a rigid plate and a force of unity to be applied at O in the direction R_1. This can be taken in any direction but will be assumed to be vertical for convenience. This force will produce no rotation of CD. From the Williot diagram for this force the direction of movement of O is determined and the second reactive force is made to act perpendicular to this movement as in the last example.

In the general case when the direction of the reactive forces are chosen arbitrarily, let a unit couple applied to CD produce a vertical deflection of any point M $=\delta_m$

a movement of O in the direction of $R_1 = \Delta_m$

a movement of O in the direction of $R_2 = \Delta'_m$

an angular rotation of CD $=\theta_m$.

Let a unit force in the line of R_1 produce

a vertical deflection of M $=\delta_1$

a movement of O in the direction of $R_1 = \Delta_1$

a movement of O in the direction of $R_2 = \Delta'_1$

an angular rotation of CD $=\theta_1$

and let a unit force in the line of R_2 produce

a vertical deflection of M $=\delta_2$

a movement of O in the direction of $R_1 = \Delta'_2$

a movement of O in the direction of $R_2 = \Delta_2$

an angular rotation of CD $=\theta_2$.

When the supports at C and D are in position and a load of unity acts vertically at M let the reactive forces consist of a moment M_0, and forces R_1 and R_2. The following equations can then be formed:

$$M_0\Delta_m+R_1\Delta_1+R_2\Delta_2'=\delta_1$$
$$M_0\Delta_m'+R_1\Delta_1'+R_2\Delta_2=\delta_2$$
$$M_0\theta_m+R_1\theta_1+R_2\theta_2=\delta_m.$$

These must then be solved simultaneously for each point on the influence line.

When the position of the point O and the directions for R_1 and R_2 are chosen as described above, however, we have

$$\theta_1=\theta_2=0$$
$$\Delta_1'=\Delta_2'=0$$
$$\Delta_m=\Delta_m'=0$$

and the equations reduce to the simple results

$$R_1=\frac{\delta_1}{\Delta_1}$$
$$R_2=\frac{\delta_2}{\Delta_2}$$
$$M_0=\frac{\delta_m}{\theta_m}$$

The whole of the data for plotting the R and M lines are available from the Williot diagrams and the calculations are of the simplest possible type.

EXERCISES

(1) A beam of length L and uniform cross-section is encastré at both ends and rests at the centre of the span on a rigid support.

Show that the equation for the influence line of reaction at this support for each half of the beam is

$$R=4\alpha^2(3-4\alpha)$$

where αL is the distance of the unit load from one end.

(2) A beam ABC of uniform cross-section is encastré at A and rests on a rigid support at B which is L from A. The end C is unsupported. If the distance of a unit rolling load from B is $x=\alpha L$ show that the influence line of reaction at B is given by the two equations

$$R=1-\frac{3\alpha}{2}+\frac{\alpha^3}{2}\text{ (when } x \text{ is between B and A)}$$

and

$$R=1+\frac{3\alpha}{2}\text{ (when } x \text{ is between B and C).}$$

(3) A beam of uniform flexural rigidity EI and length L is pinned at its ends and centre to three columns of the same material as the beam, each of height l.

The end columns each have a cross-sectional area A and the middle column 2A. If x is measured from the centre of the beam show that the influence line of reaction on the mid-support is given by

$$R=\frac{6Lx^2-4x^3-L^3+\frac{24lI}{A}}{L^3+\frac{48lI}{A}}$$

(4) A two-pinned segmental arch rib of 100 feet span has a rise of 20 feet. Plot the influence line for the horizontal thrust.

(5) If the arch in the last question is encastré at both ends plot the influence lines for the reactive forces and moments at the supports.

(6) An encastré parabolic arch rib has a span of 100 feet and a rise of 16 feet. Assuming that the second moment of area at any section is given by $I_0 \sec \alpha$ where I_0 is the value at the crown and α is the angle of slope of the rib at any point, plot the influence lines for the reactions at the supports.

(7) A Warren truss 12 feet deep consists of ten panels each 10 feet long. It rests on rigid supports at the ends and at the fourth panel point from one end. The cross-sectional areas of the members of the truss are such that if the intermediate support is removed and a load applied to that point the stress in all the loaded bars is the same.

Draw the influence line of reactions for the centre support for a load on the bottom chord.

CHAPTER 16

THE SUSPENSION BRIDGE

16.1. The hanging cable.—When a flexible cable suspended from two supports carries loads which are large compared with the weight of the cable the shape it assumes can be obtained by means of a funicular polygon provided that a third point through which the cable must pass or alternatively the horizontal reaction at one point of support is specified. The methods used are given in books on mechanics and need not be dealt with here.

When a uniform cable hangs freely under its own weight it assumes a shape known as the catenary and the chains of a suspension bridge would take this form if otherwise unloaded. The weight of the platform, suspension rods, etc., however, cause modifications.

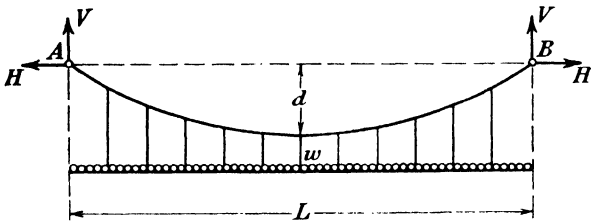

FIG. 16.1.

Suppose a cable of negligible weight carries by means of suspension rods a flexible platform upon which there is a uniformly distributed load of intensity w, as shown in Fig. 16.1.

The reactions at A and B consist of vertical forces $V=\frac{wL}{2}$ and horizontal forces H which have to be determined. H is the horizontal component of the tension in the cable and is the same everywhere since there are no external horizontal loads. Take the lowest point on the cable as origin and consider the equilibrium of a portion OC where C is a distance x horizontally from O and a distance y vertically above it, as in Fig. 16.2. The only forces acting on OC are the tensions H and T at O and C respectively and the load wx acting at $x/2$ from O.

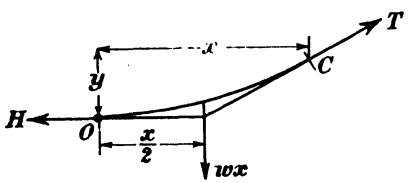

FIG. 16.2.

By taking moments about C we obtain

$$Hy=\frac{wx^2}{2}$$

or

$$y=\frac{wx^2}{2H}$$

Hence the cable under the specified condition assumes a parabolic form.

When $x=L/2$, $y=d$ and the equation becomes

$$d=\frac{wL^2}{8H}$$

so that

$$H=\frac{wL^2}{8d} \quad . \quad . \quad . \quad . \quad . \quad . \quad . \quad . \quad . \quad . \quad (1)$$

The uniformly distributed dead load of a bridge therefore causes the cables to distort from the catenary and the result is a curve which is neither catenary nor parabola. For the small ratios of d/L which occur in actual bridges, however, the difference between the curves is very slight and it is always assumed that when carrying its dead load the cable of a bridge takes a parabolic form.

If the origin of this parabola be taken at O, the lowest point, its equation can be written

$$y=\frac{4dx^2}{L^2} \quad . \quad . \quad . \quad . \quad . \quad . \quad . \quad . \quad . \quad . \quad (2)$$

It is often convenient, however, to take the origin at A and the equation is then

$$y=\frac{4d}{L^2}x(L-x) \quad . \quad . \quad . \quad . \quad . \quad . \quad . \quad . \quad . \quad (3)$$

At any point in the cable the tension T is given by

$$T=H\frac{ds}{dx}$$

and since

$$\frac{ds}{dx}=\sqrt{1+\left(\frac{dy}{dx}\right)^2},$$

$$T=H\sqrt{1+\left(\frac{dy}{dx}\right)^2}.$$

From equation (2) when the origin is at O this is

$$T=H\sqrt{1+\frac{64d^2x^2}{L^4}} \quad . \quad . \quad . \quad . \quad . \quad . \quad . \quad . \quad . \quad (4)$$

When $x=L/2$, T is a maximum and

$$T_{max}=H\sqrt{1+\frac{16d^2}{L^2}} \quad . \quad . \quad . \quad . \quad . \quad . \quad . \quad . \quad . \quad (5)$$

If the cable is supported at two points which are at different levels and carries a uniformly distributed load along a horizontal line as

shown in Fig. 16.3, its shape consists of the parabola ACB where C is the lowest point of the curve. Let the support B be a distance h above the support A and the maximum dip of the cable at C be d below A.

Also let C be x_1 from A.

Then since the horizontal component of the tension in the cable is constant we have

$$H=\frac{wx_1^2}{2d}=\frac{w(L-x_1)^2}{2(h+d)}$$

or

$$\frac{x_1^2}{d}=\frac{(L-x_1)^2}{h+d}.$$

From which we obtain

$$x_1=\frac{L}{h}\{\sqrt{d(d+h)}-d\} \quad \ldots\ldots\ldots \quad (6)$$

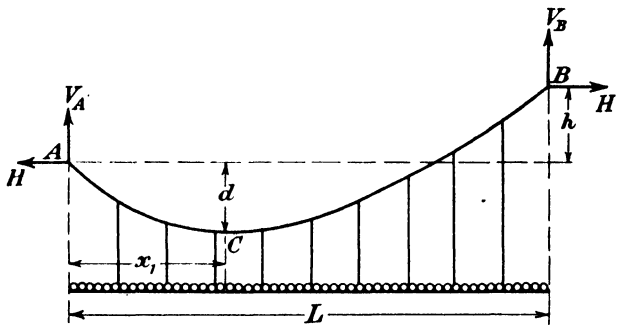

FIG. 16.3.

16.2. Stiffened suspension bridges.—Owing to the tendency to change its configuration under different load systems the simple suspension cable does not make a satisfactory bridge except for the lightest traffic and to overcome this disadvantage stiffening girders are used in conjunction with the cable. Such girders are suitably supported on the bridge piers and suspension rods connect them with the cables. Loads coming on the bridge are distributed through the stiffening girders to the suspension rods and the cables.

A reasonably simple solution of the problem of stress distribution in a stiffened suspension bridge can only be found by adopting certain assumptions as follows :—

(1) It is assumed that the suspension rods are so adjusted that under the dead weight of the bridge the cable assumes a parabolic shape and that the whole of the dead weight is carried direct to the cables through the suspension rods. The stiffening girders are thus relieved of all stress arising from the dead weight of the bridge.

(2) It is assumed that the cable retains a parabolic shape under all conditions of live loading.

Since, as was shown in the previous paragraph, the parabolic shape

can only be maintained by a uniformly distributed horizontal loading, the second assumption implies that any live load on the bridge causes a uniform pull in all the suspension rods.

The stiffening girder may be supported in various ways : if the bridge is a single span, the girder will normally be pinned or hinged to the piers. If there are, in addition, stiffened side spans, the girder may be either continuous over the piers or pinned as before. The case of pinned girders only will be considered in this book.

The suspension cable acting alone is a sufficient and statically determinate means of carrying loads and when a beam which is itself also statically determinate is connected to it the resultant structure is redundant. Hence a suspension bridge with a stiffening girder pinned at its ends exhibits one degree of redundancy. If, however, the girder is provided with an additional pinned joint or hinge somewhere in its span the bridge stiffened by such a three-pinned girder becomes statically soluble. This case will be considered first.

16.3. Suspension bridge with three-pinned stiffening girder.—Fig. 16.4 represents a suspension cable of span L and central dip d, stiffened by

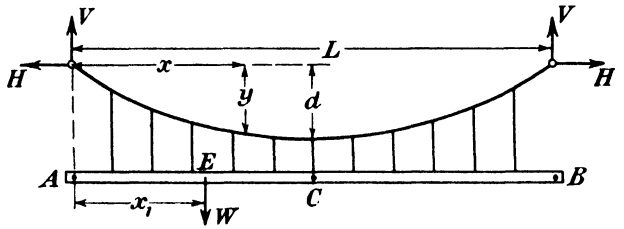

FIG. 16.4.

a girder pinned to supports at A and B and having a central hinge at C. The reactive forces from the cable loads will consist of horizontal and vertical components as shown, and since the assumption is made that however the bridge is loaded the pulls from the suspension rods will always give a uniformly distributed load on the cable, the reactive forces will be the same at each pier.

If the total dead weight of the bridge is equivalent to a uniform horizontally distributed load of intensity w_0 the horizontal component of tension in the cable due to this will be

$$H_0=\frac{w_0L^2}{8d} \quad . \quad . \quad . \quad . \quad . \quad . \quad . \quad . \quad . \quad (1)$$

and the tension in each suspension rod will be

$$t_0=\frac{w_0L}{N} \quad . \quad . \quad . \quad . \quad . \quad . \quad . \quad . \quad . \quad (2)$$

where N is the number of rods.

The equation for the cable is conveniently written in the form

$$y=\frac{4d}{L^2}x(L-x)$$

where x is measured from the support A.

When a load W is placed on the bridge at a distance x_1 from A it causes an equal tension in each suspension rod equivalent to that produced by a uniform horizontally distributed load of intensity w and the conditions of loading of the cable and girder are shown in Fig. 16.5.

The girder is subjected to bending from the downward concentrated load W and the uniformly distributed upward load of intensity w, so that at any point nL from A the bending moment on the girder is

$$M=\mu+\mu'$$

where μ is the bending moment due to W and μ' that due to w,

i.e. $$\mu=W\{-n(L-x_1)+[nL-x_1]\}$$

the second term being included only when it is positive

and $$\mu'=\frac{wnL^2}{2}(1-n).$$

The cable is subjected to a uniformly distributed downward load of

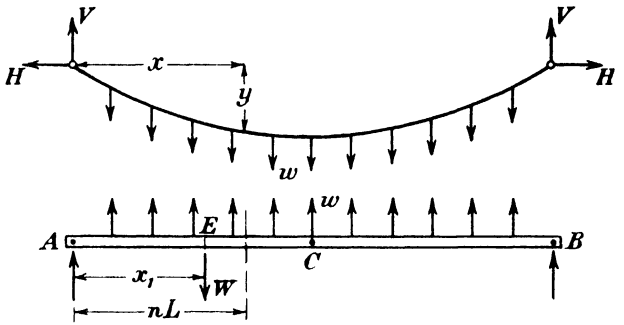

FIG. 16.5.

intensity w which causes a horizontal component of tension H so that the moment about a point in it at nL from A is

$$m=Hy-VnL+\frac{wn^2L^2}{2}$$

where y is the dip at $x=nL$.

Since the cable is flexible, $m=0$.

Also $$V=\frac{wL}{2}$$

$$\therefore\quad Hy=\frac{wnL^2}{2}(1-n)=\mu'$$

and $$M=\mu+Hy \quad \ldots\ldots\ldots\ldots \quad (3)$$

Since H is a constant and y is the ordinate to the parabolic curve of the cable the second term in this equation is represented by a parabola. The first term is represented by a triangle having its apex at $x=x_1$.

At the centre of the girder M=0 due to the presence of the hinge which is incapable of transmitting bending moment, and the bending moment diagram can be drawn as shown in Fig. 16.6.

ADB is the bending moment diagram for the concentrated load W, the maximum ordinate ED being $-\frac{Wx_1}{L}(L-x_1)$. The value of μ at the centre is CF and so if a parabola is drawn through AFB the intercepts between the two diagrams give the bending moments on the girder.

At the centre of the girder since M=0 we have

$$-\mu_c = Hd.$$

Now

$$H = \frac{wL^2}{8d}$$

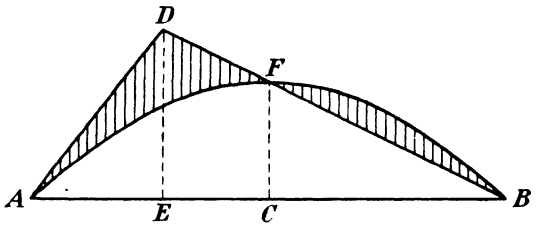

FIG. 16.6.

and if $x_1 < L/2$ $\quad \mu_c = -\frac{Wx_1}{L} \cdot \frac{L}{2} = -\frac{Wx_1}{2}$

$$\therefore \frac{wL^2}{8} = \frac{Wx_1}{2}$$

or $\quad w = \frac{4Wx_1}{L^2}$

and $\quad H = \frac{Wx_1}{2d}$ $\qquad \ldots\ldots\ldots\ldots (4)$

It will be noticed that μ_c given above is only correct provided $x_1 < L/2$, but since the bridge is symmetrical about the centre it is unnecessary to consider cases in which $x_1 > L/2$ since these can be obtained by taking the origin at the other end of the girder.

In all the work following therefore the restriction will be imposed that $x_1 < L/2$.

Having calculated w as above the shearing force diagrams for the girder can be obtained, since the shearing force at any section of the girder is the algebraic sum of the forces due to W and w. The load W as in Fig. 16.4 acts at x_1 from A and we shall calculate the shearing forces at any point nL from A.

If $nL < x_1$

$$F = -\left(\frac{L-x_1}{L}\right)W - wnL + \frac{wL}{2}$$

and substituting the value of w from equation (4) this gives

$$F = \frac{W}{L}(3x_1 - L - 4nx_1) \qquad \ldots\ldots\ldots\ldots (5)$$

This is a straight line in n.

When $n=0$, $\quad F_A=\frac{W}{L}(3x_1-L)$

and when $nL=x_1$ $\quad F_W=\frac{W}{L}\left(3x_1-L-\frac{4x_1^2}{L}\right)$.

If $nL>x_1$

$$F=\frac{W}{L}(3x_1-4nx_1) \quad \ldots\ldots\ldots \quad (6)$$

this is also a straight line in n

when $nL=x_1$ $\quad F_W=\frac{W}{L}\left(3x_1-\frac{4x_1^2}{L}\right)$

when $n=1$ $\quad F_B=-\frac{Wx_1}{L}$.

The shearing force diagram will vary according as $x_1<L/3$ or $x_1>L/3$. The two cases are shown in Fig. 16.7.

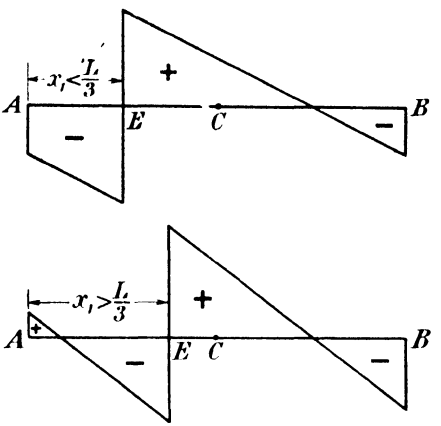

FIG. 16.7.

The maximum negative shearing force will occur at A, to the left of E, or at B.

Clearly, the value to the left of E is greater numerically than that at A.

The numerical value at E is greater than that at B if

$$-3x_1+L+\frac{4x_1^2}{L}>x_1$$

i.e. if $\quad (L-2x_1)^2>0$

which is always the case.

Hence, the maximum negative shearing force occurs just to the left of the load.

The maximum positive shearing force occurs just to the right of the load.

The equations to the curves of maximum positive and negative shearing forces as a load W rolls across the bridge are thus,

$$\left.\begin{aligned} +F_M &= \frac{W}{L}\left(3x_1 - \frac{4x_1^2}{L}\right) \\ \text{and} \quad -F_M &= -\frac{W}{L}\left(3x_1 - \frac{4x_1^2}{L} - L\right) \end{aligned}\right\} \quad \ldots\ldots (7)$$

The positions of the absolute maximum values are found by putting $\frac{dF_M}{dx_1}=0$ and this leads in each case to

$$x_1 = \tfrac{3}{8}L \quad \ldots\ldots (8)$$

The values of the absolute maximum shearing forces are then

$$\left.\begin{aligned} +F_M &= \tfrac{9}{16}W \\ -F_M &= \tfrac{7}{16}W \end{aligned}\right\} \quad \ldots\ldots (9)$$

So for a single concentrated load on the bridge the maximum shearing forces are obtained when the load is at $\frac{3}{8}$ of the span from the end and they are $\frac{9}{16}W$ and $-\frac{7}{16}W$, respectively occurring to the right and left of the load.

The maximum bending moments can be determined as follows. From the bending moment diagram of Fig. 16.6 it is clear that the maximum negative moment occurs at E and is

$$-M_M = \frac{W}{L}x_1(L-x_1) - \frac{w}{2}x_1(L-x_1).$$

Substituting for w this gives

$$-M_M = \frac{W}{L^2}x_1(L-x_1)(L-2x_1) \quad \ldots\ldots (10)$$

Differentiating this and equating to zero we find that the position of maximum negative bending moment occurs when

$$6x_1^2 - 6x_1L + L^2 = 0.$$

or when $$x_1 = \cdot 211L.$$

The value of the bending moment is then $-\cdot 096WL$. The maximum positive bending moment occurs midway between C and B and is

$$+M_M = -\frac{Wx_1}{L}\cdot\frac{L}{4} + \frac{3wL^2}{32}.$$

On substitution for w this becomes

$$+M_M = \frac{Wx_1}{8} \quad \ldots\ldots (11)$$

which has its absolute maximum value of $\frac{WL}{16}$ when x_1 has its maximum value of L/2.

Hence the greatest negative bending moment due to a concentrated load occurs at the load point when the load is $\cdot 211L$ from one end, its value being $-\cdot 096WL$. The greatest positive bending moment $\frac{WL}{16}$ occurs at the quarter span points when the load is at the centre of the span.

16.4. Influence lines for bridge with three-pinned stiffening girder.— The effect of a distributed load upon a suspension bridge is best studied by the use of influence diagrams and these will now be obtained.

Suppose a load W rolls across the bridge as shown in Fig. 16.8; the influence lines are to be drawn for the point G which is at a distance nL from A. n will be always restricted to the range of values zero to $\frac{1}{2}$: if G is on the other half of the girder the influence lines will be obtained directly from those for the coresponding position on AC.

In the first place we shall consider the variation in shearing force at G as x increases from zero to L.

If $x<n$L

$$F_G=-W\left(\frac{L-x}{L}\right)+W-wnL+\frac{wL}{2}$$

and substituting for w from equation (4) of paragraph 16.3 this reduces to

$$F_G=\frac{Wx}{L}(3-4n) \quad \ldots\ldots\ldots \quad (1)$$

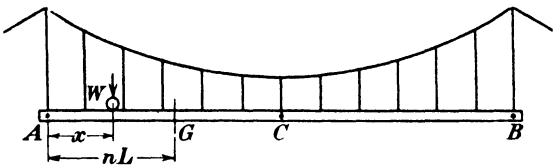

FIG. 16.8.

which is a straight line having zero value at A and a maximum ordinate $Wn(3-4n)$ at G.

If $x>n$L$<\frac{L}{2}$

$$F_G=\frac{Wx}{L}(3-4n)-W \quad \ldots\ldots\ldots \quad (2)$$

which is also a straight line having an ordinate $W(3n-4n^2-1)$ at $x=n$L and an ordinate $\frac{W}{2}(1-4n)$ at $x=L/2$.

If $x>\frac{L}{2}$ the value for w given in equation (4) of paragraph 16.3 is not valid but since loads at x and L$-x$ from A will be symmetrically placed about C they will produce the same effect and therefore when $x>L/2$ it is only necessary to replace x by L$-x$ to obtain w,

i.e. $$w=\frac{4W(L-x)}{L^2} \quad \ldots\ldots\ldots \quad (3)$$

As before $$F_G=-W\left(\frac{L-x}{L}\right)-wnL+\frac{wL}{2}$$

and substituting the value of w given above this reduces to

$$F_G=\frac{-W(L-x)}{L}(4n-1) \quad \ldots\ldots\ldots \quad (4)$$

This is also a straight line giving values of $F_G=0$ when $x=L$

and $$F_G=-\frac{W}{2}(4n-1) \quad \text{when } x=\frac{L}{2}.$$

From this last value for the shearing force when the load is at the centre of the girder it is seen that when $n<1/4$ F_G is positive and when $n>\frac{1}{4}$, F_G is negative. If $n=\frac{1}{4}$ there is no shearing force at the point G when the load has passed the centre of the span. The three influence lines for these cases are shown in Fig. 16.9.

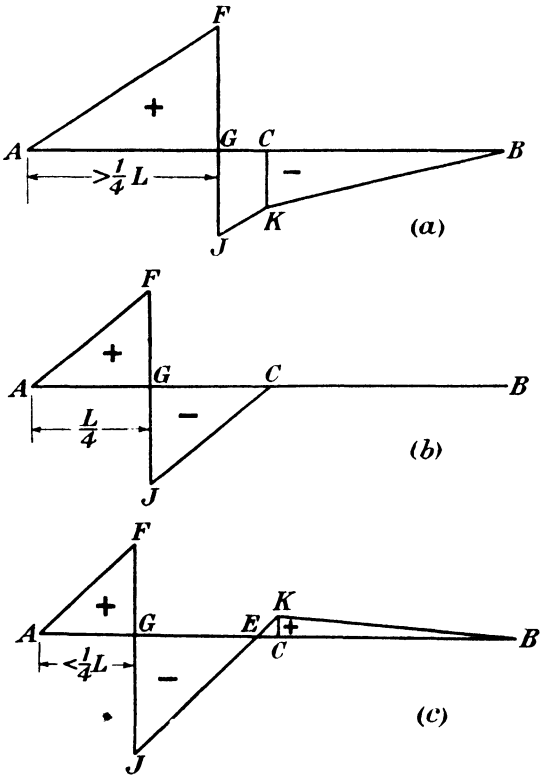

FIG. 16.9.

The influence lines of bending moments for the point G will now be considered.

The dip of the cable at point G is found from equation (3) of paragraph 16.1, by putting $x=nL$, to be $4dn(1-n)$.

Also, when $x<L/2$, $H=\frac{Wx}{2d}$ from equation (4) of paragraph 16.3.

$$\therefore \quad Hy=\frac{Wx}{2d}\cdot 4dn(1-n)=2Wxn(1-n)$$

for values of $x<L/2$.

and the bending moment at G is,

$$M=\mu+2Wxn(1-n) \quad \ldots\ldots\ldots \quad (5)$$

When $x<nL$

$$\mu=-\frac{x}{L}W(L-nL)=-Wx(1-n)$$

$$\therefore\ M=-Wx(1-n)(1-2n) \text{ from equation (5)} \quad \ldots \quad (6)$$

This is a straight line and

when $x=0$, $M=0$

when $x=nL$, $M=-WLn(1-n)(1-2n)$.

When $x>nL<L/2$

$$\mu=-\left(\frac{L-x}{L}\right)WLn=-n(L-x)W$$

and $$M=-Wn(L-x)+2Wxn(1-n)$$

or $$M=Wn\{x(3-2n)-L\}. \quad \ldots\ldots\ldots \quad (7)$$

This is also a straight line

when $x=nL$, $M=-WLn(1-n)(1-2n)$

when $x=L/2$, $M=\frac{1}{2}WLn(1-2n)$.

When $x>L/2$ the value of H previously used is not valid, but by the same argument as was used for determining w in the like case for calculating shearing forces we put

$$H=\frac{(L-x)W}{2d}.$$

Then $$Hy=2Wn(1-n)(L-x)$$

and $$M=\mu+2Wn(1-n)(L-x),$$

but $$\mu=-\left(\frac{L-x}{L}\right)WnL=-Wn(L-x).$$

$$\therefore\ M=Wn(L-x)(1-2n) \quad \ldots\ldots\ldots \quad (8)$$

This is a straight line and

when $x=L/2$, $M=\frac{1}{2}WLn(1-2n)$

when $x=L$, $M=0$.

The influence line of bending moments is then as shown in Fig. 16.10.

The maximum numerical bending moment occurs either when the load is at G or C.

The B.M. for the load at G is greater than the B.M. for the load at C if

$$Ln(1-n)(1-2n)>\frac{Ln}{2}(1-2n),$$

i.e. if $$2(1-n)>1.$$

Since $n<\frac{1}{2}$ this is always true and the maximum numerical bending moment therefore occurs when the load is over the point considered and is negative in sign.

$\therefore$ Maximum negative bending moment

$$-M_M = WnL(1-n)(1-2n) \quad \ldots\ldots\ldots \quad (9)$$

This has its absolute maximum value when $\frac{dM}{dn}=0$,

i.e. when $6n^2-6n+1=0$

or when $n=\cdot 211$.

Hence the maximum negative bending moment occurs under the load when the load is ·211L from either end and its value is —·096WL as found previously from the bending moment diagram.

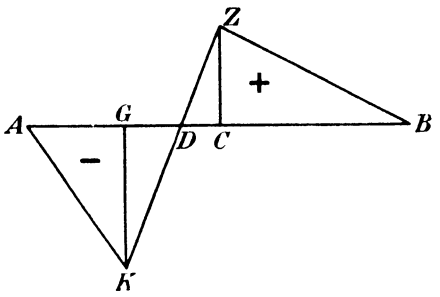

Fig. 16.10.

The maximum positive bending moment is

$$+M_M = \tfrac{1}{2}WLn(1-2n) \quad \ldots\ldots\ldots \quad (10)$$

The absolute maximum occurs when $\frac{dM}{dn}=0$,

i.e. when $1-4n=0$

or $n=\frac{1}{4}$

Its value is then $\frac{WL}{16}$.

So the greatest positive bending moment occurs when the load is at the centre of the span. Its position is at the quarter span points and its value is $\frac{WL}{16}$ as previously determined from the bending moment diagram.

16.5. Effect of uniform load on three-pinned stiffening girders.—By the use of the influence lines obtained in the preceding paragraph we can determine the maximum bending moments and shearing forces in the stiffening girder when a uniformly distributed load of intensity p crosses the bridge.

From the influence lines for shearing force given in Fig. 16.9 it will be seen that the maximum positive shearing force at G will occur either when AG in line (*a*) is covered by the rolling load or when AG and EB in line (*c*) are simultaneously covered.

Consider first the case (*a*), for which n lies between $\frac{1}{4}$ and $\frac{1}{2}$.

The value of the positive shearing force at G is

$$+F_G = p(\text{area AFG})$$

$$= \frac{p}{2} \cdot nL \cdot n(3-4n)$$

$$= \frac{pL}{2} n^2(3-4n) \quad \ldots\ldots\ldots \quad (1)$$

This is a maximum when $\frac{dF}{dn}=0$,

i.e. when $6n-12n^2=0$

or when $n=\frac{1}{2}$.

Its value is then $F_G=\frac{pL}{8}$.

When $x<\frac{1}{4}$ the line (*c*) is applicable and AG and EB must be simultaneously covered to obtain the maximum positive shearing force at G.

Now $$\frac{EC}{EG}=\frac{KC}{JG}=\frac{1-4n}{-2(3n-4n^2-1)}.$$

$$\therefore \quad \frac{EC}{EC+EG}=\frac{1-4n}{8n^2-10n+3}$$

or $$EC=\frac{(1-4n)(1-2n)L}{2(8n^2-10n+3)}$$

$$=\left(\frac{1-4n}{3-4n}\right)\frac{L}{2}$$

$$\therefore \quad EB=2L\left(\frac{1-2n}{3-4n}\right).$$

Then $$+F_G=p(\text{area AGF}+\text{area EKB}).$$

$$+F_G=\frac{pL}{2}\left\{n^2(3-4n)+\frac{(1-4n)(1-2n)}{3-4n}\right\} \quad \ldots \quad (2)$$

This value decreases steadily as n increases from 0 to $\frac{1}{4}$, and the maximum value is therefore $\frac{pL}{6}$ when $n=0$.

Hence, the maximum positive shearing force $\frac{pL}{6}$ occurs at the support A when the loaded length is EB=2/3L.

The maximum negative shearing force at G occurs either when GB in Fig. 16.9 (*a*) is covered by the load or when GE in Fig. 16.9 (*c*) is so covered.

When GB is covered the shearing force is

$$-F_G=-\frac{p}{2}\left[\{(3n-4n^2-1)L+\tfrac{1}{2}(1-4n)\}\left(\frac{L}{2}-nL\right)+\frac{L}{4}(1-4n)\right]$$

or $$-F_G=-\frac{pL}{8}(16n^3-12n^2). \quad \ldots\ldots\ldots\ldots \quad (3)$$

This is a maximum when $\frac{dF_G}{dn}=0$,

i.e. when $n=\frac{1}{2}$.

Its value is then $-\frac{pL}{8}$.

When EG is covered the negative shearing force is

$$-F_G=-\frac{p}{2}\left[\left\{(L-nL)-2L\left(\frac{1-2n}{3-4n}\right)\right\}(3n-4n^2-1)\right]$$

or
$$-F_G=-\frac{pL}{2}\frac{(4n^2-3n+1)^2}{(3-4n)} \quad \ldots\ldots\ldots\ldots \quad (4)$$

This is a maximum when $x=0$ and the value is then $-\frac{pL}{6}$ the covered length being L/3. Hence the maximum negative shearing force $-\frac{pL}{6}$ also occurs at A when the loaded length EG is L/3.

Considering now the bending moments due to a uniformly distributed load it is clear from the influence line of Fig. 16.10 that the maximum negative bending moment at G will occur when the length AD is covered by the load. This length can be found by putting the expression for M equal to zero,

or
$$Wn\{x(3-2n)-L\}=0$$

From which
$$x=AD=\frac{L}{3-2n} \quad \ldots\ldots\ldots \quad (5)$$

The value of the maximum negative bending moment at G is then

$$-M_M=p(\text{area AKD})$$
$$=-\frac{p}{2}\left(\frac{L}{3-2n}\right)Ln(1-n)(1-2n)$$

or
$$-M_M=-\frac{pL^2n(1-n)(1-2n)}{2(3-2n)} \quad \ldots\ldots \quad (6)$$

To find the position of G for which the negative bending moment has the greatest possible value we put $\frac{dM_M}{dn}=0$ and obtain

$$\frac{pL^2}{2}\left\{\frac{(3-2n)(1-6n+6n^2)+2n(1-3n+2n^2)}{(3-2n)^2}\right\}=0$$

or
$$8n^3-24n^2+18n-3=0\,;$$

from which
$$n=0{\cdot}234.$$

Substituting this value of n in equation (6) we find that the greatest negative bending moment in the girder is $-0{\cdot}01883pL^2$ which occurs at a distance of ·234L from the end of the girder. The loaded length to produce this maximum bending moment is found from equation (5) to be ·395L.

The maximum positive bending moment at G occurs when the length DB is covered by the load.

Now $$DB=L-\left(\frac{L}{3-2n}\right)$$

or $$DB=\frac{2(1-n)L}{3-2n} \quad \ldots\ldots\ldots\ldots \quad (7)$$

The bending moment at G is then

$$+M_M=\frac{p}{2}\cdot\frac{2(1-n)L}{3-2n}\cdot\frac{nL(1-2n)}{2}$$

$$=\frac{pL^2n(1-n)(1-2n)}{2(3-2n)} \quad \ldots\ldots\ldots \quad (8)$$

This is the same expression as that for the negative bending moment at G given in equation (6). Hence the greatest possible positive bending moment also occurs at ·234L from one support when the bridge is loaded for a distance of ·605L from the other support. The magnitude of this maximum value is $0{\cdot}01883pL^2$.

16.6. Suspension bridge with two-pinned stiffening girder.—The analysis of this case is complicated by the fact that the structure is redundant and also because a flexible cable does not follow a linear law for its load-deflection relation. The principle of superposition cannot therefore be applied and the effects of a live load are not calculable separately from those due to the dead load as would be the case if the structure obeyed a linear law. The methods of strain energy are not, therefore, strictly applicable to the problem but will be used here to obtain an approximate solution. The assumptions underlying this treatment must, however, be borne clearly in mind. As stated in paragraph 16.2 the initial shape of the cable is assumed to be a parabola and under all subsequent loads it is assumed to retain this shape. This is equivalent to saying that the cable will be treated as an inverted elastic parabolic arch under a load uniformly distributed along the horizontal. The resultant action in it will then consist only of axial tensions and transverse shearing forces; there will be no bending moments.

This theory of the suspension bridge is sometimes known as the elastic theory to distinguish it from the more general and accurate treatment which takes into account the deflection of the girder and cable under live loading.

The horizontal component of cable tension will be taken as the redundant force for the analysis by strain energy methods.

Then $$\frac{dU}{dH}=0.$$

The uniformly distributed pull in the suspension rods due to the load W acting at x_1 from A as in Fig. 16.11 will be represented by w.

For the girder we have

$$M=\mu+Hy$$

where μ is the bending moment on the beam AB due to the load W

so that $$\mu=-\frac{W}{L}(L-x_1)x+W[x-x_1]$$

x being the distance of any point in the girder from A. The term in square brackets only appears in the expression for μ when it is positive, *i.e.* when $x>x_1$.

Then for the girder, $$\frac{dU}{dH}=\int\frac{M}{EI}\frac{dM}{dH}dx$$

$$=\frac{1}{EI}\int(\mu+Hy)ydx.$$

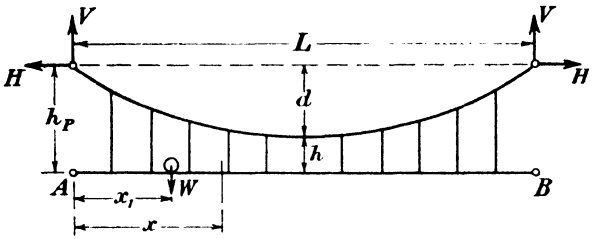

FIG. 16.11.

Taking, as before, the equation of the cable to be

$$y=\frac{4d}{L^2}x(L-x)$$

and substituting the values of μ and y in the expression for $\frac{dU}{dH}$ we have

$$\frac{dU}{dH}=\frac{W}{EI}\left[-\frac{4d}{L^3}(L-x_1)\int_0^L x^2(L-x)dx+\frac{4d}{L^2}\int_{x_1}^L x(x-x_1)(L-x)dx\right]$$
$$+\frac{H}{EI}\left[\frac{16d^2}{L^4}\int_0^L x^2(L-x)^2dx\right],$$

which reduces to

$$\frac{dU}{dH}=\frac{Wx_1d}{3EI}\left[-L+\frac{x_1^2}{L^2}(2L-x_1)\right]+\frac{8HLd^2}{15EI}. \quad . \quad . \quad . \quad . \quad (1)$$

For the cable it is convenient to transfer the origin to the mid-point and to write the equation in the form

$$y=\frac{4x^2d}{L^2}$$

Then $$\frac{dU}{dH}=\frac{1}{AE}\int T\frac{dT}{dH}ds$$

where A is the area of the cable.

At any point in the cable

$$T=H\frac{ds}{dx}$$

and $$\frac{dT}{dH}=\frac{ds}{dx}.$$

Hence $$\frac{dU}{dH}=\frac{2H}{AE}\int_{x=0}^{x=\frac{L}{2}}\left(\frac{ds}{dx}\right)^2 ds$$

Now $$\frac{dy}{dx}=\frac{8xd}{L^2}$$

and $$\left(\frac{ds}{dx}\right)^2=1+\left(\frac{dy}{dx}\right)^2=1+\frac{64x^2d^2}{L^4}$$

$$\therefore\ \frac{dU}{dH}=\frac{2H}{AE}\int_0^{\frac{L}{2}}\left(1+\frac{64x^2d^2}{L^4}\right)^{3/2}dx.$$

Substituting B for $\frac{8d}{L^2}$ and putting $Bx=\tan\theta$ this becomes

$$\frac{dU}{dH}=\frac{2H}{BAE}\int_0^{\tan^{-1}\frac{4d}{L}}\sec^5\theta d\theta$$

i.e. $$\frac{dU}{dH}=\frac{2H}{BAE}\left[\frac{1}{4}\tan\theta\sec^3\theta+\frac{3}{8}\tan\theta\sec\theta+\frac{3}{8}\log_e(\tan\theta+\sec\theta)\right]_0^{\tan^{-1}\frac{4d}{L}}$$

or, for the cable,

$$\frac{dU}{dH}=\frac{HL}{AE}\left[\frac{1}{4}\left(\frac{5}{2}+\frac{16d^2}{L^2}\right)\left(1+\frac{16d^2}{L^2}\right)^{1/2}+\frac{3}{32}\frac{L}{d}\log_e\left\{\frac{4d}{L}+\left(1+\frac{16d^2}{L^2}\right)^{1/2}\right\}\right]. \quad (2)$$

Writing K for the product of L and the terms in the brackets

$$\frac{dU}{dH}=\frac{KH}{AE}.$$

It is convenient to assume that the suspension rods are replaced by a continuous connection between the cable and stiffening girder, this being only able to transmit stress vertically.

If there are N rods each having a cross-sectional area a_r, the thickness of this continuous connecting " plate " is

$$\Delta=\frac{Na_r}{L}.$$

At x from the centre of the span the vertical distance between the girder and the cable is

$$l=h+\frac{4x^2d}{L^2}$$

where h is the distance at the centre as shown in Fig. 16.11.

The load on an element of the plate δx in length is $w\delta x$ where w is the uniform intensity of load caused by the weight W.

Then the strain energy of this element is

$$\delta U=\frac{(w\delta x)^2\left(h+\frac{4x^2d}{L^2}\right)}{2\Delta\delta xE_r}$$

where E_r is the modulus of elasticity of the plate and therefore of the rods.

Then $$U=\frac{w^2}{\Delta E_r}\int_0^{\frac{L}{2}}\left(h+\frac{4x^2d}{L^2}\right)dx.$$

But $$w=\frac{8Hd}{L^2}$$

$$\therefore \quad U=\frac{64H^2d^2}{\Delta E_rL^2}\int_0^{\frac{L}{2}}\left(h+\frac{4x^2d}{L^2}\right)dx$$

and $$\frac{dU}{dH}=\frac{64d^2H}{L^3\Delta E_r}\left(h+\frac{d}{3}\right).$$

Substituting for Δ we obtain for the rods the expression

$$\frac{dU}{dH}=\frac{64d^2H}{Na_rE_rL^2}(h+d/3) \quad \ldots\ldots\ldots \quad (3)$$

The effect of the piers is small but may be included if so desired as follows:

Let the equivalent area of the pier be A_P and its height h_P. The compression in the pier will be V, the vertical component of the cable tension at the pier,

and $$V=H\frac{dy}{dx}$$

From the equation for the cable, taking the origin at the centre, we have

$$\frac{dy}{dx}=\frac{8xd}{L^2}$$

and when $x=L/2$, *i.e.* at the pier,

$$\frac{dy}{dx}=\frac{4d}{L}$$

therefore $$V=\frac{4Hd}{L} \quad \text{and} \quad \frac{dV}{dH}=\frac{4d}{L}.$$

Then $$\frac{dU}{dH}=\frac{1}{A_PE_P}\int_0^{h_P}V\frac{dV}{dH}dx$$

$$=\frac{16d^2h_PH}{A_PE_PL^2}.$$

For the two piers therefore

$$\frac{dU}{dH}=\frac{32d^2h_PH}{A_PE_PL^2} \quad \ldots\ldots\ldots \quad (4)$$

Adding the terms from equations (1) to (4) and equating to zero the total value of $\frac{dU}{dH}$ thus found, we obtain as the value of H the expression

$$H=\frac{\frac{Wx_1d}{3EI}\left\{L-\frac{x_1^2}{L^2}(2L-x_1)\right\}}{\frac{8Ld^2}{15EI}+\frac{K}{AE}+\frac{64d^2}{Na_rE_rL^2}\left(h+\frac{d}{3}\right)+\frac{32d^2h_P}{A_PE_PL^2}} \quad \ldots\ldots \quad (5)$$

If the effect of the suspension rods and the piers be neglected this reduces to

$$H=\frac{\frac{Wx_1d}{3EI}\left\{L-\frac{x_1^2}{L^2}(2L-x_1)\right\}}{\frac{8Ld^2}{15EI}+\frac{K}{AE}} \quad . \quad . \quad . \quad . \quad . \quad . \quad (6)$$

The part of this equation affected by the load position is

$$x_1\left\{L-\frac{x_1^2}{L^2}(2L-x_1)\right\}$$

so that H varies with this expression.

Differentiating with respect to x_1 and equating to zero, we find that for a maximum value of H

$$L-\frac{6x_1^2}{L}+\frac{4x_1^3}{L^2}=0$$

or $$x_1=L/2.$$

The value is then

$$H_{max}=\frac{\frac{5WL^2d}{48EI}}{\frac{8Ld^2}{15EI}+\frac{K}{AE}} \quad . \quad . \quad . \quad . \quad . \quad . \quad (7)$$

The bending moment at any point in the girder, as for the three-hinged type, is

$$M=\mu+Hy$$

and this can be plotted after H has been calculated from equation (5).

Since $w=\frac{8Hd}{L^2}$ its value can also be found and the shearing force curve plotted as the algebraic sum of the curves due to the concentrated load W and the uniform load of intensity w.

16.7. Influence line of bending moment for two-pinned girder.—Let G in Fig. 16.12 (*a*) be the point for which the influence line of bending moment is to be drawn and let it be nL from A.

Since $$M=\mu+Hy$$

the influence line of bending moment for any point will be the algebraic sum of the influence lines for μ and for Hy where y is the particular value of the dip at $x=n$L.

Re-writing the above equation we get

$$M=\left(\frac{\mu}{y}+H\right)y$$

and $$y=\frac{4d}{L^2}nL(L-nL)=4nd(1-n).$$

The influence line for μ is a triangle with its apex at G, the ordinate at this point being

$$\frac{nL(L-nL)}{L}=nL(1-n)$$

so that the influence line for $\frac{\mu}{y}$ is also a triangle with its apex at G, the ordinate being

$$\frac{nL(1-n)}{4nd(1-n)} = \frac{L}{4d}.$$

This is independent of n so that the maximum ordinate of the influence line is the same for all positions for which such lines may be drawn.

For the load in any one position on the beam the value of H is the same throughout the cable and so the influence line of H is the same for

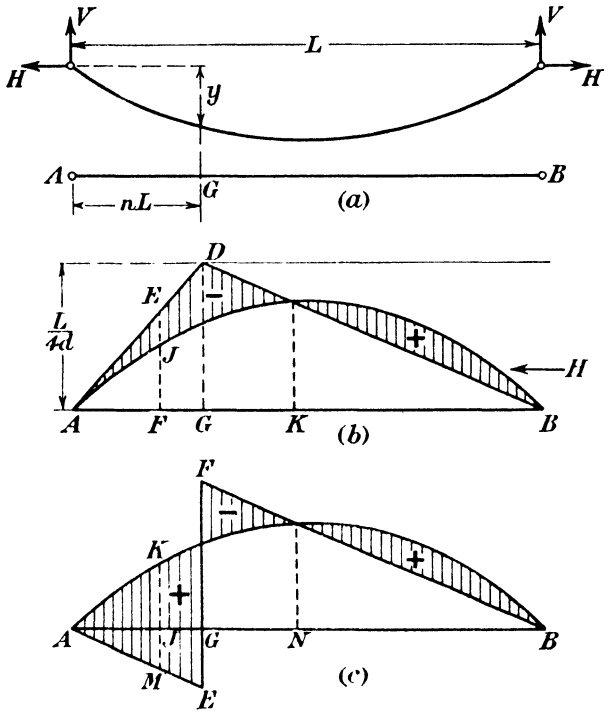

FIG. 16.12.

all points and is simply the curve obtained from equation (5) of the last paragraph.

Hence to draw the influence line of M/y, the procedure is as follows :

Re-write equation (5) of paragraph 16.6 as

$$H = CWx_1\left\{L - \frac{x_1^2}{L^2}(2L - x_1)\right\} \quad \ldots\ldots\ (1)$$

and having calculated C, which depends only on known dimensions of the bridge and its constituents, plot the curve of H when W is made equal to unity for all values of x_1 from 0 to L, as shown in Fig. 16.12 (*b*).

Draw a line parallel to AB at a distance $\frac{L}{4d}$ from it. This line will

be the locus of the apices of the influence lines of μ/y. If at any point such as G a perpendicular GD is set up to cut this locus, ADB will be the required influence line of μ/y and the influence line of M/y will be as shown shaded in the Figure.

The bending moment at G for the load at F will then be the ordinate EJ multiplied by y, *i.e.* by $4dn(1-n)$.

The maximum negative bending moment at G under a distributed load occurs when AK is covered and the maximum positive bending moment when KB is covered.

General expressions such as were obtained in the case of the three-pinned girder are not practicable, but for any particular case the results are quickly found by plotting the influence diagrams as shown.

16.8. Influence line of shearing force for two-hinged girder.— Differentiating the expression for the bending moment at any point on the girder we obtain

$$\frac{dM}{dx}=\frac{d\mu}{dx}+H\frac{dy}{dx}.$$

$\frac{dM}{dx}$ is the shearing force at any section of the girder under the action of all forces acting upon it and $\frac{d\mu}{dx}$ that due to the concentrated load only and we may re-write the expression

$$F=\left(\frac{F'}{\frac{dy}{dx}}+H\right)\frac{dy}{dx}.$$

As before we shall consider the shearing force at the point G which is a distance nL from A.

Since $$y=\frac{4d}{L^2}x(L-x)$$

$$\frac{dy}{dx}=\frac{4d}{L^2}(L-2x)$$

and at G, $$\frac{dy}{dx}=\frac{4d}{L}(1-2n)$$

$$\therefore \quad F=\left[\frac{F'L}{4d(1-2n)}+H\right]\frac{4d}{L}(1-2n).$$

The variable part of this is included in the square brackets and it is therefore only necessary to plot the influence line for this expression.

As in the case of the bending moment, the influence line for H is the curve of H with W put equal to unity. This is shown plotted in Fig. 16.12 (*c*). To balance the moment at G due to H an upward reaction will always be required at B and so the shearing force at G due to H will always be positive.

Upon this curve must be superimposed the expression involving F'. This is the influence line for a simple beam multiplied by the constant $\frac{L}{4d(1-2n)}$.

When the load is just to the left of G the shear at G is positive and the ordinate GE is

$$\frac{nL}{L}\left\{\frac{L}{4d(1-2n)}\right\}=\frac{nL}{4d(1-2n)}.$$

When the load is just to the right of G the shearing force at G is negative and the ordinate GF is

$$-\frac{L(1-n)}{L}\left\{\frac{L}{4d(1-2n)}\right\}=-\frac{(1-n)L}{4d(1-2n)}.$$

The influence line for the complete expression is then as shown in Fig. 16.12 (*c*) and to obtain the shearing force at G for a load of unity at J, for example, the ordinate KM must be multiplied by $\frac{4d(1-2n)}{L}$.

The maximum positive shearing force at G for a uniformly distributed load will occur when AG and NB are covered by the load, and the maximum negative shearing force when GN is so covered.

16.9. Length of a suspension cable.—The length of a cable hanging in a parabolic arc can be calculated as follows:

Since $$\frac{ds}{dx}=\sqrt{1+\left(\frac{dy}{dx}\right)^2}$$

we have $$\int ds=\int\left\{1+\left(\frac{dy}{dx}\right)^2\right\}^{\frac{1}{2}}dx$$

and using equation (2) of paragraph 16.1 we obtain

$$\frac{dy}{dx}=\frac{8xd}{L^2}$$

so that the total length of the cable is

$$s=2\int_0^{L/2}\left(1+\frac{64x^2d^2}{L^4}\right)^{\frac{1}{2}}dx$$

or
$$s=\frac{L}{2}\left(1+\frac{16d^2}{L^2}\right)^{\frac{1}{2}}+\frac{L^2}{8d}\log_e\left\{\frac{4d}{L}+\left(1+\frac{16d^2}{L^2}\right)^{\frac{1}{2}}\right\}. \quad . \quad . \quad . \quad . \quad (1)$$

By expanding the expression to be integrated, a solution in series can be obtained and a result sufficiently accurate for most purposes found in a simpler form.

Thus

$$s=2\int_0^{L/2}\left(1+\frac{32x^2d^2}{L^4}-\frac{512x^4d^4}{L^8}+\ldots\ldots\right)dx$$

$$=2\left[x+\frac{32x^3d^2}{3L^4}-\frac{512x^5d^4}{5L^8}+\ldots\ldots\right]_0^{L/2}$$

$$=\left[L+\frac{8}{3}\frac{d^2}{L}-\frac{32d^4}{5L^3}+\ldots\ldots\right]$$

or
$$s=L\left[1+\frac{8}{3}\left(\frac{d}{L}\right)^2-\frac{32}{5}\left(\frac{d}{L}\right)^4+\ldots\ldots\right] \quad . \quad . \quad . \quad . \quad . \quad (2)$$

For small d/L ratios it is sufficient for many purposes to take the first two terms only and write

$$s=L\left\{1+\frac{8}{3}\left(\frac{d}{L}\right)^2\right\} \quad . \quad . \quad . \quad . \quad . \quad . \quad . \quad . \quad (3)$$

16.10. Deflection theory of suspension bridges.—In the elastic theory, upon which the results so far obtained in this chapter are based, it is assumed that the cable maintains the same parabolic curve under all loading systems. This assumption is not an accurate one since under the action of any load on the girder the cables will deflect and the bending moments in the stiffening girder will be modified. The effect of the deflection is to reduce the bending moments and in long span bridges the neglect of this reduction results in the use of unnecessarily large sections in the girders. The first treatment of the problem of the suspension bridge taking account of the deflection terms was given by J. Melan * in 1888 and since then the theory has been extended by D. B. Steinmann,† S. Timoshenko,‡ Atkinson and Southwell ** and others. Space does not permit anything but a short statement of the general principles to be given here and for a full treatment reference should be made to more specialised works § and the original papers.

Under the action of the dead weight of the bridge let the dip of the cable at any point be y and the horizontal tension in it be H_w. Suppose now that additional load is placed on the bridge and that this is, as previously assumed, distributed uniformly between the hangers. Let this cause the horizontal tension to be increased to H_w+H. In the elastic theory the dip of the cable is assumed to be unaltered and the bending moment at any point is

$$M=\mu+Hy.$$

The effect of the extra load however is to increase the dip of the cable to $y+\eta$ and the bending moment in the girder is relieved by the amount $(H_w+H)\eta$.

Then $$M=\mu+Hy+(H_w+H)\eta \quad . \quad . \quad . \quad . \quad . \quad . \quad . \quad (1)$$

If it is assumed that the hangers are inextensible, the deflection of the stiffening girder at any point will be the same as that of the cable and the equation connecting bending moment and deflection in the

* "Eiserne Bogenbrücken und Hängenbrücken. Leipzig, 1888 and 1906.

† "A generalised Deflection Theory for Suspension Bridges." D. B. Steinmann. Trans. Am. Soc. C.E., Vol. 100, 1935, p. 1133.

‡ "The Stiffness of Suspension Bridges." S. Timoshenko. Trans. Am. Soc. C.E., Vol. 94, 1930, p. 377.

"Suspension Bridges with a Continuous Stiffening Truss." S. Timoshenko and S. Way. Pub. of International Assoc. for Bridges and Structural Eng. II (1934).

** "On the Problem of Stiffened Suspension Bridges and its Treatment by Relaxation Methods." R. J. Atkinson and R. V. Southwell. Journal Inst. C.E., Vol. 11, 1938–39, pp. 289–326.

§ *E.g.* "Modern Framed Structures." Johnson, Bryan and Turneaure. 9th ed. Vol. 2, pp. 276–318.

girder is therefore

$$\frac{d^2\eta}{dx^2}=\frac{M}{EI} \quad \ldots\ldots\ldots\ldots \quad (2)$$

Substituting the value of M given by (1) and putting

$$c^2=\frac{H_w+H}{EI}$$

this becomes

$$\frac{d^2\eta}{dx^2}=c^2\eta+\frac{c^2(\mu+Hy)}{H_w+H} \quad \ldots\ldots\ldots\ldots \quad (3)$$

The solution of this equation is

$$\eta=\frac{H}{H_w+H}\left\{C_1e^{cx}+C_2e^{-cx}-\left(\frac{\mu}{H}+y\right)-\frac{1}{c^2}\left(\frac{1}{H}\frac{d^2\mu}{dx^2}+\frac{8d}{L^2}\right)\right\} \quad \ldots \quad (4)$$

where d and L, as before, are respectively the centre dip and span of the cable.

Substituting this expression in (1) we obtain

$$M=H\left\{C_1e^{cx}+C_2e^{-cx}-\frac{1}{c^2}\left(\frac{1}{H}\frac{d^2\mu}{dx^2}+\frac{8d}{L^2}\right)\right\} \quad \ldots\ldots \quad (5)$$

and differentiating (5) the shearing force is given by

$$S=Hc\{C_1e^{cx}-C_2e^{-cx}\}. \quad \ldots\ldots\ldots \quad (6)$$

Since c contains the term H_w it is evident from equations (4), (5) and (6) that the deflection, bending moment and shearing force are not proportional to the additional load placed on the bridge and so it is not possible to draw influence lines for these quantities.

If the deformations are small the value of H found from the elastic theory may be used in the equations. A more exact value is given by Johnson, Bryan and Turneaure.*

The constants of integration C_1 and C_2 depend on the conditions of loading. As an example of their evaluation suppose the bridge to carry a uniformly distributed load of intensity w along its span.

Then in equation (5) $\frac{d^2\mu}{dx^2}=w$ and $M=0$ when $x=0$ and when $x=L$.

Substitution of these values gives

$$C_1+C_2-\frac{1}{c^2}\left(\frac{w}{H}+\frac{8d}{L^2}\right)=0$$

and

$$C_1e^{cL}+C_2e^{-cL}-\frac{1}{c^2}\left(\frac{w}{H}+\frac{8d}{L^2}\right)=0$$

and the solution of these simultaneous equations is

$$C_1=\frac{1}{c^2(e^{cL}+1)}\left(\frac{w}{H}+\frac{8d}{L^2}\right)$$

and

$$C_2=C_1e^{cL}.$$

If the loading is not uniform there will be different values of the constants for each section of the bridge carrying a different load intensity and their values may be found by equating the bending moments and shearing forces respectively at points of loading change on the girder.

An extension of the theory to include allowance for the elasticity of the hangers has been made by S. Timoshenko.*

16.11. Stresses in an extensible suspension cable.—Cables may be used to form the main supporting members in some types of structures. They will usually be very light compared with the loads which they support and will be initially stretched as tightly as possible so that when the loads are applied the sag will be reduced to the minimum. In such cases serious errors will be introduced if the cables are assumed to be inextensible. †

Fig. 16.13 shows a cable, of weight supposed to be negligible in comparison with the loads which it carries, supported at points A and B which are separated by a horizontal distance L and a vertical distance D.

Assume the loads on the cable to be W_1, W_2, . . . W_q, . . . W_{n-1}, acting at distances $l_1, l_2, \ldots l_q \ldots l_{n-1}$ from A, measured horizontally to their final lines of action ; and the reactions at A and B due to these loads to be $R_A+H\alpha$ and $R_B-H\alpha$ vertically, and H horizontally, where H is the constant horizontal component of tension in the cable and α is written for $\frac{D}{L}$.

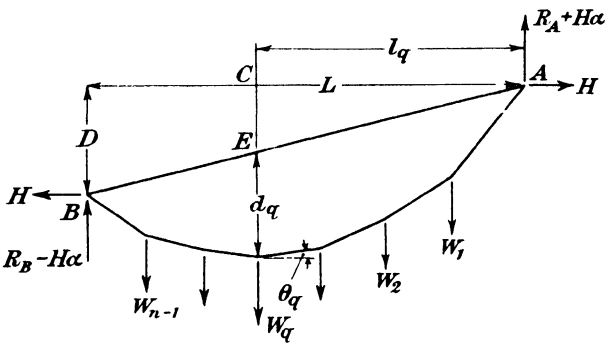

FIG. 16.13.

Let S be the original length of the cable before it is placed in position between the supports A and B ;

d_q, the dip at the load point Q when the cable is loaded, measured from the line AB ;

θ_q, the angle between the cable in the qth bay and the horizontal ;

A, the cross-sectional area of the cable ;

E, Young's modulus for the material of the cable ;

M_q, the bending moment at the qth load due to the force system if H is assumed to be zero ;

F_q, the vertical shearing force in the qth bay on the same assumption.

* Loc. cit., p. 403

† "The Stresses in an Extensible Suspension Cable." A. J. S. Pippard and L. Chitty. Journal Inst. C.E., June, 1942, pp. 322–333.

Then taking moments about Q gives

$$(d_q+\mathrm{EC})\mathrm{H}-\mathrm{H}\alpha l_q-\mathrm{M}_q=0\,;$$

and since $\mathrm{EC}=\alpha l_q$,

$$d_q=\frac{\mathrm{M}_q}{\mathrm{H}}. \qquad \ldots\ldots\ldots\ldots \quad (1)$$

Also, $$\tan\theta_q=\frac{(d_q+\alpha l_q)-(d_{q-1}+\alpha l_{q-1})}{l_q-l_{q-1}}=\frac{\mathrm{M}_q-\mathrm{M}_{q-1}}{\mathrm{H}(l_q-l_{q-1})}+\alpha\,;$$

but $$\frac{\mathrm{M}_q-\mathrm{M}_{q-1}}{l_q-l_{q-1}}=\mathrm{F}_q,$$

and so, $$\tan\theta_q=\frac{\mathrm{F}_q}{\mathrm{H}}+\alpha. \qquad \ldots\ldots\ldots\ldots \quad (2)$$

Then, if θ_q is not too large,

$$\sec\theta_q=1+\tfrac{1}{2}\left(\frac{\mathrm{F}_q}{\mathrm{H}}+\alpha\right)^2. \qquad \ldots\ldots\ldots\ldots \quad (3)$$

Subsequent results are based upon this approximation for sec θ_q, and their application should, therefore, be limited to cases in which the maximum slope of the loaded cable is comparatively small. Table 16.1 gives the error involved for different values of θ; even when $\theta=30$ degrees it is only about 1 per cent., but it increases rapidly for larger values and the results become increasingly inaccurate. The useful range is, however, considerable and probably covers most cases of cables used for structural purposes.

TABLE 16.1.

θ	Tan θ	Sec θ		Error : per cent.
		Accurate	Approximate	
0	0	1	1	0
10	0·1763	1·0154	1·0155	0·01
20	0·3639	1·0642	1·0662	0·19
30	0·5773	1·1547	1·1667	1·04
45	1·0	1·4142	1·5000	6·07
60	1·7320	2·0	2·5	25·0

The strained length of the cable in the qth bay is $(l_q-l_{q-1})\sec\theta_q$, and so the total length of the cable is

$$\sum_1^n(l_q-l_{q-1})\left\{1+\tfrac{1}{2}\left(\frac{\mathrm{F}_q}{\mathrm{H}}+\alpha\right)^2\right\}$$

$$=(1+\tfrac{1}{2}\alpha^2)\sum_1^n(l_q-l_{q-1})+\frac{1}{2\mathrm{H}^2}\sum_1^n(l_q-l_{q-1})\mathrm{F}_q{}^2+\frac{\alpha}{\mathrm{H}}\sum_1^n(l_q-l_{q-1})\mathrm{F}_q.$$

Now from equation (2),

$$\sum_1^n (l_q - l_{q-1}) \tan \theta_q = \frac{1}{H} \sum_1^n (l_q - l_{q-1}) F_q + \alpha \sum_1^n (l_q - l_{q-1})$$

or,
$$D = \frac{1}{H} \sum_1^n (l_q - l_{q-1}) F_q + D ;$$

so
$$\sum_1^n (l_q - l_{q-1}) F_q = 0.$$

The total strained length of the cable is, therefore,

$$L(1+\tfrac{1}{2}\alpha^2) + \frac{Z}{2H^2} \quad . \quad . \quad . \quad . \quad . \quad . \quad . \quad (4)$$

where
$$Z = \sum_1^n (l_q - l_{q-1}) F_q^2.$$

Now if T_q is the tension in the cable in the qth bay, the increase in its length in this bay is

$$\frac{T_q (l_q - l_{q-1}) \sec \theta_q}{AE},$$

and since $T_q = H \sec \theta_q$, the total increase in the length of the cable is

$$\frac{H}{AE} \sum_1^n (l_q - l_{q-1}) \sec^2 \theta_q,$$

and the strained length is, using equation (3),

$$S + \frac{H}{AE}\left[L(1+\alpha^2) + \frac{Z}{H^2} \right] \quad . \quad . \quad . \quad . \quad . \quad . \quad . \quad (5)$$

Equating (4) and (5) we obtain

$$2H^3 L(1+\alpha^2) + 2H^2 AE\{S - L(1+\tfrac{1}{2}\alpha^2)\} + Z(2H - AE) = 0.$$

Since AE is very large in comparison with H, this is, very nearly,

$$2H^3 L(1+\alpha^2) + 2H^2 AE\{S - L(1+\tfrac{1}{2}\alpha^2)\} - ZAE = 0, \quad . \quad . \quad . \quad (6)$$

which determines H for any specified length of cable and distribution of load.

If the cable is erected with an initial tension whose horizontal component is H_0 we have

$$L(1+\tfrac{1}{2}\alpha^2) = S\left\{ 1 + \frac{H_0(1+\tfrac{1}{2}\alpha^2)}{AE} \right\},$$

and on substituting the value obtained for S from this, equation (6) becomes

$$2L(1+\alpha^2)(H^3 - H^2 H_0) - ZAE = 0 \quad . \quad . \quad . \quad . \quad . \quad (7)$$

where H is the final tension under load.

If the cable may be assumed to be initially straight, but has no initial

tension, $S=L(1+\frac{1}{2}\alpha^2)$, and equation (6) gives

$$H^3=\frac{ZAE}{2L(1+\alpha^2)} \quad . \quad . \quad . \quad . \quad . \quad . \quad . \quad . \quad (8)$$

Some particular forms of this result may be noted.

(*a*) If the loads are unequal, but are spaced equally along the span, that is if $l_q-l_{q-1}=l$,

$$H^3=\frac{AE}{2n(1+\alpha^2)}\sum_1^n F_q^2 \quad . \quad . \quad . \quad . \quad . \quad . \quad (9)$$

where n denotes the number of equal bays in the cable.

(*b*) If the loads and spacings are both equal, that is, if $l_q-l_{q-1}=l$ and $W_1=\ldots=W_q=\ldots=W_{n-1}=\ldots=W$,

$$\sum_1^n F_q^2=\frac{W^2n(n^2-1)}{12},$$

and

$$H^3=\frac{AEW^2(n^2-1)}{24(1+\alpha^2)} \quad . \quad . \quad . \quad . \quad . \quad . \quad . \quad (10)$$

(*c*) If the loads and spacings are both equal and A and B are at the same level, that is, if $D=0$,

$$H^3=\frac{AEW^2(n^2-1)}{24} \quad . \quad . \quad . \quad . \quad . \quad . \quad . \quad (11)$$

(*d*) If the loading is continuous and of uniform intensity w along AB, the shearing force at a distance x from A is $w(\frac{1}{2}L-x)(1+\frac{1}{2}\alpha^2)$.

Then,

$$Z=w^2(1+\alpha^2)\int_0^L(\tfrac{1}{2}L-x)^2dx=\frac{w^2L^3(1+\alpha^2)}{12},$$

and

$$H^3=\frac{AEw^2L^2}{24} \quad . \quad . \quad . \quad . \quad . \quad . \quad . \quad . \quad (12)$$

In all cases, when H has been calculated, the dips may be found from equation (1) and the loaded shape of the cable thus determined.

As an example consider the case of a cable stretched tightly between two points A and B which are 100 feet apart horizontally, A being 10 feet above B so that $\alpha=0{\cdot}1$. The loads are 2 tons, 1 ton, $\frac{1}{2}$ ton, $\frac{1}{2}$ ton and 1 ton acting at distances of 20 feet, 30 feet, 50 feet, 80 feet and 90 feet respectively from A. The value of AE is 6,000 tons.

The vertical reaction at A is 2·75 tons. The shearing forces and bending moments at the load points are calculated and entered in columns (3) and (6) of Table 16.2. The values of l_q-l_{q-1} are entered in column (2), and calculated values of F_q^2 and $(l_q-l_{q-1})F_q^2$ in columns (4) and (5). The sum of the values in column (5) gives $Z=241$ foot-tons^2, and H is then found from equation (8) to be 19·3 tons. The dips are found by dividing the bending moments in column (6) by H, and are given in column (7) :

TABLE 16.2.

1	2	3	4	5	6	7
Point	$l_q - l_{q-1}$	F_q	F_q^2	$(l_q - l_{q-1})F_q^2$	M_q	d_q
A					0	0
	20	2·75	7·56	151·2		
C					55	2·85
	10	0·75	0·56	5·6		
D					62·5	3·24
	20	−0·25	0·06	1·2		
E					57·5	2·98
	30	−0·75	0·56	16·8		
F					35·0	1·81
	10	−1·25	1·56	15·6		
G					22·5	1·17
	10	−2·25	5·06	50·6		
B					0	0

EXERCISES

(1) A suspension cable is 700 feet span and 70 feet dip. Calculate the length of the cable.

(718·6 feet)

(2) A thin uniform flexible cable of weight w per unit length connects two points which are at the same level.

Treating the dip d as small compared with the span prove that the difference between the greatest and least tension is wd, and that the difference between the length of the cable and the span is given approximately by $\frac{8}{3}\frac{d^2}{l}$.

The span of such a cable is 200 feet, and the dip is 10 feet at a certain temperature. The coefficient of expansion for the cable is 12×10^{-6} per degree Centigrade. Neglecting change of length due to change of stress, calculate the percentage increase in the maximum tension due to a fall in temperature of 30° C.

(2·74 per cent.)

(3) A suspension bridge of 700 feet span has a dip of 70 feet. It carries a uniformly distributed load of 500 tons. If the chains are made of steel, the allowable stress on which is 5 tons per square inch, calculate the required cross-sectional area of the chains.

The anchor chains make an angle of 45° with the piers.

Calculate the load in one anchor chain and the overturning force on a pier,

(*a*) When the chains run over a pulley device.

(*b*) When the chains are attached to a saddle resting on rollers at the top of the pier.

(67·3 square inches.
(a) 336·5 tons ; 74·4 tons.
(b) 442·0 tons ; none.)

(4) A cable is suspended from two points separated horizontally by a distance of 60 feet and vertically by a distance of 10 feet. The maximum dip of the cable when hanging freely is 5 feet below the lower point of suspension. It is stiffened by a girder which is hinged at both ends and also at a point vertically below the lowest point of the cable.

Calculate the maximum tension in the cable when the girder carries a uniformly distributed load of 1 ton per foot over the whole span and sketch the bending moment diagram for the girder when a load of 10 tons is placed at the hinge point between the supports.

(61·4 tons.)

(5) A suspension bridge with a three-hinged stiffening girder has a span of 350 feet, a central dip of 35 feet and weighs 350 tons. It is to be designed to carry a superimposed rolling load of 1 ton per foot of span equally divided between the two sets of chains. This load may cover all or any part of the span.

Using a working stress of 8 tons per square inch calculate :

(*a*) The cross-sectional area of one suspension cable.

(*b*) The necessary modulus of section of the stiffening girder.

((a) 59 square inches.
(b) 1,731 inches³.)

CHAPTER 17

THE BEAM CURVED IN PLAN

17.1. The curved cantilever.—This chapter deals with the determination of the resultant actions at any section of a beam which is curved in plan. Such beams are often used in steel framed buildings and require special treatment. In the first place the simplest case of a curved cantilever such as shown in Fig. 17.1 will be considered. In this diagram AB represents in plan a horizontal cantilever firmly built

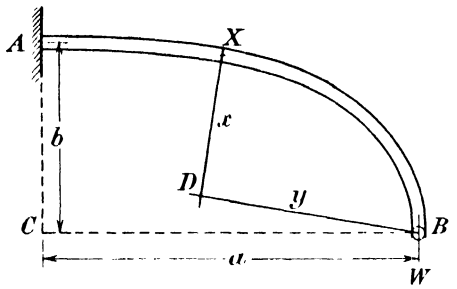

FIG. 17.1.

in at A and carrying a load W at the end B. The tangent of the slope of the beam at A is supposed to be normal to the wall to which it is fixed. If a line BC be drawn from B perpendicular to the wall the resultant actions at A will consist of :—

(*a*) A shearing force W tending to move the beam downwards at the wall section.

(*b*) A bending moment W*a* tending to bend the beam convex upwards at the wall section.

(*c*) A torque W*b* tending to twist the beam counterclockwise at the wall section.

The presence of the torque differentiates this problem from that of the straight beam.

At any other section such as X the resultant actions are similar. Through X a normal plane is drawn, its trace being XD. From B a perpendicular BD is dropped to XD. If the distances XD and DB are x and y, the bending moment and torque at X are Wy and Wx respectively.

In the case of the cantilever these are directly calculable. Suppose the curve AB to be the quadrant of a circle of radius R as shown in Fig. 17.2. The origin is taken at the centre of the circle O and the angle BOX is θ.

Then $M_x = W \cdot BD = WR \sin\theta,$

$T_x = W \cdot DX = WR(1-\cos\theta)$

and $F_x = W,$

where M_x, T_x and F_x are the bending moment, torque and shearing force at X respectively.

The diagrams for these quantities can be plotted from the above equations.

If, instead of a concentrated load W, the beam carries a uniformly-distributed load of intensity w over its whole length as shown in

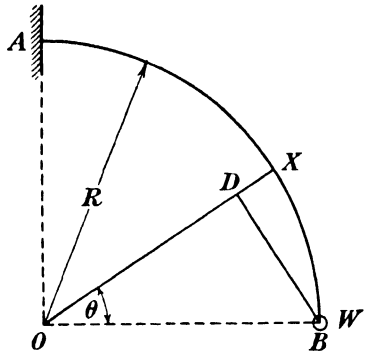

FIG. 17.2.

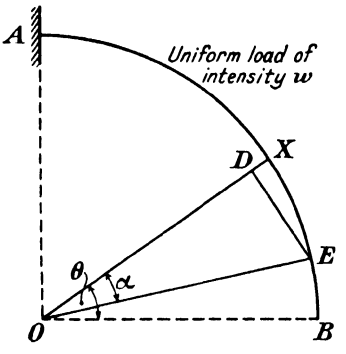

FIG. 17.3.

Fig. 17.3 the weight acting on a small element at E which is α from OX is $w\mathrm{R}d\alpha$.

The bending moment at X due to this is $w\mathrm{R}d\alpha \cdot \mathrm{DE}$ or $w\mathrm{R}^2 \sin\alpha d\alpha$, the torque is $w\mathrm{R}d\alpha \cdot \mathrm{XD}$ or $w\mathrm{R}^2(1-\cos\alpha)d\alpha$ and the shearing force is $w\mathrm{R}d\alpha$.

Hence the total resultant actions at X are

$$M_x = w\mathrm{R}^2 \int_0^\theta \sin\alpha d\alpha \qquad = w\mathrm{R}^2(1-\cos\theta),$$

$$T_x = w\mathrm{R}^2 \int_0^\theta (1-\cos\alpha)d\alpha = w\mathrm{R}^2(\theta-\sin\theta),$$

$$F_x = w\mathrm{R} \int_0^\theta d\alpha \qquad = w\mathrm{R}\theta.$$

17.2. The circular arc bow girder.—When the girder is rigidly fixed at both ends it has three degrees of redundancy since, if one support is completely released the beam becomes a cantilever and can be dealt with as described in the previous paragraph. Hence the reactions at one support are redundant. The stress analysis can be effected either by the slope deflection method or by strain energy methods. The application of the former treatment has been described by Professor A. H. Gibson and E. G. Ritchie * who used it for the particular case of the bow girder which was a circular arc in plan. It can be ex-

* "A Study of the Circular Arc Bow Girder." Constable, 1914.

tended to the general case of a girder of any plan form but the integrations must then be dealt with graphically. Treatment by strain energy methods will be adopted here.* In the first case attention will be directed to the circular arc girder of uniform cross-section since the integrations can be done by direct methods.

Fig. 17.4 represents such a girder firmly built in at A and B and carrying a load W as shown.

The angle subtended at the centre of the arc is ϕ. W acts at an angular distance α from OB. If the support at B is removed its effect can be replaced by a bending moment M_0, a torque T_0 and a shearing force F_0 and these resultant actions will be taken as the redundant

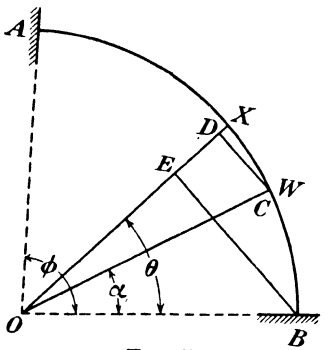

FIG. 17.4.

elements. Hence, if U is the total strain energy of the beam the conditions to be satisfied are

$$\frac{\partial U}{\partial M_0}=0,$$

$$\frac{\partial U}{\partial T_0}=0$$

and

$$\frac{\partial U}{\partial F_0}=0.$$

The total strain energy of the beam is the sum of the components due to bending, torque and shearing force. The last named is small compared with the other two and can consequently be neglected. Denoting the strain energies due to bending and torque by U_B and U_T respectively, we obtain

$$\frac{\partial U_B}{\partial M_0}+\frac{\partial U_T}{\partial M_0}=0$$

$$\frac{\partial U_B}{\partial T_0}+\frac{\partial U_T}{\partial T_0}=0$$

$$\frac{\partial U_B}{\partial F_0}+\frac{\partial U_T}{\partial F_0}=0.$$

* "The Stress Analysis of Bow Girders." A. J. S. Pippard and F. L. Barrow. H.M. Stationery Office, 1926.

If ds is a small element of the arc, EI the flexural rigidity and NJ the torsional rigidity of the girder,

$$U_B=\frac{1}{2EI}\int M_x^2 ds\,; \quad U_T=\frac{1}{2NJ}\int T_x^2 ds$$

where M_x and T_x are the bending moment and torque at any section and the integration extends round the whole girder.

The above equations can then be re-written as

$$\left.\begin{aligned}
&\frac{1}{EI}\int M_x\frac{\partial M_x}{\partial M_0}ds+\frac{1}{NJ}\int T_x\frac{\partial T_x}{\partial M_0}ds=0\\
&\frac{1}{EI}\int M_x\frac{\partial M_x}{\partial T_0}ds+\frac{1}{NJ}\int T_x\frac{\partial T_x}{\partial T_0}ds=0\\
&\frac{1}{EI}\int M_x\frac{\partial M_x}{\partial F_0}ds+\frac{1}{NJ}\int T_x\frac{\partial T_x}{\partial F_0}ds=0
\end{aligned}\right\} \quad \ldots\ldots \quad (1)$$

Before obtaining expressions for M_x, T_x and F_x a convention as to signs must be adopted. It will be taken that if AX is viewed from the front a positive moment at X is one that tends to make AX convex upwards,

a positive torque at X is one that tends to turn the viewed section clockwise,

a positive shearing force at X is one that tends to raise the viewed section.

With these conventions take M_0, T_0 and F_0 as positive and at the section X in Fig. 17.4 at an angular distance θ from OB

M_0 imposes a bending moment $= M_0\cos\theta$
and a torque $= -M_0\sin\theta$.
T_0 imposes a bending moment $= T_0\sin\theta$
and a torque $= T_0\cos\theta$.

From C, the point of application of W, and from B, perpendiculars CD and BE are dropped on OX and then

$$\left.\begin{aligned}
M_x&= M_0\cos\theta+T_0\sin\theta-F_0\,.\,BE+W\,.\,CD\\
\text{and}\quad T_x&=-M_0\sin\theta+T_0\cos\theta+F_0\,.\,XE-W\,.\,XD.
\end{aligned}\right\} \quad \ldots \quad (2)$$

When X lies between B and C the terms in W are omitted.

Then, from equation (2),

$$\left.\begin{aligned}
&\frac{\partial M_x}{\partial M_0}=\cos\theta\,; \quad \frac{\partial T_x}{\partial M_0}=-\sin\theta\,;\\
&\frac{\partial M_x}{\partial T_0}=\sin\theta\,; \quad \frac{\partial T_x}{\partial T_0}=\cos\theta\,;\\
&\frac{\partial M_x}{\partial F_0}=-BE\,; \quad \frac{\partial T_x}{\partial F_0}=XE.
\end{aligned}\right\} \quad \ldots\ldots \quad (3)$$

Now $BE=R\sin\theta$, $XD=R\{1-\cos(\theta-\alpha)\}$,
$CD=R\sin(\theta-\alpha)$ and $XE=R(1-\cos\theta)$

and equations (1) become

$$\left.\begin{aligned}
&\frac{1}{EI}\int\{M_0\cos\theta+T_0\sin\theta-F_0R\sin\theta+WR\sin(\theta-\alpha)\}\cos\theta d\theta\\
&\quad-\frac{1}{NJ}\int[-M_0\sin\theta+T_0\cos\theta+F_0R(1-\cos\theta)\\
&\qquad\qquad-WR\{1-\cos(\theta-\alpha)\}]\sin\theta d\theta=0\\
&\frac{1}{EI}\int\{M_0\cos\theta+T_0\sin\theta-F_0R\sin\theta+WR\sin(\theta-\alpha)\}\sin\theta d\theta\\
&\quad+\frac{1}{NJ}\int[\{-M_0\sin\theta+T_0\cos\theta+F_0R(1-\cos\theta)\\
&\qquad\qquad-WR\{1-\cos(\theta-\alpha)\}]\cos\theta d\theta=0\\
&-\frac{1}{EI}\int\{M_0\cos\theta+T_0\sin\theta-F_0R\sin\theta+WR\sin(\theta-\alpha)\}\sin\theta d\theta\\
&\quad+\frac{1}{NJ}\int[-M_0\sin\theta+T_0\cos\theta+F_0R(1-\cos\theta)\\
&\qquad\qquad-WR\{1-\cos(\theta-\alpha)\}](1-\cos\theta)d\theta=0
\end{aligned}\right\}\quad(4)$$

where the integrals extend from $\theta=0$ to $\theta=\phi$ for the terms in M_0, T_0 and F_0 and from $\theta=\alpha$ to $\theta=\phi$ for those in W.

These reduce to

$$\left.\begin{aligned}
&M_0\left[\frac{1}{EI}(2\phi+\sin 2\phi)+\frac{1}{NJ}(2\phi-\sin 2\phi)\right]\\
&\qquad+T_0\left[\left(\frac{1}{EI}-\frac{1}{NJ}\right)(1-\cos 2\phi)\right]\\
&\quad+F_0R\left[\frac{1}{EI}(\cos 2\phi-1)+\frac{1}{NJ}(4\cos\phi-\cos 2\phi-3)\right]\\
&\quad-WR\left[\frac{1}{EI}\{\cos(2\phi-\alpha)+2(\phi-\alpha)\sin\alpha-\cos\alpha\}\right.\\
&\quad\left.+\frac{1}{NJ}\{4\cos\phi-3\cos\alpha+2(\phi-\alpha)\sin\alpha-\cos(2\phi-\alpha)\}\right]=0\\
&M_0\left(\frac{1}{EI}-\frac{1}{NJ}\right)(1-\cos 2\phi)+T_0\left[\frac{1}{EI}(2\phi-\sin 2\phi)\right.\\
&\qquad\left.+\frac{1}{NJ}(2\phi+\sin 2\phi)\right]\\
&\quad+F_0R\left[\frac{1}{EI}(\sin 2\phi-2\phi)+\frac{1}{NJ}(4\sin\phi-\sin 2\phi-2\phi)\right]\\
&\quad+WR\left[\frac{1}{EI}\{2(\phi-\alpha)\cos\alpha+2\cos\phi\sin(\alpha-\phi)\}\right.\\
&\quad\left.-\frac{1}{NJ}\{(4\sin\phi-3\sin\alpha-2(\phi-\alpha)\cos\alpha-\sin(2\phi-\alpha)\}\right]=0\\
&M_0(1-\cos\phi)-T_0\sin\phi-F_0R(\phi-\sin\phi)+WR\{\phi-\alpha\\
&\qquad\qquad-\sin(\phi-\alpha)\}=0
\end{aligned}\right\}\quad(5)$$

and these are the general equations for the circular arc bow girder with a concentrated load at any position.

These equations are not readily soluble in algebraic terms, but if

definite values for EI, NJ, ϕ and α are substituted the determination of M_0, T_0 and F_0 is quite straightforward.*

Suppose the girder to be semi-circular in form and to carry a single load at the centre of its span, so that $\phi=\pi$ and $\alpha=\pi/2$.

The equations then reduce to

$$2\pi M_0\left(\frac{1}{EI}+\frac{1}{NJ}\right)-\frac{8F_0R}{NJ}-WR\left(\frac{\pi}{EI}-\frac{4-\pi}{NJ}\right)=0;$$

$$2\pi T_0-2\pi F_0R+2WR=0;$$

and

$$2M_0-\pi F_0R+WR\left(\frac{\pi}{2}-1\right)=0;$$

which give

$$F_0=\frac{W}{2},$$

$$M_0=\frac{WR}{2},\quad T_0=WR\left(\frac{1}{2}-\frac{1}{\pi}\right).$$

17.3. Circular arc bow girder with a distributed load.—If the girder carries a uniformly distributed load, the terms in equations (4) and (5) of paragraph 17.2 for M_0, T_0 and F_0 are unaltered, but those involving W require modification.

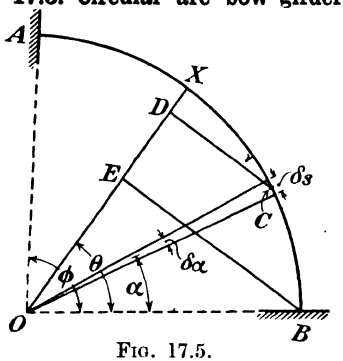

FIG. 17.5.

Let the girder shown in Fig. 17.5 carry a uniformly distributed load of intensity w. Let δm_x and δt_x be the bending moment and torque at any point X due to an element of load $w\delta s$ at C, the angular distance of C from OB being α.

Then $$\delta m_x=\text{CD}\,.\,w\delta s = R^2w\sin(\theta-\alpha)\delta\alpha$$

and $$\delta t_x=-\text{XD}\,.\,w\delta s=-R^2w\{1-\cos(\theta-\alpha)\}\delta\alpha.$$

The bending moment and torque at X due to the distributed load between B and X is then

$$m_x=R^2w\int_0^\theta\sin(\theta-\alpha)d\alpha=R^2w(1-\cos\theta).$$

$$t_x=-R^2w\int_0^\theta\{1-\cos(\theta-\alpha)\}d\alpha=-R^2w(\theta-\sin\theta).$$

Instead of the terms for W in equations (4) of paragraph 17.2 we now have

$$R^2w\left[\frac{1}{EI}\int_0^\phi(1-\cos\theta)\cos\theta d\theta+\frac{1}{NJ}\int_0^\phi(\theta-\sin\theta)\sin\theta d\theta\right],$$

$$R^2w\left[\frac{1}{EI}\int_0^\phi(1-\cos\theta)\sin\theta d\theta-\frac{1}{NJ}\int_0^\phi(\theta-\sin\theta)\cos\theta d\theta\right]$$

and

$$-R^2w\left[\frac{1}{EI}\int_0^\phi(1-\cos\theta)\sin\theta d\theta+\frac{1}{NJ}\int_0^\phi(\theta-\sin\theta)(1-\cos\theta)d\theta\right]$$

* For a solution of this problem in explicit general terms see "An Application of the Principle of Superposition to Certain Structural Problems." A. J. S. Pippard. Journal Inst. C.E., 1938–38, pp. 447–464.

respectively and the general equations for the circular arc bow girder with a uniformly distributed load are

$$\left.\begin{aligned}
&M_0\left[\frac{1}{EI}(2\phi+\sin 2\phi)+\frac{1}{NJ}(2\phi-\sin 2\phi)\right]\\
&\qquad+T_0\left[\left(\frac{1}{EI}-\frac{1}{NJ}\right)(1-\cos 2\phi)\right]\\
&\quad+F_0R\left[\frac{1}{EI}(\cos 2\phi-1)+\frac{1}{NJ}(4\cos\phi-\cos 2\phi-3)\right]\\
&\quad+wR^2\left[\frac{1}{EI}(4\sin\phi-2\phi-\sin 2\phi)+\frac{1}{NJ}(4\sin\phi-2\phi\right.\\
&\qquad\left.+\sin 2\phi-4\phi\cos\phi)\right]=0\\
&M_0\left(\frac{1}{EI}-\frac{1}{NJ}\right)(1-\cos 2\phi)+T_0\left[\frac{1}{EI}(2\phi-\sin 2\phi)\right.\\
&\qquad\left.+\frac{1}{NJ}(2\phi+\sin 2\phi)\right]\\
&\quad+F_0R\left[\frac{1}{EI}(\sin 2\phi-2\phi)+\frac{1}{NJ}(4\sin\phi-\sin 2\phi-2\phi)\right]\\
&\quad+wR^2\left[\frac{1}{EI}(3+\cos 2\phi-4\cos\phi)-\frac{1}{NJ}(\cos 2\phi+4\cos\phi\right.\\
&\qquad\left.-5+4\phi\sin\phi)\right]=0\\
&M_0(1-\cos\phi)-T_0\sin\phi-F_0R(\phi-\sin\phi)\\
&\qquad+wR^2\left(\frac{\phi^2}{2}+\cos\phi-1\right)=0
\end{aligned}\right\}\quad(1)$$

As in the case of the single concentrated load these equations do not give a simple solution in general terms but when particular values are assigned to EI, NJ and ϕ they are readily solved. In the special case of the semi-circular girder they reduce to

$$\begin{aligned}
&\pi M_0\left(\frac{1}{EI}+\frac{1}{NJ}\right)-\frac{4F_0R}{NJ}-\pi wR^2\left(\frac{1}{EI}-\frac{1}{NJ}\right)=0\\
&\pi T_0-\pi F_0R+4wR^2=0\\
&2M_0-\pi F_0R+\frac{wR^2}{2}(\pi^2-4)=0
\end{aligned}$$

and the solution is

$$\begin{aligned}
F_0&=\frac{\pi Rw}{2},\\
M_0&=wR^2,\\
T_0&=wR^2\left(\frac{\pi}{2}-\frac{4}{\pi}\right),
\end{aligned}$$

which are independent of the values of EI and NJ.

17.4. The bow girder of any shape with a concentrated load.—If the girder is not a circular arc the necessary integrals cannot generally

be solved by direct mathematical methods and it is necessary to obtain their values graphically.

Suppose, for example, the girder shown in Fig. 17.6 has to be

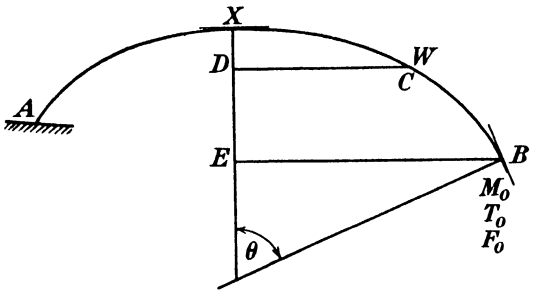

FIG. 17.6.

analysed. The whole of the work of paragraph 17.2 up to and including equations (3) will be applicable, but we cannot express BE, XE, XD and CD as functions of θ and α as in the case of the circular arc girder.

Equations (4) must now be expressed in the following form:

$$\left.\begin{aligned}
&M_0\left[\frac{1}{EI}\int_B^A \cos^2\theta ds+\frac{1}{NJ}\int_B^A \sin^2\theta ds\right]+\frac{T_0}{2}\left[\left(\frac{1}{EI}-\frac{1}{NJ}\right)\int_B^A \sin 2\theta ds\right]\\
&\quad -F_0\left[\frac{1}{EI}\int_B^A BE\cos\theta ds+\frac{1}{NJ}\int_B^A XE\sin\theta ds\right]\\
&\quad +W\left[\frac{1}{EI}\int_C^A CD\cos\theta ds+\frac{1}{NJ}\int_C^A XD\sin\theta ds\right]=0\\
&\frac{M_0}{2}\left[\left(\frac{1}{EI}-\frac{1}{NJ}\right)\int_B^A \sin 2\theta ds\right]+T_0\left[\frac{1}{EI}\int_B^A \sin^2\theta ds+\frac{1}{NJ}\int_B^A \cos^2\theta ds\right]\\
&\quad -F_0\left[\frac{1}{EI}\int_B^A BE\sin\theta ds-\frac{1}{NJ}\int_B^A XE\cos\theta ds\right]\\
&\quad +W\left[\frac{1}{EI}\int_C^A CD\sin\theta ds-\frac{1}{NJ}\int_C^A XD\cos\theta ds\right]=0\\
&-M_0\left[\frac{1}{EI}\int_B^A BE\cos\theta ds+\frac{1}{NJ}\int_B^A XE\sin\theta ds\right]\\
&-T_0\left[\frac{1}{EI}\int_B^A BE\sin\theta ds-\frac{1}{NJ}\int_B^A XE\cos\theta ds\right]\\
&\qquad +F_0\left[\frac{1}{EI}\int_B^A (BE)^2 ds+\frac{1}{NJ}\int_B^A (XE)^2 ds\right]\\
&\quad -W\left[\frac{1}{EI}\int_C^A CD\,.\,BE ds+\frac{1}{NJ}\int_C^A XD\,.\,XE ds\right]=0
\end{aligned}\right\} \quad (1)$$

The first three terms in each equation depend only on the shape of the girder and are the same whatever is the position of the load. If more than one load acts on the girder each will appear in the several equations. Suppose, for example, that loads W_1, W_2 . . . W_n act at

points denoted by 1, 2 . . . n. Then the term giving the coefficient of W in the first equation must be replaced by

$$W_1\left[\frac{1}{EI}\int_1^A C_1D_1\cos\theta ds+\frac{1}{NJ}\int_1^A XD_1\sin\theta ds\right]$$
$$+W_2\left[\frac{1}{EI}\int_2^A C_2D_2\cos\theta ds+\frac{1}{NJ}\int_2^A XD_2\sin\theta ds\right]$$
$$+\ \ldots\ +W_n\left[\frac{1}{EI}\int_n^A C_nD_n\cos\theta ds+\frac{1}{NJ}\int_n^A XD_n\sin\theta ds\right]$$

where $C_1D_1 \ldots C_nD_n$, $XD_1 \ldots XD_n$ represent the lengths corresponding to CD, XD drawn for the points 1, 2 . . . n. Similar terms replace the coefficients of W in the other two equations.

The graphical treatment is best described by an example which will be taken from the paper previously mentioned.*

Fig. 17.7 shows the centre line of a bow girder drawn to scale. It is rigidly built in at A and B and carries a load W at C.

The perimeter is divided into a number of equal parts which should

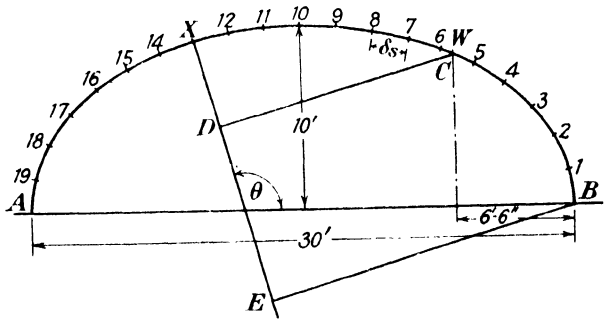

Fig. 17.7.

be as small as practicable since the greater the number the more accurate will be the results obtained. At each of these points, numbered 1–19 on the diagram, draw normals to the curve and from B drop perpendiculars to each of these normals. Taking point X as an example, XE is the normal and BE is perpendicular to XE. From C, the point of application of the load, draw similar perpendiculars such as CD. Since the terms in W only appear between C and A, the perpendiculars from C are only required for points on the curve lying between C and A.

Equations (1) show that the integrals which must be evaluated involve a number of trigonometrical functions of θ and the lengths BE, XE, CD and XD. A list of these integrals will be found in Table 17.3.

The various terms in these integrals can be obtained from the drawing and the necessary products calculated. The integrals can then be evaluated graphically.

As an example of the method the term $\int_B^A BE\sin\theta ds$ will be considered in detail.

* Loc. cit., p. 413

BE and θ are measured for each point from 0–19 and entered as in Table 17.1, columns 2 and 3. Sin θ is taken from trigonometrical tables and BE sin θ calculated (column 5).

TABLE 17.1.—EVALUATION OF $\int_B^A BE \sin\theta ds$.

1	2	3	4	5	6	
					Area by Simpson's rule	
Point	BE	θ	sin θ	BE sin θ	Multiplying factor	—
B	0	0	0	0	1	0
1	1·95	15·5	0·2672	0·52	4	2·08
2	3·78	30·0	0·5	1·89	2	3·78
3	5·44	43·8	0·6922	3·74	4	14·96
4	7·00	53·0	0·7986	5·59	2	11·20
5	8·50	60·7	0·8721	7·42	4	14·84
6	9·92	67·5	0·9239	9·17	2	18·34
7	11·29	73·8	0·9603	10·84	4	43·36
8	12·60	79·6	0·9835	12·40	2	24·80
9	13·84	84·8	0·9959	13·80	4	55·20
10	15·00	90·0	1·0	15·00	2	30·00
11	16·05	95·2	0·9959	16·00	4	64·00
12	16·92	100·4	0·9835	16·65	2	33·30
13	17·55	106·2	0·9603	16·87	4	67·48
14	17·85	112·5	0·9239	16·50	2	33·00
15	17·66	129·3	0·8721	15·40	4	61·60
16	16·95	127·0	0·7986	13·53	2	27·06
17	15·13	136·2	0·6922	10·48	4	41·92
18	11·31	150·0	0·5	5·65	2	11·31
19	6·27	164·5	0·2672	1·68	4	6·72
20	0	180·0	0	0	1	0
						564·96

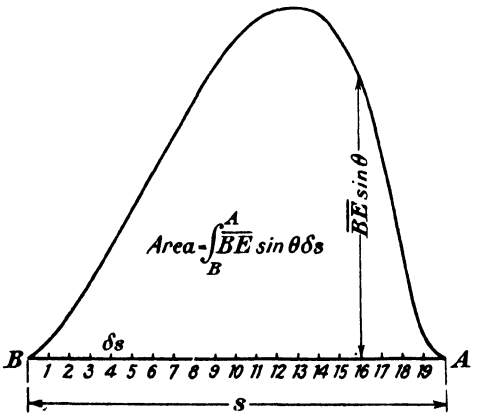

FIG. 17.8.

A base proportional in length to the perimeter of the girder is now set out and divided into the same number of parts as the girder (Fig. 17.8). At each point the appropriate value of BE sin θ is plotted as an ordinate and a smooth curve drawn through the points thus obtained. The area of the resulting curve is found either by a planimeter or by the use of Simpson's rule. In the latter case plotting is not essential but is advisable since it helps in the detection of calculation errors. The calculation, if Simpson's rule is used, may be set out as in column 6 of Table 17.1. In the case under consideration $\frac{\delta s}{3}=0{\cdot}6633$.

Therefore, $\int_B^A \text{BE} \sin\theta ds = 0{\cdot}6633 \times 564{\cdot}96 = 374{\cdot}8$.

A similar method is adopted for the remaining integrals but in the case of such terms as $\int_C^A \text{CD} \cos\theta ds$ the integration only extends from A to C. The calculations for this integral are given in Table 17.2.

TABLE 17.2.—EVALUATION OF $\int_C^A \text{CD} \cos\theta ds$.

1	2	3	4	5	6	
					Area by Simpson's rule	
Point	CD	θ	cos θ	CD cos θ	Multiplying factor	—
C	0			0		
6	0·82	67·5	0·3827	0·31	1	0·31
7	2·79	73·8	0·2790	0·77	4	3·11
8	4·75	79·6	0·1805	0·86	2	1·72
9	6·63	84·8	0·0907	0·60	4	2·40
10	8·54	90·0	0	0	1	0
						+7·55
10	8·54	90·0	0	0	1	0
11	10·38	95·2	−0·0907	− 0·94	4	− 3·76
12	12·07	100·4	−0·1805	− 2·18	2	− 4·36
13	13·61	106·2	−0·2790	− 3·80	4	− 15·20
14	14·98	112·5	−0·3827	− 5·74	2	− 11·50
15	16·06	119·3	−0·4894	− 7·90	4	− 31·60
16	16·76	127·0	−0·6018	−10·10	2	− 20·20
17	16·70	136·2	−0·7217	−12·06	4	− 48·24
18	15·39	150·0	−0·8700	−13·37	2	− 26·74
19	12·41	164·5	−0·9636	−11·98	4	− 48·00
20	8·23	180·0	−1·0	− 8·23	1	− 8·23
						−217·83
						+ 7·55
						−210·28

Again $\frac{\delta s}{3}=0{\cdot}6633$,

therefore $\int_C^A \text{CD} \cos\theta ds = {\cdot}6633 \times (-210{\cdot}28) = -139{\cdot}3$.

The area of the diagram between C and 6 has been neglected, as Simpson's rule has been applied for an odd number of ordinates. The error is seen to be small compared with the total area

Care must be observed if different scales are used for plotting the curves to reduce them all to equivalent values.

The scale to which the diagram of the girder is drawn is immaterial: the values of M_0, F_0 and T_0 will be the same for all geometrically similar girders similarly loaded, provided the ratio EI/NJ is kept constant.

Suppose the base BA of Fig. 17.8 is drawn n times the length of the perimeter in Fig. 17.7 and the ordinates BE are drawn m times their real values as scaled from that Figure.

Then the area of the curve will be mn times the true value and should be reduced accordingly. If this be done, different integral curves can be plotted to different scales, a matter of some convenience in many cases. The calculated values of the various integrals without the coefficients $\frac{1}{EI}$ and $\frac{1}{NJ}$ are given in Table 17.3.

TABLE 17.3.

Integral	Value	Integral	Value
$\int_B^A \cos^2\theta ds$	14·19	$\int_B^A XE\cos\theta ds$	— 215·3
$\int_B^A \sin^2\theta ds$	25·63	$\int_C^A CD\sin\theta ds$	243·5
$\int_B^A \sin 2\theta s$	0	$\int_C^A XD\cos\theta ds$	— 143·9
$\int_B^A BE\cos\theta ds$	— 67·86	$\int_B^A BE^2 ds$	6,122·0
$\int_B^A XE\sin\theta ds$	339·12	$\int_B^A XE^2 ds$	8,951·9
$\int_C^A CD\cos\theta ds$	—139·30	$\int_C^A CD\,.\,BE\,.\,ds$	4,540·3
$\int_C^A XD\sin\theta ds$	118·40	$\int_C^A XD\,.\,XE\,.\,ds$	4,726·7
$\int_B^A BE\sin\theta ds$	374·80		

If the equations are multiplied throughout by EI the necessity for knowing the absolute values of EI and NJ vanishes since only the ratio $\frac{EI}{NJ}=\gamma$ appears.

Making this alteration in the form of the equations and substituting the values of the integrals from Table 17.3, the following are obtained,

$$M_0(14{\cdot}19+25{\cdot}63\gamma)+T_0(0)-F_0(-67{\cdot}86+339{\cdot}12\gamma)$$
$$+W(-139{\cdot}3+118{\cdot}4\gamma)=0$$
$$M_0(0)+T_0(25{\cdot}63+14{\cdot}19\gamma)-F_0(374{\cdot}8+215{\cdot}3\gamma)$$
$$+W(243{\cdot}5+143{\cdot}9\gamma)=0$$
$$-M_0(-67{\cdot}86+339{\cdot}12\gamma)-T_0(374{\cdot}8+215{\cdot}3\gamma)$$
$$+F_0(6{,}122+8{,}951{\cdot}9\gamma)-W(4{,}540{\cdot}3+4{,}726{\cdot}7\gamma)=0.$$

If the cross-section is such that $\gamma=10$ these equations give the values

$$M_0=\cdot204WL,$$
$$T_0=\cdot077WL,$$
$$F_0=\cdot815W,$$

where L is the span AB.

The bending moment, torque and shearing force at any point can then be obtained directly.

17.5. Bow girder of any shape with distributed load.—If the girder carries a uniformly distributed load, the terms in M_0, T_0 and F_0 in equations (1) of the last paragraph are unaltered but those in W must be replaced. As in paragraph 17.3 the bending moment and torque at any point X due to the element of load $w\delta s$ at a point C are respectively

$$\delta m_x=\mathrm{CD}w\delta s$$

and

$$\delta t_x=-\mathrm{XD}w\delta s$$

but whereas in the case of the circular arc girder these could be expressed as functions of θ and integrated to find the bending moment and torque at X due to the distributed load, in the general case we have

$$m_x=\int_{\mathrm{B}}^{\mathrm{X}} w\mathrm{CD}ds,$$
$$t_x=-\int_{\mathrm{B}}^{\mathrm{X}} w\mathrm{XD}ds$$

and these integrals must be evaluated graphically. The equations for M_x and T_x can now be written

$$M_x=M_0\cos\theta+T_0\sin\theta-F_0\,.\,\mathrm{BE}+m_x$$
$$T_x=-M_0\sin\theta+T_0\cos\theta+F_0\,.\,\mathrm{XE}+t_x,$$

and instead of equations (1) of paragraph 17.4 we obtain

$$\left.\begin{aligned}
&M_0(A_1)+T_0(B_1)-F_0(C_1)+\frac{1}{EI}\int m_x\cos\theta ds-\frac{1}{NJ}\int t_x\sin\theta ds=0\\
&M_0(A_2)+T_0(B_2)-F_0(C_2)+\frac{1}{EI}\int m_x\sin\theta ds+\frac{1}{NJ}\int t_x\cos\theta ds=0\\
&-M_0(A_3)-T_0(B_3)+F_0(C_3)-\frac{1}{EI}\int m_x\mathrm{BE}ds+\frac{1}{NJ}\int t_x\mathrm{XE}ds=0
\end{aligned}\right\}\quad(1)$$

where A_1, B_1, C_1, etc., represent the coefficients of those equations.

The values of m_x and t_x must first be obtained graphically for all the

points such as 1, 2 . . . 19 in the example of the previous paragraph. The integrals $\int m_x \cos\theta ds$, etc., of equations (1) can then be found by graphical methods as previously described, the limits of integration being appropriate to the distribution of w. If this is uniform over the whole girder these limits are from A to B; if it extends over part of the girder only they are modified accordingly.

17.6. Deflection of a bow girder.—The deflection of a girder at any loaded point can be found by an application of the first theorem of Castigliano. Suppose the deflection of point C in Fig. 17.6 is required.

The girder may be supposed to be a cantilever supported at A and loaded at B by a couple M_0, a torque T_0 and an upward force F_0 and at C by a concentrated load W.

Then, whatever values are assigned to M_0, T_0 and F_0 the deflection at C is $\frac{\partial U}{\partial W}$

or
$$\Delta_C=\frac{1}{EI}\int M_x\frac{\partial M_x}{\partial W}ds+\frac{1}{NJ}\int T_x\frac{\partial T_x}{\partial W}ds.$$

Between B and C
$$\frac{\partial M_x}{\partial W}=0,\quad \frac{\partial T_x}{\partial W}=0$$

and between C and A
$$\frac{\partial M_x}{\partial W}=CD,\quad \frac{\partial T_x}{\partial W}=-XD.$$

Substituting the expressions for M_x, T_x, $\frac{\partial M_x}{\partial W}$ and $\frac{\partial T_x}{\partial W}$ we obtain

$$\Delta_C=M_0\left[\frac{1}{EI}\int_C^A CD\cos\theta ds+\frac{1}{NJ}\int_C^A XD\sin\theta ds\right]+T_0\left[\frac{1}{EI}\int_C^A CD\sin\theta ds-\frac{1}{NJ}\int_C^A XD\cos\theta ds\right]$$
$$-F_0\left[\frac{1}{EI}\int_C^A BE\,.\,CD ds+\frac{1}{NJ}\int_C^A XE\,.\,XD ds\right]+W\left[\frac{1}{EI}\int_C^A CD^2 ds+\frac{1}{NJ}\int_C^A XD^2 ds\right] \quad . \quad . \quad . \quad (1)$$

Again, in the general case, these integrals must be evaluated graphically but in the particular case of the circular arc girder they can be dealt with by direct methods.

Taking the case shown in Fig. 17.4 we obtain by substitution of the values for CD, XD, etc., given in paragraph 17.2, the value of the deflection:

$$\Delta_C=M_0\left[\frac{R^2}{EI}\int_\alpha^\phi \sin(\theta-\alpha)\cos\theta d\theta+\frac{R^2}{NJ}\int_\alpha^\phi\{1-\cos(\theta-\alpha)\}\sin\theta d\theta\right]$$
$$+T_0\left[\frac{R^2}{EI}\int_\alpha^\phi \sin(\theta-\alpha)\sin\theta d\theta-\frac{R^2}{NJ}\int_\alpha^\phi\{1-\cos(\theta-\alpha)\}\cos\theta d\theta\right]$$

$$-F_0\left[\frac{R^3}{EI}\int_\alpha^\phi \sin(\theta-\alpha)\sin\theta d\theta + \frac{R^3}{NJ}\int_\alpha^\phi \{1-\cos(\theta-\alpha)\}(1-\cos\theta)d\theta\right]$$

$$+W\left[\frac{R^3}{EI}\int_\alpha^\phi \sin^2(\theta-\alpha)d\theta \quad + \frac{R^3}{NJ}\int_\alpha^\phi \{1-\cos(\theta-\alpha)\}^2 d\theta\right],$$

which on integration becomes

$$\frac{\Delta_C}{R^2}=M_0\left[\frac{1}{EI}\left\{\frac{\cos\alpha-\cos(2\phi-\alpha)}{4}-\frac{(\phi-\alpha)\sin\alpha}{2}\right\}+\frac{1}{NJ}\left\{\cos\alpha-\cos\phi - \frac{\cos\alpha-\cos(2\phi-\alpha)}{4}-\frac{(\phi-\alpha)\sin\alpha}{2}\right\}\right]$$

$$+T_0\left[\frac{1}{EI}\left\{\frac{(\phi-\alpha)\cos\alpha}{2}+\frac{\sin\alpha-\sin(2\phi-\alpha)}{4}\right\}+\frac{1}{NJ}\left\{\sin\alpha-\sin\phi - \frac{\sin\alpha-\sin(2\phi-\alpha)}{4}+\frac{(\phi-\alpha)\cos\alpha}{2}\right\}\right]$$

$$-F_0R\left[\frac{1}{EI}\left\{\frac{(\phi-\alpha)\cos\alpha}{2}+\frac{\sin\alpha-\sin(2\phi-\alpha)}{4}\right\}+\frac{1}{NJ}\left\{\phi-\alpha+\sin\alpha-\sin\phi -\sin(\phi-\alpha)-\frac{\sin\alpha-\sin(2\phi-\alpha)}{4}+\frac{(\phi-\alpha)\cos\alpha}{2}\right\}\right]$$

$$+WR\left[\frac{1}{EI}\left\{\frac{\phi-\alpha}{2}-\frac{\sin 2(\phi-\alpha)}{4}\right\}+\frac{1}{NJ}\left\{\frac{3(\phi-\alpha)}{2}-2\sin(\phi-\alpha) +\frac{\sin 2(\phi-\alpha)}{4}\right\}\right] \quad . \quad . \quad . \quad (2)$$

This is the general equation for the deflection of any point C carrying a load W on any circular arc bow girder.

In the special case of a semi-circular arc loaded at the centre $\phi=\pi$, $\alpha=\pi/2$, and

$$\frac{\Delta_C}{R^2}=\frac{M_0}{4}\left[-\frac{\pi}{EI}+\frac{4-\pi}{NJ}\right]+\frac{T_0}{2}\left[\frac{1}{EI}+\frac{1}{NJ}\right]-\frac{F_0R}{2}\left[\frac{1}{EI}+\frac{\pi-1}{NJ}\right] +\frac{WR}{4}\left[\frac{\pi}{EI}+\frac{3\pi-8}{NJ}\right].$$

The values of M_0, T_0 and F_0 have already been determined for this case and on substituting them we obtain

$$\Delta_C=WR^3\left[\frac{1}{EI}\left(\frac{\pi}{8}-\frac{1}{2\pi}\right)+\frac{1}{NJ}\left(\frac{3\pi}{8}-\frac{1}{2\pi}-1\right)\right]. \quad . \quad . \quad . \quad (3)$$

If the girder carries more than one load the deflections can be found under the several load points in the same way as for a single load, by the first theorem of Castigliano. They are, under loads W_1, W_2 . . . W_n, given respectively by

$$\frac{\partial U}{\partial W_1}, \quad \frac{\partial U}{\partial W_2} \quad . \quad . \quad . \quad . \quad \frac{\partial U}{\partial W_n}.$$

If the deflection at any point on a girder carrying a uniformly distributed load is required it can be found by placing a load W_0 at

the point, determining $\frac{\partial U}{\partial W_0}$ and then putting $W_0=0$ in the final result as already described in Chapter 5.

17.7. Bow girders having symmetry about an axis.—If a bow girder is symmetrical and symmetrically loaded about one axis the analysis is considerably simplified. Suppose, for instance, we have a girder

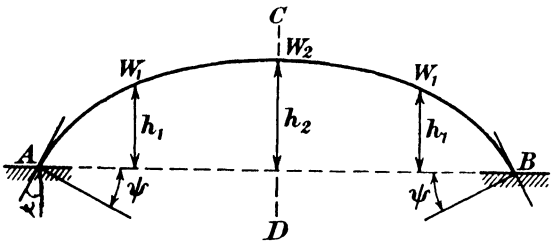

FIG. 17.9.

as shown in Fig. 17.9 which is symmetrical about CD, the loading also being symmetrical about this line.

The reactions F_A and F_B will be equal, as will also be the bending moments M_A and M_B and the torques T_A and T_B.

By equating vertical forces on the girder we have

$$F_A+F_B=2W_1+W_2$$

or

$$F_A=F_B=\tfrac{1}{2}(2W_1+W_2)$$

and, by taking moments about the line AB, we have

$$(M_A+M_B)\cos\psi=2W_1h_1+W_2h_2+(T_A+T_B)\sin\psi$$

or

$$M_A=M_B=\tfrac{1}{2}(2W_1h_1+W_2h_2)\sec\psi+T_B\tan\psi$$

where ψ is the angle between AB and the normal to the girder at A or B.

Now F_B, M_B and T_B are the actions we have hitherto denoted by F_0, M_0 and T_0 and the only indeterminate term in the symmetrical case is therefore T_0.

Equations derived from the conditions $\frac{\partial U}{\partial M_0}=0$ and $\frac{\partial U}{\partial F_0}=0$ are not required and it is only necessary to substitute the above values of M_0 and F_0 in the equation $\frac{\partial U}{\partial T_0}=0$ to obtain the solution: thus, for the general case, only the second equation of (1) paragraph 17.4 is required.

Applying these results to the case of the circular arc bow girder dealt with in paragraph 17.2, we put $\alpha=\phi/2$ giving a single load at the centre of the span, $\psi=\frac{\pi-\phi}{2}$ and we have

$$F_0=\frac{W}{2}$$

and

$$M_0=\frac{WR}{2}\left(1-\cos\frac{\phi}{2}\right)\operatorname{cosec}\frac{\phi}{2}+T_0\cot\frac{\phi}{2}.$$

On substituting for F_0, M_0 and α the second equation of (5) of that paragraph gives

$$2T_0\left[\frac{1}{EI}(\phi+\sin\phi)+\frac{1}{NJ}(\phi-\sin\phi)\right]$$
$$+WR\left(\frac{1}{EI}+\frac{1}{NJ}\right)\left(1-\cos\frac{\phi}{2}\right)\left(2\sin\frac{\phi}{2}-\phi\right)=0.$$

In the special case of the semi-circular girder $\phi=\pi$ and

$$F_0=\frac{W}{2}$$
$$T_0=WR\left(\frac{1}{2}-\frac{1}{\pi}\right)$$
$$M_0=\frac{WR}{2}$$

agreeing with the previous result obtained for this case.

17.8. Bow girder with intermediate supports.— In some cases a bow girder is supported at points along its span by columns or by cantilevers. These supports may give restraint of two types.

In the first place the column may be so attached to the girder that it effectively restrains it against vertical movement and change of slope. This would occur in a monolithic construction such as reinforced concrete if the columns were of such dimensions that their shortening and changes of slope under loads on the beam were negligible. The girder is then divided into a number of separate units each of which can be dealt with as described in the foregoing paragraphs.

In the second type of restraint the connection between the column and beam may be such that little or no restraint is imposed upon the slope of the latter and vertical movement only is affected. This may be entirely or partially prevented, depending upon the elastic properties of the supports.

In this case we can proceed as if the vertical reactions from the supports are applied forces opposite in direction to the normal loads on the girder. The magnitudes of these forces must be determined from the conditions

$$\frac{\partial U}{\partial R_1}=-\delta_1$$
. . . .
$$\frac{\partial U}{\partial R_n}=-\delta_n$$

where $R_1 \ldots R_n$ are the reactive forces to be found and $\delta_1 \ldots \delta_n$ are the amounts by which the supports sink, the negative sign denoting movement against the direction of the force.

If there is no vertical movement of the supports, $\delta_1 \ldots \delta_n$ are zero.

These equations, together with the usual ones for the determination of the reactive forces at the end of the girder viz. $\frac{\partial U}{\partial M_0}=\frac{\partial U}{\partial T_0}=\frac{\partial U}{\partial F_0}=0$,

enable a complete analysis of the girder to be made. The last equations referred to are as in paragraph 17.4 with the W term expanded to include expressions for R_1, R_2 . . . R_n. It must be remembered that these reactions act in the opposite direction to the applied loads and will therefore have negative signs in the equations.

The expressions for $\frac{\partial U}{\partial R_1}$ . . . $\frac{\partial U}{\partial R_n}$ are obtained as described in paragraph 17.6 for the deflection of loaded points and these expressions, equated to the appropriate values of δ_1 . . . δ_n, provide the remaining equations.

EXERCISES

(1) A solid circular steel rod of diameter d is bent into the quadrant of a circle of mean radius R and firmly fixed at one end. A couple and a torque each of magnitude C are applied to the free end. Show that if $N=\frac{2}{5}E$ the change of slope and the angular twist are each equal to $\frac{4}{\pi}\frac{CR}{Ed^4}(9\pi-2)$.

(2) A straight circular bar is bent at right angles, each leg of the angle being L. One end is firmly fixed and the other is supported by a spherical bearing. A load W acts normally to the axis of the bar at a distance $\frac{L}{2}$ from the spherical bearing.

Assume that $N=\frac{2}{5}E$ and calculate the reactions at the supports.

$$\left(\text{Fixed end } M_0=\frac{41}{92}WL\right.$$

$$T_0=\frac{5}{92}WL$$

$$F_0=\frac{41}{92}W$$

$$\left.\text{Pinned end } F_0=\frac{51}{92}W\right)$$

(3) A steel tube of 2 inches outside diameter and wall thickness $\frac{1}{8}$ inch is bent into the arc of a circle of radius 30 inches subtending 120° at the centre. It is rigidly held at the ends. Calculate the restraining moment and torque at the supports when a load of 100 lb. acts at the centre of the beam thus formed. $N=\frac{1}{3}E$.

($M_0=942$ *inch-lb.*
$T_0=135$ *inch-lb.*)

(4) Calculate the support reactions in the last question if the load is uniformly distributed along the beam.

($M_0=604$ *inch-lb.*
$T_0=69$ *inch-lb.*)

(5) A beam is bent in plan view to form three sides of a regular octagon each side being of length s. It is firmly held at both ends and carries a load W at the centre. If the flexural rigidity of the beam is α times the torsional rigidity show that the bending moment at the loaded point is

$$-\frac{Ws}{8}\left\{\frac{(2\sqrt{2}+3)+2\alpha}{2+\alpha}\right\}.$$

(6) Using the graphical method described in this Chapter plot the bending moment, torque and shearing force diagrams for a bow girder of segmental plan form. The radius is 10 feet, the subtended angle is 150° and a load W is carried at a third-point of the girder.

Take EI=15NJ.

Check the results obtained by direct calculation.

CHAPTER 18

NOTES ON FLAT SLABS AND PLATES

18.1. General.—The flat slab or plate is an important structural element. In modern buildings the floors consist, in the majority of cases, of rectangular concrete slabs reinforced with bars or with rolled steel sections. In tanks, containers and machines circular plates are common. A knowledge of the deflections and stresses in plates when loads are applied normal to their surfaces is, therefore, of importance for design purposes.

No satisfactory treatment of the bending of plates such as reinforced concrete slabs made up of materials which are not homogeneous and isotropic has yet been given. The general theory of the bending of uniform thick plates * is difficult and the simpler approximate theory commonly used for the derivation of design data is sufficiently involved to make it impossible in the space available here to show the detailed application. Nothing more will be given in this chapter therefore than expressions for the deflections and stresses in the more common forms of plates together with sufficient references to published work to enable the reader to study the subject in greater detail.

In deriving the expressions given here it has been assumed that the deflection of the plate is small compared with its thickness. The difference between this and the assumptions made in paragraph 3.8 for the bending of a beam, that the deflection may be large so long as the slope of the beam is everywhere small, arises from the fact that while the neutral layer of a beam may take up any curvature without stretching, no layer in a bent plate remains unstretched unless the bent form is that of a developable surface. If the deflections of the neutral layer or middle surface of the plate are not small compared with the thickness of the plate the strains set up in the middle surface cannot be neglected. The theory admitting these strains is difficult but fortunately it is of little importance in engineering problems since the deflections allowed in practice are usually small, while the properties of engineering materials and the conditions of support at the edges of the plate can seldom be specified with sufficient exactness to warrant the use of a more accurate method. Other assumptions made in deriving the expressions are that the plate is of uniform material and thickness and that elements of the plate originally straight and perpendicular to the neutral layer remain so after straining.

* See "The Bending of Moderately Thick Circular Plates." J. Vint. Proc. London Math. Soc. Ser. 2, Vol. 39, 1935, p. 32.

18.2. The circular plate.—The treatment of the circular plate is comparatively simple and is given very clearly by Case.* For the circular plate of radius a freely supported at the edge carrying a uniform load of intensity p over its whole area the deflection w at a radius r is

$$w=\frac{3p(m^2-1)}{16m^2Et^3}(a^2-r^2)\left(\frac{5m+1}{m+1}a^2-r^2\right) \quad . \quad . \quad . \quad . \quad (1)$$

where E is Young's modulus

$\frac{1}{m}$ is Poisson's ratio

and t is the thickness of the plate.

The radial and hoop stresses at the surface of the plate are respectively

$$\left.\begin{aligned} p_r&=\frac{3(3m+1)}{8mt^2}p(a^2-r^2)\\ p_\theta&=\frac{3p}{8mt^2}\{(3m+1)a^2-(m+3)r^2\}\end{aligned}\right\} \quad . \quad . \quad . \quad . \quad . \quad (2)$$

The maximum values occur when $r=0$ and are

$$p_r(\max)=p_\theta(\max)=\frac{3(3m+1)}{8mt^2}pa^2 \quad . \quad . \quad . \quad . \quad . \quad (3)$$

For the circular plate with edge clamped, carrying a uniform load p over its whole area, the corresponding expressions are

$$\left.\begin{aligned} w&=\frac{3(m^2-1)p}{16m^2Et^3}(a^2-r^2)^2\\ p_r&=\frac{3p}{8mt^2}\{(m+1)a^2-(3m+1)r^2\}\\ p_\theta&=\frac{3p}{8mt^2}\{(m+1)a^2-(m+3)r^2\}\end{aligned}\right\} \quad . \quad . \quad . \quad . \quad . \quad (4)$$

These stresses are also a maximum at $r=0$ their values being

$$p_r(\max)=p_\theta(\max)=\frac{3(m+1)pa^2}{8mt^2} \quad . \quad . \quad . \quad . \quad . \quad (5)$$

For the circular plate with its edge freely supported carrying a concentrated load W at the centre of the plate, the deflection and stresses at all points not in the immediate neighbourhood of the applied load are given by

$$\left.\begin{aligned} w&=\frac{3W(m^2-1)}{2\pi m^2Et^3}\left\{-r^2\log_e\frac{a}{r}+\tfrac{1}{2}\frac{3m+1}{m+1}(a^2-r^2)\right\}\\ p_r&=\frac{3W}{2\pi t^2}\left(1+\frac{1}{m}\right)\log_e\frac{a}{r}\\ p_\theta&=\frac{3W}{2\pi t^2}\left\{\left(1+\frac{1}{m}\right)\log_e\frac{a}{r}+\left(1-\frac{1}{m}\right)\right\}\end{aligned}\right\} \quad . \quad . \quad (6)$$

* "Strength of Materials." J. Case. Arnold, 1932.

For the circular plate with edge clamped carrying a concentrated load W at the centre of the plate

$$\left.\begin{aligned} w&=\frac{3W(m^2-1)}{2\pi m^2 E t^3}\left\{-r^2\log_e\frac{a}{r}+\tfrac{1}{2}(a^2-r^2)\right\}\\ p_r&=\frac{3W}{2\pi t^2}\left\{\left(1+\frac{1}{m}\right)\log_e\frac{a}{r}-1\right\}\\ p_\theta&=\frac{3W}{2\pi t^2}\left\{\left(1+\frac{1}{m}\right)\log_e\frac{a}{r}-\frac{1}{m}\right\}\end{aligned}\right\} \quad . \quad . \quad . \quad (7)$$

18.3. The rectangular slab.—The treatment of the rectangular slab is considerably more difficult than that of the circular plate. A full account of the solution for a slab supported at the same level along its four edges and carrying a uniform load of intensity p is given by Prescott.*

If the axes of x and y are taken along one pair of edges, the other pair being $x=a$ and $y=b$, the deflection at any point is given by

$$\begin{aligned} w=\frac{192a^4b^4p(m^2-1)}{\pi^6t^3m^2E}\Bigg[&\frac{\sin\frac{\pi x}{a}\sin\frac{\pi y}{b}}{(a^2+b^2)^2}+\frac{1}{3}\frac{\sin\frac{\pi x}{a}\sin\frac{3\pi y}{b}}{(3^2a^2+b^2)^2}\\ &+\frac{1}{3}\frac{\sin\frac{3\pi x}{a}\sin\frac{\pi y}{b}}{(a^2+3^2b^2)^2}+\frac{1}{3^2}\frac{\sin\frac{3\pi x}{a}\sin\frac{3\pi y}{b}}{(3^2a^2+3^2b^2)^2}\\ &+\frac{1}{5}\frac{\sin\frac{5\pi x}{a}\sin\frac{\pi y}{b}}{(a^2+5^2b^2)^2}+\frac{1}{15}\frac{\sin\frac{5\pi x}{a}\sin\frac{3\pi y}{b}}{(3^2a^2+5^2b^2)^2}\\ &+\ldots\ldots\ldots\Bigg] \quad . \quad . \quad . \quad . \quad . \quad . \quad . \quad . \quad (1)\end{aligned}$$

The flexural couples M_x and M_y per unit length of sections perpendicular to the axes of x and y can be found from the expressions

$$\left.\begin{aligned} M_x&=\frac{m^2Et^3}{12(m^2-1)}\left[\frac{\partial^2w}{\partial x^2}+\frac{1}{m}\frac{\partial^2w}{\partial y^2}\right]\\ \text{and}\quad M_y&=\frac{m^2Et^3}{12(m^2-1)}\left[\frac{\partial w^2}{\partial y^2}+\frac{1}{m}\frac{\partial^2w}{\partial x^2}\right]\end{aligned}\right\} \quad . \quad . \quad . \quad . \quad . \quad (2)$$

When these couples are known the flexural stresses follow since, from the assumption that elements of the slab originally straight and perpendicular to the middle surface remain so after bending, we have at the surface of the slab

$$\left.\begin{aligned} p_x&=\frac{6M_x}{t^2}\\ \text{and}\quad p_y&=\frac{6M_y}{t^2}\end{aligned}\right\} \quad . \quad . \quad . \quad . \quad . \quad . \quad . \quad . \quad (3)$$

* "Applied Elasticity." J. Prescott. Longmans, 1924.

A most lucid account of the problem of the rectangular plate clamped at the edges has been given by Professor C. E. Inglis.*

The general expression for the deflection of the rectangular plate is too long to be reproduced here, but for a square plate bounded by the planes $x=\pm a$, $y=\pm a$ a very close approximation to the deflections is given by

$$w=\frac{3(m^2-1)}{2m^2}\frac{a^4p}{Et^3}\left[\left(1-\frac{x^2}{a^2}\right)\left(1-\frac{y^2}{a^2}\right)+0{\cdot}090995\left\{f_1\left(\frac{x}{a}\right)\cos\frac{\pi y}{2a}+f_1\left(\frac{y}{a}\right)\cos\frac{\pi x}{2a}\right\}+\frac{1{\cdot}4741}{10^6}\left\{f_3\left(\frac{x}{a}\right)\cos\frac{3\pi y}{2a}+f_3\left(\frac{y}{a}\right)\cos\frac{3\pi x}{2a}\right\}\right] \quad . \quad (4)$$

where $$f_n\left(\frac{x}{a}\right)=\frac{1}{a}\left[(x-a)\sinh\frac{n\pi}{2a}(x+a)+(x+a)\sinh\frac{n\pi}{2a}(x-a)\right].$$

The pressure per unit length on the boundary edge may be calculated from the formula

$$S_x=\frac{1}{12}\frac{m^2}{(m^2-1)}Et^3\left[\frac{\partial^3 w}{\partial x^3}+\frac{\partial^3 w}{\partial y^2\partial x}\right] \quad . \quad . \quad . \quad . \quad . \quad (5)$$

Inglis has plotted a curve showing the variation of pressure and it will be seen that the maximum pressure per unit length ($0{\cdot}9182pa$) occurs at the centre of the edge, while at the corners the pressure becomes negative reaching the value $-0{\cdot}1561pa$. Details are also given of the flexural couples and deflections in the square plate and similar information is given for a rectangular plate in which the lengths of the sides are in the ratio 2 : 1.

The case of a rectangular plate freely supported along two parallel edges ($x=0$ and $x=a$) the other two edges ($y=0$ and $y=b$) being free has received some attention. The deflection of such a plate when subjected to a uniform load of intensity p is †

$$w=\frac{(m^2-1)p}{2m^2Et^3}\left[a^3x-2ax^3+x^4\right]+\frac{48(m^2-1)p}{am^2Et^3}\sum\frac{\sin\alpha x}{\alpha^5 Z}\left[\frac{m+1}{m(m-1)}\{\sinh\alpha y+\sinh\alpha(b-y)\}-\frac{1}{m}\{\alpha(b-y)\cosh\alpha y+\alpha y\cosh\alpha(b-y)\}\right] \quad . \quad . \quad . \quad . \quad . \quad . \quad (6)$$

where $\alpha=\dfrac{n\pi}{a}$, n representing all odd numbers

and $$Z=\frac{3m+1}{m}\sinh\alpha b-\frac{m-1}{m}\alpha b.$$

The case of such a plate subjected to a point load at the centre has been treated by Professor A. E. H. Love ‡ while the expressions for

* "Stresses in Rectangular Plates Clamped at their Edges and Loaded with a Uniformly Distributed Pressure." Transactions of the Institution of Naval Architects, 1925.

† C. A. Garabedian. Comptes Rendus, Vol. 181.

‡ "The Bending of a Centrally-Loaded Isotropic Rectangular Plate Supported at Two Opposite Edges." Proc. Roy. Soc., Series A., Vol. 118.

the stresses in such a plate have been considered in detail by M. Pigeaud * and made more readily available by W. L. Scott.†

The expressions given above are of little value to the designer who has to estimate the maximum stress in a particular slab. The arithmetical computation involved in such an estimate is extremely long and simpler expressions must be found.

H. M. Westergaard and W. A. Slater,‡ in a paper which should be studied by all engineers concerned with the design of slabs, have calculated the bending moments in thin plates supported in a variety of ways and have set out the results in a simple form which is reproduced in Table 18.1.

It will be seen that the stresses in a plate, due to the application of an external load, depend on the value of Poisson's ratio for the material of the plate. In order to make the data as general as possible the formulas for moments, set out in Table 18.1, have been deduced for the case when Poisson's ratio $\left(\frac{1}{m}\right)$ is zero and from them the moments can be calculated for any other particular case by means of the following expressions

$$M'_x = M_x + \frac{1}{m} M_y \quad \text{and} \quad M'_y = M_y + \frac{1}{m} M_x,$$

where, for a slab having a Poisson's ratio of zero, at any point M_x and M_y are the bending moments per unit length about perpendicular axes xx and yy and M'_x and M'_y are the corresponding bending moments in a similar slab having a Poisson's ratio of $\frac{1}{m}$.

While the stress distribution in reinforced concrete slabs is extremely complex there is considerable evidence to show that under normal design conditions the deflections are close to those given by the simpler approximate theory of the bending of thin plates. It is fair to assume, therefore, that the bending moment per unit length at any point deduced by means of that theory is a close approximation to the corresponding bending moment present in the reinforced concrete slab. As pointed out above, Poisson's ratio must be known before the bending moment can be estimated. A low value should be assumed for this in a concrete slab; W. L. Scott has suggested a value of ·15 but there is evidence that a value more nearly zero is justified.

* Annales des Ponts et Chaussées. Feb., 1921.

† "Design of Reinforced Concrete Slabs." Concrete and Constructional Engineering, Vol. 25, 1930.

‡ "Moments and Stresses in Slabs." Proceedings of the American Concrete Institute, Vol. 17, 1921.

TABLE 18.1.

APPROXIMATE FORMULAS FOR BENDING MOMENT PER UNIT LENGTH IN SLABS.

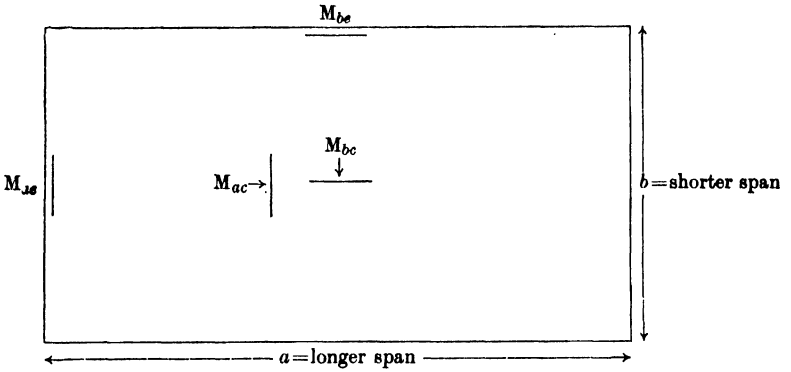

$\alpha = \frac{b}{a}$; Poisson's ratio = 0.

p = uniformly distributed load per unit area.

		Moments in span b		Moments in span a	
		At centre of edge $-M_{be}$	At centre of slab M_{bc}	At centre of edge $-M_{ae}$	At centre of slab M_{ac}
RECTANGULAR SLABS	Four edges simply supported	0	$\frac{1}{8}pb^2 \over 1+2\alpha^2$	0	$\frac{pb^2}{48}(1+\alpha^2)$
	Span "b" fixed. Span "a" simply supported.	$\frac{1\frac{1}{2}pb^2}{1+0{\cdot}2\alpha^4}$	$\frac{2\frac{1}{4}pb^2}{1+0{\cdot}4\alpha^4}$	0	$\frac{pb^2}{80}(1+0{\cdot}3\alpha^2)$
	Span "a" fixed. Span "b" simply supported.	0	$\frac{\frac{1}{8}pb^2}{1+0{\cdot}8\alpha^2+6{\cdot}0\alpha^4}$	$\frac{\frac{1}{8}pb^2}{1+0{\cdot}8\alpha^4}$	$0{\cdot}015pb^2\frac{1+3\alpha^2}{1+\alpha^4}$
	All edges fixed.	$\frac{1\frac{1}{2}pb^2}{1+\alpha^4}$	$\frac{\frac{1}{8}pb^2}{3+4\alpha^4}$	$2\frac{1}{4}pb^2$	$0{\cdot}009pb^2(1+2\alpha^2-\alpha^4)$
Elliptic slab with fixed edge. Diameters a and b.		$\frac{1\frac{1}{2}pb^2}{1+\frac{2}{3}\alpha^2+\alpha^4}$	$\frac{2\frac{1}{4}pb^2}{1+\frac{2}{3}\alpha^2+\alpha^4}$	$\frac{1\frac{1}{2}pb^2\alpha^2}{1+\frac{2}{3}\alpha^2+\alpha^4}$	$\frac{2\frac{1}{4}pb^2\alpha^2}{1+\frac{2}{3}\alpha^2+\alpha^4}$

CHAPTER 19

THE DESIGN OF STEEL FRAMED BUILDINGS

19.1. Introduction.—A form of structure which has become increasingly important during the last thirty years is the building frame consisting, in the main, of lines of vertical stanchions joined by horizontal beams which support the floors and panel walls. While for many years almost all such frames were constructed of structural steel, reinforced concrete has recently entered the field. Many of the problems met in design and discussed here are common to both forms of construction, but attention will be mainly directed in this chapter to steel frames, since a comprehensive enquiry into their design was completed recently by the Steel Structures Research Committee,* while the behaviour of reinforced concrete frames has not yet been so fully investigated. This chapter consists primarily of a description of the work carried out by that Committee and their suggestions for the practical design of building frames.

As far back as 1909 regulations were drawn up governing the use of steel frames in London. These regulations, contained in the London County Council (General Powers) Act, 1909, not only served as the model on which the Codes of Practice governing the use of steel in buildings of almost all other countries in the world were based, but remained in force for twenty-three years. Long before the expiration of that period, the development in the manufacture of steel and the advance in the technique of steelwork made engineers feel that the regulations were unduly restrictive and that they did not allow full advantage to be taken of the excellent qualities which steel possesses as a material for building construction. It was in response to this feeling that the Steel Structures Research Committee was appointed.

The first task undertaken was a review of the regulations governing the design of steel framed buildings throughout the world. This showed that, although there were some striking discrepancies in detail, the method of design implied in every case was the same. The differences in detail are no longer of interest to the engineer practising in this country, since as an outcome of the Committee's First Report a uniform Code of Practice is now adopted by almost all authorities in Great Britain, and in considering the design method used to-day this Code alone need be studied.

So unsatisfactory at the time of the Committee's inception were the rules governing the use of steel in buildings that it was felt desirable,

* First, Second and Final Reports of the Steel Structures Research Committee, published by H.M. Stationery Office, 1931, 1934 and 1936.

in view of the considerable period which would elapse before the results of the full research programme were available, to draw up recommendations for a Code of Practice, based on knowledge existing then, which would remove many restrictions. It must be emphasised that these recommendations were not based on any investigations carried out for the Committee, but on the available knowledge and experience of practising engineers. These recommendations have been accepted practically unchanged by the London County Council and have been embodied in the British Standard Specification No. 449 issued in April, 1932, by the British Standards Institution; they have also been recommended to local authorities by the Ministry of Health, and a study of them will show the method of design in general use to-day.

19.2. Existing design methods.—The relevant clauses in the Code of Practice mentioned above are as follows:

(12) The steel framework of a building, in combination with the floors, bearing walls and bearing structures (if any) and the foundations shall be capable of safely and independently sustaining the whole dead and superimposed load of the building together with all forces due to wind, earth or other pressures acting upon it.

(35) (*a*) The dead load of a building shall consist of the actual weight of walls, floors, roofs, partitions and all other permanent construction comprised in such building, etc.

(*b*) The superimposed load in respect of a building shall consist of all loads other than the dead load.

(*c*) For the purpose of calculating the loads on foundations, pillars, brick or stone piers, walls and beams in buildings, the minimum superimposed load on each floor and on the roof shall be estimated as equivalent to the following dead load:—

	lb. per sq. ft. of floor area.
Rooms used for domestic purposes, hotel bedrooms, hospital rooms and wards . . .	40
Offices, floors above entrance floor	50
Offices, entrance floor and floors below entrance floor	80

etc., etc.

(*e*) For the purpose of calculating the total load to be carried on foundations, pillars, brick piers and walls in buildings of more than two storeys in height the superimposed loads for the roof and the topmost storey shall be calculated in full in accordance with the schedule of loading, but for the lower storeys a reduction of the superimposed loads may be allowed in accordance with the following table:—

Next storey below topmost storey.	10 per cent. reduction of superimposed load.
Next storey below	20 per cent. reduction of superimposed load.

Next storey below	30 per cent. reduction of superimposed load.
Next storey below	40 per cent. reduction of superimposed load.
All succeeding storeys	50 per cent. reduction of superimposed load.

The above reduction may be made by estimating the proportion of floor area carried by each foundation, pillar, pier and wall. No such reductions shall be allowed on any floor scheduled for an applied loading of 100 lb. or more per sq. ft.

(*f*) All buildings, other than those indicated below, shall be so designed as to resist safely a wind pressure in any horizontal direction of not less than 15 lb. per sq. ft. of the upper two-thirds of the vertical projection of the surface of such buildings with an additional pressure of 10 lb. per sq. ft. upon all projections above the general roof level. On the sea coast and in similarly very exposed situations a further provision not exceeding 10 lb. per sq. ft. shall be made.

If the height of a building is less than twice its average width, wind pressure in general may be neglected, provided that the building is adequately stiffened by floors and walls.

(36) (This clause contains particulars of the permissible working stresses for steel of Quality A ; for flexural stresses the value being 8 tons per square inch.)

(40) The working stresses on pillars and other compression members of Quality A steel due to all loads and forces other than wind pressure shall not exceed those specified in Table 7.4 (p. 129).

(41) The effective pillar length, l, to be assumed in determining the working stresses for pillars of one storey height shall be the actual pillar length.

(42) The effective pillar length to be assumed in determining the working stresses for the topmost and lowest lengths of a pillar which is continuous through two or more storeys shall be measured from floor level to floor level.

The effective pillar length to be assumed for any intermediate length of such a pillar may be taken at ·70 of the floor to floor length for any pillar which is effectually restrained at both its upper and lower ends. For any intermediate length of such a pillar in which the restraint at one or both ends is not entirely effectual, an intermediate value between ·70 and 1·00 shall be assessed, depending upon the degree of actual restraint.

(43) In all cases of eccentric loading on pillars, the bending moment about each principal axis is to be calculated and the resulting bending stresses added to the axial stress. The permissible stress may then be increased, for cases where the ratio of effective pillar length to least radius of gyration is less than 150, beyond the

figure specified in Clause 40 up to a limit of $\left[C_d+7{\cdot}2\left(1-\frac{C_d}{C_s}\right)\right]$, where C_s denotes the stress specified in Clause 40, and C_d denotes the compressive stress due to direct or axial load.

(44) In cases where a beam is connected to a continuous pillar, the bending moment in the pillar due to the eccentricity of the reaction from the girder may be regarded as divided between the pillar lengths above and below the level of the girder in direct proportion to the stiffnesses (moment of inertia/length) of the upper and lower lengths.

(45) In continuous pillars all bending moments due to eccentricities of loading at any one floor level may be considered as entirely dissipated at the levels of the floor beams immediately above and below, provided that the pillar at these latter levels is effectually restrained in the direction of the eccentricity.

These clauses do not set out the actual method to be used in proportioning the members of the frame, which consists in the main of lines of horizontal beams connected to vertical stanchions by brackets attached to the top and bottom flanges of the beams, but there is no doubt of the method implied. When considering the effect of the vertical loads arising from the dead and superimposed loads applied to the structure, it is usual to assume that the beam is simply supported or connected to the stanchion by perfectly free hinges which apply no bending restraint. This assumption makes the choice of the necessary beam sections easy, the vertical loads being known. Since it is assumed that the ends of the beams are attached to the vertical stanchions by hinges, the only load exerted on a stanchion by a beam is taken to be a vertical reaction. When the beam is attached to the flange of a stanchion of I section this acts at some distance from the centre-line ; conservative engineers take it to act at a distance of 2 inches outside the face of the stanchion, representing approximately the position of the centre of the bottom bracket on which the beam rests. The stanchion is designed, by means of Clauses 40–45, to carry the eccentric reactions applied to it.

The frame, as Clause 35 (*f*) indicates, may be called upon to withstand other than vertical loads. Horizontal loads may be applied due to wind action. The stresses brought about by a horizontal load acting on the frame with hinged joints can be found without difficulty but they will be excessive, since the stanchions merely behave as cantilevers of the same length as the height of the building. Practical experience has shown that the actual stresses are not excessive, so that when considering the effect of horizontal wind loads, it is customary to consider the connections between beams and stanchions to be perfectly rigid joints capable of transmitting bending moments. The fundamental assumptions are, therefore, diametrically opposite, and depend on the direction of loading. With these assumptions the design of the beams is straightforward ; that of the compression members is a more difficult problem.

The permissible loads per unit area (working stresses) on pillars referred to in Clause 40, have been deduced from the Perry formula which is derived and discussed in paragraph 7.9.

These loads are based on the consideration of a pin-ended compression member. The stanchion lengths in a steel frame are not hinged at their ends but are continuous through many floors and in an attempt to allow for this continuity Clauses 41 and 42 have been introduced. If a compression member is continuous through a number of storeys and a truly axial load is applied, then, as the member deflects under this load, restraining moments are induced at the ends of each storey length, due to the beams which frame into the stanchion at the floor levels offering resistance to the change of slope of the stanchion at those points. This restraining moment allows a member of given section to carry safely a greater axial load than would have been possible had it been pin-ended. To take the restraints into account it was assumed that the effective length of the member was less than its actual length, and then, by means of Clause 40, the pin-ended member having a length equal to this effective pillar length was designed. Clauses 41 and 42 were drafted before any reliable information of the effective length of pillars in steel frames was available, and they do not help the designer as no definition is given of " effectual restraint." In applying this method of design it appears to be common to-day to estimate the ratio of effective to actual length for intermediate stanchion lengths as follows :—

where three or four beams frame into the stanchion at each floor	0·750
where two beams frame into the stanchion at each floor	0·875
where one beam frames into the stanchion at each floor	1·000

For top lengths under the same conditions the figures are ·875, 1·000 and 1·250 respectively. Although these values are probably on the safe side for most frames they are at best rough approximations, since the number of beams alone cannot govern the restraint.

The magnitudes of the restraining moments at the ends of a stanchion length depend not only on the beam stiffness but also on the type of connection between the beams and the stanchion. If the beams are connected to the stanchion by perfectly free hinges no restraining moments can be transmitted from the beams to the stanchion and the effective length of the stanchion is not decreased by the presence of the beams. If, on the other hand, the connections between the members have considerable rigidity, appreciable restraining moments are induced and it has been found possible * to estimate the value of the ratio of effective length to actual pillar length for a member in a frame with rigid joints as shown in Table 19.1.

* " Note on the Effective Length of a Pillar Forming Part of a Continuous Member in a Building Frame." J. F. Baker. Second Report of the Steel Structures Research Committee (1934), p. 13.

TABLE 19.1.—SUGGESTED VALUES OF THE RATIO OF EFFECTIVE LENGTH TO ACTUAL PILLAR LENGTH FOR A MEMBER IN A FRAME WITH RIGID JOINTS.

$\frac{\text{Stiffness of beam}}{\text{Stiffness of pillar length}}$	0·25	0·50	1·00	1·50 and above
$\frac{\text{Effective length}}{\text{Actual pillar length}}$	0·90	0·75	0·65	0·60

Where the usual types of semi-rigid steelwork connections are used the variables are so many that it is impossible to formulate a concise rule. The designer is forced, therefore, to depend on the unsatisfactory approximations already mentioned.

Clauses 43, 44 and 45 deal with the effect of the bending moment induced by the reactions coming from the beams. If the loads on the beams at a floor level produce reactions R_1 and R_2 on either side of the stanchion at eccentricities e_1 and e_2 (usually taken as half the width of the stanchion plus 2 inches), the total moment applied to the stanchion at that floor level is taken to be $R_1e_1 - R_2e_2$, and, according to Clause 45, no account is taken of the effect on this moment of loads on the floors above and below. The end bending moments in the stanchion lengths above and below the floor level under consideration are found, according to Clause 44, by dividing the total moment between them in the ratio of their stiffnesses. The end bending moment applied to a stanchion length produces bending stresses in the member and it must be decided whether they can be safely sustained. The working stresses referred to in Clause 40 were deduced from a consideration of a pillar subjected to axial load only, so that some alteration is required when an end moment also is present. The alteration is made by means of the formula in Clause 43.

This formula is open to severe criticism. The total maximum stress in a pin-ended pillar of cross-sectional area A, carrying an axial load P, is the sum of the unit compressive stress P/A, and the maximum bending stress developed by a bending moment Py where y is the greatest deflection of the pillar due to the action of P. Clause 40 gives the value of P which makes the maximum stress in the member rise to a certain limiting value. The reasoning behind the formula of Clause 43 is that if an axial load P′, less than P, acts together with an end bending moment, then, since the greatest deflection of the strut due to the action of P′ alone is less than y, the end bending moment may develop a bending stress somewhat greater than (P—P′)/A without the maximum stress in the member rising above its limiting value. The fault in this reasoning is that the effect of the end bending moment on the magnitude of y is neglected. As will be seen later, when the end bending moment produces " single curvature " bending (p. 429) y is increased, so that Clause 43 overestimates the permissible stress. There are other objections to the formula, its only virtue in fact being that of simplicity.

One other point needs emphasising. In the present method of design

it is assumed, when estimating stresses, that all members are loaded, but this may not produce the worst stress conditions. For instance, in calculating the bending moment on a stanchion, a greater moment (R_1e_1) is produced when the beam on one side only is loaded than that ($R_1e_1 - R_2e_2$) when both are loaded.

The designer's task is by no means an easy one and reasonably simple formulas must be derived for his use, but it is evident from a study of existing design methods that there has been a tendency in the past to base the formulas on assumptions which make some calculation possible rather than on those justified by the actual behaviour of the frame.

19.3. Preliminary investigations by the Steel Structures Research Committee.—The use of the design method reviewed above results in the production of safe structures. This is due, in the main, to the assumption of values for the superimposed loads which are greater than those actually carried by the structure. It was clear to those who had taken part in the drafting of the recommendations for a Code of Practice that a limit had been reached in the reduction of these values, below which it would be unsafe to venture while the existing unsatisfactory methods of estimating the stresses in the structure were in use. It was equally clear that, as the existing method did produce safe structures, there were opportunities of effecting economies in material. These, however, could only be exploited if a method of design having a rational basis could be produced.

No information of any value existed as to the real behaviour of framed structures, but the contradictory assumptions made in design had drawn attention to the beam-to-stanchion connections. One of the first tasks undertaken by the Committee therefore was an investigation of their behaviour, the results of which have been outlined in Chapter 11. At the same time it was realised that as a step towards a rational design method a sound method of stress analysis was essential.

It would have been of little value to embark on an elaborate mathematical investigation without the aid of experiment and it was decided, therefore, to erect a steel framework the stress distribution in which could be measured to serve as a guide to mathematical analysis.

The frame consisted of six stanchions, the bases of which were bolted down to a concrete raft, and twenty-one beams, all 8-inch by 4-inch by 18-pound steel joists. Provision was made for the use of various types of bolted and riveted beam-to-stanchion connections. Three of the stanchions were arranged with their webs parallel to the length of the frame and three with their webs perpendicular to the length of the frame, so that a large variety of one and two bay, three storey frames could be built up.

The object of the tests on this frame was the determination of the stress distribution in the members due to the application of external loads. It was arranged that a central concentrated load could be applied to each beam in turn by means of a spring and turnbuckle and the stress distribution was found by measuring the strains at a number of sections of the members.

One of the first tests carried out was on the symmetrical single bay frame shown in Fig. 19.1. The beams were connected to the webs of the stanchions by type A connections consisting of top and bottom flange-cleats made up of $3\frac{1}{2}$-inch by 3-inch by $\frac{5}{16}$-inch angle, 4 inches long and secured with $\frac{1}{2}$-inch diameter bolts. The distribution of observed stresses when a central concentrated load of 2 tons was applied to the beam at the first floor is shown in Fig. 19.1 and in Table 19.2.

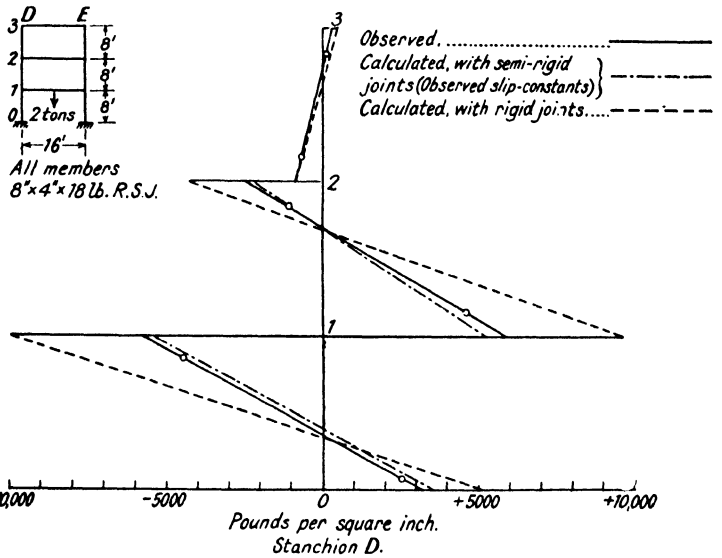

FIG. 19.1.—Maximum Fibre Stresses due to Bending in Plane of Frame. Load: 2 tons at centre of D_1E_1.

TABLE 19.2.—COMPARISON OF BENDING STRESSES. SYMMETRICAL SINGLE BAY FRAME, FITTED WITH TYPE A CONNECTIONS. CONCENTRATED LOAD OF 2 TONS AT CENTRE OF BEAM D_1E_1.

Section	Observed, with type A connections: lb. per square inch	Calculated, with semi-rigid joints (observed slip constants): lb. per square inch	Calculated, with rigid joints: lb. per square inch
D_0D_1	+3,100	+3,345	+ 5,176
D_1D_0	−6,075	−5,775	−10,352
D_1D_2	+5,800	+5,354	+ 9,916
D_2D_1	−2,450	−2,364	− 4,302
D_2D_3	− 850	− 890	− 831
D_3D_2	+ 200	+ 244	+ 350

The Table gives the maximum stresses (+denoting tension, −compression, at the inside edge of the member) at the top and bottom of each stanchion length due to bending about the YY axis of the stanchion.

The stresses in the stanchion for this condition of loading have been calculated on the assumption that the joints are perfectly rigid. They are shown in Fig. 19.1 and Table 19.2 (column 4). The fact is revealed that, although the bending stresses actually induced in the stanchion

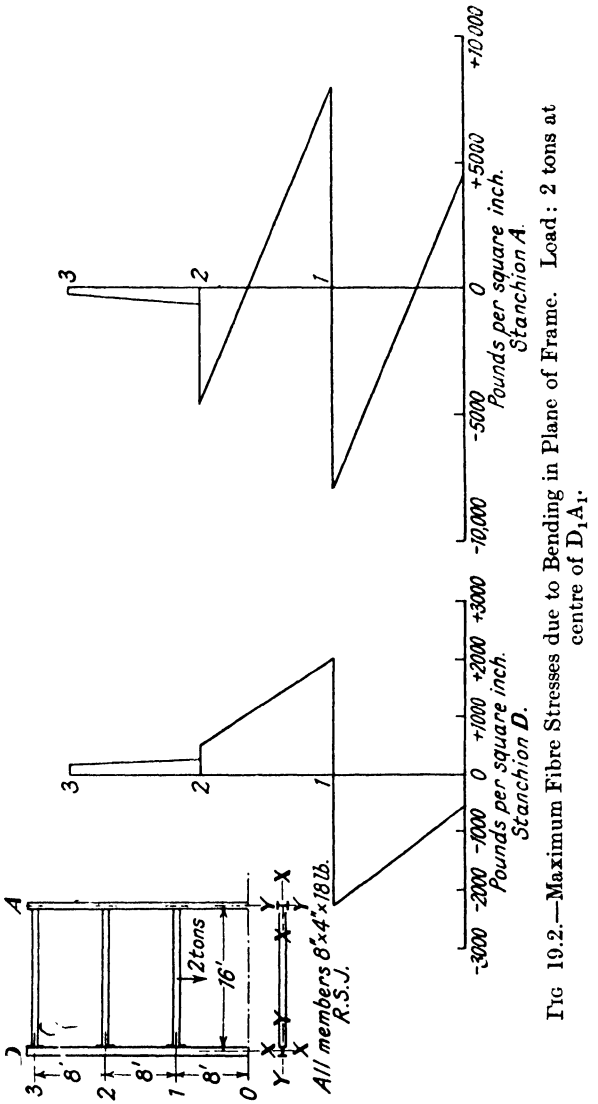

FIG 19.2.—Maximum Fibre Stresses due to Bending in Plane of Frame. Load: 2 tons at centre of D_1A_1.

lengths are smaller than those which would have been found had the joints been perfectly rigid, the distributions of stress in the two cases are exactly similar in form, with the result that appreciable bending stresses are found in the top length 2–3 of the stanchion which is two storeys above the applied load. The magnitude of the observed bending stress is considerable. It must be remembered that the beam-to-

stanchion connections were not of a particularly rigid type and would in any case have been assumed in the existing design method to have been pin-ended so far as vertical loads on the beam were concerned. As the connection was made to the web of the stanchion the eccentricity would have been taken by many designers as zero and by the conservative designer as not more than 2 inches. In actual fact the "equivalent eccentricity" of the connection to stanchion D at the level of the first floor (that is to say, the distance from the axis of the stanchion at which the reaction arising from a similarly loaded simply supported beam would have had to act to produce the observed bending stresses in the stanchion) was 9·3 inches. The form of the bending stress or bending moment diagrams observed for these stanchion lengths are typical for a frame in which sway, relative horizontal deflection of the beams in the plane of the frame, does not exist. The condition of bending in such stanchion lengths may be defined as "double curvature" bending.

A different condition is found when sway is present and this can be most easily seen from the results of tests on an unsymmetrical frame, Fig. 19.2, in which the beams were joined by type A connections to the flange of one stanchion D and to the web of another stanchion A. The stresses observed in stanchions D and A due to the application of a central concentrated load of 2 tons to the beam at the first floor are shown in Fig. 19.2 and Table 19.3.

TABLE 19.3.—OBSERVED BENDING STRESSES. UNSYMMETRICAL SINGLE BAY FRAME FITTED WITH CONNECTIONS OF TYPE A.

Concentrated load of 2 tons at centre of Beam D_1A_1.

Section	Observed, with type A connections: lb. per square inch
A_0A_1	+4,560
A_1A_0	−8,120
A_1A_2	+8,100
A_2A_1	−4,520
A_2A_3	− 600
A_3A_2	− 200
D_0D_1	− 700
D_1D_0	−2,275
D_1D_2	+2,000
D_2D_1	+ 525
D_2D_3	+ 250
D_3D_2	+ 150

It will be seen that the forms of the bending stress diagrams in the two stanchions are quite different, due to the sway which has arisen from the lack of symmetry in the structure. In the lengths 0–1 1–2 of stanchion A, double curvature bending has resulted as before from

the application of the load to the beam, whereas in stanchion D the form of bending can be designated " single curvature " bending. The difference in these forms was found to be of the first importance when the rational design of a stanchion length was under consideration.

In addition to measurements of strains in these frames the characteristics of the beam-to-stanchion connections were found. Relative rotation of the ends of the members joined was measured by a simple arrangement of dial indicators and a curve obtained showing the relation between the moment transmitted by a connection and the relative rotation of the members joined. It was found that this relation (the characteristic curve for the connection) was by no means linear, and that, on the removal of load from a beam, reverse bending moments remained at the ends of the beam. These points have been

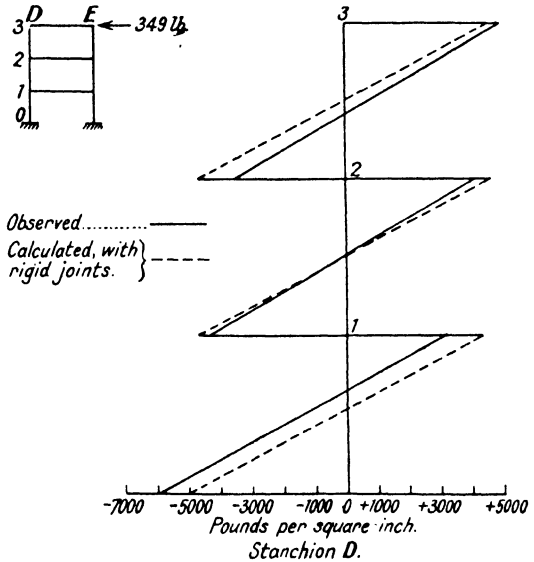

FIG. 19.3.—Maximum Fibre Stresses due to Bending in Plane of Frame. Horizontal Load of 349 lb.

discussed in Chapter 11 where it is also shown how the methods of stress analysis given in paragraph 9.4 can be used when the characteristic curves for the connections are not straight lines. An example of the stresses calculated in this way is shown in Table 19.2 (column 3).

One other test carried out on the experimental frame must be mentioned. A horizontal load of 349 lb. was applied to the top of the symmetrical single bay frame (Fig. 19.1). The observed stresses are plotted in Fig. 19.3, and are set out in Table 19.4. It will be seen that, while the distribution of stress was of the same form, the maximum bending stress observed at the foot of each stanchion was greater than would have been predicted on the assumption of perfectly rigid joints.

TABLE 19.4.—COMPARISON OF BENDING STRESSES DUE TO A HORIZONTAL LOAD OF 349 LB.

Symmetrical Single Bay Frame.

Section	Observed stress: lb. per square inch	Calculated stress, with rigid joints: lb. per square inch
D_0D_1	−5,700	−4,990
D_1D_0	+3,600	+4,590
D_1D_2	−4,600	−4,780
D_2D_1	+5,050	+4,780
D_2D_3	−4,250	−4,690
D_3D_2	+5,150	+4,880

A reliable method of design could only be produced if the behaviour of the complex structure, consisting of the steel frame and the clothing of walls and floors which makes up the finished building, was understood. It was decided, therefore, in view of the success of the work on the experimental frame, to test actual buildings. Details of these tests cannot be given here but the data collected on two buildings, an hotel and an office, will be reviewed.

19.4. Review of tests on buildings.—The buildings tested behaved normally under load. Appreciable restraining moments were developed at the ends of the beams and corresponding bending moments in the stanchion lengths. It was found that the method of stress analysis developed could be made to give a reliable estimate of the stresses in a frame even when it was clothed.

The magnitudes of the restraining moments can be gauged from the fact that the equivalent eccentricity of a connection lay between 30·0 and 44·6 inches for the bare frame of the hotel building and between 16·0 and 34·3 inches for the office building. These restraining moments, while reducing the maximum stresses in the beams by from 17 per cent. to 25 per cent. of those which would be found in similarly loaded simply supported beams, were at the same time responsible for large bending stresses in the stanchions, in some cases as much as 9 times those which would be estimated by the existing methods.

Sway of the bare unsymmetrical frames was detected but it was eliminated after the addition of floors and casing. The presence of sway makes it difficult to formulate simple expressions for the bending moments in the members of a frame adjacent to a loaded beam. In frames which are not to be clothed, therefore, great care must be exercised in drafting design rules, particularly for stanchions, since the distribution of bending stresses will depend very largely on the proportions of quite distant members. Evidence, both from these tests and by calculation, shows that it should be safe, in all but the most extreme cases, to neglect sway when the frame has floors of hollow tile or similar construction, brick walls and even light stanchion casings.

The opportunity was taken, after the hollow-tile floors had been laid in the buildings, of measuring the stresses induced in adjacent stanchions by the application of a central concentrated load to a beam not framing into those stanchions. These stresses, produced by the slab effect of the floor, were appreciable. The bending stress developed in an adjacent stanchion was found to be as much as 20 per cent. of the stress in the stanchion into which the loaded beam framed. Considerably more data will be needed before advantage can be taken of the fact in design but there is no doubt that, as far as the stresses in the stanchions are concerned, each bay of a hollow-tile floor should be considered as a slab capable of bending a stanchion about both principal axes.

Among the many smaller matters illustrated by the tests was an indication of the considerable local stress which can be set up in a stanchion by unequal bearing on its base. The foot of one stanchion in the hotel building rested on a 5-inch thick steel slab. Strain readings taken 12 inches above the foot of the stanchion showed that the stress at one corner of a flange was 17 times as great as that at any other corner. Examination of the base showed that the holding-down bolts had not been screwed home as far as they might have been. A further test, made after these bolts had been tightened, showed that some redistribution of stress had taken place over the cross section but that the stanchion was still unevenly bedded since at the one corner the stress was still more than 3 times that at any other. The load applied to this stanchion length by the placing of the floors must have been sufficient to produce local yielding in the foot of the stanchion, as when a test was carried out after the floors were in position the distribution of stress at the section 12 inches above the base was quite normal.

One of the main objects of the tests was the collection of data which would throw light on the variability of the behaviour of beam-to-stanchion connections made to the same design under normal conditions on the site.

If, in designing beams, advantage is to be taken of the restraining moments transmitted by the connections, a complete knowledge of the characteristics of the connections is necessary. This was obtained for the Committee mainly by means of laboratory tests, where a number of specimens with connections made to the same design by different fabricators were tested, so that a measure of the variability of behaviour could be made. It would have been unwise, however, to depend on this information alone. One of the most probable causes of variability appeared to be differences in workmanship. The method of fabricating the laboratory specimens was by no means the same as that which would normally be used on the site. Apart from the more difficult conditions there it is usual for stanchions to be erected and for a beam to be brought between them, the connection at one end being made before that at the other. While the first connection might be represented faithfully by a laboratory specimen, the conditions of fabrication at the other end would in all probability be so different

that appreciable variation in behaviour might result. The only way of investigating this was by tests on connections to the beams of actual building frames. Fig. 19.4 shows the relation between the moment transmitted by a connection and the relative rotation $\theta - \phi$ of the members joined for the class of connections found in the hotel building

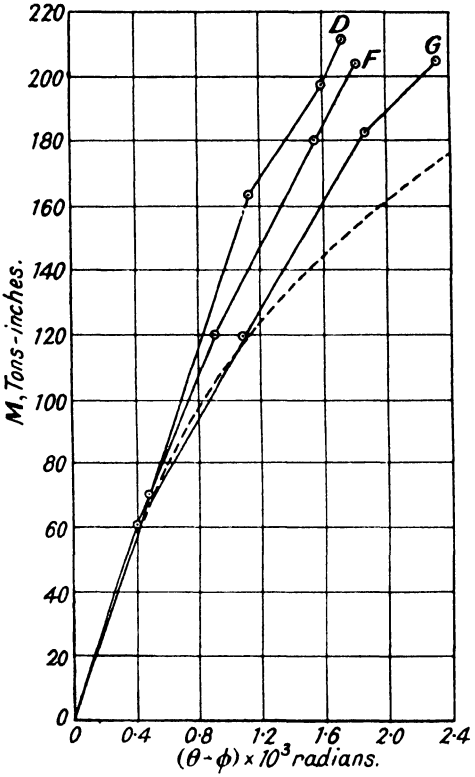

FIG. 19.4.

and illustrated in Fig. 19.5. Similar agreement was found between the curves for the other classes of connections used in the two buildings tested and there is no indication that the effect of workmanship on the site is likely to cause greater variation than that found in the laboratory tests.

The curves given above referred to bare connections. In the great majority of important buildings the connections will be covered by the concrete of the floors or of the fire resisting stanchion casing. An attempt was made in the tests to find the effect of this concrete casing on the behaviour of the connections. It did not prove an easy matter as the moment transmitted through the connection could only be deduced from the stresses produced in the stanchion and it was found impossible to measure the relative rotation of the members. Characteristic curves could not, therefore, be drawn. A comparison of the stresses developed in the stanchions before and after the connections were cased

gave some indication that the variability of the connections was decreased by the casing.

Clause 44 (p. 422) of the existing method of design states that the bending moment coming on a continuous pillar from a loaded beam may be regarded as divided between the pillar lengths above and below

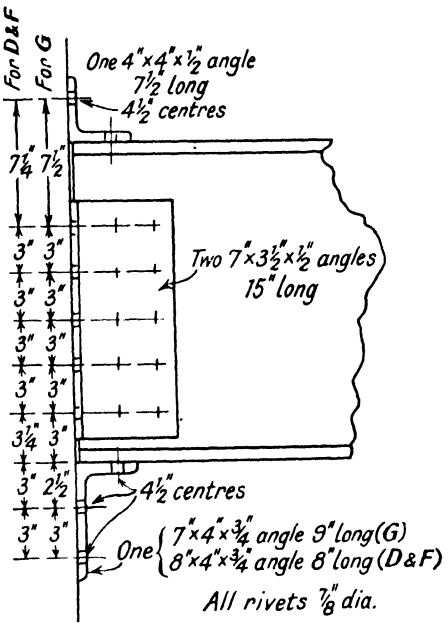

FIG. 19.5.

the level of the beam in direct proportion to the stiffnesses of the upper and lower lengths.

The tests showed that the actual partition of moment is very different from this. In all cases, except that of an internal stanchion of the hotel building, it was found that in the bare frame the lower stanchion length received more of the bending moment coming from the beam than the simple rule allows. Table 19.5 shows typical values of the true partition.

When the floors were laid and the stanchions were cased the partition of moment approached much more nearly that of the ratio of the stiffnesses of the stanchion lengths, as can be seen from Table 19.5 (columns 5 and 6). In the internal stanchion of the hotel building the state of affairs was very different. Table 19.6 shows that the upper stanchion length received more than its share of moment and that the partition was not seriously modified when floors were laid.

The rule of Clause 44 was based on a consideration of the simplest possible frame in which the top and bottom ends of the stanchion lengths were encastré and in which horizontal sway was prevented. In an actual frame there would be some rotation of the ends of the

stanchion lengths remote from the loaded beam and there would also in general, in a bare frame, be some sway. Neither of these effects could produce the change in the partition shown by the tests and it must, therefore, arise from the axial thrust developed in a loaded beam by the behaviour of the end connections. When a beam is connected to supports by a flange-cleat connection the bottom or

TABLE 19.5.—A COMPARISON OF THE RATIOS OF STANCHION STIFFNESSES AND BENDING MOMENTS IMMEDIATELY ABOVE AND BELOW THE NEUTRAL AXIS OF THE LOADED BEAM. (OFFICE BUILDING, SINGLE BAY PORTION.)

Loaded beam	Stanchion	Ratio of stiffnesses of stanchion lengths	Ratio of bending moments		
			With frame bare	With floors laid	With stanchions cased and floors laid
200 D	S. 20	0·95	0·54	0·95	—
	S. 34	0·99	0·46	0·70	1·10
200 C	S. 20	0·78	—	0·47	—
	S. 34	0·94	—	0·73	0·96
200 E	S. 20	0·85	0·71	—	—
	S. 34	1·00	0·56	—	—

TABLE 19.6.—A COMPARISON OF THE RATIOS OF THE STANCHION STIFFNESSES AND BENDING MOMENTS IMMEDIATELY ABOVE AND BELOW THE NEUTRAL AXIS OF THE LOADED BEAM. (HOTEL BUILDING, INTERNAL STANCHION NO. 8A.)

Loaded beam	Ratio of stiffnesses of stanchion lengths	Ratio of bending moments		
		With frame bare	With floors laid	With stanchions cased and floors laid
81 D	1·00	1·21	1·13	—
81 F	0·75	1·24	0·96	1·01
81 G	0·89	1·34	1·42	—
81 H	0·67	1·35	1·39	—

tension flange tends to increase in length while the top or compression flange decreases as transverse load is applied to the beam. Since the distortion of the bottom brackets cannot take place as freely as that of the top cleats, thrust is developed in the beam when the supports are not perfectly free to move. This thrust could produce the ratios of moments observed in the stanchions of the single bay frames, where it was less than the ratio of the stiffnesses of the members.

In a multi-bay frame thrusts will be developed both in the loaded beam and in the beam on the other side of the internal stanchion to which they are connected. If the sections of the beams are not very different, the thrust in the loaded beam will be the greater and the effect on the moments in the internal stanchion will be similar to that in the stanchions of a single bay frame. This was the case in the two bay frame of the office building. Where, as in the multi-bay portion of the hotel building, the loaded beam is of a much smaller section than that on the other side of the internal stanchion, the thrust in it may be less than that in the unloaded beam. This will produce a different form of partition of stanchion moment, the ratio of moments above and below the level of the beam being greater than the corresponding ratio of stanchion stiffnesses.

In the present state of knowledge it is impossible to predict with any accuracy the ratio of the stanchion moments, but the important fact remains that, if a close estimate of the total moment coming on to the stanchion is made, the use of the simple Code of Practice rule will, in most cases, result in an under estimate of the maximum end bending stress in the stanchion since the greatest total moment will, in general, arise when the heavier beam attached to the stanchion is loaded.

A knowledge of the effect of the clothing added to the steel frame is essential. The placing of floors influences the stanchion stresses in three ways as follows :—

(*a*) The presence of beam casing or of hollow-tile floors increases the effective stiffness of the beam in the frame, and so, other influences being unaltered, tends to decrease the bending stresses in the stanchions.

(*b*) The concrete which is placed around the connections when the floors are laid increases, to some extent, the rigidities of the connections, with the result that the moments transmitted to the stanchions and the bending stresses induced in them tend to increase.

(*c*) The floors form slabs connecting all the bents of the framework, so that the effect of a load on one beam is felt not only in the stanchions to which the beam frames, as in the bare framework, but in adjacent stanchions also. Due to this slab effect, the stanchion stresses produced by the application of a concentrated load to a beam are likely to decrease.

It was not easy to study all these influences separately.

In the single bay portion of the hotel building the addition of floors decreased appreciably the bending stresses induced in the stanchions when a central concentrated load was applied to a beam framing into them. In ten of the twelve stanchion lengths tested the decrease in maximum bending stress varied from 37·5 to 21·1 per cent. Since in practice the applied load would be distributed over a considerable floor area it was essential to evaluate the slab effect. This was done by measuring the stresses in adjacent stanchions when a concentrated

load was applied to a beam. From such measurements it was deduced that, in this particular structure, had a distributed load been applied to the whole floor area the maximum stanchion bending stresses in the frame with floors laid would, with two exceptions, have varied between 10·8 per cent. less and 14·7 per cent. more than the corresponding stresses in the bare frame under the same load. In two stanchion lengths, however, increases of as much as 40 per cent. and 62·5 per cent. would have been found. Where the internal stanchion of the hotel building was concerned the presence of floors decreased in every case the bending stresses induced when a concentrated load was applied to the beams framing into it.

A very different state of affairs was found in the office building, a considerable increase in stanchion bending stress occurring when the floors were in position. As measured by the equivalent eccentricity of a connection, an increase of 53 per cent. was found in one stanchion of the single bay portion when a concentrated load was applied to a beam, that is to say without allowance for slab effect. When, as was fortunately possible in this building, a distributed load was applied to the floor so that the slab effect was automatically included, the increase in stress was as much as 66·5 per cent. over that which would have been estimated in the bare frame carrying the same load.

When the floor was laid in the two bay portion of the office building, casing was at the same time poured around the internal stanchion. In spite of this and the fact that the floor was continuous past the internal stanchion, the increase of stanchion bending stress was no less than 61·3 per cent.

Although these effects are so different from those found in the case of the hotel building the reason is not difficult to find. In the hotel the bare beam-to-stanchion connections were much less flexible than those of the office building. The addition of concrete would therefore increase the rigidity of the former far less than that of the latter and would make it much more likely for the decrease in stress, due to the added stiffness of the beams, to prevail.

Floors are not the only clothing likely to affect the stresses in the steel framework ; the fire-resisting casings added to the stanchions and the external walls will also play their part.

Apart from any effect due to the reduction in sway, the presence of casings and walls will tend to stiffen the stanchions and so increase the moments developed in them. These increased moments may not, however, produce increased bending stresses in the steelwork since the total section of the stanchion is increased by the addition of casing. For the investigations of these effects additional tests were carried out after walls and stanchion casings had been built.

Although the stanchion casing of the hotel building was very light in form, two tests made on the fully clothed single bay portion showed that its presence decreased the maximum bending stress in each stanchion length below that observed when the floors alone were in place. The decrease in the five stanchion lengths concerned varied

from 10 per cent. to 35·5 per cent. In one test, strain measurements were made on adjacent stanchions also, so that the slab effect could be evaluated. It was found that the stresses in the bare frame would have been approximately 31 per cent. more than the corresponding stresses in the completely clothed frame subjected to a distributed load. Only one test was carried out on the internal stanchion of the hotel building after the casing was in position. There, again, small but quite definite reductions in the stanchion stresses were found. From this it appears that the addition of clothing to this particular frame relieved the stresses in the steel framework appreciably.

Once more very different conditions were found in the office building. In one test on the single bay portion the presence of walls and casing, which were more substantial than those of the hotel building, brought about an increase in the total bending moment in the steel core of 19 per cent. of the value it would have had in the frame with floors alone in position. In one stanchion length the increase in the maximum bending stress was 47·2 per cent.

In the two bay portion of the office building the increase in stress was more striking. In one length of the internal stanchion the maximum bending stress increased by 97 per cent. above the value it would have had in the frame without external walls and external stanchion casing. In other lengths of the same stanchion the corresponding increases were 41 and 27 per cent.

These tests have shown that the effect of clothing cannot be ignored. In a frame such as the hotel building, with a rigid type of bare steelwork connection, the effect of the clothing may, in general, be to reduce the stresses somewhat below the values which would be estimated, by an accurate method of stress analysis, in the bare frame. In a frame, such as the office building, with more flexible connections the stresses may be very appreciably increased. The bending stress found in a certain stanchion length of the fully clothed building was 2·89 times that which would have been set up in the bare frame. In other cases the increase in bending stress was as much as 60 per cent. It appears from this that, until more is known of the effect of cased connections, the assumption must be made in the design of stanchions that, where a frame is encased in concrete, all connections are perfectly rigid.

19.5. The problem of design.—The more important points brought out by the experimental investigations can be summarised as follows :—

(*a*) Standard types of riveted and bolted connections are capable of transmitting large bending moments, and appreciable restraining moments are developed at the ends of a loaded beam in a steel framed building.

(*b*) Although there was some variation due to workmanship in the behaviour of connections made to the same design, it was possible to produce a lower-limit curve for each type of connection similar to those shown in Fig. 11.4, enabling a safe estimate of the restraining moment to be made.

(*c*) The moment transmitted through a connection from a loaded

beam develops bending moments in the stanchion which are many times greater than those taken into account to-day.

(*d*) The bending moments developed in a stanchion due to load applied to a beam are appreciable, not only in the stanchion lengths to which the beam is attached but also in those more remote.

(*e*) The ratio of maximum bending moments in the stanchion lengths above and below a loaded beam may be very different from that of the stiffnesses of the stanchion lengths.

(*f*) The addition of floors, walls and stanchion casing to a frame does not bring about any fundamental change in the behaviour of the frame.

(*g*) Concrete casing can appreciably increase the rigidity of connections in the working range.

(*h*) The presence of clothing decreases the maximum stresses in the steel beams of a frame but it may increase the bending stresses in the steel cores of the stanchions.

(*i*) The methods of stress analysis developed could be depended upon to give a true picture of the distribution of stress in the steelwork of a frame even when it was clothed.

The investigations thus showed that the stress calculations made by existing methods give a very faulty representation of the distribution of stress in a frame. They emphasise shortcomings in stanchion design and the extravagance of the present method of beam design, in which restraining moments are neglected. They also disprove the assumption that the worst conditions are provided for each member when every member carries its full load.

It is not easy to calculate the stresses in such a complicated structure as a building frame. Simplified assumptions must be made but if they are so sweeping that the true behaviour of the frame is disguised, economy of material and evolution of the method of construction are impossible. The Steel Structures Research Committee endeavoured to produce a method of design which, while simple enough to be applied in ordinary practice, was based on an accurate estimate of conditions in the structure.

It is not difficult to see that the restraining moment developed at the end of a loaded beam joined to a stanchion by a certain connection depends not only on the characteristics of the connection but on the stiffness of the stanchion. If the stanchion can be assumed to be rigid, the restraining moment developed will have its maximum value; as the stiffness decreases so does the restraining moment. The maximum stress in the beam is influenced by the magnitude of the restraining moment so that the suitability of a beam to carry a given load depends on the connections at its ends and on the stanchion to which it is attached. In the same way the bending moment applied to the stanchion by a loaded beam is influenced by the proportions of the beam.

As a designer cannot afford to make a tentative design of the whole structure and then to modify each member as the effect of the remainder of the frame is appreciated, some means had to be found which would

enable one member to be designed economically without reference to the actual properties of the rest of the structure. It was found that, while the stresses in each member are affected to some extent by the conditions of the rest of the frame, the maximum stress in a loaded beam fitted with a certain semi-rigid beam-to-stanchion connection is not particularly sensitive to changes in the stiffnesses of the members into which it frames. A safe design without serious loss of economy would, therefore, result if a lower limit was assumed for the stiffnesses of these members when the restraining moment on the beam was estimated. From the evidence supplied by a large number of frames designed under existing methods it was seen that the sum of the stiffnesses of the stanchion lengths into which a beam framed would not, except in special cases, be less than two-thirds of the stiffness of the beam. Assuming the stiffness of the stanchion lengths to be two-thirds that of the beam, it was possible to find, by the graphical method described on p. 237, the restraining moments at the ends of any loaded beam fitted with any type of standard connection, and therefore, taking account of the relief given by these moments, to design a beam which would be safe and more economical than those obtained by existing methods, whatever the actual sizes of the adjacent members in the structure. With the beams designed in this way the design of the stanchions could be approached with some confidence.

The difficulty in designing a stanchion length is to decide what conditions give rise to the greatest stress in the member. Fig. 19.6 gives diagrams showing the bending stresses in a symmetrically placed stanchion length, AB, deduced from the results of the tests on existing buildings, due to various arrangements of superimposed load on the beam. In the existing method of design it is usual to choose a stanchion section from a consideration of the conditions existing when all floors are loaded, Fig. 19.6 (*a*), making the usual reduction in live load allowed in Clause 35 (*e*). This load will not, however, give rise to the greatest stress in the stanchion since, by removing load from the floors below on alternate sides of the stanchion, as shown in Fig. 19.6 (*b*), considerable end bending moments are developed in AB. This removal does not reduce the magnitude of the end load on AB, but it does appreciably increase the maximum bending stress in the stanchion length.

The conditions shown in Fig. 19.6 (*b*) do not necessarily develop the absolute maximum stanchion stress. If load is removed from part of the floor immediately above the stanchion length as shown in Fig. 19.6 (*c*) the end bending stresses are increased further and the decrease in axial end load arising from the removal of the load from the floor above may not compensate for this increase, leaving the maximum total stress greater than in Fig. 19.6 (*b*). A further increase in end bending stress arises if other floors are unloaded as in Fig. 19.6 (*d*), but in most structures the reduction in axial end load which follows outweighs this further increase. In these last three arrangements of load, shown in Fig. 19.6 (*b*), (*c*) and (*d*), the bending moments applied by the beams to the ends of the stanchion length bend it in double

curvature. Another condition has to be considered in which the stanchion length bends in single curvature. An arrangement of load

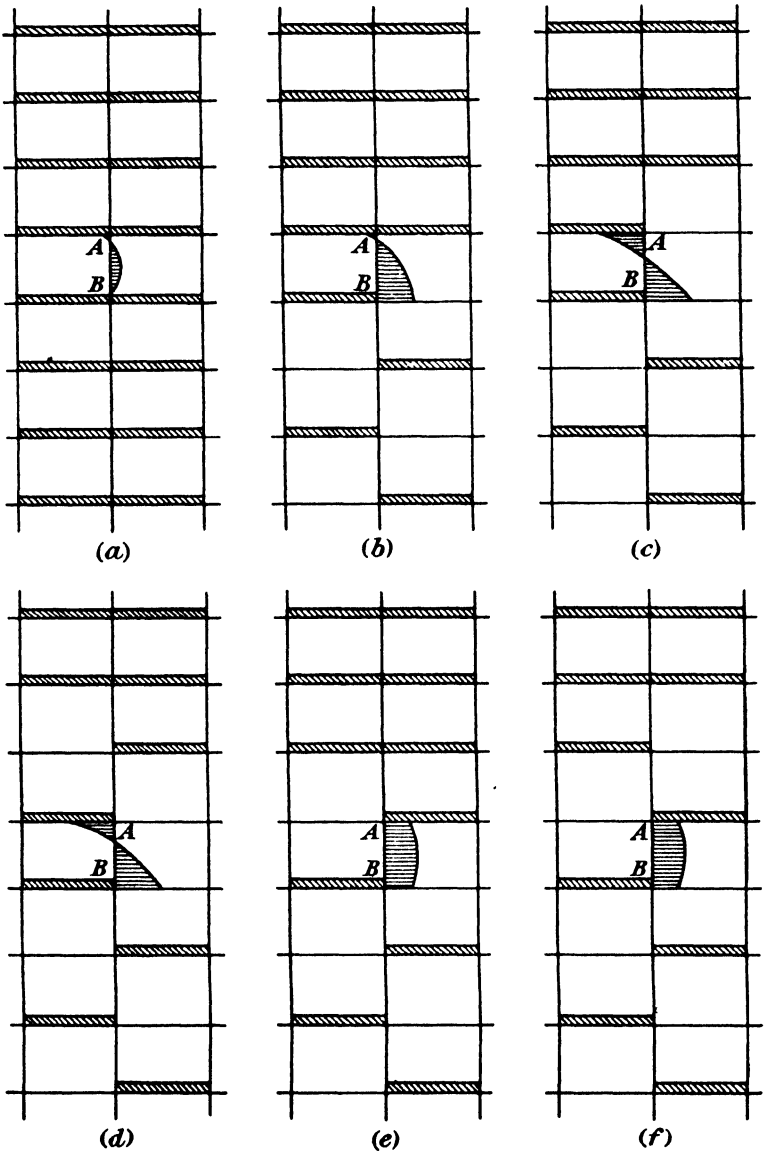

FIG. 19.6.

which brings this about is shown in Fig. 19.6 (*e*), together with the resulting form of the bending stress diagram.

As before, the removal of further load, Fig. 19.6 (*f*), increases the bending stress but decreases the axial stress.

It is impossible to say from inspection which of the arrangements of

load shown in Fig. 19.6 (*b*)-(*f*) will give the absolute maximum stress in the stanchion length, but it is certain that one or other of them will give a greater value than the arrangement of load hitherto used (Fig. 19.6 (*a*)). It is clear that, for a complete treatment, the behaviour of a stanchion length under axial end load and end moments, producing both single and double curvature, must be studied. The arrangement of load which must be used in design depends on the relative values of the end moments for the various cases which in turn depend on the layout and dimensions of the frame concerned. This will be dealt with later.

The design of a stanchion length, therefore, resolves itself into two steps, (1) the determination of the end reactions applied to the member by that arrangement of load on the structure which produces the worst conditions in the member, and (2) the estimate of the maximum stress developed in the member by those reactions which enables the suitability of the member to be judged.

19.6. Evolution of a method of design.—Before the details of design for either beams or stanchions could be settled, a method of obtaining a definite margin of safety in the structure had to be considered. It will be seen from the discussion of the behaviour of the beam-to-stanchion connections that if the load on a beam in a steel building frame is doubled, the maximum flexural stress in the loaded beam occurring at some section remote from the ends is more than doubled. The same conditions exist in the stanchions as is recognised in the existing method of design (p. 129). To obtain an approximately uniform margin of safety it was decided, therefore, to adopt the basis of load factor commonly used in aeronautical engineering and to design each member so that if the design load was increased in a given ratio (the load factor) failure would be imminent. The simplest way of ensuring this would be to design the structure so that when it carried a load equal to the design load multiplied by the load factor, the failing stress of the material would be reached. This was considered to be too radical a departure from existing ideas, but the same result was obtained by other means. As a basis of strength the load factor was taken as 2 and the failing stress of the material as 18 tons per square inch.

In the existing method of design it is usual to assume a beam to be simply supported, to calculate the maximum bending moment produced in it by the application of the full dead and superimposed load and to design the member to a given working stress.

It was felt to be desirable to retain this general method, but since a constant load factor had to be maintained it was impossible to use, in calculating the maximum moment, the real values of the restraining moments given by the lower limit curves. The following method, due to Mr. E. W. Butler of H.M. Office of Works, was used to obtain, from the lower-limit curves, other curves which would give the required load factor.

As explained in paragraph 11.2 a curve OP'Q' (Fig. 11.9) can be

drawn giving the relation between the moment and rotation at the end of a symmetrically loaded beam from which, by the use of the beam-line AB, the restraining moment under the full design load can be found. If the load on the beam were doubled the restraining moment Q'N' (Fig. 19.7) would be given by the new beam-line A_1B_1 parallel to AB and such that $OA_1=2OA$. OQ' is drawn, cutting AB in R. Then, if the end restraining moment allowed for in the design of the beam is RN and if a nominal permissible flexural stress of 9 tons per square inch is worked to, the stress in the beam when the load is doubled will be 18 tons per square inch. A curve ORR' can be drawn by this construction, to be used as the standard in design to replace the lower-limit curve.

The lower-limit curves, and those of the type ORR', were deduced from the behaviour of connections on beams of 12 inches depth. Since it was found that the moment required to produce a given deformation

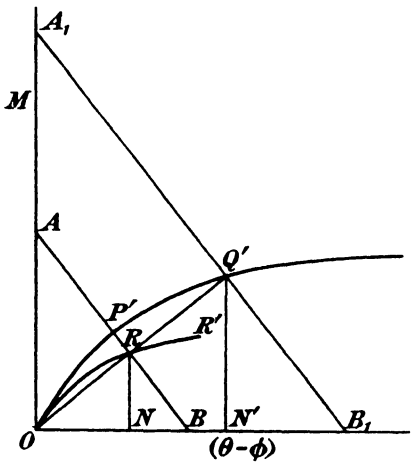

FIG. 19.7.

in the connection was approximately proportional to the depth of the beam and that the angle of rotation for a given deformation was very nearly inversely proportional to the depth of the beam, it was possible to plot from each curve another showing the behaviour of the same connection when attached to a beam of any depth. This was most easily done by plotting M/D against $D(\theta-\phi)$ where D denotes the depth of the beam; this gives a curve showing the relation between the nominal pull P, equal to M/D, on the top cleat and the relative linear movement of the ends of the upper and lower faces of the beam. The restraining moment provided by a connection attached to a beam of depth D can be found, using such a curve, by the beam-line method, the intercepts on the axes being OA, equal to M_F/D, and OB, equal to $\frac{M_F D l}{2EI}$, where M_F denotes the fixed-end moment (that is, the moment present at the end of a similarly loaded beam with completely fixed ends), and equals

$\frac{1}{12}wl^2$ when the load is uniformly distributed and of intensity w. As the restraining moment is being determined so that the beam can be designed, it is undesirable to have the second moment of area appearing in the expression for OB. Trial designs can be avoided at a slight sacrifice of economy if a simplified method, due to Professor Batho, is used and a lower limit is taken for OB independent of the actual section of the beam.

If f_F is the maximum flexural stress in the beam section produced by the moment M_F, then $M_F = \frac{2f_F I}{D}$

and $$OB = \frac{M_F D l}{2EI} = \frac{f_F l}{E}.$$

When a single concentrated load acts on the span, f_F has its lowest value, equal to $f_s/2$, where f_s denotes the maximum stress which would be found in the beam if it were simply supported. This stress f_s cannot be less than 9 tons per square inch when the yield stress of the material and the load factor are taken to be 18 tons per square inch and 2 respectively so that if, in drawing the beam-line, OB is made equal to $\frac{f_s l}{2E}$, f_s having the value of 9 tons per square inch, a safe restraining moment is found, depending only on the length of the beam, the depth of the section and the load carried expressed in the form of M_F. By drawing beam-lines in this way it is a simple matter to prepare tables or to plot families of design curves for each type of connection showing the relation between $M_F/2D$, l and P. Such design curves for standard connections of classes B and C, formed of 6-inch by 4-inch by $\frac{1}{2}$-inch and 6-inch by 4-inch by $\frac{3}{4}$-inch flange-cleats respectively, are given in Fig. 19.8.

The argument given above was based on the consideration of a beam carrying a symmetrical load and with equal restraints at its ends. The results can, however, be applied when this symmetry does not exist. If the load is unsymmetrical but the restraints are equal, safety will be ensured if M_F is taken as the mean of the two fixed-end moments, so that the design curve of Fig. 19.8 gives the mean of the end moments, which is taken to be the restraining moment at each end of the beam. When the restraints are unequal and the load is unsymmetrical an error on the unsafe side may occur, but even in an extreme case it is so small as to be negligible.

The lower-limit and standard curves used above give the restraint provided by a bare beam-to-stanchion connection. When the connections are encased in concrete it is possible that the restraint, under the design load, will be considerably greater than that shown by the curve. The lower limit for the cased connection depends upon the transmitted moment which produces cracks in the casing and if there is no reinforcement this moment may be comparatively low. No allowance should therefore be made for the extra restraint which might be provided by the casing.

This is the basis of the main clauses dealing with the design of beams in the Committee's recommendations, which read:-

Clause 2.—Where a beam of uniform web depth throughout its length is attached at one end to the flange of a stanchion, allowance

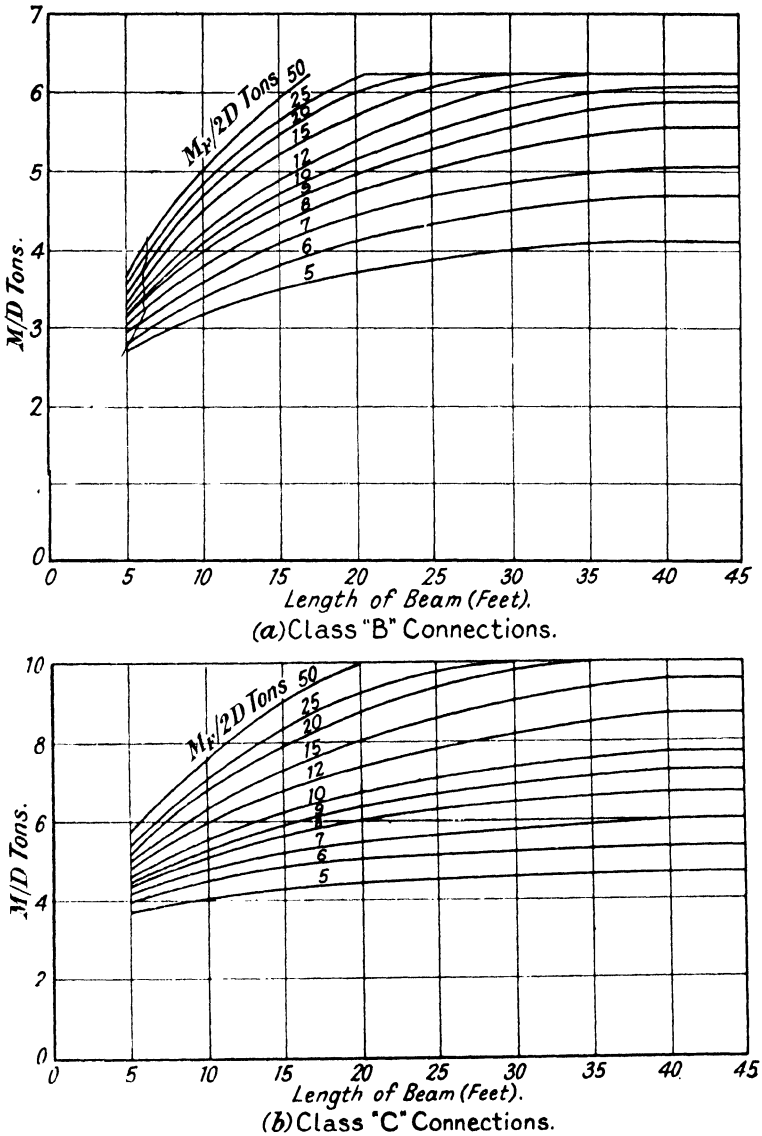

FIG. 19.8.—Standard Design Curves giving Restraining Moments at End of Beam.

may be made for the restraining moment present at that end of the beam in the following manner:—

The value of $\frac{M_F}{2D}$ shall be calculated, D being the depth of the

beam and M_F the mean of the fixed-end moments (*i.e.* the moments present at the ends of a similarly loaded beam with completely fixed ends) and the appropriate table or curve (for example Fig. 19.8) used for the determination of the restraining moment M at the end of the beam.

Where in extreme cases, such as the upper storeys of certain frames, $\frac{K_B}{K_U+K_L}$ (K_B is the stiffness of the beam and K_U and K_L are the stiffnesses of the stanchion lengths above and below the beam) is found to exceed 1·5, no allowance shall be made for the restraining moment unless the procedure of *Clause* 3 (1) is followed. In calculating the stiffness of a member the gross moment of inertia shall be used, no deduction being made for rivet holes. For a plated beam the stiffness shall be taken as the maximum gross moment of inertia of the beam divided by its length.

Clause 3.—Where a beam is connected to the web of a member, either stanchion or beam, no allowance may be made for the restraining moment at that end except in the following cases :—

(1) Where a beam frames into one side of the web of a stanchion, there being no beam on the other side, and special provision is made to stiffen the web of the stanchion, allowance may be made for the restraining moment provided that the value of $\frac{K_B}{K_U+K_L}$ does not exceed 1·5. If $\frac{K_B}{K_U+K_L}$ exceeds 1·5 the value of $q=\frac{1}{1+\frac{2K_B}{3(K_U+K_L)}}$ shall be calculated, the restraining moment M being determined as in *Clause* 2, $\frac{qM_F}{D}$ being substituted for $\frac{M_F}{2D}$ in the appropriate table or curve (for example Fig. 19.8).

(2) Where the connection is balanced by a connection of the same class to a beam on the opposite side of the member, the rivets or bolts in the vertical legs of the cleats serving both connections, allowance may be made for the restraining moment as set out in *Clause* 2, the fixed end moment being taken as that portion which is balanced by the fixed end moment due to dead load only in the beam on the opposite side of the member.

Reference has already been made (p. 439) to the arrangements of live or superimposed load which are likely to produce the most rigorous conditions of stress in a stanchion length. The worst possible moment that can occur in any stanchion length is made up of two parts, one due to the dead load on all the beams and the other due to the most unfavourable combination of live loads, Fig. 19.6. The first step in the production of a method of design is, therefore, the collection of data which will enable these moments to be estimated. The magnitudes of the moments are affected by the proportions of the members making up the frame and by the characteristics of the connections joining the

members. The tests on existing buildings, while indicating that the methods of stress analysis derived earlier in the investigation were reliable, showed that the casing of a connection could increase its rigidity very considerably. Since the end moments in a stanchion length increase as the rigidity of the connections between the members increases, it was decided that, for the normal type of clothed steel frame, it would be necessary, in estimating stanchion moments, to assume that the joints in the frame were perfectly rigid. Making this assumption, which while giving the maximum possible moments had the additional advantage of removing one of the variables from the calculations, it was possible to draw up tables giving the desired information in a fairly compact form. Any exact determination of these worst moments can only be made, however, if the proportions of all the members in the frame are known. As the whole structure is not yet designed these proportions cannot be known, so that the data to be provided must be such that an upper limit value of the moment can be estimated from the meagre knowledge of the frame already possessed by the designer. All that has been determined at this stage is the sizes of the beams. It has been shown that the moments developed in the stanchions depend on the relation between beam and stanchion stiffness so that, if an economical upper-limit value for the moment is to be found, the designer must, as he does in the existing method of design, first choose a stanchion section and then, by the methods to be described later (p. 457), find whether his choice is satisfactory. The sections of the beams at one floor level and of the stanchion lengths above and below that level being known, it was found possible to compile tables giving the maximum value of the bending moment which could be applied to the stanchion at that level, no matter what the arrangement of loaded beams or the proportions and layout of more distant members in the structure might be.

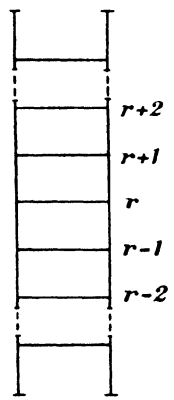

FIG. 19.9.

The calculations * which had to be made before the tables of worst moments could be compiled were somewhat arduous and only a brief account of them can be given here.

The first step was to derive general expressions for the bending moments in all the members of a frame due to a load on any beam. For this the symmetrical single bay frame shown in Fig. 19.9 was considered. It was assumed that the stanchions were of uniform section, continuous through an infinite number of storeys and that all the beams were of the same section.

If a distributed load of intensity w_r per unit length is applied to the rth beam of such a frame a consideration of the equilibrium of the joint A_r gives, with the notation of paragraph 9.3,

* "Study of the Critical Loading Conditions in Building Frames." J. F. Baker and E. Leader Williams. Final Report, Steel Structures Research Committee. H.M. Stationery Office, 1936.

$$2EK_A\theta_{A(r-1)}+\left[\frac{2EK_r(3\alpha+2)}{3\alpha^2+4\alpha+1}+8EK_A\right]\theta_{Ar}+2EK_A\theta_{A(r+1)}$$
$$+\frac{2EK_r}{3\alpha^2+4\alpha+1}\theta_{Br}-\frac{w_rl^2}{12(\alpha+1)}=0. \quad . \quad . \quad . \quad . \quad . \quad (1)$$

From symmetry $\theta_{Br}=-\theta_{Ar}$ and equation (1) may be written

$$2\theta_{A(r-1)}+\left[\frac{2Q}{\alpha+1}+8\right]\theta_{Ar}+2\theta_{A(r+1)}-\frac{w_rl^2}{12EK_A(\alpha+1)}=0 \quad . \quad . \quad (2)$$

where $$Q=\frac{K_r}{K_A}=\frac{\text{stiffness of beam}}{\text{stiffness of stanchion length}}.$$

Let $$\theta_{A(r-1)}=a\theta_{Ar},$$

then it follows that $\theta_{A(r-2)}=a\theta_{A(r-1)}=a^2\theta_{Ar}$ etc.

and $\theta_{A(r+1)}=\theta_{A(r-1)}$; $\theta_{A(r+2)}=\theta_{A(r-2)}$, etc. Substituting for $\theta_{A(r-1)}$ and $\theta_{A(r+1)}$ in equation (1) we obtain

$$4a\theta_{Ar}+\left[\frac{2Q}{\alpha+1}+8\right]\theta_{Ar}-\frac{w_rl^2}{12EK_A(\alpha+1)}=0 \quad . \quad . \quad . \quad . \quad (3)$$

Similarly, from a consideration of the equilibrium of the $(r-1)$th joint,

$$2\theta_{A(r-2)}+\left[\frac{2Q}{\alpha+1}+8\right]\theta_{A(r-1)}+2\theta_{Ar}=0$$

or

$$a^2+a\left[\frac{Q}{\alpha+1}+4\right]+1=0.$$

Let

$$\left[\frac{Q}{\alpha+1}+4\right]=D,$$

then

$$a^2+aD+1=0$$

and one solution is

$$a=\frac{-D+\sqrt{D^2-4}}{2}.$$

From (3)

$$\theta_{Ar}=\frac{1}{2\sqrt{D^2-4}}\cdot\frac{w_rl^2}{12EK_A(\alpha+1)}$$

and writing F for $\frac{1}{\sqrt{D^2-4}}$ and W_r for $\frac{w_rl^2}{12(\alpha+1)}$

we have

$$\theta_{Ar}=\frac{F}{2}\cdot\frac{W_r}{EK_A}.$$

When beam $(r-1)$ is loaded

$$\theta_{Ar}=\frac{aF}{2}\cdot\frac{W_{(r-1)}}{EK_A}$$

and for loads on all beams

$$\theta_{Ar}=\ldots+\frac{a^2F}{2}\cdot\frac{W_{(r-2)}}{EK_A}+\frac{aF}{2}\cdot\frac{W_{(r-1)}}{EK_A}+\frac{F}{2}\cdot\frac{W_r}{EK_A}+\ldots$$

and

$$\theta_{A(r-1)}=\ldots+\frac{aF}{2}\cdot\frac{W_{(r-2)}}{EK_A}+\frac{F}{2}\cdot\frac{W_{(r-1)}}{EK_A}+\frac{aF}{2}\cdot\frac{W_r}{EK_A}+\ldots$$

But

$$M^A_{r(r-1)}=2EK_A[2\theta_{Ar}+\theta_{A(r-1)}],$$
$$=F[\ldots+a(2a+1)W_{(r-2)}+(2a+1)W_{(r-1)}$$
$$+(2+a)W_r+a(2+a)W_{(r+1)}+\ldots].$$

The moment at the end of any stanchion length of such an infinite frame can therefore be obtained directly. In Table 19.7 the end moments for values of $\frac{Q}{\alpha+1}$ between 0 and 16 in an intermediate stanchion length are given in terms of $\frac{M_F}{\alpha+1}$ (where M_F is the fixing moment at the end of an encastré beam similarly loaded) for loads on three beams above and three below the stanchion length under consideration.

TABLE 19.7.—BENDING MOMENT $M_{r(r-1)}$ IN AN INTERMEDIATE STANCHION LENGTH OF A SYMMETRICAL SINGLE BAY FRAME. (STANCHIONS OF UNIFORM SECTION THROUGHOUT THEIR LENGTH.)

$\frac{Q}{\alpha+1}$	$M_{r(r-1)} \Big/ \frac{M_F}{\alpha+1}$					
	Beam $(r-3)$ Loaded	Beam $(r-2)$ Loaded	Beam $(r-1)$ Loaded	Beam r Loaded	Beam $(r+1)$ Loaded	Beam $(r+2)$ Loaded
16	+0·0001	−0·0023	+0·0452	+0·0980	−0·0049	+0·0003
8	+0·0005	−0·0059	+0·0703	+0·1619	−0·0136	+0·0011
4	+0·0015	−0·0122	+0·0963	+0·2418	−0·0307	+0·0039
2	+0·0034	−0·0199	+0·1131	+0·3232	−0·0555	+0·0095
1	+0·0055	−0·0265	+0·1271	+0·3909	−0·0816	+0·0170
0·5	+0·0072	−0·0309	+0·1318	+0·4380	−0·1027	+0·0241
0	+0·0096	−0·0359	+0·1340	+0·5000	−0·1340	+0·0359

Similar expressions for the moments in the bottom and in the top-most stanchion length of an infinite symmetrical single bay frame can be derived. The end moments in these members are collected in Tables 19.8 and 19.9, for various values of $\frac{Q}{\alpha+1}$.

These tables give the moments in a frame consisting of an infinite number of storeys. A close estimate of the moments in the members of a finite frame can, however, be obtained directly from them. To show that the error involved is small the moments at the ends of the stanchion lengths of a six storey symmetrical single bay frame have been calculated by solving the six simultaneous slope deflection equations for this particular frame. The stanchion sections are the same throughout, all beams are identical, the ratio $Q=1$ and joints rigid ($\alpha=0$), while the load on the beams is uniformly distributed. These moments are shown in Table 19.10 together with the corresponding moments collected from Tables 19.7, 19.8 and 19.9.

The assumption that each member of the frame is most severely stressed when the structure is fully loaded gives results very far from the truth as the curves of Fig. 19.6 show. The worst possible moment

TABLE 19.8.—BENDING MOMENT M_{10} IN BOTTOM STANCHION LENGTH OF A SYMMETRICAL SINGLE BAY FRAME. (STANCHIONS OF UNIFORM SECTION THROUGHOUT THEIR LENGTH.)

$\frac{Q}{\alpha+1}$	$M_{10}/\frac{M_F}{\alpha+1}$		
	Beam 1 loaded	Beam 2 loaded	Beam 3 loaded
16	+0·1003	−0·0050	+0·0002
8	+0·1678	−0·0141	+0·0012
4	+0·2540	−0·0323	+0·0041
2	+0·3431	−0·0589	+0·0101
1	+0·4174	−0·0871	+0·0182
0·5	+0·4689	−0·1099	+0·0258
0	+0·5359	−0·1436	+0·0385

TABLE 19.9.—BENDING MOMENT $M_{n(n-1)}$ IN TOPMOST STANCHION LENGTH OF A SYMMETRICAL SINGLE BAY FRAME. (STANCHIONS OF UNIFORM SECTION THROUGHOUT THEIR LENGTH.)

$\frac{Q}{\alpha+1}$	$M_{n(n-1)}/\frac{M_F}{\alpha+1}$			
	Beam n Loaded	Beam $(n-1)$ Loaded	Beam $(n-2)$ Loaded	Beam $(n-3)$ Loaded
16	+0·1086	+0·0447	−0·0022	+0·0001
8	+0·1932	+0·0677	−0·0057	+0·0005
4	+0·3189	+0·0865	−0·0110	+0·0014
2	+0·4776	+0·0896	−0·0154	+0·0026
1	+0·6417	+0·0748	−0·0156	+0·0033
0·5	+0·7790	+0·0517	−0·0121	+0·0028
0	+1·0000	0	0	0

that can occur in any stanchion length is made up of two parts, one due to the dead load on all the beams, and the other due to the most unfavourable combination of live load. Thus the dead load moment M_{34} for the case given in Table 19.10 is $-\cdot0362w_D l^2$ and the greatest possible live load moment due to live load on beams 1, 3, 4 and 6, is $-\cdot0453w_L l^2$. It should be noticed that the signs of both the dead and live load moments M_{43} are opposite to those of M_{34}, *i.e.* the stanchion is bent in double curvature.*

The data already given in Tables 19.7, 19.8 and 19.9 may be arranged

* The sign convention used will be readily appreciated from the tables. The sign given to a moment is that of the fibre stress produced by it in the left-hand side of the member, tensile stress being positive.

TABLE 19.10.

COMPARISON OF MOMENTS IN SYMMETRICAL SINGLE BAY SIX STOREY FRAME.

Moment		M/M_F					
		Beam 1 loaded	Beam 2 loaded	Beam 3 loaded	Beam 4 loaded	Beam 5 loaded	Beam 6 loaded
M_{10}	Calculated by more exact method	+0·4175	−0·0871	+0·0182	+0·0040	+0·0010	−0·0002
	Read from Table 19.8 . . .	+0·4174	−0·0871	+0·0182	—	—	—
M_{21}	Calculated by more exact method	+0·1216	+0·3920	−0·0818	+0·0169	−0·0036	+0·0013
	Read from Table 19.7 . . .	+0·1271	+0·3909	−0·0816	+0·0170	—	—
M_{34}	Calculated by more exact method	−0·0163	+0·0815	−0·3907	−0·1273	+0·0274	−0·0091
	Read from Table 19.7 . . .	−0·0170	+0·0816	−0·3909	−0·1271	+0·0265	−0·0055
M_{43}	Calculated by more exact method	+0·0053	−0·0265	+0·1270	+0·3914	−0·0839	+0·0279
	Read from Table 19.7 . . .	+0·0055	−0·0265	+0·1271	+0·3909	−0·0816	+0·0170
M_{54}	Calculated by more exact method	−0·0012	+0·0054	−0·0260	+0·1249	+0·4018	−0·1339
	Read from Table 19.7 . . .	—	+0·0055	−0·0265	+0·1271	+0·3909	−0·0816
M_{65}	Calculated by more exact method	+0·0001	−0·0006	+0·0032	−0·0156	+0·0748	+0·6418
	Read from Table 19.9 . . .	—	—	+0·0033	−0·0156	+0·0748	+0·6417

so as to give, at any joint in a symmetrical single bay frame, the sum ΣM of the maximum bending moments due to live or dead load, at the sections of a stanchion just above and just below a beam for any value of $\frac{K_B}{K_U+K_L}$. It should be noted that, while it is convenient to add these moments, those due to live load do in fact occur separately under different arrangements of loaded beams. Tables 19.11 and 19.12, in which M_F^D and M_F^L are the fixed-end moments of a beam due to dead load and live load respectively, can then be used to determine the worst possible live and dead moments in any stanchion length of a symmetrical single bay frame in which the stanchions are of uniform section throughout their length.

TABLE 19.11.—$\Sigma M/M_F^D$ DUE TO DEAD LOAD.

$\frac{K_B}{K_U+K_L}$	Bottom length	Intermediate length	Topmost length
0	0·8616	1·0000	1·0000
0·5	0·6970	0·8648	0·8217
1·0	0·5886	0·7536	0·7041
2·0	0·4516	0·6012	0·5545
4·0	0·3098	0·4286	0·3958
8·0	0·1910	0·2728	0·2557

TABLE 19.12.—$\Sigma M/M_F^L$ DUE TO LIVE LOAD.

$\frac{K_B}{K_U+K_L}$	Bottom length	Intermediate length	Topmost length
0	1·1488	1·3590	1·0000
0·5	0·8712	1·0810	0·8338
1·0	0·7064	0·9044	0·7197
2·0	0·5162	0·6870	0·5699
4·0	0·3380	0·4676	0·4068
8·0	0·2010	0·2872	0·2614

In practice the stanchion will rarely be of the same section in all storeys. Fortunately the sum of the moments in the upper and lower stanchion lengths, given in Tables 19.11 and 19.12, depends almost entirely on the ratio $\frac{K_B}{K_U+K_L}$ at the beam level under consideration and these tables may therefore be used to determine the sum of the moments ΣM even though the stanchion changes section at that level. The designer is, however, not interested in this sum so much as in the individual moments in the stanchion lengths. The exact expression for the ratio of the moments in the upper and lower stanchion lengths at any level is complex and depends on the stiffnesses

of all the members in the frame. A safe approximation to the greatest moment that can occur at the end of any stanchion length, leaving out of account the effect of axial load in the beams shown by the tests on existing buildings, is however given by dividing ΣM between the upper and lower stanchion lengths in proportion to their stiffnesses.

The basic fact which made possible the evaluation of the large number of cases necessary for the preparation of Tables 19.7, 19.8 and 19.9 was that in a single bay frame carrying symmetrically disposed loads the slopes at the ends of each beam were equal in magnitude. This is not so when the beams frame at one end into an internal stanchion. It is, however, possible to represent any multi-bay frame by a number of equivalent single bay frames and in this way to obtain the moments in an internal stanchion from the data already given for a stanchion forming part of a single bay frame.

The analogy between the single bay and the multi-bay frame is best seen from a consideration of the simple frames shown in Figs. 19.10 and 19.11. The first represents part of a multi-bay frame in which

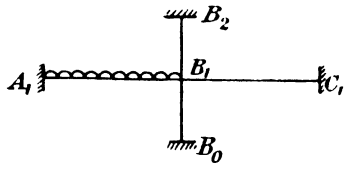

FIG. 19.10.

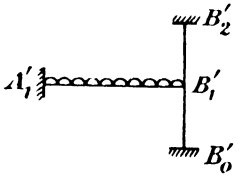

FIG. 19.11.

the members are so proportioned that the remote ends of the four members meeting at the joint B may be assumed to be encastré.

Fig. 19.11 represents part of the equivalent single bay frame, that is the single bay frame in which the moments in the stanchion $B'_0B'_1B'_2$ due to load on beam $A'_1B'_1$ are the same as the moments in the stanchion $B_0B_1B_2$ of the two bay frame due to the same intensity of load on beam A_1B_1.

With the usual notation, from the equilibrium of the joint B_1 in the two bay frame, we obtain

$$\left[\frac{2EK_1(3\alpha_1+2)}{3\alpha_1\beta_1+2\alpha_1+2\beta_1+1}+\frac{2EK_2(3\beta_2+2)}{3\alpha_2\beta_2+2\alpha_2+2\beta_2+1}+8EK_B\right]\theta_{B1}=\frac{w_1l_1^2(3\alpha_1+2)}{3\alpha_1\beta_1+2\alpha_1+2\beta_1+1}$$

and, similarly, for the single bay frame

$$\left[\frac{2EK'(3\alpha'+2)}{3\alpha'\beta'+2\alpha'+2\beta'+1}+8EK_B\right]\theta'_{B1}=\frac{w_1l_1^2(3\alpha'+2)}{3\alpha'\beta'+2\alpha'+2\beta'+1}.$$

If the desired similarity between these two frames is to be obtained, θ'_{B1} in the single bay must be equal to θ_{B1} in the two bay frame or

$$\frac{2EK'(3\alpha'+2)}{3\alpha'\beta'+2\alpha'+2\beta'+1}$$

must be equal to $\left(\frac{2EK_1(3\alpha_1+2)}{3\alpha_1\beta_1+2\alpha_1+2\beta_1+1}+\frac{2EK_2(3\beta_2+2)}{3\alpha_2\beta_2+2\alpha_2+2\beta_2+1}\right)$.

TABLE 19.21

BEAM SHEET

1	2	3	4	5	6	7	8	9	10	11	12	13	14
Beam Mark	Span	Left Hand: Restraining Moment	Left Hand: Class of Connection	Left Hand: Fixed End Moment	Left Hand: Reaction	Details of Loading	Right Hand: Reaction	Right Hand: Fixed End Moment	Right Hand: Class of Connection	Restraining Moment	$\frac{M_F}{2D}$	Calculations for Max. B.M.	Section Selected
162 172 182 192	19′ 3″		Eccentric Web Connection No Restraint	33 226	0·85 5·85 6·7	LIVE LOAD Floor 1·7 DEAD LOAD Floor 3·3 Wall 7·4 B & C 1·0	0·85 5·85 6·7	33 226				Max. B.M. $= \frac{13{\cdot}4 \times 19{\cdot}25 \times 12}{8} = 387$ ton-ins. Z Required $= 48{\cdot}4$ ins.^{3}	I 14″×5½″×40♯ K=19·4
41 51	17′ 6″	64	Flange Connection Class B	35 35 82·5 87·5 240	0·7 1·0 1·6 2·5 5·8	LIVE LOAD From 42 1·2 Floor 2·0 DEAD LOAD From 42 2·8 Floor 4·0 B & C 1·0 1·2 2·8 ←7·5′→ ←10·0′→ 2·0 and 5·0	0·5 1·0 1·2 2·5 5·2	26 35 62 88 211	Flange Connection Class B	8·7 64		Max. B.M. $= 5{\cdot}2 \times 10 \times 12 = 624$ $- 4{\cdot}0 \times 5 \times 12 = -240$ $-64 \quad -64$ $= 320$ ton-ins. Z Required $= \frac{320}{9} = 35{\cdot}6$ ins.^{3}	I 13″×5″×35♯ K=16·7

In the simple case when all joints are rigid,

$$K' \text{ must be equal to } K_1+K_2.$$

That is to say, the stiffness of the beam in the equivalent single bay frame must be equal to the sum of the stiffnesses of the beams of the two bay frame. If this condition, deduced from a consideration of the simplest possible frame, is fulfilled the equivalent single bay frame may be used with a fair degree of accuracy to determine the moments in a multi-storey, multi-bay frame.

It is now a simple matter to determine the worst live and dead load moments in any length of an internal stanchion from tables similar to, and prepared from, Tables 19.11 and 19.12. The procedure will be most easily followed if a particular frame is considered. The case chosen is the unsymmetrical two bay frame, six storeys in height, shown in Fig. 19.12.

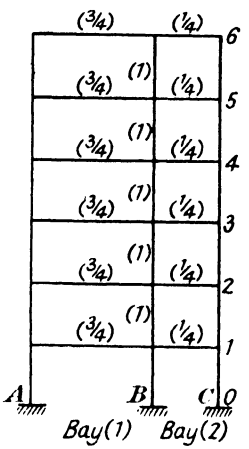

FIG. 19.12.

All beams in each bay identical, all stanchions identical and of uniform section throughout. Rigid joints. The figures in brackets on the diagram represent the relative stiffnesses of the members.

The moments in the stanchion length B_3B_4 will be considered. When any beam in bay (1) is loaded with a uniformly distributed load of intensity w_1 the moments induced, M^B_{43} and M^B_{34}, will be approximately the same as the corresponding moments in a six storey single bay frame in which Q=1, since the ratio of the sum of the stiffnesses of the beams to the stiffness of the stanchion length in the two bay frame is $\frac{\frac{3}{4}+\frac{1}{4}}{1}=1$. These moments in the single bay frame have already been given in Table 19.10 and therefore the moments required in the two bay frame can be written down as in Table 19.13 where $M_{F1}=\frac{w_1 l_1^2}{12}$ and the length of a beam in bay (1) is l_1.

By exactly the same reasoning it follows that when any beam in bay (2) is loaded with a uniformly distributed load of intensity w_2 the moments induced in the stanchion length B_3B_4 of the two bay frame will be as set out in Table 19.14 where $M_{F2}=\frac{w_2 l_2^2}{12}$, the length of a beam in bay (2) being l_2. Thus Tables 19.13 and 19.14 provide all the necessary information from which the moments at the ends of the stanchion length B_3B_4 can be deduced for any arrangement of loaded beams.

When all beams are loaded, the condition under dead load, the moments M^B_{34} and M^B_{43} will clearly be $-\cdot435(M^D_{F1}-M^D_{F2})$ and $+\cdot441$ $(M^D_{F1}-M^D_{F2})$ respectively. This procedure is quite general and it has been possible to collect in Table 19.15 the total bending moments due to dead load for any length of an internal stanchion. This table is,

TABLE 19.13.—MOMENTS IN INTERMEDIATE STANCHION LENGTH, BAY (1) LOADED.

	Beam 1 loaded	Beam 2 loaded	Beam 3 loaded	Beam 4 loaded	Beam 5 loaded	Beam 6 loaded
M^B_{34} = . . .	$+0{\cdot}0163\ M_{F1}$	$-0{\cdot}0815\ M_{F1}$	$+0{\cdot}3907\ M_{F1}$	$+0{\cdot}1273\ M_{F1}$	$-0{\cdot}0274\ M_{F1}$	$+0{\cdot}0091\ M_{F1}$
M^B_{43} = . . .	$-0{\cdot}0053\ M_{F1}$	$+0{\cdot}0265\ M_{F1}$	$-0{\cdot}1270\ M_{F1}$	$-0{\cdot}3914\ M_{F1}$	$+0{\cdot}0839\ M_{F1}$	$-0{\cdot}0279\ M_{F1}$

TABLE 19.14.—MOMENTS IN INTERMEDIATE STANCHION LENGTH, BAY (2) LOADED.

	Beam 1 loaded	Beam 2 loaded	Beam 3 loaded	Beam 4 loaded	Beam 5 loaded	Beam 6 loaded
M^B_{34} = . . .	$-0{\cdot}0163\ M_{F2}$	$+0{\cdot}0815\ M_{F2}$	$-0{\cdot}3907\ M_{F2}$	$-0{\cdot}1273\ M_{F2}$	$+0{\cdot}0274\ M_{F2}$	$-0{\cdot}0091\ M_{F2}$
M^B_{43} = . . .	$+0{\cdot}0053\ M_{F2}$	$-0{\cdot}0265\ M_{F2}$	$+0{\cdot}1270\ M_{F2}$	$+0{\cdot}3914\ M_{F2}$	$-0{\cdot}0839\ M_{F2}$	$+0{\cdot}0279\ M_{F2}$

in fact, derived directly from Table 19.11 by writing $\frac{K_{BR}+K_{BL}}{K_U+K_L}$ (where K_{BR} and K_{BL} are the stiffnesses of the beams meeting at a joint) instead of $\frac{K_B}{K_U+K_L}$ and $(M^D_{F1}-M^D_{F2})$ instead of M^D_F.

When the moments due to live load are considered, that arrangement of loaded beams which gives rise to the most rigorous conditions must be chosen. It will be seen from Tables 19.13 and 19.14 that the maximum moment at both ends of the stanchion length B_3B_4 will occur when beams (1) 1, (2) 2, (1) 3, (1) 4, (2) 5 and (1) 6 are loaded. The moments M^B_{34} and M^B_{43} will then be $+(\cdot545M^L_{F1}+\cdot109M^L_{F2})$ and $-(\cdot551M^L_{F1}+\cdot110M^L_{F2})$ respectively. Since these moments are of opposite sign bending will be in double curvature. If, however, beams (1) 1, (2) 2, (1) 3, (2) 4, (1) 5 and (2) 6 are loaded the moments at the ends of the stanchion length will be $+(\cdot380M^L_{F1}-\cdot055M^L_{F2})$ and $+(\cdot392M^L_{F2}-\cdot048M^L_{F1})$ respectively. Since in this case the moments are of the same sign, bending thus being in single curvature, these smaller moments combined with the same axial load may give rise to a higher stanchion stress than the larger moments which caused bending in double curvature.

TABLE 19.15.—TOTAL BENDING MOMENT DUE TO DEAD LOAD.

$\frac{K_{BR}+K_{BL}}{K_U+K_L}$	Bottom length; $\left(\frac{\text{total moment}}{M^D_{F1}-M^D_{F2}}\right)$	Intermediate length; $\left(\frac{\text{total moment}}{M^D_{F1}-M^D_{F2}}\right)$	Topmost length; $\left(\frac{\text{total moment}}{M^D_{F1}-M^D_{F2}}\right)$
0·0	0·862	1·000	1·000
0·2	0·783	0·950	0·918
0·6	0·671	0·842	0·794
1·0	0·589	0·754	0·704
2·0	0·452	0·601	0·555
4·0	0·310	0·429	0·396
8·0	0·191	0·273	0·256

As with dead load it is possible here again to prepare from Tables 19.7, 19.8 and 19.9 a table, similar to Table 19.12, giving the total bending moment in both double and single curvature for any length of an internal stanchion and for any value of the stiffness ratio $\frac{K_{BR}+K_{BL}}{K_U+K_L}$. It should be noted that this table (Table 19.16) may also be used for an external stanchion by putting K_{BR} and M^L_{F2} equal to zero.

The reactions at the ends of the stanchion length are now known and the next step is to find a convenient way of checking the suitability of the section chosen for the member. This entails finding the maximum total stress in the member or, more conveniently, demonstrating that the maximum stress does not exceed a certain permissible value. The

TABLE 19.16.—TOTAL BENDING MOMENT DUE TO LIVE LOAD.

$\frac{K_{BR}+K_{BL}}{K_U+K_L}$	Bottom length	Intermediate length		Topmost length	
	Double curvature	Double curvature	Single curvature	Double curvature	Single curvature
0·0	$1{\cdot}149M^L_{F1}+0{\cdot}287M^L_{F2}$	$1{\cdot}359M^L_{F1}+0{\cdot}340M^L_{F2}$	$1{\cdot}000M^L_{F1}-0{\cdot}000M^L_{F2}$	$1{\cdot}000M^L_{F1}+0{\cdot}000M^L_{F2}$	$1{\cdot}000M^L_{F1}-0{\cdot}000M^L_{F2}$
0·2	$1{\cdot}017M^L_{F1}+0{\cdot}231M^L_{F2}$	$1{\cdot}230M^L_{F1}+0{\cdot}280M^L_{F2}$	$0{\cdot}887M^L_{F1}-0{\cdot}064M^L_{F2}$	$0{\cdot}925M^L_{F1}+0{\cdot}007M^L_{F2}$	$0{\cdot}891M^L_{F1}-0{\cdot}027M^L_{F2}$
0·6	$0{\cdot}834M^L_{F1}+0{\cdot}159M^L_{F2}$	$1{\cdot}043M^L_{F1}+0{\cdot}200M^L_{F2}$	$0{\cdot}731M^L_{F1}-0{\cdot}110M^L_{F2}$	$0{\cdot}807M^L_{F1}+0{\cdot}013M^L_{F2}$	$0{\cdot}734M^L_{F1}-0{\cdot}061M^L_{F2}$
1·0	$0{\cdot}706M^L_{F1}+0{\cdot}118M^L_{F2}$	$0{\cdot}904M^L_{F1}+0{\cdot}151M^L_{F2}$	$0{\cdot}626M^L_{F1}-0{\cdot}128M^L_{F2}$	$0{\cdot}720M^L_{F1}+0{\cdot}016M^L_{F2}$	$0{\cdot}626M^L_{F1}-0{\cdot}078M^L_{F2}$
2·0	$0{\cdot}516M^L_{F1}+0{\cdot}065M^L_{F2}$	$0{\cdot}687M^L_{F1}+0{\cdot}086M^L_{F2}$	$0{\cdot}467M^L_{F1}-0{\cdot}134M^L_{F2}$	$0{\cdot}570M^L_{F1}+0{\cdot}015M^L_{F2}$	$0{\cdot}462M^L_{F1}-0{\cdot}092M^L_{F2}$
4·0	$0{\cdot}338M^L_{F1}+0{\cdot}028M^L_{F2}$	$0{\cdot}468M^L_{F1}+0{\cdot}039M^L_{F2}$	$0{\cdot}314M^L_{F1}-0{\cdot}114M^L_{F2}$	$0{\cdot}407M^L_{F1}+0{\cdot}011M^L_{F2}$	$0{\cdot}308M^L_{F1}-0{\cdot}088M^L_{F2}$
8·0	$0{\cdot}201M^L_{F1}+0{\cdot}010M^L_{F2}$	$0{\cdot}287M^L_{F1}+0{\cdot}014M^L_{F2}$	$0{\cdot}192M^L_{F1}-0{\cdot}081M^L_{F2}$	$0{\cdot}261M^L_{F1}+0{\cdot}006M^L_{F2}$	$0{\cdot}188M^L_{F1}-0{\cdot}068M^L_{F2}$

method of checking adopted is based on the work set out in paragraph 7.20. There equation (14) shows the necessary values of the end bending stresses, f_A and f_B, arising from end moments M_A and M_B in the plane in which buckling would occur, acting on a practical strut, subjected also to a given end load P, if the total maximum stress is not to exceed a certain permissible value p'. As explained in that paragraph the expression is too complex for design purposes, but it is a simple matter to present the results in families of curves showing, for any ratio of f_B/f_A and therefore of M_B/M_A, the value the maximum end bending stress f_A can have without raising the total maximum stress above the permissible value. When M_B and M_A are known from Tables 19.15 and 19.16, together with P, the axial load, which is easily estimated, the suitability of the section can be tested.

This method of testing is complicated by the necessity of determining the ratio M_B/M_A and it is worth while to introduce a simplification by considering only the moment at the top end of the stanchion length which, in the type of frame under consideration, is always greater than that at the bottom end and by assigning to the moment at the bottom end a limiting value such that safety is ensured. It is not difficult to see that in the case of single curvature bending the limit is given by assuming $M_B/M_A=1$. In the case of double curvature bending the value to be assumed is not so obvious. Reference to Fig. 19.6 shows that when the loads are so arranged as to produce bending in double curvature a decrease in the magnitude of the moment at the lower end of the stanchion length may increase the maximum stress in the stanchion. For safety in this case the ratio f_B/f_A must be based on a consideration of the conditions which make the ratio of the corresponding end moments a minimum. This minimum (−·268) is found in the topmost length of an external stanchion when the topmost beam only is loaded and when the ratio of beam to stanchion stiffness approaches zero. The relevant information given by the families of curves can now be embodied in only two sets, Figs. 19.13 and 19.14. The former refers to single curvature bending and is made up of curves for $f_B/f_A=1$, while the latter refers to double curvature bending and is made up of curves for $f_B/f_A=-\cdot 268$. Both sets are based on a load factor of 2 and a yield stress in the material of 18 tons per square inch, that is to say the curves are plotted from the expressions

$$\frac{18-2p+f'}{2f_A+f'}=\frac{\sin\mu(l-x)}{\sin\mu l}+\frac{\sin\mu x}{\sin\mu l}\cdot\frac{2f_B+f'}{2f_A+f'} \quad . \quad . \quad . \quad . \quad (4)$$

and

$$\tan\mu x\,.=\operatorname{cosec}\mu l\left[\frac{2f_B+f'}{2f_A+f'}-\cos\mu l\right] . \quad . \quad . \quad . \quad . \quad (5)$$

where

$$\mu=\sqrt{\frac{2P}{EI}}$$

and the notation is that of paragraph 7.20.

With these curves, which also make allowance for the effects of imperfections in the stanchions not included in the calculation of the end

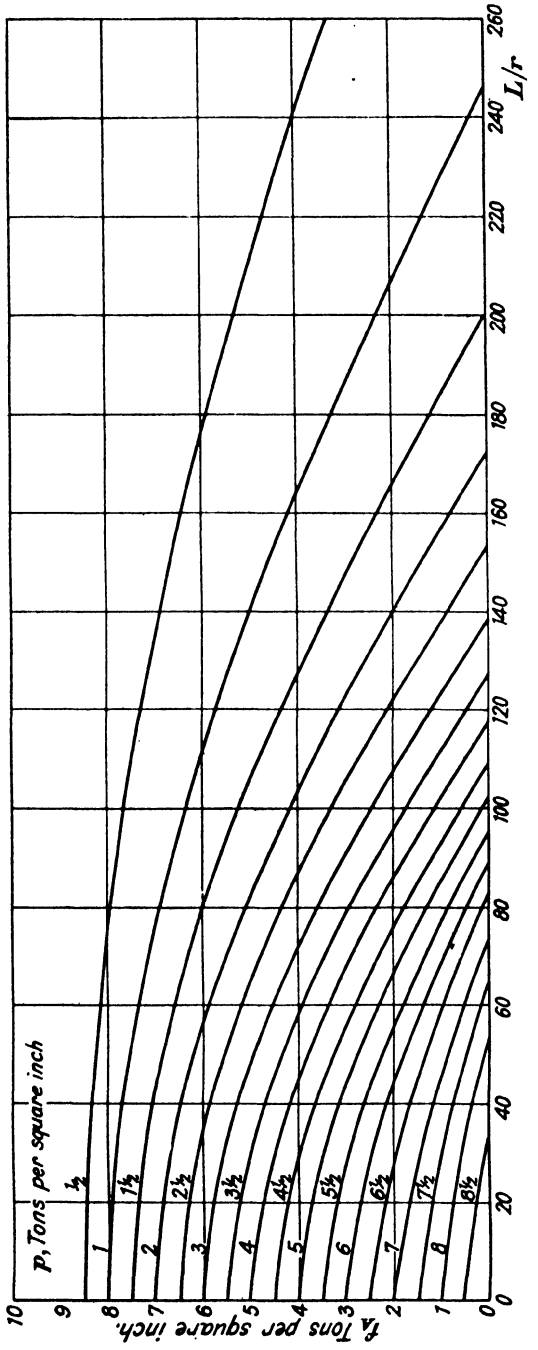

FIG. 19.13.—Permissible end bending stress. Single curvature bending.

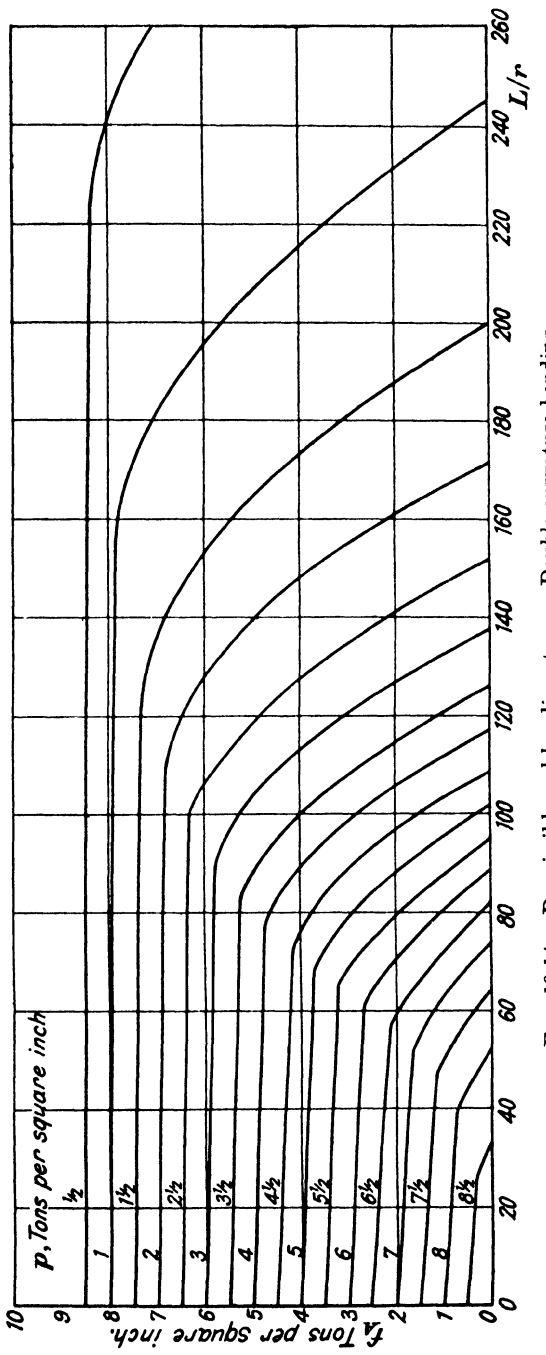

FIG. 19.14.—Permissible end bending stress. Double curvature bending.

moments,* and with the list of end moments given in Tables 19.15 and 19.16, a stanchion can be designed with comparative ease. The method will be most easily appreciated if an intermediate length is considered, the stanchion lengths above it having been already designed.

The first step is the choice of a provisional section for the stanchion length and the determination of the axial load per unit area (p) arising from the loads applied to the structure. The beams will have been designed by the method already described, so before a start is made with the stanchion design the stiffnesses of the beams framing into the upper end of the stanchion length, the fixed end moments, M_{F1} and M_{F2}, and the reactions at the ends of these beams, will be known. The stiffness ratios $\frac{K_{BR}+K_{BL}}{K_U+K_L}$ about both axes of the stanchion can also be calculated. These enable the total bending moments on the stanchion due to dead load and to both critical arrangements of live load to be read off from Tables 19.15 and 19.16, and it is essential that the ability of the section selected to sustain both these arrangements of load should be checked.

Single curvature loading will first be considered. Using the appropriate value of the stiffness ratio, the total bending moment about the XX axis of the stanchion at the top end due to live load is read from Table 19.16 (column 4), and to this is added the dead load total bending moment read from Table 19.15 (column 3). The dead load will actually cause bending of the stanchion length in double curvature, but if serious complications are to be avoided some economy must be sacrificed and the dead load moment be assumed to produce bending in single curvature. The sum of these total moments is now divided between the stanchion length under consideration and that above in the ratio of their relevant stiffnesses, thus giving the end moment in single curvature about the XX axis at the top end of the stanchion length. The maximum fibre stress due to this end moment is calculated and similarly the maximum fibre stress due to that arrangement of load producing bending in single curvature about the YY axis of the stanchion. The sum of these fibre stresses is the maximum single curvature end bending stress in the stanchion length. If this stress is less than the permissible end bending stress (f_A) given in Fig. 19.13 for the stanchion length, as defined by its slenderness ratio (L/r) and axial load per unit area (p), the section selected will be adequate to carry the forces imposed on it when the loads are such as to produce bending in single curvature.

The suitability of the section to resist double curvature bending is checked in a similar way. The sum of the total bending moments about the XX axis of the stanchion at its top end due to live loads (Table 19.16, column 3) and dead loads (Table 19.15, column 3) is, as before, divided between the stanchion lengths in proportion to their relevant stiffnesses, thus giving the bending moment and hence the

* "The Behaviour of a Pillar forming part of a Continuous Member in a Building Frame." J. F. Baker and P. D. Holder. Final Report, Steel Structures Research Committee. H.M. Stationery Office, 1936.

bending stress in double curvature about the XX axis at the top end of the stanchion length. In the same way the bending stress, due to double curvature loading, about the YY axis of the stanchion, is determined. The sum of these stresses is the maximum double curvature end bending stress and the suitability of the section is checked from Fig. 19.14.

It might be thought that two other combinations of load, producing single curvature bending about one axis and double curvature about the other, should be considered. A comprehensive investigation,* in which the true maximum stress in the stanchion under such loading has been found in a number of particular cases, makes it appear that the cases dealt with above will always be critical.

The fact that the end bending stresses about both principal axes are added in the above needs some explanation. Expressions (4) and (5), p. 457, refer only to bending in the plane in which buckling would occur but it can be proved that, if the end stresses arising from bending in a plane at right angles are assumed to arise from bending in the plane in which buckling would occur, safety is ensured.

A design method is of little value, however sound it may be, if it is too complex to be used conveniently in the design office. A number of practising engineers gave the method described above a trial in their offices. They were of the opinion that while designers had no difficulty in applying it the time taken in proportioning a stanchion was prohibitive. The reason was that the two critical loading conditions had to be considered separately for each stanchion length. To produce a method acceptable to the designer further simplification was essential.

It was desirable to arrange the data so that, while the principle of the original method would not be sacrificed, only one loading condition would, in effect, have to be considered. It was found possible, without serious loss of economy, to prepare a single set of curves giving the permissible end bending stress, which would ensure safety whether bending was in single or double curvature.

For a symmetrical frame in which $M_{F2}=M_{F1}$, the bending moment in single curvature is never greater than 1/1·7 times the moment in double curvature. If, therefore, the ordinates of Fig. 19.13 for any value of p are multiplied by 1·7, the composite lower-limit curve, formed from this and the corresponding double curvature curve of Fig. 19.14 by taking that portion of each which gives the lower value of the permissible end bending stress (f_A), will, if used in conjunction with the double curvature moments, ensure safety in all cases whether the critical loading is such as to produce bending in double or single curvature. Such composite lower-limit curves are shown in Fig. 19.15.

These composite strut curves are so drawn that safety is ensured provided that the moment in single curvature is not greater than 1/1·7 times the moment in double curvature. It must be remembered

* "The Design of Stanchions in Building Frames." J. F. Baker and E. Leader Williams. Final Report, Steel Structures Research Committee. H.M. Stationery Office, 1936.

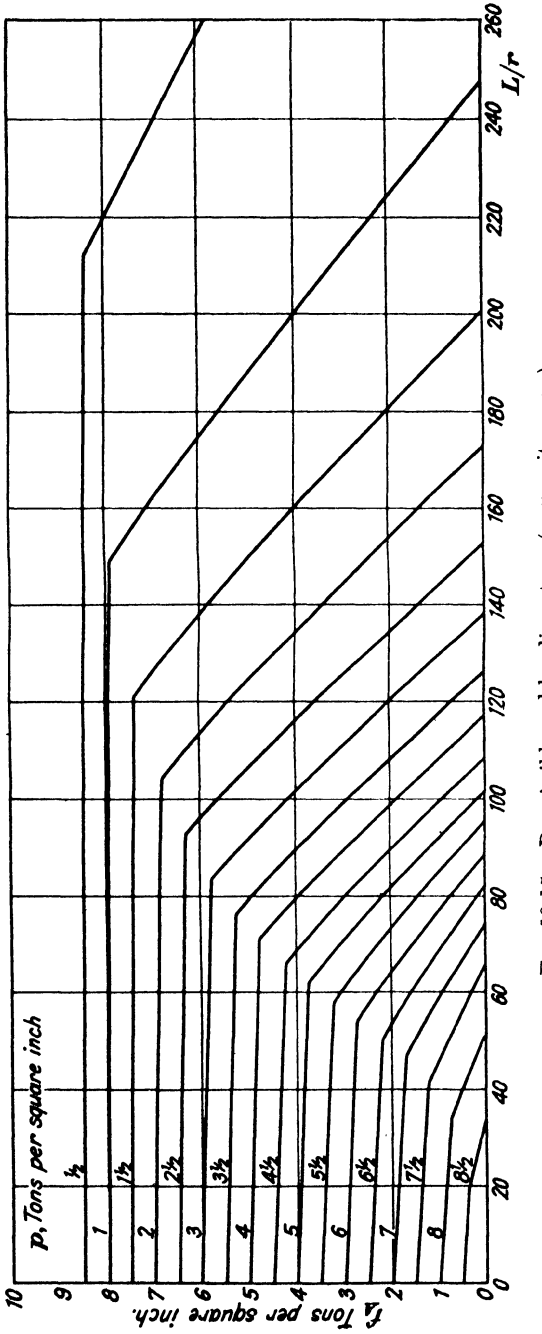

FIG. 19.15.—Permissible end bending stress (composite curve).

that the curve giving the permissible end bending stress (f_A) in single curvature is based on the assumption that the bending moments at the ends of the stanchion length are equal. This is important since as a result, although in an unsymmetrical frame the bending moment for single curvature loading may be more than 1/1·7 times that due to double curvature, the composite strut curves are always satisfactory.

Some further consideration must now be given to the moments of Tables 19.15 and 19.16. It is not easy to assess the axial load in a stanchion length resulting from the arrangement of load on the beams which produces these moments, but it is known to be less than that when all beams are loaded. The conditions arising when a stanchion length is subjected to this full axial load, together with the end moments deduced from Table 19.15 or 19.16, are therefore more rigorous than the real worst conditions. The combination of circumstances giving rise to the latter is likely to arise but rarely in practice, so that if rather worse conditions are assumed, a satisfactory stanchion section could be produced if the load factor chosen was reduced, for example, from 2 to 1·25. The stanchion, while safe under these impossibly rigorous conditions, would have a load factor greater than 1·25 under more normal loads. It was considered inadvisable to set out the method of design in this way; instead, it was decided to retain the load factor of 2 used in plotting the curves in Figs. 19.13, 19.14 and 19.15, but to follow the lead set by existing codes, and to reduce the specified live axial load assumed in all storeys below the topmost. If this reduction in the live axial load is justifiable, similar reduction is justifiable in the end moments due to the live load. This was arranged by omitting all the terms in M_{F2} from Table 19.16, thus giving a reduction which varies with the stiffness ratio but which never exceeds 20 per cent. This omission of the M_{F2} term is merely a device to secure a reduction in the total moment, while at the same time simplifying the calculation of that moment, and does not mean that the critical arrangements of load, which form the whole basis of this work, have in any way been altered.

The moments in topmost lengths of internal stanchions and in external stanchions need special treatment, which will not be discussed here, but it was not difficult to produce a table of suitably reduced moments which, if used in conjunction with the composite strut curve, brings about a considerable saving of labour as compared with the first method described.* The amended moments are given in Tables 19.17 and 19.18.

In addition to the foregoing, provision had to be made for designing frames of all types. The Tables given above could only be compiled in their simple form on the assumption that all stanchion lengths in the same storey were of the same stiffness. It was found possible to specify correction factors for use when this condition did not exist, by which the tabulated moments could be multiplied to give safe values of the moments in any unsymmetrical frame (*Clause* 18

* Loc. cit., p.477

below). A further correction factor was needed when the intensity of load on the beam framing into the lower end of a stanchion length was greater than that on the beam framing into the upper end (*Clause* 17 below).

TABLE 19.17.—TOTAL BENDING MOMENT DUE TO DEAD LOAD.

$\frac{K_{BR}+K_{BL}}{K_U+K_L}$.	Bottom length; $\left(\frac{\text{total moment}}{M_F^D}\right)$.	Intermediate length; $\left(\frac{\text{total moment}}{M_F^D}\right)$.	Topmost length; $\left(\frac{\text{total moment}}{M_F^D}\right)$.
0	0·862	1·000	1·000
0·1	0·820	0·975	0·957
0·2	0·783	0·950	0·918
0·3	0·752	0·920	0·882
0·4	0·725	0·893	0·852
0·5	0·697	0·865	0·822
0·6	0·671	0·842	0·794
0·7	0·648	0·820	0·769
0·8	0·627	0·798	0·745
0·9	0·606	0·776	0·722
1·0	0·589	0·754	0·704
1·25	0·545	0·709	0·659
1·5	0·511	0·669	0·619
1·75	0·482	0·632	0·583
2·0	0·452	0·601	0·555
2·5	0·405	0·546	0·503
3·0	0·367	0·500	0·461
3·5	0·336	0·462	0·426
4·0	0·310	0·429	0·396
5·0	0·268	0·375	0·349
6·0	0·236	0·333	0·310
7·0	0·211	0·300	0·279
8·0	0·191	0·273	0·256
10·0	—	—	0·227
12·0	—	—	0·197
14·0	—	—	0·174
16·0	—	—	0·156

The more important clauses in the Committee's recommendations setting out the method are :—

(11) For each stanchion length a steel section shall be chosen and its adequacy shall be tested by the method set out in Clauses 12–18.

(12) The total load (P) carried by each stanchion length shall be determined on the assumption that all beams are freely hinged at their ends.

(13) For the purpose of calculating the total load the live load for the roof and topmost storey shall be calculated in full, but for the lower storeys a reduction of the live loads may be allowed in accordance with the following Table :—

Next storey below topmost storey . 10 per cent. reduction of live load.
Next storey below . . . . . 20 per cent. reduction of live load.
Next storey below . . . . . 30 per cent. reduction of live load.
Next storey below . . . . . 40 per cent. reduction of live load.
All succeeding storeys . . . . 50 per cent. reduction of live load.

No such reduction shall be allowed on any floor scheduled for an applied loading of 100 lb. or more per square foot.

TABLE 19.18.—TOTAL BENDING MOMENT DUE TO LIVE LOAD.

$\frac{K_{BR}+K_{BL}}{K_U+K_L}$.	Bottom length; $\left(\frac{\text{total moment}}{M_F^L}\right)$.	Intermediate length; $\left(\frac{\text{total moment}}{M_F^L}\right)$.	Topmost length; (total moment/M_F^L).	
			Internal stanchion	External stanchion
0	1·149	1·359	1·360	1·000
0·1	1·080	1·290	1·261	0·961
0·2	1·017	1·230	1·175	0·925
0·3	0·961	1·175	1·098	0·892
0·4	0·912	1·125	1·031	0·861
0·5	0·871	1·082	0·968	0·834
0·6	0·834	1·043	0·915	0·807
0·7	0·796	1·004	0·869	0·781
0·8	0·763	0·968	0·823	0·759
0·9	0·732	0·934	0·782	0·738
1·0	0·706	0·904	0·746	0·720
1·25	0·648	0·837	0·669	0·673
1·5	0·596	0·780	0·602	0·635
1·75	0·554	0·729	0·548	0·601
2·0	0·516	0·687	0·503	0·570
2·5	0·456	0·615	0·431	0·517
3·0	0·408	0·556	0·390	0·474
3·5	0·370	0·508	0·358	0·436
4·0	0·338	0·468	0·334	0·407
5·0	0·289	0·404	0·293	0·357
6·0	0·252	0·356	0·261	0·318
7·0	0·224	0·318	0·235	0·287
8·0	0·210	0·287	0·214	0·261
10·0	—	—	0·181	0·222
12·0	—	—	0·157	0·193
14·0	—	—	0·139	0·171
16·0	—	—	0·124	0·153

(14) The axial load in tons per square inch of gross cross-sectional area of steel (p) shall be determined.

(16) Where the fixed end moments of the beams framing into the upper and lower ends of a stanchion length are the same in each bay and where each of these beams is attached at its remote end to a stanchion having a relevant stiffness at least as great as that of the stanchion under consideration, the procedure shall be as follows :—

(1) M_{FX}^D, the moment about the XX axis of the stanchion

due to dead load on the beams attached to the upper end of the stanchion length, shall be calculated. M^D_{FX} shall be the algebraic sum of the resolved components, about the XX axis of the stanchion, of the fixed end moments at the ends, attached to the stanchion, of these beams and of the moments about the XX axis of the stanchion due to the reactions at their ends. The total moment on the stanchion about its XX axis at the upper end of the stanchion length due to the dead load shall then be determined from Table 19.17 for the appropriate value of the stiffness ratio $\frac{K_{BR}+K_{BL}}{K_U+K_L}$, where K_L and K_U are the relevant stiffnesses, that is in this case about the XX axis, of the stanchion length under consideration and of the one above, and K_{BR} and K_{BL} are the relevant stiffnesses of the beams, that is in this case the stiffnesses of the beams framing into the upper end of the stanchion length at right angles to the XX axis of the stanchion.

(2) In the same way the maximum moment M^L_{FX} about the XX axis of the stanchion due to the most unfavourable arrangement of live load on the beams attached to the upper end of the stanchion length shall be calculated. The total moment on the stanchion about its XX axis at the upper end of the stanchion length due to live load shall then be determined from Table 19.18.

(3) The end bending moment in the stanchion length about its XX axis shall be taken as the sum of the dead and live load total moments determined in *Clause* 16 (1)–(2) multiplied by the ratio of the relevant stiffness of the stanchion length under consideration to the sum of the relevant stiffnesses of that stanchion length and of the one above. The maximum bending stress in the steel section at the upper end of the stanchion length due to this end bending moment shall be calculated.

(4) The same procedure as that set out in *Clause* 16 (1)–(3) shall be adopted for the determination of the maximum end bending stress due to the moments about the YY axis.

(5) Where a beam makes a skew connection to a stanchion the fixed end moment at the end of the beam shall, for the determination of M^D_F and M^L_F, be resolved into its components about the XX and YY axes of the stanchion, and the relevant stiffnesses of the beam shall be the stiffness of the beam multiplied by the sines of the angles between the axis of the beam and the XX and YY axes of the stanchion respectively.

(6) The total end bending stress shall be taken as the sum of the maximum end bending stresses calculated under *Clause* 16 (1)–(5). The magnitude of this total end bending stress shall not exceed the value given for the stanchion length, as defined by its slenderness ratio (L/r_y), by the curve of Fig. 19.15 appropriate to the axial load per unit area (p).

(17) Where the fixed end moment of a beam framing into the lower end of a stanchion length is greater than the fixed end moment

of the corresponding beam framing into the upper end, the fixed end moment of the upper beam shall be increased in the ratio $\frac{2+V}{3}$, where V is the ratio of the fixed end moment of the lower beam to that of the upper. This increased moment shall be used in the determination of the total end bending stress at the upper end of the stanchion length. The total end bending stress at the lower end of the stanchion length shall also be determined using the actual values of the fixed end moments of the beams framing into the lower end of the stanchion length. The greater of these two end bending stresses shall then be taken as the total end bending stress to be used in determining the adequacy of the section as in *Clause* 16 (6).

(18) (1) Where a beam frames at its remote end into the web of another beam, the fixed end moment at the end of the beam attached to the stanchion shall be increased by the appropriate correction factor as given in Table 19.19.

TABLE 19.19.—CORRECTION FACTOR (CONNECTION TO BEAM AT REMOTE END).

$\frac{K_{BR}+K_{BL}}{K_U+K_L}$.	Factor.
0·1	1·47
0·5	1·36
1·0	1·29
2·0	1·20
4·0	1·13
8·0	1·07
16·0	1·04

(2) Where a beam frames at its remote end into a stanchion of less stiffness than the stanchion under consideration, the fixed end moment shall be increased by the appropriate correction factor (Table 19.20). Where the stiffness of the stanchion at the remote end is not less than one-half that of the stanchion under consideration no correction factor need be used. Where the beam frames into the flange of the stanchion under consideration and is attached at its remote end to the web of another stanchion, the section of which is not known, the ratio (S) shall be taken as $\frac{1}{16}$.

No mention has so far been made of the steps to be taken when dealing with horizontal or wind loads.

It was recommended by the Steel Structures Research Committee that the method of design described above should apply " to the steel framework of building structures formed with horizontal girders and vertical columns and provides only for the stresses caused by vertical forces. Any structure for which the method of design is used must be

so constructed as to resist horizontal forces due to wind or other causes, without significant horizontal sway, by means of its floor slabs in association with vertical walls or braced vertical frames."

TABLE 19.20.—CORRECTION FACTOR (CONNECTION TO STANCHION AT REMOTE END).

$\frac{K_{BR}+K_{BL}}{K_U+K_L}$	Stiffness ratio, S.			
	$\frac{1}{16}$	$\frac{1}{8}$	$\frac{1}{4}$	$\frac{1}{2}$
0·1	1·27	1·18	1·10	1·04
0·5	1·30	1·25	1·18	1·09
1·0	1·25	1·22	1·17	1·09
2·0	1·18	1·16	1·14	1·08
4·0	1·11	1·10	1·09	1·05
8·0	1·07	1·06	1·05	1·03
16·0	1·04	1·03	1·03	1·02

$$S=\frac{\text{sum of stiffnesses of upper and lower stanchion lengths at remote end of beam}}{\text{sum of stiffnesses of upper and lower stanchion lengths at end under consideration}}.$$

This decision was based on the evidence provided by a lengthy investigation of the effect of wind loads on frames having semi-rigid connections.* It was found that the bending moments in the stanchions due to wind loads increased rapidly in magnitude as the connections departed from the condition of complete rigidity. This tendency is shown in the tests on the experimental frame, p. 429. It was considered desirable to relieve such frames of the stresses arising from wind shear and therefore, where floors and walls do not supply adequate bracing, special wind bents are demanded.

The investigation showed also that the assumptions usually made to-day when wind loads are taken into account are not satisfactory for use in the design of these special bents. For this reason the subject of designing for wind loads, which is being studied by a Committee of the American Society of Civil Engineers, will not be discussed here. An examination of the somewhat unsatisfactory methods commonly used to-day, which is also outside the scope of this chapter, has been adequately dealt with elsewhere.†

The most satisfactory way of showing the ease with which the method of design described in this chapter can be applied is to give detailed calculations for a particular case.

Fig. 19.16 shows a typical floor plan for a seven storey frame. In Table 19.21 the sections of certain beams have been calculated. In the first column is entered the beam mark and in the second the span

* "The Effect of Wind Loads on Frames with Semi-Rigid Connections." J. F. Baker and E. Leader Williams. Final Report, Steel Structures Research Committee. H.M. Stationery Office, 1936.

† "Wind Stresses in Buildings." R. Fleming. John Wiley & Sons, New York, 1930.

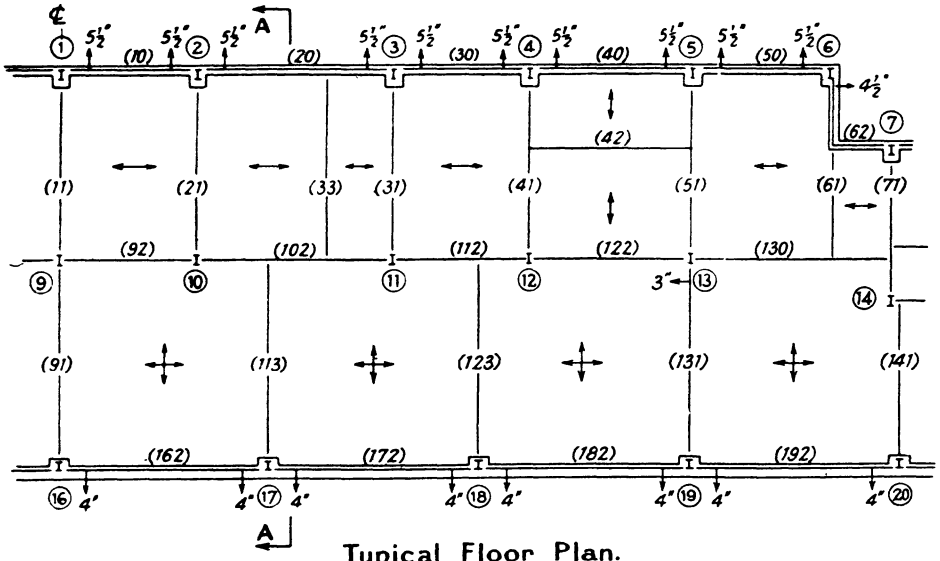

Typical Floor Plan.

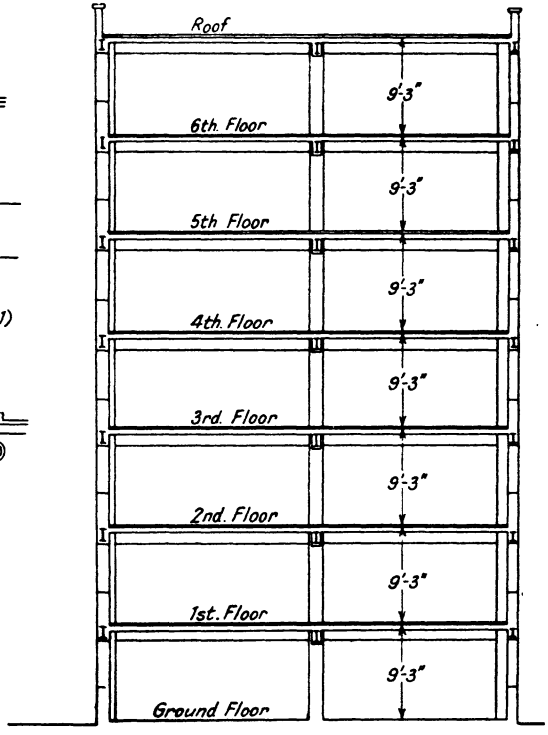

Section AA.

LOADING DATA

ROOF:—

Garden superimposed	40 lb./sq. ft.	= 1/56 tons.
Constructional slab	45 ,,	,,
Screed	12 ,,	,,
Asphalt	10 ,,	,,
Flower boxes	10 ,,	,,
Ceiling	5 ,,	,,
	82 ,,	,, = 1/27·2 tons.

DOMESTIC FLOORS:—

Superimposed	40 lb./sq. ft.	= 1/56 tons.
Constructional slab	45 ,,	,,
Finish (boards and battens)	5 ,,	,,
Ceiling	5 ,,	,,
Partitions	27 ,,	,,
	82 ,,	,, = 1/27·2 tons.

WALLS:—

Main frontage, 13½" brick = 1/16 tons.

Garden court, 9" brick = 1/23·5 tons.

FIG. 19.16.

of the beam between supporting faces. The next four columns refer to the left-hand end of the beam, giving the restraining moment, class of connection, fixed end moment and reaction respectively. In the 7th column are the details of the loads. The next four columns refer to the right-hand end of the beam.

The first step, the loads having been entered in column 7, is to write down in columns 6 and 8 the reactions at the left- and right-hand ends of the beam. The fixed-end moments are then entered in columns 5 and 9. These moments are, of course, those which would be present at the ends of a similarly loaded beam with completely fixed ends. The classes of the connections are entered, for convenience of checking, in columns 4 and 10. A provisional beam section is now chosen so that D, the web depth, may be used in the calculation of $\frac{M_F}{2D}$ to be entered in column 12. M_F is the mean of the total fixed-end moments at the ends of the beams entered in columns 5 and 9. When $\frac{M_F}{2D}$ is known, the restraining moments at the ends of the beam to be entered in columns 3 and 11 can be read off the curve (p. 444) appropriate to the class of connection. The maximum bending moment must now be calculated in column 13 and from it the modulus of section required. The final section is then selected and entered in column 14. It will be found convenient in the design of the stanchion if the stiffness of the beam is entered in this column.

The arrangement of the stanchion calculations, Table 19.22, like that for the beam, has been made to conform as nearly as possible to existing practice. Normally the same section will be used for the two topmost lengths of a stanchion. In Table 19.22 this section has been chosen from a consideration of the conditions in the stanchion length next below the topmost. In certain cases more rigorous conditions may occur in the topmost length and the adequacy of the section there should be tested. The first step is to enter on the loading diagram the reactions and fixed-end moments due to both live and dead load for each beam framing into the stanchion. The loads coming on to the stanchion are entered in column 4. In the cases illustrated these loads are made up of the weight of the stanchion and casing and of the beam reactions, since for simplicity in the beam calculations the load carried by each was assumed to be that due to the full area of floor between stanchion centres. The load carried by a beam may, however, be taken as due to that part of the floor between stanchion flanges and where use is made of this refinement the loads entered in column 4, which must give the total load coming on the stanchion, will be greater than the reactions from the beams. An improvement might also be made by providing separate columns for dead load and live load which would enable the permitted reduction in the latter to be made simply.

A stanchion section, which in the case illustrated in Table 19.22 is an I, 10 ins. $\times$ 6 ins. $\times$ 40 lbs., is chosen and the axial load per square inch of cross-section and the slenderness ratio are entered in column 5.

These being known, the permissible end bending stress (f_A) may now be read off from the appropriate curve (Fig. 19.15) and entered on the sheet. The stiffness ratios $\frac{K_{BR}+K_{BL}}{K_U+K_L}$ about both the XX and YY axes of the stanchion are calculated and entered in column 8. The next step is the calculation (column 6) of the moments about the principal axes of the stanchion, due to the reactions and fixed-end moments entered on the loading diagram. In the case illustrated in Table 19.22 the moment due to dead load about the XX axis is made up as follows: 150 tons-inches (the fixed-end moment of beam 51) plus $3{\cdot}7\times5$ tons-inches (the dead load reaction at the end of beam 51 multiplied by the distance of that reaction from the XX axis of the stanchion) minus 141 tons-inches (the fixed-end moment of beam 131) minus $3{\cdot}8\times5$ tons-inches (the dead load reaction at the end of beam 131 multiplied by its distance from the XX axis of the stanchion). The maximum live load moment must now be found. It will be seen at a glance that about the XX axis it occurs when beam 131 is loaded and beam 51 is unloaded, its value then being $(66+1{\cdot}7\times5)$ tons-inches. The detailed calculations of the moments about the YY axis are given in the Table.

All the data needed for the determination of the actual total end bending stress in the stanchion are now available and the method used will be clear from the formula in general terms printed at the top of column 7. In this formula Z is the relevant modulus of section of the stanchion length, $\frac{K_L}{K_U+K_L}$ is the ratio of the relevant stiffness of the stanchion length under consideration to the sum of the relevant stiffnesses of that stanchion length and of the one above. C^D and C^L are the coefficients obtained from the tables of total bending moments due to dead load and due to live load (Tables 19.17 and 19.18). M_F^D and M_F^L are the moments found in column 6 due to dead and live load.

The actual total end bending stress is the sum of the end bending stresses about the XX and YY axes. These are calculated separately by the formula as shown in detail in column 7. The actual total end bending stress, in this case 3·84 tons per square inch, must be less than f_A the permissible end bending stress (4·7 tons per square inch) if the stanchion section chosen is adequate.

CHAPTER 20

THE THEORY OF GRAVITY DAMS

20.1. Function and types of dam.—In the conservation of water either for domestic or power purposes it is often necessary to form an artificial lake by constructing a barrier across a valley and thus raising the natural water level. Such a barrier is termed a dam and may be one of various types. Perhaps the simplest is the earth dam, which consists of a bank of earth supporting a central core wall of impervious clay which is carried down in a trench to an impervious foundation. The design of such dams is a matter of experience based on previous examples of the type which have stood satisfactorily and no attempt will be made to discuss them in this book.

Dams built of masonry or concrete are, however, designed on more definite scientific principles and may be divided into two main types: the gravity dam and the arched dam. The former relies on the weight and disposition of the material of which it is constructed to resist the forces produced by the water pressure. The latter is in plan either a single arch spanning the valley and abutting on the sides of it, or else a number of arches with buttresses to take the thrusts of the intermediate spans.

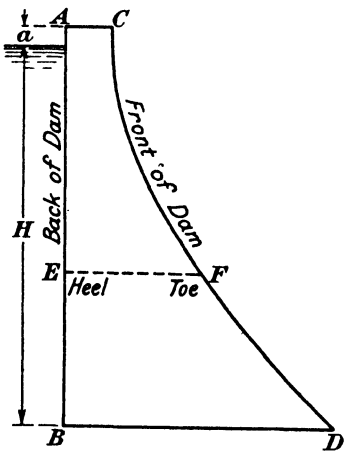

FIG. 20.1.

Fig. 20.1 shows the profile of a gravity dam. The water pressure due to a maximum head H acts on the face AB which is known as the back of the dam: the free face, CD, is the front. The points at which any horizontal section cuts the front and back are known respectively as the toe and heel of that section. The distance *a* by which the level of the top of the dam exceeds the maximum water level is the freeboard.

20.2. Possible types of failure of a gravity dam.—Certain ways in which a dam may fail can be stated as follows with reference to Fig. 20.1.

(*a*) Under the action of the overturning moment of the water the whole dam may turn bodily about the toe D.

(*b*) The section above a plane such as EF may slide relative to the lower section.

(*c*) The compressive stress at some point in the masonry may exceed the safe value: this may occur either when the reservoir is full or empty.

(*d*) Tensile stress may be developed at some point in the masonry and cause failure due to the inability of the mortar joints to withstand it.

The earliest conditions laid down for the design of dams were those of Sazilly (1853). He only stated the possibilities of failures under (*b*) and (*c*), rejecting serious consideration of (*b*) since no failure of this type had ever been recorded. The importance of eliminating tensile stress was not appreciated until Professor W. M. Rankine pointed it out as an essential feature of design in a report dealing with the construction of a dam in India. Since that time it has always been considered a primary factor in design.

Rankine was concerned with the possibility of tension occurring at the heel of a horizontal joint due to the resultant force on that joint, compounded of the weight of masonry resting on it and the water pressure above it, falling outside the middle third and this was the only aspect of the matter considered by most later designers. In 1904, however, L. W. Atcherley and Karl Pearson propounded a theory that tensile stress might also be developed due to the resultant of the water pressure and the vertical shearing force falling outside the middle third of vertical sections. They suggested that this was of equal importance with the earlier consideration and that its effect, if taken into account, would modify a profile considerably.

The elimination of tensile stress by keeping resultant actions within the middle third of a horizontal section automatically provides a large factor against overturning of the dam about the toe and so it is usual to consider only the last two possibilities, (*c*) and (*d*).

Another factor, however, which has not so far been mentioned, must be given serious consideration, *i.e.* the uplift pressure or upward force exerted on the base of the dam due to the transmission of pressure through fissures in the foundation, porous concrete in the dam, cracks, etc. This question was discussed by B. Hellstrom in a course of lectures given at the University of London in November, 1935,* and we cannot do better than quote his views. He says in reference to concrete dams :—

" A controversial question in connection with the design of gravity dams is the uplift pressures. It is no exaggeration to say that many failures of such dams are due to the fact that no account was taken of uplift pressure. In my opinion, it is a crime not to pay due attention to uplift pressure, even if the foundation of the dam is first-class hard rock without visible fissures, and even if grouting has been carried out.

" The measures generally taken to reduce the uplift pressure are as follows :—Providing the dam with a cut-off trench filled with concrete near the upstream face of the dam, placing drains along the downstream

* " Recent Practice in Hydro-Electric Power Development." " The Engineer." February 14th to April 17th, 1936 (inclusive).

side of this trench and along the foundation where fissures exist and providing drainage in the dam itself, either in the form of vertical drain pipes near the upstream face at a comparatively short distance from each other or arranging for large drainage galleries through the whole body of the dam.

"Measurements of uplift pressure at existing dams have shown conclusively that, so far as foundation level is concerned, uplift forces do exist, even in cases where the foundation rock has been grouted and drainage has been provided for.

"The uplift force with which the designer of dams is principally concerned is a product of pressure and area. It is often argued that the latter factor is of greater importance than the former, but the determination of the area over which uplift pressure is exerted is far more difficult than the measurement of the pressure itself. So far no satisfactory information has been obtained regarding the proportion of the total horizontal base area on which the measured uplift pressures act. All that is known is that they cannot act on more than the full area, but nothing is known of the effective area at the base of the dam where concrete comes into contact with rock."

After a discussion of suggested methods for allowing for this effect Hellstrom continues :—

"Other American engineers calculate with 100 per cent. uplift intensity at the upstream face, reducing it to 50 per cent. at the drainage gallery, if any, near the upstream face, and taking it as varying by a straight line to zero or tail water pressure at the downstream face, assuming the uplift pressure as acting on the full area at all points.* This is, in my opinion, a far better mode of calculation than the other method referred to.

"Terzaghi has made certain interesting experiments to determine the uplift pressure.† These experiments and investigations have shown that the effective area on which uplift may act in concrete is practically 100 per cent.

"Horizontal construction joints in a dam are always vulnerable points. Moreover, there is never any guarantee that some more or less horizontal layers in a concrete between such joints may not occasionally be of inferior quality and more or less porous. Water may get into such layers directly, or through vertical cracks which are often found in dams near the foundation. As it has been found that also horizontal cracks may occur, and that, as will be referred to later, deterioration of the concrete particularly near the upstream face is possible, there seems to be no reason why, if all these circumstances are taken into account, safe assumptions should not be made for the

* "Uplift Pressure in Masonry Dams." I. E. Houk. Civil Engineering, New York, September, 1932.

† Karl v. Terzaghi. "Die wirksame Flachenporositat des Betons, Zeitschrift des Osterr." Ingenieur- und Architekten-Vereines, Nr. 1-2, 1934.

"Beanspruchung von Gewichtstaumauern durch das strömende Sickerwasser." Die Bautechnik, Nr. 29, 1934.

"Zur Statischen Berechnung der Gewichtstaumauern." Die Bautechnik, Nr. 45, 1934.

design of all dams and especially for such important dams where large quantities of water, if suddenly released, would cause appreciable damage. In Sweden for the last three decades or so, gravity dams have been designed to withstand uplift pressure varying in a straight line from 100 per cent. water pressure at the upstream face to 100 per cent. tail water pressure at the downstream face, acting upon 100 per cent. of the base area. The additional quantity of concrete required to make the dam able to withstand such uplift pressure calculated over the whole area is not considerable, and the extra margin of safety from failure that may thereby be attained is to be recommended."

20.3. Assumptions as to stress distribution in masonry.—If a masonry dam and its foundation be assumed to consist of a homogeneous mass of elastic material the stresses at any point in it can, theoretically at least, be calculated provided that the conditions of loading on all the faces are known exactly. The calculation would be laborious and difficult and in the absence of exact knowledge of the boundary conditions hardly worth while.

It may be assumed with reasonable accuracy for all sections of a dam except in the immediate neighbourhood of the abutments that there are little or no shearing forces on transverse vertical sections, or, in other words, any section of the dam between two such sections may be assumed to be in equilibrium under its own weight, the fluid pressure on the back and the reactive forces from the foundation.

The forces from the water pressure are known accurately and since the face of the dam is exposed to the air there can be no normal or tangential stresses at any point on this boundary. There remain the reactive forces from the foundation and, from the nature of the problem, it is quite impossible for these to be known accurately.

If the dam is assumed to be rigid it can sink bodily or rotate from the action of the forces on it but no movements it may experience can distort the base boundary; if this was initially a straight line it will remain straight. If the foundation is perfectly elastic it follows, since the reaction at any point is proportional to the displacement, that the vertical reactive stresses upon the base of the dam follow a linear law. If the dam is not rigid, or the foundation not perfectly elastic, this distribution will be modified, but since it is impossible to state the elastic condition of the foundation an exact distribution cannot be determined. Under these circumstances it is customary always to assume a linear variation of normal stress across any horizontal section of the profile. It should be realised that this is no more than assumption and the whole of the existing theory of masonry dams is built upon it.

In Fig. 20.2 let AB be any horizontal section of a dam and let the resultant of the weight and water pressure for unit length of the dam be R, the line of action of R cutting AB at u from A. Let the length of AB be l.

R can be resolved into its two components W, acting normal to AB and P, acting along BA. P is a shearing force and its effect will be considered later. W is a load applied normally to a rectangular section

of width unity and depth l; the eccentricity is $\frac{l}{2}-u$. The direct compressive stress on this base section is $\frac{W}{l}$ and the maximum stress due to the bending moment $W\left(\frac{l}{2}-u\right)$ is

$$\pm\frac{6W}{l^2}\left(\frac{l}{2}-u\right)=\pm\frac{3W}{l}\left(1-\frac{2u}{l}\right).$$

Hence the maximum compressive stress at A is $\frac{2W}{l}\left(2-\frac{3u}{l}\right)$ and the minimum compressive stress at B is $\frac{2W}{l}\left(\frac{3u}{l}-1\right)$. If $\frac{3u}{l}-1=0$, *i.e.* if $u=l/3$ the minimum compressive stress is zero and the maximum compressive stress is $\frac{2W}{l}$. If $\frac{2l}{3}>u>\frac{l}{3}$ the stress everywhere is compressive and if $u<l/3$ tensile stress is developed at the point B. The three cases are shown in Fig. 20.2.

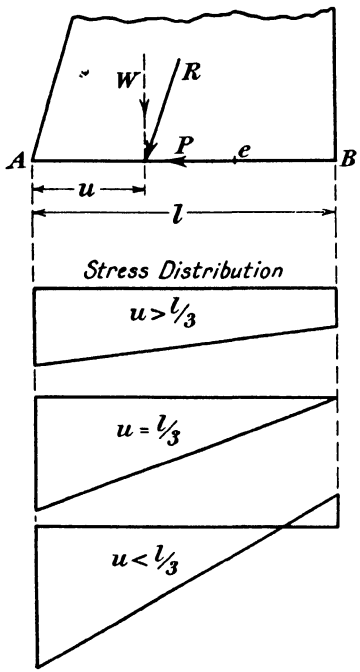

FIG. 20.2.

Hence, if tensile stress is to be eliminated, the line of action of the resultant force must cut the base section within the middle third of its length.

This rule follows directly from the assumption of a linear stress distribution: it is not true for any other. It was pointed out by L. W. Atcherley and Karl Pearson in a paper * which will be referred to later that if this assumption be adopted it follows with almost equal validity that the distribution of shear stress across the horizontal section arising from the pressure must be parabolic in form. This result is well known for a beam subjected to bending and if the dam were of rectangular profile the cases would be parallel. If either the back or front of the dam is vertical at the section considered, the shearing stress there must be zero, but if it is battered this is not necessary.

This question of shear stress distribution caused considerable controversy after the publication of the paper referred to above, the chief disputants being Professor Karl Pearson and Professor W. C. Unwin. Unwin produced a treatment for the determination of shear stress distribution which appeared to confute the result obtained by Atcherley and

* "Some disregarded points in the stability of masonry dams." Drapers Company Research Memoirs. Technical Series II, 1904.

Pearson, but in an article in "Engineering" * the latter discussed the situation and pointed out that the results achieved were the same. These were briefly that in the general case of a dam the distribution is parabolic, but the parabola is not symmetrically placed with zero shears at the front and back of the dam; in the special case of a rectangular profile the parabola is symmetrical, with zero shears at front and back, and in the special case of a triangular dam the parabola degenerates into a triangle.

In this same article Karl Pearson emphasised the fact that the basis of the analysis is the assumption of linear stress distribution which he contended is wholly erroneous.

20.4. Analysis of an existing profile.—Before proceeding to a discussion of the various profiles which have been suggested it will be

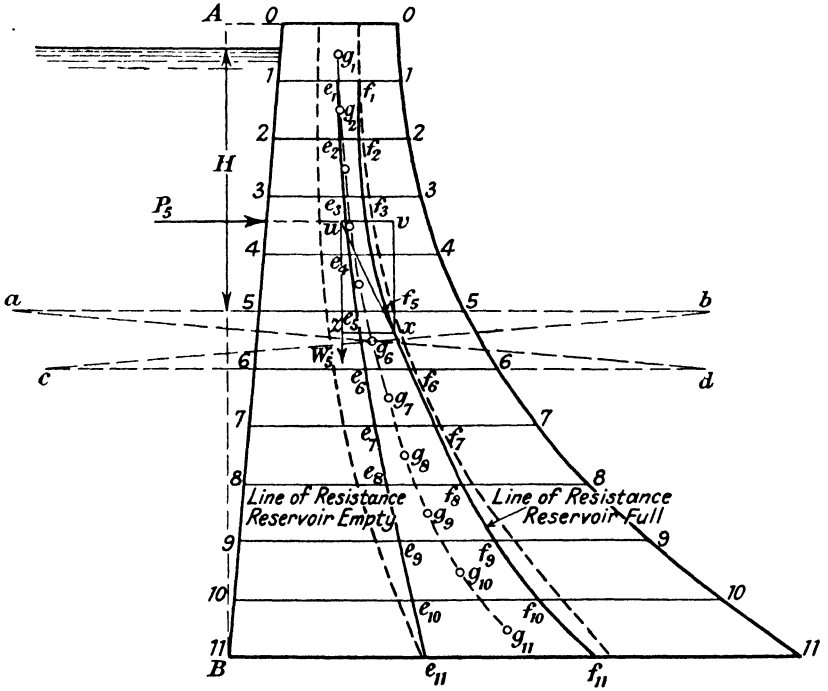

FIG. 20.3.

advisable to examine the method for analysing a section already proposed since it is quite usual procedure to draw a profile, analyse it to determine whether the essential points have been adequately covered and modify it by a process of trial and error until a satisfactory design is achieved.

Suppose that the profile in Fig. 20.3 is to be analysed, the procedure is as follows. Divide the profile into a number of sections by horizontal lines 11, 22, . . . etc., sufficiently closely spaced for the front and

* July 14th, 1905, p. 35.

back of the dam to be considered as formed by straight lines between successive sections.

Find the centre of gravity of each of the trapeziums thus formed: this may be done graphically as shown for 5566 by making $5a=5b=66$ and $6c=6d=55$ and joining ad and bc. The intersection of these lines at g_6 is the centre of gravity.

Consider now a length along the dam of one foot and calculate the weights of the portions of the dam between successive sections: these weights act through the centres of gravity g_1, g_2, etc., and will be denoted by w_1, w_2, etc. If a vertical be dropped from g_1 to meet 11 at e_1, e_1 is the point where w_1, the resultant of the weights above 11, acts when the reservoir is empty and its position determines the distribution of stress across 11 for this case. The resultant of w_1 and w_2 acting through g_1 and g_2 respectively must now be found and this is done most accurately by taking moments of these weights about a line such as AB. It may be found graphically by a link polygon but direct calculation is preferable. This resultant cuts 22 at e_2 and the process is continued for each section in turn to find e_3, e_4 . . . e_{11}. The line through e_1, e_2 . . . e_{11} is known as the line of resistance for the reservoir empty and must cut any section within the middle third of its width if tension at the toe is to be eliminated when the reservoir above that section is empty.

A corresponding line of resistance for the reservoir full must also be found and we will consider section 55 as an example of the method. The resultant weight $w_1+w_2+w_3+w_4+w_5=W_5$ say, above this section, acts through the centre of gravity of 0055 which has been already found. The pressure on the back of the dam above section 55 due to the head H is $P_5=\frac{wH^2}{2}$ where w is the density of the water, and this acts at H/3 above 55. It is usual to assume this to be always horizontal and to make no allowance for the fact that there is a downward component due to the batter of the back; this assumption is on the side of safety. The line of action of the pressure P_5 is produced to cut that of W_5 at u; uv and uz are made proportional to P_5 and W_5 respectively and the resultant given by ux cuts the section 55 at f_5 which is a point on the line of resistance for the reservoir full. This is done for all sections and the complete line f_1, f_2 . . . f_{11} is obtained.

For the elimination of tension at the heel when the reservoir is full this line must cut every section within the middle third.

The maximum compressive stress at any section can be obtained once these lines of resistance are found: let the appropriate line of resistance for the reservoir empty cut any section, say, 55 at c from the mid-point of the section. Then if l_5 is the width of that section the direct compressive stress on it is W_5/l_5 lbs. per square foot, since we consider one foot of the dam.

The bending stress is given by

$$\frac{My}{I}=\frac{6cW_5}{l_5^2}.$$

Hence the maximum compressive stress is

$$\frac{W_5}{l_5}\left(1+\frac{6c}{l_5}\right).$$

20.5. The Rankine profile.—The profile suggested by Rankine is described in a Report made by him in connection with the design of a high dam for Bombay * and it is in this report that the importance of eliminating tensile stress is first introduced as fundamental in the design of masonry dams.

Rankine rejects the view of the earlier French engineers, Graeff and Delocre, that the intensity of vertical compressive stress allowable should be the same both at the toe and at the heel. The argument is best given in the words of the Report, " The direction in which the pressure is exerted amongst the particles close to either face of the masonry is necessarily that of a tangent to that face ; and, unless the face is vertical, the vertical pressure found by means of the ordinary formula is not the whole pressure, but only its vertical component ; and the whole pressure exceeds the vertical pressure in a ratio which becomes the greater the greater the ' batter,' or deviation of the face from the vertical. The outer face of the wall has a much greater batter than the inner face ; therefore, in order that the masonry of the outer face may not be more severely strained when the reservoir is full, than that of the inner face when the reservoir is empty, a lower limit must be taken for the intensity of the vertical pressure at the outer face than at the inner face."

He points out further that the same reasoning shows that the intensity of the vertical component ought gradually to diminish at the lower part of the front of the dam where the batter gradually increases. Since the existing state of knowledge did not warrant any definite theory as to the law which such diminution should follow, he was guided by the example of the dam across the Furens and made the vertical component of pressure at a depth of 150 feet approximately the same as in that dam, viz. that due to 107 feet of masonry.

The maximum intensities of pressure adopted by Rankine were 20,000 lbs. per square foot on the back and 15,625 lbs. per square foot on the front of the dam, or, expressed in height of masonry, 160 feet and 125 feet respectively.

The argument used as a basis for the design is given in detail in the Report and the result is a particular design for specific conditions as to height, stress intensities and density of material. This design is shown in Fig. 20.4. The same method could be used for another set of conditions, but the calculations would be rather complicated.

The front, back and centre line of the profile all consist of logarithmic curves having the vertical line OX in Fig. 20.4 as a common asymptote and having one common constant subtangent.

* Miscellaneous Scientific Papers. W. M. Rankine. No. XXXIV. " Report on the Design and Construction of Masonry Dams."

The following formulas are then deduced :—

Let t =the thickness of the profile at any depth x from the top.
t_1=a given thickness at a given depth x_1.
y =the distance from OX of the centre line of any section.
$c = y/t$.

Then $$t = t_1 e^{\frac{x-x_1}{a}}$$

or, in common logarithms,

$$\log t = \log t_1 + \cdot 4343 \frac{x-x_1}{a}$$

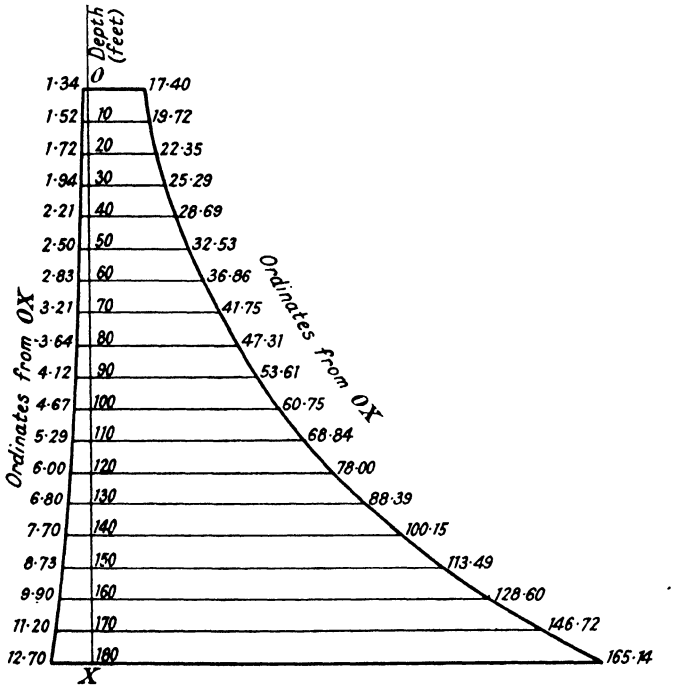

FIG. 20.4.

In the actual profile given by Rankine and shown in Fig. 20.4,

a, the subtangent was taken as 80 feet,
t_1 as 84 feet,
and x_1 as 120 feet.

The top width of the dam is found from these data to be 18·74 feet. At the depth 120 feet, the heel was 6 feet and the toe 78 feet from OX.

Hence $$y = 36$$
$$c = \frac{36}{84} = \frac{3}{7}.$$

So for the particular profile $\frac{y}{t} = \frac{3}{7}$ and at any depth the heel is $t/14$ and the toe $\frac{13t}{14}$ from the axis OX.

The necessary dimensions for plotting this profile are given on Fig. 20.4.

20.6. The Wegmann profile.—A direct method for determining the profile of a gravity dam is due to E. Wegmann * and was used by him in the design of actual structures. It is claimed that this method gives the minimum weight of material to withstand any specified head of water. The equations deduced appear in some instances rather cumbersome, but their solution is quite simple. Every dam, according to its height, is divided into five or less stages, the controlling condition in each stage being different. These stages and conditions are :

Stage I.—This is a top section rectangular in profile. The top width of the dam, fixed by such considerations as the size of roadway to be built across it and the amount of freeboard, will govern the height of this section. The limit of this stage will be reached when the line of resultant action for the reservoir full cuts the base section at the middle third point since, if the rectangular profile be continued beyond this, tensile stress will be developed at the heel.

Stage II.—In this stage the front of the dam is battered sufficiently to ensure that the line of resultant action for the reservoir full always cuts a horizontal section at the front middle third point. The limit of this stage is reached when the line of resultant action for the reservoir empty cuts the base at the back middle third point. If the back of the dam is still made vertical below this section, tensile stress will be developed at the toe when the reservoir is empty.

Stage III.—The front of the dam is battered to comply with the condition in Stage II and the back to a sufficient extent to eliminate tensile stress at any section when the reservoir is empty above that section. The limit of this stage is reached when the compressive stress at the toe of the dam when the reservoir is full reaches a prescribed value.

Stage IV.—In this stage the batter on the front of the dam is increased to a sufficient extent to keep the compressive stress at the toe at the prescribed value while the batter on the back is made sufficient to eliminate tension at the toe as in Stage III. The limit of this stage is reached when the compressive stress at the heel for the reservoir empty reaches its prescribed value. This value is generally higher than that for the toe for the reasons given earlier in this chapter.

Stage V.—The batters for both front and back of the dam are governed in this final stage by the necessity of keeping the compressive stresses in the masonry to the prescribed values when the reservoir is empty or full.

The general method of design is to fix the required top width of the dam and the necessary freeboard. An equation is then available for determining the height of Stage I. A horizontal section at some arbitrary depth below the bottom section of Stage I is considered and

* "The Design and Construction of Dams," E. Wegmann. John Wiley.

another formula determines the width of the dam at this point. The process is repeated until the application of a criterion for the position of the line of resultant action for the reservoir empty shows that the limit of Stage II has been reached.

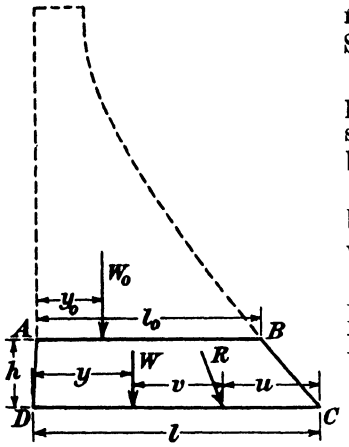

FIG. 20.5.

Corresponding formulas and appropriate criteria for the other stages are similarly used until the required depth below top water level has been reached.

The details of the method will be best understood by a study of the worked example given later.

Fig. 20.5 represents a section of the profile of a dam in any stage.

Let l_0 be the width of the dam already determined,

l, the width of the section to be calculated,

h, the arbitrary distance between these sections,

u, the distance from the toe to the line of resultant action for the reservoir full on the lower section,

v, the distance between the lines of resultant action for the reservoir full and empty measured along the lower section,

y, the distance from the heel to the point where the line of resultant action for the reservoir empty cuts the lower section,

y_0, the corresponding distance for the upper section,

A_0, the area of the profile above AB,

A, the area of the profile above DC,

W_0, the weight of masonry above AB per unit length of dam,

W, the weight of masonry above DC per unit length of dam,

ρ, the specific gravity of the material of the dam,

w, the density of water

and H, the head of water above the section of width l.

Then
$$l=u+v+y,$$
$$A=A_0+\left(\frac{l+l_0}{2}\right)h$$

and
$$W=\rho w\left\{A_0+\left(\frac{l+l_0}{2}\right)h\right\}.$$

By equating the overturning moment of the water pressure about the point where the line of resultant action for the reservoir full cuts the lower section to the restoring moment of W about the same point we have

$$\frac{wH^3}{6}=Wv,$$

or
$$v=\frac{H^3}{6\rho\left\{A_0+\left(\frac{l+l_0}{2}\right)h\right\}}.$$

Stage I.—Let the top width of dam=L
and the freeboard=a.

In this stage, which is rectangular as shown in Fig. 20.6,

$$l=l_0=\mathrm{L}.$$

Also $y=l/2$,

and u must not be less than $l/3$.

At a depth of water H let u reach the minimum limiting value of $l/3$.

Then since $l=u+v+y$

we have $$l=\frac{l}{3}+\frac{\mathrm{H}^3}{6\rho\left\{\mathrm{A}_0+\left(\frac{l+l_0}{2}\right)h\right\}}+\frac{l}{2}$$

and substituting $h=\mathrm{H}+a$,

$\mathrm{A}_0=0$

and $l=l_0=\mathrm{L}$

we obtain $$\mathrm{H}^3=\rho\mathrm{L}^2(\mathrm{H}+a) \quad . \quad . \quad . \quad . \quad . \quad . \quad . \quad . \quad (1)$$

which determines H.

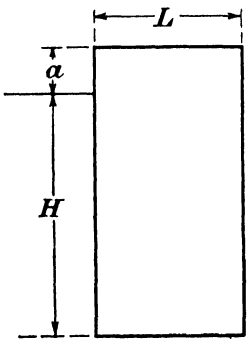

FIG. 20.6.

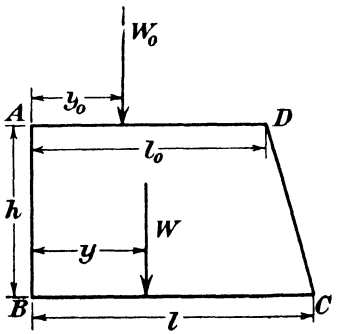

FIG. 20.7.

In the special case when $a=0$ this equation reduces to

$$\mathrm{H}=\mathrm{L}\sqrt{\rho}.$$

Stage II.—The back is vertical and the front battered to keep the line of resultant pressure on the middle third point when the reservoir is full.

So $u=l/3$

and $y>l/3$ with a limiting value $y=l/3$.

To determine an expression for y we take moments of the area of profile as shown in Fig. 20.7 about the vertical face of the dam and obtain

$$\mathrm{A}y=\mathrm{A}_0y_0+\text{moment of trapezium ABCD}.$$

But moment of ABCD $=\frac{hl_0^2}{2}+\frac{(l-l_0)h}{2}\left\{l_0+\frac{l-l_0}{3}\right\}$

$$=\frac{h}{6}(l_0^2+ll_0+l^2).$$

$$\therefore \quad Ay=A_0y_0+\frac{h}{6}(l_0^2+ll_0+l^2).$$

or
$$y=\frac{A_0y_0+\frac{h}{6}(l_0^2+ll_0+l^2)}{A_0+\left(\frac{l+l_0}{2}\right)h} \quad \ldots\ldots\ldots (2)$$

which must be not less than $l/3$.

Since $l=u+v+y$

$$l=\frac{l}{3}+\frac{H^3}{6\rho\left\{A_0+\left(\frac{l+l_0}{2}\right)h\right\}}+\frac{A_0y_0+\frac{h}{6}(l_0^2+ll_0+l^2)}{A_0+\left(\frac{l+l_0}{2}\right)h}$$

which reduces to

$$l^2+l\left(\frac{4A_0}{h}+l_0\right)=\frac{1}{h}\left(\frac{H^3}{\rho}+6A_0y_0\right)+l_0^2. \quad \ldots\ldots (3)$$

This quadratic is solved to determine l for any arbitrary value of h. The value thus found is substituted in the expression for y given above and if y is greater than $l/3$ the value of h chosen is such as to lie within Stage II.

This l is then taken as l_0 and a new value of h is selected. The calculation is repeated and the width of the dam for the new section is determined. The process is continued until a depth is reached where $y=l/3$, which denotes that the limit of Stage II has been found.

Stage III.—In which the no-tension condition is observed both for the reservoir full and empty. At each section in this stage therefore the limiting values are

$$y=l/3$$

and
$$u=l/3.$$

$$\therefore \quad l=\frac{l}{3}+\frac{H^3}{6\rho\left\{A_0+\left(\frac{l+l_0}{2}\right)h\right\}}+\frac{l}{3}.$$

which gives
$$l^2+l\left(\frac{2A_0}{h}+l_0\right)=\frac{H^3}{\rho h} \quad \ldots\ldots\ldots (4)$$

When the reservoir is full, since there is no stress at the heel, the maximum compressive stress at the toe is

$$p'=\frac{2W}{l}=\frac{2\rho w\left\{A_0+\left(\frac{l+l_0}{2}\right)h\right\}}{l} \quad \ldots\ldots\ldots (5)$$

and this must not exceed the prescribed stress for the toe of p tons per square foot.

As before, an arbitrary value of h is chosen and l calculated from (4). This is substituted in the expression for p' and provided $p'<p$ the calculated width is allowable. A new value of h is taken and the design carried a section lower. This process is repeated until $p'=p$, which indicates that the limit of Stage III has been reached.

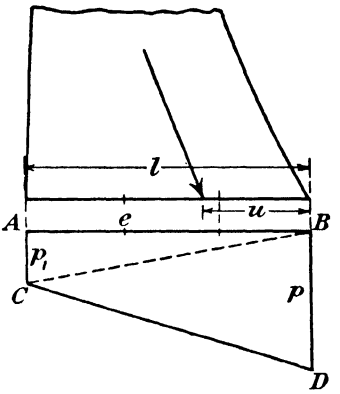

FIG. 20.8.

Stage IV.—In this stage the maximum compressive stress at the toe is limited to p. The line of resultant pressure for the reservoir full will fall within the middle third as shown in Fig. 20.8 giving a stress distribution across the section under consideration as shown, p_1 being the compressive stress at the heel and p that at the toe.

Let e be the middle third point nearer the heel. Since the moment of the load which produces the given stress distribution about any point is equal to the moment of the diagram we have, by taking moments about e,

$$W(\tfrac{2}{3}l-u)=\frac{pl^2}{6},$$

since the moment of the triangle ACB about e is zero.

So
$$p=\frac{2W}{l}\left(2-\frac{3u}{l}\right)$$

and
$$u=\frac{2l}{3}-\frac{pl^2}{6A\rho w}.$$

Also
$$y=l/3$$

$$\therefore \quad l=\frac{2l}{3}-\frac{pl^2}{6A\rho w}+\frac{H^3}{6\rho\left\{\Lambda_0+\left(\frac{l+l_0}{2}\right)h\right\}}+\frac{l}{3}$$

which gives
$$l^2=\frac{wH^3}{p} \qquad \ldots\ldots\ldots\ldots \quad (6)$$

If q' is the compressive stress at the heel when the reservoir is empty we can write by analogy with the above expression for p,

$$q'=\frac{2W}{l}\left(2-\frac{3y}{l}\right)$$

and the limit of Stage IV is reached when l is of such a value that $q'=q$, the prescribed stress for the heel.

Stage V.—The compressive stresses at the heel and toe for the reservoir empty and full are kept to the values q and p respectively.

As in Stage IV, $$u=\frac{2l}{3}-\frac{pl^2}{6A\rho w}$$

and by symmetry $$y=\frac{2l}{3}-\frac{ql^2}{6A\rho w}$$

$$\therefore \quad l=\frac{2l}{3}-\frac{pl^2}{6A\rho w}+\frac{H^3}{6\rho\left\{A_0+\left(\frac{l+l_0}{2}\right)h\right\}}+\frac{2l}{3}-\frac{ql^2}{6A\rho w}$$

or $$l^2\left(\frac{p+q}{\rho w h}-1\right)-l\left(\frac{2A_0}{h}+l_0\right)=\frac{H^3}{\rho h} \quad . \quad . \quad . \quad . \quad . \quad (7)$$

from which l is found.

Distribution of batter between front and back of dam.—In Stages III, IV and V both the front and back of the dam are battered and it is necessary to determine how much is to be given to each.

Fig. 20.9 represents a section of the dam in any of these Stages, O being the heel and t the projection of the lower section beyond the vertical through the heel of the upper section.

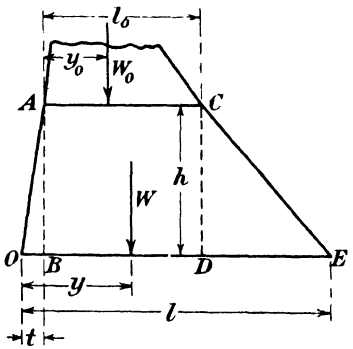

FIG. 20.9.

Divide the trapezium into the triangles OAB, CDE and the rectangle ACDB and take moments for the whole profile about O.

Then $$Ay=A_0(y_0+t)+\frac{ht^2}{3}+l_0h\left(t+\frac{l_0}{2}\right)+h\left(\frac{l-l_0-t}{2}\right)\left(\frac{l+2l_0+2t}{3}\right).$$

In Stages III and IV, $y=l/3$ and on substituting this value and that of A we obtain

$$t=\frac{2A_0(l-3y_0)-hl_0^2}{6A_0+h(2l_0+l)} \quad . \quad . \quad . \quad . \quad . \quad . \quad . \quad (8)$$

and since all the terms in the right-hand expression are known, t is calculable.

In Stage V, $$y=\frac{2l}{3}-\frac{ql^2}{6A\rho w}$$

$$\therefore \quad Ay=\frac{2l}{3}\left\{A_0+\left(\frac{l+l_0}{2}\right)h\right\}-\frac{ql^2}{6\rho w}$$

TABLE 20.1.

h	H	H+a	y_0	v_0	u_0	l_0	A_0	y	v	u	l	A	p'	q'	t	
ft.	ft.	ft.	ft.	ft.	ft.	ft.	sq. ft.	ft.	ft.	ft.	ft.	sq. ft.	tons per sq. ft.	tons per sq. ft.	ft.	
38·65	32·65	38·65	0	0	0	20·0	0	10·0	3·3	6·7	20·0	773	—	—	—	Stage I
10	42·65	48·65	10·0	3·3	6·7	20·0	773	10·2	5·8	8·0	24·0	993	—	—	—	
10	52·65	58·65	10·2	5·8	8·0	24·0	993	10·7	8·8	9·7	29·2	1,259	—	—	—	
10	62·65	68·65	10·7	8·8	9·7	29·2	1,259	11·8	11·5	11·7	35·0	1,580	—	—	—	Stage II
1	63·65	69·65	11·8	11·5	11·7	35·0	1,580	11·9	11·9	11·9	35·7	1,615	—	—	—	
10	73·65	79·65	11·9	11·9	11·9	35·7	1,615	14·7	14·7	14·7	44·1	2,014	5·7	—	1·3	
10	83·65	89·65	14·7	14·7	14·7	44·1	2,014	17·4	17·4	17·4	52·2	2,495	6·0	—	1·0	
10	93·65	99·65	17·4	17·4	17·4	52·2	2,495	19·9	19·9	19·9	59·7	3,054	6·4	—	0·7	
10	103·65	109·65	19·9	19·9	19·9	59·7	3,054	22·4	22·4	22·4	67·2	3,688	6·9	—	0·4	Stage III
10	113·65	119·65	22·4	22·4	22·4	67·2	3,688	24·7	24·7	24·7	74·1	4,395	7·4	—	0·3	
10	123·65	129·65	24·7	24·7	24·7	74·1	4,395	27·1	27·1	27·1	81·3	5,172	8·0	—	0·2	
10	133·65	139·65	27·1	27·1	27·1	81·3	5,172	30·4	29·3	31·5	91·2	6,034	8·0	8·3	1·1	
10	143·65	149·65	30·4	29·3	31·5	91·2	6,034	33·9	31·4	36·4	101·7	6,998	8·0	8·6	1·1	
10	153·65	159·65	33·9	31·4	36·4	101·7	6,998	37·5	33·3	41·6	112·4	8,068	8·0	9·0	1·1	
10	163·65	169·65	37·5	33·3	41·6	112·4	8,068	41·2	35·1	47·3	123·6	9,248	8·0	9·0	1·0	Stage IV
10	173·65	179·65	41·2	35·1	47·3	123·6	9,248	45·0	36·8	53·2	135·0	10·541	8·0	9·8	1·0	
5	178·65	184·65	45·0	36·8	53·2	135·0	10,541	47·0	37·6	56·4	141·0	11,231	8·0	10·0	0·5	
10	188·65	194·65	47·0	37·6	56·4	141·0	11,231	53·1	39·1	63·2	155·4	12,713	8·0	10·0	3·2	
10	198·65	204·65	53·1	39·1	63·2	155·4	12,713	59·8	40·5	70·7	171·0	14.345	8·0	10·0	3·6	
10	208·65	214·65	59·8	40·5	70·7	171·0	14,345	67·1	41·8	78·7	187·6	16,138	8·0	10·0	4·2	Stage V
10	218·65	224·65	67·1	41·8	78·7	187·6	16,138	75·0	42·7	87·3	205·0	18,101	8·0	10·0	4·7	

which gives, on equating to the expression for Ay above, the result

$$t=\frac{A_0(4l-6y_0)+l^2\left(h-\frac{q}{\rho w}\right)+l_0h(l-l_0)}{6A_0+h(2l_0+l)} \quad . \quad . \quad . \quad (9)$$

As an example of the calculation for a profile by the foregoing treatment a case has been worked out in detail from the following data :—

Total head=218·65 feet.
Freeboard = 6 feet.
Top width = 20 feet.
Specific gravity of masonry=2·25.
Density of water=62·4 lb. per cubic foot.
Allowable compressive stress at toe = 8 tons per square foot.
Allowable compressive stress at heel =10 tons per square foot.

The work is arranged as shown in Table 20.1. In the first place the value of h is calculated for the rectangular portion of Stage I by the use of equation (1). The values of u, v and y for this value of h, namely 38·65 feet, are entered in the appropriate columns. We are now in a position to design Stage II and h is chosen as 10 feet. The

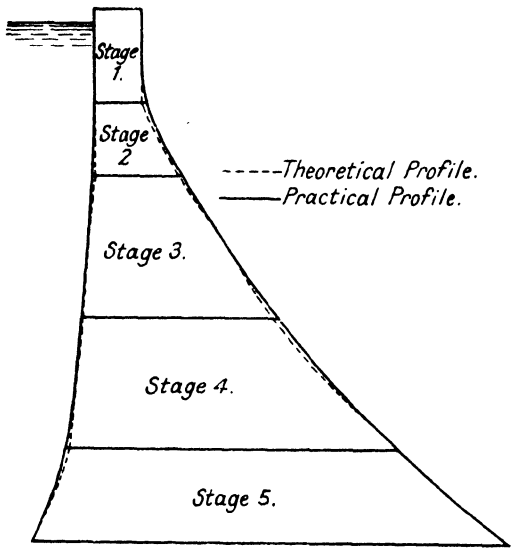

FIG. 20.10.

values of u, v, y, l and A for h=38·65 are the values of u_0, v_0, y_0, l_0 and A_0 for the level we are now considering and are entered in the appropriate columns. The values of l and y are determined from equations (3) and (2) respectively. v is found from the standard equation. A new section, still keeping h=10 feet so that H=52·65 feet, is dealt with in a similar manner and the process is continued until the calculated value of y becomes nearly $\frac{1}{3}$ of the calculated value of l. It will be seen that this occurs in the present case when H=62·65 feet. The next section is taken 1 foot below this level and y is then exactly

$l/3$, indicating that the limit of Stage II is reached with a head of water of 63·65 feet. We now enter Stage III and h is again taken as 10 feet. The value of l is calculated from equation (4). u, v and y are all equal to $\frac{1}{3}$ of this value and are entered in the appropriate columns. The maximum compressive stress at the toe is calculated from equation (5) and entered under p'. The process is continued in sections for which h=10 feet until when H=123·65 feet, p'=8 tons per square foot, which is the allowable limit for the toe stress. Stage IV is now entered with a further increase in depth of 10 feet, l, u and q' are calculated from the appropriate equations for this stage and the limit is reached at H=178·65 feet at which depth q'=10 tons per square foot, the allowable compressive stress at the heel. In Stage V the values of l are calculated from equation (7) and u, y and v from the equations for Stage V. The only remaining calculations to be made are those to determine the amount of batter, the appropriate equations being (8) in Stages III and IV and (9) in Stage V. The theoretical profile obtained in this way is plotted in Fig. 20.10 which also shows the faired profile which would actually be used.

20.7. Distribution of shearing stress in a masonry dam.—In a paper previously cited, L. W. Atcherley and Karl Pearson showed from the

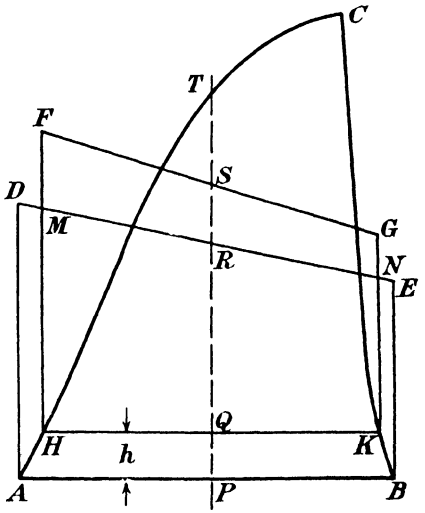

FIG. 20.11.

elastic equations that the assumption of linear distribution of normal stresses on a horizontal section of a dam leads to a parabolic distribution of shear stress across that section except for the special case of a triangular profile, when the distribution is linear. Unwin subsequently gave a treatment* which produced the same results and his method, somewhat modified, will be followed here.

Fig. 20.11 represents one foot length of a dam ABC. Let ADEB be the normal stress distribution on the section AB, assumed linear.

* "Engineering," June 30th, 1905, p. 825.

The weight of one cubic foot of masonry will be taken as the unit of force. The stress at any point in masonry units per square foot can then be represented as a *column* of masonry and if this is drawn to the same scale as the profile, the area ADEB will be equal to the area ABC.

If PT is any vertical section, the shearing force along PT is the difference between the weight and upward thrust on either side of PT,

i.e. PTCB—PREB.

Let HK be another horizontal section at a height h above AB and HFGK the stress distribution curve for this section. The shearing force on QT is then

QTCK—QSGK.

Therefore the shearing force on the length PQ is

(PTCB—PREB)—(QTCK—QSGK).

i.e. (PTCB—QTCK)—(PREB—QSGK).

or PQKB—(PQKB+KNEB—RSGN)

i.e. RSGN—KNEB.

Hence the average shear stress on PQ is

$$\frac{\text{RSGN}-\text{KNEB}}{h}.$$

If h is small this is the vertical shear stress at P and therefore the complementary horizontal shear stress at the same point.

If the back of the dam is vertical over the length h the area KNEB is zero and the shear stress is $\frac{\text{RSGN}}{h}$. In modern dams the back is either vertical or only slightly battered and so the area KNEB can usually be neglected.

Take the point N in Fig. 20.12 as origin. Then the equations of the lines ND and GF are

$$y=m_1x$$

and $y=m_2x+c$, where c=NG.

Let TP be x from N.

Then $\text{RS}=(m_2x+c)-m_1x,$

the area $$\text{RSGN}=\frac{(m_2-m_1)x^2}{2}+cx$$

and the shear stress $$s=\frac{(m_2-m_1)x^2}{2h}+\frac{cx}{h}.$$

This is a parabola except in the special case when $m_2=m_1$. It is then a straight line.

Let f_h=normal stress at the heel on section AB,

f'_h=normal stress at the heel on section δh above it

and f_t=normal stress at the toe on section AB.

Then $$m_1=\frac{f_t-f_h}{\text{AB}}$$

and $$c=f'_h+\delta h-f_h=-(f_h-f'_h)+\delta h.$$

Since δh is very small

$$m_1 - m_2 = \frac{dm}{dh}\delta h$$

and

$$f_h - f'_h = \frac{df}{dh}\delta h.$$

The area of RSGN obtained above can therefore be expressed in the form

$$-\frac{x^2}{2}\frac{dm}{dh}\delta h + x\left(1 - \frac{df_h}{dh}\right)\delta h$$

and the shear stress

$$s = -\frac{x^2}{2}\frac{dm}{dh} + x\left(1 - \frac{df_h}{dh}\right).$$

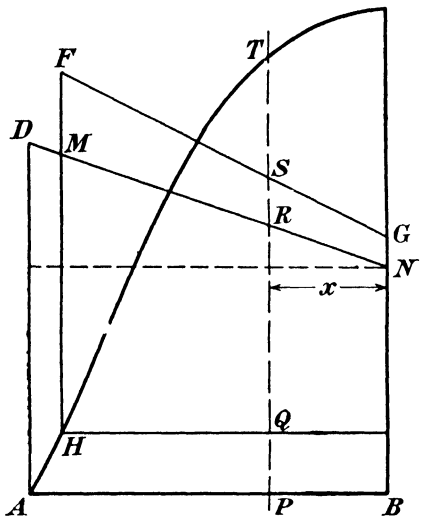

FIG. 20.12.

In the case of the triangular profile with vertical back of height h and base width nh

$$W = \frac{nh^2}{2} \text{ masonry units}$$

and

$$P = \frac{h^2}{2\rho} \text{ masonry units.}$$

The eccentricity of loading from the mid-point of the base is $\frac{h}{6}\left(\frac{2}{\rho n} - n\right)$.

Then

$$f_t = \frac{h}{\rho n^2}$$

$$f_h = h\left(1 - \frac{1}{\rho n^2}\right)$$

$$m = \frac{2}{\rho n^3} - \frac{1}{n}$$

$$\therefore \qquad \frac{dm}{dh}=0.$$

Also $$\frac{df_h}{dh}=1-\frac{1}{\rho n^2}$$

and $$s=\frac{x}{\rho n^2}$$

which is a triangle with its maximum ordinate $\frac{h}{\rho n}$ at the toe where $x=nh$.

If the profile is rectangular of base width b and height h,

$$W=bh \text{ masonry units,}$$

$$P=\frac{h^2}{2\rho} \text{ masonry units}$$

and the eccentricity of loading on the base is given by

$$\frac{3e}{h}=\frac{P}{W}=\frac{h}{2\rho b}$$

i.e. $$e=\frac{h^2}{6\rho b}.$$

Then $$f_t=h\left(1+\frac{h^2}{\rho b^2}\right)$$

and $$f_h=h\left(1-\frac{h^2}{\rho b^2}\right)$$

so that $$m=\frac{2h^3}{\rho b^3}$$

and $$\frac{dm}{dh}=\frac{6h^2}{\rho b^3}.$$

Also $$\frac{df_h}{dh}=1-\frac{3h^2}{\rho b^2},$$

so that $$s=\frac{3h^2}{\rho b^2}\left(x-\frac{x^2}{b}\right).$$

This is a parabola with $s=0$ at $x=0$ and $x=b$ and a maximum ordinate $\frac{3h^2}{4\rho b}$ at $x=b/2$.

In any other profiles the curves of shearing stress can be obtained graphically. It should be noticed that there can be no shearing stress at any point where the boundary of the profile is vertical. This is shown in the case of the triangular section where the back is vertical and in the rectangular where both front and back are vertical. It frequently happens that the bottom part of a dam, which is under the ground, is rectangular in profile: in this section horizontal sections will give shearing curves with zero values at both the toe and the heel.

20.8. Stresses on vertical sections of masonry dams.—Reference has already been made * to a paper by L. W. Atcherley and Professor Karl

* Loc. cit., p. 476.

Pearson in which the authors put forward a new point of view in the theoretical study of masonry dams. Their contention was that the method of guarding against tensile stress by a consideration of horizontal sections only was completely inadequate as in most existing dams an examination of stress distribution along vertical sections showed serious tensile stresses over a large part of the profile. Fig. 20.13 is the profile of a masonry dam of base width $2b$. The weight is W and the water pressure P. The line of resultant action for the reservoir full cuts the base at a distance e from the mid-point.

The distribution of normal stresses on the base is assumed as usual to be linear and to be represented by the diagram ACGB. The stresses

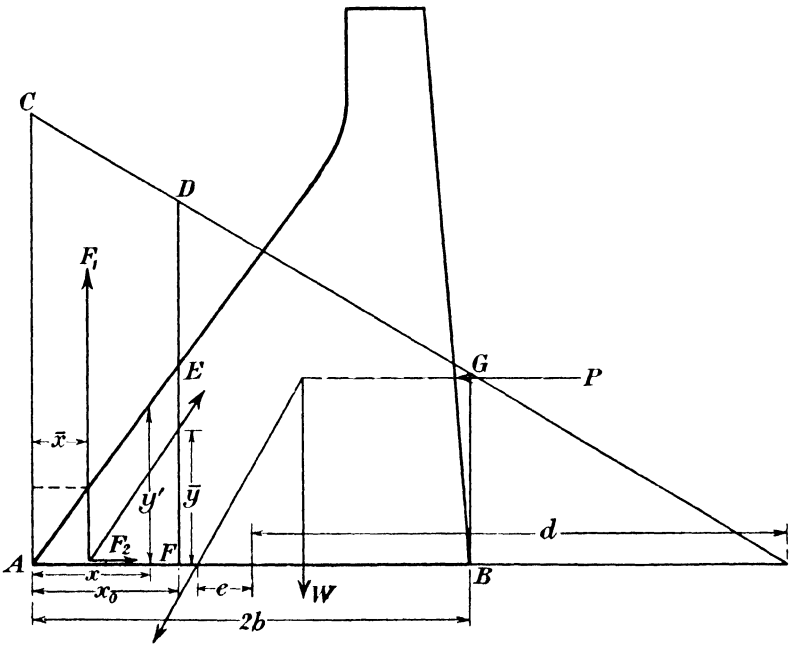

FIG. 20.13.

are in masonry units so that this diagram is the same area as the profile.

CG is produced to cut the line of AB and the distance from the intersection to the mid-point of the base is denoted by d.

If the normal stress at the mid-point of the base is f,

the stress at B is $$f\left(1-\frac{3e}{b}\right)$$

and $$\frac{d}{d-b}=\frac{f}{f\left(1-\frac{3e}{b}\right)}$$

from which $$d=\frac{b^2}{3e}.$$

The stress at a distance x from the toe is then

$$\frac{W}{2b}\left(\frac{d+b-x}{d}\right).$$

The assumption, which is very nearly true, that the front of the dam is linear for some distance from the base enables us to express the height at the distance x in the form

$$y'=mx.$$

The intercept between the front of the dam and the stress distribution curve is then, for this linear range,

$$y=\frac{W(d+b)}{2bd}-x\left(m+\frac{W}{2bd}\right)$$

and this represents the resultant upward intensity of stress on the base at x from the toe. The upward force on a length x_0 of the base is then $\int_0^{x_0} y\,dx$ so that

$$F_1=\frac{W(d+b)x_0}{2bd}-\frac{x_0^2}{2}\left(m+\frac{W}{2bd}\right).$$

Its vertical line of action is given by $\bar{x}=\frac{1}{F_1}\int_0^{x_0} yx\,dx$, or

$$\bar{x}=x_0\frac{\frac{1}{2}W(d+b)-\frac{1}{3}x_0(2bdm+W)}{W(d+b)-\frac{1}{2}x_0(2bdm+W)}.$$

The distribution of shear stress on the base is assumed to be parabolic in accordance with the principles discussed in paragraph 20.7 and to be represented by the equation

$$s=\frac{3P}{4b}\left(\frac{2bx-x^2}{b^2}\right).$$

Since this gives a zero value at the toe it would apply more accurately to a profile having a rectangular base section as indicated by the dotted line on the diagram. This is quite usual so that the assumed shear stress distribution is probably reasonably close to the actual. The total shearing force over a length of base x_0 is $\int_0^{x_0} s\,dx$, or

$$F_2=\frac{3P}{4b}\left(\frac{bx_0^2-\frac{1}{3}x_0^3}{b^2}\right).$$

The forces F_1, F_2 and the resultant forces on the face EF are in equilibrium, hence :—

Total shearing force on EF$=F_1$
and total thrust on EF$=F_2$.

If the line of action of the resultant of these two forces cuts EF at $\bar{y}$ from the base

$$\frac{\bar{y}}{x_0-\bar{x}}=\frac{F_1}{F_2}$$

which gives, upon substituting the values of $\bar{x}$, F_1 and F_2,

$$\bar{y}=\frac{b^2}{3\bar{P}d}\,\frac{W(d+b)-\frac{1}{3}x_0(2bdm+W)}{b-\frac{1}{3}x_0}.$$

This is the equation of the line of resistance for vertical sections for that portion of the dam over which the front face is approximately the straight line $y'=mx$. It is a hyperbola, the asymptotes of which are

$$x=3b$$

and

$$y=\frac{2bdm+W}{P}e.$$

The average shear stress on the vertical section is $\frac{F_1}{mx_0}$ since mx_0 is the height of the section EF. If the reasonable assumption is made that the maximum shear on the section is 50 per cent. greater than the mean,

$$s_{max}=\frac{3}{2}\,\frac{W(d+b)-\frac{1}{2}x_0(2bdm+W)}{2bdm}$$

which is a linear expression having its maximum value of $\frac{3}{4}\,\frac{W(d+b)}{bdm}$ masonry units at the toe of the dam. This emphasises the importance of thickening the toe as indicated by the dotted line in Fig. 20.13.

The maximum tensile stress on the section EF occurs at F and is

$$t=\frac{F_2}{mx_0}\left(\frac{6c}{mx_0}-1\right)$$

where $c=\bar{y}-\frac{mx_0}{2}$ is the eccentricity of loading on this section.

If the value of t is negative it indicates that the stress at F is compressive.

Substituting for c, F_2 and $\bar{y}$ the expression becomes

$$t=\frac{3}{2bdm^2}\{W(d+b)-\tfrac{1}{3}x_0(2bdm+W)\}-\frac{3P}{b^3m}x_0(b-\tfrac{1}{3}x_0),$$

which is a parabola with a vertical axis.

The value of t when $x_0=0$, *i.e.* at the toe, is

$$t_0=\frac{3W(d+b)}{2bdm^2}.$$

The maximum value occurs when $\frac{dt}{dx_0}=0$, *i.e.* when

$$-\frac{1}{2bdm^2}(2bdm+W)=\frac{3P}{b^3m}\left(b-\frac{2x_0}{3}\right)$$

or when

$$x_0=\frac{b^2}{2P}\left(\frac{2bdm+W}{2dm}\right)+\frac{3b}{2}$$

and is

$$t_{max}=t_0\left\{1-\frac{1}{12\epsilon}\left(3\epsilon+\frac{b}{x_0}\right)^2\right\}$$

where

$$\epsilon=\frac{3P}{bmt_0}.$$

The values of t_0 and t_{max} having been calculated the parabola can be plotted.

After the front of the dam departs from the linear a graphical method must be used to determine further points on the curves if these are found to be necessary. The procedure is as follows :—a vertical section is taken and the area bounded by this section, the normal stress curve and the front of the dam is obtained by a planimeter or otherwise. This gives the value of F_1, its line of action being through the centre of gravity of the area which is determined graphically. F_2 can be calculated directly from the formula. These two forces are compounded graphically and the value of $\bar{y}$ thus found. The stresses are then calculated in the usual way.

The authors of the paper which has been outlined above also considered the effect of assuming a linear distribution of shear stress across the horizontal section and found substantially the same qualitative results viz. that considerable tensile stresses existed in vertical sections for more than half the width of the dam measured from the toe. Their conclusions were tested by means of models. In one of these the profile was divided into horizontal laminas and in the other into vertical laminas. Under load applied to the back to represent fluid pressure the behaviour of these models was in accordance with their expectation from the theoretical considerations. Their general conclusions, given in the words of the paper itself, are as follows :—

" (1) The current theory of the stability of dams is both theoretically and experimentally erroneous, because :—

" (*a*) Theory shows that the vertical and not the horizontal sections are the critical sections.

" (*b*) Experiment shows that a dam first gives by tension of the vertical sections near the tail.

" (2) An accepted form of profile is shown to be stable as far as the horizontal sections are concerned, but unstable by applying the same conditions of stability to the vertical sections.

" (3) The distribution of shear over the base must be more nearly parabolic than uniform, but as no reversal of our statements follows when we pass from the former to the latter extreme hypothesis, it is not unreasonable to assume the former distribution will describe fairly closely the facts until we have greater knowledge.

" (4) In future we hold that in the first place masonry dams must be investigated for the stability of their vertical sections. If this be done we feel pretty certain that most existing dams will be found to

fail, if we accept the criteria of stability usually adopted for their horizontal sections. This failure can be met in two ways :—

"(*a*) By a modification of the customary profile. We think it probable that a profile like that of Vyrnwy dam would give better results than more usual forms.

"(*b*) By a frank acceptance that masonry, if carefully built, may be trusted to stand a definite amount of tensile stress. It is perfectly idle to assert that it is absolutely necessary that the line of resistance shall lie in the middle third for a horizontal treatment, when it lies well outside the middle third for at least half the dam for a vertical treatment."

CHAPTER 21

PRESSURE OF EARTH AND RETAINING WALLS

21.1. The general problem of earth pressure.—In the previous chapter it has been shown that the only physical property which has to be considered in the calculation of the pressure due to water on a dam is the weight of the water and, in consequence, the problem of external forces is a simple one. When, however, the retained material is earth the difficulty is increased very considerably, since earth possesses other physical characteristics which seriously influence its behaviour. Characteristics common to all earths are friction and cohesion; the relative importance of these depends upon the type of material under consideration. The term earth is comprehensive and includes materials as diverse as dry sand and stiff clay and elementary observation is sufficient to show that the behaviour of these two is very different. If, for example, dry sand is piled the sides of the heap will assume a definite angle and further material placed on these slopes will roll down the inclined surface. This angle is known as the angle of repose or the angle of friction for the material. A dry, undisturbed clay on the other hand can be cut to a steep, even a vertical, slope and in the absence of any change in moisture conditions will remain at that slope. The difference in behaviour of these two materials is explained by the cohesion which exists in the clay and is absent in the sand. Cohesion may be looked upon as a resistance to shear comparable with viscosity in a fluid. Not only, however, do earths which are fundamentally different in their constituents behave in different ways, but the same material under different conditions will behave just as diversely. If, for example, dry clay be pulverised, it will act like a granular material and assume a natural angle of repose when an attempt is made to pile it. If this pulverised clay be then mixed with varying quantities of water it can be given varying degrees of cohesion. As the amount of water is increased the cohesion increases to a maximum and then decreases until the mixture becomes so wet as to form a slurry. For purposes of pressure calculation it can then be treated as liquid.

Thus, while frictional effects are always present in a mass of earth those of cohesion may in extreme cases either be negligible or be the predominating factor. It will be evident that variations such as those described render problems connected with earth pressures very indeterminate and any attempt at a theoretical discussion must of necessity include assumptions which apply only to an idealised material.

Theories of earth pressure were formulated very early in the history of engineering science but in all cases it has been assumed that the material is dry and granular, free from cohesion and possessing only the

physical characteristics of weight and friction. Granular material, however, possesses certain distinctive features of its own which are known as dilatancy and arching and these exercise such a profound influence that no theory which neglects them can offer a satisfactory solution to the problem. It is essential to realise the strict limitations of existing classical theories of earth pressure and the various factors which may modify a design for a retaining wall in practice. Recently, through the work of Professor C. F. Jenkin, F.R.S., a real attempt has been made to discover the influence exerted by dilatancy on the behaviour of granular material. His work, which will be discussed later, is a definite step towards a real understanding of some of the factors which must be taken into account when dealing with problems of earth pressure.

21.2. Dilatancy.—A discussion of the principles of dilatancy has been given by Jenkin * in a paper in which he describes the difficulties he met in attempting to measure the coefficient of friction of sand. He found that it was impossible to get repeat results by the experimental methods which he adopted. One of these was to rotate a horizontal cylindrical disc immersed in sand and it was noticed that the moment the disc moved the surface of the sand heaved up, although the disc was six inches below the surface ; this indicated that the sand was expanding. To verify this phenomenon a test was made as follows :—a closed cylindrical vessel in which a second cylinder rotated had the space between the outer and inner cylinders completely filled with sand without ramming. When an attempt was made to rotate the inner cylinder it was found to be locked and 270 times the ordinary friction couple was needed to move it. Examination of the sand after the test revealed a quantity of fine dust, showing that rotation had not occurred until the sand was crushed. It was evident, therefore, that the closeness of packing of the grains of sand was an essential factor in determining its behaviour and small changes in packing can produce large effects. This phenomenon of expansion is known as dilatancy and was first observed by Osborne Reynolds in 1885.† He said, " As regards any results which may be expected to follow from the recognition of this property of dilatancy : in a practical point of view it will place the theory of earth pressure on a true foundation."

The principle of dilatancy is expressed by Jenkin as follows :—" The pressure in a granular mass depends on its weight, on the geometry of the boundaries and the geometry of all the points of contact between the grains and on the coefficient of friction on the points of contact. The term ' geometry of the points of contact ' is meant to include the composition and the inclinations of the minute surfaces of contact.

* " The Pressure exerted by Granular Material: an Application of the Principles of Dilatancy." C. F. Jenkin. Proc. Royal Society, Vol. 131, 1931, p. 54.

† " The Dilatancy of Media composed of Rigid Particles in Contact." Osborne Reynolds. Philosophical Magazine. December, 1885.

Changes in the geometry is the fundamental fact of dilatancy, the most striking fact being an increase in volume."

To demonstrate the importance of changes in geometry, Jenkin made two-dimensional models in which circular discs took the place of spherical grains and his paper contains an exhaustive discussion of experiments carried out by means of these models. The discs could be arranged in his apparatus in different modes of packing and he found that the forces exerted varied considerably with the mode.

This study enabled him to approach the problem of earth pressure from a different standpoint and to design apparatus which led to a new conception of the behaviour of granular material when held by a retaining wall. This theory will be dealt with at a later stage in this chapter.

21.3. Arching of granular material.—The phenomenon known as arching is best illustrated by a well-known experiment ascribed by P. M. Crosthwaite * to C. J. Meem. The latter enclosed sand in a long box open at the top and having a false bottom. This box was filled with sand which was tightly rammed and after consolidation the false bottom was removed. The sand remained in position supported by the friction of the sides of the box and, in addition, was able to carry a considerable surface load. Meem came to the conclusion that this could only be accounted for by the formation in the material of arches carrying the load to the sides of the box which acted as abutments.

A variation of this experiment is to fill a box with sand and to bore a small hole in the bottom. A small quantity of sand will then trickle out but even when considerable pressure is applied to the free surface of the sand no more will be forced out. This is again due to the formation by the grains of the material of a natural arch which is sufficiently strong to carry the superimposed load over the opening.

In a deep grain silo the pressure on the bottom is much less than would be expected from calculation made on the usual assumption of a linear relation between depth and pressure. After a certain depth is reached there is no increase in the bottom pressure, the load being taken by the arching of the grain to the sides of the silo.

This action has been relied upon by R. N. Stroyer in the design of flexible retaining walls.† These walls are firmly held at the base and anchored at the top so that these two points are fixed: the slight bulging of the wall between them is sufficient to allow arching to take place and a considerable amount of the earth pressure is transmitted directly to the top and bottom anchorages.

It is evident from these examples that arching exercises an important effect upon the distribution of pressure in a mass of granular material: unfortunately, it is not one that can readily be allowed for and no existing theory takes it into account.

We shall now discuss some of the theories of earth pressure which have been advanced, but it must be remembered that all of these are

* Proc. Inst. C.E., Vol. 203, p. 130.

† "Earth Pressure on Flexible Walls." R. N. Stroyer. Proc. Inst. C.E., Vol. 226, p. 116.

based upon certain assumptions which impose definite limitations upon their direct application to practical problems.

21.4. Rankine's theory of earth pressure.—One of the best known theories of earth pressure, due to Professor W. M. Rankine, is based on the assumption that the stresses in a mass of granular material obey the same laws as those in an elastic solid. The mass of earth under consideration is supposed to be unlimited in extent and free from cohesion; dilatancy and arching are neglected and pressures are assumed to increase linearly with the depth of material as in a fluid. In spite of the limitation imposed by these assumptions, the results obtained have been extensively used for the design of retaining walls.

Fig. 21.1 represents an elementary mass of granular material at a depth h below the horizontal earth surface.

It is assumed that the vertical pressure p at this depth is, following

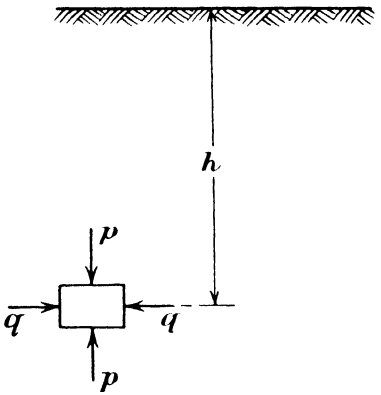

FIG. 21.1.

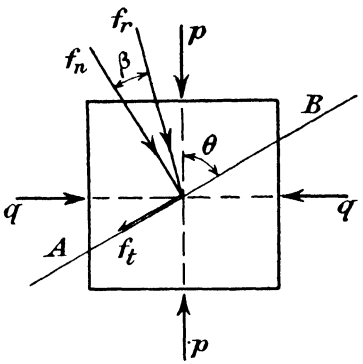

FIG. 21.2.

the hydrostatic law, equal to $\rho_e h$ where ρ_e is the density of the material. This pressure acting normally to a horizontal plane is a principal stress: there will be another principal stress q acting horizontally and it is first necessary to determine the ratio between them.

If AB in Fig. 21.2 is a plane through the elementary mass inclined at an angle θ to the direction of p, the component stresses normal and tangential to this plane are respectively *

$$f_n = p \sin^2 \theta + q \cos^2 \theta$$

and

$$f_t = (p-q) \sin \theta \cos \theta.$$

The resultant of these will be inclined to the normal to the plane at an angle β given by

$$\cot \beta = \frac{f_n}{f_t} = \frac{1}{p-q}(p \tan \theta + q \cot \theta).$$

* See any text-book on Strength of Materials.

When this has a minimum value, β is a maximum. Hence the greatest inclination of the resultant stress to the normal occurs when

$$\frac{d\,(\cot\beta)}{d\theta}=0$$

or when $$p\sec^2\theta-q\,\mathrm{cosec}^2\,\theta=0,$$

i.e., when $$\frac{p}{q}=\cot^2\theta.$$

Substitution of the values $\sqrt{\frac{p}{q}}$ and $\sqrt{\frac{q}{p}}$ for $\cot\theta$ and $\tan\theta$ in the general expression for $\cot\beta$ gives

$$\cot\beta_{max}=\frac{2\sqrt{pq}}{p-q}$$

If β_{max} is less than ϕ the angle of internal friction of the material, or the angle of repose, no slipping will occur along the plane BA : if it is equal to this angle slipping is just about to occur. Hence, just before slip occurs q is given by

$$\cot\phi=\frac{2\sqrt{pq}}{p-q}$$

or $$\mathrm{cosec}^2\,\phi=1+\cot^2\phi=\left(\frac{p+q}{p-q}\right)^2$$

i.e. $$\sin\phi=\frac{p-q}{p+q}$$

or $$\frac{q}{p}=\frac{1-\sin\phi}{1+\sin\phi}.$$

This value of q is thus the minimum lateral pressure which will maintain the equilibrium of the element and so, in a mass of granular material of unlimited extent,

$$q=\rho_e h\left(\frac{1-\sin\phi}{1+\sin\phi}\right).$$

21.5. Application of Rankine's theory to depth of foundation.—A simple application of this theory gives the depth of foundation necessary in such a material to sustain a given intensity of loading.

Suppose at a depth h, Fig. 21.3, a horizontal plane AB is loaded by external means to a stress of intensity f.

If f is less than $\rho_e h$ the plane will tend to rise due to the force exerted by the surrounding earth, and the earth at the sides of the plane will tend to sink. If f is greater than $\rho_e h$ the tendency will be for the plane to sink and for the earth at the sides to rise.

Consider two elementary contiguous masses of earth, one immediately under the plane having vertical and lateral stresses f and q' respectively and the other just away from the plane having stresses p and q where $p=\rho_e h$.

If $f > \rho_e h$ the minimum value of the lateral stress required to prevent downward movement is

$$q' = f\left(\frac{1-\sin\phi}{1+\sin\phi}\right).$$

Also the maximum value of the lateral stress, if upward movement of the earth at the sides is to be prevented, is

$$q = p\left(\frac{1+\sin\phi}{1-\sin\phi}\right).$$

But since the elements are contiguous q and q' are equal and the downward tendency has just been arrested if

$$f\left(\frac{1-\sin\phi}{1+\sin\phi}\right) = \rho_e h\left(\frac{1+\sin\phi}{1-\sin\phi}\right)$$

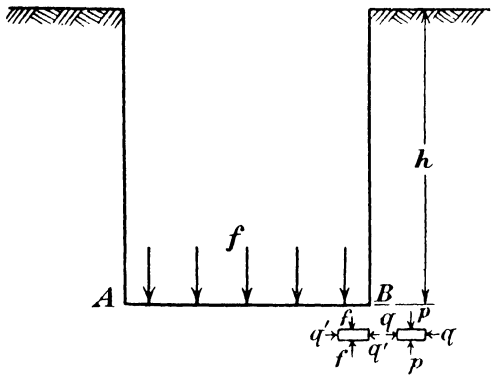

FIG. 21.3.

i.e. the minimum depth necessary to sustain f is

$$h_{\min} = \frac{f}{\rho_e}\left(\frac{1-\sin\phi}{1+\sin\phi}\right)^2.$$

If $f < \rho_e h$ the maximum lateral pressure which can be applied if no upward movement of the plane is to take place is

$$q' = f\left(\frac{1+\sin\phi}{1-\sin\phi}\right)$$

and the minimum lateral pressure if no downward movement of the earth at the side is to occur is

$$q = p\left(\frac{1-\sin\phi}{1+\sin\phi}\right).$$

As before $q = q'$

so

$$f\left(\frac{1+\sin\phi}{1-\sin\phi}\right) = \rho_e h\left(\frac{1-\sin\phi}{1+\sin\phi}\right)$$

and the maximum depth necessary to sustain f is therefore

$$h_{\max} = \frac{f}{\rho_e}\left(\frac{1+\sin\phi}{1-\sin\phi}\right)^2.$$

There are thus two limiting values for h between which a stress f can be maintained.

If h is less than the smaller value the plane will sink, if more than the larger value it will rise.

In the case of a fluid these two values are coincident, since $\phi=0$, and there is only one equilibrium position for a floating body: if it is lifted from that position it will sink back; if it is depressed it will rise.

If the stress f is applied by the pressure from a foundation the smaller value of h gives the minimum depth for equilibrium.

21.6. Application of Rankine's theory to retaining walls with no surcharge.—Fig. 21.4 shows a vertical plane through a mass of granular

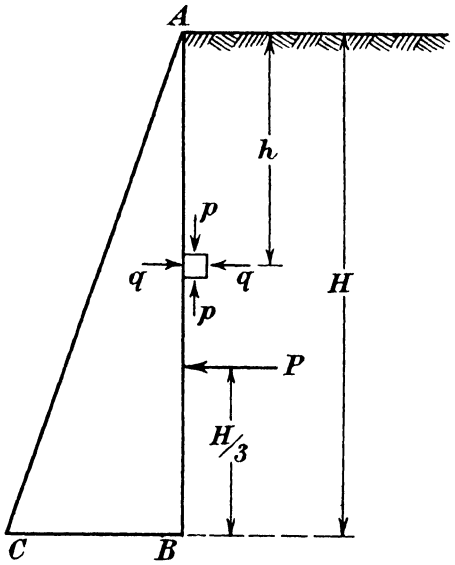

FIG. 21.4.

material. The lateral stress q at any depth on this plane is given by

$$q=\rho_s h\left(\frac{1-\sin\phi}{1+\sin\phi}\right)$$

which is represented by a straight line AC.

Rankine assumed that if the earth to the left of AB were removed and a wall built to retain the material to the right of the section the pressures on this wall would be the same as those on the ideal plane AB.

He therefore took the total pressure on a wall of height H to be given by the area of the triangle ABC,

or

$$P=\frac{\rho_s H^2}{2}\left(\frac{1-\sin\phi}{1+\sin\phi}\right)$$

and this was assumed to act through the centre of gravity of the triangle, *i.e.* at H/3 from the bottom of the wall.

Later work has shown that this assumption is not correct: the centre of pressure is not necessarily at the third point and in some cases departs considerably from it. The presence of the wall invalidates the initial assumption of an unlimited extent of earth and the pressure distribution on the wall is considerably modified.

The result just obtained was only applied by Rankine to walls in which the surface of the earth was level with the top of the wall, that is when there was no surcharge. The treatment for surcharged walls will be dealt with in succeeding paragraphs.

21.7. Theory of conjugate stresses.—Before proceeding to Rankine's theory of surcharged retaining walls it is necessary to deal with certain problems of complex stress.

Fig. 21.5 shows principal stresses f_x and f_y acting on an element: in (*a*) the stresses are alike, in (*b*) they are opposite in sign.

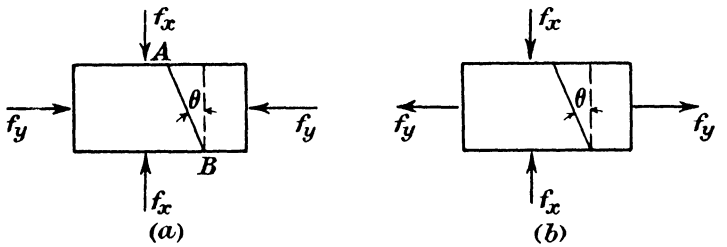

FIG. 21.5.

On any plane AB inclined at an angle θ to the direction of f_x, the normal and tangential stresses are

Case (*a*)
$$f_n = f_y \cos^2\theta + f_x \sin^2\theta$$
$$f_t = \frac{f_y - f_x}{2} \sin 2\theta$$

Case (*b*)
$$f_n = -f_y \cos^2\theta + f_x \sin^2\theta$$
$$f_t = -\frac{f_y + f_x}{2} \sin 2\theta.$$

The resultant stress is given in either case by

$$f_r = \sqrt{f_n^2 + f_t^2}$$

and this is inclined to the normal to AB at an angle β given by

$$\tan\beta = f_t/f_n.$$

If f_x and f_y are numerically equal, f_r and β are given in the two cases by the following:—

Case (*a*)
$$f_r = f_x$$
$$\beta = 0.$$

Case (*b*)
$$f_r = f_x$$
$$\beta = 2\theta.$$

Suppose now we have two unequal stresses p_x and p_y acting normally to the faces of the element.

These stresses can be written

$$p_x = \frac{p_x+p_y}{2} + \frac{p_x-p_y}{2}$$

$$p_y = \frac{p_x+p_y}{2} - \frac{p_x-p_y}{2}.$$

The resultant stresses on any plane at θ to the direction of p_x can then be found by superimposing the effects of two equal, like stresses $\frac{p_x+p_y}{2}$ upon the effects of two equal and unlike stresses $\frac{p_x-p_y}{2}$.

The compounding of these is most readily done by the use of vectors as shown in Fig. 21.6 where AB represents to scale the resultant $\frac{p_x+p_y}{2}$ of the two equal like stresses: this acts normal to the plane. BC represents the resultant $\frac{p_x-p_y}{2}$ of the equal unlike stresses, acting at 2θ to the plane. Then AC represents the resultant of these two, inclined at the angle α to the normal.

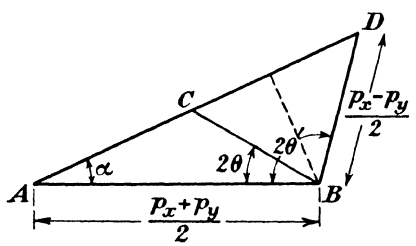

FIG. 21.6.

If we produce AC to D such that BD=BC, it is clear that AD is also a resultant of two stresses $\frac{p_x+p_y}{2}$ and $\frac{p_x-p_y}{2}$ and there must therefore, if angle ABD$=2\theta'$, be another plane inclined at θ' to the direction of p_x upon which the resultant acts at α to the normal. The two planes inclined at θ and θ' to the direction of p_x upon which the resultant stress is inclined at the same angle to the normal are called conjugate planes and the stresses represented by AC and AD are called conjugate stresses.

21.8. Rankine's theory of surcharged walls.—In Fig. 21.7 let AB be the back of a vertical wall retaining earth surcharged at an angle i.

It is assumed that the pressure acts parallel to the surface of the earth so that at any depth h the stresses p_1 and p_2 act as shown. p_1 and p_2 are resultant stresses and since they both act at an angle i to the normals on their respective planes they are conjugate and can be represented by the vectors AC and AD of Fig. 21.6.

At the point we are considering let the principal stresses be p_x and p_y. It should be noted that these are not vertical and horizontal; their directions are unknown.

Then, as before,

$$p_x = \frac{p_x+p_y}{2} + \frac{p_x-p_y}{2}$$

and

$$p_y = \frac{p_x+p_y}{2} - \frac{p_x-p_y}{2}.$$

Also $$\frac{p_2}{p_1}=\frac{AC}{AD}.$$

The vertical intensity of pressure on a horizontal face is $\rho_e h$, and p_1 which acts on a face at i to the horizontal is therefore given by

$$p_1=\rho_e h \cos i.$$

Hence $$p_2=\frac{AC}{AD}\rho_e h \cos i.$$

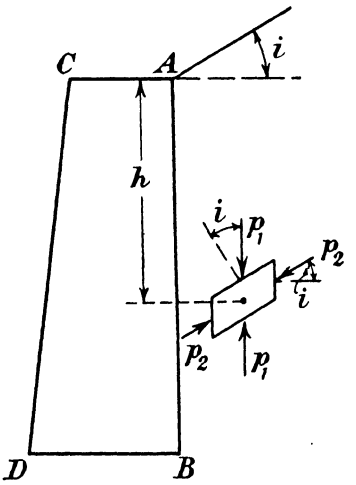

FIG. 21.7.

From the vector diagram of Fig. 21.6

$$BC^2=AC^2+AB^2-2AB \cdot AC \cdot \cos i$$

$$\therefore \quad AC^2-AC(p_x+p_y)\cos i+\left(\frac{p_x+p_y}{2}\right)^2-\left(\frac{p_x-p_y}{2}\right)^2=0,$$

i.e. $$AC^2-AC(p_x+p_y)\cos i+p_x p_y=0.$$

and $$AC=\frac{(p_x+p_y)\cos i-\sqrt{(p_x+p_y)^2\cos^2 i-4p_x p_y}}{2}.$$

In a similar manner

$$AD=\frac{(p_x+p_y)\cos i+\sqrt{(p_x+p_y)^2\cos^2 i-4p_x p_y}}{2}$$

so $$\frac{AC}{AD}=\frac{(p_x+p_y)\cos i-\sqrt{(p_x+p_y)^2\cos^2 i-4p_x p_y}}{(p_x+p_y)\cos i+\sqrt{(p_x+p_y)^2\cos^2 i-4p_x p_y}}$$

$$=\frac{\cos i-\sqrt{\cos^2 i-\frac{4p_x p_y}{(p_x+p_y)^2}}}{\cos i+\sqrt{\cos^2 i-\frac{4p_x p_y}{(p_x+p_y)^2}}}.$$

The ratio of the principal stresses at the moment when slipping is about to occur is

$$\frac{p_x}{p_y}=\frac{1+\sin\phi}{1-\sin\phi}$$

$$\therefore \qquad \left(\frac{p_x-p_y}{p_x+p_y}\right)^2=\sin^2\phi$$

and $$\frac{(p_x-p_y)^2-(p_x+p_y)^2}{(p_x+p_y)^2}=\sin^2\phi-1$$

or $$\frac{4p_xp_y}{(p_x+p_y)^2}=\cos^2\phi.$$

Therefore $$\frac{AC}{AD}=\frac{\cos i-\sqrt{\cos^2 i-\cos^2\phi}}{\cos i+\sqrt{\cos^2 i-\cos^2\phi}}$$

and $$p_2=\rho_e h\cos i\,\frac{\cos i-\sqrt{\cos^2 i-\cos^2\phi}}{\cos i+\sqrt{\cos^2 i-\cos^2\phi}}.$$

The total pressure on a wall of height H is then

$$P=\frac{\rho_e H^2}{2}\cos i\,\frac{\cos i-\sqrt{\cos^2 i-\cos^2\phi}}{\cos i+\sqrt{\cos^2 i-\cos^2\phi}}$$

$$=\frac{\rho_e H^2}{2}K$$

where $$K=\cos i\,\frac{\cos i-\sqrt{\cos^2 i-\cos^2\phi}}{\cos i+\sqrt{\cos^2 i-\cos^2\phi}}.$$

When the wall is unsurcharged, *i.e.* when $i=0$, this reduces to the previous result,

$$P=\frac{\rho_e H^2}{2}\left(\frac{1-\sin\phi}{1+\sin\phi}\right).$$

When i has its maximum possible value ϕ,

$$P=\frac{\rho_e H^2}{2}\cos\phi.$$

In each case P acts at H/3 from the base of the wall and parallel to the earth surface.

Retaining wall with battered back.—If the back of the wall, AB in Fig. 21.8, is battered at an angle α the pressure on the face AB is compounded of the weight of the wedge ACB and the pressure P on CB the vertical through B.

The height $CB=h=H(1+\tan\alpha\tan i)=mH$, say.

Then $$P=\frac{\rho_e m^2 H^2}{2}K$$

and the weight of the wedge ACB is

$$W=\frac{\rho_e m H^2}{2}\tan\alpha.$$

The vector diagram for these two forces is shown in Fig. 21.8 and the resultant is given by

$$R^2=P^2+W^2+2WP\sin i$$
$$=\left(\frac{\rho_e H^2 m}{2}\right)^2\{m^2K^2+\tan^2\alpha+2Km\tan\alpha\sin i\}$$

i.e. $$R=\frac{\rho_e H^2 m}{2\cos\alpha}\sqrt{m^2K^2\cos^2\alpha+\sin^2\alpha+2Km\sin\alpha\cos\alpha\sin i}.$$

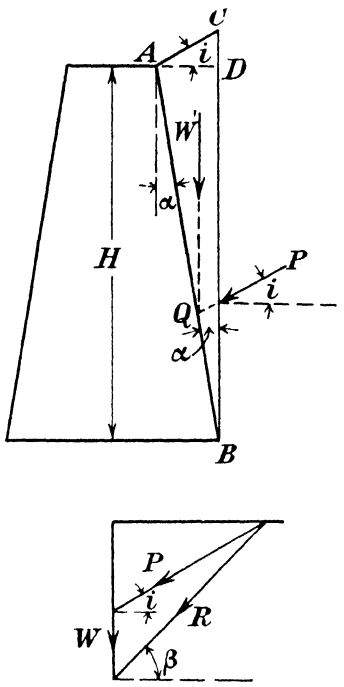

FIG. 21.8.

Substituting $m=1+\tan\alpha\tan i=\frac{\cos(i-\alpha)}{\cos i\cos\alpha}$ we find

$$R=\frac{\rho_e H^2}{2}\cos(i-\alpha)\sec i\sec^2\alpha$$
$$\times\sqrt{K^2\cos^2(i-\alpha)\sec^2 i+\sin^2\alpha+2K\cos(i-\alpha)\tan i\sin\alpha}.$$

If β is the angle which R makes with the horizontal

$$\tan\beta=\frac{W+P\sin i}{P\cos i}=\frac{W}{P}\sec i+\tan i$$
$$=\frac{\tan\alpha}{mK\cos i}+\tan i$$

or $$\tan\beta=\frac{1}{K}\sec(i-\alpha)\sin\alpha+\tan i.$$

The line of action of P is parallel to AC and cuts BC at $h/3$ from B. It therefore cuts BA at Q, *i.e.* H/3 from B measured vertically.

The line of action of W is one-third of DA from D and is parallel to CB and also meets AB at Q.

Hence the reaction R acts at Q, *i.e.* at H/3 measured vertically above the base.

21.9. The wedge theory of earth pressure.—In Fig. 21.9, BA represents the back of a wall retaining earth at a slope BC. The natural slope of the material is AC making an angle ϕ, the angle of repose, with the horizontal. In the absence of the wall the earth is supposed to slide

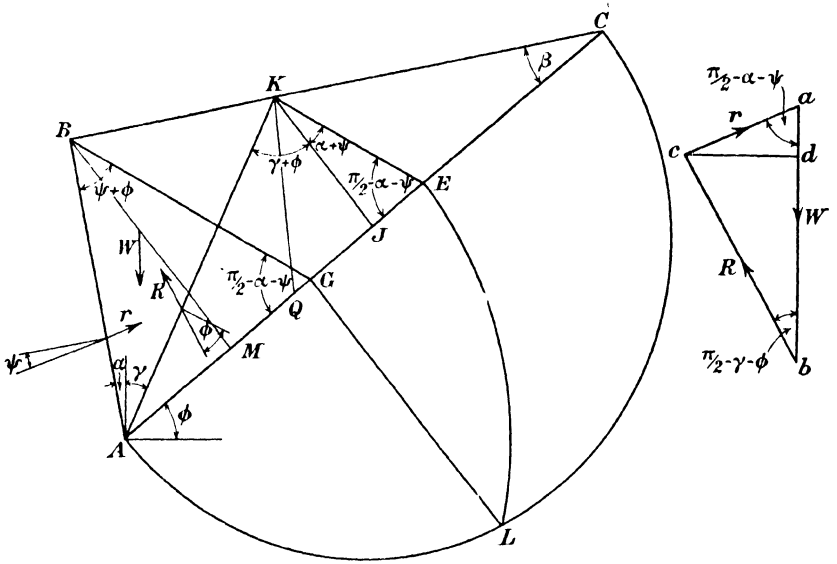

FIG. 21.9.

along some plane represented by AK, known as the plane of rupture, which is chosen so that the pressure due to the wedge BAK on the wall has the greatest possible value.

The wedge is in equilibrium under the action of W, the weight of earth forming it, the reaction R from the main mass of earth behind the plane of rupture and the reaction r from the wall. R is inclined at ϕ to the normal to the plane AK and r is inclined at ψ to the normal to the wall where $\tan\psi$ is the coefficient of friction between the material and the wall. Let BC and AC meet at C where angle $BCA=\beta$. From B draw BG at $\psi+\phi$ to AB and draw KE parallel to BG.

Let the batter of the wall be α and the angle between the plane of rupture and the vertical be γ.

From K and B draw KJ and BM perpendicular to AC.

Then angle $KAJ=90-\gamma-\phi$,

$AKJ=\gamma+\phi$,

$KEJ=BGA=90-(\alpha+\psi)$

and $EKJ=\alpha+\psi$.

The vector diagram for the three forces W, R and r is shown in the figure whence

$$ad = r \sin(\alpha+\psi)$$

$$bd = cd \tan(\gamma+\phi) = r \cos(\alpha+\psi) \tan(\gamma+\phi)$$

$$\therefore \quad W = ad+bd = r\{\sin(\alpha+\psi)+\cos(\alpha+\psi)\tan(\gamma+\phi)\}$$

or
$$r = \frac{W}{\sin(\alpha+\psi)+\cos(\alpha+\psi)\tan(\gamma+\phi)}.$$

If we consider a unit thickness of wedge,

$$r = \frac{\rho_e \cdot ABK}{\sin(\alpha+\psi)+\cos(\alpha+\psi)\tan(\gamma+\phi)}.$$

Writing a, x and b for the lengths BG, KE and AC respectively this becomes

$$r = \frac{\rho_e b(a-x)\cos(\alpha+\psi)}{2\{\sin(\alpha+\psi)+\cos(\alpha+\psi)\tan(\gamma+\phi)\}}$$

since $BM = a\cos(\alpha+\psi)$

and $KJ = x\cos(\alpha+\psi)$.

On reduction
$$r = \frac{\rho_e b(a-x)}{2\{\tan(\alpha+\psi)+\tan(\gamma+\phi)\}}.$$

Now
$$\tan(\gamma+\phi) = \frac{AJ}{JK} = \frac{b-KJ\cot\beta}{x\cos(\alpha+\psi)}$$

and substituting for KJ we have

$$\tan(\gamma+\phi) = \frac{b}{x\cos(\alpha+\psi)} - \cot\beta$$

$$\therefore \quad r = \frac{\rho_e b\cos(\alpha+\psi)}{2}\left\{\frac{x(a-x)}{x\sin(\alpha+\psi)+b-x\cos(\alpha+\psi)\cot\beta}\right\}.$$

For a maximum
$$\frac{dr}{dx} = 0$$

or
$$ab - x^2\sin(\alpha+\psi) - 2bx + x^2\cos(\alpha+\psi)\cot\beta = 0$$

which can be expressed in the form

$$b(a-x) = x\{b - x\cos(\alpha+\psi)\cot\beta + x\sin(\alpha+\psi)\}.$$

Now the area ABK
$$= \frac{b}{2}(a-x)\cos(\alpha+\psi),$$

and the area AKE
$$= \frac{KJ}{2}(b-CE)$$

$$= \frac{KJ}{2}(b-CJ+JE)$$

$$= \frac{KJ}{2}(b-KJ\cot\beta+JE),$$

or, substituting for these lengths,

$$\text{Area AKE}=\frac{x\cos(\alpha+\psi)}{2}\{b-x\cos(\alpha+\psi)\cot\beta+x\sin(\alpha+\psi)\}.$$

Hence the condition that r shall be a maximum is

$$\frac{2(\text{area ABK})}{\cos(\alpha+\psi)}=\frac{2(\text{area AKE})}{\cos(\alpha+\psi)}$$

or for a maximum thrust on the wall

$$\text{Area ABK}=\text{area AKE}.$$

To find the position of K which will satisfy this condition we proceed as follows :

Let the length AG be represented by m,
and AE by n.

Then since area ABK=AKE,

$$\frac{b}{2}(a-x)\cos(\alpha+\psi)=\frac{\text{KJ}}{2}(b-\text{CE})$$

or
$$b(a-x)=x(b-\text{CE})=xn$$

$\therefore$
$$\frac{b}{n}=\frac{x}{a-x}.$$

But
$$\frac{x}{a}=\frac{\text{CE}}{\text{CG}}$$

$\therefore$
$$\frac{x}{a-x}=\frac{\text{CE}}{\text{CG}-\text{CE}}=\frac{b-n}{n-m}.$$

Hence
$$\frac{b}{n}=\frac{b-n}{n-m},$$

or
$$n^2=bm,$$

from which n is calculable and so K may be found.

The triangle AKE and the vector diagram are similar figures.

$\therefore$
$$\frac{\text{AE}}{\text{EK}}=\frac{ab}{ac}=\frac{\text{W}}{r}.$$

Make EQ=EK.

Then
$$\frac{\text{AE}}{\text{EQ}}=\frac{\text{W}}{r}$$

and
$$\frac{\text{area AEK}}{\text{area EQK}}=\frac{\text{W}}{r}$$

therefore
$$\frac{\text{area EQK}}{\text{area ABK}}=\frac{r}{\text{W}}$$

and the area of the triangle EQK represents the resultant pressure on the wall to the same scale that ABK represents the weight of the wedge. EQK is called the pressure triangle.

This pressure is assumed to act at one-third of the height of the wall from the base as in the Rankine theory, but it will be shown later that this is not a justifiable assumption.

The resultant pressure is most readily found graphically by the following construction.

Describe a semi-circle on AC. Draw BG at $\psi+\phi$ to AB and from G draw GL perpendicular to AC to meet the semi-circle at L.

With A as centre and AL as radius strike the arc LE to cut AC. From E draw EK parallel to GB. KA is the required line of rupture. Make EQ=EK and EQK is the pressure triangle.

Since
$$AG \cdot GC = GL^2$$
$$AG^2 + AG \cdot GC = AG^2 + GL^2$$
$$AG(AG+GC) = AL^2 = AE^2$$
or
$$mb = AE^2$$
$\therefore$
$$AE = n \text{ as required.}$$

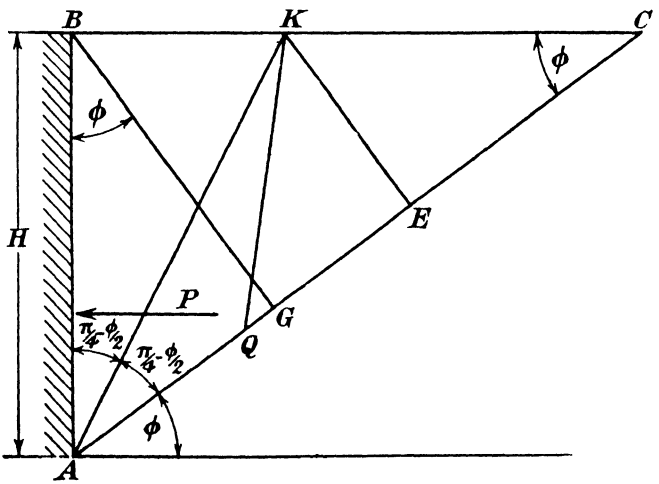

FIG. 21.10.

The value of ψ is often taken as ϕ, a reasonable assumption in the absence of more exact data, but on the grounds that the value may be lessened if the material in contact with the wall is wet it may be taken as $\phi/2$, which is also a common value to assign to it. In the early form of the wedge theory due to Coulomb the friction on the wall was neglected, *i.e.* ψ was made zero; this, however, leads to very thick walls and is clearly not a justifiable assumption.

In the particular case when there is no surcharge and the back of the wall is vertical and $\psi=0$ as shown in Fig. 21.10.

BG is perpendicular to AC,

KE is perpendicular to AC

and AK therefore bisects BAC.

Then the pressure on the wall is

$$P=\rho_e \text{ (area of pressure triangle)}$$

or $$P=\frac{\rho_e}{2}.KE^2.$$

But $$KE=EC\tan\phi$$
$$=(AC-AE)\tan\phi$$
$$=H(\operatorname{cosec}\phi-1)\tan\phi$$
$$=H\left(\frac{1-\sin\phi}{\cos\phi}\right)$$

$$P=\frac{\rho_e H^2}{2}\left(\frac{1-\sin\phi}{\cos\phi}\right)^2=\frac{\rho_e H^2}{2}\frac{(1-\sin\phi)^2}{1-\sin^2\phi}$$

or $$P=\frac{\rho_e H^2}{2}\left(\frac{1-\sin\phi}{1+\sin\phi}\right)$$

as given by the Rankine theory for this case.

21.10. Jenkin's revised wedge theory.—As a result of the experimental work previously mentioned, Professor Jenkin has advanced a new form of the wedge theory * which takes into account phenomena arising from the dilatancy of granular material.

He found that when a model retaining wall was allowed to move away slightly from the granular material which it supported, a plane

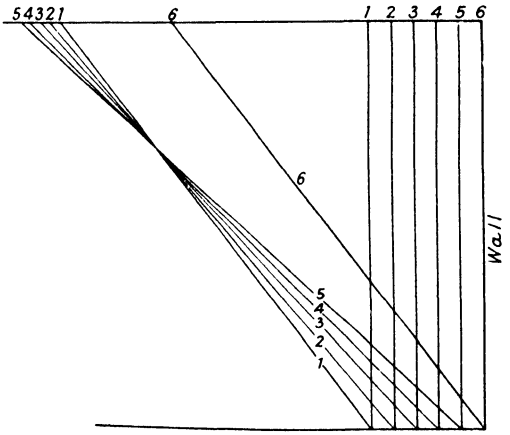

FIG. 21.11.

of rupture developed in accordance with the original wedge theory ot the behaviour of such material. This rupture showed that the interlocking of the particles had been destroyed and the material was then in a state when slip could occur. The surface behind the wall was then brought up to its original level by the addition of material and the wall allowed to move slightly again. A new plane ot rupture then developed

* "The Pressure on Retaining Walls." C. F. Jenkin. Proc. Inst. C.E., Vol. 234, 1931-2, Part 3, p. 103.

at a different angle from the first and it was found that when the process of making good the surface and moving the wall was continued there was a definite cycle of events. The angle of the plane of rupture became flatter until a certain limiting angle was reached, when it returned suddenly to the original value; the cycle then repeated. The variation of the force required to maintain the equilibrium was also cyclical. This is illustrated in Fig. 21.11 where the numbers denote consecutive positions of the wall and the corresponding planes of rupture.

It is necessary therefore to find the particular plane of rupture which will produce the maximum force on the wall since this will be the criterion in design.

When the back of the wall had a large positive batter the experiments showed that another plane of rupture developed as shown at BA in

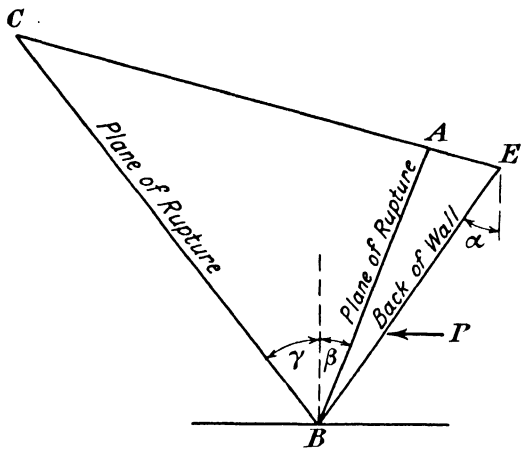

FIG. 21.12.

Fig. 21.12. The existence of this plane has usually been ignored in theories of earth pressure, but Jenkin shows that it has an important influence upon the value of the thrust on the wall. Clearly this second plane of rupture can only occur if α is greater than β. The modified wedge theory taking account of these factors will now be discussed. The symbols used are as follows: reference should be made to Fig. 21.13.

α=The batter of a plane wall, *i.e.* the angle between the back of the wall BE and the vertical plane.

β=The angle between the front plane of rupture, BA, and the vertical plane.

γ=The angle between the back plane of rupture, BC, and the vertical plane.

i=The angle of surcharge (+when above the horizontal
−when below the horizontal).

ρ_s=The weight per cubic foot of the granular material.

W=The weight of the wedge of sand, 1 foot thick. When there are two planes of rupture, it is contained between the two

planes of rupture : when there is only one plane of rupture, it is contained between the plane of rupture and the wall.

ϕ=The minimum friction angle between two faces of sand when moving past each other.

Φ=The maximum friction angle between two faces of sand just before rupture occurs.

ψ=The friction angle between the sand and the back of the wall. In most cases $\psi=\phi$.

z_1 and z_2=The friction angles on the front and back faces of the wedge.

z_1 may have the values of ϕ, Φ or ψ

z_2 may have the values ϕ or Φ but since ϕ gives the worst case it is taken in design.

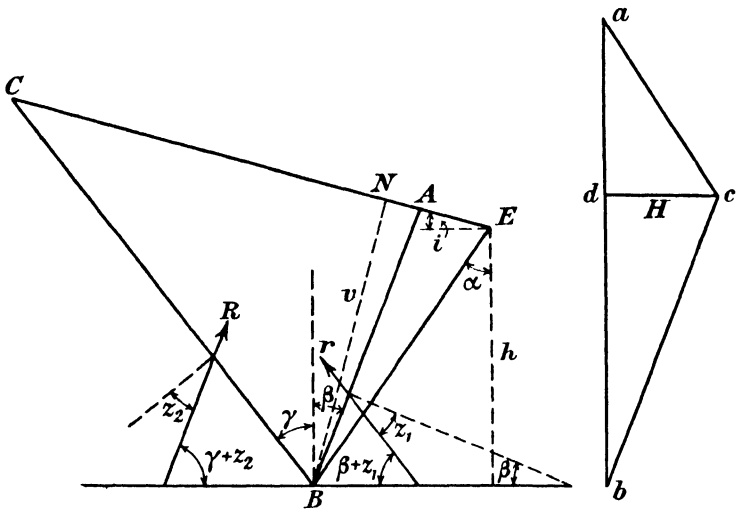

FIG. 21.13.

θ=The angle between the resultant force on the wall and the normal to the wall. When there is only one plane of rupture $\theta=\psi$. When there are two planes of rupture $\theta<\psi$.

H=The horizontal force exerted by the sand. It has the same value on the back plane of rupture, on the front plane of rupture and on the wall.

V=The vertical component of the force exerted by the sand on the wall. For plane walls V=H tan $(\theta+\alpha)$.

h=The height of the wall, measured vertically.

x=The ratio of the height of the centre of pressure to the height of the wall.

v=The length of the normal from the foot of a plane wall on to the surface of the sand,

i.e. $$v=\frac{h\cos(\alpha-i)}{\cos\alpha}.$$

The first case to be considered is that of a wall in which there is no second plane of rupture, *i.e.* when the batter is such that $\alpha < \beta$.

This case is exactly similar to that discussed in the earlier wedge theory. The minimum angle of repose is taken for the value of ϕ and ψ is either found experimentally or assumed. Unless the wall is very smooth ψ may be taken as equal to ϕ.

The magnitude of the greatest horizontal thrust may be found by assuming a number of planes of rupture, calculating H for each and then plotting a curve of H against γ, and by direct mathematical calculation, or graphically as described in paragraph 21.9.

The point on the back of the wall at which this thrust may be assumed to act, that is the centre of pressure, varies considerably according to the conditions of the problem and will be discussed later.

When there are two planes of rupture the simple methods of determining the maximum thrust H, used in the foregoing case, are not applicable and a more complicated analysis is necessary. EB in Fig. 21.13 represents the battered face of a wall retaining granular material. EC is the surface of the sand, BC is the back plane of rupture and BA the front plane of rupture.

R, the resultant force on BC, acts at an angle z_2 to the normal to BC and r the resultant force on AB at an angle z_1 to the normal to AB. The points of application of these forces are not known but only their directions.

Draw BN normal to CE and let its length be v.

The weight of the wedge CAB is

$$W = \frac{\rho_e v}{2}(CA)$$

$$= \frac{\rho_e v^2}{2}\{\tan(\gamma + i) + \tan(\beta - i)\}.$$

The vector polygon for the forces W, R and r is shown in Fig. 21.13 and cd represents H.

From triangles acd and bcd we have

$$\frac{H}{\sin a} = \frac{ad}{\sin acd}$$

and

$$\frac{H}{\sin b} = \frac{bd}{\sin bcd},$$

from which

$$ab = ad + bd = H\left\{\frac{\sin acd}{\sin a} + \frac{\sin bcd}{\sin b}\right\}$$

or

$$\frac{ab}{H} = \frac{\sin a \sin bcd + \sin b \sin acd}{\sin a \sin b}$$

$$= \frac{\cos acd \sin bcd + \cos bcd \sin acd}{\sin a \sin b}$$

$$= \frac{\sin c}{\sin a \sin b}.$$

Hence $$H=\frac{W \sin a \sin b}{\sin c}.$$

From the diagram it is clear that angle

$$a=\frac{\pi}{2}-(\beta+z_1)$$

$$b=\frac{\pi}{2}-(\gamma+z_2)$$

$$c=\beta+\gamma+z_1+z_2$$

so that substituting for W, a, b and c we have

$$H=\frac{\frac{\rho_e v^2}{2}\{\tan(\gamma+i)+\tan(\beta-i)\}\cos(\beta+z_1)\cos(\gamma+z_2)}{\sin(\beta+\gamma+z_1+z_2)} \qquad (1)$$

The values of z_1 and z_2 are assumed to be known and we have to determine what values of β and γ will give the maximum value of H.

The conditions for H to be a maximum are

$$\left.\begin{aligned}\frac{\partial H}{\partial \beta}&=0\\ \frac{\partial H}{\partial \gamma}&=0\end{aligned}\right\}$$

Partially differentiating the expression for H with respect to β and equating to zero gives

$$\sin(\beta+\gamma+z_1+z_2)[\sec^2(\beta-i)\cos(\beta+z_1)-\{\tan(\gamma+i)+\tan(\beta-i)\}\sin(\beta+z_1)]-\{\tan(\gamma+i)+\tan(\beta-i)\}\cos(\beta+z_1)\cos(\beta+\gamma+z_1+z_2)=0$$

which reduces simply to

$$\frac{\sec^2(\beta-i)\cos(\beta+z_1)\sin(\beta+\gamma+z_1+z_2)}{\cos(\gamma+z_2)\{\tan(\gamma+i)+\tan(\beta-i)\}}=1. \quad \therefore \quad (2)$$

Similarly, $\frac{\partial H}{\partial \gamma}=0$ gives

$$\frac{\sec^2(\gamma+i)\cos(\gamma+z_2)\sin(\beta+\gamma+z_1+z_2)}{\cos(\beta+z_1)\{\tan(\gamma+i)+\tan(\beta-i)\}}=1 \quad . \quad . \quad . \quad (3)$$

The simultaneous solution of these two equations for β and γ is laborious, but in his paper Jenkin gives a short table of their values for various values of i and ϕ. This is reproduced (Table 21.1), but it must be remembered that it only applies to cases where there are two planes of rupture, *i.e.* when $\alpha>\beta$. The values of z_1 and z_2 have been taken as ϕ. Full tables have since been prepared by the Department of Scientific and Industrial Research * and these should be used for design purposes.

To obtain the maximum magnitude of the thrust on such a wall as we have discussed, the values of β and γ are found from Table 21.1. If $\alpha>\beta$ the table is valid: if $\alpha<\beta$ the wall should be designed as

* "Earth Pressure Tables." H.M. Stationery Office.

explained for the case when there is only one plane of rupture. Using these values of β and γ, H is calculated from equation (1).

TABLE 21.1.

If $i>0$, γ is the larger angle and β the smaller angle.
If $i<0$, β is the larger angle and γ the smaller angle.

i	$\phi=45°$						$\phi=40°$						$\phi=35°$					
$\pm°$	°	′	″	°	′	″	°	′	″	°	′	″	°	′	″	°	′	″
45		0		45	0	0		—			—			—			—	
40	9	48	50	35	11	10		0		50	0	0		—			—	
35	12	53	45	32	6	15	10	55	0	39	5	0		0		55	0	0
30	15	0	0	30	0	0	14	28	5	35	31	55	12	10	15	42	49	45
25	16	38	55	28	21	5	16	56	45	33	3	15	16	16	10	38	43	50
20	18	2	10	26	57	50	18	55	35	31	4	25	19	11	50	35	48	10
15	19	15	55	25	44	5	20	37	40	29	22	20	21	35	20	33	24	40
10	20	23	30	24	36	30	22	9	50	27	50	10	23	41	20	31	18	40
5	21	27	35	23	32	25	23	36	15	26	23	45	25	37	45	29	22	15
0	22	30	0	22	30	0	25	0	0	25	0	0	27	30	0	27	30	0

i	$\phi=30°$						$\phi=25°$						$\phi=20°$					
$\pm°$	°	′	″	°	′	″	°	′	″	°	′	″	°	′	″	°	′	″
30		0		60	0	0		—			—			—			—	
25	13	38	25	46	21	35		0		65	0	0		—			—	
20	18	25	10	41	34	50	15	29	10	49	30	50		0		70	0	0
15	21	54	45	38	5	15	21	6	5	43	53	55	17	54	40	52	5	20
10	24	50	20	35	9	40	25	22	10	39	37	50	24	44	40	45	15	20
5	27	28	50	32	31	10	29	3	0	35	57	0	30	7	5	39	52	55
0	30	0	0	30	0	0	32	30	0	32	30	0	35	0	0	35	0	0

i	$\phi=15°$						$\phi=10°$						$\phi=5°$					
$\pm°$	°	′	″	°	′	″	°	′	″	°	′	″	°	′	″	°	′	″
15		0		75	0	0		—			—			—			—	
10	21	25	50	53	34	10		0		80	0	0		—			—	
5	30	9	40	44	50	20	27	26	10	52	33	50		0		85	0	0
0	37	30	0	37	30	0	40	0	0	40	0	0	42	30	0	42	30	0

The actual force on the front plane of rupture is

$$r=\text{H sec } (\beta+\phi)$$

which acts at an angle $\beta+\phi$ with the horizontal. The weight of dead sand represented by the area ABE is calculated and added vectorially to r to give the actual resultant thrust on BE.

Position of centre of pressure.—As already stated it has been usual in theories of earth pressure to assume that the centre of pressure was at one-third of the height from the bottom of the wall by analogy

with fluid pressure. The experiments upon which the revised wedge theory is based show that this is not the case and that the centre of pressure varies between wide limits. Recorded values in the tests ranged from about ·25 to ·54 of the height of the wall. Until further experimental work has made the position more certain Jenkin recommends that the following values should be used :—

For batters from −10° to 25° assume 0·04.
For larger positive batters assume 0·45.
For batters of −15° to −30° assume 0·33.

A special case arises when the surcharge is nearly the same as the angle of repose and it is recommended that when it is within 3° of that angle x shall be taken as ·55.

21.11. Determination of profiles for retaining walls.—In paragraph 20.2 the methods by which a gravity dam may fail were described and a retaining wall may fail in any of these ways. The method of analysis is the same except that in the case of a retaining wall the earth pressure, calculated from one of the theories described in this chapter, is used instead of the water pressure. For a trapezoidal section, which is the common profile except in reinforced concrete construction the process is generally one of trial and error but it is possible, working on the Rankine theory, to design such a profile directly.* The method gives the profile which eliminates tensile stress at the toe of the wall and must be checked to ensure that it is safe against other possible types of failure.

The late Sir Benjamin Baker stated † that:

" Experiment has shown the actual lateral thrust of good filling to be equivalent to that of a fluid weighing about 10 lb. per cubic foot, and allowing for variations in the ground, vibration, and contingencies, a factor of safety of 2, the wall should be able to sustain at least 20 lb. fluid pressure, which will be the case if ¼ of the height in thickness.

" It has been similarly proved by experience that under no ordinary conditions of surcharge or heavy backing is it necessary to make a retaining wall on a solid foundation more than double the above, or ½ of the height in thickness. Within these limits the engineer must vary the strength in accordance with the conditions affecting the particular case."

The assumption of a fluid pressure of 20 lb. per cubic foot only gives the same result as a design based on the Rankine hypotheses for certain specific combinations of earth density and angle of repose. Thus, if ρ_e is the unit weight of earth fill, ϕ the angle of repose and H the height of the wall, the lateral pressure on the vertical face of a non-surcharged wall is, by the Rankine theory,

$$P = \frac{\rho_e H^2}{2}\left(\frac{1-\sin\phi}{1+\sin\phi}\right). \quad \ldots\ldots\ldots \quad (1)$$

* " Determination of Trapezoidal Profiles for Retaining Walls." A. J. S. Pippard. Trans. Am. Soc. C.E., Vol. 100 (1935), p. 116.

† " The Actual Lateral Pressure of Earthwork," Sir Benjamin Baker. Minutes of Proceedings, Inst. C.E., Vol. LXV, p. 183.

whereas that on a wall retaining a fluid of density ρ_L is

$$P = \frac{\rho_L H^2}{2} \quad . \quad . \quad . \quad . \quad . \quad . \quad . \quad . \quad . \quad . \quad (2)$$

For these to be equal it is necessary that

$$\rho_L = \rho_e \left(\frac{1 - \sin \phi}{1 + \sin \phi} \right) \quad . \quad . \quad . \quad . \quad . \quad . \quad . \quad . \quad . \quad (3)$$

This is a general relationship but if ρ_L is made equal to 20 lbs. per cubic foot, equation (3) becomes

$$\frac{1 - \sin \phi}{1 + \sin \phi} = \frac{20}{\rho_e} \quad . \quad . \quad . \quad . \quad . \quad . \quad . \quad . \quad . \quad (4)$$

and for any value of ρ_e there will be a corresponding value of ϕ, which will give the same pressure as that calculated from equation (1).

Fig. 21.14 shows the range of combinations of ρ_e and ϕ that will satisfy equation (4), and it is evident that only a small region on this

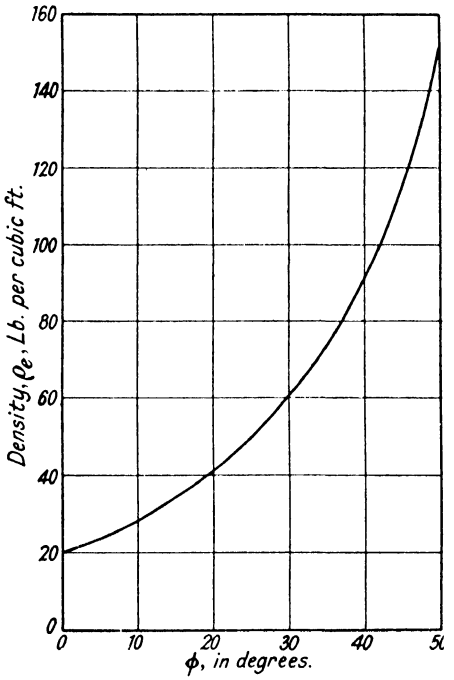

FIG. 21.14.

curve gives simultaneous values of ρ_e and ϕ which are likely to be associated in practical material.

This method of viewing the problem can be used more generally, however, since for any values of ρ_e and ϕ, a value of ρ_L can be found from equation (3), which will give the same " Rankine " pressure as the earth considered.

This equation can be written in the form :

$$\log \rho_L = \log \rho_e + \log \left(\frac{1 - \sin \phi}{1 + \sin \phi} \right) \quad . \quad . \quad . \quad . \quad . \quad (5)$$

which lends itself to simple nomographic representation as shown in Fig. 21.15.

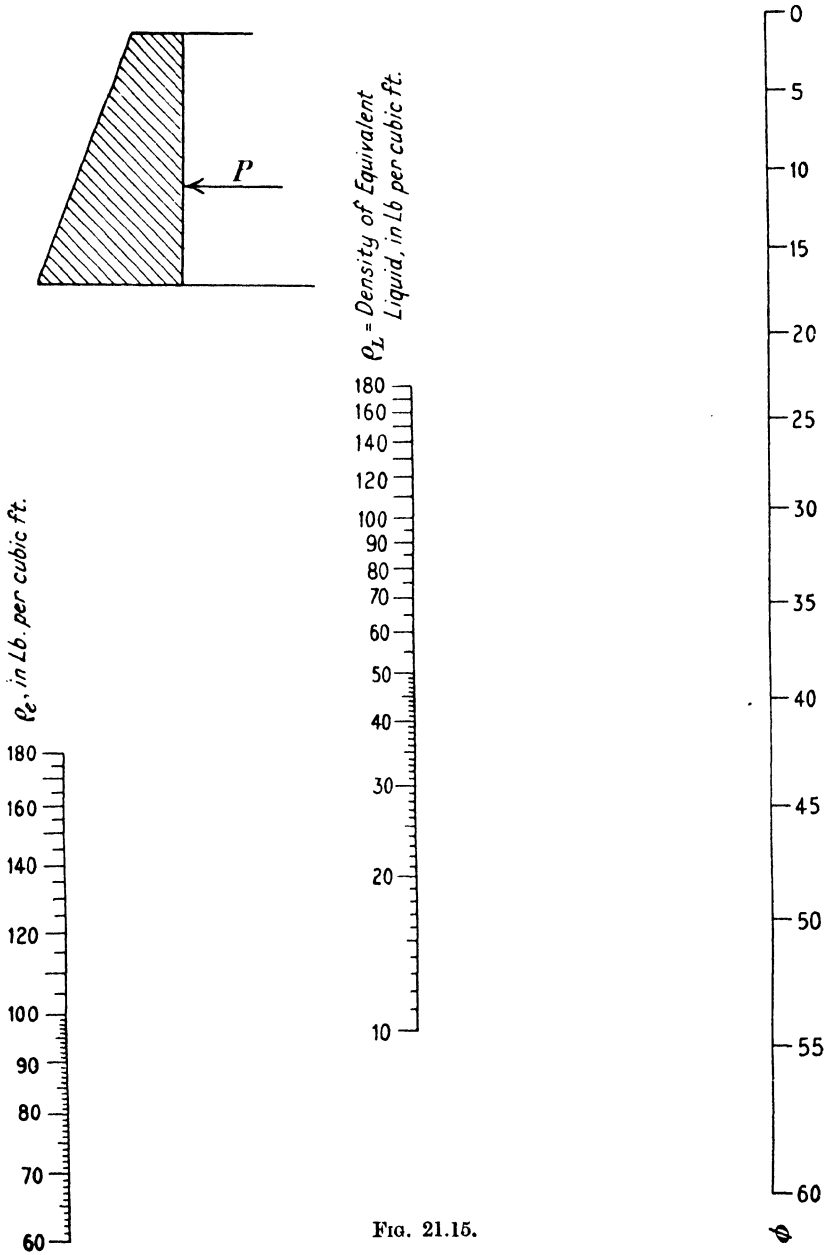

FIG. 21.15.

If a line is drawn on this diagram joining the known values of ρ_e and ϕ on the two outside lines, its intersection with the middle line gives ρ_L. As will be shown later, however, there is no need to calculate the value of P from equation (2) because a suitable profile can be obtained directly from the value of ρ_L thus found.

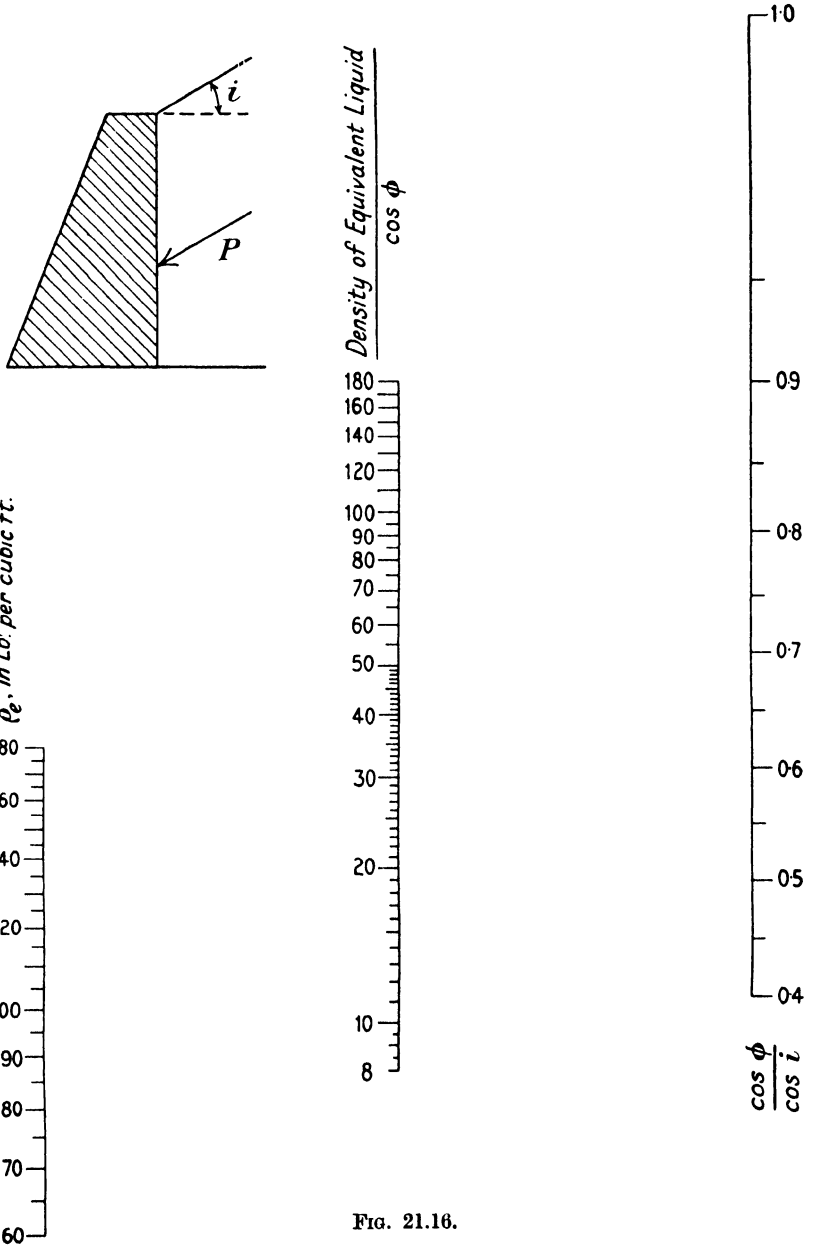

FIG. 21.16.

The case of the surcharged wall is not quite so simple as that just dealt with but can be exhibited in a similar form. If i is the angle of surcharge, the earth pressure acting at one-third the height from the base is, according to the Rankine theory,

$$P=\frac{\rho_e H^2}{2}\cos i\frac{\cos i-\sqrt{\cos^2 i-\cos^2\phi}}{\cos i+\sqrt{\cos^2 i-\cos^2\phi}} \quad . \quad . \quad . \quad . \quad (6)$$

and this pressure is assumed to act parallel to the earth surface. The unit weight of the equivalent liquid is now

$$\rho_L=\rho_e\cos i\frac{\cos i-\sqrt{\cos^2 i-\cos^2\phi}}{\cos i+\sqrt{\cos^2 i-\cos^2\phi}} \quad . \quad . \quad . \quad . \quad . \quad (7)$$

and if $\frac{\cos\phi}{\cos i}=a$ this becomes

$$\frac{\rho_L}{\cos\phi}=\frac{\rho_e}{a}\left(\frac{1-\sqrt{1-a^2}}{1+\sqrt{1-a^2}}\right) \quad . \quad . \quad . \quad . \quad . \quad . \quad (8)$$

Writing equation (8) in the logarithmic form

$$\log\frac{\rho_L}{\cos\phi}=\log\rho_e+\log\frac{1-\sqrt{1-a^2}}{a(1+\sqrt{1-a^2})} \quad . \quad . \quad . \quad . \quad (9)$$

which can also be expressed as a nomogram as shown in Fig. 21.16.

To use this diagram the value of $\frac{\cos\phi}{\cos i}$ is first calculated and the point on the right-hand line corresponding to it is joined by a straight line to the value of ρ_e on the left-hand line. The intersection of this connecting line with the middle line of the diagram gives $\frac{\rho_L}{\cos\phi}$ and this needs only to be multiplied by the value of $\cos\phi$ already found to give ρ_L.

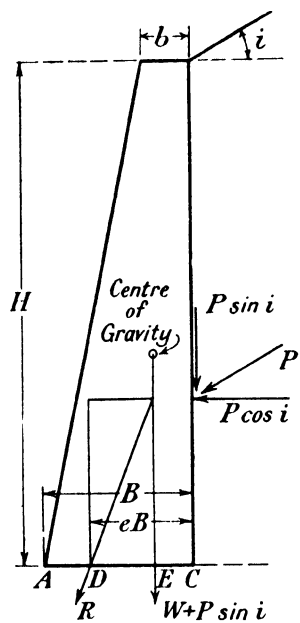

FIG. 21.17.

The value of ρ_L having thus been found either from Fig. 21.15 or Fig. 21.16 as appropriate, the profile of the wall must be determined. Fig. 21.17 shows the section of a trapezoidal wall of height H. The known top width is b and the base width, to be determined, is B.

The pressure P acts at one-third of the height from the base and is parallel to the earth surface. The resultant of the inclined pressure P and the weight of the wall, acting through the centre of gravity of the profile, cuts the base joint at point D, a distance eB from point C, the heel of the wall. It is convenient to resolve the inclined pressure P into a horizontal force, P cos i and a vertical force P sin i.

By taking moments about C, the distance of the centre of gravity of the vertical forces from C is found to be :

$$CE=\frac{B^2+Bb+b^2}{3(B+b)+\frac{6P\sin i}{\rho_m H}}$$

in which ρ_m is the unit weight of the masonry of which the wall is built. Then, $DE=eB-CE$; and $\frac{\text{total vertical force}}{P\cos i}=\frac{H}{3DE}$. When P is made equal to $\frac{\rho_L H^2}{2}$ this leads to the result :

$$B^2(3e-1)+Bb(3e-1)-b^2+3e\sigma BH\sin i=\sigma H^2\cos i \qquad (10)$$

in which σ is the ratio $\frac{\rho_L}{\rho_m}$.

If the usual condition is adopted, that there shall be no tensile stress at the back of the wall, e must be two-thirds and equation (10) then becomes

$$B^2+B(b+2\sigma H\sin i)-(\sigma H^2\cos i+b^2)=0$$

and the solution of this equation is :

$$2B=-(b+2\sigma H\sin i)+\sqrt{5b^2+4\sigma H(H\cos i+\sigma H\sin^2 i+b\sin i)} \qquad (11)$$

If b is made zero the profile of the wall is a triangle and

$$\frac{B}{H}=\sqrt{\sigma^2\sin^2 i+\sigma\cos i}-\sigma\sin i \qquad (12)$$

With $i=0$, equation (12) reduces to the well-known result for a non-surcharged wall,

$$B=H\sqrt{\sigma} \qquad (13)$$

The family of curves plotted in Fig. 21.18 enables $\frac{B}{H}$ to be found for any values of σ and i and the profile of a triangular wall, to satisfy the Rankine theory, is thus determined directly from the value of ρ_L found from Fig. 21.16 without the necessity of calculating the value of P.

To determine the trapezoidal profile of top width b, let B_b be the necessary width of the base of the trapezoidal section given by equation (11), and B the base width of the triangular wall, which would satisfy the conditions and which can be found as explained previously. Then, the reduction in the base that can be made, due to the provision of a top width, is $B-B_b=B'$. Substituting from equations (11) and (12) we obtain

$$\frac{B'}{H}=\frac{n}{2}-\frac{1}{2}\sqrt{4\sigma(\cos i+\sigma\sin^2 i)}\left\{\sqrt{\frac{5n^2+4\sigma n\sin i}{4\sigma(\cos i+\sigma\sin^2 i)}+1}-1\right\}$$

in which n is written for $\frac{b}{H}$. Expanding the root in the bracket and retaining only the first two terms as giving a sufficiently accurate result,

$$\frac{B'}{H}=\frac{n}{2}-\frac{1}{8}\left(\frac{5n^2+4\sigma n\sin i}{\sqrt{\sigma^2\sin^2 i+\sigma\cos i}}\right).$$

Substituting for $\sqrt{\sigma^2 \sin^2 i + \sigma \cos i}$ from equation (12) this reduces to

$$B' = \frac{b}{2}\left(\frac{\frac{B}{H} - \frac{5b}{4H}}{\frac{B}{H} + \sigma \sin i}\right) \quad \ldots \ldots \quad (14)$$

In this connection $\frac{B}{H}$ is taken from the curves of Fig. 21.18. Owing to the omission of terms in the expansion of the root of the equation

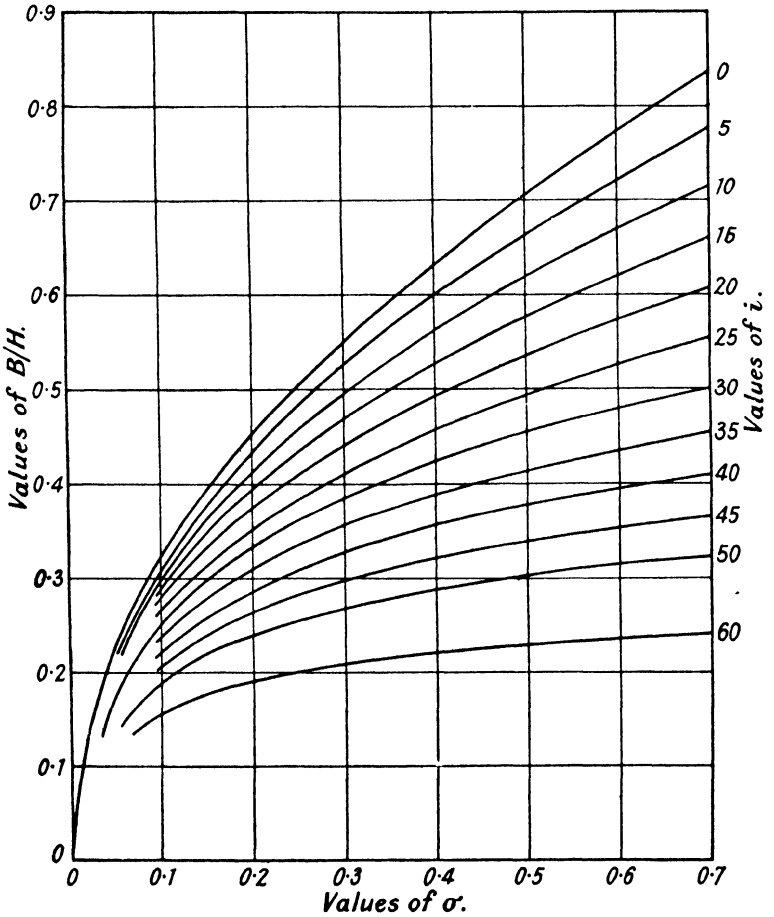

FIG. 21.18.

for $\frac{B'}{H}$, the correction is slightly smaller than an exact result would give but the small error introduced is negligible in view of the nature of the problem and, in any case, is on the right side.

Rankine suggested that the resultant action in the case of earth-retaining walls might be allowed to cut the base within the middle

three-eighths instead of the middle third. This makes $e=\frac{11}{16}$ in equation (10) and it is found that the resulting base width of the wall is 3 per cent. less than that determined by the curves in this paragraph.

As an example of the method suppose a profile is required for a wall 20 feet high, retaining earth weighing 120 lb. per cubic foot and having an angle of repose of 45°. The surcharge angle is 30°, the weight of the masonry 140 lbs. per cubic foot and the top width 2 feet.

Since $\cos i=\cdot866$ and $\cos\phi=\cdot707$, $\frac{\cos\phi}{\cos i}=\cdot816$. Then, from Fig. 21.16,

$$\frac{\rho_L}{\cos\phi}=39\cdot5 \text{ and } \rho_L=39\cdot5\times\cdot707=27\cdot9 \text{ lb. per cubic foot.}$$

Then
$$\sigma=\frac{\rho_L}{\rho_m}=\frac{27\cdot9}{140}=\cdot199.$$

Thus, from Fig. 21.18, the value of $\frac{B}{H}$ for a triangular wall is ·328; that is, $B=\cdot328\times20=6\cdot56$ feet. Since the top width is 2 feet a correction may be applied as found by equation (14), or

$$B'=\frac{\cdot328-\cdot125}{\cdot328+\cdot098}=\cdot48$$

and the base width is $6\cdot56-\cdot48=6\cdot0$ feet, say.

This profile is shown in Fig. 21.19 and a graphical analysis has been made to check it; thus, the weight of the wall $=4\cdot0\times20\times140=11{,}200$ lb. per foot. The earth pressure, by equation (6), is equal to

$$\frac{60\times400\times\cdot866\times\cdot366}{1\cdot366}=5{,}560 \text{ lb. per foot.}$$

The resultant of these forces is shown in Fig. 21.19 and cuts the base just inside the middle third, thus checking the result obtained by the use of the curves.

When the back of the wall is battered the problem is more complicated but the treatment to be given has the advantage of being a direct design method which is easily applied. In Fig. 21.20 let AC be the back of the wall battered at an angle α to the vertical Then, the resultant action on the back AC is compounded of the weight of earth represented by CDA and the earth pressure on AD of height $h=H(1+\tan i\tan\alpha)=mH$.

If AE is made equal to rh, in which r is the ratio $\frac{\rho_e}{\rho_m}$, the masonry triangle CEA is equivalent to the earth triangle CDA, both as regards weight and moment about A. Hence the section FCEAM is the equivalent wall to resist the earth pressure on the face DA.

The pressure on DA is proportional to $\rho_e m^2H^2$ and is equal in magnitude to the pressure that would be exerted on JA if the filling had a density $\rho'_e=\rho_e m^2$ and was surcharged to the angle i. The earth surface for this equivalent filling is JK in Fig. 21.20.

The procedure adopted is to design a wall of trapezoidal profile

FJAM (Fig. 21.20) by the methods previously explained and to correct the base width thus found to allow for the inaccuracies involved. These inaccuracies are as follows: (*a*) The absence of the masonry triangle CJE from the section reduces the weight of the wall from that designed and also moves the centre of gravity away from the back and (*b*)

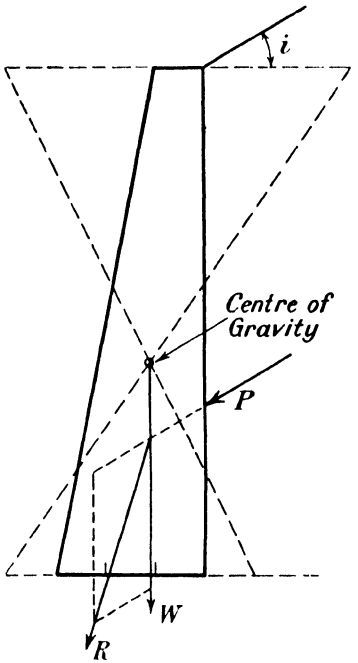

Fig. 21.19.

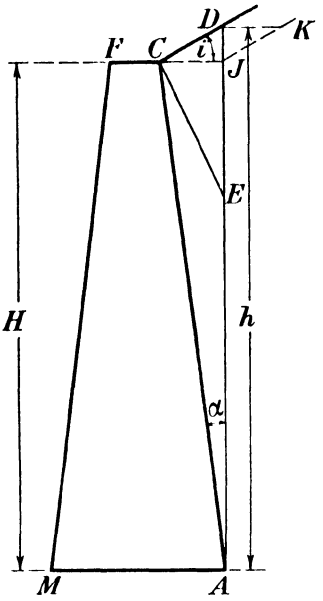

Fig. 21.20.

the centre of pressure of the force acting on DA is at a height of $\frac{h}{3}$ from A, instead of $\frac{H}{3}$ as assumed in the design.

The effects are small and can be dealt with as follows: In Fig. 21.21 let l be the height of the centre of pressure above point A, k the distance of the centre of gravity of vertical forces from line AJ and V, the total vertical force acting through the centre of gravity $=\rho_m\left(\frac{B+b}{2}\right)H + P \sin i$.

Taking moments about point K we have

$$lP \cos i = V\left(\frac{2B}{3} - k\right)$$

since $MK = \frac{B}{3}$. The effect of small changes in V, l and k on B is given by

$$\delta B = \frac{\partial B}{\partial V}\delta V + \frac{\partial B}{\partial l}\delta l + \frac{\partial B}{\partial k}\delta k$$

in which $\frac{\partial B}{\partial V}$, $\frac{\partial B}{\partial l}$ and $\frac{\partial B}{\partial k}$ are the partial differential coefficients of B with respect to V, l and k, and δV, δl and δk are the small increments of these quantities. It follows that $\frac{\partial B}{\partial V}=\frac{3k-2B}{2V}$, $\frac{\partial B}{\partial l}=\frac{3P\cos i}{2V}$ and $\frac{\partial B}{\partial k}=\frac{3}{2}$. In the present case :

$$\delta V=-\frac{\rho_m}{2}(1-mr)H^2\tan\alpha$$

$$\delta l=\frac{H}{3}(m-1)$$

$$\delta k=\frac{\rho_m(1-mr)H^3\tan^2\alpha}{6V}$$

$$k=\frac{\rho_m H(B^2+Bb+b^2)}{6V}$$

$$l=\frac{H}{3}$$

and

$$\frac{P\cos i}{V}=\frac{2B-3k}{H}$$

Substituting these values and reducing we obtain

$$\frac{\delta B}{H}=\frac{\tan\alpha}{2}\left\{\frac{(1-mr)\left(\tan\alpha+\frac{2B-3k}{H}\right)}{\sigma'\sin i+\frac{B}{H}+\frac{b}{H}}+\frac{2B-3k}{H}\tan i\right\} \quad . \quad . \quad (15)$$

in which σ' is the value of σ for the equivalent filling, that is

$$\frac{\rho_L}{\rho_m}(1+\tan\alpha\tan i)^2.$$

The terms in this expression are readily found from the designed profile FJAM (Fig. 21.21) and the increase in base width thus determined.

As an example of the method, consider a wall to the following requirements : Height H=20 feet ; top width b=2 feet ; batter of back =1 in 8 (that is, α=7·1°) ; weight of masonry ρ_m=140 lb. per cubic foot ; weight of earth fill ρ_e=100 lb. per cubic foot ; angle of repose ϕ=45° and angle of surcharge i=45°.

The necessary width of base B is to be determined. The equivalent unit weight of earth is $\rho_e'=100(1+\frac{1}{8})^2=126{\cdot}5$ lb. per cubic foot. In the first place the curves are used to find the necessary width of a wall with a vertical back and a top width of (2+H tan α)=4·5 feet. From Fig. 21.16, $\rho_L=126{\cdot}5\cos\alpha=89{\cdot}5$ lb. per cubic foot and $\sigma'=\frac{89{\cdot}5}{140}={\cdot}64$. From Fig. 21.18 $\frac{B}{H}$ for a triangular wall=·36, or B=7·2 feet. The

correction to be applied for the width is, from equation (14),

$$B' = \frac{4{\cdot}5}{2}\left(\frac{{\cdot}36-{\cdot}281}{{\cdot}36+{\cdot}452}\right) = {\cdot}22 \text{ feet.}$$

The base width of the vertical back wall is thus: 7·2—·22=7·0 feet. The pressure of earth acting at 45° on the vertical back is $P=\frac{\rho_e' H^2}{2}\cos i = 17{,}900$ lb. per foot of wall. The vertical component

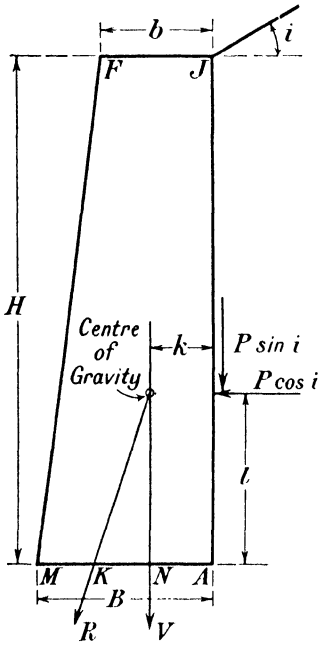

Fig. 21.21.

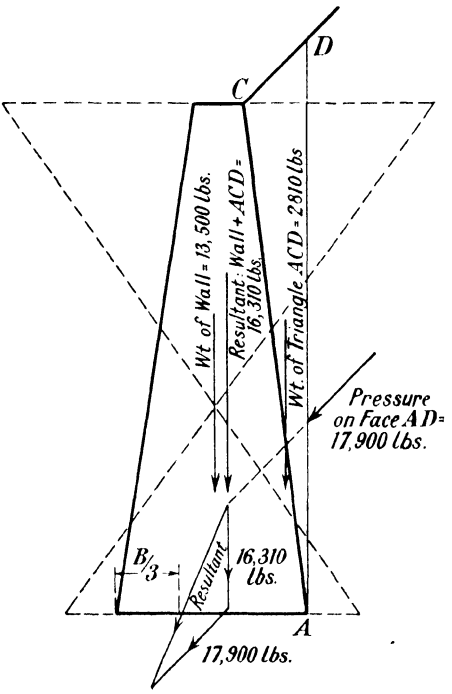

Fig. 21.22.

of this is 17,900×·707=12,650 lb. per foot. The weight of the wall is 140×11·5×10=16,100 lb. per foot. Therefore V=28,750 lb. and

$$k = \frac{\rho_m H(B^2+Bb+b^2)}{6V} = \frac{140\times 20\times 100{\cdot}75}{6\times 28{,}750} = 1{\cdot}64 \text{ feet,}$$

which, if desired, could have been found graphically.

Now $\tan\alpha=\frac{1}{8}$; $(1-mr)=1-\frac{5}{7}(1+\tan i\tan\alpha)=1-\frac{5}{7}(1{\cdot}125)={\cdot}196$; $\frac{B}{H}={\cdot}35$; $\frac{b}{H}={\cdot}225$; and $k=1{\cdot}64$. Substituting these values in equation (15) we have $\frac{\delta B}{H}={\cdot}034$; or, $\delta B={\cdot}68$ feet. The necessary base width is thus 7·0+·68=7·68 feet.

As a check this profile (shown in Fig. 21.22) will be examined graphically. The weight of the wall per foot of run is (2+7·68) ×10×140 lb.=13,500 lb. The weight of the wedge of earth resting

on the battered back is $(2{\cdot}5\times22{\cdot}50)50=2{,}810$ lb. The line of action of the resultant of these two vertical forces is found graphically. The force acting on the vertical earth back is $P=\frac{\rho_e h^2}{2}\cos i=50\times22{\cdot}5^2\times{\cdot}707=17{,}900$ lb., and is inclined at 45° to the vertical. Combining these forces the resultant is found to cut the base closely to $\frac{B}{3}$ from the toe of the wall as required.

EXERCISES

(1) A retaining wall 15 feet high is built of masonry weighing 140 lb. per cubic foot, the profile being triangular and the back vertical.

The filling weighs 120 lb. per cubic foot, has an angle of repose of 45° and is surcharged 30°. Determine the thickness of the wall at the base using the wedge theory and assuming that the mortar joints cannot withstand tension.

(*6·7 feet.*)

(2) A masonry retaining wall, trapezoidal in section, has a top width of 2 feet. It is 15 feet high and retains earth level with its top. If the masonry weighs 140 lb. per cubic foot and the earth filling 120 lb. per cubic foot, calculate the necessary width at the base. $\phi=45°$.

(*5·15 feet.*)

(3) A retaining wall of triangular profile is 20 feet high and is built of masonry weighing 140 lb. per cubic foot. The earth it retains weighs 120 lb. per cubic foot, has an angle of repose of 45° and is surcharged to an angle of 30°.

Calculate the width of base required if there is to be no tension at the back of the wall.

(*a*) By Rankine's theory ;

(*b*) by the wedge theory, assuming the back of the wall is perfectly smooth.

((*a*) *6·55 feet.*
(*b*) *8·97 feet.*)

(4) The floor of a reservoir is 20 feet below ground level. The reservoir may be empty or full to ground level. The earth weighs 120 lb. per cubic foot and has an angle of repose of 45°.

Calculate the necessary width of a reservoir wall which is made of masonry weighing 140 lb. per cubic foot and is rectangular in section.

What would be the difference in thickness if Sir Benjamin Baker's empirical rule for earth pressure were used ?

(*10·92 feet. No difference.*)

(5) A wall 27 inches wide carrying 10 tons per foot run has a foundation 4 feet below the ground level. The ground is sandy and weighs 120 lb. per cubic foot, its angle of repose being 30°.

Calculate the necessary width of the concrete foundation upon which the wall is built.

(*5·2 feet.*)

CHAPTER 22

MECHANICAL METHODS OF STRESS ANALYSIS

22.1. Introduction.—If the preceding chapters have been studied and examples worked it will be realised that the determination, by mathematical methods, of the distribution of stress in many engineering structures is a laborious task and that there are many opportunities for arithmetical errors. The same difficulty in arriving at the stress distribution is not experienced by the structures, which adjust themselves, on the application of load, rapidly and without any difficulty or distress except when overstrain occurs. It is not surprising, therefore, that engineers have turned to a physical study of the behaviour of the structures themselves in the hope of determining the stresses induced on the application of load. This movement, which is comparatively recent, is likely to be of the greatest use to engineers and though nothing like a complete treatment can be attempted in the space available here, some of the better known methods used will be described.

The most straightforward way of attacking the problem of stress distribution would appear to be by the direct measurement of strains in an actual loaded structure but owing to the expense and magnitude of the task, comparatively little along these lines has been done. This is regrettable as there is no other way of finding the true assumptions which should be made in subsequent mathematical or model analyses of the stresses in similar structures. That valuable general information for use in design can be obtained is shown by the results of tests on full scale frames and existing steel framed buildings carried out for the Steel Structures Research Committee, mentioned in Chapter 19 and fully described in the Committee's Reports. Such tests, however, are not undertaken for the purpose of collecting data relating to the design of one particular structure and are therefore outside the scope of this chapter which is concerned with the more simple mechanical means which are available for stressing as alternatives to the mathematical methods already outlined. No attempt will be made to describe the more elaborate methods such as that of photo-elasticity,* which are primarily used for the design of details rather than for the main members of a structure and which need apparatus not readily available.

22.2. Mechanical analysis of stresses in pin-jointed frames.—Straightforward mechanical methods, similar to those used in measuring the

* For a full description of this method of analysis see "Photo Elasticity," by E. G. Coker and L. N. G. Filon (Camb. Univ. Press).

strains of actual structures, but applied to model or small scale structures, are sometimes valuable aids in design, and were used by the authors,* among other purposes, to investigate the validity of general formulas to be used in the design of rigid airships. The high degree of redundancy possessed by an airship structure makes the application of the more usual mathematical methods of analysis described in Chapter 6 a practical impossibility and it was necessary to produce, for design purposes, approximate formulas of a generalised type to enable the internal forces in the various members to be determined from a knowledge of the resultant actions at any section of the hull. Before

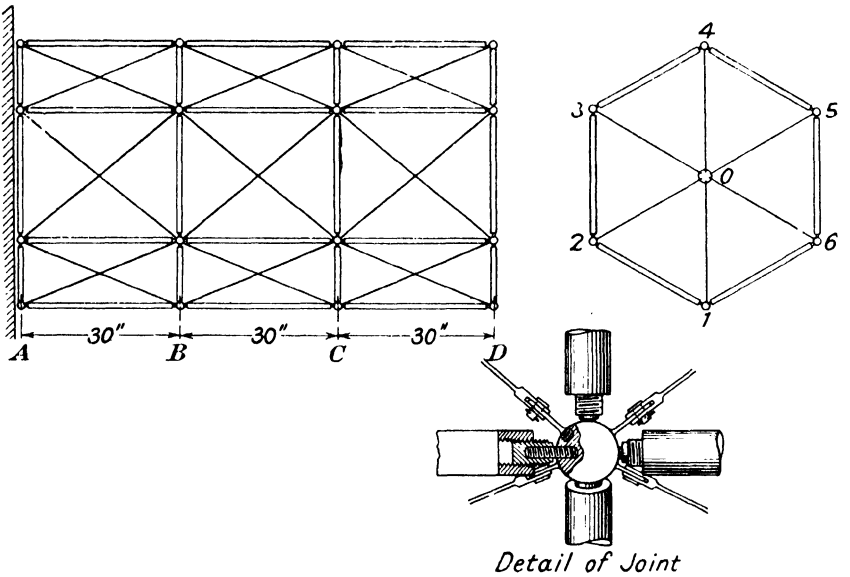

FIG. 22.1.

these formulas could be used with confidence their accuracy had to be checked and as this could not be done against results obtained by more accurate mathematical analysis recourse had to be made to experimental methods.

The experimental structure and some details of its construction are shown in Fig. 22.1. The framework was 3 bays in length, each bay being 30 inches long and of hexagonal cross-section, the side of the hexagon being 25 inches. With the object of the experimental work in view the structure was built to conform as nearly as possible to the assumptions made in deriving the formulas to be tested. Fig. 22.1 shows the design of joint adopted so that the members would be subjected to as little end bending restraint as possible, the assumption having been made in the analytical work that the structure was pin-jointed. The joints were 1¼-inch diameter Hoff-

* "On an Experimental Verification of Castigliano's Principle of Least Work and of a Theorem relating to the Torsion of a Tubular Framework." A. J. S. Pippard and J. F. Baker. Phil. Mag., July, 1925, pp. 97–112.

mann steel balls, partially softened to receive $\frac{7}{32}$-inch diameter steel dowels, the other ends of which were screwed into plugs in the ends of the members, leaving $\frac{1}{16}$-inch between the faces of the joint and the plug. While these dowels had the necessary strength their small flexural rigidity ensured that the amount of restraint offered by them would be small. To test the efficacy of the arrangement a strut 24 inches long and ·75 inch diameter fitted with the dowel ends was tested in compression and failed at a load of 7,645 lbs., the calculated Euler critical load being 7,905 lbs.

The transverse and longitudinal members of the structure were made of steel tube $\frac{7}{8}$-inch outside diameter and 22 gauge thick while all cross bracing members were 4 B.A. swaged rods, ability to resist compression being obtained by initially tensioning them.

TABLE 22.1.

Member	Measured load, lbs.	Calculated load, lbs.
A_1B_1	335·5	343·0
A_2B_2	200·0	206·0
A_3B_3	−196·1	−206·0
A_4B_4	−352·0	−343·0
A_1B_2	73·0	70·7
A_2B_1	− 26·5	− 27·2
A_2B_3	105·0	106·0
A_3B_2	−110·0	−106·0
A_3B_4	25·5	27·2
A_4B_3	− 74·0	− 70·8
B_1C_1	188·4	206·0
B_2C_2	123·5	123·6
B_3C_3	−115·5	−123·6
B_4C_4	−211·0	−206·0
B_1C_2	68·0	62·0
B_2C_1	− 35·0	− 36·0
B_2C_3	103·2	106·0
B_3C_2	−110·0	106·0
B_3C_4	36·2	36·0
B_4C_3	− 63·0	− 62·0

The strains in the members were measured by means of a simple type of extensometer. Along each member of the structure was placed a gauge of thin aluminium, corrugated for the sake of stiffness. It was attached to the member at one end by a hardened steel knife-edge and small set screw. At the other end of the gauge was a small circle of glass marked on the underside with a fine cross hair at right angles to the axis of the member. The glass was held in contact with the member by rubber bands. A fine line was scratched on the member to coincide as nearly as possible with the line on the glass. The distance between the scratches on the member and on the glass was measured by a special micrometer microscope and the alteration

in this distance under different conditions of loading was the magnitude of the elongation produced. The gauges were 15 inches long between the point of attachment to the member and the line on the glass. Actual calibration curves obtained by direct loading tests were used to reduce the micrometer-head readings to loads in the member and it was found that for the $\frac{7}{8}$-inch$\times$22 gauge tube a movement of the cross hair represented by one division of the micrometer head was equivalent to a load of 7·84 lbs. and for a 4 B.A. swaged rod one division corresponded to a load of 1·02 lbs. in the member. Dead loads were applied to the structure and the strains, and therefore the stresses, were found in all the members. Table 22.1 shows a typical set of experimental results obtained when a radial load of 400 lbs. was applied at joint D of the end bulkhead. It will be seen from a comparison between the measured loads and those obtained by calculation that the mechanical method gave satisfactory results.

This work is quoted simply as an example of a method of research or particular investigation which has been used in a very wide field.

22.3. Mechanical slope deflection method of analysis.—Another simple method of analysis in which loads are applied to experimental structures makes use of the slope deflection relations derived in Chapter 9 and is of particular value in the determination of the internal reactions of structures such as building frames which are made up in the main of straight members of uniform cross-section. This mechanical method does not call for the use of elaborate and extensive apparatus or any very refined technique and might well be employed in the design office. The model structure can be made up quickly and cheaply since it is only necessary to ensure that the centre lines of its members represent to some convenient scale the centre lines of the members of the structure to be analysed and that the second moments of area of its members are proportional to those of the members of the structure. As a result of this last stipulation if the whole of the model is made of material of the same thickness, the depths of the members must be made proportional to the cube roots of the second moments of area of the members of the structure. Additional refinement may be obtained by making the model of material of different thicknesses, so that both the second moments of area and the depths are proportional to those of the actual sections used in the structure. Any load may be applied which does not overstrain the model and will be governed by the dimensions of the members and the type of microscope used.

W. M. Wilson and G. A. Maney * have described tests which they carried out on a xylonite model in order to check the deflections and the changes in slope calculated by the slope deflection method for wind loads on a building frame. The agreement obtained by them between theory and practice made it appear worth while to attempt the analysis of the stresses in such frames by the direct measurement of the slopes and deflections of models under load.

* "Wind Stresses in the Steel Frames of Office Buildings." University of Illinois. Engineering Experiment Station Bulletin, No. 80. Urbana, 1915.

When the usual assumptions are made, viz. (1) that the members are represented by their neutral axes, (2) that the deformations due to shear and direct stress in the members and also the effect of the direct thrust due to the flexure of the stanchions are negligible, and (3) that the applied load on any beam of a frame is symmetrical about the centre of that beam, the bending moment at the end of any member may be expressed as

$$\begin{aligned} M = {} & a_1\frac{A_{11}}{l_{11}} + b_1\frac{A_{21}}{l_{21}} + \text{ . . . . .} \\ & + a_2\frac{A_{12}}{l_{12}} + b_2\frac{A_{22}}{l_{22}} + \text{ . . . . .} \\ & + \text{ . . . . . .} \\ & + a_r\frac{A_{1r}}{l_{1r}} + b_r\frac{A_{2r}}{l_{2r}} + \text{ . . . . .} \\ & + \text{ . . . . . .} \end{aligned} \qquad (1)$$

where a_1, b_1, . . . a_2, b_2, . . . a_r, b_r . . . are constants, A_{1r} denotes the area of the bending moment diagram for a simply supported beam having the same length and carrying the same load as the member $1r$ and l_{1r} denotes the length of the member $1r$, which member is the first beam from the left at the rth floor level.

The notation used here is given in full in Chapter 9 and is shown diagrammatically in Fig. 9.12. The sign convention adopted is

(1) The rotation of a joint is positive when clockwise.
(2) The deflection of one end of a member relative to the other is positive when the line joining the ends rotates clockwise.
(3) The end moments applied by the joints to the members are positive when they tend to cause a clockwise rotation.

The bending moments at the ends A and B of a member AB of uniform cross-section throughout its length are also given by

$$M_{AB} = \frac{2EI_{AB}}{l_{AB}}\left[2\phi_A + \phi_B - 3\frac{\delta_{AB}}{l_{AB}}\right] - \frac{A_{AB}}{l_{AB}} \text{ . . . . .} \qquad (2)$$

and

$$M_{BA} = \frac{2EI_{AB}}{l_{AB}}\left[\phi_A + 2\phi_B - 3\frac{\delta_{AB}}{l_{AB}}\right] + \frac{A_{AB}}{l_{AB}} \text{ . . . . .} \qquad (3)$$

where E denotes the modulus of elasticity of the material,
I_{AB} denotes the second moment of area of the member AB,
ϕ_A and ϕ_B denote the changes of slope at A and B
and δ_{AB} is the deflection of one end of the member relative to the other, due to the applied loads.

If, therefore, means are available for measuring the changes of slope and the deflections of points on a frame under load, the bending moment in that frame can be evaluated from equations (2) and (3), and from equation (1) the bending moments in any similar frame under any similar load system can be obtained.

Following the lead given by Wilson and Maney, tests were carried out by one of the present authors on xylonite models but they were not

satisfactory as it was impossible to obtain readings with any accuracy owing to the creep of the xylonite. Brass was therefore substituted for xylonite. Fig. 22.2 shows the arrangement of the apparatus for the determination of the internal reactions in a two storey two bay frame having perfectly rigid joints. The model frame was cut out of sheet brass $\frac{1}{32}$-inch thick. The foot of each stanchion was held in a steel clamp A, representing the foundation slab and a double row of $\frac{1}{8}$-inch diameter steel balls under each beam and stanchion supported the model in a horizontal position, but left it free to move under load. The load was applied at each beam through a turnbuckle and spring balance, B. Small clamps, E, carrying aluminium pointers 6 inches long could be fixed at any point on the model. When load was applied the

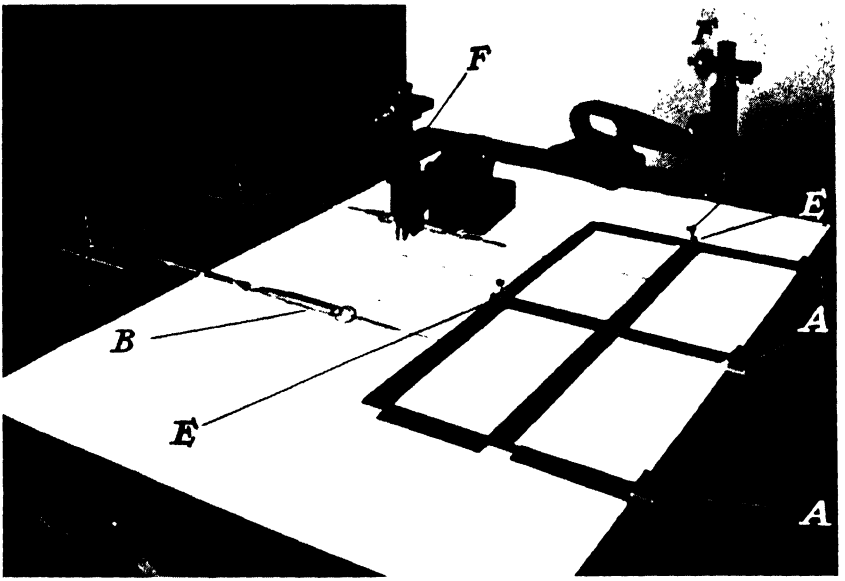

FIG. 22.2.

horizontal deflections of the frame and of the free ends of the pointers were measured by means of the micrometer microscopes, F.

The brass models behaved satisfactorily under load. There was no appreciable creep and repeat readings always coincided with the originals within two divisions of the micrometer head which represented an actual deflection of 0·000187 inch or a slope of 0·000031. The standard increment of load was 7 lbs. which could be adjusted to within 2 ozs. The only serious trouble likely to arise when working with models of this type is the buckling of the members out of the plane of the frame but this can be prevented by placing small weights on top of the frame sufficient to keep it in contact with the steel balls. In America successful use has been made of models constructed of I-section bars having sufficient rigidity to prevent buckling.

This slope deflection method has advantages over all others when

used to determine the stresses in building frames. It has been of the greatest service in throwing light on the behaviour of frames with semi-rigid connections,* but its sphere of usefulness is strictly limited and when curved members or those of varying cross-section are encountered, recourse must be had to one of the methods described in a later paragraph.

Another direct loading method of some interest is due to C. Rieckhof.† For this the models, which may be of such structures as continuous beams, portal frames and building frames with rigid joints, are made up of steel splines capable of sustaining appreciable deflections without any danger of being overstressed. Loads representing those to be borne by the full-sized structure are applied to the members and the positions of the points of contraflexure are found experimentally by means of a spherometer. At a point of contraflexure the curvature of the member changes sign; it is not difficult, therefore, by moving the spherometer along the spline, to find the position of such a point with considerable accuracy. In certain structures, such as continuous beams, the values of the bending moment and shearing forces at any cross-section can be obtained easily once the positions of the points of contraflexure are known and in these cases Rieckhof's method is capable of giving very accurate results. In other structures, however, the shearing forces at the points of contraflexure must be known before the reactions at other cross-sections can be obtained. To find these shears a special instrument is used to measure the perpendicular distance y of the point of contraflexure from the tangent to the member at any point distant x from the point of contraflexure. When no load acts upon the member in this distance x the shearing force at the point of contraflexure is $\frac{3EIy}{x^3}$, where E and I are the modulus of elasticity and the relevant second moment of area of the member. There appears to be some difficulty in obtaining an accurate measure of the shearing force in this way so that for complicated structures the method is not altogether satisfactory.

22.4. Mechanical methods of plotting influence lines.—The use of influence lines in the study of structures has been discussed in Chapters 14 and 15. These useful diagrams can in many cases be obtained without difficulty by mechanical methods and the credit for drawing attention to this fact is due to Professor G. E. Beggs.‡ The fundamental basis of all such methods in Clerk Maxwell's reciprocal theorem as stated in the general form in paragraph 4.10.

Fig. 22.3 shows an elastic structure which has three redundant reactions. If the support B is removed the initial conditions may be restored by the application of a vertical force V_0, a horizontal force H_0

* "The Mechanical and Mathematical Stress Analysis of Steel Building Frames." J. F. Baker. Selected Engineering Paper No. 131, Institution of Civil Engineers.

† "Experimentelle Statik." Darmstadt, 1927.

‡ "The Use of Models in the Solution of Indeterminate Structures." Journal of the Franklin Institute, March, 1927.

and a moment M_0. These redundant reactions must be determined before the resultant actions at any section can be found.

Suppose the load W to be removed and *a purely vertical* displacement of known amount Δ_B imposed at B. This will necessitate the application of unknown actions V', H' and M' at B in the directions of V_0, H_0 and M_0.

Under this distortion let the point of application of W move in the direction of W by an amount Δ_W. Then we have two distinct force and displacement systems, one relating to the loaded structure in its

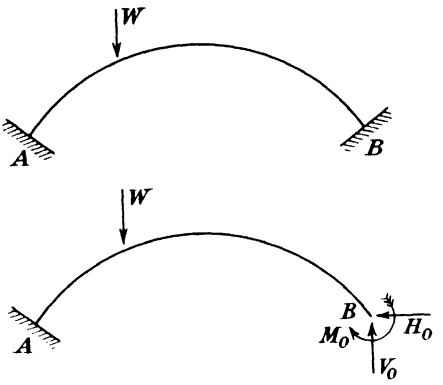

FIG. 22.3.

original condition and the other to the displaced structure with no load acting at W.

Tabulating these we have

System 1 (*Original conditions*)

Force	V_0	H_0	M_0	W
Displacement	0	0	0	δ

System 2 (*Displaced structure*)

Force	V'	H'	M'	0
Displacement	Δ_B	0	0	Δ_W

Then by the reciprocal theorem,

$$V_0\Delta_B+H_0(0)+M_0(0)+W\Delta_W=V'(0)+H'(0)+M'(0)+0(\delta)$$

or

$$V_0\Delta_B+W\Delta_W=0.$$

If W is unity

$$V_0=-\frac{\Delta_W}{\Delta_B}. \quad . \quad . \quad . \quad . \quad . \quad . \quad . \quad . \quad . \quad (1)$$

Hence to determine V_0 due to a unit load in the direction of W it is only necessary to impose a purely vertical displacement at B and to measure this displacement, Δ_B, and the resulting displacement of the point of application of W, Δ_W.

The negative sign in equation (1) indicates that the displacement Δ_W is in the opposite direction to W.

If instead of applying a vertical displacement Δ_W at B, a *purely horizontal* displacement δ_B is imposed, the same argument leads to

$$H_0 = -\frac{\Delta_W'}{\delta_B} \quad . \quad . \quad . \quad . \quad . \quad . \quad . \quad . \quad . \quad (2)$$

where Δ_W' is now the displacement of W in its line of action due to δ_B.

Similarly, if a *pure rotation* θ is imposed at B we find

$$M_0 = -\frac{\Delta_W''}{\theta} \quad . \quad . \quad . \quad . \quad . \quad . \quad . \quad . \quad . \quad (3)$$

where Δ_W'' is the displacement of W due to the imposition of θ.

It should be noted that the results of equations (1), (2) and (3) are correct as long as the structure obeys a linear law between deformations and the forces causing them. In many cases quite large displacements can be imposed without violating this condition and the use of special apparatus such as micrometer microscopes for measuring displacements is unnecessary.

Beggs, however, used a special instrument which he called a deformeter for applying small displacements, the resulting deflections of the model being measured by microscopes.

A modified form of this instrument is shown in Fig. 22.4.

The lower plate of the instrument is screwed to a drawing board and the top plate is held against it by means of two springs. Two circular plugs of equal diameter a are inserted between the notches, and the cut

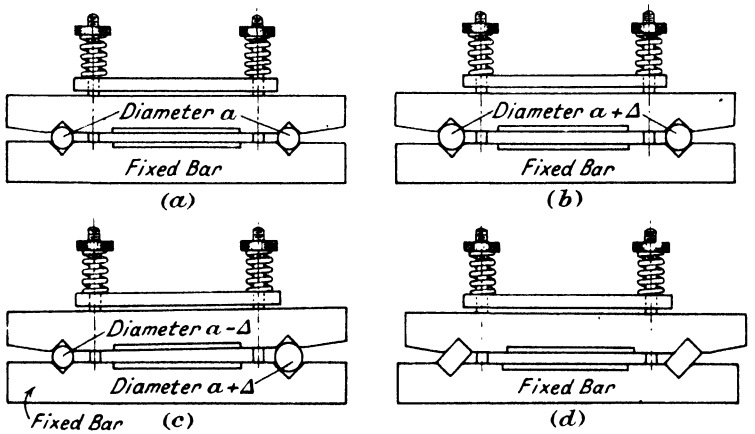

FIG. 22.4.

sections of the model are clamped, one to the top plate, and the other to the bottom plate.

If these plugs are replaced by others whose diameters are $a+\Delta$, a displacement Δ, normal to the line joining the centres of the plugs is applied between the cut faces of the model (Fig. 22.4*b*).

If the first plugs are replaced by two whose diameters are $a-\Delta$, an equal displacement in the opposite direction is applied. When one of the small plugs is inserted in one notch, and one of the large plugs in the other, a pure rotation is applied (Fig. 22.4*c*).

A relative shear displacement of the faces is obtained if two equal rectangular plugs are first placed in the notches so that the movable arm of the deformeter is moved say to the right of the fixed arm, and the plugs then reversed (Fig. 22.4*d*).

The Beggs deformeter method is the most generally useful of all mechanical methods. It gives, with comparative ease, influence lines for any structure no matter what the variation in section of a member or the shape of its axis. There are, however, certain precautions which have to be observed if accuracy is to be obtained. The deformations are small and, particularly when xylonite is used for the model, temperature changes can affect the results seriously.* Appreciable errors can also arise as a result of slight inaccuracy in orienting the microscope.

Other methods, similar in principle, are used in which the deformations are very much greater, the object being to avoid the use of expensive microscopes. It will be realised that in so deforming a model care must be taken to avoid overstraining the material. In the first successful method of this kind † the material used was steel strip which could undergo large deformations without overstrain. The strips are clamped together to the form of the structure to be analysed, are placed on a drawing board and fixed in position at the supports. A line diagram is made by plumbing down from the strip to the drawing board at frequent intervals. The model is then deformed by giving displacements to the section at which reactions are to be found. The deformations for thrust and shear are of the order of $\frac{1}{8}$th of the span of the member concerned and for moments from 0·5 to 1·0 radian. A line diagram of the deformed structure is made and the displacement of any point can then be measured by means of a graduated scale.* This method can, for such structures as continuous beams and portals, give satisfactory results but it will be realised that large deflections may, particularly in complicated structures, give results which are far from accurate.

Another method involving comparatively large displacements, which is particularly useful for finding the horizontal reactions for such structures as two-hinged arch ribs, portals, etc., has recently been described.† In this, a model of the structure to be analysed is cut out

* "Mechanical Methods of Solution of Stresses in Frames." C. H. Lobban. Inst. of Eng. and Shipbuilders in Scotland. 1934.

† "An Experiment in Statics." O. Gottschalk. Journal of the Franklin Institute, Vol. 207.

* This and other methods are fully described in a paper, "Mechanical Methods for the Analysis of Statically Indeterminate Structures," by H. A. Whittaker. Structural Engineer, April, 1934.

† "Simple Experimental Solutions of Certain Structural Design Problems." A. J. S. Pippard and S. R. Sparkes. Journal of the Institution of Civil Engineers, November, 1936.

of xylonite, as for Beggs' method and, for example, in the case of a two hinged arch rib is pinned at the hinge points A and B to a sheet of paper. Initial positions of points on one edge of the rib are marked on the paper. The pin B is then removed and given a small displacement in the direction BA and the new positions marked. On removing the model from the paper the vertical distances between the two positions of the rib can be measured and these, divided by the displacement given to B, give the values of the ordinates of the influence line for the thrust in the arch. The displacement given is such that the resulting deflection is great enough to be measured by an ordinary finely divided scale. In the case of an arch rib of uniform cross-section, depth $\frac{1}{4}$ inch, with the ratio of rise to span of one to four and a span of 12 inches it was possible, without overstraining the xylonite, to give a hinge displacement which produced a maximum vertical deflection of about $\frac{1}{4}$ inch. The method can be used conveniently in the drawing office where micrometer microscopes are not available. It has the advantage over the similar method used by Gottschalk that, since the models are cut from xylonite instead of being made from steel splines, it can deal with a greater variety of problems, including structures with variable cross-sections and curved axes and also with structures such as braced spandrel arches.

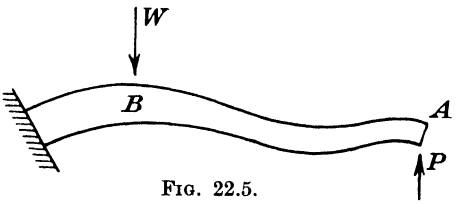

FIG. 22.5.

In general the use of these methods requires the construction of a scale model of the structure to be analysed and the influence of the scales needs consideration.

Let Fig. 22.5 represent an elastic structure in which the bending strain energy is such a large proportion of the whole that the contributions due to direct and shearing stresses may be neglected. If Δ_P and Δ_W are the displacements of the points A and B respectively under the action of loads P and W we have

$$\frac{\Delta_P}{\Delta_W} = \frac{\dfrac{\partial U}{\partial P}}{\dfrac{\partial U}{\partial W}} = \frac{\displaystyle\int \frac{M}{EI}\frac{\partial M}{\partial P}\,ds}{\displaystyle\int \frac{M}{EI}\frac{\partial M}{\partial W}\,ds}.$$

If a model of the structure is made so that the geometrical configuration is m times full size and the flexural rigidity of the model at any point is n times that of the prototype at the corresponding point, we have

$$\frac{\Delta'_P}{\Delta'_W} = \frac{\dfrac{m^2}{n}\displaystyle\int \frac{M}{EI}\frac{\partial M}{\partial P}\,ds}{\dfrac{m^2}{n}\displaystyle\int \frac{M}{EI}\frac{\partial M}{\partial W}\,ds} = \frac{\Delta_P}{\Delta_W}$$

where Δ'_P and Δ'_W are the displacements of points on the model corresponding to A and B on the prototype.

So, in making a model for experimental analysis, the scales adopted for the geometrical configuration and for the flexural rigidities are independent and can be chosen as convenient. This is often a matter of importance as will be indicated later.

It is clear that the result is independent of the absolute values of P and W, providing their ratio is constant.

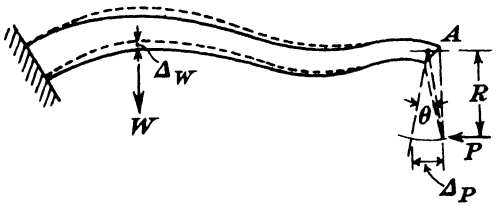

FIG. 22.6.

Suppose now that a couple M_0 is applied to A and that A is restrained against all movements except that of rotation. If, in the model, the flexural rigidities only are changed, the ratio $\frac{\Delta_W}{\theta}$ will be the same both in the model and in the prototype. To investigate the effect of a scale change m in the geometry of the model, it is convenient to replace the couple M_0 by a force P acting at the end of a rigid arm at a radius R (Fig. 22.6). Then, in the actual structure, from equation (1)

$$\frac{R\Delta_W}{\Delta_P}=-\frac{RP}{W}$$

and, since $R\theta=\Delta_P$,

$$\frac{\Delta_W}{\theta}=-\frac{M_0}{W}.$$

If W is made equal to unity

$$M_0=-\frac{\Delta_W}{\theta}.$$

In the model

$$\frac{mR\Delta'_W}{\Delta'_P}=-\frac{mRP}{W}$$

or

$$\frac{\Delta'_W}{\theta'}=-\frac{mM_0}{W}.$$

Hence

$$M_0=-\frac{\Delta'_W}{m\theta'}.$$

Thus the model results must be corrected for scale before they are applied to the full-sized structure.

In structures such as braced frameworks the strain energy due to bending is often very small in comparison with that due to axial forces

and in such cases the *cross-sectional areas* of members in the model are made proportional to those of the prototype. If the structure is one in which both bending moments and axial forces contribute appreciably to the strain energy the model must be such that both the flexural rigidities and the cross-sectional areas of the various parts bear the same relationship to the prototype. This necessitates a true scale model of the actual structure and will, in many cases, prohibit experimental analysis since the chief value of such a method lies in its cheapness and the quickness with which it can be done. In the case of a structure which is incalculable, however, the expense of making a correct model may be justified since it is the only method of analysis available.

To illustrate the results which may be achieved by these experimental methods a few actual examples will be described. These were done by the large displacement method but a deformeter and measuring microscopes could equally well have been used. In all the following examples the unit of displacement was $\frac{1}{48}$ inch, and measurements were made directly by a scale.

1. *Influence line for reaction in a continuous beam.*—The first case is that of a continuous beam, which is given as the simplest possible illustration. A small strip of xylonite of uniform cross-section (as shown in Fig. 22,7), was pinned at the three supporting points C, A, and B to a sheet of paper on a drawing-board, and a sharp pencil used to mark the position of the upper edge of the beam. The pin at C was

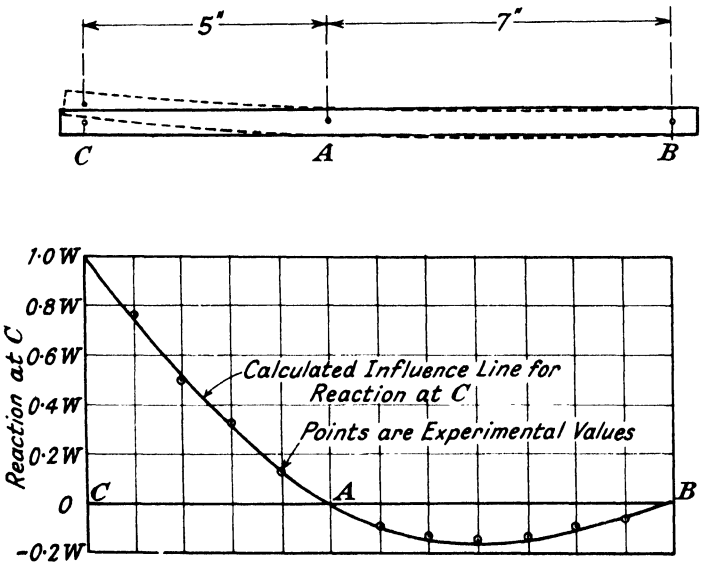

FIG. 22.7.

removed, the point displaced by a small amount, and the pin replaced. The new position of the beam was then marked and the beam removed from the paper. The vertical distance between the two curves at any

point when divided by the vertical displacement imposed at C gave a point on the influence line for the reaction at C, and a sufficient number of such points were calculated and the required influence line was plotted. The experimental points are shown in Fig. 22.7 together with the calculated influence line, and the agreement is seen to be very good.

2. *The influence line of thrust for a two-pinned segmental arch.*—An arch of uniform cross-section was represented by a model having a span of 12 inches and a rise of 3 inches. Fine scratches were made on one side of the model normal to the surface and were used as guides for pricking positions on the paper. The initial positions of the scratches were marked, and the pin at one end of the model was then given a small displacement in the line joining the supports. The new positions of all points around the model were then marked. On removing the model from the paper the vertical distances between the marks at each point were measured and divided by the displacement given to the pin. These values, given in Table 22.1, are points on the experimental influence line and the table also gives the theoretical values for comparison.

TABLE 22.1.

ANGLE SUBTENDED BY ARCH AT CENTRE=ϕ. HORIZONTAL DISPLACEMENT OF B=12·5.

Angular displacement from A		0	$\frac{\phi}{8}$	$\frac{\phi}{4}$	$\frac{3\phi}{8}$	$\frac{\phi}{2}$	$\frac{5\phi}{8}$	$\frac{3\phi}{4}$	$\frac{7\phi}{8}$	ϕ
Vertical displacement.		0	3·0	5·8	7·9	8·8	7·8	5·7	2·9	0
H	Experimental .	0	0·24	0·47	0·63	0·71	0·62	0·46	0·23	0
	Calculated . .	0	0·261	0·508	0·688	0·746	0·688	0·508	0·261	0

3. *Two-pinned arch with a variable cross-section.*—The same procedure as above was used to determine the influence line of thrust for a two-

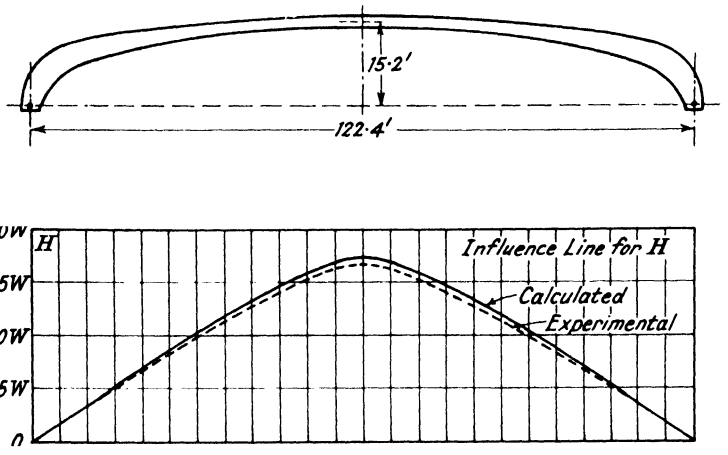

FIG. 22.8.

pinned arch in which the cross-section varied. The depth of the model was made proportional at every section to the cube root of the true second moment of area at that section. Fig. 22.8 shows the actual dimensions of the prototype and also the experimental and calculated influence lines.

4. *Influence line of thrust for a spandrel-braced arch.*—The arch shown in Fig. 22.9 is the Lengue bridge designed by Mr. Ralph Freeman * for which he gave the calculated influence line of thrust. The structure is braced and it was assumed that the forces in all bars were axial. The areas of the bars in the model were therefore made proportional to the areas in the actual bridge and this example differs from the others given, in which resistance to applied loads was obtained by bending actions. The experimental influence line is compared with that given by Mr. Freeman in Fig. 22.9.

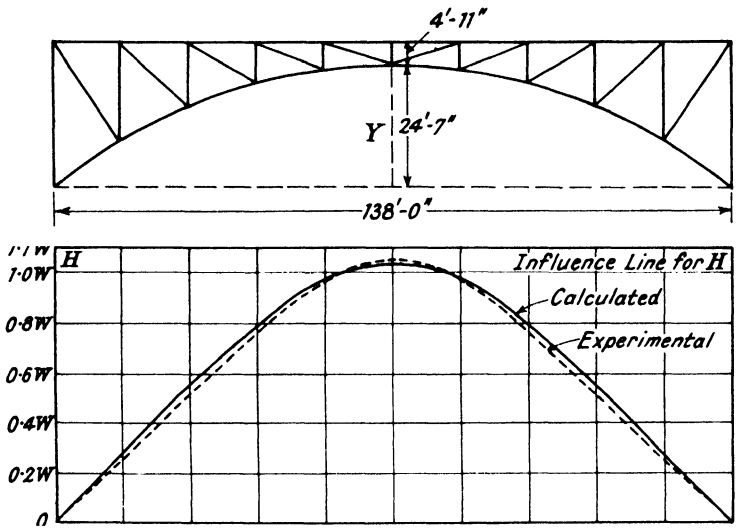

FIG. 22.9.

22.5. Experimental Analysis of stresses in rings.—The methods given in the preceding paragraph may be used to analyse the stresses in rings of any shape, and are particularly useful for such members as the frames of aeroplane fuselages. The examples to be given † were done by imposing displacements sufficiently large to be measurable by an ordinary scale but the same general procedure would be followed if a Beggs' deformeter were used.

If the ring shown in Fig. 22.10 be cut at any section A, the original

* "The Design of a Two-hinged Spandrel-braced Steel Arch." Minutes of Proceedings Inst. C.E., vol. clxvii (1906–7, Part I), p. 343.

† "Simple Experimental Analysis of the Stresses in Rings." Aeronautical Research Committee, Reports and Memoranda No. 1851. A. J. S. Pippard and S. R. Sparkes, 1938.

conditions of equilibrium can be restored by the application to this section of unknown forces H_0 and V_0, and an unknown couple M_0.

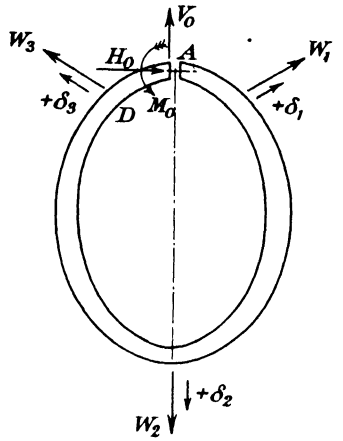

FIG. 22.10.

These may be calculated or determined experimentally in the following way. A model of the ring is made of xylonite, the second moments of area at all sections being proportional to the second moments of area of the prototype at corresponding sections. The model is cut at the section where the redundant reactions are required. To determine H_0 a known deformation Δ_H is imposed between the faces at A in the direction of H_0 in such a way that there is neither vertical nor angular displacement of the section. The displacement δ_{1H}, δ_{2H} and δ_{3H} of B, C and D in the directions of W_1, W_2 and W_3 respectively are measured and then

$$H_0=\frac{W_1\delta_{1H}+W_2\delta_{2H}+W_3\delta_{3H}}{\Delta_H}.$$

Similarly, to determine V_0, a displacement Δ_V is imposed between the cut faces in the direction of V_0 and, if δ_{1V}, δ_{2V} and δ_{3V} are the displacements of B, C and D respectively in the direction of W_1, W_2 and W_3,

$$V_0=\frac{W_1\delta_{1V}+W_2\delta_{2V}+W_3\delta_{3V}}{\Delta_V}.$$

The reaction M_0 is found by imposing a known angular displacement between the cut faces at A and, as before, measuring the appropriate displacements δ_{1M}, δ_{2M} and δ_{3M}. Then,

$$M_0=\frac{W_1\delta_{1M}+W_2\delta_{2M}+W_3\delta_{3M}}{m\theta}$$

where m is the linear scale of the model.

A satisfactory experimental procedure is as follows: the xylonite model is made with an arm $\frac{1}{2}$ inch wide and $4\frac{1}{4}$ inches long, normal to the model at A, as shown in Fig. 22.11. Two holes, $\frac{1}{8}$ inch diameter,

are drilled, one on the axis of the ring at A, and the other on the centre line of the arm about 3 inches from the first hole. The arm is stiffened by screwing to it two narrow strips of 16 gauge brass after the surfaces in contact have been treated with a strong adhesive. A saw cut is then made along the line AB (Fig. 22.11) and the two cut faces are filed parallel.

One arm of the model is screwed to a drawing board * and $\frac{1}{8}$ inch

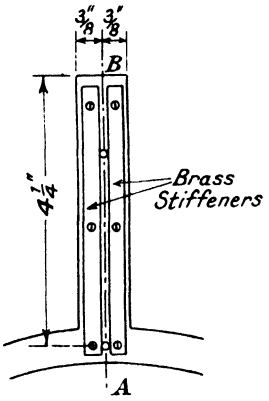

FIG. 22.11.

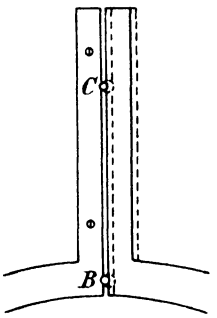

FIG. 22.12.

diameter steel balls are inserted between the notches at B and C (Fig. 22.12). A scratch on the outside of the movable arm and normal to the board is used to guide a pin point to a piece of paper under the model, thus marking the first position of the arm. The balls are then replaced by two equal but larger balls. The new position of the scratch on the movable arm is marked and the distance between the two pin pricks is the displacement imposed in the direction of H_0.

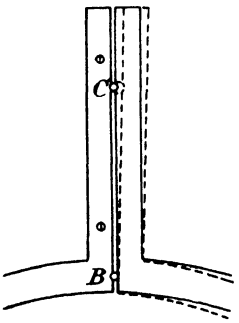

FIG. 22.13.

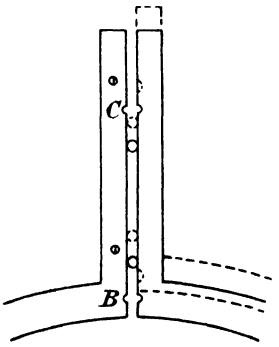

FIG. 22.14.

An angular displacement is obtained by inserting $\frac{1}{8}$ inch diameter

* It is advisable to place a thin packing piece of paper between the arm and the board to prevent friction between the model and the board when the former is displaced.

balls at B and C (Fig. 22.13) and marking the position of the scratch. The ball at C is then removed and a larger one inserted thus causing the movable arm to rotate about B. The new position is marked and the rotation is then the distance between the two pricks divided by the distance between B and C.

A displacement in the direction V_0 is obtained by inserting the $\frac{1}{8}$ inch diameter balls between the cut faces as shown in Fig. 22.14. The position of the scratch on the movable arm is marked as before. Using the balls as rollers, the movable arm is displaced in the direction of V_0 and the new position of the scratch marked. The distance between the pricks is the displacement.

The procedure will be illustrated by the case of a circular ring of constant section, under the system of loading shown in Fig. 22.15. The ring was 12 inches mean diameter, 0·5 inches wide and 0·18 inches thick. Scratches were made on the inner edge of the model and normal to the face at the load points A, B and C, and one arm was screwed to a drawing board. Using the scratches to guide a needle point to paper

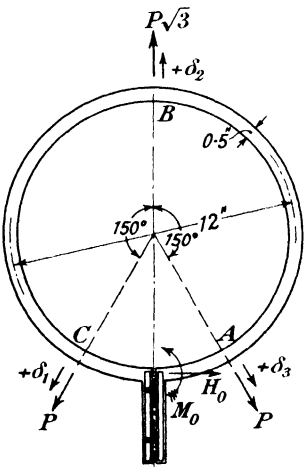

FIG. 22.15.

placed under the model, the positions of A, B and C were marked before and after the appropriate displacement of the movable arm had been made. Very fine lines were drawn through the pricks at right angles to the direction in which the displacement was required, and the distances between the lines measured with a finely divided scale. The following results were obtained. Δ is the displacement of the scratch on the movable arm and d is the distance of the scratch from the centre of rotation. The angular rotation between the cut faces of the ring is then $\frac{\Delta}{d}$.

VALUES OF M_0.

Test No.	Δ	δ_1	δ_2	δ_3	$-M_0=\frac{d}{\Delta}(\delta_1+\delta_3+\sqrt{3}\delta_2)P$
1	13·5	1·3	6·3	−8·6	1·06P
2	13·8	1·2	6·4	−8·8	1·02P
3	13·0	1·1	5·9	−8·0	1·02P

Average value of M_0 = 1·03P.
Calculated value of M_0 = 1·067P. Difference = 3½ per cent.

VALUES OF H_0.

Test No.	Δ	δ_1	δ_2	δ_3	$-H_0=\frac{(\delta_1+\delta_3+\sqrt{3}\delta_2)P}{\Delta}$
1	5·7	−0·4	0	2·7	0·404P
2	5·8	−0·2	0	2·6	0·414P
3	5·7	−0·4	0	2·7	0·404P

Average value of H_0 = 0·407P
Calculated value of H_0 = 0·417P. Difference = 2·4 per cent.

For other examples of this method reference should be made to the paper quoted on p. 562, but one experiment is of special interest and will be outlined.

To illustrate the advantage of a suitable choice of scales, the link shown in Fig. 22.16 was investigated.

To apply measurable deformations to a true scale model of the link, considerable force would have to be used and would cause yielding or buckling. Only very small deformations could safely be applied and a Beggs' deformeter would be necessary.

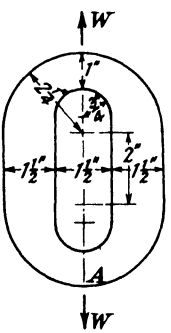

FIG. 22.16.

The methods already described can, however, be used if the scales of the model are altered to produce a more flexible ring and by making the linear scale twice full size (*i.e.* $m=2$), and the width of the model at all sections ⅜ths of the width of the actual link, a sufficiently flexible

model was obtained as shown in Fig. 22.17. Angular deformations were

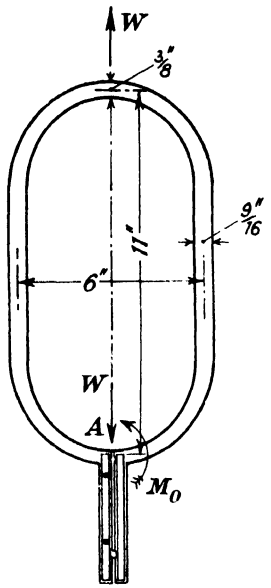

FIG. 22.17.

applied and measurements made as before to obtain M_0 at the section A for loads of magnitude W acting along the major axis of the link.

The results were :

Test No.	Δ	δ_W	$-M_0=\frac{d}{\Delta m}(\delta_W)W$
1	12·1	2·7	0·446W
2	13·2	3·0	0·454W
3	11·0	2·4	0·436W

Average value of M_0 $= -0{\cdot}445W$.
Calculated value of $M_0 = -0{\cdot}460W$. Difference = 3 per cent.

CHAPTER 23

THE VOUSSOIR ARCH

23.1. Description and definitions.—In Chapter 12 we dealt with arches formed by continuous members, *i.e.* arched ribs or members connected to form braced structures. These are comparatively recent developments in the history of engineering, but many centuries before it would have been feasible to build such structures the arch form was in common use in building construction. The early arches were made of a number of wedge-shaped blocks of masonry which were usually set in a jointing material of mortar or cement, although this is not essential to their stability. This type of structure is still commonly used for such diverse purposes as relieving the loads on a lintel over a window opening or bridging a wide gap to carry road or rail traffic.

Fig. 23.1 shows such an arch with the names of the various parts.

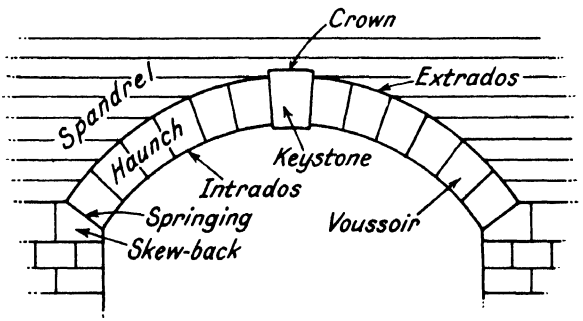

FIG. 23.1.

Many of these terms are of ancient origin.

The wedge-shaped blocks of which the arch is built are known as *voussoirs*. They are usually symmetrically disposed about a central voussoir known as the *key-stone* from a mistaken idea on the part of early builders that it had a special function to perform. As will be seen later, no single voussoir is of more importance structurally than any other, and a key-stone is not essential, as shown by the occasional occurrence of arches with an even number of voussoirs. This, however, is unusual and while its rarity mainly arises from the belief in the importance of the key-stone, it is due to some extent to the prejudice of the mason against allowing a joint instead of a block of stone.

occupy the central position. The key-stone in fact is an aesthetic and traditional feature rather than a structural requirement. The blocks in the abutments of the arch upon which the end voussoirs rest are known as *skew-backs* and the surface between a skew-back and an end voussoir is the *springing*. The highest point of the arch is the *crown* and the lower sections are the *haunches*. This is a general term and there is no hard and fast definition of how much of the structure is comprised in a haunch. The upper boundary line of the arch ring is known as the *extrados* and the inner line as the *intrados*. The under surface of the structure is the *soffit*. When this type of arch is used for a bridge and a more or less level roadway is required, the *spandrels*, *i.e.* the spaces between the top of the arch and the roadway, are built up by *filling*. The weight of this filling has an important effect upon the load which the arch can carry as will appear in later discussion.

An arched bridge of steel or reinforced concrete usually consists of a number of ribs which are suitably bridged transversely to carry the road or railway. In a masonry bridge, on the other hand, the arch is the full width of the road. The under surface (or soffit) is often referred to as the *barrel* of the arch.

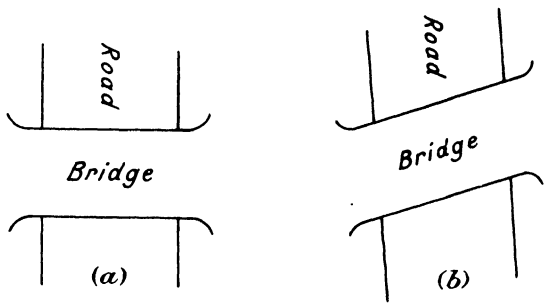

FIG. 23.2.

The simplest type of masonry arch occurs when the bridge crosses the gap to be spanned at right angles, as shown in Fig. 23.2 (*a*). Often, however, the crossing is not right-angled as shown at (*b*) in the same figure. Such a structure is known as a *skew arch* and if it is built of solid blocks of masonry the setting-out and cutting of the voussoirs is more complicated and expensive than in the case shown at (*a*).

Many arches are built of brickwork instead of masonry and the arch then consists of a sufficient number of rings to give the necessary depth, as shown in Fig. 23.3.

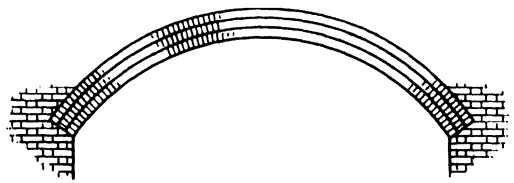

FIG. 23.3.

23.2. Historical.—The voussoir arch is a structure of great antiquity, and speculation upon its behaviour must have been the concern of many of the early builders. The earliest attempts at a formal explanation appear to have been made by French mathematicians.

As might be expected, the first arguments were based on the properties of the inclined plane and the wedge. Some writers approached the problem theoretically, assuming that the interacting surfaces of the voussoirs were polished and that the arch would fail by slipping. This line of argument assumed that the pressure acted normal to the face of each voussoir and led to the conclusion that the voussoirs must be of increasing depth towards the springings in order that the arch might be equilibrated.

As late as 1801, Atwood in England made experiments on two models of arches with polished metal voussoirs, in which he measured the pressure perpendicular to the face of certain voussoirs in order to prove formulas based on the wedge theory. Rennie's bridges at the beginning of the last century were designed more or less on these assumptions.

An alternative assumption was that the voussoirs were infinitely rough. The arch must then fail by the rotation of some of the voussoirs about their edges, and this was actually shown to occur in certain model experiments made by the French engineer, Couplet, in 1730. He, however, arrived at the erroneous conclusion that the joints of rupture for all arches were at the key-stone and at 30° to the horizontal.

A third line of attack, enunciated by Hooke but little developed during the eighteenth century, was derived from analogy with the loaded catenary.

Meanwhile, a number of important voussoir arches were being designed and erected in France under Perronet who initiated a number of experiments. In particular, in connection with a bridge at Nemours, Chief Engineer Boistard made a number of model experiments in 1800 which led him to the conclusion that all bridges failed by opening of joints at the crown, at the haunches and at the abutments, and that in general the joints at the crown and abutments would open at the intrados and those at the haunches at the extrados. These experiments, together with others made by Rondelet about the same time, were of considerable importance, as they led to new theories of the behaviour of the arch.

In 1826 Navier, having propounded a straight line law for the pressure distribution across the face of voussoirs in contact, showed that if the resultant pressure at the crown and joints of rupture acted at one-third of the depth of the ring from the extrados and the intrados respectively, the joints would be just on the point of opening. This was re-introduced by Mery as a new idea in 1840 and is the beginning of the doctrine of the middle-third of which more will be said later.

Much of the Continental work seems to have remained unknown in England for a long time. Professor Robison of Edinburgh recorded the collapse of a bridge made in rather soft stone, the failure of which was ascribed to overloading at the crown. About a fortnight before final failure occurred, it was noticed that the stones on the soffit of the arch at 10 feet on either side of the centre and also at 20 feet on one side

were cracking badly and it was considered by the masons that ultimate failure would take place at these points. Actually, it occurred by pivotting of segments of the arch about a point at the crown and at points about 15 feet or 16 feet on either side of the centre : the arch hovered for a short time and finally pivotted about points at the abutments. Professor Robison experimented on a model made of chalk and by overloading the crown was able to reproduce this type of failure.

It is uncertain when the idea of the line of pressure or linear arch,* which is the outcome of the third line of attack, was introduced on the Continent as a means of studying the voussoir arch, but in this country it was developed by Professor Moseley in 1835, who showed that this line must lie within the arch ring.

In 1846 Snell determined the joints of rupture and the amount of thickening of voussoirs required in the neighbourhood of the abutments of certain arches to keep the line of pressure inside the arch ring. He also introduced the question of the failure of the materials of the arch and the necessary bearing area as modifying the position of the line of pressure.

In the same year Barlow pointed out that in most cases more than one line of pressure could be drawn for an arch, all of which had equal validity. He proposed as a criterion the line of pressure which passed through the centres of the crown and haunches.

In a sense this marks an advance in the formal approach to the problem ; interest was no longer centred on a state of limiting stability which no actual arch would reach, but on the correct choice of the line of pressure, assuming the arch to be of dimensions admitting of choice. The prevailing view seems to have been that since any line of pressure which could be drawn within the prescribed limits was a possible one, the matter of selection was simply one of convenience.

This is not the case ; each possible line of pressure corresponds to a definite condition at the abutments as will be shown later.

Woodbury in America, and Rankine in this country, adopted the doctrine that the line of pressure must like within the middle-third, thus eliminating tensile stresses. This is nowadays advocated by most writers, many of whom assume that if any line of pressure for the given load can be drawn within the middle-third, the arch is satisfactory.

Rankine's design method is a compromise and, since it affords a key to many other design methods to be found in text books, it will be outlined here. He assumed that the load system consists of vertical forces distributed in any symmetrical manner along the span. A linear arch which will carry this system is selected in a more or less arbitrary manner. Generally this linear arch is the same shape as that of the intrados of the completed arch.

The horizontal thrust at the crown is calculated from a formula, due to Navier, for an arch under normal pressure, viz., the product of the intensity of pressure and the radius of curvature at the point considered.

The equilibrium of this linear arch can only be maintained by a system of horizontal pressures applied along its length ; between the crown and

* See paragraph 12.10.

some point on the haunches these pressures must be directed outwards ; below that point they must be directed inwards. Rankine called these conjugate pressures, and the point where the pressures change sign he termed the point of rupture. If the pressures were omitted below this point the voussoirs of the actual arch would be forced outward and freed, while omission of the pressures above it would only tend to wedge them together. The point of rupture corresponds to the position of maximum horizontal thrust, which is the sum of the Navier thrust at the crown and the conjugate pressure applied between the crown and that point.

Having determined the point of rupture and the maximum horizontal thrust, the arbitrary linear arch is abandoned and the real design is begun. That part of the arch below the point of rupture is included in the abutment and is given suitable horizontal backing ; the part above, which is the real arch, is designed to carry the vertical loads and a horizontal thrust equal to the maximum already determined. With regard to this, Rankine stated : " The stability of an arch is secure if a linear arch balanced under the forces which act on the real arch can be drawn within the middle-third of the arch ring." He emphasised the point thus : " It is true that arches have stood, and still stand, in which the centres of resistance of joints fall beyond the middle-third of the depth of the arch ring ; but the stability of such arches is either now precarious, or must have been precarious while the mortar was fresh."

Since stability of a voussoir arch is not dependent upon fulfilment of the no-tension condition and since a condition of instability only occurs under much larger loads than those which just violate this condition, it must be assumed that Rankine used the word " stability " in a different sense from that now understood.

Meanwhile speculation as to the " true " line of pressure continued on the Continent and various theories were advanced.

Hagen defined the most probable line as that for which the vertical projections of the minimum distances between the line of pressure and the boundaries of the arch ring were a minimum. Another theory advanced in a slightly varying form by various writers, was that the true line gave minimum stresses at the critical sections.

Winkler suggested that the true line was that for which the sum of the squares of its distances from the centre line of the arch ring was a minimum. These distances are proportional to the bending moments in the ring, and the proposal is practically equivalent to stating that the strain energy due to bending must be a minimum. This is consistent with the work of Castigliano who analysed a masonry voussoir arch on the basis of his newly enunciated theorems.

Castigliano assumed that the abutments were rigid and so long as the line of pressure of the arch ring was everywhere within the middle-third the ring would behave as a continuous elastic rib. The thrust was first calculated for the complete arch by the method of minimum strain energy. If the resulting line of pressure fell outside the middle-third at any section, the portions of the arch ring which were thereby put into tension were assumed to be removed and a second approximation was made using the modified arch ring. This process was continued until

no tension was found at any point and the stresses were then calculated by the usual methods.

One objection to the use of Castigliano's method was the doubt as to whether a masonry arch exhibited a linear relationship between load and displacement. This point will be discussed later.

Although in the light of more recent work Castigliano's method appears to provide the soundest basis of design, it has not hitherto been generally accepted and reliance is usually placed on a combination of older theories, which will be summarised in the next paragraph.

23.3. The accepted basis of design.—It is generally assumed that a voussoir arch may fail in any of four ways :

(1) By the development of excessive tensile stress in the jointing material.
(2) By the development of excessive compressive stress in the material.
(3) By the sliding of one voussoir over another.
(4) By spreading of the abutments.

The last of these can only be prevented by the provision of adequate stability in the abutments and foundations. This is necessary for all arches and must be treated as a separate problem distinct from that of the design of the arch itself. The sliding of a voussoir depends upon the angle which the resultant of the normal and transverse forces at any joint makes with the normal to the joint. If this angle is less than the angle of friction the joint is safe against such failure. If it is greater than the angle of friction, the joint between voussoirs may need a mechanical key.

The calculation of the stresses at any section of the arch would be simple if the correct linear arch or line of pressure could be drawn, but as already shown in the preceding paragraph, the selection of the correct line has given rise to considerable controversy in the past. Only one point has been generally agreed upon—that if tension is to be avoided the linear arch must fall within the middle-third of the depth of the arch ring at every point. If it is assumed that the stress distribution is linear across any section this must be true, but within this limitation any number of linear arches can be drawn.

It does not appear to have been recognised until recently * that each of these possible linear arches is intimately associated with the condition of fixity at the abutments and this needs emphasising.

Suppose that Fig. 23.4 represents a voussoir arch with fixed ends, which carries any system of external loads. Since it is assumed, as a basis of design, that no tension shall be developed in the ring, the structure can be treated as an arch-rib, as will be shown.

Such a rib has three redundant reactions represented by the couple M_0, the vertical force V_0, and the horizontal force H_0, at the support B. The forces V_0 and H_0 act at the centre of the springing.

These three reactions can be replaced by a single force R acting at some point in the springing line, and this is the point through which the

* "An Experimental Study of the Voussoir Arch." A. J. S. Pippard and R. J. Ashby. Journal Inst. C.E., 1938–39, pp. 383–404.

line of resistance passes. Since the structure is complete in itself if the end B is unsupported, the actions M_0, H_0 and V_0 may be assigned any arbitrary values without causing a collapse. For each set of values, however, there will be a different position of the resultant action R; that is, the line of resistance will start at a different point in each case.

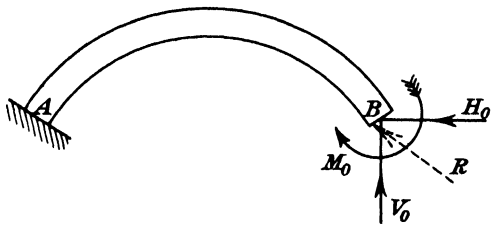

FIG. 23.4.

These actions will, however, in general, cause component displacements of the end B which may be calculated by an application of the first theorem of Castigliano. Thus if U denotes the total strain-energy of the structure due to the external system, then

$\frac{\partial U}{\partial M_0}$ = the angular rotation of section B in the direction of M_0,

$\frac{\partial U}{\partial H_0}$ = the horizontal movement of section B in the direction of H_0, and

$\frac{\partial U}{\partial V_0}$ = the vertical movement of section B in the direction of V_0.

For one particular set of values of M_0, H_0 and V_0 these movements will be zero; that is, there will be no displacement of the support. For any other set of values, however, the end B will be displaced and a different linear arch will be obtained. The arbitrary assumption of a particular linear arch thus tacitly assumes certain movements of the abutments, and it is therefore inconsistent to assume absolute fixity and at the same time to select a linear arch arbitrarily.

It is customary, however, to make such an arbitrary choice and thus determine the thrust and bending moment at all sections of the arch. The stresses in the material are calculated from these data and must not exceed the prescribed safe values.

23.4. The voussoir arch as an elastic structure.—The method of analysis used by Castigliano depends for its validity upon the assumption that a voussoir arch shows a linear relationship between load and displacement and in 1890 the Austrian Society of Engineers carried out an exhaustive series of experiments to determine this point, among others. A number of arches were loaded to destruction and it was found that until cracks started to develop, the measured displacements were approximately proportional to the applied loads. The development of cracks did not cause much alteration to the arch shape.

From these experiments it was rightly deduced that elastic theory was applicable to such structures. There appears to have been, however, an unwarranted deduction that the arches behaved as solid ribs and that the thrust could, therefore, be calculated by the method of minimum strain energy. This does not follow from the mere fact of a linear relationship between displacement and loading, since such a relationship would equally be observed if the structure were a three-pinned arch, and, therefore, statically determinate.

In order to prove that the structure behaves as a solid rib it is necessary to show that the thrust of a voussoir arch is the same as that of a continuous rib of the same dimensions. As part of an experimental research recently carried out upon voussoir arches * this point was tested and found to be true

For a study of the behaviour of the arch, as distinct from an investigation of design problems, it was desirable to experiment upon a structure made of material whose elastic properties were definite, and for this purpose a segmental arch was made of steel voussoirs. The span was 4 feet and the rise 1 foot. The voussoirs, fifteen in number, were each 3 inches deep and $1\frac{1}{2}$ inch in width ; they were very carefully machined so that the bearing was as perfect as possible. In some cases a very thin rubber insertion was placed between them to distribute any slight inequalities, but this did not appreciably affect the results obtained. The arch was made so that it could either be mounted on pins at each abutment or on skew-backs. The design is shown in Fig. 23.5.

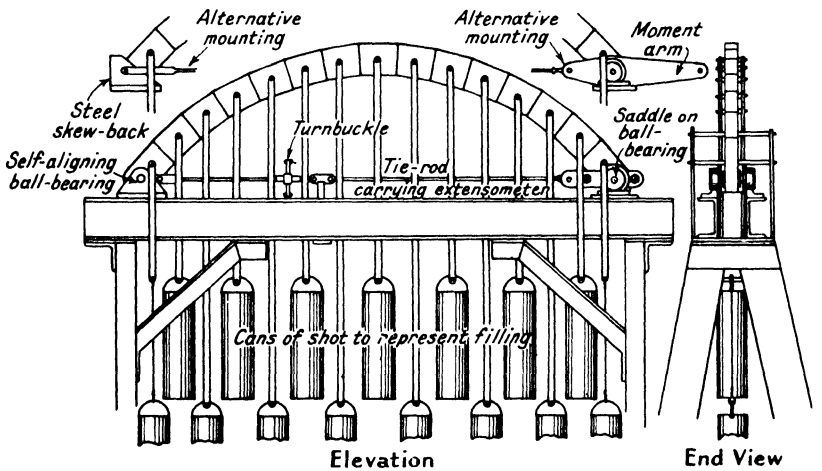

FIG. 23.5.

In either case, whether the ends were pinned or mounted on skew-backs, one support was fixed in position and the other was attached to a saddle which could move on ball bearings in a horizontal direction. The movable end was anchored by a No. 4 B.A. tie-rod, to which was attached

* "The Mechanics of the Voussoir Arch." A. J. S. Pippard, E. Tranter, and L. Chitty. Journal Inst. C.E., 1936–37, pp. 281–306.

an extensometer of the mirror type which enabled the horizontal thrust to be measured. The span of the arch was controlled by a turnbuckle and a delicate mirror indicator. The tie-rod was calibrated by direct loading and the extensometer allowed the load in it to be measured to about 0·1 lb. The centre of each voussoir carried a spindle from which weights were hung to represent the filling of the arch, and an extra load representing the live load could be suspended from any of these points. The voussoirs were provided with slots and pins to prevent relative rotation but no other constraint was given.

In the experiment to test the point now under discussion the span of the arch was kept constant and the variation of thrust was measured when a point load of increasing amount was applied to a particular voussoir.

The curve of Fig. 23.6 shows the increase of the horizontal thrust due to the applied concentrated load, and it consists of two straight lines joined by a short transition curve. The slope of the lower line gives H=0·458W, which agrees well with the value H=0·455W for a similar solid arch-rib, similarly loaded. The upper line gives H=0·720W and

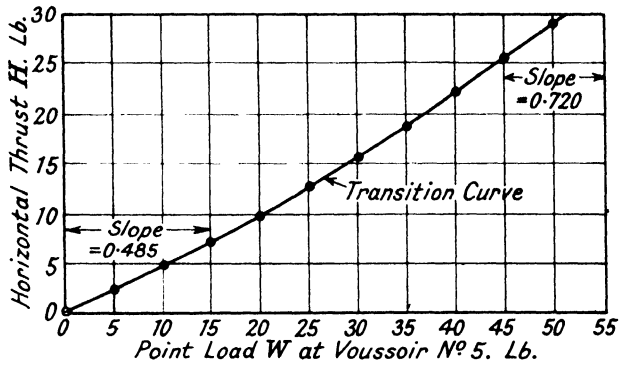

FIG. 23.6.

this is very close to the value of H=0·716W for an arch-rib pinned at the supports and also at a point on the extrados of the joint nearest the load between the centre of the arch and the loaded point.

Similar results were obtained when the load was applied to other voussoirs and shows conclusively that in the earlier stages of loading a voussoir arch behaves in a similar way to a solid arch-rib of the same dimensions. The small differences observed were probably due to imperfections in the bearing surfaces. The significance of the curves obtained in the later stages of loading will be examined later, but they indicate clearly the development of a " virtual pin joint," by hinging of adjacent voussoirs.

Later, evidence of the elastic behaviour of masonry arches was obtained during the course of a long series of tests on actual bridges carried out by the Building Research Station of the Department of Scientific and Industrial Research for the Ministry of Transport just before the war of 1939. These tests were made on stone and brick

arches of varying ages and spans, and deflections under load were carefully measured. The results showed beyond doubt that all the structures exhibited good linear relationship between load and displacement.

These and the earlier Austrian tests provide ample justification for treating the voussoir arch as a structure which obeys Hooke's law and the laboratory tests mentioned above show that the structure is equivalent in behaviour to a solid rib during the earlier stages of loading.

23.5. Mechanics of the voussoir arch.—Reference was made in paragraph 23.4 to laboratory experiments to determine the thrust of a voussoir arch. These particular tests were made as part of a wider study of the mechanics of this type of structure and a description of the results obtained will help towards an understanding of the way in which the loads are supported by the interactions of the voussoirs. The experimental arch is shown in Fig. 23.5 and the transition of the arch from a two-pinned to a three-pinned structure has already been described. The next step in the research was to find the position of the points of hinging between voussoirs, *i.e.* of the virtual pins under different conditions of loading, and to determine the way in which ultimate collapse occurred. It had already been established that when the span was kept constant the virtual pins always formed, if the point load were sufficiently great, although it was not possible to see the actual hinging as the voussoirs were so well fitted. A series of experiments was, therefore, made in which the model, after being erected correctly, was given a definite increase or decrease in span. This served the double purpose of enabling visual observations to be made of the hinge points or pins and also provided evidence of what would happen to an arch if small movements of the abutments occurred. The ends of the arch were mounted on practically frictionless pins. The arch was first erected as accurately as possible without the insertion of rubber between the joints and was loaded with weights representing the dead load of the filling. The turnbuckle controlling the span was then adjusted to give a small spread. Visual observations showed that under these conditions the key-stone was held only at the extrados of the two joints, and that there was a slight gap in both these joints at the intrados. This is shown in Fig. 23.7. A small additional concentrated load was applied to a particular voussoir (for the purpose of illustration, this was No. 6) and the effect was to cause the joint on the farther side of the key-stone to close, leaving a single " pin " at the extrados between the key-stone and voussoir No. 2. An increase in the concentrated load caused this " pin " to move to the extrados of the next joint towards the load and a progressive increase in the magnitude of the applied load caused the joint to move nearer and nearer towards the loaded voussoir. The sequence of events is shown in Fig. 23.7. When the pin had taken up a position on the joint next to the load, between the load and the centre of the arch, it did not change its position again until failure occurred.

When the load was removed the cycle of events was reversed and the pin-joint assumed the same series of positions as during loading; the process could be repeated over and over again with perfectly consistent

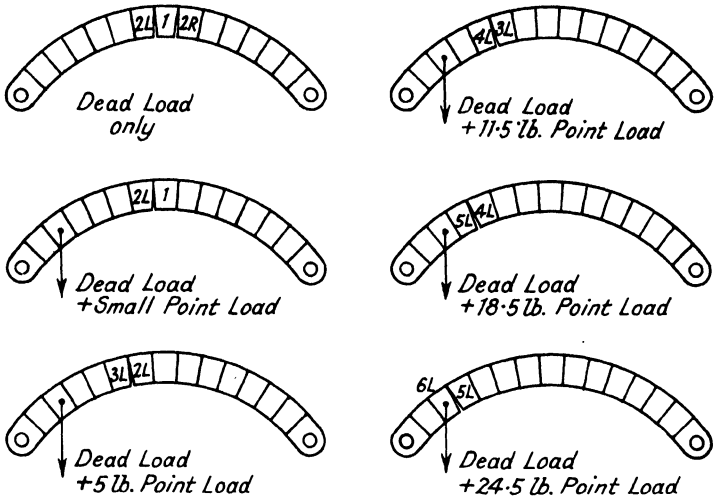

FIG. 23.7.

results. It is therefore clear that in a pin-ended voussoir arch a spread of the abutments produces what is effectively a three-pinned arch in which the third pin ultimately assumes a position at the extrados of the joint next to the load, between the load and the centre of the arch. Having observed this behaviour it was verified by measuring the value of the thrust for definite values of the point load, and Fig. 23.8 shows,

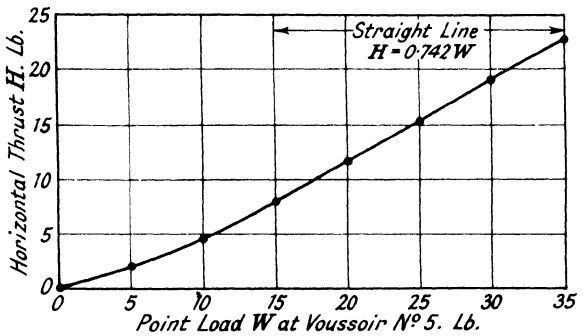

FIG. 23.8.

as an example, the curve when voussoir No. 5 was loaded. It will be seen that the first portion of the curve is not straight, due to the changing position of the pin as it moves from the centre of the arch towards its final position.

When this final point has been reached, however, the curve becomes linear and its slope corresponds to the thrust for the corresponding three-pinned arch, which can be calculated statically. In Fig. 23.9 the theoretical influence line of thrust is shown for the three-pinned arch, the third pin being assumed to be in the appropriate position next to the

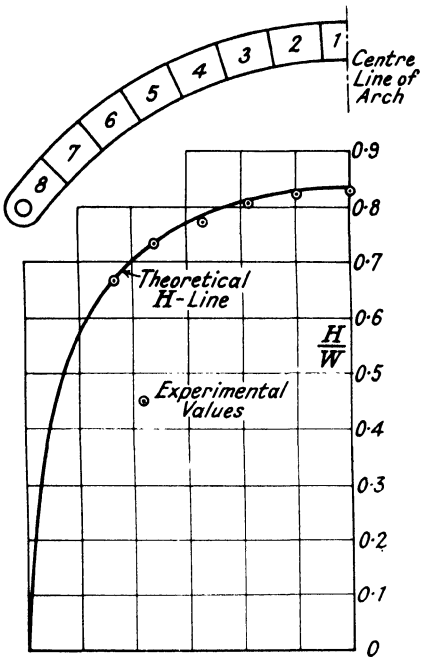

FIG. 23.9.

load, and experimental values obtained from the slopes of curves such as that of Fig. 23.8 show excellent agreement. If the abutments, instead of being spread, are contracted, a pin forms on the intrados of the arch between the key-stone and the next voussoir. As the live load increases, the pin travells away from the loaded point, as shown in Figs. 23.10, instead of towards it as in Figs. 23.7 ; the final position, in this particular case, is 3–4.

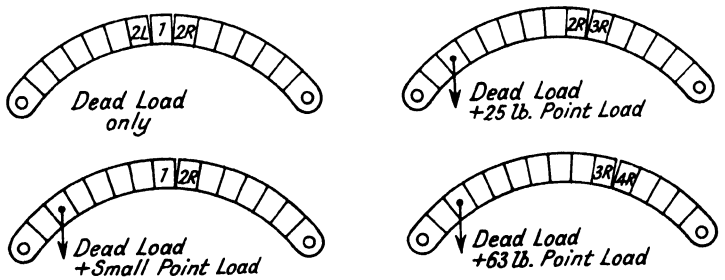

FIG. 23.10.

When the span is kept correct the pins, althougn not visually detectable, still form in the same positions, and for a certain value of the point load on a particular voussoir the final position of the pin on the extrados is reached, *i.e.* at the joint next to the loaded voussoir. If the load is

increased beyond this value no chance occurs in the pin position but at another, possibly a considerably higher, value a pin develops at the intrados somewhere in the other half of the arch. The three-pinned structure is now turned into a four-bar mechanism and complete collapse occurs. The four-bar mechanism is the same whatever the original conditions as regards the span.

An actual voussoir arch is not supported on pinned ends as in the experiments just described, but on skew-backs which may, on the assumption of perfect fixity, be supposed to provide encastré ends. The changes of slope at the ends of a pinned arch under load are, however, extremely small, and a very slight movement of skew-backs would be sufficient to transform a nominally fixed end into a virtually pinned arch. It is therefore likely that the case of the pinned arch, just described, is in many cases a closer approximation to the true conditions in an actual structure than when the ends are assumed to be encastré. It was clearly necessary, however, to examine the latter case, and the experimental structure was modified by the provision of special end blocks to take the place of the pinned ends previously used. At one end a steel skew-back, carefully machined to the correct angle, was bolted to the framework supporting the arch; the other end was mounted as in the earlier structure, its horizontal movement being restrained by the No. 4 B.A. tie-rod as before, but in this case an extension arm rigidly attached to it allowed moments to be applied by adding weights to the end of the arm. The angle of the voussoir at this end could thus be controlled.

Preliminary experiments showed that this arch also behaved for small loads in the same way as a solid encastré rib of the same cross-section.

As in the arch with pinned ends, it is probable that the most important practical case occurs when a slight movement of the abutment takes place, and this was the next case to be investigated. There are several possibilities to be considered, as follows :—

(*a*) The abutments may spread and at the same time rotate in such a way that the ends of the arch are free to take any angular positions.

(*b*) There may be a spread of the abutments with no angular movements.

(*c*) The abutments may approach each other.

The last of these cases is possibly only of academic interest, but the first two can, and probably do, occur frequently in practice.

In the model it was only possible to adjust the movement of one skew-back, but visual observation showed clearly what occurs under the different conditions. When the abutments were spread and the adjustable skew-back was allowed to rotate freely, the arch behaved exactly as in the case of the pin-ended structure previously described. In this case the " pins " were at the centre of rotation of the adjustable skew-back, at the intrados of the joint between the end voussoir and the fixed skew-back, and at the extrados of some other joint, the position as before being governed by the magnitude of the point load.

When the abutments were spread and rotation was restrained, " pins " developed at the intrados of the two joints next to the skew-backs and at the extrados of another joint, as before. If the abutments were brought closer together than the designed span, " pins " appeared at the extrados of joints near the skew-backs (not always at the joints next to them) and at the intrados of some other joint as in the pin-ended arch. These cases are shown in Fig. 23.11.

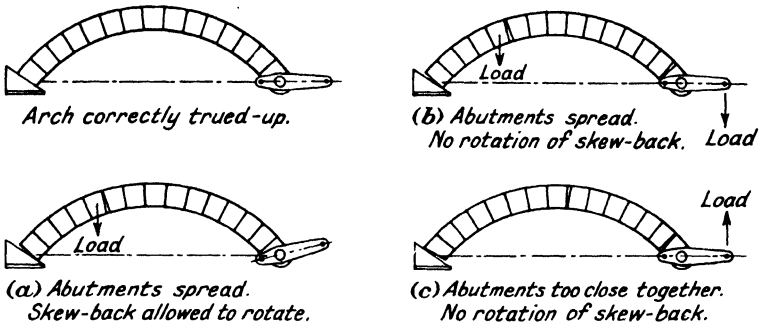

FIG. 23.11.

It is therefore clear that the fixed-end arch, if there is any movement of the abutments, becomes in effect a three-pinned arch, and can be treated as already described. The general results may be summarised as follows :—

(*a*) *Two-pinned arch with span kept constant.*—When the span was kept constant the two-pinned arch behaved like a solid rib of the same dimensions until a certain value of the point load was reached. As this load was increased the ratio $\frac{H}{W}$ also increased, until it reached the value corresponding to that for a three-pinned arch in which the third pin was at the extrados of the joint nearest the load, between the load and the centre of the arch. At this value it remained constant.

(*b*) *Two-pinned arch with abutments slightly spread.*—A virtual pin-joint was found to develop at the extrados. When there was no live load the pin was at the crown, but its position changed with the magnitude of the live load, moving in turn to joints nearer the load, the final position (when the load was sufficiently large) being at the joint next to the load, between the load and the centre of the arch.

(*c*) *Two-pinned arch with abutments brought nearer together.*—A virtual pin-joint developed at the intrados. When there was no load the pin was at the crown, but its position changed with the magnitude of the live load, moving successively to joints farther away from the load.

The position of the third pin for any system of loads could be determined for either case (*b*) or (*c*), whilst the load which produced instability of the structure in cases (*a*), (*b*) or (*c*) could also be determined.

(*d*) *Fixed-end arch with span kept constant.*—In this case the arch behaved for low loads approximately as a solid rib.

(*e*) *Fixed-end arch with abutments spread.*—Virtual pins were found

to develop at the intrados of the skew-backs and at the extrados of some other joint, the position of this third pin being the same as that described in case (*b*).

(*f*) *Fixed-end arch with abutments brought nearer together.*—Virtual pins were found to develop at the extrados, at or near the skew-backs and at the intrados of some other joint, the position of this third pin being the same as that described in case (*c*).

(*g*) *Design assumptions for fixed-end arch.*—In many actual arches there will be a spread of abutments corresponding to cases (*e*) and (*f*) above, and the problem will be statically determinate. Any design method should therefore take into account the possibility of the structure assuming the three-pinned form.

23.6. Behaviour of a masonry arch.—In the experiment described in the last paragraph the arch was constructed without jointing material between the voussoirs, and the usual assumption made in design, that no tensile stresses can be transmitted, was exactly satisfied. It was shown that under these conditions, provided the correct linear arch fell everywhere within the middle-third of the arch ring, the structure behaved exactly like an arch-rib and could be analysed by the standard methods applicable to such structures.

An increase in the point load finally produced a condition in which adjacent voussoirs were in contact only at the extreme edges, and a succession of virtual pin-joints were formed, which reduced the problem to comparatively simple statical terms. Failure occurred when sufficient of these pins formed to transform the structure into a mechanism.

Between the two extremes of an arch-rib and a pinned structure there was an intermediate stage in which the bearing surface between adjacent voussoirs extended over a diminishing depth of the joint, but owing to the nature of the material used in the voussoirs this transition stage was not very marked

If a jointing material is used in the construction of an arch the adhesion between this material and the voussoirs, and the nature of the material itself, may enable the joint to offer some resistance to tensile stress. Also, the material may be such that it will fail in compression before the virtual pin can form at the extreme edge of the joint.

The general effects of the presence of jointing material of the type referred to will be to increase the magnitude of the point load under which the structure still behaves as an arch-rib, since the linear arch can fall outside the middle-third without causing the opening of a joint, and to lower the magnitude of the load at which instability occurs, since the " pin " cannot reach the extreme edge of the joint.

If the material of which the voussoirs are made cannot withstand the compressive stresses set up, premature failure of the structure will occur.

Further experiments were carried out * to determine the applicability of the results of the previous work to actual structures and for this purpose an arch having a clear span of 10 feet and a rise of 2 feet 6 inches

* " An Experimental Study of the Voussoir Arch." A. J. S. Pippard and R. J. Ashby. Journal Inst. C.E., 1938–39, pp. 384–404.

was built. This is shown in Fig. 23.12.

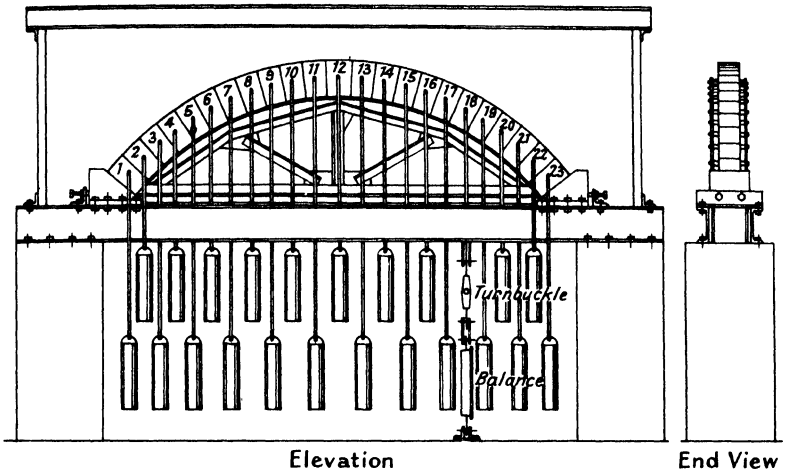

FIG. 23.12.

Two sets of cast concrete voussoirs made of rapid hardening cement with limestone and granite chippings respectively were used. The compressive strengths of the two concretes at 28 days were 1,740 lb. per square inch and 6,700 lb. per square inch. The voussoirs were 10 inches deep, 6 inches thick and tapered from 6·18 inches to 5·41 inches in elevation. The arch, with $\frac{1}{4}$ inch mortar joints, contained twenty-three voussoirs. The load representing the arch filling was provided by lead shot carried in cans from the individual voussoirs. Most of the tests were made with a light loading estimated on a depth of filling of 6 inches over the crown, the density being 70 lb. per cubic foot. One test, however, was made with heavier loading estimated on a depth of filling of 12 inches over the crown, the density being 140 lb. per cubic foot.

Seven series of tests were made on arches built and loaded to the specifications shown in Table 23.1.

TABLE 23.1.

Series	Voussoirs	Jointing material	Loading
1	Limestone	Non-hydraulic lime mortar	Light
2	,,	None	,,
3	,,	Rapid-hardening Portland cement mortar	,,
4	Granite	Non-hydraulic lime mortar	,,
5	,,	None	,,
6	,,	Rapid-hardening Portland cement mortar	,,
7	,,	,, ,,	Heavy

The non-hydraulic lime gives a mortar with practically no tensile

strength, and it was used solely to form a bedding for the voussoirs. It is also weak in compression compared with cement mortar. The cement mortar was a mixture of rapid-hardening Portland cement and sand in the proportion 1 : 3 by weight.

In every test an increasing load was applied to a particular voussoir and observations were made of the initiation and development of cracks in the jointing material.

The test was continued until complete failure occurred, usually by the development of a fourth " pin-joint " causing the structure to become unstable, or in some cases by spalling of the voussoirs, or by slipping along a joint. It was found that the load could be steadily increased to the value at which a fourth pin developed, when a sudden collapse occurred. The centering of the arch, left in position a few inches clear of the soffit, prevented a complete break-up, and on removing the point load it was generally found that the structure returned to its original position unless slipping between voussoirs had occurred.

For full details of the test results reference should be made to the original paper, but they are shown in diagrammatic form in Figs. 23.13 and 23.14.

Fig. 23.13 gives the tests on both limestone and granite voussoir arches when jointed in lime mortar, and Fig. 23.14 those when cement mortar was used. Reference curves are plotted in each figure as follows. Curve A shows the concentrated load which must be applied to any voussoir to cause the linear arch to reach the middle-third point of any joint. Curves B and C show the load which cause the linear arch to reach the middle-half and middle-three-quarter points respectively of any joint. Curve D gives the loads which cause the linear arch to touch the extrados of the arch ring at any joint. All of these curves are obtained on the assumptions that no cracking of a joint occurs ; that is, that the arch can be treated as a rib, and that the abutments are completely rigid. Curve E gives the maximum loads for which an *arbitrary* linear arch can be drawn wholly within the middle-third of the arch ring. As already shown, this involves the tacit assumption that the abutments are free to move as required, and although this method is widely used it is incorrect if the abutments are rigid, as they are assumed to be. For the particular proportions of the experimental arch it is of interest to note that this curve coincides very closely with curve B, which shows the maximum loads keeping the linear arch within the middle-half, the abutments being rigid. The middle-half rule has been advocated by various authors and, at any rate in the test arch, its correct application would lead to the same results as the usual and incorrect application of the middle-third rule. Curve G gives the loads which would cause the arch to fail due to instability. The method of calculation is given in detail in paragraph 23.8.

Curve F is similar to curve G but is based on the assumption that the arch ring is 9 inches deep instead of its real value of 10 inches. This assumption was made as it was found in a number of the experiments with lime mortar that the tension crack only extended to within $1\frac{1}{2}$ inch of the edge of the ring at failure. If a linear distribution of stress is

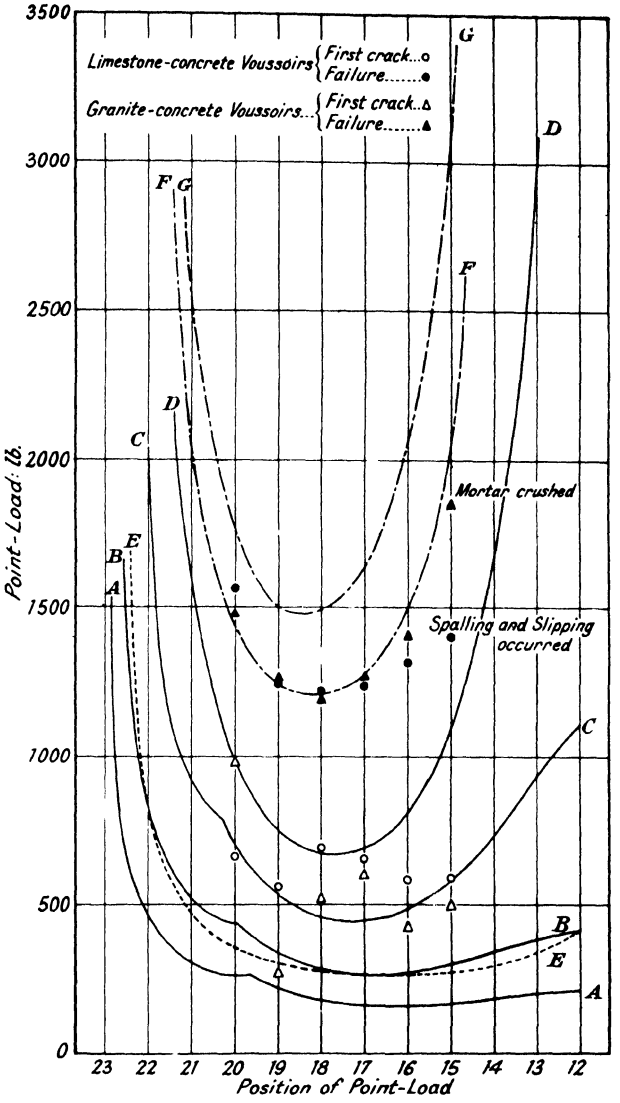

FIG. 23.13.

assumed, the centre of pressure is then ½ inch from the edge.

It will be seen from Fig. 23.13 that only in one case did the first crack appear at a load below that of curve B. The majority of arches in this series did not show any sign of cracking until the linear arch almost reached the extrados. The ultimate failures were grouped closely around curve F. Those giving low values of ultimate load failed by crushing of the mortar or spalling of the voussoirs. It should be noticed that the

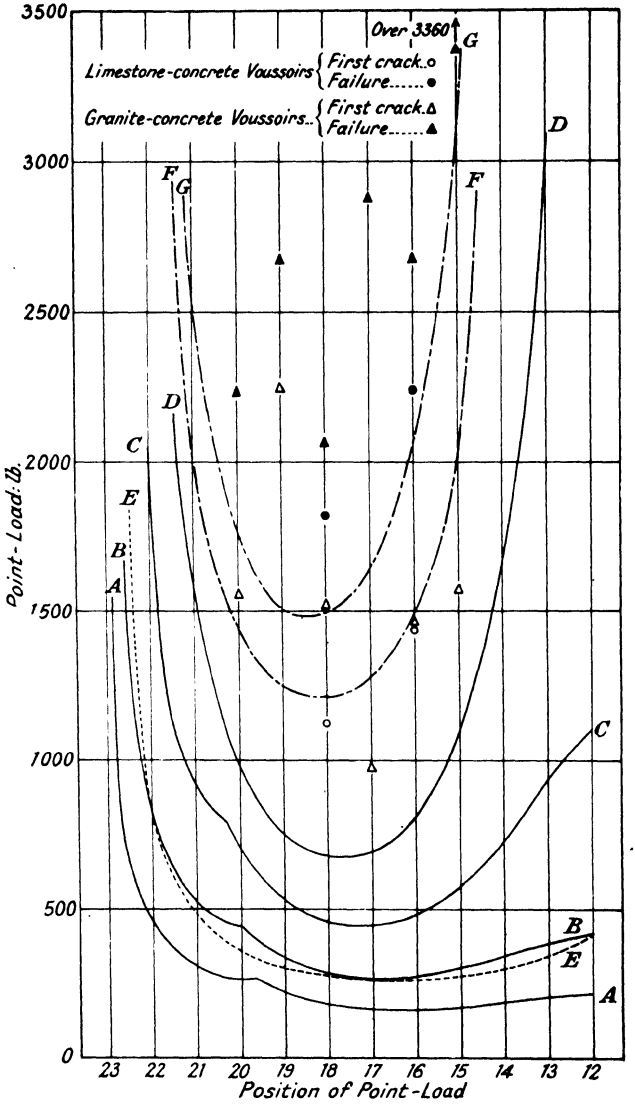

FIG. 23.14.

results of the tests are not dependent to any marked extent upon the material of the voussoirs, indicating that the behaviour of the arch depends primarily on the jointing material.

Fig. 23.14, relating to tests with cement-mortar joints, shows that in every case the linear arch came well outside the arch ring before the first crack appeared, and in the majority of cases ultimate failing loads were much higher than those based on the stability calculation for unjointed

voussoirs. These results indicate that cement-mortar joints have an appreciable strength in resisting tension, which could well be taken into account in design.

The results are shown in Figs. 23.15 and 23.16 by a series of linear arches for lime- and cement-mortar jointed arches respectively. These are drawn for the loads at which the first crack appeared, and show the conservative nature of the middle-third rule. They were obtained by strain-energy analysis on the assumption that there was no movement of the abutments.

These tests were all carried out for light loading, since the point loads required to cause failure under heavy loading would have been inconveniently large. For comparison, however, one test was made with the heavy dead load. This arch showed no sign of failure until a point load of 3,545 lb. was applied, when it collapsed suddenly with a typical instability failure. The spalling was no worse than in previous tests. Under light loading the arch failed at 2,075 lb. applied to the same point. The ratio of the failing loads is 1.71, which is practically the ratio of the dead loading including the weight of the voussoirs.

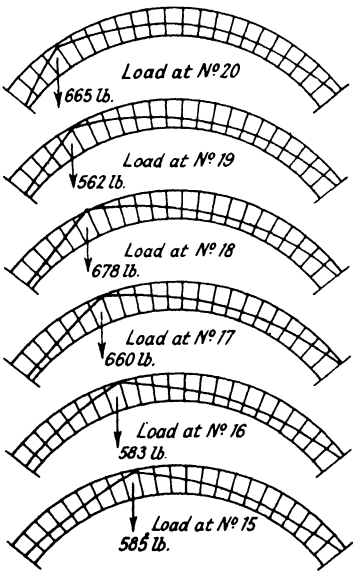

FIG. 23.15.

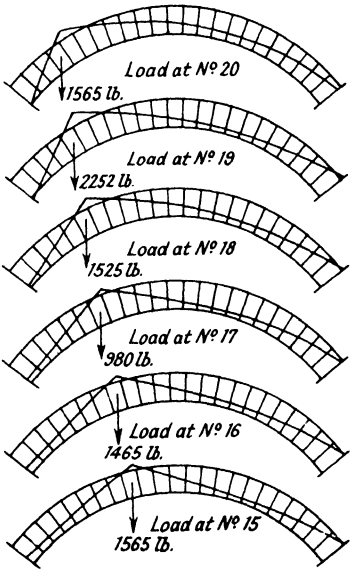

FIG. 23.16.

It is evident from these tests that, even when weak mortar is used, the middle-third criterion is pessimistic. This has been recognised by various authors, who have suggested that the middle-half core should be considered as the safe region for the linear arch. With good cement mortar, however, even this is on the safe side, and there is little doubt that no cracking of joints would occur if a wide margin still were adopted. It must be emphasised, in this connection, that the development of tension at a single joint does not indicate that the structure is unsafe, since a very large margin of strength is available before instability occurs.

23.7. Effect of repeated loads on a voussoir arch.—It was shown in the last paragraph that under static loads the voussoir arch is considerably stronger than is generally assumed ; under actual conditions, however, the live loads upon the structure will be applied, not once, but many times. Two series of tests were therefore carried out to determine the effect of repeated application and removal of the load.*

The arch was that already described and the dead load was applied as in the static tests.

A sketch of the arrangement for applying the live load is shown in Fig. 23.17. The rocking lever was pivoted to a bracket bolted to two joists at right angles to the centre plane of the arch. The other end of the lever was attached to a slider link, connected to a cam driven through gearing from an electric motor. A spring-balance was attached to a voussoir, but at its lower end it was provided with a link which passed through the rocking lever and was guided by a plate fastened to it. The lower end of this link was screwed for a considerable length, and a stop which rested on a hand-wheel was attached, so that the effective length of the link could be altered by adjusting the position of the wheel. When the rocking lever made contact with this stop a load was applied through the spring-balance to the voussoir. The position of the stop governed the magnitude of the load. The rocking lever was placed in its lowest position and the hand-wheel adjusted until the spring-balance recorded the load to be applied to the arch. For each revolution this load was then applied and taken off ; the cam was driven approximately 65 revolutions per minute

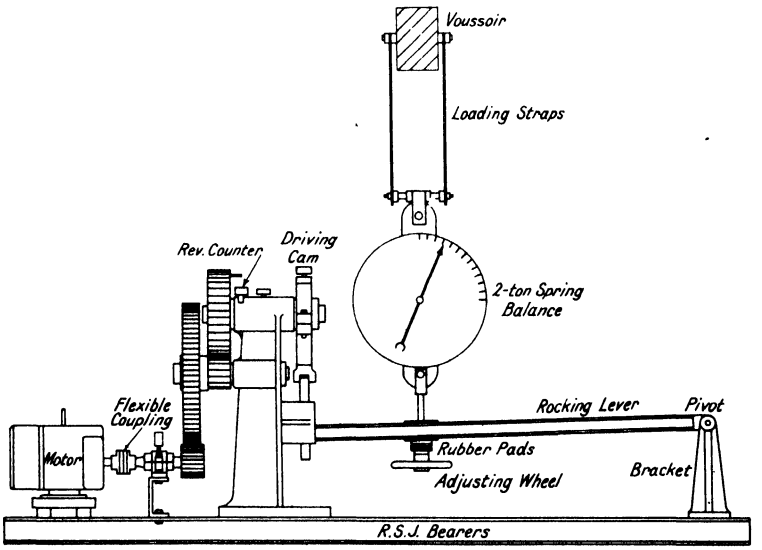

FIG. 23.17.

* " Repeated Load Tests on a Voussoir Arch." A. J. S. Pippard and L. Chitty. Journal of Inst. C.E., 1941–42, pp. 79–86.

A revolution-counter was connected to the cam driving-shaft to furnish a record of the number of reversals and a cut-out device was used to stop the motor when a particular joint cracked.

The first series of tests was made on an arch of granite-concrete voussoirs with cement-mortar joints. Particulars of the tests are given in Table 23.2.

TABLE 23.3.

Test	Period: days	Voussoir loaded	Repeated load: lb.	Number of repetitions	Driving speed: revolutions per minute
1	21	18	430	over 10^6	30-40
2	13	,,	530	,,	41-65
3	11	,,	670	,,	65
4	11	,,	700	,,	,,
5	11	,,	720	,,	,,
6	11	,,	750	,,	,,
7	11	,,	830	,,	,,
8	11	,,	880	,,	,,
9	11	,,	970	,,	,,
10	—	,,	1,050	8,380	,,

The dead load was the light loading referred to in paragraph 23.6.

Since the load at which the first crack appeared in the static tests was lowest when the live load was applied to voussoir No. 18 (that is, at about the quarter-point in the span of the arch) the alternating load was applied to this voussoir and the circuit was arranged to detect a crack on the intrados of joint 17–18.

The alternating load at which the first crack appeared was 1,050 lb.; the corresponding static load was 1,525 lb.

Particulars of the second series of tests are given in Table 23.3. The same arch was used, *i.e.* granite-concrete voussoir with cement-mortar joints, except for joint 17–18, which was of lime mortar.

TABLE 23.3.

Test	Period: days	Voussoir loaded	Repeated load: lb.	Number of repetitions	Driving speed: revolutions per minute
1	12	18	330	over 10^6	65
2	11	,,	400	,,	64
3	11	,,	480	,,	,,
4	11	,,	540	,,	,,
5	1	,,	580	over 10^5	,,
6	1	,,	630	,,	,,
7	1	,,	670	,,	,,
8	1	,,	720	,,	,,
9	2	,,	830	,,	,,
10	2	,,	900	,,	,,
11	2	,,	980	171,089	,,

As the joint proved stronger than was anticipated, the later tests were shortened by making 100,000 instead of 1 million reversals at each load. During test No. 10 two cracks developed, one at the intrados of joint 14–15 and the other at the left abutment 0–1. The load was increased to 980 lb. for test No. 11 and the motor was left to run. After 171,089 reversals a definite crack developed at joint 17–18.

The load was then increased by increments of roughly 100 lb. and the motor was run for a few minutes at each load. At about 1,030 lb. a definite crack appeared at 7–8 (extrados) and at 1,850 lb. the arch failed in the usual manner by the formation of four pins. The joints opened at 0–1 *i*; 7–8 *e*; 17–18 *i*; 23–0 *e*.

It is interesting to note that this failing load is practically equal to the load (1,825 lb.) at which failure occurred in the static test for an arch made with limestone-concrete voussoirs and cement-mortar joints.

These results indicate that, whilst the first crack in a joint appears at a definitely lower load than in the static tests, the strength of this type of structure is still much greater than is usually assumed in traditional methods of design. The thrust-line, even with lime-mortar joints, was well outside the central middle-third of the ring depth when tension failure first occurred, and was, in fact, outside the middle-three-quarters; but until further tests are possible it may not be advisable to extend the "core" quite to that extent.

23 8. Calculation of the stability of a voussoir arch.—In an earlier paragraph it was shown that a voussoir arch increasingly loaded at a point may reach a state of instability due to the development of four virtual hinges which occur alternately at the intrados and extrados. The structure is thus turned into a four-bar mechanism and collapses. A method of calculating the magnitude of the load which must be applied at any point to cause this will now be described.

Fig. 23.18 shows an arch carrying any specified dead loading denoted by w_1, w_2 and w_3. The load W is just sufficient to put the structure into a state of unstable equilibrium. The unknown reactions are then V_A, V_B and H, as shown.

In the first place it will be assumed that the positions of the four virtual pins A, B, C and D are known. The section of the structure CDB is in equilibrium under the forces acting upon it, which do not

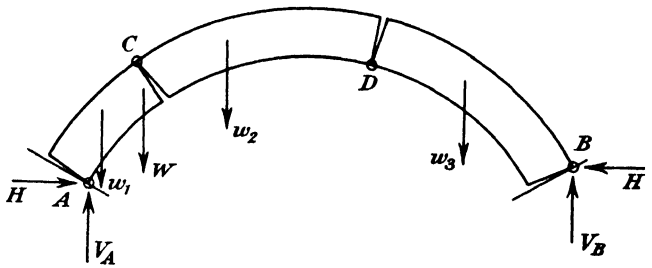

FIG. 23.18.

include the unknown W. Hence, by taking moments of these forces

about C and D, two equations in H, V_B and the appropriate part of the dead-load system, are obtained. By eliminating V_B from these, the value of H is determined.

If moments of the forces on the structure are taken about A, an equation is obtained which contains W, V_B, H and the terms for the dead load. V_B is again eliminated by using the equation of moments about C, and since H has been found, W can be determined.

In an actual case the positions of two of the pins are not precisely known, and some trial and error is necessary, but certain general rules reduce the uncertainty considerably. Thus, pin C always forms at the extrados of the joint adjacent to W, lying between W and the crown of the arch ; pin B always forms at the extrados of the springing farther away from W ; pin A is on the intrados, either at the other springing or on a joint near it, and the position of pin D can in most cases be judged very nearly.

To find W it is therefore necessary to make a few trials for different pin-positions. H is calculated from a consideration of the equilibrium of the section CB as before, but for a few (perhaps two or three) different positions of D. That giving the lowest value of H will be the correct one, since it will give the lowest value of W whatever the position of A. After finding H, a few alternative positions for A are taken and the corresponding values of W calculated as already described. The lowest will be the correct one.

Since in most cases the critical values of W will be needed for all points on the arch the work should be done systematically, and the following method is recommended. The arch ring considered is shown in Fig. 23.19 and consists of 23 voussoirs 3·33 inches deep. The span is 10 feet and the rise 2 feet 6 inches.

Take B as origin with Ox as horizontal and Oy as vertical axes of reference. Starting from the left-hand abutment, the co-ordinates of the extrados and intrados of each joint are tabulated (in this particular

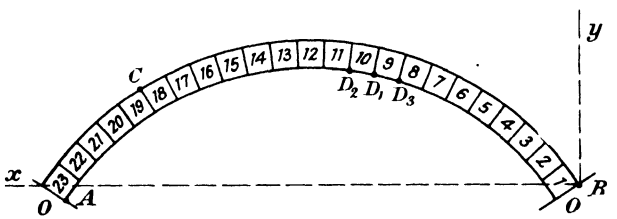

FIG. 23.19.

case in terms of the mean radius) as shown in Table 23.4. The x co-ordinate of the centre of each voussoir is entered in column 4 of the Table, the dead load applied to it in column 6, and the moment of this dead load about the origin in column 7. The sum of all dead loads to the right of a joint and the sum of their moments are entered in columns 8 and 9.

As an example we will determine the load which must be applied to voussoir No. 19 to cause the arch to become unstable.

TABLE 23.4.

(1)	(2)	(3)	(4)	(5)	(6)	(7)	(8)	(9)
Reference-points			x	y	Load, w	Moment, wx	Σw	Σwx
Int.	Mid.	Ext.						
23, 0			1·600	−0·027				
		23, 0	1·636	0			2,016	1,649
	23		1·593		108	172		
22, 23			1·550	0·035				
		22, 23	1·584	0·064			1,908	1,477
	22		1·540		106	163		
21, 22			1·496	0·091				
		21, 22	1·526				1,802	1,314
	21		1·481		107	159		
20, 21			1·437	0·144				
		20, 21	1·465	0·178			1,695	1,155
	20		1·419		100	142		
19, 20			1·369	0·191				
		19, 20	1·399	0·228			1,595	1,013
	19		1·353		94	127		
18, 19			1·307	0·233				
		18, 19	1·329	0·272			1,501	886
	18		1·283		86	110		
17, 18			1·237	0·270				
		17, 18	1·256	0·310			1,415	776
	17		1·210		83	100		
16, 17			1·165	0·301				
		16, 17	1·181	0·342			1,332	676
	16		1·135		77	88		
15, 16			1·090	0·326				
		15, 16	1·102	0·368			1,255	588
	15		1·057		74	78		
14, 15			1·013	0·345				
		14, 15	1·022	0·388			1,181	510
	14		0·978		71	69		
13, 14			0·936	0·357				
		13, 14	0·941	0·401			1,110	441
	13		0·898		68	61		
12, 13			0·857	0·364				
		12, 13	0·859	0·408			1,042	380
	12		0·818		68	56		
11, 12			0·778	0·364				
		11, 12	0·777	0·408			974	324
	11		0·737		68	50		
10, 11			0·700	0·357				
		10, 11	0·694	0·401			906	274
	10		0·657		71	47		
9, 10			0·622	0·345				
		9, 10	0·613	0·388			835	227
	9		0·578		74	43		
8, 9			0·545	0·326				
		8, 9	0·533	0·368			761	184
	8		0·501		77	39		
7, 8			0·471	0·301				
		7, 8	0·455	0·342			684	145

TABLE 23.4—*continued.*

(1)	(2)	(3)	(4)	(5)	(6)	(7)	(8)	(9)
Reference-points			x	y	Load, w	Moment, wx	Σw	Σwx
Int.	Mid.	Ext.						
	7		0·425		83	35		
6, 7			0·398	0·270				
		6, 7	0·379	0·310			601	110
	6		0·353		86	30		
5, 6			0·328	0·233				
		5, 6	0·306	0·272			515	80
	5		0·283		94	27		
4, 5			0·267	0·191				
		4, 5	0·237	0·228			421	53
	4		0·217		100	22		
3, 4			0·199	0·144				
		3, 4	0·171	0·178			321	31
	3		0·154		107	16		
2, 3			0·140	0·091				
		2, 3	0·109	0·123			214	15
	2		0·096		106	10		
1, 2			0·085	0·035				
		1, 2	0·052	0·064			108	5
	1		0·043		108	5		
0, 1			0·036	−0·027				
		0, 1	0	0				

Taking moments about C for the part of the arch between C and B we obtain

$$x_C V_B = y_C H + x_C \sum_C^B w - \sum_C^B wx.$$

Point C is 18–19e, and on substituting numerical values from the Table we have

$$1{\cdot}329 V_B = 0{\cdot}272 H + (1{\cdot}329 \times 1501) - 886,$$

whence $$V_B = 0{\cdot}204 H + 835 \quad . \quad . \quad . \quad . \quad . \quad . \quad . \quad . \quad . \quad (1)$$

For a first trial assume pin D to be at 9–10i. The moment equation for the part of the arch between D and B about this point is

$$0{\cdot}622 V_B = 0{\cdot}345 H + (0{\cdot}622 \times 835) - 227,$$

whence $$V_B = 0{\cdot}554 H + 471 \quad . \quad . \quad . \quad . \quad . \quad . \quad . \quad . \quad . \quad (2a)$$

Eliminating V_B between (1) and (2a),

$$H = 1{,}040 \text{ lb.} \quad . \quad . \quad . \quad . \quad . \quad . \quad . \quad . \quad . \quad (3a)$$

For a second trial assume pin D at 10–11i;

then $$0{\cdot}700\ V_B = 0{\cdot}357 H + (0{\cdot}700 \times 906) - 274,$$

whence $$V_B = 0{\cdot}511 H + 516 \quad . \quad . \quad . \quad . \quad . \quad . \quad . \quad . \quad . \quad (2b)$$

From (1) and (2*b*)

$$H=1{,}042 \text{ lb.} \quad . \quad . \quad . \quad . \quad . \quad . \quad . \quad . \quad . \quad (3b)$$

Similarly, if pin D is at 8–9*i*

$$H=1{,}045 \text{ lb.} \quad . \quad . \quad . \quad . \quad . \quad . \quad . \quad . \quad . \quad (3c)$$

The position 9–10*i* is correct since it gives the lowest value for H. Selecting the left abutment (that is, 23–0*i*) as the pin A, we obtain by taking moments about A,

$$1{\cdot}600V_B=-0{\cdot}027H+(1{\cdot}600\times0{\cdot}2016)-1{,}649+0{\cdot}247W,$$

whence $$V_B=-0{\cdot}017H+986+0{\cdot}155W \quad . \quad . \quad . \quad . \quad . \quad . \quad . \quad . \quad (4)$$

Eliminating V_B between (1) and (4), and substituting for H from (3*a*),

$$W=512 \text{ lb.}$$

If pin A is at 23–22

$$W=534 \text{ lb.}$$

The correct pins are, therefore, 0–1*e*; 9–10*i*; 18–19*e*; and 23–0*i*, and the corresponding values for the load and horizontal thrust are W=512 lb. and H=1,040 lb. respectively.

It should be noticed that W is directly proportional to the dead load and so, from the standpoint of stability, a heavy filling is preferable to a light. The compressive stresses, however, are naturally increased in the same proportion and there is more danger of a failure from this cause.

23.9. Analysis and design methods for a voussoir arch.—As we showed in paragraph 23.3, the existing methods of design for voussoir arches are based on a combination of principles some of which are applied in a way which is open to criticism. The work of Castigliano in this field appears to have received little attention although it was the first attempt to treat the subject rationally as an elastic problem. The experimental work done since the publication of his treatment, both in the laboratory and on actual structures, shows without doubt that the general line of approach which he advocated is sound and its adoption would lead to the more scientific design of these structures. There is, however, one aspect which so far has not been considered but is of importance. Hitherto in this chapter attention has been directed to the location of the linear arch within the actual ring without reference to the stresses developed in the material, and it is obvious that to specify limitations in position alone would be inadequate.

Suppose that at any joint the linear arch cuts the ring at a distance *e* from the centre line. The maximum and minimum stresses are then given by $\frac{P}{A}\left(1\pm\frac{6e}{d}\right)$ where P is the thrust on the joint, A is its cross-sectional area, and *d* is the depth of the joint. Hence the ratio of maximum to minimum stress occurring at the edges of the joint is

$\frac{1+\frac{6e}{d}}{1-\frac{6e}{d}}$. When this ratio is negative a tensile stress occurs. If $e=\frac{d}{6}$, the minimum stress is zero and the middle-third rule is obtained. If $e=\frac{d}{4}$, the ratio is -5 and a tensile stress of one-fifth of the intensity of the compressive stress occurs. So, if a maximum compressive stress of 13 tons per square foot is permitted and reached at such a joint, the tensile stress at the other edge will be 2·6 tons per square foot or about 40 lb. per square inch. The compressive stress quoted is a reasonable one and the accompanying tensile stress is low for good cement mortar and probably quite safe for any kind of lime mortar likely to be used for this class of structure. In many cases, therefore, it would be undoubtedly safe to permit the linear arch to fall outside the middle-half as was shown in the experiments described in paragraph 23.6. It is, however, wise to adopt a conservative attitude in view of the uncertainties as to the effect of prolonged repetition of stress, the weathering of the materials and the possibilities of future heavier traffic than contemplated in design. Taking all these into consideration, however, it appears reasonable to adopt the middle half criterion, as advocated by some writers in the past.

The proposed arch ring should be treated as a solid rib with known or assumed conditions at the abutments and the true linear arch for these conditions should be found by a strain energy analysis. The linear arch should not fall outside the middle half of the actual ring but should lie as closely as possible to the boundaries of this core. Trial-and-error methods may be necessary to determine the minimum depth of ring to meet this requirement. The compressive stresses should then be calculated to ensure that the allowable limit is not exceeded anywhere.

The resulting arch should be safe for all normal conditions and will have a large margin of strength against ultimate failure by instability. This may be calculated by the method described in the last paragraph.

The above treatment is suggested on the assumption that the arch can be divided into separate ribs as would be the case in steel or reinforced concrete structures. This is seldom so in masonry or brick arches which are generally of barrel construction. It then becomes necessary to make an assumption as to the effective width of the rib for design purposes and this depends on the type of load and on the type and depth of filling.

It is commonly assumed in similar problems that a filling distributes a concentrated load through a cone of 90° apex angle so that a point load acting on a filling of 12 inches depth would be spread over a circular area of 12 inches radius at the bottom of the filling. Thus a point load on a barrel arch with this depth of filling could be assumed to be resisted by a rib 24 inches wide. This is, of course, only an assumption and is quoted simply to show one method of dealing with the problem ; special cases require individual treatment and there are unfortunately little data available to assist the designer.

CHAPTER 24

THE BEHAVIOUR OF STRUCTURES IN THE ELASTO-PLASTIC RANGE

24.1. Introduction.—With the exception of the steelwork connections (Chapter 11), this book has so far been concerned only with the behaviour of structures within the elastic range. While it is usual to assume in design that the limit of proportionality of the material is nowhere exceeded, it must be remembered that a redundant structure of ductile material can often support a considerable increase of load after yield has occurred at one section.

Much attention has been given in recent years to the development of a theory to explain the behaviour of structures in the plastic range.* The theory is, however, still incomplete and speculative. No attempt will be made here to deal exhaustively with the subject though it is hoped that enough will be said to show the possibilities of work in this field and the need for more complete data.

24.2. The simply supported beam.—Robertson and Cook † were the first to give a satisfactory explanation of the way in which a mild steel beam fails in flexure. If the material of the beam is normalised mild steel it will have a stress-strain relation in tension as shown in Fig. 24.1.

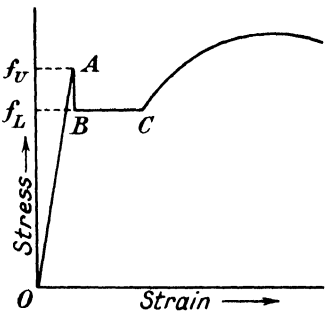

FIG. 24.1.

The point A represents the upper yield of the material, the upper yield

* A bibliography and a number of papers on the subject will be found in the Preliminary Publication, 2nd Congress, International Association for Bridge and Structural Engineering. Berlin, 1936.

† Proc. Roy. Soc., **88A**, 462, 1913.

stress being f_U. As straining of the test piece continues an immediate drop in stress to B, the lower yield point, stress f_L, will occur. From B the material extends without any increase in load to C, BC being the region of complete plasticity. After C the plastic flow ceases and load has to be added before any further extension is produced.

It will be assumed that the stress-strain relation in compression is identical with that in tension, that, as in the simple elastic theory of bending, plane sections before bending remain plane after bending and that longitudinal fibres are free to expand and contract laterally.

When a member is subjected to pure bending about a principal axis of inertia the distribution of stress across the section will be of the form shown in Fig. 24.2 (*a*) so long as the applied bending moment is small. This form will persist as the bending moment increases until the stress at the extreme fibres eventually reaches the value f_U, the upper yield stress of the material. As the bending moment is increased further a drop in stress to f_L, the lower yield value, must occur in these

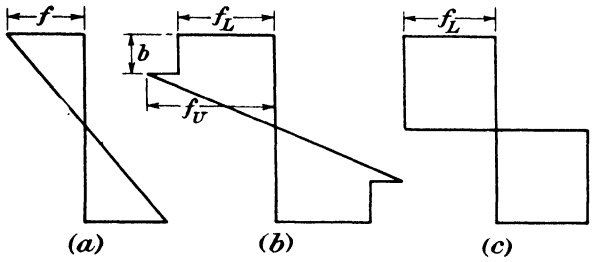

FIG. 24.2.

extreme fibres in accordance with the stress strain relation of Fig. 24.1. The stress in more and more fibres will reach the upper yield value and will drop back to the lower as shown in Fig. 24.2 (*b*). Eventually, under a certain bending moment, the whole of the section will have yielded, giving the stress distribution shown in Fig. 24.2 (*c*). A further simplifying assumption has been made in this argument, that the extreme fibres and all others after reaching the lower yield stress remain in a state of complete plasticity, *i.e.* within the range BC, Fig. 24.1, until the whole section has yielded.

An expression for the moment of resistance can be derived as in paragraph 3.4. For a rectangular section of depth d and width w the moment of resistance will be

$$M=\frac{w}{6}\{6b(d-b)f_L+(d-2b)^2f_U\} \quad . \quad . \quad . \quad . \quad . \quad . \quad (1)$$

when the fibres to a depth b, Fig. 24.2 (*b*), have reached the plastic state.

The " carrying capacity," that is the moment which produces complete plasticity throughout the whole section of this member, Fig. 24.2 (*c*), is

$$M_p=\frac{wd^2}{4}f_L \quad . \quad . \quad . \quad . \quad . \quad . \quad . \quad . \quad . \quad (2)$$

That the simple assumptions set out above are adequate for many design purposes is indicated by the agreement between the observed and calculated load deflection curves shown in Fig. 24.3 (*a*) and (*b*). These results were obtained from a simply supported beam, 10 inches long, of normalised steel $1\frac{1}{4}$ inches wide and $\frac{3}{8}$ inches deep subjected to a central point load.

The observed deflections are compared in Fig. 24.3 (*a*) with deflections (Curve (1)) calculated on the assumptions set out above, the values of yield stress (f_U=24·7 tons per square inch; f_L=19·5 tons per square inch) being deduced from the behaviour of the beam. Curve (2) shows that the calculated deflections are not seriously affected if it is assumed that there is no drop in stress at yield and that f_U=f_L=19·5 tons per square inch.

As can be seen from the curves, a very large deflection of the beam takes place without any drop in the applied load when complete plasticity has been developed at the centre. This is of great importance.

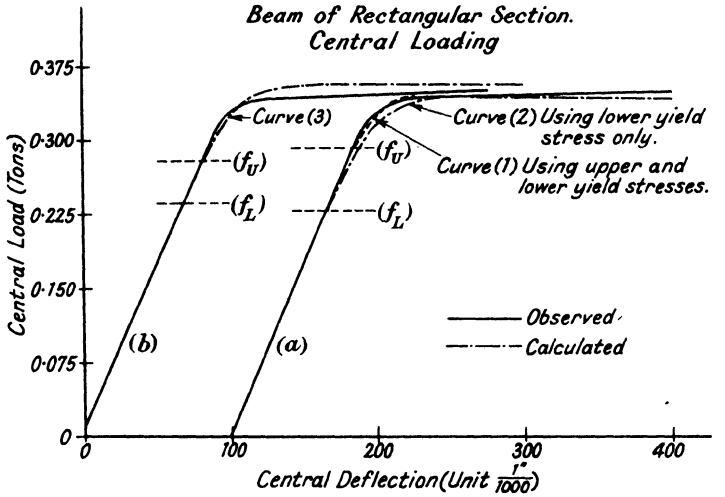

FIG. 24.3.

The designer must, of course, be able to estimate the strength and behaviour of any member he wishes to use without tests on the actual member. That this is possible, within reasonable limits, is shown by Curve (3), Fig. 24.3 (*b*). To calculate this curve, a tension test was made on the steel from which the beam was to be fabricated. The yield stresses obtained from this tension test were f_U=23·52 tons per square inch, f_L=20·32 tons per square inch.

Using these values, Curve (3) was obtained by calculation. It gives a rather higher load for the " collapse " of the beam than was observed. This is probably attributable to some slight difference in the effect of the heat treatment upon the small tension specimen and the larger beam.

It must be remembered that there is a wide difference in the forms of the stress-strain curves and in the yield stresses of material cut from

different parts of the web and flanges of a rolled steel joist taken from stock * and, what is more often forgotten, that there is no value for yield stress laid down in the British specification for structural steel. It is not possible, therefore, to give a close estimate of the " carrying capacity " of a standard rolled section. When the plastic theory is used more generally in design it will be necessary to have the yield stress specified. It will probably be found most practicable to do this by defining limits for the " carrying capacity " in bending of each section rather than by specifying a minimum yield stress for the material tested in tension.

It must not be assumed that, because there is variation in the yield stress across the section, the behaviour of a rolled steel joist which has not been heat treated is fundamentally different from that of the normalised beam discussed above. Fig. 24.4, which is the load deflection

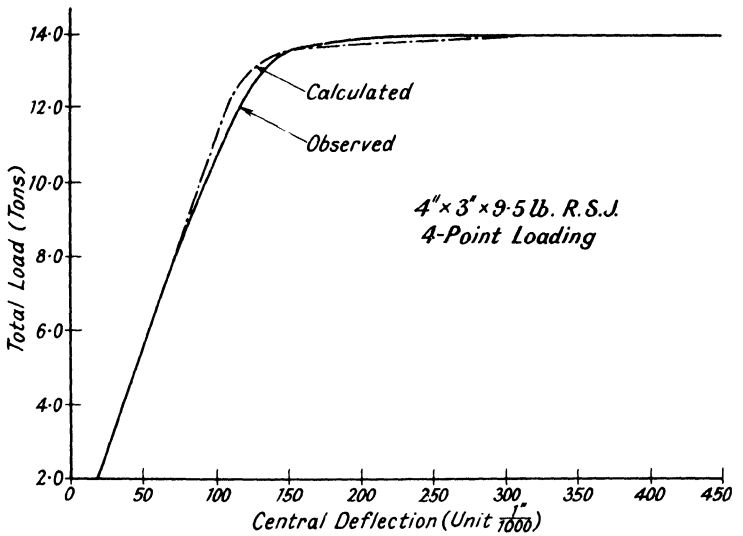

FIG. 24.4.

curve for a 4 inch by 3 inch by 9·5 lb. R.S.J. of span 40 inches, shows that this is not so. The ratio of moment producing complete plasticity to that producing the first yield in the material of this beam is 1·23. This ratio, or " shape factor " as it is called, since it depends only upon the geometrical shape of the section, is given for a number of other standard sections in Table 24.1.

TABLE 24.1.

I section.	4″×3″	6″×3″	9″×4″	12″×5″	15″×6″	22″×7″	24″×7½″
Shape factor	1·23	1·17	1·17	1·15	1·16	1·15	1·15

* " The Use of Small Specimens in the Testing of Mild Steel." A. Robertson. First Report Steel Structures Research Committee, H.M. Stationery Office, 1931.

24.3. The portal frame.—Although the knowledge of the behaviour of simple beams carried into the plastic range has already proved most useful in design, particularly where impact loads have to be considered, its chief value lies in the help it gives in explaining the behaviour of continuous structures.

Fig. 24·5 shows the load deflection curve for a small scale portal frame made up of $1\frac{1}{4}$ inches by $1\frac{1}{4}$ inches mild steel H section throughout.

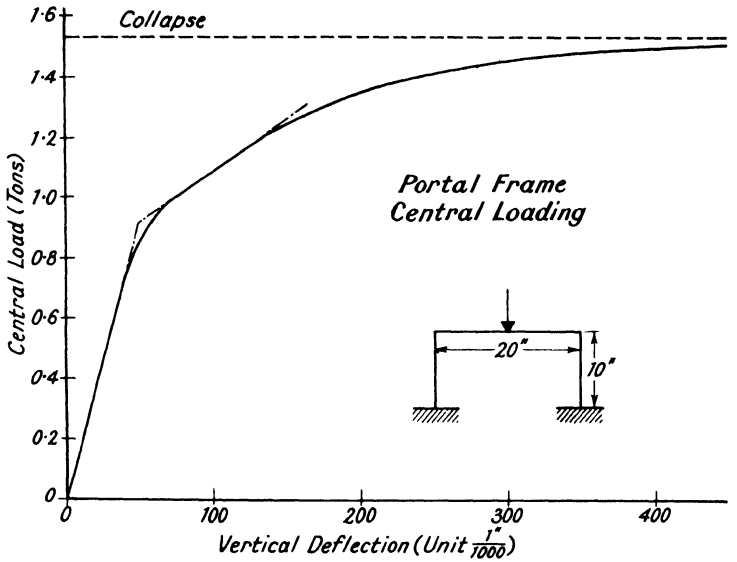

FIG. 24.5.

Details of the experimental methods used in determining this curve, together with accounts of other tests on portals and beams, will be found in Reports made to the Institute of Welding.*

The span of the beam was 20 inches and the stanchion height was 10 inches, welded joints of considerable rigidity were made between the beam and the stanchions and the feet of the latter were firmly fixed to a base. A central concentrated load was applied to the beams in increments of approximately 70 lb. It will be seen that there was a linear relationship between the applied load and the deflection until a load of approximately 0·8 tons was reached. After this the rate of change of deflection increased until a load of 1·0 tons had been applied. From this up to a load of about 1·22 tons the relation once more became linear. As the load was increased beyond this value the deflections grew at an increasingly rapid rate until " collapse " of the portal took place under a load of 1·54 tons when a very large central deflection was experienced.

The behaviour of this portal can be easily explained. It was

* " Investigation into the Behaviour of Welded Rigid Frame Structures." J. F. Baker, and J. W. Roderick. First Interim Report, Trans. Inst. of Welding, Vol. I, No. 4, 1938. Second Interim Report, Trans. Inst. of Welding, Vol. III, No. 2, 1940.

elastic until the applied load reached 0·8 tons; this was sufficient to cause yield of the outer fibres at the centre of the beam. As the applied load was increased from 0·8 to 1·0 tons a plastic zone was formed at the centre of the beam, the condition of the centre section passing through the stages shown in Fig. 24.2 (*a*)–(*c*). At a load of 1·0 tons the centre section of the beam had become completely plastic, Fig. 24.2 (*c*), thereby developing the maximum moment of resistance or plastic moment which would, owing to the ductile nature of the material, remain unchanged as further load was added. In the next stage each half of the portal behaved as a post carrying a cantilever subjected at its end to an increasing vertical load and a constant restraining moment equal to the full plastic moment at the centre section. As a result, the load deflection relation once more became linear and remained so until the stresses in the outer fibres at the ends of the beam reached yield. This occurred when the applied load was 1·22 tons. As further load was added plastic zones were formed at the ends of the beam, passing through the stages shown in Fig. 24.2 (*a*)–(*c*) until, at 1·54 tons, the material at the ends of the beam as well as at the centre became completely plastic. There was no castrophic failure of the structure at this load since the maximum restraining moments developed at the ends and centre could be maintained while the beam suffered very large deflections. Had the load been slightly reduced in this range the growth of deflection would have ceased and the portal would have maintained almost its full " collapse " load without difficulty

Had the beam carried such an arrangement of symmetrical load that yield occurred first at the ends,the " collapse " condition would have been the same. At a certain load plasticity would be developed, in this case at the ends of the beam, and thereafter, for a second linear load deflection range, the behaviour would be that of a symmetrically loaded beam subjected to unchanging restraining moments at its ends. This would continue until the bending moment at the centre reached such a magnitude that yield began at the outer fibres. After this, further load could be carrried until full plasticity was developed at the centre as well as at the ends of the beam. In these cases, and in fact for any portal where the stanchions are not sufficiently slender to yield before the beam, the maximum load carried would be approximately twice that which the similar simply supported beam could support.

It can, in fact, be stated generally that for any symmetrical loading, collapse will only take place when the bending moments at both the centre and the ends of the beam become equal to the moment for complete plasticity of the section under consideration. It should be noted that yield at the end of the beam can take place in two ways, depending upon the relative properties of stanchion and beam sections. If the stanchion is the heavier then yield will occur at the section of the beam in line with the inner face of the stanchion. On the other hand if the stanchion is of lighter section, then yield will take place at the top of the stanchion.

For any condition of symmetrical loading on these portal frames the

sum of the end and centre moments is known and can be expressed as

$$M_e+M_c=KPl \quad \ldots\ldots\ldots \quad (1)$$

where M_e is the bending moment at the end of the beam, M_c that at the centre, l is the span, P the total applied load and K a constant depending on its arrangement. When the stanchions are of heavier section than the beam, collapse of the frame will take place when both M_e and M_c are equal to M_p, the moment of resistance for complete plasticity of the beam section. The total applied load at collapse is

$$P=\frac{2M_p}{Kl} \quad \ldots\ldots\ldots \quad (2)$$

If the stanchions are of lighter section than the beam then collapse will occur when the moment at the centre is M_p and the moment at the ends is M_p^s, the moment for complete plasticity of the stanchion, when

$$P=\frac{(M_p+M_p^s)}{Kl} \quad \ldots\ldots\ldots \quad (3)$$

Verification of the reliability of these formulas will be found in Table 24.2 which is a summary of the tests on portals described in the Institute of Welding Reports. The span of the beam was 20 inches

TABLE 24.2.

1	2	3	4	5	6
Portal frame test No.	Section of beam	Section of stanchion	Control test "carrying capacity" M_p (ton-inches)	Collapse loads for steel portal frames (tons)	
				Calculated	Observed
F.3	1¼″×1¼″ H	1¼″×1¼″ H strong way	3·90	1·56	1·54
F.6	1¼″×1¼″ H	1¼″×1¼″ H strong way	3·71	2·91	3·03
F.8	1¼″×1¼″ H	1¼″×1¼″ H weak way	4·44 2·38	2·72	2·79
F.9	1¼″×1¼″ H	1¼″×¼″ flat weak way	4·44 0·09	1·81	1·70
F.10	1¼″×1¼″ H	1¼″×¼″ flat weak way	4·44 0·30	1·89	1·81

and the stanchion height 10 inches except in portal F.8, where the height was 11.25 inches. The beam-to-stanchion connections were made by

welding and were of considerable, but not complete, rigidity ; perfectly rigid joints are very difficult to produce in practice. The stanchion bases were bolted to heavy supporting joists, but slight rotation of the bases and relative horizontal movements were detected during the tests. A central point load was applied to portal No. F.3, but in all other cases four point loading was used. The beam and stanchion sections for each portal are given in Table 24.2, Columns 2 and 3. Specimens of the materials used in making up these members were tested so that an estimate could be made of the " carrying capacity " or moment of resistance for complete plasticity ; these moments are given in Column 4. In Column 5 are the loads calculated from equation (3) to produce collapse of the portals and in Column 6 those observed in the tests.

The agreement between Columns 5 and 6 is within the limits of experimental error, with the possible exception of the results for frame No. F.9, but in that instance very slender stanchions, $1\frac{1}{4}$ inch by $\frac{1}{8}$ inch, gave rise to high axial stresses which were not taken into account in the simple calculations.

It would have been difficult, even in the case of these single span portals, to calculate with any exactness the stress distribution during the elastic range and so to estimate, for instance, the load which would first produce the yield stress of the material. This was due to such complications as deflections at the stanchion bases, the relaxation, or semi-rigidity, of the beam-to-stanchion connections and so on. It would, that is to say, using the elastic theory, be impossible to make any close estimate of the load which would bring about failure of these structures. The reassuring fact emerges from Table 24.2, however, that, in spite of the doubts about the exact behaviour of the connections, the plastic theory affords an accurate method of forecasting collapse load.

24.4. Propped beams.—The value of the plastic theory can be further demonstrated by considering the particular problem of the propped beam.

If a steel beam of uniform cross-section and length l with ends encastré were subjected to its full design load of intensity w under which the permissible working stress was developed at the end sections, where the highest stresses occurred, the bending moment diagram would be as in Fig. 24.6 (*a*). If now a prop were inserted at the centre and a further uniformly distributed load of intensity w_1 were added, the additional bending moment induced would be as shown in Fig. 24.6 (*b*). It is clear that no load could be added to the propped beam without inducing at the encastré ends stresses exceeding the permissible working stress. Therefore, according to normal design methods, it would not be possible to add any load to the beam after propping. Consideration of the real strength of the member shows, however, that it is possible for it to support an appreciable additional load while retaining what is considered the usual factor of safety.

Suppose the carrying capacity of the beam section is $\frac{wl^2}{6}$, that is to say the moment producing complete plasticity is twice that producing

the permissible working stress, a conservative estimate. When load is applied to the propped beam the bending moments at the encastré

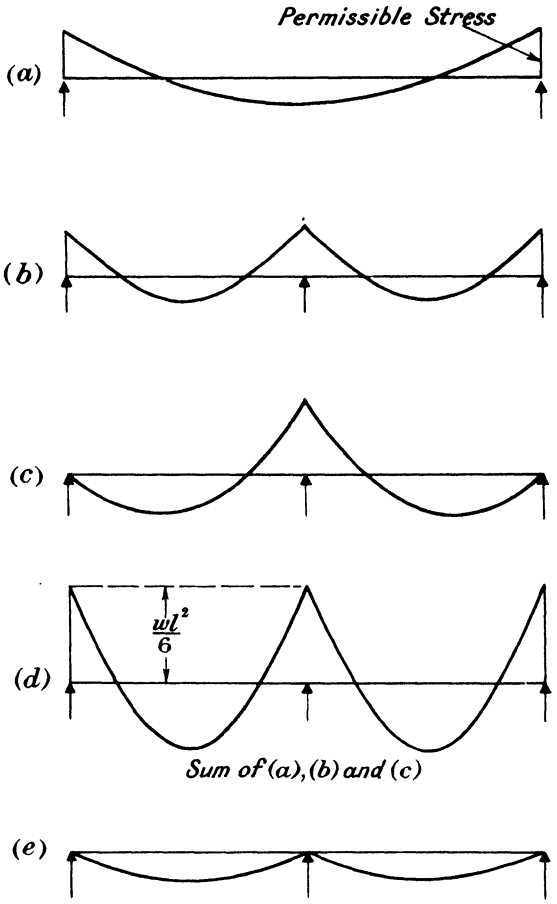

FIG. 24.6.

ends increase until when $w_1=4w$ complete plasticity is produced there. As was seen in the case of the portals, paragraph 24.3, this does not mean that failure of the beam is imminent but merely that the restraining moments at the ends cannot increase further. When more uniformly distributed load of intensity w_2 is added to the beam, while the bending moments at all other sections increase, those at the encastré ends remain constant at the value $\frac{wl^2}{6}$. The additional bending moments in the beam due to the application of a load of intensity w_2, shown in Fig. 24.6 (*c*), can therefore be calculated by considering the beam as continuous over three simple supports. When $w_2=4w$ the total hogging bending moment over the prop reaches the limiting value of $\frac{wl^2}{6}$,

Fig. 24.6 (*d*). The beam is still far from failure; while a further additional uniformly distributed load of intensity w_3 is added the bending moments at the encastré ends and over the prop remain at the limiting value of $\frac{wl^2}{6}$. The additional moments at all other sections due to w_3 can be calculated by considering the beam as made up of two simply supported lengths each of span $\frac{l}{2}$, Fig. 24.6 (*e*). Collapse of the beam, or rather the growth of large deflections, is not brought about until the total bending moment reaches the limiting value at the centre of each span. This occurs when $w_3=\frac{5w}{3}$, so that the total intensity of load which can be carried by the beam is $w+4w+4w+\frac{5w}{3}=10\frac{2}{3}w$.

The calculation above shows, therefore, that while according to the usual permissible stress method of design no additional load should be allowed on this beam after propping, it could, in fact, carry a further intensity of load $9\frac{2}{3}w$ before large deflections were produced. By considering such cases as this it is possible, by making use of the load-factor method referred to in paragraph 1.3 and adopting a factor of 2, to lay down a design rule that where a steel beam designed normally to a working stress of not more than 8 tons per square inch for an intensity of load w per unit length, is to be strengthened by the insertion of a central prop, it will be satisfactory so long as the total intensity of load to which it is to be subjected does not exceed $5\frac{1}{3}w$ per unit length and so long as the usual permissible working stress in shear is not exceeded.

24.5. The continuous stanchion.—A discussion of the loading conditions to which a stanchion in a rigidly jointed steel building frame can be subjected is given in Chapter 19. A method to determine the end bending moments which can be applied to a stanchion length is explained and families of curves, Figs. 19.13 and 19.14, give the permissible end bending stress for any intensity of axial load. In deriving these curves the load factor method was used, but instead of working to the load which caused real collapse of the stanchion it was assumed that elastic conditions persisted throughout and that the stanchion became unsafe when the total stress at any point reached 18 tons per square inch. This is virtually the same assumption as was made in deriving the familiar British strut formula (paragraph 7.9). Though this formula has served well enough for design purposes it does not represent the behaviour of the continuous stanchion accurately and may well be extravagant. Stanchions designed by the more exact method described in Chapter 19 also tend to be extravagant because, though a load factor of 2 was used in deriving the curves of Figs. 19.13 and 19.14, the collapse load assumed was almost certainly low. Much work has still to be done before it will be possible to base stanchion design on the load which would cause real collapse, but a little at any rate is now known about the mechanics of failure.

The moments acting at the ends of a length of continuous stanchion usually have the same sense, so bending it in double curvature (see Fig. 19.6 (*c*)). This condition was reproduced in the portal tests described in paragraph 24.3 and certainly gives the stanchion length a considerable degree of stability. In an internal stanchion, however, it is also possible, as pointed out in paragraph 19.5, for the end moments to produce bending in single curvature. This may often be the most rigorous loading condition.

It is a common error to consider the behaviour of a length of a continuous stanchion, bent in single curvature by the beams framing into it, to be the same as that of a pin-ended strut carrying an axial load and end moments. If, in the case of the pin-ended strut, the axial load and the end moments are increased in the same proportion at a certain rate, the maximum moment and, therefore, the maximum total stress increases at a greater rate. In the continuous stanchion, on the other hand, as the axial load and the loads on the beams are increased, the beams at the ends of the stanchion length restrain that length, so that the rate of increase of the end moments is less than that of the loads and the rate of increase of the maximum total stress is less than in the case of the pin-ended strut.

It was impossible, owing to the complications involved, to take advantage of this when developing the general design method described in paragraph 19.6 but, had it been possible, useful economies would have resulted. To quote one particular case,* where a 10-inch by 8-inch by 55 lb. R.S.J., 10 feet long, had 22-inch by 7 inch by 75 lb. R.S.J., 20 feet long rigidly connected to its web, an axial load of 6 tons per square inch applied to the stanchion was sufficient to reduce the end moments coming in from the loaded beams by 20 per cent. If the safe axial load on a stanchion were based on that necessary to cause collapse, this reduction of end moment night well have an even more marked effect than in the case quoted, since the restraint from the beams increases at an accelerated rate as the axial load increases. Tests on small-scale frames which demonstrate this and throw some light on the mechanics of failure of a stanchion length bent in single curvature are described in a further report † published by the Institute of Welding.

It is not difficult to describe in general terms the behaviour of a steel stanchion forming part of a rigidly jointed frame and subjected to the quite practical loading conditions, shown in Fig. 19.6 (*f*), used in the tests. These were equal end moments produced by constant loads applied to the beams at the top and bottom of the stanchion length and an increasing axial load, which would in practice come from the loads added to the higher floors in the building. When loads are applied to the beams at the upper and lower ends of a stanchion length the beams

* "The Behaviour of a Pillar forming part of a Continuous Member in a Building Frame." J. F. Baker and P. D. Holder. Final Report, Steel Structures Research Committee, H.M. Stationery Office, 1936.

† "The Behaviour of Stanchions Bent in Single Curvature." J. F. Baker and J. W. Roderick. Third Interim Report, Trans. Inst. of Welding, Vol. V., No. 3, 1942.

bend and, since the joints of the frame are rigid, induce bending in the stanchion. Due to the presence of axial load the bending moment is not the same at all sections of the stanchion length but is a maximum at the centre as shown by the full line (*a*) in Fig. 24.7. As axial load is

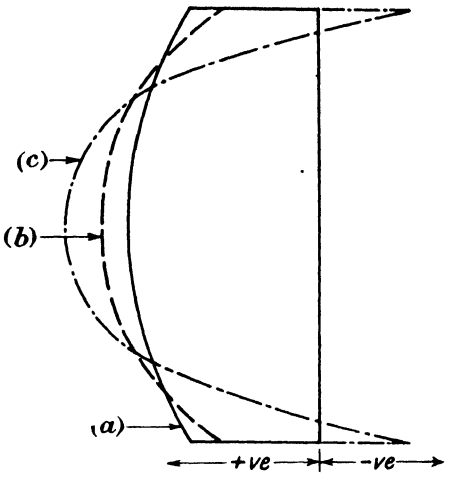

FIG. 24.7.

added, the loads on the beams being kept constant, the bending moment at the centre of the stanchion increases and the end moments decrease, as shown by the broken line (*b*) in Fig. 24.7, so that even in this range the action of the beam is to restrain the bending of the stanchion. In some frames the bending-moment diagram is similar in form to (*b*), Fig. 24.7, throughout the elastic range, but in others, when the stanchion is more slender, the end moments actually change sign and the form of the diagram eventually becomes that shown by line (*c*), Fig. 24.7.

The yield stress of the material will first be reached on the compression face at the centre of length under a certain axial load P_1. The member does not collapse under this load. The mere fact that the yield stress of the material has been reached at an outer fibre does not in general inconvenience the member unduly. This can be seen from the typical load deflection curve, Fig. 24.8, where the upper yield stress of the material was reached at an axial load of 3 tons. As in the case of beams and portals (paragraphs 24.2 and 24.3), no appreciable change in the behaviour of the stanchion is found until a considerable portion of the material across the section has reached its yield stress. Further, the load producing collapse is not determined by the condition of the centre section alone. Before collapse can occur the end section of the member as well as the centre must be incapable of resisting further moment. As the axial load is increased above P_1, which first produced yield, a plastic zone is formed at the centre of length of the stanchion, its extent depending on the dimensions of the cross-section of the member and on the proportions of the frame. The formation of this plastic zone tends to produce an increase in the rate of change of stanchion deflection

with respect to axial load, but this is offset to some extent by the increase in the restraining moments offered by the beams to the stanchions. As the axial load is increased further, these restraining moments grow until the nett moments at the ends become of opposite sign to those of the moments initially applied by the beams to the stanchion. Under some axial load P_2, the maximum total stress in the extreme fibre at the end of the member, on the opposite face to that at which yield first occurred at the centre, reaches the yield stress of the material. On the addition of further axial load, plastic zones are formed at the ends, and collapse of the member is brought about when the end sections, like the centre section, are unable to resist any additional moment.

That this is a reasonable explanation of the behaviour can be demonstrated by analysis of the experimental data. The load deflection curve, Fig. 24.8, was obtained from a stanchion of rectangular cross-section

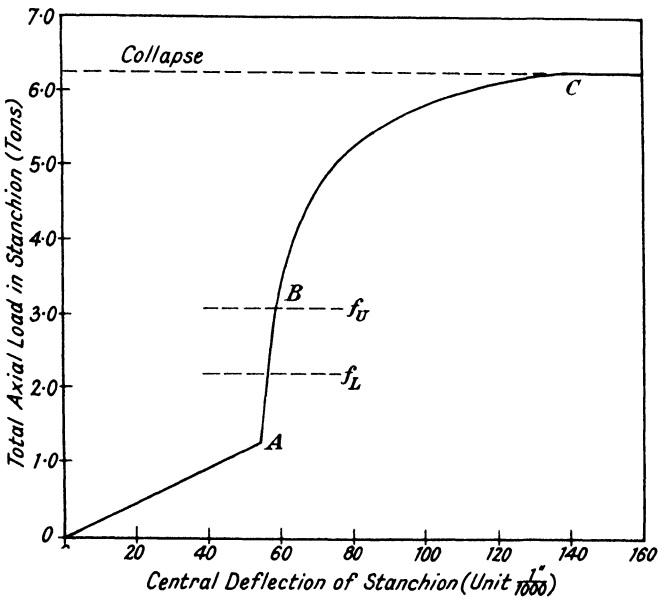

FIG. 24.8.

1¼ inch by ⅜ inch and storey height 10 inches The material was normalised mild steel with an upper yield stress, f_U=22·88 tons per square inch, and a lower yield stress, f_L=20·32 tons per square inch. Load was first added to the beams at the ends of a stanchion length, producing a bending stress in the stanchion of 14·97 tons per square inch. OA, Fig. 24.8, represents the range when the beam load was being applied. Beyond A, axial load alone was added to the stanchion, the loads on the beams being unchanged. It will be seen that from A to B the rate of increase of stanchion deflection was small. When the axial load reached 3 tons (6·4 tons per square inch) the upper yield stress of the material was developed in the extreme fibres at the centre of the stanchion. Far

from failing, the stanchion carried an additional axial load of 3·25 tons (6·9 tons per square inch) before collapsing under a total axial load of 6·25 tons (13·3 tons per square inch).

The bending moments and maximum total fibre stresses at the centre and ends of the stanchion length have been deduced from the test results and are plotted in Figs. 24.9 and 24.10. It will be seen that

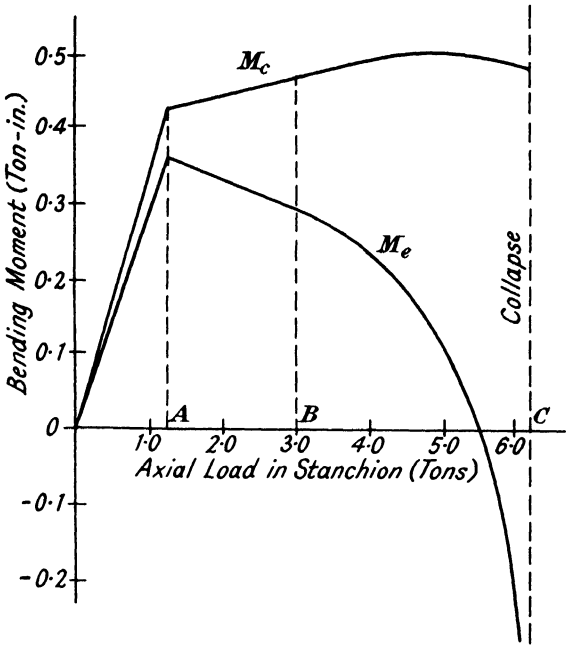

FIG. 24.9.

during the first range OA, when the beam loads were being added, the bending moments at both the ends and centre of the stanchion increased, the latter having the greater value. When the beam loading ceased and further axial load was added to the stanchion, range AB, the centre moment M_c still increased, though at a lesser rate, and the end moment M_e decreased. After an axial load of 3 tons had been reached, the point at which yield began at the centre of the stanchion, the rate of change of the centre bending moment decreased slightly but that of the end moment increased until, when the axial load was about 5·5 tons, the end moment was zero. Thereafter as more axial load was added the end moment changed sign and increased rapidly.

The total stresses f_c, in the extreme fibre on the compression side at the centre of length, and f_e at the end, on the opposite side of the stanchion, have been deduced from these bending moments and from the axial load, Fig. 24.10. They call for no comment in the elastic range OB. At B, when the axial load was 3 tons, f_c reached the upper yield stress of the material and then immediately dropped to the lower yield stress and remained at that value. The trend of the stress f_e is

of great interest in the range BC. It fell to zero when the axial load on the stanchion was approximately 4 tons and therefter increased

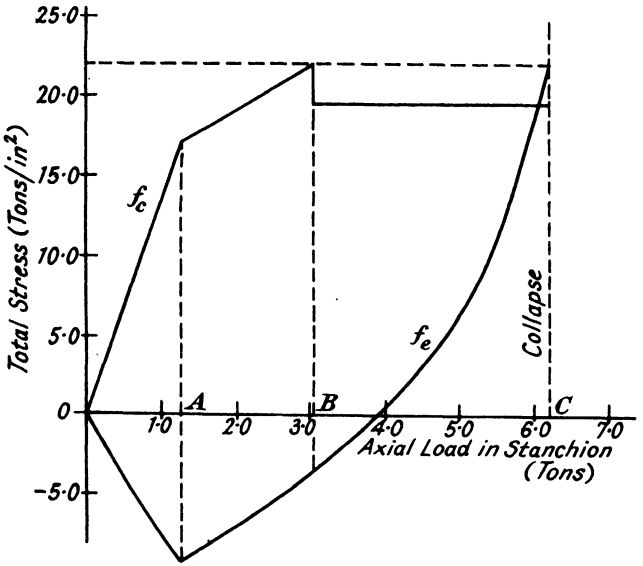

FIG. 24.10.

until it reached almost exactly the upper yield stress of the material at the collapse load, 6·25 tons. This shows that the stanchion length was capable of supporting additional axial load after yield had been developed at the centre until the material at the ends reached the plastic state.

Similar frames were tested and it is of interest to note that in spite of great differences in the beam loads applied, the largest of which produced an initial bending stress in the stanchion of 18·24 tons per square inch and the smallest 8·70 tons per square inch, the axial loads causing collapse only differed by 0·69 tons, ranging from 6·17 tons to 6·86 tons. They were all greater than the crippling load, 5·74 tons, for a pin-ended strut without end moments, given by the strut formula of paragraph 7·9, suitably adjusted to take account of the higher yield stress of the material used in the stanchion lengths tested.

Professor C. E. Inglis * has studied the problem of the behaviour of a compression member in a braced framework with stiff joints. He has drawn attention to the fact that, just as in the building frames discussed above, the terminal bending moments, giving rise to the secondary stresses, Chapter 10, may in many cases diminish, and even change sign, as the loading increases. This enables a compression member to withstand a much greater thrust than would be expected, according to ordinary theory. Professor Inglis points out that, even when an initial ratio of secondary to primary stress of 40 per cent. exists, the actual crippling primary stress is almost double that prescribed by the usual

* "The Crippling Load of a Compression Member in a Framework with Stiff Joints." Journal Inst. of Civil Engineers, No. 6, 1939–40.

formulas for struts with riveted ends. The tests carried out indicated that whereas in the case of exceptionally slender struts complete failure seemed to occur as soon as the yield stress was reached at the centre, for shorter struts general failure did not occur until that limit had been considerably surpassed.

24.6. Reinforced concrete structures.—The load deflection curve for a simply supported concrete beam lightly reinforced, so that failure takes place by yield of the mild steel reinforcement, is of the same form as that for the mild steel beam discussed in paragraph 24.2 and illustrated in Fig. 24.3. The mechanics of failure of reinforced concrete members are much more complex than those of rolled steel joists. Though they are not yet fully understood it is known that even in the case of the beam carrying a central point load, yield of the reinforcement takes place over a considerable length of the beam.

When a concrete beam is over-reinforced so that failure of the beam takes place by crushing of the concrete, the load deflection curve does not exhibit such a typical " ductile " form. Instead of maintaining the maximum or " collapse " load for a very large deflection (which can be as much as one-fifth of the span in the case of a concrete beam with 1 per cent. tensile reinforcement and much more in the case of rolled steel joists) the load falls after a small, though real, deflection to as low as one-quarter of the maximum. This lower load is, however, maintained for a large deflection, the beam thus acquiring a belated " ductile " quality. It is clear, therefore, that continuous reinforced concrete structures, like those of mild steel, can be designed capable of supporting a considerable increase of load after the condition which is usually considered as failure has occurred. An interesting series of tests demonstrating this fact is reported in a Building Research Paper * wherein references will also be found to similar work carried out abroad.

The first test was made on a single span portal frame 5 feet span and 5 feet high. The cross-section of the beam was 4 inches by 7 inches with bottom reinforcement consisting of two $\frac{3}{8}$-inch diameter bars. Two bars $\frac{7}{8}$ inch diameter were carried up from the stanchions to form top reinforcement at the ends of the beam ; $\frac{1}{4}$-inch diameter stirrups were provided at every 4 inches. A central point load was applied to the beam and measurements were made of the bending moments in the frame. It was found that there was an initial elastic range when the bending moments were reasonably proportional to the applied load. This persisted until the load was 3·2 tons and the bending moment at the centre of the span reached about 25 ton-inches. At this load, what would normally be considered failure took place in the beam at the centre. Further load was added and, just as was found in the case of the steel portals, paragraph 24·3, the moment at the centre of the span remained practically constant at 25 ton-inches, while the end moments continued to increase. Collapse did not occur until the load reached 5 tons. This load was not sufficient to induce bending failure at the ends of the

* " Moment Redistribution in Reinforced Concrete." W. H. Glânville and F. G. Thomas. Building Research Technical Paper, No. 22, London, H.M. Stationery Office, 1939.

beam or in the columns owing to earlier shear failure. This is important since it indicates that increased load carrying capacity can only be relied upon when the new shear condition induced can be resisted.

Tests were also made on two-span continuous beams which were reinforced so that incipient failure would occur over the central support, either by yield of the steel or by crushing of the concrete. In the former the behaviour was very similar to that estimated for the propped steel beam of paragraph 24.4. That is to say, after yield had occurred over the central support, the moment there remained practically constant until the system collapsed due to failure at the centres of the spans. In those beams which were so made that crushing of the concrete first occurred over the central support this was not the case and the behaviour of the system cannot be so easily explained. The concrete at the support continued to carry load in an apparently undistressed condition long after the load calculated to produce a maximum fibre stress equal to the cube strength of the concrete (u lb. per square inch). However, the use of the assumption that the moment remained constant over the central support, at a value corresponding with a modular ratio of $40{,}000/u$, leads to a fair estimate of the collapse load of the system, except in the case where compression reinforcement was provided over the central support. The failing loads observed are given in Table 24.3 together with those calculated, (*a*) on the usual elastic theory, (*b*) on the simple plastic theory with the assumptions stated above and (*c*) on the simple plastic theory using the plastic moments found from tests on similar simply supported beams, as were the calculated results given in Table 24.2 for the steel portals. It will be seen from Table 24.3 that, apart from the case with

TABLE 24.3.

Cause of incipient failure at central support	Collapse loads for reinforced concrete continuous beams (tons)			
	Calculated			Observed
	(*a*) Elastic theory	(*b*) Plastic theory $\left(m = \frac{40{,}000}{u}\right)$	(*c*) Plastic theory (observed M_p)	
Steel failure	5·0	23·0	26·5	29·1
Concrete failure (no compression steel) . . .	7·8	28·5	30·7	28·6
Concrete failure (compression steel) . . .	19·8	36·3	36·3	28·9
Concrete failure (no compression steel, increased span length) .	2·5	11·8	13·4	13·0

compression steel over the support, the plastic theory gave a much better estimate of the collapse load than did the usual elastic theory.

Four further tests were carried out on portals to determine the load carrying capacity of a frame when the column head section was weak in either tension or compression. In each case the beam was considerably stronger than the columns, the designs representing extreme differences in column and beam strengths. The observed loads are given in Table 24.4, together with those calculated on the usual elastic theory and according to the simple plastic theory. It will be

TABLE 24.4.

Cause of incipient failure at column head section	Collapse loads for reinforced concrete portals (tons)		
	Calculated		Observed
	Elastic theory	Plastic theory	
Steel failure (1)	19·5	75·5	65·0
Steel failure (2)	19·5	75·5	67·8
Concrete failure (1)	24·7	46·8	47·1
Concrete failure (2)	18·8	42·6	43·2

seen that when incipient failure was by concrete weakness the agreement between the plastic theory loads and the observed loads was good but that it was not quite so good for the frames with incipient steel failure. In every case, however, the actual collapse load was far above that calculated on the usual elastic theory to produce failure at the column head. As was emphasised in the report of the tests, the results were obtained with frames specially designed, *i.e.* the shear reinforcement and the anchorage of the reinforcement were arranged to be sufficient for the actual shear and bond conditions developed in the plastic range. When such precautions are not taken, the extent to which the plastic range can increase the ultimate load carrying capacity of a reinforced concrete framework may be seriously reduced.

24.7. Conclusions.—There are many gaps in this short account of the behaviour of structures in the plastic range. Some, such as the effect of shear on the carrying capacity of a member, can be partially bridged by reference to the various papers listed in the footnotes. To fill others, further experimental data and mathematical analysis are required. There is, in fact, scope for many investigators in this field.

Though there is still much to learn, the information already available has made it possible to design successfully, by the plastic method, a variety of structures of the rigidly jointed single storey portal type.

Many difficulties have still to be resolved before a really simple procedure can be evolved for the design of multi-storey frames. It is doubtful whether it is in the best interests of the community to reduce all structural design methods to such simple terms that they can be applied without any knowledge of the fundamental theory of structural behaviour, since inevitably economy of material and progress must be sacrificed. However, if such a procedure is necessary the plastic theory seems likely to provide the most satisfactory basis.

The complication of deriving a rational method of design based on the behaviour of building frames in the elastic range will be apparent from Chapter 19. It has been shown in paragraphs 24.2–24.6 that for beams and portals close estimates can be made by the plastic method of the loads causing collapse, *i.e.* the growth of large deflections. The work on stanchions mentioned in paragraph 24·5 gives some hope that it may be possible to estimate the strength of these somewhat intractable members more accurately than has been the case in the past. It will eventually be possible to make an estimate of the collapsing load of any structure much more easily and accurately by the plastic than by the usual elastic theory. When this is so, a relatively simple method of designing any structure to support a given load without collapse should follow. By using for this design or collapse load the working load multiplied by a certain factor, it will be possible to ensure that the structure will not fail under accidental overload or due to variations in workmanship. Such a check as is usual in present-day methods will still have to be made to see that deflections under the working load are kept within the limits which experience shows to be necessary.

APPENDIX

BERRY FUNCTIONS

TABLE I

$f(\alpha)=6(2\alpha \operatorname{cosec} 2\alpha-1)/(2\alpha)^2$, $\varphi(\alpha)=3(1-2\alpha \cot 2\alpha)/(2\alpha)^2$,
$\psi(\alpha)=3(\tan\alpha-\alpha)/\alpha^3$. ($\alpha$ in radians)

$\alpha°$	$f(\alpha)$	$\varphi(\alpha)$	$\psi(\alpha)$	$\alpha°$	$f(\alpha)$	$\varphi(\alpha)$	$\psi(\alpha)$
0	1·0000	1·0000	1·0000	35	1·2065	1·1161	1·1759
1	1·0001	1·0001	1·0001	36	1·2208	1·1241	1·1880
2	1·0006	1·0003	1·0005	37	1·2359	1·1324	1·2007
3	1·0013	1·0007	1·0011	38	1·2517	1·1412	1·2140
4	1·0023	1·0013	1·0019	39	1·2683	1·1503	1·2281
5	1·0036	1·0020	1·0030				
6	1·0051	1·0029	1·0044	40	1·2858	1·1600	1·2429
7	1·0070	1·0040	1·0060	41	1·3042	1·1701	1·2584
8	1·0092	1·0052	1·0078	42	1·3236	1·1807	1·2747
9	1·0116	1·0066	1·0099	43	1·3440	1·1918	1·2918
				44	1·3654	1·2035	1·3099
10	1·0144	1·0082	1·0123	45	1·3880	1·2158	1·3289
11	1·0175	1·0100	1·0150	46	1·4118	1·2288	1·3489
12	1·0209	1·0120	1·0179	47	1·4370	1·2425	1·3700
13	1·0246	1·0140	1·0210	48	1·4635	1·2568	1·3922
14	1·0286	1·0163	1·0245	49	1·4915	1·2720	1·4157
15	1·0329	1·0188	1·0282				
16	1·0376	1·0214	1·0322	50	1·5211	1·2879	1·4405
17	1·0427	1·0243	1·0365	51	1·5524	1·3048	1·4666
18	1·0481	1·0273	1·0411	52	1·5856	1·3226	1·4944
19	1·0538	1·0306	1·0460	53	1·6208	1·3415	1·5237
				54	1·6582	1·3615	1·5549
20	1·0599	1·0341	1·0512	55	1·6979	1·3827	1·5880
21	1·0664	1·0377	1·0568	56	1·7403	1·4052	1·6232
22	1·0734	1·0416	1·0628	57	1·7853	1·4291	1·6607
23	1·0807	1·0458	1·0690	58	1·8335	1·4546	1·7007
24	1·0884	1·0502	1·0756	59	1·8850	1·4818	1·7434
25	1·0966	1·0548	1·0825				
26	1·1052	1·0596	1·0898	60	1·9401	1·5109	1·7891
27	1·1143	1·0647	1·0976	61	1·9994	1·5421	1·8381
28	1·1239	1·0701	1·1058	62	2·0631	1·5755	1·8908
29	1·1340	1·0758	1·1144	63	2·1318	1·6115	1·9476
				64	2·2060	1·6503	2·0089
30	1·1446	1·0817	1·1234	65	2·2865	1·6922	2·0753
31	1·1558	1·0879	1·1329	66	2·3741	1·7377	2·1474
32	1·1675	1·0945	1·1428	67	2·4695	1·7872	2·2260
33	1·1799	1·1013	1·1533	68	2·5739	1·8412	2·3119
34	1·1928	1·1086	1·1643	69	2·6886	1·9005	2·4061

TABLE I (*continued*)

$\alpha°$	$f(\alpha)$	$\varphi(\alpha)$	$\psi(\alpha)$	$\alpha°$	$f(\alpha)$	$\varphi(\alpha)$	$\psi(\alpha)$
70·0	2·8152	1·9657	2·5100	75·0	3·7083	2·4225	3·2409
70·1	2·8286	1·9725	2·5210	75·1	3·7323	2·4348	3·2606
70·2	2·8421	1·9795	2·5321	75·2	3·7568	2·4472	3·2806
70·3	2·8557	1·9865	2·5433	75·3	3·7815	2·4598	3·3008
70·4	2·8695	1·9936	2·5546	75·4	3·8066	2·4726	3·3213
70·5	2·8835	2·0008	2·5660	75·5	3·8321	2·4855	3·3421
70·6	2·8976	2·0080	2·5776	75·6	3·8579	2·4987	3·3631
70·7	2·9118	2·0153	2·5893	75·7	3·8841	2·5120	3·3845
70·8	2·9262	2·0227	2·6011	75·8	3·9107	2·5255	3·4062
70·9	2·9407	2·0302	2·6130	75·9	3·9376	2·5392	3·4282
71·0	2·9554	2·0378	2·6250	76·0	3·9650	2·5531	3·4505
71·1	2·9703	2·0454	2·6372	76·1	3·9927	2·5672	3·4731
71·2	2·9853	2·0531	2·6495	76·2	4·0208	2·5814	3·4961
71·3	3·0005	2·0609	2·6620	76·3	4·0494	2·5959	3·5194
71·4	3·0159	2·0688	2·6746	76·4	4·0784	2·6107	3·5431
71·5	3·0314	2·0767	2·6873	76·5	4·1078	2·6256	3·5671
71·6	3·0471	2·0848	2·7001	76·6	4·1376	2·6408	3·5914
71·7	3·0630	2·0929	2·7131	76·7	4·1680	2·6561	3·6162
71·8	3·0790	2·1011	2·7263	76·8	4·1987	2·6718	3·6412
71·9	3·0953	2·1095	2·7396	76·9	4·2300	2·6876	3·6667
72·0	3·1117	2·1179	2·7530	77·0	4·2617	2·7037	3·6926
72·1	3·1283	2·1264	2·7666	77·1	4·2940	2·7201	3·7189
72·2	3·1451	2·1350	2·7804	77·2	4·3267	2·7367	3·7456
72·3	3·1621	2·1437	2·7943	77·3	4·3600	2·7535	3·7727
72·4	3·1792	2·1524	2·8084	77·4	4·3938	2·7707	3·8003
72·5	3·1966	2·1614	2·8226	77·5	4·4281	2·7881	3·8283
72·6	3·2142	2·1704	2·8370	77·6	4·4631	2·8058	3·8568
72·7	3·2320	2·1795	2·8516	77·7	4·4986	2·8237	3·8857
72·8	3·2500	2·1887	2·8663	77·8	4·5346	2·8420	3·9151
72·9	3·2683	2·1980	2·8812	77·9	4·5713	2·8606	3·9450
73·0	3·2867	2·2074	2·8963	78·0	4·6086	2·8795	3·9754
73·1	3·3054	2·2170	2·9116	78·1	4·6465	2·8987	4·0063
73·2	3·3243	2·2266	2·9270	78·2	4·6851	2·9182	4·0377
73·3	3·3434	2·2364	2·9427	78·3	4·7243	2·9380	4·0697
73·4	3·3627	2·2463	2·9585	78·4	4·7643	2·9582	4·1022
73·5	3·3823	2·2563	2·9746	78·5	4·8049	2·9788	4·1353
73·6	3·4022	2·2664	2·9908	78·6	4·8462	2·9997	4·1690
73·7	4·4223	2·2767	3·0072	78·7	4·8883	3·0210	4·2032
73·8	3·4426	2·2871	3·0238	78·8	4·9311	3·0426	4·2381
73·9	3·4632	2·2976	3·0407	78·9	4·9748	3·0647	4·2737
74·0	3·4841	2·3082	3·0577	79·0	5·0192	3·0871	4·3098
74·1	3·5052	2·3190	3·0750	79·1	5·0644	3·1100	4·3467
74·2	3·5266	2·3299	3·0925	79·2	5·1105	3·1333	4·3842
74·3	3·5483	2·3410	3·1102	79·3	5·1575	3·1570	4·4224
74·4	3·5702	2·3522	3·1282	79·4	5·2053	3·1812	4·4613
74·5	3·5925	2·3635	3·1464	79·5	5·2541	3·2058	4·5010
74·6	3·6150	2·3750	3·1648	79·6	5·3038	3·2309	4·5415
74·7	3·6379	2·3866	3·1834	79·7	5·3545	3·2565	4·5828
74·8	3·6610	2·3984	3·2023	79·8	5·4062	3·2826	4·6248
74·9	3·6845	2·4104	3·2215	79·9	5·4589	3·3092	4·6677

TABLE I (*continued*)

$\alpha°$	$f(\alpha)$	$\varphi(\alpha)$	$\psi(\alpha)$	$\alpha°$	$f(\alpha)$	$\varphi(\alpha)$	$\psi(\alpha)$
80·0	5·5127	3·3363	4·7115	84·2	9·4578	5·3198	7·9168
80·1	5·5675	3·3640	4·7561	84·3	9·6229	5·4026	8·0508
80·2	5·6235	3·3922	4·8017	84·4	9·7939	5·4884	8·1896
80·3	5·6807	3·4211	4·8482	84·5	9·9711	5·5773	8·3335
80·4	5·7390	3·4505	4·8957	84·6	10·1549	5·6694	8·4827
80·5	5·7986	3·4805	4·9442	84·7	10·3457	5·7651	8·6375
80·6	5·8595	3·5112	4·9937	84·8	10·5438	5·8644	8·7982
80·7	5·9217	3·5426	5·0442	84·9	10·7497	5·9677	8·9653
80·8	5·9853	3·5746	5·0959				
80·9	6·0502	3·6073	5·1488	85·0	10·9638	6·0750	9·1391
				85·1	11·1867	6·1867	9·3200
81·0	6·1166	3·6408	5·2028	85·2	11·4189	6·3031	9·5084
81·1	6·1845	3·6750	5·2580	85·3	11·6610	6·4245	9·7049
81·2	6·2540	3·7100	5·3145	85·4	11·9137	6·5511	9·9098
81·3	6·3251	3·7458	5·3722	85·5	12·1776	6·6833	10·1239
81·4	6·3978	3·7824	4·4314	85·6	12·4535	6·8215	10·3478
81·5	6·4722	3·8199	5·4919	85·7	12·7423	6·9662	10·5821
81·6	6·5485	3·8582	5·5538	85·8	13·0448	7·1178	10·8275
81·7	6·6265	3·8975	5·6173	85·9	13·3621	7·2767	11·0849
81·8	6·7065	3·9378	5·6823				
81·9	6·7885	3·9790	5·7489	86·0	13·6954	7·4436	11·3552
				86·1	14·0457	7·6190	11·6394
82·0	6·8725	4·0213	5·8172	86·2	14·4144	7·8037	11·9384
82·1	6·9587	4·0646	5·8873	86·3	14·8032	7·9984	12·2537
82·2	7·0471	4·1091	5·9591	86·4	15·2135	8·2038	12·5865
82·3	7·1378	4·1547	6·0328	86·5	15·6473	8·4210	12·9384
82·4	7·2309	4·2015	6·1084	86·6	16·1067	8·6510	13·3109
82·5	7·3265	4·2496	6·1861	86·7	16·5939	8·8949	13·7060
82·6	7·4246	4·2989	6·2658	86·8	17·1116	9·1541	14·1259
82·7	7·5255	4·3496	6·3478	86·9	17·6627	9·4299	14·5727
82·8	7·6292	4·4017	6·4320				
82·9	7·7359	4·4553	6·5186	87·0	18·2506	9·7241	15·0495
				87·1	18·8791	10·0387	15·5592
83·0	7·8456	4·5104	6·6077	87·2	19·5525	10·3757	16·1052
83·1	7·9584	4·5671	6·6994	87·3	20·2758	10·7375	16·6917
83·2	8·0746	4·6255	6·7938	87·4	21·0548	11·1273	17·3233
83·3	8·1943	4·6856	6·8910	87·5	21·8961	11·5483	18·0054
83·4	8·3176	4·7475	6·9911	87·6	22·8076	12·0043	18·7444
83·5	8·4447	4·8114	7·0944	87·7	23·7983	12·5000	19·5478
83·6	8·5759	4·8772	7·2008	87·8	24·8792	13·0408	20·4240
83·7	8·7112	4·9451	7·3107	87·9	26·0631	13·6330	21·3839
83·8	8·8508	5·0152	7·4241				
83·9	8·9951	5·0876	7·5412	88·0	27·3653	14·2844	22·4396
84·0	9·1442	5·1624	7·6622				
84·1	9·2983	5·2398	7·7874				

Between 88° and 90° the functions can be calculated by the approximate formulas—

$$f(\alpha)=\frac{54{\cdot}71}{90-\alpha},\quad \varphi(\alpha)=\frac{27{\cdot}36}{90-\alpha}+0{\cdot}61,\quad \psi(\alpha)=\frac{44{\cdot}35}{90-\alpha}+0{\cdot}26,$$

α being in degrees.

TABLE II

$F(\alpha)=6(1-2\alpha \text{ cosech } 2\alpha)/(2\alpha)^2$, $\Phi(\alpha)=3(2\alpha \coth 2\alpha-1)/(2\alpha)^2$,
$\Psi(\alpha)=3(\alpha-\tanh \alpha)/\alpha^3$.

α Radians	$F(\alpha)$	$\Phi(\alpha)$	$\Psi(\alpha)$	α Radians	$F(\alpha)$	$\Phi(\alpha)$	$\Psi(\alpha)$
·00	1·0000	1·0000	1·0000	·50	·8945	·9391	·9092
·01	0·9999	1·0000	0·9999	·51	·8906	·9369	·9059
·02	·9998	0·9999	·9998	·52	·8868	·9346	·9026
·03	·9996	·9998	·9996	·53	·8828	·9323	·8992
·04	·9992	·9996	·9994	·54	·8789	·9300	·8957
·05	·9988	·9993	·9990	·55	·8748	·9276	·8922
·06	·9983	·9990	·9986	·56	·8708	·9253	·8887
·07	·9977	·9987	·9981	·57	·8667	·9229	·8851
·08	·9970	·9983	·9975	·58	·8626	·9204	·8815
·09	·9962	·9979	·9968	·59	·8584	·9180	·8779
·10	·9953	·9973	·9960	·60	·8542	·9155	·8743
·11	·9944	·9968	·9952	·61	·8500	·9130	·8706
·12	·9933	·9962	·9943	·62	·8457	·9105	·8669
·13	·9922	·9955	·9933	·63	·8414	·9080	·8632
·14	·9909	·9948	·9922	·64	·8371	·9054	·8595
·15	·9896	·9940	·9910	·65	·8328	·9028	·8557
·16	·9882	·9932	·9898	·66	·8284	·9003	·8519
·17	·9867	·9924	·9886	·67	·8240	·8977	·8481
·18	·9851	·9915	·9872	·68	·8196	·8950	·8442
·19	·9834	·9905	·9857	·69	·8151	·8924	·8403
·20	·9816	·9895	·9842	·70	·8107	·8897	·8364
·21	·9798	·9884	·9826	·71	·8062	·8871	·8325
·22	·9779	·9873	·9810	·72	·8017	·8844	·8286
·23	·9758	·9862	·9793	·73	·7972	·8817	·8247
·24	·9738	·9850	·9775	·74	·7927	·8790	·8207
·25	·9716	·9837	·9756	·75	·7881	·8762	·8167
·26	·9693	·9824	·9736	·76	·7835	·8735	·8127
·27	·9670	·9811	·9717	·77	·7790	·8708	·8087
·28	·9646	·9797	·9696	·78	·7744	·8680	·8047
·29	·9621	·9783	·9675	·79	·7698	·8653	·8007
·30	·9595	·9768	·9653	·80	·7652	·8625	·7967
·31	·9569	·9753	·9630	·81	·7606	·8597	·7927
·32	·9542	·9737	·9607	·82	·7560	·8569	·7887
·33	·9514	·9721	·9583	·83	·7513	·8541	·7847
·34	·9486	·9705	·9558	·84	·7467	·8513	·7807
·35	·9457	·9688	·9533	·85	·7421	·8485	·7766
·36	·9427	·9671	·9507	·86	·7374	·8457	·7725
·37	·9396	·9653	·9481	·87	·7328	·8429	·7684
·38	·9365	·9635	·9454	·88	·7282	·8400	·7643
·39	·9333	·9617	·9427	·89	·7235	·8372	·7601
·40	·9301	·9598	·9399	·90	·7189	·8344	·7560
·41	·9268	·9579	·9371	·91	·7143	·8315	·7519
·42	·9234	·9559	·9342	·92	·7096	·8287	·7478
·43	·9200	·9539	·9312	·93	·7050	·8259	·7437
·44	·9165	·9519	·9282	·94	·7004	·8230	·7396
·45	·9129	·9499	·9252	·95	·6958	·8202	·7355
46	·9094	·9478	·9221	·96	·6912	·8173	·7314
·47	·9057	·9456	·9189	·97	·6866	·8145	·7273
·48	·9020	·9435	·9157	·98	·6820	·8117	·7232
·49	·8983	·9413	·9125	·99	·6774	·8088	·7192

TABLE II (*continued*)

α Radians	F(α)	Φ(α)	Ψ(α)	α Radians	F(α)	Φ(α)	Ψ(α)
1·00	·6728	·8060	·7152	1·30	·5429	·7229	·5985
1·01	·6683	·8031	·7112	1·31	·5389	·7202	·5948
1·02	·6637	·8003	·7072	1·32	·5349	·7175	·5912
1·03	·6592	·7975	·7031	1·33	·5309	·7149	·5875
1·04	·6547	·7946	·6991	1·34	·5269	·7123	·5839
1·05	·6501	·7918	·6950	1·35	·5230	·7097	·5803
1·06	·6456	·7890	·6910	1·36	·5191	·7071	·5767
1·07	·6411	·7861	·6870	1·37	·5152	·7045	·5732
1·08	·6367	·7833	·6830	1·38	·5114	·7019	·5697
1·09	·6322	·7805	·6790	1·39	·5075	·6993	·5662
1·10	·6278	·7777	·6750	1·40	·5037	·6967	·5627
1·11	·6233	·7749	·6711	1·41	·4999	·6942	·5593
1·12	·6189	·7721	·6672	1·42	·4962	·6916	·5559
1·13	·6145	·7693	·6633	1·43	·4924	·6891	·5525
1·14	·6102	·7665	·6594	1·44	·4887	·6866	·5491
1·15	·6058	·7637	·6555	1·45	·4851	·6840	·5457
1·16	·6015	·7609	·6516	1·46	·4814	·6815	·5423
1·17	·5972	·7582	·6477	1·47	·4778	·6790	·5389
1·18	·5929	·7554	·6438	1·48	·4742	·6766	·5355
1·19	·5886	·7527	·6399	1·49	·4706	·6741	·5321
1·20	·5843	·7499	·6360	1·50	·4670	·6716	·5288
1·21	·5801	·7472	·6322	1·51	·4635	·6692	·5255
1·22	·5759	·7444	·6284	1·52	·4600	·6668	·5222
1·23	·5717	·7417	·6246	1·53	·4565	·6643	·5189
1·24	·5675	·7390	·6208	1·54	·4530	·6619	·5157
1·25	·5633	·7363	·6170	1·55	·4496	·6595	·5125
1·26	·5592	·7336	·6133	1·56	·4462	·6571	·5093
1·27	·5551	·7309	·6096	1·57	·4428	·6547	·5061
1·28	·5510	·7282	·6059	1·58	·4395	·6524	·5030
1·29	·5469	·7255	·6022	1·59	·4361	·6500	·4999
				1·60	·4328	·6476	·4968

TABLE III

Tanh α.

α Radians	Tanh α	α Radians	Tanh α	α Radians	Tanh α	α Radians	Tanh α
0·00	·00000	0·50	·46212	1·00	·76159	1·50	·90515
·01	·01000	·51	·46995	·01	·76576	·51	·90694
·02	·02000	·52	·47770	·02	·76987	·52	·90870
·03	·02999	·53	·48538	·03	·77391	·53	·91043
·04	·03998	·54	·49299	·04	·77789	·54	·91212
·05	·04996	·55	·50052	·05	·78181	·55	·91379
·06	·05993	·56	·50798	·06	·78566	·56	·91542
·07	·06989	·57	·51536	·07	·78946	·57	·91703
·08	·07983	·58	·52267	·08	·79320	·58	·91860
·09	·08976	·59	·52990	·09	·79688	·59	·92015
0·10	·09967	0·60	·53705	1·10	·80050	1·60	·92167
·11	·10956	·61	·54413	·11	·80406	·61	·92316
·12	·11943	·62	·55113	·12	·80757	·62	·92462
·13	·12928	·63	·55805	·13	·81102	·63	·92606
·14	·13909	·64	·56490	·14	·81441	·64	·92747
·15	·14888	·65	·57167	·15	·81775	·65	·92886
·16	·15865	·66	·57836	·16	·82104	·66	·93022
·17	·16838	·67	·58498	·17	·82427	·67	·93155
·18	·17808	·68	·59152	·18	·82745	·68	·93286
·19	·18775	·69	·59798	·19	·83058	·69	·93415
0·20	·19738	0·70	·60437	1·20	·83365	1·70	·93541
·21	·20697	·71	·61068	·21	·83668	·71	·93665
·22	·21652	·72	·61691	·22	·83965	·72	·93786
·23	·22603	·73	·62307	·23	·84258	·73	·93906
·24	·23550	·74	·62915	·24	·84546	·74	·94023
·25	·24492	·75	·63515	·25	·84828	·75	·94138
·26	·25430	·76	·64108	·26	·85106	·76	·94250
·27	·26362	·77	·64693	·27	·85380	·77	·94361
·28	·27291	·78	·65271	·28	·85648	·78	·94470
·29	·28213	·79	·65841	·29	·85913	·79	·94576
0·30	·29131	0·80	·66404	1·30	·86172	1·80	·94681
·31	·30044	·81	·66959	·31	·86427	·81	·94783
·32	·30951	·82	·67507	·32	·86678	·82	·94884
·33	·31852	·83	·68048	·33	·86925	·83	·94983
·34	·32748	·84	·68581	·34	·87167	·84	·95080
·35	·33638	·85	·69107	·35	·87405	·85	·95175
·36	·34521	·86	·69626	·36	·87639	·86	·95268
·37	·35399	·87	·70137	·37	·87869	·87	·95359
·38	·36271	·88	·70642	·38	·88095	·88	·95449
·39	·37136	·89	·71139	·39	·88317	·89	·95537
0·40	·37995	0·90	·71630	1·40	·88535	1·90	·95624
·41	·38847	·91	·72113	·41	·88749	·91	·95709
·42	·39693	·92	·72590	·42	·88960	·92	·95792
·43	·40532	·93	·73059	·43	·89167	·93	·95873
·44	·41364	·94	·73522	·44	·89370	·94	·95953
·45	·42190	·95	·73978	·45	·89569	·95	·96032
·46	·43008	·96	·74428	·46	·89765	·96	·96109
·47	·43820	·97	·74870	·47	·89958	·97	·96185
·48	·44624	·98	·75307	·48	·90147	·98	·96259
·49	·45422	·99	·75736	·49	·90332	·99	·96331
						2·00	·96403

INDEX

NOTE.—*References are to page numbers.*